

Iron and Manganese Homeostasis in Marine Bacteria

Robert Green

A thesis submitted to the University of East Anglia for the Degree of
Doctor of Philosophy

2012

© This copy of the thesis has been supplied on condition that anyone who consults it is understood to recognise that its copyright rests with the author and that use of any information derived there from must be in accordance with current UK Copyright Law. In addition, any quotation or extract must include full attribution.

I declare that the work in this thesis has not been previously submitted for a degree at the University of East Anglia or any other university, and all research has been carried out by myself, unless otherwise stated.

Signed,

Robert Tristan Green

Acknowledgements

Firstly I have to thank Andy Johnston for everything he has taught me, for his enthusiasm for my work, and for taking me on as an orphan PhD student. You will always be a voice in my head (in a good way)!

I must also thank Arnoud van Vliet, for being my very patient secondary supervisor; without your help this project would not have been possible.

To call all the other members of my lab, past and present, 'my colleagues' would be inaccurate. You are all my friends, and cannot stress enough the importance every single one of you had on my project, both in helping with my work, and in making the lab a great place to come, every single day.

I must also thank Claire, who has been such an incredible support at home; I wouldn't have done so well without you!

And to everyone along the way, friends past and present, thank you for whatever parts you played.

Finally, to my family, who are truly my best friends in life, you gave me so much support these last few years, through some tough times, and I am very thankful for that.

I would like to dedicate this thesis to my Mum; you started my 'academic career' all those years ago in York. Look where it ended up!

Abstract

Using a mixture of bioinformatic analyses, microarrays on cells that were grown in media that were either replete or depleted for manganese or for iron, and by making targeted mutations and reporter fusions, several important observations were made on the mechanisms of Mn and Fe homeostasis in the marine α -proteobacterium *Ruegeria pomeroyi* (the main species studied here), and in other important marine bacteria.

R. pomeroyi lacks most of the known Fe uptake systems, including TonB and outer-membrane receptors, but has a predicted, but incomplete iron uptake ABC-class transporter operon, whose expression is much enhanced in Fe-depleted conditions, although a strain lacking these genes was unaffected in growth. The Fe-specific regulatory network of *R. pomeroyi* was found to involve the Irr transcriptional regulator, which controlled the expression of several genes. Microarrays revealed many other genes whose expression was enhanced or diminished in Fe-replete conditions, providing material for future work on the iron regulon of this bacterium,

Turning to manganese, here too the expression of many genes was affected (up or down) by Mn availability. These included an operon corresponding to *sitABCD*, an effective ABC-type Mn^{2+} transporter in many other bacteria. This was confirmed, directly, to be the case for *Ruegeria*. Bioinformatic analyses showed that some other Roseobacter strains lacked any previously known Mn^{2+} transporter, but instead, had a gene that likely encoded an inner membrane protein and was preceded by a motif (MRS box) that was known to be recognised by the Mn^{2+} -responsive transcriptional regulator Mur. It was confirmed that this gene, termed *mntX*, did indeed encode a manganese transporter and that MntX orthologues occurred in several other, unrelated marine bacteria, notably most strains of the pathogenic genus *Vibrio* (including *V. cholerae*) and some of the most abundant bacteria in the oceans, namely the SAR11 clade (*Pelagibacter*).

Index

Acknowledgements.....	2
Abstract.....	3
Index.....	4
Figure Index.....	12
Table Index.....	14
Chapter 1 – General Introduction.....	16
1.1 Iron.....	16
1.1.1 Dependence of bacteria on iron.....	16
1.1.2 Iron chemistry.....	16
1.1.3 Iron catalyses the formation of oxygen free-radicals.....	17
1.2 Manganese.....	18
1.2.1 Dependence of Bacteria on Manganese.....	18
1.2.2 Manganese chemistry.....	18
1.2.3 Manganese helps protect cells from oxidative damage.....	19
1.3 The ocean environment.....	19
1.3.1 Ocean Geochemical Cycles.....	19
1.3.2 Marine Snow.....	20
1.3.3 Input of metals into the ocean.....	21
1.3.4 Iron and manganese availability in the ocean.....	23
1.3.5 Iron limitation for life in the ocean.....	23
1.4 Bacterial Iron Uptake Systems.....	25
1.4.1 Feo.....	25
1.4.2 Ferric reductases.....	25
1.4.3 Siderophores.....	26
1.3.4 Other bacterial sources of iron.....	27
1.3.5 Outer membrane receptors.....	28

1.3.6 TonB	29
1.3.7 ABC Transporters	29
1.3.8 Marine siderophores.....	31
1.4 Iron storage	33
1.4.1 Ferritins	33
1.4.2 Fe-S.....	34
1.5 Manganese uptake.....	35
1.5.1 MntH	35
1.5.2 SitABCD	35
1.5.3 MnoP	36
1.6 Iron and manganese –responsive regulatory systems	36
1.6.1 Fur	36
1.6.2 DtxR.....	37
1.7 Iron and manganese gene regulation in the α -proteobacteria	38
1.7.1 Fur	38
1.7.2 Irr.....	38
1.7.3 RirA.....	39
1.7.4 IscR.....	40
1.7.5 Mur.....	40
1.7.6 MntR	41
1.8 Marine metagenomics	42
1.8.1 The GOS dataset.....	42
1.9 The model Roseobacters.....	42
1.9.1 The Roseobacter Clade	42
1.9.2 The Ruegeria and Silicibacter Genera	44
1.10 Thesis aims	45
Chapter 2 - Iron Uptake in the Roseobacters – A Bioinformatic Approach	46
2.0 Introduction	46

2.1.1 Comparative genomics - bioinformatic analysis of iron uptake systems in the Roseobacters	46
2.1.2 The distribution of TonB-dependent outer membrane receptors in the Roseobacters	54
2.1.3 The search for TonB	56
2.1.4 Haeme and Ferrous iron ABC-class transporters are poorly conserved in the Roseobacters	65
2.2 Siderophore biosynthetic genes in the Roseobacters	66
2.2.1 Homologues of vicibactin and aerobactin biosynthesis genes in the Roseobacters	67
2.2.2 Vibriobactin biosynthetic genes in the Roseobacters	67
2.2.3 Enterobactin biosynthesis genes in the Roseobacters	68
2.3 Siderophore export and uptake in the Roseobacters	70
2.3.1 Enterobactin export genes in the Roseobacters	70
2.3.2 Aerobactin uptake genes in the Roseobacters	70
2.3.3 Rhodochellin uptake genes in the Roseobacters	71
2.4 Iron responsive regulators in the Roseobacters	71
2.4.1 Mur	71
2.4.2 Irr and RirA	72
2.4.3 IscR	72
2.4.4 The Roseobacters likely do not use ferric reductases	72
2.4.5 The Roseobacters may not import ferrous iron	73
2.4.6 Other genes linked to iron	73
2.7 Discussion	74
Chapter 3 - <i>in silico</i> study of putative iron regulated genes of <i>R. pomeroyi</i>	76
3.0 Introduction	76
3.1.1 Irr and its target ICE sequences and genes in <i>Ruegeria pomeroyi</i>	77
3.1.2 SPO3842, MbfA	78
3.1.3 SPO0382 FssA	79
3.1.4 SPO0330; CcpA	79

3.1.5 SPO2025–SPO2014; – the iscR-suf operon	79
3.2.1 Iron-Rhodo (IR) boxes	80
3.2.2 SPO0086 - irpA	82
3.2.3 SPO0087 – irpB.....	84
3.2.4 SPO0088	85
3.2.5 SPO0089	86
3.2.6 SPO0090	86
3.2.7 SPO3139 – A truncated haemoglobin protein	88
3.2.8 SPO0789- hemP	89
3.2.9 Components of an iron specific ABC-class transporter – FbpA and FbpB	89
3.3.1 Concluding comments	91
Chapter 4 - <i>in vivo</i> studies on iron uptake in <i>R. pomeroyi</i>	93
4.0.1 Introduction	93
4.1.1. <i>R. pomeroyi</i> does not produce siderophores	93
4.1.2 Iron deficiency limits growth of <i>R. pomeroyi</i>	94
4.1.3 The fbp iron transport genes of <i>R. pomeroyi</i>	95
4.1.4 Disruption of the fbpAB genes does not affect growth of <i>R. pomeroyi</i>	96
4.1.5 Growth phenotype of the Δ FbpAB strain of <i>R. pomeroyi</i>	103
4.1.6 Analysis of fbpA-lacZ and fbpB-lacZ transcriptional fusions	104
4.1.7 IR motifs preceding fbpA and fbpB are important for their Fe-responsive transcription .	107
4.1.8 ‘The “Irp” operon of <i>Ruegeria pomeroyi</i>	113
4.1.9 Expression of irpA is repressed by iron in <i>R. pomeroyi</i>	114
4.1.10 Construction of an IrpA ⁻ strain of <i>R. pomeroyi</i>	116
4.1.11 Phenotypic analysis of the IrpA ⁻ strain of <i>R. pomeroyi</i>	120
4.1.12 Iron-responsive expression of the hemP and iscR genes of <i>R. pomeroyi</i>	121
4.2 Discussion.....	122
Chapter 5 - Iron-Responsive transcriptional regulators in <i>R. pomeroyi</i> DSS-3	124
5.1 Introduction	124

5.2 <i>in vivo</i> analysis of iron responsive regulators of <i>R. pomeroyi</i>	124
5.2.1 The Rrf2 family of proteins in <i>Ruegeria pomeroyi</i> and the Roseobacters.....	124
5.2.2 Construction and analysis of mutations in genes for Rrf2-family proteins in <i>Ruegeria</i>	126
5.2.3 <i>Ruegeria pomeroyi</i> Irr – a global iron-responsive regulator in other α -proteobacteria ...	127
5.2.4 Phenotype of Irr ⁻ mutant of <i>R. pomeroyi</i>	131
5.2.5 Expression of mbfA in the Irr ⁻ strain of <i>R. pomeroyi</i>	131
5.2.6 Expression of iscR in the Irr ⁻ strain of <i>R. pomeroyi</i>	133
5.3 Discussion.....	134
Chapter 6 _a - Manganese Uptake and Regulation in <i>R. pomeroyi</i>	137
6.1 Introduction	137
6.1.1 <i>Ruegeria pomeroyi</i> has a homologue of the SitABCD manganese transporter.....	137
6.1.2 The expression of sitABCD responds to manganese levels.....	138
6.1.3 A SitA ⁻ strain of <i>R. pomeroyi</i> requires manganese for growth	139
6.1.4 Two cis-acting motifs regulate expression of sitABCD.....	141
6.1.5 Mur regulates sitABCD in <i>Ruegeria pomeroyi</i>	143
6.1.6 Mur regulates another Fur-family transcriptional regulator, irr in <i>R. pomeroyi</i>	144
Chapter 6 _b - Manganese uptake in other Marine Bacteria.....	146
6.2 Diversity of <i>mur</i> , <i>sitABCD</i> and other genes involved in Mn uptake and sensing in the Roseobacters.....	146
6.2.1 Mur.....	146
6.2.2 SitABCD	150
6.2.3 The Mn ²⁺ specific transporter MnH is also found in the Roseobacters	152
6.2.4 A novel class of Marine Mn uptake systems, MntX.....	155
6.2.5 Expression of mntX of <i>Roseovarius nubinhibens</i> is regulated by Mn levels via the Mur transcriptional regulator	155
6.2.6 Cloning and complementation of mntX of <i>R. nubinhibens</i>	156
6.2.7 The distribution of MntX in other bacteria	156
6.2.8 The γ -proteobacterial MntX.....	156

6.2.9 The α -proteobacterial MntX	163
6.2.10 MntX in the GOS	163
6.2.11 Structural predictions for mntX	166
6.2.12 Correction of the SitA ⁻ mutant of <i>Ruegeria pomeroyi</i> DSS-3 with the cloned mntX genes of <i>Candidatus Pelagibacter</i> sp. IMCC9063 and of <i>Vibrio cholerae</i>	167
6.3 Discussion.....	170
Chapter 7 - Microarray study of the Fe- and Mn-responsive transcriptome of <i>Ruegeria pomeroyi</i> .. 173	
7.1 Introduction	173
7.1.1 Methodology.....	173
7.1.2 Performing the microarray	174
7.2.1 Venn diagrams of gene expression patterns	176
7.3.1 Effects of manganese availability and mutations in mur on the transcriptome of <i>Ruegeria pomeroyi</i>	179
7.3.2 Class I – expression repressed in Mn-replete medium, and enhanced in Mur ⁻ mutant....	180
7.3.3 Class II – expression enhanced in Mn-replete medium, and enhanced in wild type, compared to Mur ⁻ mutant	182
7.3.4 Class III – expression repressed in Mn-replete medium, independent of mur genotype .	186
7.3.5 Class IV – expression enhanced in Mn-replete medium, independent of the mur genotype	188
7.4.1 Genes regulated by iron in <i>Ruegeria pomeroyi</i>	196
7.4.2 Effects of iron availability and mutations in irr on the transcriptome of <i>Ruegeria pomeroyi</i>	197
7.5.1 Genes that enhance the story already told in this thesis – regulation and uptake of Mn and Fe.....	199
7.5.2 Irr.....	200
7.5.3 MbfA	200
7.5.4 IscR.....	201
7.5.5 RRF-2 family proteins.....	201
7.5.6 The fbpAB genes	202

7.5.7 The irp genes.....	202
7.6.1 Genes highly regulated by iron and manganese limitation	203
Chapter 8 - General Discussion	208
8.1 Iron - Bioinformatically based outcomes	208
8.1.1 Paucity of ferrous iron and Fe-reductase genes	208
8.1.2 Marine siderophore production and uptake	210
8.1.3 TonB	211
8.1.4 Iron transporters in <i>R. pomeroyi</i>	212
8.2 Iron - Experimentally based outcomes	214
8.2.1 Regulation of the fbpAB genes of <i>R. pomeroyi</i>	214
8.2.2 The IR box cognate regulator.....	214
8.2.3 The marine Irr story	215
8.2.4 Pigment production by Irr- <i>R. pomeroyi</i>	216
8.3 Manganese - Bioinformatically based outcomes.....	217
8.3.1 MntX.....	217
8.3.2 Manganese uptake and regulation in the Roseobacters	217
8.4 Manganese - Experimentally based outcomes	218
8.4.1 SitABCD	218
8.4.2 MntX is a functional Mn transporter	218
8.5 The transcriptome of <i>R. pomeroyi</i> – some conclusions.....	220
8.5.1 Future microarray studies.....	221
8.5.2 Other targets for study	222
Chapter 9 - Materials and Methods.....	223
9.0 Media and General Growth Conditions	223
9.0.1 Luria-Bertani (LB) medium	223
9.0.2 Half-YTSS (HY) Medium.....	223
9.0.3 Marine Basal Medium (MBM).....	224
9.0.4 Rob's Sea Salts (RSS) Medium.....	224

9.0.5 Growth experiments	225
9.1.1 Glycerol storage	225
9.1.2 DMSO storage	226
9.2.1 Bacterial Conjugations	226
9.2.2 Conjugation via patch crosses.....	226
9.2.3 Conjugation via filter crosses	226
9.3.1 Purification of plasmid DNA using QIAGEN Miniprep kit.....	227
9.3.2 Mini-preparation of plasmid DNA by alkaline lysis and phenol-chloroform purification..	228
9.3.3 Purification of plasmid DNA using QIAGEN Midi kit	229
9.3.4 Purification of genomic DNA.....	231
9.3.5 RNA purification for microarrays	232
9.4 Microarrays	235
9.4.1 Performing microarray experiments.....	235
9.4.2 Microarray analysis	238
9.5 Manipulation and in vitro analysis of nucleic acids – DNA amplification and plasmid construction	238
9.5.1 Design of oligonucleotides used for PCR and SDM.....	238
9.5.2 Polymerase chain reaction (PCR) amplification of DNA	239
9.5.3 Colony PCR	239
9.5.4 Southern blot	240
9.5.5 Purification of PCR-amplified DNA.....	244
9.5.6 Restriction enzyme digestion.....	244
9.5.7 Dephosphorylation of plasmid DNA	245
9.5.8 Ligation of DNA fragments.....	245
9.5.9 DNA gel electrophoresis	245
9.5.10 Extraction of DNA from agarose gels.....	246
9.5.11 Site-directed mutagenesis (SDM)	246
9.6 Generation of genomic insertion mutants of <i>R. pomeroyi</i>	248

9.6.1 pK19 derivatives.....	248
9.6.2 pEX18Ap derivatives	248
9.7 Transformation of <i>E. coli</i> with plasmid DNA.....	249
9.7.1 Preparation of competent cells	249
9.7.2 Transformation of competent cells	249
9.7.3 DNA sequencing.....	250
9.7.4 β -Galactosidase assays.....	250
9.7.5 CAS assay plates.....	252
9.8 <i>in silico</i> analyses	252
9.8.1 DNA sequence analysis	252
9.8.2 Sequence alignments and phylogenetic trees	253
9.8.3 Database searches	253
9.8.4 Other bioinformatic tools	253
Appendix	258
Chapter 10 - Bibliography	204

Figure Index

Figure 1.1 Diagram of marine nutrient cycling	21
Figure 1.2 Mechanism of iron transport in bacteria.....	30
Figure 1.3 The structure and properties of three marine siderophores.....	32
Figure 1.4 Tree of selected members of the α -proteobacteria, to show the taxonomic distribution of the Roseobacters [adapted from (Williams et al. 2007)].....	43
Figure 2.1 Histogram of TBDR numbers in Roseobacters species	55
Figure 2.2 The enterochelin biosynthetic pathway	69
Figure 3.1 Logos of iron responsive regulator binding sites in <i>Ruegeria pomeroyi</i>	77
Figure 3.2 The <i>iscR-suf</i> operon of <i>R. pomeroyi</i>	80
Figure 3.3 Logos of iron responsive regulator binding sites in <i>Ruegeria pomeroyi</i>	81
Table 3.2 <i>Ruegeria pomeroyi</i> genes with predicted IR motifs.....	82

Figure 3.4 <i>SPO0086-SPO0090</i> Operon Map.....	83
Figure 3.5 IrpA, IrpB, OmpF and FhuA modelled in the outer membrane	85
Figure 3.6 STRING 9.0 Co-occurrence analysis of <i>SPO0086-SPO0090</i>	88
Figure 3.7 Arrangement of <i>fbpA</i> and <i>fbpB</i> genes in <i>R. pomeroyi</i>	91
Figure 4.1 Siderophore production by different strains and species of the Roseobacter clade	94
Figure 4.2 Growth of <i>R. pomeroyi</i> in MBM with iron limitation	95
Figure 4.3 Map of plasmid pEX18Ap.....	97
Figure 4.4 pBIO2103, and pBIO2104.....	99
Figure 4.5 Creating a mutagenic pEX18Ap derivative pBIO2105.....	100
Figure 4.6 Screening FbpAB ⁻ strains of <i>R. pomeroyi</i> using PCR.....	102
Figure 4.7 The effect of iron limitation on growth of FbpAB ⁻ strains of <i>R. pomeroyi</i>	104
Figure 4.8 Generation of wide host range <i>fbpA</i> - and <i>fbpB-lacZ</i> fusion plasmids pBIO1845 and pBIO1846	106
Figure 4.9 Expression of iron availability on the expression of <i>fbpA-lacZ</i> and <i>fbpB-lacZ</i> fusions.....	107
Figure 4.10 The IR boxes upstream of <i>fbpA</i> and <i>fbpB</i> of <i>R. pomeroyi</i>	109
Figure 4.11 Effects of mutations in the IR boxes on the expression of <i>fbpA</i> and <i>fbpB</i>	112
Figure 4.12 The <i>irpA</i> promoter region showing IR box location and sequence.....	113
Figure 4.13 Gel photos of clone, and site-directed mutant clone, of the promoter region of <i>irpA</i> into pBIO1878	115
Figure 4.14 Effects of Fe and the IR motif on the expression of <i>irpA-lacZ</i>	116
Figure 4.15 Insertion and ratification of insertion mutation into <i>R. pomeroyi irpA</i>	118
Figure 4.16 Verification by Southern blot of an insertional mutation into <i>irpA</i>	120
Figure 4.17 Effect of iron limitation on expression of <i>hemP</i> - and <i>iscR-lacZ</i> fusions.....	122
Figure 5.1 Phylogenetic tree of Rrf2 family transcriptional regulator peptide sequences.....	125
Figure 5.2 Map of Irr ⁻ recombinant mutant.....	129
Figure 5.3 PCR screening of potential Irr ⁻ mutants of <i>R. pomeroyi</i>	130
Figure 5.4 Effect of iron limitation and <i>irr</i> on expression of <i>mbfA</i> in <i>R. pomeroyi</i>	132
Figure 5.5 Effect of Fe on a <i>iscR</i> fusion in both wild type, and Irr ⁻ <i>R. pomeroyi</i>	134
Figure 6.1 Map of the <i>sit</i> locus of <i>R. pomeroyi</i>	138
Figure 6.2 Effects of mutating <i>Ruegeria pomeroyi sitA</i> on growth in manganese-depleted media... 140	
Figure 6.3 Mur-box (MRS) of the Rhodobacteraceae and an alignment of the two MRS boxes upstream of <i>sitA</i> in <i>R. pomeroyi</i>	141
Figure 6.4 β -galactosidase activity of <i>sitA-lacZ</i> fusion in <i>R. pomeroyi</i> and the effect of mutating the MRS boxes.....	142

Figure 6.5 Effects of Mn-limitation of the expression of the <i>irr-lacZ</i> fusion.....	145
Figure 6.6 Phylogenetic tree of Mur peptides in the α -proteobacteria	147
Figure 6.7 Phylogenetic tree of SitA-like peptides.....	151
Figure 6.8 Comparison of MRS sequences that precede the <i>sitA</i> and <i>mntX</i> genes of selected Roseobacter strains	152
Figure 6.9 Phylogenetic tree of all MntX peptides	165
Figure 6.10 Prediction of TM domains in MntX proteins, with MntH for reference	167
Figure 6.11 Growth defect of the <i>R. pomeroyi</i> SitA ⁻ strain J529 is corrected by the cloned <i>mntX</i> genes of <i>Pelagibacter</i> , <i>Roseovarius nubinhibens</i> and <i>Vibrio cholerae</i>	169
Figure 7.1 Scanned microarray slide from this work	175
Figure 7.2 Venn diagram showing numbers of genes that were differentially expressed depending on availability of Mn and/or Fe and/or the <i>mur</i> or <i>irr</i> genotype.....	177
Table 7.1 Lists of <i>Ruegeria pomeroyi</i> genes in the categories in the Venn diagram in Figure 7.2	178
Figure 7.3 <i>sitABCD</i> map with expression ratios	180
Figure 7.4 <i>SPOA0392-SPOA0399</i> map with expression ratios.....	181
Figure 7.5 <i>SPO1789-SPO1791</i> map with expression ratios.....	183
Figure 7.6 <i>SPO0833-SPO0834</i> map with expression ratios.....	184
Figure 7.7 <i>SPO1555-SPO1556</i> map with expression ratios.....	185
Figure 7.8 Map of <i>SPO2250-SPO2264</i>	187
Figure 7.9 Map of <i>SPOA0339-SPOA0347</i>	188
Figure 7.10 Map of <i>SPO2394-SPO2399</i>	190
Figure 7.11 Map of <i>SPO1500-SPO1508</i>	191

Table Index

Table 2.1. Bioinformatic study of iron uptake genes in the Roseobacters	47
Table 2.2 Functions and genbank identities of all peptides used in Table 2.1	52
Table 2.3 Presence of TonB Homologues in Genome-Sequenced Strains of the Roseobacter Clade ..	58
Table 3.1 Genes with ICE boxes	78
Table 4.1 Oligonucleotide primer sequences for IR box site directed mutagenesis	110
Table 5.1 Prevalence of Rrf2 gene homologues of <i>Ruegeria</i> in the Roseobacters.....	126
Table 5.2 Primer sequences used to generate mutant strains of <i>R. pomeroyi</i>	127

Table 6.1 The effect of a Mur ^r mutation on the expression of a <i>sitA-lacZ</i> fusion.....	144
Table 6.2 Distribution of sub-types of the SitA, MntX, MntH and Mur polypeptides in genome-sequenced Roseobacter strains.....	153
Table 6.3 Distribution of manganese transporters in α -proteobacterial genera that have at least one strain with a homologue of MntX.....	158
Table 7.2 Genes whose expression is affected by the Mur regulator and/or Mn ²⁺ availability.....	192
Table 7.3 Genes affected by both Fe limitation and the <i>irr</i> mutation.....	198
Table 7.4 <i>Ruegeria pomeroyi</i> genes whose expression was altered >5-fold in response to iron limitation; predicted function, cellular location, structural prediction and prevalence in the Roseobacters.....	203
Table 9.1 Details of Strains, Plasmids and Oligonucleotide primers used in this work.....	255

Chapter 1 – General Introduction

1.1 Iron

On Earth, iron is the second most common metal, and the fourth most plentiful element in the Earth's crust (Emsley 2001). It predominantly exists in two oxidised states, the extremely water-soluble ferrous iron (Fe^{2+}) and the extremely insoluble ferric iron (Fe^{3+}) (Crichton and Boelaert 2001). Fe found in seawater is nearly all in the ferric form, due to the oxic and slightly alkaline conditions.

1.1.1 Dependence of bacteria on iron

Iron (Fe) is required for growth of almost all microorganisms. It is used as a catalytic cofactor in many biological processes including photosynthesis, respiration, the citric acid cycle of central metabolism, gene regulation and DNA biosynthesis (Andrews *et al.* 2003). There are some examples of bacteria that do not require iron; these include *Lactobacillus*, which uses manganese and cobalt in place of iron (Archibald 1983; Pandey *et al.* 1994), *Borrelia burgdorferi*, a genome-reduced endosymbiotic parasite that utilises its host's metabolism to replace its own iron dependency (Posey and Gherardini 2000) and some species of Streptococci that can grow in the absence of Fe (Niven *et al.* 1999; Spatafora and Moore 1998). All bacteria that do not require Fe for growth have an absolute requirement for Mn (Jakubovics and Jenkinson 2001).

1.1.2 Iron chemistry

The coordination stereochemistry of both Fe^{2+} and Fe^{3+} means that they are often found as octahedral complexes in nature. Dependent on the associated ligand, a coordinated iron atom can exist in a high or low spin state. Weak field ligands such as F^- or OH^- increase the frequency of paired electrons in the iron-ligand interaction and are described as a low spin complex, whereas strong field ligands such as CO or CN^- maximise unpaired electrons and cause high spin complexes (Crichton and Boelaert 2001). Both the ferric and ferrous forms of iron are Lewis acids, the ferric state being stronger than the ferrous (Crichton and Boelaert 2001). The range of redox potential of both Fe^{2+} and Fe^{3+} is huge, and can be fine-tuned by various ligands. The iron site of any molecule or complex can

almost span the entire range of biologically relevant redox potentials, from -0.5 V to +0.6 V (Crichton and Boelaert 2001). Furthermore, iron complexes can catalyse electron transfer and acid-base reactions, making iron a hugely important and adaptable element for many physiological processes.

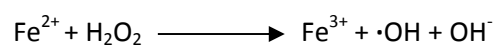
All these chemical properties make iron the ideal cofactor for many enzymes (Andrews *et al.* 2003), and the near-ubiquitous iron-dependency of all living things suggests that this has been the case since life evolved (Beinert *et al.* 1997) and may even have contributed to the emergence of life (Wachtershauser 2000).

Molecular oxygen was not present on Earth when life emerged, so all the iron present was in the reduced form. This iron was soluble, and easily accessible to all forms of emerging life. As early cyanobacteria 'breathed' oxygen into our atmosphere, the great majority of the dissolved iron became oxidised and precipitated out of the oceans, leaving huge deposits of iron hydroxides in the Precambrian fossil layer (Crichton and Boelaert 2001).

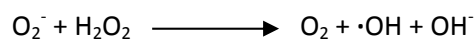
1.1.3 Iron catalyses the formation of oxygen free-radicals

Ferrous iron can participate in the heterolytic fission of the dioxygen bond in hydrogen peroxide (H₂O₂) leading to the generation of a hydroxyl radical and a hydroxide ion. This process involves both Fenton chemistry and the Haber-Weiss reaction, as shown below:

Fenton chemistry (Fenton 1894).



Iron can also catalyse the formation of a hydroxyl radical through the Haber-Weiss reaction (Haber and Weiss 1932):



The lone unpaired electron in the hydroxyl radical makes it highly reactive, and this hydroxyl species can damage proteins, carbohydrates, lipids and nucleic acids, so it is genotoxic, and mildly mutagenic (Sies 1993). This means that this essential metal can also be lethal. It follows that Fe homeostasis in bacteria (and, indeed, all organisms) is tightly regulated, so that cells have neither too little, nor too much Fe.

1.2 Manganese

Manganese is the twelfth most common element in the Earth's crust (Emsley 2001), and exists in a range of oxidised states (+1 - +7), the most common being Mn^{4+} in MnO_2 (pyrolusite). Manganese in sea water is found in the soluble state Mn^{2+} , although it also occurs as the insoluble oxides Mn^{3+} and Mn^{4+} (Stumm and Morgan 1981). In the oceans, soluble Mn oxides are reduced to Mn^{2+} by sunlight (Sunda *et al.* 1998), making them biologically available. Dissolved Mn levels are in the low nanomolar range in surface waters of the ocean (Landing and Bruland 1987; Middag *et al.* 2011).

1.2.1 Dependence of Bacteria on Manganese

Manganese (Mn) is also an essential metal, being critical for photosynthesis, gluconeogenesis, glycolysis, amino acid and aromatic acid metabolism, peptide cleavage, nucleic acid degradation, signal transduction and the stringency and oxidative stress responses in a variety of bacteria (Jakubovics and Jenkinson 2001). In bacteria, there is a clear biological, as well as a chemical, link between the two very similar transition metals Mn and Fe. Thus, Mn can regulate intracellular levels of Fe in *Bradyrhizobium japonicum* (Puri *et al.* 2010) and the expression of Mn uptake systems is under the control of Fe and Mn in *Escherichia coli* (Patzner and Hantke 2001), *Salmonella enterica* serovar Typhimurium (Kehres *et al.* 2002) and *Bacillus subtilis* (Que and Helmann 2000).

1.2.2 Manganese chemistry

$Mn(II)$ has an ionic radius of 0.8\AA , which is very similar to that of Fe^{2+} (0.76\AA), and indeed other transition metals such as calcium and magnesium (Jakubovics and Jenkinson 2001). Because of this size similarity, Mn will often substitute for Fe in the metal-binding sites of proteins; Mn also commonly incorporates into Mg-specific ligands due to their similar binding properties (Jakubovics and Jenkinson 2001).

Mn has a major role in biological systems by catalysing redox reactions. These Mn-containing enzymes can have 1, 2 or 4 Mn atoms to facilitate redox chemistry. Mononuclear Mn containing enzymes include the Mn-containing superoxide dismutase, Mn-dependant peroxidase, and Mn-

dioxygenase. Bacterial catalase and Mn-ribonucleotide reductase enzymes utilise a binuclear Mn redox site, and the oxygenic catalytic centre of photosystem II has 4 Mn atoms (Law *et al.* 1998).

1.2.3 Manganese helps protect cells from oxidative damage

In contrast to iron, the reactions between Mn^{2+} and O_2^- , H_2O_2 or $\cdot OH$ do not form hydroxyl radicals (Cheton and Archibald 1988; Stadtman *et al.* 1990). Indeed, being a co-factor in the Mn-superoxide dismutase SodA, Mn is essential in detoxifying reactive oxygen species (Keele *et al.* 1970), and several groups of lactic acid bacteria use millimolar levels of intracellular Mn^{2+} to “mop up” and detoxify superoxides (Archibald 1986).

1.3 The ocean environment

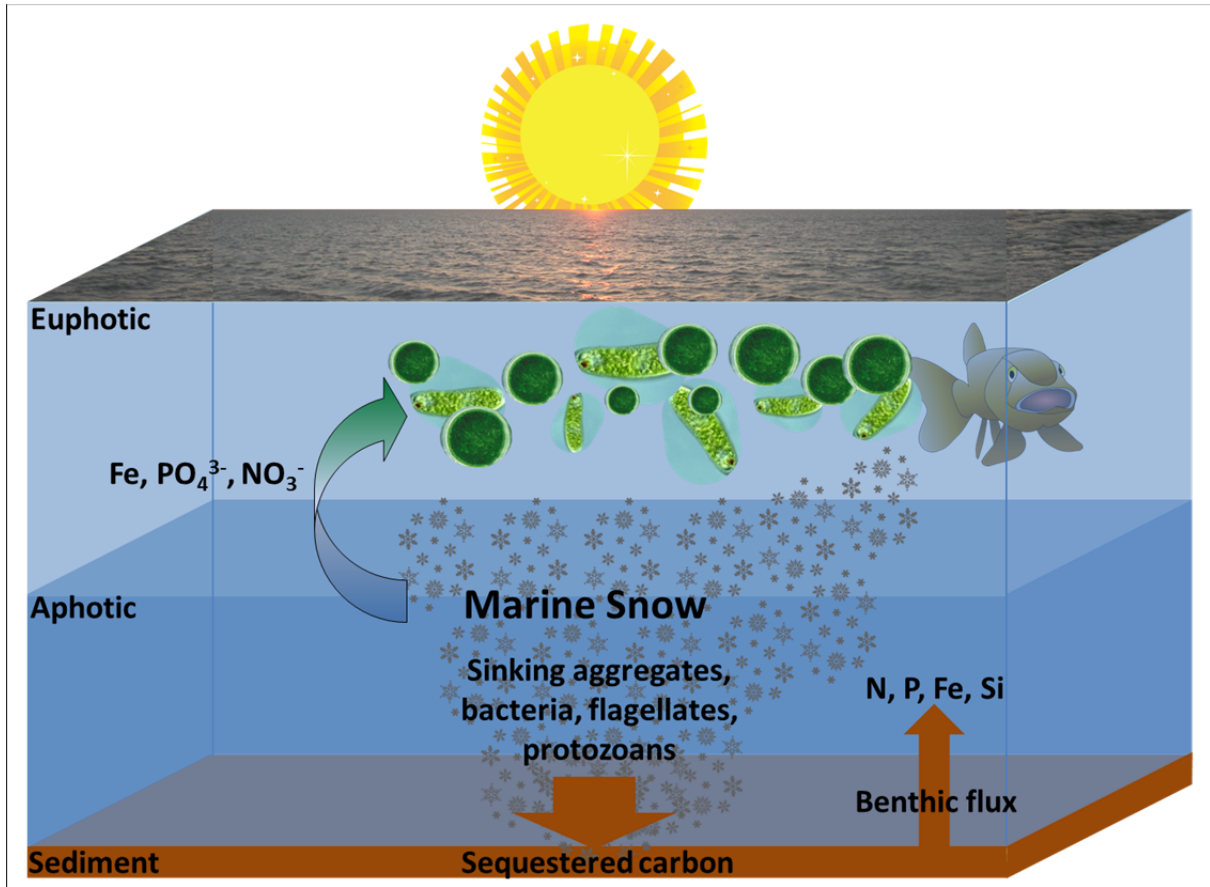
1.3.1 Ocean Geochemical Cycles

Cycling of organic molecules within the epipelagic zone (<200 m) occurs readily by mixing due to wind action, thermohaline current (Millero 2006), and through the abundant aquatic microbes (Whitman *et al.* 1998) constituting the ‘biological pump’ (Buesseler and Boyd 2009). Below the epipelagic, the mesopelagic (< 1000m) zone contains water that remains in place for decades, yet bacteria and archaea (Karner *et al.* 2001; Kirchman *et al.* 2007), protists (Peter *et al.* 2007) and nanoflagellates (Hideki *et al.* 2007) found here contribute extensively to ocean metabolism (Aristegui *et al.* 2009). Further down still, the bathypelagic (1000–4000-m depth) and abyssal zones (>4000 m) contain extremely high pressure water which remains *in situ* for centuries (Aristegui *et al.* 2009). In these ecosystems, very little is known about the biology, although a study by Sogin *et al.* (Sogin *et al.* 2006), revealed that 80% of mesopelagic and bathypelagic organisms were from uncharacterised genera. Movement of nutrients, metabolites and sequestered compounds down the water column is also caused by gravity – in the form of marine snow.

1.3.2 Marine Snow

Marine snow consists of organic material, excreted waste and inorganic solids falling from the densely populated euphotic zone, settling on the ocean floor in benthic sludge depositions. Phytoplankton, bacteria, flagellates and protozoans form part of clumping snow particles, which can measure many centimetres across, and are considered an important part of nutrient cycling in the water column (Alldredge and Silver 1988). Bacteria can reach densities of 10^8 – 10^9 per ml of marine snow (Alldredge *et al.* 1986). These break down organic material, releasing plumes of small molecules and ions from the snow particles (Azam and Malfatti 2007; Kioerboe and Jackson 2001). These plumes play a major role in recycling iron, phosphate and nitrates back to the higher water column (Kioerboe and Jackson 2001), and also lead to a net loss of carbon from the upper ocean compared to these compounds; refer to figure 1.1 (Azam and Malfatti 2007).

Figure 1.1 Diagram of marine nutrient cycling



Marine snow falling from the euphotic zone is colonised by microorganisms which contribute to the flux of nutrients. Plumes of nutrients, Fe , PO_4^{3-} and NO_3^- , are released by grazing bacteria, flagellates and protozoans from marine snow. These are recycled back into the phytoplankton rich euphotic zone; the remaining snow falls through the aphotic zone where it is sequestered into the benthic sediment. Over time, elemental nitrogen, phosphorus, iron and silicon are reabsorbed by the water column where they re-join the cycle. Also, a net loss of carbon occurs from the water as marine snow enters the sediment (Azam and Malfatti 2007).

1.3.3 Input of metals into the ocean

The influx of Fe and Mn into the oceans is mainly from erosion of sediments, which are washed into terrestrial waterways (Johnson *et al.* 1997), and the metal laced dust that is carried around in the atmosphere (Coale *et al.* 1996; Duce and Tindale 1991). Dust is considered to be the major pathway of marine iron input (Jickells *et al.* 2005), only 10 % of which is soluble in seawater (Zhuang *et al.* 1990). However, Mn concentrations in surface seawater are nearly entirely due to dust deposition

(Mendez *et al.* 2010). There are extremely low levels of Fe and Mn in the Southern Oceans due to a lack of dust input into this body of water (Martin *et al.* 1990).

Global iron deposition into the oceans is estimated to be between 131 and $487 \times 10^9 \text{ mol yr}^{-1}$ (Duce and Tindale 1991; Mahowald *et al.* 1999; Tegen and Fung 1995), fuelling blooms of life in both coastal and offshore waters (Archer and Johnson 2000). Iron availability in the oceans contributes directly to both the strength of the biological pump, and the amount of dissolved CO_2 (Archer and Johnson 2000), both of which are vital to a stable climate (Sunda 2010).

The global input of Mn into the oceans has not been determined, but some initial estimates for the flux of Mn to the Southern Ocean indicate that that $\sim 2 \mu\text{mol Mn m}^{-2}\cdot\text{yr}^{-1}$ of Mn is deposited by dust, which is less than the estimate of Mn flux from marine and land sediments into the same water system - $3.3 \mu\text{mol Mn m}^{-2}\cdot\text{yr}^{-1}$ (Middag *et al.* 2011)

Iron cycling within oceans is complex. Fe(III) is almost entirely bound to organic ligands (Gledhill and van den Berg 1994; Rue and Bruland 1995; Rue and Bruland 1997; van den Berg 1995; Wu and Luther 1995). The precise makeup of these Fe-containing materials is poorly understood; thus Hopkinson (2009) states that the ligand pool '*is likely to be a mixture of siderophores, organic exudates and humic material*'. Any Fe(II) is either used by bacteria and phytoplankton, or falls to the ocean floor in marine snow, where benthic flux slowly returns metals to the water by diffusion (Azam and Malfatti 2007). The mechanical stirring of water via waves, and currents such as the Gulf Stream, and transport of iron via feeding and migrating macroscopic life leads to its movement both horizontally and vertically around the water column, so both physical and biological factors impact on the distribution of this metal (Morel and Price 2003).

The iron cycle is directly linked to the 'biological pump': 25 % of all CO_2 released into the atmosphere is absorbed into the oceans (Feely *et al.* 2009), causing a decrease in pH (Sunda 2010). By the end of the century, current trends show that the global pH of seawater will drop from 8.2 to 7.7 (Feely *et al.* 2009; Millero *et al.* 2009). Increasing acidification of surface water will decrease the bioavailable (Fe(II)) iron, less phytoplankton will grow, and less CO_2 will be fixed, with real potential for increasing global warming further – a dangerous feedback loop (Shi *et al.* 2010).

1.3.4 Iron and manganese availability in the ocean

Total dissolved iron concentrations in the oceans range from 20 pM to 1 nM in pelagic, offshore zones (Bruland *et al.* 1994; Gordon *et al.* 1982; Martin *et al.* 1991), and 100 pM to 10 nM around the coastlines (Gordon *et al.* 1982; Wu and Luther 1995). Iron availability is sensitive to pH, a particularly relevant factor, given the increasing atmospheric CO₂, and consequent acidification of the oceans (Shi *et al.* 2010). Modelled increases in irradiation or decreases in temperature were both shown to enhance levels of Fe(II) (Tagliabue *et al.* 2009), the biologically available form of iron. More than 99% of dissolved iron is in complex with unidentified ligands (Gledhill and van den Berg 1994; Rue and Bruland 1995; Rue and Bruland 1997; van den Berg 1995; Wu and Luther 1995), thereby reducing free iron concentration to low picomolar quantities (Bruland *et al.* 1994; Gordon *et al.* 1982; Martin *et al.* 1991; Wu and Luther 1995), although there is ongoing debate about iron availability in seawater (Hutchins *et al.* 1999; Wells *et al.* 1995). It is strongly suggested that the ligands responsible for most of the iron chelation are bacterial siderophore pools (Granger and Price 1999; Haygood *et al.* 1993; Hutchins *et al.* 1999; Rue and Bruland 1995; Tortell *et al.* 1999; Wilhelm *et al.* 1998).

Even though Mn is, overall, an abundant element on Earth, it only exists in low nanomolar concentrations in seawater - < 1nM in the Southern Ocean, though somewhat higher (~ 20 nM) in the Arctic Ocean (Middag *et al.* 2011a). Mn is found as both insoluble Mn oxides, and soluble Mn ions, which are rapidly lost from the upper water column by sinking, and by uptake by cells (Sunda and Huntsman 1994). Therefore, Mn concentrations fall with increasing depth (Middag *et al.* 2011).

1.3.5 Iron limitation for life in the ocean

Bacterial communities in the euphotic zone are hugely abundant (Hobbie *et al.* 1977; Whitman *et al.* 1998) and diversity is rich (Rusch *et al.* 2007; Shaw *et al.* 2008). Competition for nutrients, including iron (Measures *et al.* 2008), is therefore extremely high (Hutchins *et al.* 1999), as has been extensively modelled by Moore *et al.* (2001). Iron limits growth of bacteria in certain parts of the oceans (Martin *et al.* 1991; Moore *et al.* 2001), as graphically revealed by the iron fertilisation experiments, IRONEX I and II (Coale *et al.* 1996; Martin *et al.* 1994). In IRONEX I, Martin *et al.* (1994) increased iron concentration 2-fold (to around 4 nM) over a 64 km² area in the equatorial Pacific. Subsequently, IRONEX II (Coale *et al.* 1996) expanded this work by using three separate iron fertilisation events (2 nM, then two subsequent additions of 1 nM) over a 7 day period. Both studies

produced large-scale blooms of phytoplankton, with a 27-fold increase in chlorophyll concentration in the case of IRONEX II. Recent research in the eastern Pacific (Boyd *et al.* 2004; Tsuda *et al.* 2003) and the Southern Ocean (Blain *et al.* 2007; Boyd *et al.* 2000; Coale *et al.* 2004; Pollard *et al.* 2009) showed massive variation in this phenomenon: persistence of blooms lasted from 2 – 50 days, and sequestered carbon levels were inconsistent. None of the studies purported to discover the fate of sequestered carbon but are considered good early studies into the principle of iron fertilisation (Güssow *et al.* 2010). The amount of iron chelation by organic ligands increased by an average of 4-fold after iron fertilisation, suggesting that these molecules are biological in origin (Rue and Bruland 1997). This increase in organic ligand production is likely due to the increase in bacterial numbers.

Since iron is so poorly available, various physiological strategies have evolved to acquire this limited nutrient. Morphological adaption to low iron conditions is exemplified by a very small cell size in the abundant cyanobacterium, *Synechococcus* (Rueter and Unsworth 1991) and in the highly abundant SAR11 (Morris *et al.* 2002). Furthermore, a 20-50 % decrease in cell volume, in response to low Fe, was reported in both coastal (*Thalassiosira weissflogii*, *T. pseudonana*, *Prorocentrum minimum*) and offshore species (*Emiliania huxleyi*, *Pelagomonas calceolata*, *T. oceanica* (Sunda and Huntsman 1995)) of eukaryotic phytoplankton.

Bactivory by the phytoplankton *Ochromonas* was shown by (Maranger *et al.* 1998) to be a major source of this flagellate's iron requirements: 'let someone else do the hard work...'.

On a molecular level, several species of phytoplankton and bacteria show adaptations in metalloprotein use under low iron conditions, replacing the photosynthetic electron transfer chain component cytochrome c-553 with a copper-containing plastocyanin, for example (Wood 1978). In the cyanobacterium *Synechocystis* 6803, this switch is regulated by the availability of copper (Zhang *et al.* 1992).

Another Fe-S-containing protein, ferredoxin, was shown to be replaced *in vivo* with flavodoxin in cyanobacteria (Lin *et al.* 2009; Mitsui and Arnon 1971; Smillie 1965), in diatoms (Pankowski and McMinn 2009; Roche *et al.* 1995), and other phytoplankton (Doucette *et al.* 1996; Entsch *et al.* 1983; Erdner *et al.* 1999; Sandmann *et al.* 1990). This phenomenon is also found in terrestrial bacteria, demonstrating that the ability of bacteria to adapt to Fe availability is clearly well conserved and likely very important.

1.4 Bacterial Iron Uptake Systems

As introduced above, Fe is a limiting resource, and may be especially scarce in marine environments. As a result, bacteria have evolved a variety of iron acquisition strategies. Most of what we know about Fe uptake is from a number of mostly terrestrial bacteria, most notably *E. coli* and the enterics, though with others as well. These include high affinity transporters, employment of iron chelating molecules and reduction of ferric iron to the ferrous form.

1.4.1 Feo

In anaerobic conditions, iron is found in the reduced ferrous form. Obligate and facultative anaerobic species of bacteria can use Fe²⁺-specific transporters to obtain this iron (Schroder *et al.* 2003). Bacteria such as *E. coli*, *Salmonella*, and *Shigella*, which can reside in the micro-oxic conditions of the gut, use the Feo polypeptide transporters to obtain ferrous iron. The *feo* locus consists of three genes, *feoABC*. Deletion mutants in *feoB* causes lower survival rates in a mouse colon in both *Salmonella typhimurium* (Tsolis *et al.* 1996) and *E. coli* (Stojiljkovic *et al.* 1993).

The C-terminal domain of FeoB is a helix rich transmembrane domain thought to be the permease for ferrous iron transport. The N-terminus is homologous to a GTP-binding G-protein, which is proposed to provide the active transport energy (Cartron *et al.* 2006). The functions of FeoA and FeoC are unresolved, but are not required for expression of *feoB*, but are needed for iron transport functionality. FeoA interacts directly with FeoB in *Salmonella enterica* (Kim *et al.* 2012), and is homologous to the C-terminal domain of the DtxR regulator (Braun and Killmann 1999; Kammler *et al.* 1993). The sequence of FeoA is predicted to be a GTPase activating protein, and is possibly an Fe-dependant transcriptional regulator (Cartron *et al.* 2006). FeoC is homologous to a winged-helix domain protein, only found in the γ -proteobacteria. An alignment of FeoC proteins found 4 conserved cysteine residues, which are believed to be involved in iron-sulphur cluster binding (Cartron *et al.* 2006).

1.4.2 Ferric reductases

In aerobic conditions, the availability of ferrous iron is too low to support optimal growth of bacteria (Andrews *et al.* 2003). Bacteria can use ferric reductases to convert the relatively insoluble ferric iron

into highly soluble and more easily transported ferrous iron. All bacteria (except some *Lactobacilli*) contain iron assimilatory pathways, of which ferric reductases are a component (Schroder *et al.* 2003). All bacterial assimilatory ferric reductases are flavin reductases, using either flavin mononucleotide (FMN), flavin adenine nucleotide (FAD) or riboflavin as a cofactor. They use NADH or NADPH as an electron donor to reduce ferric iron to the ferrous form (Schroder *et al.* 2003). The localisation of the ferric reductase in the bacterial cell is linked to the assimilatory function. For the reduction of ferric iron and subsequent uptake, reductases are located on the outer membrane, or even secreted, such as in *Mycobacterium paratuberculosis* (Homuth *et al.* 1998).

Thus, a wide range of bacterial species can reduce extracellular Fe^{3+} to Fe^{2+} , which they can then transport into the cytoplasm (see below). Several pathogenic bacteria (such as *E. coli*, *Salmonella typhimurium*, *Listeria* spp. and *Pseudomonas aeruginosa*), use ferric reductases to liberate Fe^{2+} from chelates such as haemoglobin and lactoferrin, enabling them to scavenge iron from their hosts during infection (Deneer *et al.* 1995; Vartivarian and Cowart 1999) and see review by (Schroder *et al.* 2003).

1.4.3 Siderophores

A commonly utilised bacterial iron acquisition strategy is *via* the secretion and uptake of siderophores. These are low molecular weight iron chelating compounds that bind strongly to Fe(III) (Braun *et al.* 1998). They were first isolated and characterised in 1952 (Neilands), and these molecules were initially called siderochromes, due to their spectroscopic properties when in complex with Fe. They exhibit significant structural diversity, but can be classified into three major groups:

The hydroxamates, these contain N-hydroxamated amide bonds and bind to iron with a hydroxamic acid functional group. This family includes desferrioxamine B, which is used as a drug to treat any iron surplus following a blood transfusion (Fernandes 2012). Hydroxamate siderophores have been shown to be produced by several marine γ -proteobacteria (Armstrong and Van Baalen 1979; Trick 1989).

The catechols which form co-ordinate bonds with iron using catecholate hydroxyl groups. These include the major siderophore of *E. coli*, enterobactin (Pollack and Neilands 1970)

Both types above have been shown to be produced in response to low iron conditions in many bacteria (Lewis *et al.*, 1995; Wilhelm *et al.*, 1998; Trick, 1989; Reid & Butler, 1991; Haygood *et al.*, 1993).

The carboxylates, which are based on the structure of citric acid, and bind to iron with carboxy- or hydroxy-groups. Examples include Rhizobactin, produced by *Rhizobium meliloti* (Smith *et al.* 1985), Staphyloferrin, produced by Staphylococcus (Drechsel *et al.* 1993) and a fungal equivalent, Rhizoferrin (Drechsel *et al.* 1995), which is the main siderophore of the Zygomycetes.

Despite their variation in structure, all siderophores bind to Fe (III) with six co-ordinate bonds with very high stability. The biosynthesis of siderophores involves several enzyme catalysed steps, and usually begins with a non-ribosomal peptide synthetase, from a variety of different non-protein amino acids (Wandersman and Delepelaire 2004). For a review of the structure and biosynthesis of siderophores see Crosa and Walsh (Crosa and Walsh 2002).

1.3.4 Other bacterial sources of iron

ferric citrate

Citrate forms the basis of most hydroxamate-type siderophores, but can also act as an iron chelator. Bacteria secrete citrate, and then use active transport systems to recover the chelated Fe (III)-citrate complex. This transport is mediated by the products of the *fec* genes in *E. coli*. Here, FecA is an outer membrane receptor which binds and internalises citrate, and FecBCDE make an inner membrane complex responsible for the inner membrane transport of the Fe-citrate (Harle *et al.* 1995).

haeme-containing proteins

Haeme uptake is best studied in pathogenic bacteria, but can also be found in bacteria which dwell in the soil, such as *Rhizobium* (Noya *et al.* 1997) and *Bradyrhizobium* (Nienaber *et al.* 2001). Pathogenic bacteria require iron to cause infection, and have a vast amount of Fe available to them in the form of haeme, which they can obtain from host haemoglobin or haemopexin (Tong and Guo

2009). Haeme can be imported in the same way as citrate, via a cognate outer membrane receptor, such as HmbR of *Neisseria* (Stojiljkovic *et al.* 1996) or HasR of *Serratia marcescens* (Letoffe *et al.* 1994). The latter produces a haeme-binding hemophore (Cescau *et al.* 2007), which is secreted out of the cell, where it scavenges haeme, and can be taken up by the bacterium using HasR. This has also been demonstrated in *Haemophilus influenzae*, which produces a haemophore, HxuA, which leaves the cell, binds haemopexin, and is returned inside the bacterium using an outer membrane receptor HxuC (Cope *et al.* 1995).

transferrin, lactoferrin and ferritin

In addition to haeme, bacterial pathogens can obtain host Fe from transferrin, lactoferrin and ferritin, all host Fe-storage molecules (Cornelissen and Sparling 1994). In *Neisseria*, receptors for the uptake of transferrin and lactoferrin have been identified, and are known to remove Fe at the outer membrane, before transporting it into the cell (Legrain *et al.* 1993; Schryvers and Morris 1988).

1.3.5 Outer membrane receptors

The outer membrane of gram-negative bacteria contains various porins, which allow passive transport of small molecules (<600 Daltons). However, to transport molecules against a concentration gradient, or for molecules >600 Da in size, active transport must take place. In the case of ferric iron uptake an outer membrane receptor binds to a Fe-associated molecule, requiring physical association of the receptor and Fe. Once bound, the Fe-ligand is internalised into the periplasm, through the internal barrel structure of the receptor, using the proton motive force present on the inner membrane. This coupling of proton motive force from the inner to outer membrane requires the action of a protein called TonB (see below). These TonB dependent, outer membrane receptors (TBDR) are well conserved throughout gram negative bacteria, and are responsible for transporting a wide range of substrates – including haem, siderophores, vitamin B₁₂ (Noinaj *et al.* 2010) and even some carbohydrates such as sucrose (Schauer *et al.* 2008).

The biosynthesis of TBDR is tightly regulated, to enable a fast response to varied ligand concentrations in the environment (Noinaj *et al.* 2010).

Structurally, all TBDR's are similar, they all possess a 22-stranded β -barrel transmembrane domain, which is closed by a plug domain. The N-terminus of the TBDR has a peptide sequence which has been identified as a point of TonB interaction – the Ton box (see below) (Noinaj *et al.* 2010).

1.3.6 TonB

The proton motive force of the inner membrane in gram-negative bacteria is used to power the active transport of siderophores and other iron complexes through the outer membrane. Here, a multimeric complex consisting of 1-2 copies of TonB, and many copies of two other proteins, ExbB and ExbD, assemble on the inner membrane, but with the C-terminus of TonB extending into the periplasm (see Figure 1.1). Higgs *et al.* (2002) showed that in *E. coli*, the exact proportion of TonB:ExbB:ExbD in each cell was 1:7:2, although this may not be indicative of the actual conformation of the TonB:ExbBD complex. When a TBDR is loaded with its substrate, a signal is transduced across the membrane, where a conformational change occurs in 5 periplasmic residues of the TBDR – the Ton box. This signal induces the binding by β -sheet pairing of the C-terminus of TonB to the N-terminus of the TBDR, at the site of the Ton box (Noinaj *et al.* 2010). However, the exact mechanism of how energy is transduced into the TBDR is still unresolved.

The TonB of *E. coli* provides energy for all known TBDR expressed in this species, however, some bacteria have multiple copies of TonB, each of which is specific for a subset of their TBDR's (Gresock *et al.* 2011). We have noted, though, that TonB is also extremely poorly conserved across bacterial genera and much still needs to be done on this important protein in non-model bacteria (see Chapter 2).

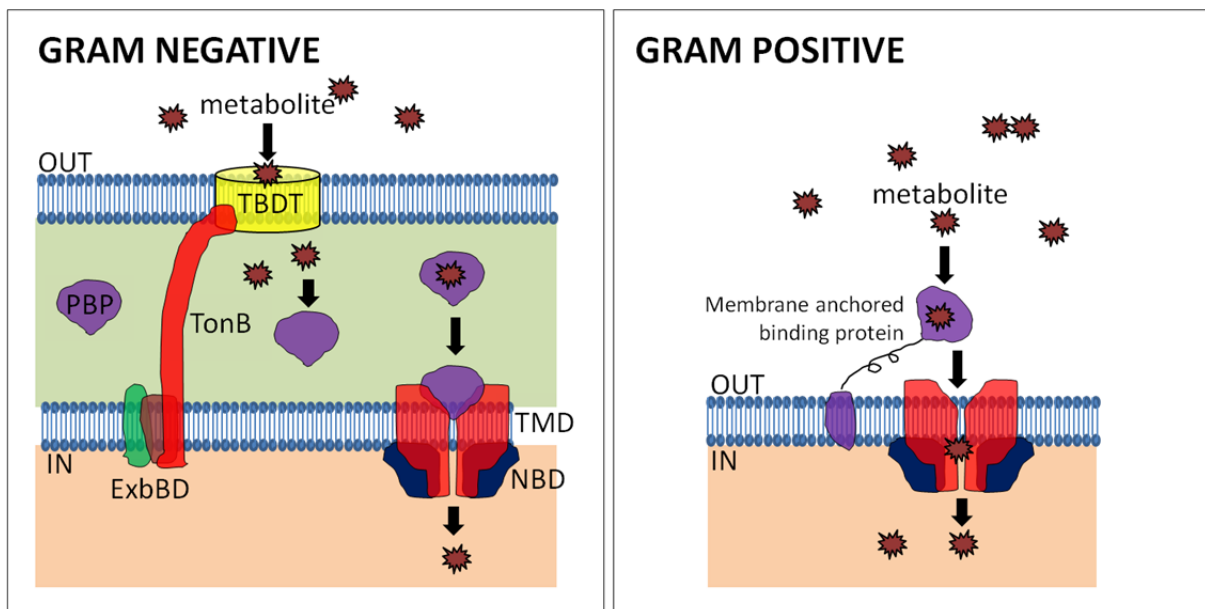
1.3.7 ABC Transporters

Once iron, or iron chelates, are in the periplasm, bacteria use cognate Fe/Fe-complex-binding protein dependent ABC-class transporters to import the iron into the cytoplasm (Köster 2001). Such systems include Fbp (*Neisseria* spp.); Hit (*Haemophilus influenza*); Yfu (*Yersinia* spp.); Afu (*Actinobacillus pleuropneumoniae*); Piu (*Streptococcus pneumoniae*); and Sit (*S. typhimurium*) (Adhikari *et al.* 1996; Adhikari *et al.* 1995; Berish *et al.* 1990; Chin *et al.* 1996; Rakin and Heesemann 1995; Tai *et al.* 2003; Zhou *et al.* 1999). The *Salmonella* iron transporter SitABCD has since been

shown to have a far higher affinity for manganese and is likely the inner membrane transporter for this metal (Kehres *et al.* 2002).

During inner membrane transport, a specific periplasmic binding protein binds to either free ferrous Fe, or to the Fe-ligand complex, and delivers them to a cognate ABC-class transporter. Here, the ligand is transported through a dimer of transmembrane permease proteins (sometimes comprising a single “intra-molecular” dimer), powered by the hydrolysis of ATP via a specific nucleotide binding protein – see figure 1.2.

Figure 1.2 Mechanism of iron transport in bacteria



Fe, (star) is transported into a Gram-negative bacterial cell via a TonB-dependent outer membrane transporter (TBDT), powered by the proton motive force of the inner membrane, which is coupled to the TBDT by TonB and ExbBD. Once in the periplasm, the method of iron import into the cytoplasm is similar in both Gram negative and Gram-positive bacteria. Here, a cognate binding protein binds to iron (PBP), and delivers it to a permease – (a transmembrane domain protein – TMD). This internalises the iron using the energy from ATP hydrolysis via a nucleotide-binding domain protein – NBD. The entire inner membrane transport complex is known as an ABC class transporter.

In *E. coli*, the transport of Fe-siderophore complexes through the cytoplasmic membrane is performed by three different ABC-class transporters, namely Fhu, Fec and Fep, with each system comprising its cognate periplasmic binding protein, trans-membrane transporter and ATPase, and

each system having specificity to the cognate class of siderophore/Fe-ligand. The genes *fhuDCB* encode an ABC-class transporter which has specificity for aerobactin and ferrichrome uptake; The Fep transporter encoded by *fepBDGC* is specific for enterobactin (there are two genes which make up the permease domain of this transporter) and the Fec transporter, encoded by *fecBCDE* has specificity for ferric citrate uptake.

There are examples of ABC class transporters which are capable of TonB-independent iron uptake, iron deficient growth of an *E. coli* TonB⁻ EntF⁻ strain (ARM100) was enhanced when the cloned *Vibrio fbpABC* genes were introduced (Wyckoff *et al.* 2006). This is especially interesting given that another FbpA homologue in *Neisseria shayeganii* 871 is possibly extracellular, meaning some bacteria may have the capacity to import iron through both membranes without the need for TonB – indeed this is the case for the Feo system.

1.3.8 Marine siderophores

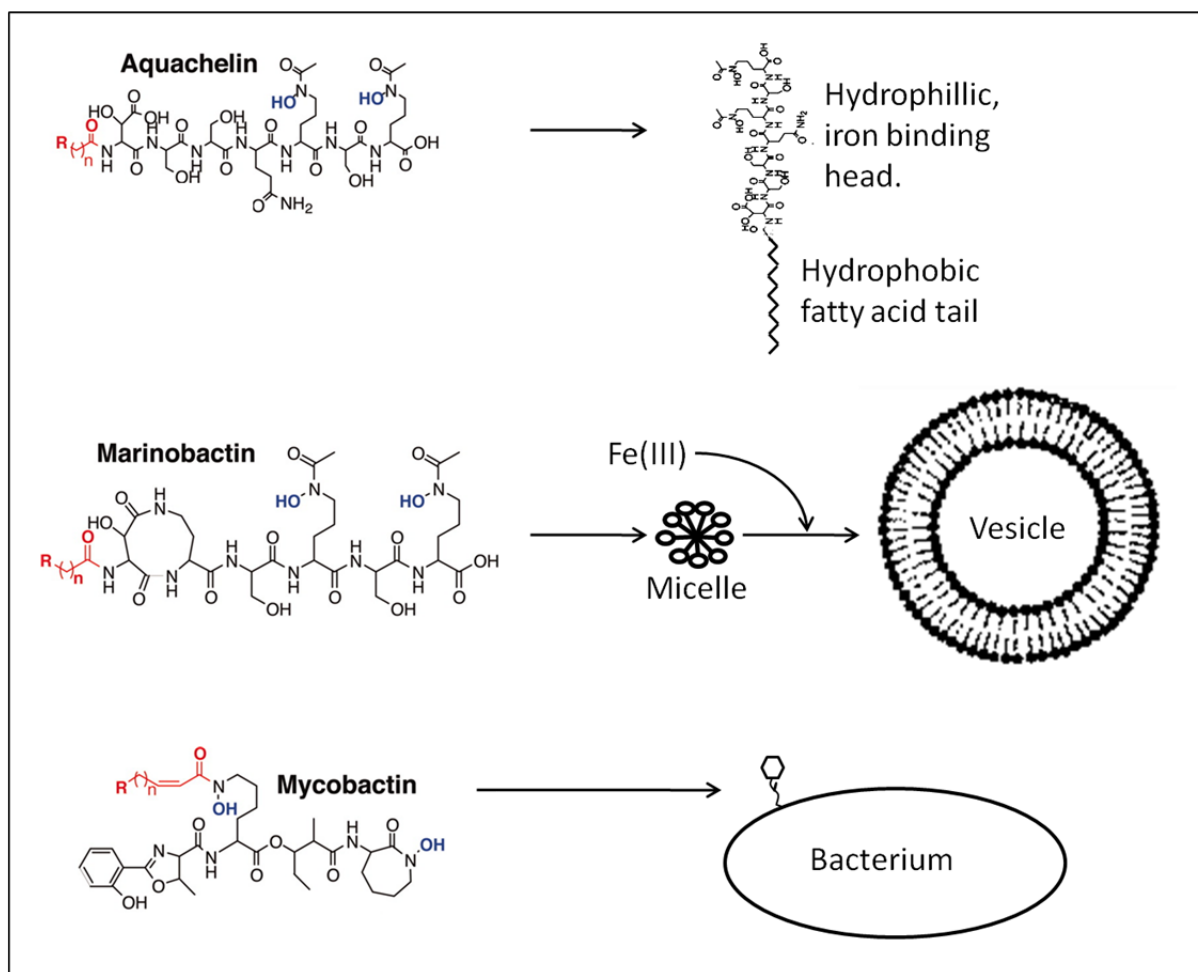
The production and uptake of siderophores has been described in some heterotrophic marine bacteria, such as *Alteromonas luteoviolacea*, *Halomonas aquamarina* and *Marinobacter* sp. strains (Granger and Price 1999; Hopkinson and Morel 2009; Martinez *et al.* 2000; Reid *et al.* 1993); the lab of Alison Butler has been instrumental in furthering our understanding of siderophore production in the marine environment.

Siderophore production in the turbulent environment of the ocean is an expensive strategy for bacteria (Hutchins *et al.* 1991) and especially for smaller cells, as modelled by Völker and Wolf-Gladrow (1999). However, siderophore production increases under iron limitation (Buck and Bruland 2007); the concentration of a specific ferroxamine siderophore was found to correlate exactly with increasing bacterial abundance (Mawji *et al.* 2008), showing that bacteria do choose to use this seemingly wasteful strategy.

Interestingly, many marine siderophores are amphiphilic (Butler and Theisen 2010), containing an Fe³⁺-binding head group attached to a series of fatty acids. These include the aquachelins (Martinez *et al.* 2000), the loihichelins from the γ -proteobacteria *Halomonas* (Homann *et al.* 2009) and marinobactins from *Marinobacter* (Martinez *et al.* 2000), synechobactins from the cyanobacteria *Synechococcus* (Ito and Butler 2005) and ochrobactin from the rhizobiales species - *Ochrobactrum* (Martin *et al.* 2006). Intriguingly, Marinobactins can form micelles, which become compacted when bound to Fe (III). Both marinobactins and aquachelins are structurally similar to mycobactin and

exochelin siderophores produced by terrestrial mycobacteria; all have a fatty acid tail, although in the mycobacteria, these remain associated with the bacterial membrane, serving as an anchor (Martinez *et al.* 2000) – refer to Figure 1.3.

Figure 1.3 The structure and properties of three marine siderophores.



Aquachelin and marinobactin have long fatty acid tail moieties, which in the latter, can form micelles. These can aggregate in the presence of iron, to form vesicles containing large amounts of iron. Of similar structure, mycobactin contains a lipid membrane-bound fatty acid tail (shown in red) which anchors it to the cell surface. Adapted from (Martinez et al. 2000).

Remarkably, multiple Fe(III)-marinobactin complexes can aggregate into multimellular vesicles, enhanced through addition of Zn(II), Cd(II), or La(III) to Fe(III) (Butler 2005). Whether these chemical properties occur in the oceanic bacterial communities is unknown, but the phenomenon of concentrating siderophores into discrete bundles of metals for passing bacteria is intriguing.

Many marine siderophores contain a photoreactive α -hydroxy-carboxylic acid when bound to Fe(III), so that near-UV light can cause the release of CO₂ and the reduction of Fe(III) to Fe(II) (Butler and Theisen 2010), thus contributing to iron cycling in the euphotic zone (Martin *et al.* 2006).

As far as is known, it is uncommon for marine cyanobacteria to produce siderophores, and there have been no reported examples of siderophores made by eukaryotic phytoplankton (Hopkinson and Morel 2009). Siderophore uptake in gram negative bacteria has evolved to require an analogue of the TonB protein (Faraldo-Gomez and Sansom 2003), but many offshore marine cyanobacteria lack this polypeptide (Palenik *et al.* 2003; Palenik *et al.* 2006; Webb *et al.* 2001), as does the subject of this work, *Ruegeria pomeroyi* (see chapter 2). Even though these bacteria are predicted to lack the ability to transport iron-siderophore complexes, they may still acquire iron from siderophores – possibly by reducing the bound Fe(III) to Fe(II) on the cell surface as is the case in *Trichodesmium erythraeum* (Hopkinson and Morel 2009) – or these species may use a TonB independent system for siderophore uptake.

1.4 Iron storage

Bacteria cannot survive with high levels of ‘free’ intracellular iron, and so have evolved methods of iron storage, thus preventing iron from participating in toxic reactions. These are detailed below.

1.4.1 Ferritins

One such class of storage molecule are ferritins, which are called bacterioferritins if they contain haeme *B* (Andrews 1998; Carrondo 2003). Ferritins are multimeric cage-like structures usually comprising 12 or 24 individual subunits (Arosio *et al.* 2009), which can store up to 4500 Fe ions within a central cavity (Carrondo 2003). Ferritins can supply the cell with iron when uptake is insufficient, and can also help to buffer against oxidative damage by sequestering iron (Carrondo 2003).

In *E. coli*, a strain which contains a bacterial ferritin FtnA was shown to grow better in iron limited conditions than a strain which lacked FtnA (Abdul-Tehrani *et al.* 1999). Although, it has also been reported that many ferritin deletion mutations have no growth phenotype (Arosio *et al.* 2009).

The controlled release of Fe from the central core of ferritins is poorly understood, but is likely to involve both reduction, and chelation of the Fe (III) contained within the ferritin. In *E. coli* bacterioferritin haeme functions as a redox centre during the release of iron (Yasmin *et al.* 2011).

1.4.2 Fe-S

Iron sulphur clusters - [Fe-S] are one of the most common protein prosthetic groups in polypeptides and serve many functions (Beinert 2000). They consist of multinuclear Fe and sulphur atoms, and are variously capable of catalysing electron transfer, enzymatic activity, proton transfer, and are also used as a sulphur donor and as a regulatory sensor for iron availability (Beinert 2000). Since both free Fe and S are toxic, the biosynthesis of [Fe-S] is carefully coordinated *in vivo* (Ayala-Castro *et al.* 2008). The biosynthesis of [Fe-S] occurs via the Suf pathway, or the Isc pathway in *E. coli*.

Here, a sulphur source (cysteine) is used to generate sulphur by a desulphurase enzyme, which cleaves cysteine to form alanine. This sulphur is delivered to the scaffold proteins (either IscA and IscU, or SufA and SufB). Next, Fe is generated from an iron source, brought to the scaffold by a chaperone protein, and both Fe and S are coordinated in the scaffold complex. This generates an [Fe-S] cluster, most commonly either [2Fe-2S] or [4Fe-4S], ready to be integrated into the apo form of an enzyme (Fontecave and Ollagnier-de-Choudens 2008; Peters and Broderick 2012).

Regulation of the [Fe-S] synthesis operon *suf* and *isc* in *E. coli* is well characterised, and has been shown to be mediated by the Rrf2 family transcriptional regulator IscR, which is in the same operon as the structural [Fe-S] biosynthesis genes; IscR binds to [2Fe-2S] and can repress the *iscRSUA* operon. This causes a negative feedback loop where *iscR* is repressed by IscR, thus limiting further repression (Ayala-Castro *et al.* 2008). However, it has been shown that apo-IscR can *induce* the *suf* [Fe-S] biosynthetic genes in response to oxidative stress. Thus, *E. coli* uses both [Fe-S] operons under different conditions; *isc* is for homeostasis of a nominal level of [Fe-S], whereas the *suf* operon is used in response to oxidative stress. Furthermore, in *E. coli*, both the *isc* and *suf* operons are

controlled by the global iron regulator Fur in response to cellular iron levels. The *suf* promoter is a binding site for Fur, so the *suf* operon is repressed in high iron conditions.

1.5 Manganese uptake

Studies on Mn import in a range of different terrestrial bacteria have revealed two, widely used, but very different transporters, termed MntH and SitABCD, with some bacteria (e.g. *Salmonella*) harbouring both systems (Boyer *et al.* 2002).

1.5.1 MntH

The Nramp family (Natural resistance-associated macrophage proteins) of transporters transports metals, with particular affinity for Fe and Mn, in many eukaryotic species. MntH-like proteins exist in bacteria, where they are termed MntH (Makui *et al.* 2000). In gram-negative bacteria, MntH homologues are responsible for high affinity Mn uptake through the inner membrane, but can also transport iron with lower efficiency (Kehres *et al.* 2000; Makui *et al.* 2000). In the α -proteobacteria *Bradyrhizobium japonicum*, a homologue of MntH was shown to be required for Mn²⁺ uptake, and is essential for growth in Mn-limited conditions (Hohle and O'Brian 2009). The gene encoding MntH was shown to be regulated by Mn via the Mur transcriptional regulator (see below). In contrast, MntH from *Bacillus subtilis* is also required for growth in Mn limited media (Que and Helmann 2002) and is regulated by Mn availability, but via a different transcriptional regulator – MntR (see below).

1.5.2 SitABCD

SitABCD is an ABC-transporter type system (see above), initially thought to be involved in iron uptake - hence its somewhat misleading acronym of *Salmonella* iron transporter (Zhou *et al.*, 1999). Expression of *sit* genes is strongly repressed by Mn in the α -proteobacteria *Sinorhizobium meliloti* (Platero *et al.* 2004), and *Rhizobium leguminosarum* (Diaz-Mireles *et al.* 2004) but by both Fe and Mn in the γ -proteobacteria *Shigella flexerii* (Runyen-Janecky *et al.* 2006) and *E. coli* (Sabri *et al.* 2006). In

the α -proteobacteria, this Mn-dependant regulation is mediated by a Fur homologue – Mur (see below).

1.5.3 *MnoP*

Hohle *et al.* (2011) recently described a novel outer membrane ion channel, MnoP, which facilitates Mn^{2+} transport across the outer membrane of *Bradyrhizobium japonicum*. Here, they showed that growth of an MnoP mutant strain required the addition of extra Mn^{2+} to the medium, although the mutant was not as severely compromised for growth in low levels of Mn as was an MntH⁻ mutant.

1.6 Iron and manganese –responsive regulatory systems

The importance of regulating iron uptake is paramount for bacteria; too little and the cells are starved of an essential metal, too much and they run the risk of oxidative and/or free radical damage. Here I will describe several examples of transcriptional regulators which mediate this balance.

1.6.1 *Fur*

The paradigm system of iron-responsive regulation in many bacteria is that of the Ferric uptake regulator (*Fur*), which has been characterised in many bacterial phyla, including the γ - and β -proteobacteria, bacilli and cyanobacteria, actinomycetes (Alahari *et al.* 2006; Delany *et al.* 2001; Fuangthong and Helmann 2003; Grifantini *et al.* 2003; Hantke 2001; Hernandez *et al.* 2004; Parker *et al.* 2005; Quatrini *et al.* 2005; Rodionov *et al.* 2006; Wan *et al.* 2004; Zhou *et al.* 2006).

Fur exists *in vivo* as a dimer, with each monomer binding to one Zn^{2+} and one regulatory Fe^{2+} ion (Cornelis and Andrews 2010). Once bound to Fe, *Fur* will recognise and bind to a well conserved DNA sequence– the *Fur* box (Escolar *et al.* 1999). $Fe(II)$ -*Fur* dimers bind to a conserved 19bp sequence consisting of 3 identical and adjacent 6 bp regions. It is thought that 2 $Fe(II)$ -*Fur* dimers bind to each *Fur* box in a ‘tandem head-to-tail fashion’ (Cornelis *et al.* 2009; Oeffelen *et al.* 2008; Pohl *et al.* 2003).

Fur boxes are usually found overlapping the promoter sequences of a gene, so when Fur is present, it blocks RNA polymerase therefore repressing expression of that gene (Cornelis *et al.* 2009).

The primary role of Fur is therefore that of an iron-responsive transcriptional repressor. The list of genes found to be Fur-repressed is usually large in any given bacterial strain and so Fur is known as the global iron-uptake regulator in these species. The genes found to be Fur-repressed usually include siderophore biosynthesis and Fe-uptake systems, acid and oxidative stress responses, energy metabolism and virulence, all of which are therefore activated in low iron conditions (Bijlsma *et al.* 2002; Cornelis and Andrews 2010; Hassett *et al.* 1996; Ochsner and Vasil 1996).

Fur can also act indirectly, by repressing secondary regulators. These include sigma factors, two component sensors, AraC-type regulators and small regulatory RNA molecules (Cornelis and Andrews 2010), and so Fur can act as an indirect activator of iron-responsive genes.

In *E.coli*, several genes were found to be positively regulated by Fur, including those encoding bacteroferritin and SodB (Andrews *et al.* 2003). These genes are post-transcriptionally regulated by a small RNA called RyhB, which is Fur repressed (Cornelis and Andrews 2010; Masse and Gottesman 2002). RyhB is a 90 nucleotide RNA, which can bind to complementary sequences in mRNA targets, this binding requires Hfq. RyhB has been shown to act both positively and negatively on the regulation of target genes, either by causing RNase E mediated degradation, or stabilisation of the transcript (Masse and Gottesman 2002).

There are other known examples of metal responsive Fur-superfamily regulators: Zinc – Zur (Patzner and Hantke 1998); Mn – Mur (see below), Nickel – Nur (Ahn *et al.* 2006), peroxidase - PerR, and Fe again by Irr (see below), showing that this protein family has a key role in metal metabolism across many genera of bacteria.

1.6.2 DtxR

Some members of the DtxR-like (Diphtheria toxin repressor) proteins have been shown to be global iron-responsive regulators, acting much like Fur in *E. coli*, but do not have any sequence similarity. These include DtxR of *Corynebacterium*, and IdeR of *Mycobacterium tuberculosis*. DtxR of *Corynebacterium diphtheria* has been shown to regulate the expression of the diphtheria toxin, but also biosynthesis and export of siderophores, iron uptake, and haem utilisation genes (Brune *et al.*

2006). Similarly, IdeR was found to regulate genes involved in siderophore biosynthesis and iron storage (Rodriguez *et al.* 2002).

1.7 Iron and manganese gene regulation in the α -proteobacteria

Recently, the α -proteobacteria have been shown to be dramatically different in their Fe homeostasis, compared to the canonical systems that have been described for *E. coli*, and other taxa. These differences are introduced below.

1.7.1 Fur

There are homologues of Fur found throughout the α -proteobacteria, however, it has become apparent that *Rhizobium*, *Sinorhizobium* and *Bradyrhizobium* Fur homologues are responsible for regulation of manganese uptake (Chao *et al.* 2004; Diaz-Mireles *et al.* 2004; Diaz-Mireles *et al.* 2005; Hohle and O'Brian 2009), even though these proteins are capable of binding to Fur boxes, and complimenting Fur mutants in *E. coli* (Wexler *et al.* 2003).

These so-called Mur regulators are introduced below.

In the Rhizobiales, the role of Fur is performed by two other regulators, the Fur-family protein Irr (Iron response regulator) and the Rrf2 family protein RirA (Rhizobial iron regulator).

1.7.2 Irr

Irr was originally identified as the repressor of haeme biosynthesis gene *hemB* during iron limitation in *B. japonicum* (Hamza *et al.* 1998). Since its discovery, Irr has been studied in other α -proteobacteria, firstly in *Rhizobium* (Singleton *et al.* 2010; Todd *et al.* 2005; Todd *et al.* 2006; White *et al.* 2011). In *Rhizobium*, Irr binds to Fe (III)-haeme at two sites. This causes an allosteric shift in the protein which prevents it binding to DNA. Irr binds to specific sequences upstream of genes, called ICE boxes - Iron Control Element (Singleton *et al.* 2010). The deduced regulon of Irr in *Rhizobium*

includes the membrane-bound ferritin gene *mbfA*, the haeme biosynthesis gene *hemA*, and the [Fe-S] biosynthesis *suf* genes (Todd *et al.* 2006).

Secondly, Irr of *Agrobacterium* has been shown to repress Fe utilisation genes in low Fe conditions, via binding to ICE boxes and repressing the upstream genes (Hibbing and Fuqua 2011). This Irr protein also binds to two haeme molecules (Yang *et al.* 2005), thus sensing the intracellular concentration of haeme to determine iron availability.

Thirdly, Irr in *Brucella abortis* has also been shown to bind to haeme, and to regulate haeme uptake (Anderson *et al.* 2011; Martinez *et al.* 2005). However, this Irr protein appears to be unstable, and degrades in the presence of haeme, therefore alleviating repression of its target genes (Martinez *et al.* 2005).

Finally, Irr of *B. japonicum* has also been shown to be degraded when interacting with haeme (Qi and O'Brian 2002; Yang *et al.* 2005). This protein recognises ICE boxes, and represses haeme biosynthesis and iron storage genes under iron sufficient conditions (Rudolph *et al.* 2006). In addition, this Irr protein has been shown to positively regulate siderophore biosynthesis in *B. japonicum*, under iron depleted conditions (Small *et al.* 2009).

Irr appears to be a signature regulator of the α -proteobacteria, with ICE box motifs found in the genomes of many different genera (Rodionov *et al.* 2006). However, another iron responsive regulator is found within the Rhizobiales – RirA.

1.7.3 RirA

In a complex complementary set-up, Rhizobium has a copy of an Rrf2 family protein – RirA (Todd *et al.* 2002). This essentially has the function of Fur, but is absolutely not related in sequence. RirA is a transcriptional repressor of iron uptake genes in *Rhizobium* and *Sinorhizobium* (Chao *et al.* 2005; Todd *et al.* 2002). The RirA protein binds to [Fe-S] clusters and so can sense the availability of iron (Johnston *et al.* 2007). The extent of the RirA regulon in these bacteria has been shown by transcriptomic (Chao *et al.* 2005) and proteomic analyses (Todd *et al.* 2005). These revealed that, in high Fe conditions, RirA represses many genes, including those involved in [Fe-S] biosynthesis (*suf*), and siderophore and haem uptake.

The DNA sequence which is recognised by RirA was termed the IRO (Iron Responsive Operator) box (Yeoman *et al.* 2004). This is very different from the Fur box described earlier, and is shown in more detail in chapter 3.

Bioinformatic analysis of potential IRO boxes found upstream of genes revealed that there are likely many RirA regulated genes found in strains of *Agrobacterium*, *Brucella*, *Bartonella*, *Mesorhizobium*, *Rhizobium* and *Sinorhizobium*. However, the range of bacteria is limited since there were no IRO box homologues found in *Bradyrhizobium* (Johnston *et al.* 2007; Rodionov *et al.* 2006) – and indeed this strain lacks a copy of RirA (Rodionov *et al.* 2006).

Together, Irr and RirA act to regulate homeostasis of Fe uptake, and usage. Irr is active under low Fe conditions, whereas RirA is active under high Fe conditions. Together, these iron-responsive repressors can respond to the level of iron in a highly controlled and sensitive fashion.

1.7.4 *IscR*

The regulation of [Fe-S] biosynthesis (see above) in bacteria has been shown to be mediated by IscR, an Rrf-2 family transcriptional regulator (Schwartz *et al.* 2001). IscR has been shown to be an [Fe-S] containing protein, which, when in complex with this co-factor, can bind to target sequences. Homologues of IscR are found throughout the eubacteria, and form part of the [Fe-S] biosynthetic *suf* operon in the Rhodobacterales, Rhodospirillales, Sphingomonadales, Rickettsiales, and Caulobacterales (Rodionov *et al.* 2006). However, despite there being *suf* homologues in the Rhizobiales, these genes are regulated by Irr and RirA (Rodionov *et al.* 2006; Todd *et al.* 2005) and not by IscR.

1.7.5 *Mur*

The regulation of iron uptake and utilisation in the α -proteobacteria is vastly different from that of *E. coli* – Fur has become a manganese responsive regulator and is termed Mur.

The Mur of *Rhizobium* and *Sinorhizobium* regulates the expression of SitABCD, a Mn²⁺ specific transporter (Chao *et al.* 2004; Diaz-Mireles *et al.* 2004; Diaz-Mireles *et al.* 2005), and is not involved

in the regulation of iron uptake. The promoter of *sitABCD* contains a binding sequence for Mur – The MRS box (Mur Recognition Sequence) (Diaz-Mireles *et al.* 2005). Homologous sequences to the MRS box are found upstream of another gene in *Rhizobium* – the manganese transporter MntH (see below). Furthermore, MRS motifs are found in the promoter regions of *sitABCD/mntH* in many other members of the Rhizobiaceae and Rhodobacterales. The prevalence of Mur, and MRS boxes has been predicted by Rodionov *et al.* (2006), and shows that Mn-responsive regulation via Mur likely extends further, to the Roseobacters, a taxonomically distinct group of marine α -proteobacteria.

Finally, *Bradyrhizobium* sp. BTAi1 has a copy of both Mur, and another class of Mn-responsive regulators – MntR (see below) (Rodionov *et al.* 2006).

1.7.6 MntR

A member of the DtxR family of transcriptional regulators, MntR was found to regulate Mn uptake in response to Mn availability. In *Bacillus subtilis*, MntR is a Mn^{2+} dependent repressor of *mntH*, and therefore Mn uptake via this transporter (Que and Helmann 2002). Furthermore, repression of both *SitABCD* and MntH in the enterobacteria is mediated by MntR in response to high Mn levels (Kehres *et al.* 2002; Patzer and Hantke 2001). Contrastingly, MntR can also act as a positive regulator of the expression of MntABCD under Mn limitation (Sabri *et al.* 2006).

In the α -proteobacteria, there are few homologues of MntR, but there are several interesting exceptions.

Both *Rhodobacter capsulatus* and *Mesorhizobium loti* lack Mur, and instead have a homologue of MntR, unlike the other sequences strains within those genera (Rodionov *et al.* 2006). Here, the copies of MntR are found next to a copy of MntH – and the bioinformatic searches performed in Rodionov *et al.*, (2006) have shown the presence of MntR boxes, homologous to those found in the enterobacteria, upstream of MntH in these strains.

1.8 Marine metagenomics

1.8.1 The GOS dataset

The recent metagenomic studies produced by the Venter institute's GOS (Global Ocean Sampling) expeditions and others have produced a staggering amount of data on microbial diversity, gene frequency and indeed species and gene discovery in the marine environment (Rusch *et al.* 2007; Venter *et al.* 2004; Yooseph *et al.* 2007). The Venter institute has created a compendium of sequence data, species identification and protein families called CAMERA (Community Cyberinfrastructure for Advanced Marine Microbial Ecology Research and Analysis) (available online at: <http://camera.calit2.net/>), which prove extremely useful in producing data about the abundance, and diversity of marine iron transport systems. These data are easily searchable using a nucleotide, or peptide query, and the resultant homologous genes/proteins returned are accompanied by data about the sampling site location, depth, temperature and other features. This really is an amazing resource to have when studying marine bacterial genetics.

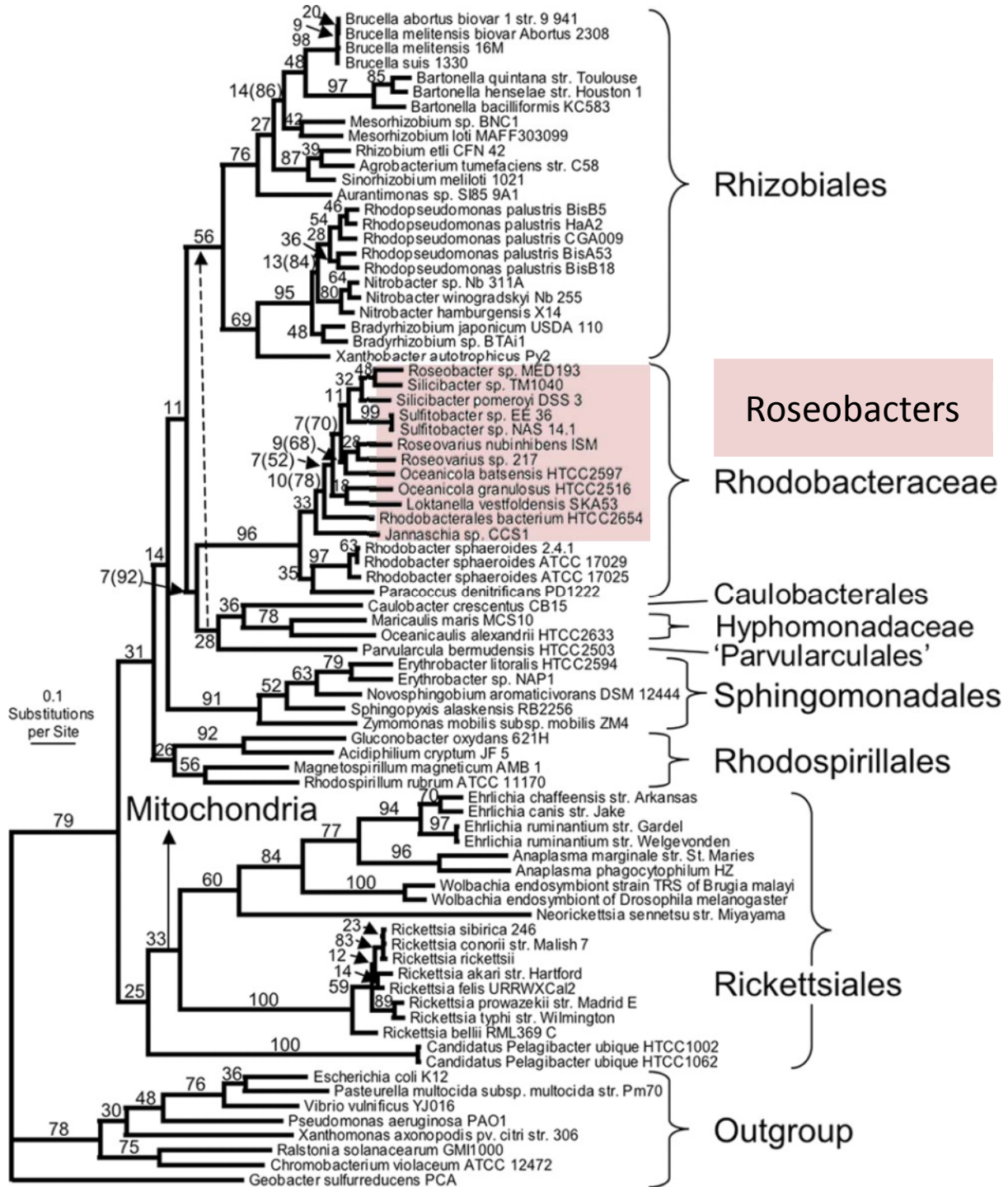
1.9 The model Roseobacters

1.9.1 The Roseobacter Clade

A subset of the α -proteobacterial Rhodobacteriaceae (refer to figure 1.4) were found to be abundant in the coastal waters of south-eastern USA (Gonzalez and Moran 1997); up to 28% of all isolated 16S ribosomal DNA sequences were identified as belonging to this group, consequently named the **Roseobacters** (Gonzalez *et al.* 1999).

The genomes of many of the Roseobacters have been fully sequenced (available at <http://www.roseobase.org/>), and many are easily culturable (Gonzalez *et al.* 1999; Gonzalez *et al.* 2000), making this group amenable to *in vivo* and *in silico* research. The Roseobacters are therefore a model group of marine α -proteobacteria for the study of marine iron and manganese uptake and regulation.

Figure 1.4 Tree of selected members of the α -proteobacteria, to show the taxonomic distribution of the Roseobacters [adapted from (Williams et al. 2007)].



Phylogenetic tree adapted from Williams et al., (2007) showing the taxonomic relationship of selected Roseobacters to a selection of the α -proteobacteria.

1.9.2 The *Ruegeria* and *Silicibacter* Genera

Members of the *Ruegeria* genus was originally classified as *Agrobacterium*, but 16S DNA sequence analysis, chemotaxonomic, morphological, and physiological studies suggested that these marine species were significantly different and were reassigned (Uchino *et al.* 1998). The phylogeny of the *Ruegeria* genus is shown below:

Bacteria → Proteobacteria → Alphaproteobacteria → Rhodobacterales → Rhodobacteraceae → *Ruegeria*

The main focus of this study, *Ruegeria pomeroyi* was isolated in 2003 (Gonzalez *et al.*) from seawater collected off the coast of Georgia. Originally termed *Silicibacter pomeroyi* it was the first member of the Roseobacters to have its genome sequenced (Moran *et al.* 2004), prior to its allocation to the genus *Ruegeria*, in 2007 (Yi *et al.*). Since then it has become something of a model for the genetic and genomic studies of the Roseobacters, with much of this work having been done in the Moran lab at the University of Georgia and here in Norwich. Indeed, several of the tools that were to be used for the planned work on the metallo-ome of this strain were already in place at UEA.

The closely related *Silicibacter* genus (refer to figure 1.4) includes *Silicibacter* sp. TM1040, 96% identity in 16S rDNA sequence to *R. pomeroyi* (Moran *et al.* 2007). Isolated from the dinoflagellate *Pfiesteria piscicida*, cultures of *P. piscicida* require *Silicibacter* sp. TM1040 to survive (Alavi *et al.* 2001; Miller and Belas 2004).

Despite their natural abundance in the oceans, the metal acquisition systems of the Roseobacters and SAR11 are yet to be investigated using functional genetic techniques. The deduced proteome of *Ruegeria pomeroyi* reveals has no identifiable iron transport systems other than *fbpAB* and there are no TonB homologues or any recognisable siderophore biosynthetic pathways (Rodionov *et al.* 2006). The following work sets out to identify how *R. pomeroyi* acquires Fe and Mn, and how the homeostasis of these metals is regulated.

1.10 Thesis aims

- To conduct a full study of potential iron and manganese uptake and regulatory genes in the Roseobacters using homology based searches.
- To study the predicted iron and manganese regulated genes in the Roseobacter *Ruegeria pomeroyi*.
- To elucidate the regulatory networks controlling iron and manganese uptake in *R. pomeroyi*.
- To analyse the transcriptional response to both iron and manganese limitation in *R. pomeroyi*.

Chapter 2 - Iron Uptake in the Roseobacters – A Bioinformatic Approach

2.0 Introduction

There has been remarkably little direct study of iron uptake genes in marine bacteria, with two, very recent, exceptions being on *Pelagibacter ubique* (Smith *et al.* 2010) and *Rhodobacter sphaeroides* (Peuser *et al.* 2011). A small scale bioinformatically-based study was performed by Hopkinson and Barbeau (2012) on the diversity of bacterial iron uptake genes in the oceans.

The work of Rodionov *et al.* (2006) provided a useful background to the work set out in this chapter, which uses bioinformatic approaches to infer some information on iron homeostasis in the Roseobacter clade of marine bacteria, Rodionov *et al.* identified a range of *cis*-acting DNA regulatory motifs upstream of genes involved in iron homeostasis in the alpha-proteobacteria, including several examples of the Roseobacters. That paper also helped to expand the range of genes shown to be involved in iron homeostasis through *in silico* identification of the iron-responsive regulon of many alpha-proteobacteria.

2.1.1 Comparative genomics - bioinformatic analysis of iron uptake systems in the Roseobacters

The genes/polypeptides that were examined were in the following general classes:

Regulatory: including, Irr (iron-response regulator), Fur (Ferric uptake regulator) and RirA (Rhizobial iron regulator).

Receptors for siderophores, haem and haem-containing molecules, citrate and vitamin B₁₂.

Siderophore biosynthetic genes, including those for enterobactin (Ent), vibriobactin (Vbs), aerobactin (Iuc), rhodochellin (Rhc) and vibriobactin (Vib).

TonB and ExbBD - energy-transducing proteins.

Ferrous uptake (Feo) and ferric reductase (Mtr and Fer) polypeptides.

Others, which include the 'iron regulated protein' IrpA.

These are presented and described in more detail, below. Note that a similar survey was presented by Hopkinson and Barbeau (2012) but with much less scope and detail as far as the Roseobacters are concerned.

Table 2.1. Bioinformatic study of iron uptake genes in the Roseobacters

The protein-coding sequences of each gene listed were used to interrogate the Roseobase BLAST database for each of the organisms shown in the table. The resultant 'E-value' output was used to populate the table, and colour-coded according to the level of homology: red for "poor", yellow for "moderate", and green for "good".

Gene Name	TonB dependant outer membrane receptors																	ABC Transporters					Ferric Reductases					Energy Transfer																		
	<i>fhuA</i>	<i>fhuE</i>	<i>btuB</i>	<i>hmuU</i>	<i>cirA</i>	<i>feca</i>	<i>fepA</i>	<i>viaA</i>	<i>viaB</i>	<i>fuv/yhl</i>	<i>fprA</i>	<i>fya</i>	<i>hasR</i>	<i>shaA</i>	<i>yiaR</i>	<i>Maqu_2192</i>	<i>hmrA</i>	<i>fepB</i>	<i>fepC</i>	<i>fepD</i>	<i>fepE</i>	<i>fepF</i>	<i>fepG</i>	<i>fepH</i>	<i>fprB</i>	<i>fprC</i>	<i>yjua</i>	<i>hmuT</i>	<i>yqhH</i>	<i>fcrA</i>	<i>fcrB</i>	<i>mtrA</i>	<i>mtrB</i>	<i>tolA</i>	<i>tolR</i>	<i>tolQ</i>	<i>tonB</i>	<i>exbB</i>	<i>exbD</i>							
Species																																														
<i>Roseobacter</i> sp. MED193	11.00	9.04	71.01	31.50	18.11	21.10	21.20	4.00	21.10	31.20	31.10	67.13	21.11	11.42	71.00	2.00	2.00	21.00	21.20	21.20	21.20	21.20	21.20	21.20	21.20	21.20	21.20	21.20	21.20	21.20	21.20	21.20	21.20	21.20	21.20	21.20	21.20	21.20	21.20	21.20	21.20					
<i>Roseobacter</i> sp. SK209-2-6	21.10	21.10	21.10	21.10	21.10	21.10	21.10	21.10	21.10	21.10	21.10	21.10	21.10	21.10	21.10	21.10	21.10	21.10	21.10	21.10	21.10	21.10	21.10	21.10	21.10	21.10	21.10	21.10	21.10	21.10	21.10	21.10	21.10	21.10	21.10	21.10	21.10	21.10	21.10	21.10	21.10	21.10				
<i>Roseovarius nubinhibens</i> ISM	11.00	9.04	71.01	31.50	18.11	21.10	21.20	4.00	21.10	31.20	31.10	67.13	21.11	11.42	71.00	2.00	2.00	21.00	21.20	21.20	21.20	21.20	21.20	21.20	21.20	21.20	21.20	21.20	21.20	21.20	21.20	21.20	21.20	21.20	21.20	21.20	21.20	21.20	21.20	21.20	21.20	21.20	21.20			
<i>Roseovarius</i> sp. 217	11.00	9.04	71.01	31.50	18.11	21.10	21.20	4.00	21.10	31.20	31.10	67.13	21.11	11.42	71.00	2.00	2.00	21.00	21.20	21.20	21.20	21.20	21.20	21.20	21.20	21.20	21.20	21.20	21.20	21.20	21.20	21.20	21.20	21.20	21.20	21.20	21.20	21.20	21.20	21.20	21.20	21.20	21.20	21.20		
<i>Roseovarius</i> sp. TM1035	11.00	9.04	71.01	31.50	18.11	21.10	21.20	4.00	21.10	31.20	31.10	67.13	21.11	11.42	71.00	2.00	2.00	21.00	21.20	21.20	21.20	21.20	21.20	21.20	21.20	21.20	21.20	21.20	21.20	21.20	21.20	21.20	21.20	21.20	21.20	21.20	21.20	21.20	21.20	21.20	21.20	21.20	21.20	21.20		
<i>Ruegeria lacuscaerulensis</i> ITI-1157	11.00	9.04	71.01	31.50	18.11	21.10	21.20	4.00	21.10	31.20	31.10	67.13	21.11	11.42	71.00	2.00	2.00	21.00	21.20	21.20	21.20	21.20	21.20	21.20	21.20	21.20	21.20	21.20	21.20	21.20	21.20	21.20	21.20	21.20	21.20	21.20	21.20	21.20	21.20	21.20	21.20	21.20	21.20	21.20	21.20	
<i>Ruegeria pomeroyi</i> DSS-3	11.00	9.04	71.01	31.50	18.11	21.10	21.20	4.00	21.10	31.20	31.10	67.13	21.11	11.42	71.00	2.00	2.00	21.00	21.20	21.20	21.20	21.20	21.20	21.20	21.20	21.20	21.20	21.20	21.20	21.20	21.20	21.20	21.20	21.20	21.20	21.20	21.20	21.20	21.20	21.20	21.20	21.20	21.20	21.20	21.20	
<i>Ruegeria</i> sp. R11	11.00	9.04	71.01	31.50	18.11	21.10	21.20	4.00	21.10	31.20	31.10	67.13	21.11	11.42	71.00	2.00	2.00	21.00	21.20	21.20	21.20	21.20	21.20	21.20	21.20	21.20	21.20	21.20	21.20	21.20	21.20	21.20	21.20	21.20	21.20	21.20	21.20	21.20	21.20	21.20	21.20	21.20	21.20	21.20	21.20	
<i>Ruegeria</i> sp. TM1040	11.00	9.04	71.01	31.50	18.11	21.10	21.20	4.00	21.10	31.20	31.10	67.13	21.11	11.42	71.00	2.00	2.00	21.00	21.20	21.20	21.20	21.20	21.20	21.20	21.20	21.20	21.20	21.20	21.20	21.20	21.20	21.20	21.20	21.20	21.20	21.20	21.20	21.20	21.20	21.20	21.20	21.20	21.20	21.20	21.20	
<i>Ruegeria</i> sp. Trich CH48	11.00	9.04	71.01	31.50	18.11	21.10	21.20	4.00	21.10	31.20	31.10	67.13	21.11	11.42	71.00	2.00	2.00	21.00	21.20	21.20	21.20	21.20	21.20	21.20	21.20	21.20	21.20	21.20	21.20	21.20	21.20	21.20	21.20	21.20	21.20	21.20	21.20	21.20	21.20	21.20	21.20	21.20	21.20	21.20	21.20	21.20
<i>Sagittula stellata</i> E-37	11.00	9.04	71.01	31.50	18.11	21.10	21.20	4.00	21.10	31.20	31.10	67.13	21.11	11.42	71.00	2.00	2.00	21.00	21.20	21.20	21.20	21.20	21.20	21.20	21.20	21.20	21.20	21.20	21.20	21.20	21.20	21.20	21.20	21.20	21.20	21.20	21.20	21.20	21.20	21.20	21.20	21.20	21.20	21.20	21.20	
<i>Sulfitobacter</i> NAS-14.1	11.00	9.04	71.01	31.50	18.11	21.10	21.20	4.00	21.10	31.20	31.10	67.13	21.11	11.42	71.00	2.00	2.00	21.00	21.20	21.20	21.20	21.20	21.20	21.20	21.20	21.20	21.20	21.20	21.20	21.20	21.20	21.20	21.20	21.20	21.20	21.20	21.20	21.20	21.20	21.20	21.20	21.20	21.20	21.20	21.20	
<i>Sulfitobacter</i> sp. EE-36	11.00	9.04	71.01	31.50	18.11	21.10	21.20	4.00	21.10	31.20	31.10	67.13	21.11	11.42	71.00	2.00	2.00	21.00	21.20	21.20	21.20	21.20	21.20	21.20	21.20	21.20	21.20	21.20	21.20	21.20	21.20	21.20	21.20	21.20	21.20	21.20	21.20	21.20	21.20	21.20	21.20	21.20	21.20	21.20	21.20	
<i>Thalassiosibium</i> RZA62	11.00	9.04	71.01	31.50	18.11	21.10	21.20	4.00	21.10	31.20	31.10	67.13	21.11	11.42	71.00	2.00	2.00	21.00	21.20	21.20	21.20	21.20	21.20	21.20	21.20	21.20	21.20	21.20	21.20	21.20	21.20	21.20	21.20	21.20	21.20	21.20	21.20	21.20	21.20	21.20	21.20	21.20	21.20	21.20	21.20	21.20

Gene Name	Siderophore Biosynthesis / Transport														Iron Responsive Regulators					Other														
	HYDROXAMATES														CATECHOLATES																			
Species	vb3c	vb3g	vb3a	luca	lucb	luc	lucd	lhuc	lhuc	lhud	lhcb	rmo	vlbf	vlba	ybda / ents	enta	entb	entc	entd	ente	entf	rira	mur	irr	isr	fur	lrpa	lrpb	lrpa	lrpb	lrpa	lrpb	lrpa	lrpb
<i>Citricella</i> SE45	2.0E-14	0.0	0.0	1.4			0.007	0.001	1.0E-13	0.000	1.0E-13	5.3	1.8E-12	1.8E-12	5.5	48.5	56.8	56.8	56.8	56.8	56.8	56.8	56.8	56.8	56.8	56.8	56.8	56.8	56.8	56.8	56.8	56.8	56.8	56.8
<i>Dinoroseobacter shibae</i> DFL12	0.00	0.0	0.0	0.0			0.0	0.0	0.0	0.0	0.0	0.0	0.0	0.0	0.0	0.0	0.0	0.0	0.0	0.0	0.0	0.0	0.0	0.0	0.0	0.0	0.0	0.0	0.0	0.0	0.0	0.0	0.0	0.0
<i>Jannaschia</i> sp. CCS1	0.000	0.000	0.000	0.000			0.000	0.000	0.000	0.000	0.000	0.000	0.000	0.000	0.000	0.000	0.000	0.000	0.000	0.000	0.000	0.000	0.000	0.000	0.000	0.000	0.000	0.000	0.000	0.000	0.000	0.000	0.000	0.000
<i>Loktaneella vestfoldensis</i> SKA53	0.00	0.00	0.00	0.00			0.00	0.00	0.00	0.00	0.00	0.00	0.00	0.00	0.00	0.00	0.00	0.00	0.00	0.00	0.00	0.00	0.00	0.00	0.00	0.00	0.00	0.00	0.00	0.00	0.00	0.00	0.00	0.00
<i>Maritimibacter alkaliphilus</i> HTC22654	0.00	0.00	0.00	0.00			0.00	0.00	0.00	0.00	0.00	0.00	0.00	0.00	0.00	0.00	0.00	0.00	0.00	0.00	0.00	0.00	0.00	0.00	0.00	0.00	0.00	0.00	0.00	0.00	0.00	0.00	0.00	0.00
<i>Oceanibulbus indolifex</i> HEL45	0.00	0.00	0.00	0.00			0.00	0.00	0.00	0.00	0.00	0.00	0.00	0.00	0.00	0.00	0.00	0.00	0.00	0.00	0.00	0.00	0.00	0.00	0.00	0.00	0.00	0.00	0.00	0.00	0.00	0.00	0.00	0.00
<i>Oceanicola batsensis</i> HTC22597	0.00	0.00	0.00	0.00			0.00	0.00	0.00	0.00	0.00	0.00	0.00	0.00	0.00	0.00	0.00	0.00	0.00	0.00	0.00	0.00	0.00	0.00	0.00	0.00	0.00	0.00	0.00	0.00	0.00	0.00	0.00	0.00
<i>Oceanicola granulosus</i> HTC22516	0.00	0.00	0.00	0.00			0.00	0.00	0.00	0.00	0.00	0.00	0.00	0.00	0.00	0.00	0.00	0.00	0.00	0.00	0.00	0.00	0.00	0.00	0.00	0.00	0.00	0.00	0.00	0.00	0.00	0.00	0.00	0.00
<i>Octadecabacter antarcticus</i> 307	0.00	0.00	0.00	0.00			0.00	0.00	0.00	0.00	0.00	0.00	0.00	0.00	0.00	0.00	0.00	0.00	0.00	0.00	0.00	0.00	0.00	0.00	0.00	0.00	0.00	0.00	0.00	0.00	0.00	0.00	0.00	0.00
<i>Octadecabacter arcticus</i> 238	0.00	0.00	0.00	0.00			0.00	0.00	0.00	0.00	0.00	0.00	0.00	0.00	0.00	0.00	0.00	0.00	0.00	0.00	0.00	0.00	0.00	0.00	0.00	0.00	0.00	0.00	0.00	0.00	0.00	0.00	0.00	0.00
<i>Pelagibaca bermudensis</i> HTC2601	0.00	0.00	0.00	0.00			0.00	0.00	0.00	0.00	0.00	0.00	0.00	0.00	0.00	0.00	0.00	0.00	0.00	0.00	0.00	0.00	0.00	0.00	0.00	0.00	0.00	0.00	0.00	0.00	0.00	0.00	0.00	0.00
<i>Phaeobacter gallaeciensis</i> 2.10	0.00	0.00	0.00	0.00			0.00	0.00	0.00	0.00	0.00	0.00	0.00	0.00	0.00	0.00	0.00	0.00	0.00	0.00	0.00	0.00	0.00	0.00	0.00	0.00	0.00	0.00	0.00	0.00	0.00	0.00	0.00	0.00
<i>Phaeobacter gallaeciensis</i> BS107	0.00	0.00	0.00	0.00			0.00	0.00	0.00	0.00	0.00	0.00	0.00	0.00	0.00	0.00	0.00	0.00	0.00	0.00	0.00	0.00	0.00	0.00	0.00	0.00	0.00	0.00	0.00	0.00	0.00	0.00	0.00	0.00
<i>Phaeobacter</i> sp. Y41	0.00	0.00	0.00	0.00			0.00	0.00	0.00	0.00	0.00	0.00	0.00	0.00	0.00	0.00	0.00	0.00	0.00	0.00	0.00	0.00	0.00	0.00	0.00	0.00	0.00	0.00	0.00	0.00	0.00	0.00	0.00	0.00
<i>Rhodobacteriales bacterium</i> HTC22083	0.00	0.00	0.00	0.00			0.00	0.00	0.00	0.00	0.00	0.00	0.00	0.00	0.00	0.00	0.00	0.00	0.00	0.00	0.00	0.00	0.00	0.00	0.00	0.00	0.00	0.00	0.00	0.00	0.00	0.00	0.00	0.00
<i>Rhodobacteriales bacterium</i> HTC22150	0.00	0.00	0.00	0.00			0.00	0.00	0.00	0.00	0.00	0.00	0.00	0.00	0.00	0.00	0.00	0.00	0.00	0.00	0.00	0.00	0.00	0.00	0.00	0.00	0.00	0.00	0.00	0.00	0.00	0.00	0.00	0.00
<i>Rhodobacteriales bacterium</i> HTC22255	0.00	0.00	0.00	0.00			0.00	0.00	0.00	0.00	0.00	0.00	0.00	0.00	0.00	0.00	0.00	0.00	0.00	0.00	0.00	0.00	0.00	0.00	0.00	0.00	0.00	0.00	0.00	0.00	0.00	0.00	0.00	0.00
<i>Rhodobacteriales bacterium</i> KLH11	0.00	0.00	0.00	0.00			0.00	0.00	0.00	0.00	0.00	0.00	0.00	0.00	0.00	0.00	0.00	0.00	0.00	0.00	0.00	0.00	0.00	0.00	0.00	0.00	0.00	0.00	0.00	0.00	0.00	0.00	0.00	0.00
<i>Roseobacter denitrificans</i> Och 114	0.00	0.00	0.00	0.00			0.00	0.00	0.00	0.00	0.00	0.00	0.00	0.00	0.00	0.00	0.00	0.00	0.00	0.00	0.00	0.00	0.00	0.00	0.00	0.00	0.00	0.00	0.00	0.00	0.00	0.00	0.00	0.00
<i>Roseobacter litoralis</i> Och 149	0.00	0.00	0.00	0.00			0.00	0.00	0.00	0.00	0.00	0.00	0.00	0.00	0.00	0.00	0.00	0.00	0.00	0.00	0.00	0.00	0.00	0.00	0.00	0.00	0.00	0.00	0.00	0.00	0.00	0.00	0.00	0.00
<i>Roseobacter</i> sp. A2wk-3b	0.00	0.00	0.00	0.00			0.00	0.00	0.00	0.00	0.00	0.00	0.00	0.00	0.00	0.00	0.00	0.00	0.00	0.00	0.00	0.00	0.00	0.00	0.00	0.00	0.00	0.00	0.00	0.00	0.00	0.00	0.00	0.00
<i>Roseobacter</i> sp. CCS2	0.00	0.00	0.00	0.00			0.00	0.00	0.00	0.00	0.00	0.00	0.00	0.00	0.00	0.00	0.00	0.00	0.00	0.00	0.00	0.00	0.00	0.00	0.00	0.00	0.00	0.00	0.00	0.00	0.00	0.00	0.00	0.00
<i>Roseobacter</i> sp. GAI101	0.00	0.00	0.00	0.00			0.00	0.00	0.00	0.00	0.00	0.00	0.00	0.00	0.00	0.00	0.00	0.00	0.00	0.00	0.00	0.00	0.00	0.00	0.00	0.00	0.00	0.00	0.00	0.00	0.00	0.00	0.00	0.00

Gene Name	Siderophore Biosynthesis and Transport														Iron Responsive Regulators					Other														
	HYDROXAMATES														CATECHOLATES																			
Species	vbsC	vbsG	vbsA	icaA	icaB	icaC	icaD	fhbB	fhbC	fhbD	rhbB	rmo	vibF	vibA	ybdA / ents	entA	entB	entC	entD	entE	entF	rirA	mur	irr	isrC	fur	rirA	irpA	irpB	feaA	feoB			
<i>Roseobacter</i> sp. MED193	0.03 0.48 0.62			7.4	9.7	9.4	1.4	3.0E-33	2.0E-54	0.005	1.0E-32	33	32.0	47.37		72.9	8.09	71.07	6.63	31.40	32.81	21.33	38.48	91.32	45.20	31.41	11.17	7.0E-83				2.1	5.0E-07	
<i>Roseobacter</i> sp. SK209-2-6	0.31 0.48 0.38							2.0E-33	1.0E-51	0.005	2.0E-34	53	24.50	28.31	44.27	90.02	25.08	11.68	74.42	45.51	11.01	38.48	91.32	45.20	31.41	11.17	7.0E-83					5.0E-07		
<i>Roseovarius nubinihibens</i> ISM	0.001							2.0E-31	2.0E-47	0.005	5.0E-49	51	51.48	13.33	44.42	11.17	51.43	35.34	74.47	51.52	11.33	38.48	91.32	45.20	31.41	11.17	7.0E-83					3.0E-08		
<i>Roseovarius</i> sp. 217								1.0E-34	3.0E-28	0.005	9.0E-34	6	11.33	28.37	44.42	11.17	51.43	35.34	74.47	51.52	11.33	38.48	91.32	45.20	31.41	11.17	7.0E-83					3.0E-08		
<i>Roseovarius</i> sp. TM1035	2.0E-04							4.0E-32	3.0E-32	0.005	3.0E-33	60	81.59	47.38	24.50	30.08	30.58	31.33			11.17	38.48	91.32	45.20	31.41	11.17	7.0E-83					3.0E-08		
<i>Ruegeria lacuscaerulensis</i> ITI-1157	0.002							3.0E-34	1.0E-57	0.21	7.0E-60	31	11.33	47.38	11.27	66.03	31.37					31.33	38.48	91.32	45.20	31.41	11.17	7.0E-83				1.1	4.0E-07	
<i>Ruegeria pomeroyi</i> DSS-3	0.002							3.0E-34	1.0E-57	0.21	7.0E-60	31	11.33	47.38	11.27	66.03	31.37					31.33	38.48	91.32	45.20	31.41	11.17	7.0E-83					1.1	4.0E-07
<i>Ruegeria</i> sp. R11	0.004							2.0E-35	3.0E-40	5.1	8.0E-54	67	31.00	38.48	31.33	61.29	11.16	34.44	21.48	11.16	11.33	31.37	38.48	91.32	45.20	31.41	11.17	7.0E-83					1	2.0E-07
<i>Ruegeria</i> sp. TM1040	1.0E-04							3.0E-34	1.0E-57	0.21	7.0E-60	31	11.33	47.38	11.27	66.03	31.37					31.33	38.48	91.32	45.20	31.41	11.17	7.0E-83					1.1	4.0E-07
<i>Ruegeria</i> sp. Trich CH4B	0.011							3.0E-33	3.0E-34	0.005	7.0E-35	1.4	36.55	28.34	11.40	66.03	31.37	10.11				31.33	38.48	91.32	45.20	31.41	11.17	7.0E-83					1	4.0E-07
<i>Sagittula stellata</i> E-37	0.02							2.0E-31	2.0E-31	1.4	6.0E-54	0.21	71.45	38.48	51.38	24.29	80.07	51.08	42.01	61.50	31.33	38.48	91.32	45.20	31.41	11.17	7.0E-83						3.0E-07	
<i>Sulfitobacter</i> NAS-14.1	0.002							3.0E-33	3.0E-34	0.005	7.0E-35	1.4	36.55	28.34	11.40	66.03	31.37	10.11				31.33	38.48	91.32	45.20	31.41	11.17	7.0E-83						3.0E-07
<i>Sulfitobacter</i> sp. EE-36	0.005							3.0E-33	3.0E-34	0.005	7.0E-35	1.4	36.55	28.34	11.40	66.03	31.37	10.11				31.33	38.48	91.32	45.20	31.41	11.17	7.0E-83						3.0E-07
<i>Thalassiosira</i> R2A62								3.0E-34	3.0E-34	0.005	7.0E-35	1.4	36.55	28.34	11.40	66.03	31.37	10.11				31.33	38.48	91.32	45.20	31.41	11.17	7.0E-83						3.0E-07

Table 2.2 Functions and genbank identities of all peptides used in Table 2.1

Gene	Genbank Accession	Function	Gene	Genbank Accession	Function
<i>fhuA</i>	NP_414692	ferrichrome	<i>vbsC</i>	CAK12032	
<i>fhuE</i>	AC136233	ferric-rihodotorulic acid, ferric siderophores coprogen and ferrioxamine B	<i>vbsG</i>	CACA48061	<i>Rhizobium vicibactin</i>
<i>btuB</i>	AA23524	vitamin B12, E colicins	<i>vbsA</i>	CAC48060	
<i>hmuU</i>	AA064869	heme/haemoglobin receptor	<i>iucA</i>	AAK71631.1	
<i>cirA</i>	NP_416660	ferric iron-catecholate-colicins	<i>iucB</i>	AAK71632.1	aerobactin synthesis - <i>Shigella boydii</i>
<i>fecA</i>	AC145941	ferric citrate	<i>iucC</i>	AAK71633.1	
<i>fepA</i>	YP_002269216.1	Ferrienterobactin permease	<i>iucD</i>	AAK71634.1	
<i>viuA</i>	AET27297	vibriobactin receptor	<i>fhuB</i>	YP_406700.1	aerobactin uptake
<i>viuB</i>	AET27296	ferric vibriobactin utilization	<i>fhuC</i>	YP_406698.1	
<i>fhuY/bil</i>	NP_415326	believed to facilitate the uptake of the siderophore dihydroxybenzoylserine	<i>fhuD</i>	YP_406699.1	
<i>fptA</i>	AA063213	pyochelin receptor - <i>Pseudomonas aeruginosa</i>	<i>rhcB</i>	ABG94125.1	rhodochelin synthesis - <i>Rhodococcus jostii</i>
<i>fpuA</i>	AA017439	ferric pyoverdine receptor	<i>rmo</i>	YP_704660.1	
<i>hasR</i>	EGT69989	Yersinia bacterin receptor	<i>vibF</i>	YP_001217726	vibriobactin synthesis
<i>shuA</i>	CAE46936	<i>Serratia marcescens</i> heme receptor	<i>vibA</i>	ACP08808	1st step in vibriobactin synthesis
<i>yiur</i>	AA027809	heme/hemoglobin receptor - <i>Shigella dysenteriae</i>	<i>ybdA / entS</i>	YP_003076595	Enterobactin exporter
<i>hmuR</i>	ADV99409	catecholate siderophores - <i>Yersinia pestis</i>	<i>entA</i>	NP_415128.1	Enterobactin biosynthesis
<i>fepB</i>	ABM19271.1	Mariobactin receptor - <i>Mariobacter</i>	<i>entB</i>	NP_286322	Enterobactin biosynthesis
<i>fepC</i>	ABX87333	TonB-dependent heme/hemoglobin uptake - <i>Yersinia pestis</i>	<i>entC</i>	AC136818	Enterobactin biosynthesis
<i>fepD</i>	EGT6731	Ferrienterobactin-binding periplasmic protein	<i>entD</i>	AC136635.1	Enterobactin biosynthesis
<i>fepE</i>	AC138323	ATPase	<i>entE</i>	YP_002269228	Enterobactin biosynthesis
<i>fepF</i>	CAA42043	Ferrienterobactin transporter, permease	<i>entF</i>	YP_002269220	Enterobactin biosynthesis
<i>fepG</i>	CAA40708	Ferrienterobactin transporter, permease	<i>rirA</i>	YP_766387	Rhizobial iron regulator
<i>fbpA</i>	NP_286103	Ferric iron permease	<i>mur</i>	CAK05888	Manganese uptake regulator
<i>fbpB</i>	YP_002400786	Ferric iron periplasmic binding protein	<i>irr</i>	AAC32183	Iron responsive regulator
<i>fbpC</i>	YP_003076376	ATPase	<i>iscR</i>	EGT66035	Iron sulphur clusters
<i>yfuA</i>	NP_668846.1	iron(III)-binding periplasmic protein	<i>fur</i>	AAR12905	Ferric uptake regulator
<i>hmuT</i>	AA064868	hemin periplasmic binding protein	<i>irpA</i>	SP00086	Iron regulated protein
<i>yqjH</i>	NP_417541	ferric reductase	<i>irpB</i>	AAV93418.1	Iron regulated protein
<i>ferA</i>	YP_913877	<i>Paracoccus denitrificans</i> ferric reductase	<i>fecA</i>	CA450386.1	ferrous iron transporter
<i>ferB</i>	YP_917833	<i>P. denitrificans</i> ferric reductase	<i>fecB</i>	YP_001732246.1	ferrous iron transporter
<i>mtrA</i>	NP_717386	<i>Shewanella</i> iron reduction			
<i>mtrB</i>	NP_717385	<i>Shewanella</i> iron reduction			
<i>tolA</i>	YP_769548				
<i>tolR</i>	YP_002977283				
<i>tolQ</i>	YP_769550	Couples proton motive force from inner to outer membrane for energising transport into periplasm			
<i>tonB</i>	YP_001730249				
<i>exxB</i>	AAA69173				
<i>exxD</i>	AAA69172				

2.1.2 The distribution of TonB-dependent outer membrane receptors in the Roseobacters

As presented in the Introduction, many iron-containing compounds are imported via an active transport process, whose initial step involves the recognition and uptake of the Fe-ligand across the outer membrane via a receptor that has a highly conserved basic structure, comprising a beta barrel. Such systems are used to import many siderophores, ferric-citrate complexes and haem, either alone, or complexed in carrier proteins, such as hemoglobin. This process also requires energy, which is transduced via the TonB/ExbBD polypeptides, so are termed, collectively “TonB-dependent outer membrane receptors” (TBDR).

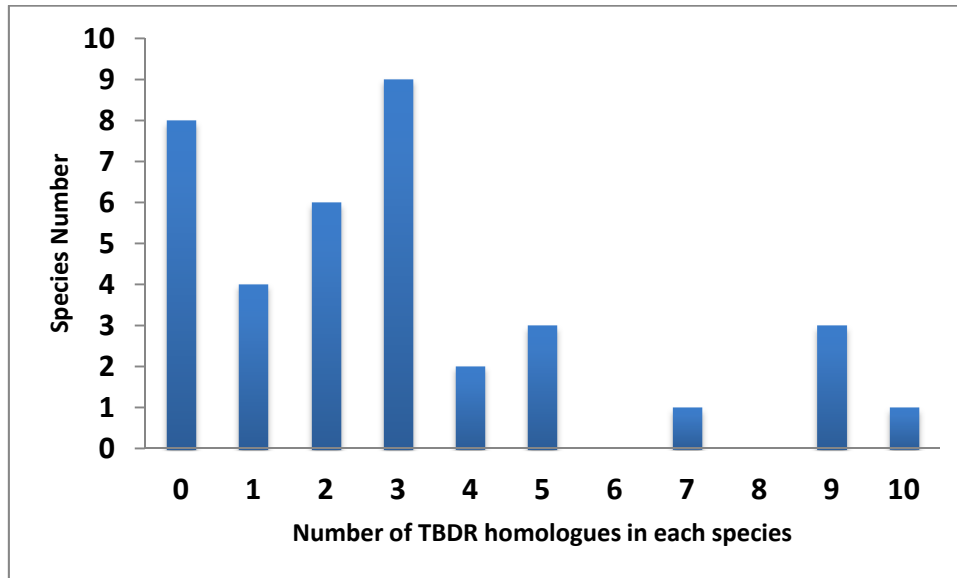
A glance at Table 2.1 shows that there are few close homologues to the various receptors.

However, it is apparent that there are significant matches to members of this super-family, but at a low level of similarity. Importantly, too, there are remarkable differences in the portfolios of different strains and even in the numbers that they have.

To infer function based on homology would be unwise given the significant diversity of the TBDR peptides; when a FhuA homologue is shown to be present in any given Roseobacter in Table 2.1, this does not mean we know the identity of the molecule which it likely imports.

As shown in Table 2.1, there is a remarkable diversity in the distribution of the types and numbers of TBDRs in the different Roseobacters. Thus, as shown in the histogram in Figure 2.1, the numbers range from zero (in eight different strains) to ten (in *Ruegeria* sp. Trich CH4B), but with only a minority of strains (10 out of 37) having four or more polypeptides in this family.

Figure 2.1 Histogram of TBDR numbers in Roseobacters species



Histogram of the numbers of TBDR gene homologues found in genome sequenced Roseobacters, as shown in Table 2.1.

The list below sets out the names of the strains with their total numbers of receptors and of the types that they most closely resemble shown in brackets: (C = citrate; H = haem; S = siderophore and B = vitamin B₁₂) are as follows: Only those with close homologues, i.e. shown as green in Table 2.1, were used for these analyses.

0 receptors: *Oceanicola granulosus* HTCC2516, *Octadecabacter arcticus* 238, *Rhodobacterales bacterium* HTCC2150, *Rhodobacterales bacterium* KLH11, *Roseobacter litoralis* Och 149, *Roseobacter* sp. AzwK-3b, *Roseobacter* sp. CCS2 and *Ruegeria pomeroyi* DSS-3.

One receptor: *Oceanibulbus indolifex* HEL45 (S), *Rhodobacterales bacterium* HTCC2083 (S), *Rhodobacterales bacterium* HTCC2255 (S), *Sagittula stellata* E-37 (S),

Two receptors *Dinoroseobacter shibae* DFL 12 (H), *Loktanella vestfoldensis* SKA53 (H), *Roseobacter* sp. GAI101 (SB), *Roseovarius nubinihibens* ISM (H), *Roseovarius* sp. TM1035 (H), *Ruegeria* sp. R11 (SH) and *Ruegeria* sp. TM1040 (H).

Three receptors : *Maritimibacter alkaliphilus* HTCC2654 (HS), *Oceanicola batsensis* HTCC2597 (S), *Phaeobacter gallaeciensis* 2.10 (S), *Phaeobacter gallaeciensis* BS107 (S), *Phaeobacter* sp. Y4I (S), *Roseobacter denitrificans* OCh 114 (H), *Ruegeria lacuscaerulensis* ITI-1157 (S)

Four receptors: *Jannaschia* sp. CCS1 (HS), *Octadecabacter antarcticus* 307 (HB) and *Thalassibium* R2A62 (SH).

Five receptors: *Roseobacter* sp. MED193 (SH), *Roseobacter* sp. SK209-2-6 (SH) and *Roseovarius* sp. 217 (SH).

Seven receptors: *Sulfitobacter* sp. EE-36 (CHS).

Nine receptors: *Citricella* SE45 (CHSB), *Pelagibaca bermudensis* HTCC2601 (CHSB) and *Sulfitobacter* NAS-14.1 (CHS).

Ten receptors: *Ruegeria* sp. Trich CH4B (CHS).

Indeed, some species possess a wide complement of receptors, such as *Citricella* SE45, which has two copies of both “*fhuA*” and “*fpvA*” and single copies of *btuB*-, *hmuU*- and *hmuR*-like genes in its genome (see Table 2.1). *Ruegeria* sp. Trich CH4B also has a large complement of homologues to iron specific receptors – *fhuA*, *hmuU*, *fecA*, *fpvA* and *hmuR*, but this is surpassed by *Sulfitobacter* NAS-14.1 and *Sulfitobacter* EE36, both of which also have a homologue of *fiu*, an enterochelin breakdown-product receptor. But, the TBDR record-holder, to date, is *Pelagibaca bermudensis* HTCC2601 which has homologues of *fhuA*, *hmuU*, *fecA*, *fpvA*, *btuB* and two catecholate siderophore receptors – *cirA* and *yiur*.

In contrast, several *Roseobacters* lack homologues to any known TBDRs; these are *R. pomeroyi* DSS-3, *Oceanicola granulosus* HTCC2516, *Octadecabacter arcticus* 238 and *Rhodobacterales* bacterium HTCC2150. Several other *Roseobacters* lack all TBDR genes, except a weak homologue to *hmuU*.

2.1.3 The search for TonB

The presence of TBDRs at least in some *Roseobacters*, points, not unreasonably to the need for a TonB polypeptide in such strains. However, using the *bone fide* TonB of *Rhizobium leguminosarum* as the BLASTP probe, none of the *Roseobacter* proteomes yielded a convincing homologue ($e < 10^{25}$). But, given the hyper-variability of TonBs in bacteria, I decided to search for TonB in the *Roseobacters* using a different approach.

I used the sequence of the TonB peptides of *E. coli*, *Rhizobium leguminosarum* and *Rhodobacter sphaeroides* as probes to interrogate all *Roseobacter* genomes, and discovered a homologue in

Roseovarius nubinhibens – the product of the *ISM_04245* gene (30% ID to TonB of *Rhizobium leguminosarum*). Although not a *bone fide* TonB gene, *ISM-04245* is next to putative haem uptake genes *hmuR* and a putative *exbB* gene, so I added the *ISM_04245* gene product to the *in silico* probes used for my TonB search.

I used all the TonB probes against the proteomes of all the Roseobacters. The resulting matches are shown in table 2.3. Since each putative TonB polypeptide is targeted by four probes (four different colours), any gene locus with analogous to **most** of the probes was considered to be a *bona fide* TonB. Even with this approach, none of the TonBs was >45% identical to any of the probes, except, of course for *R. nubinhibens* itself. Although this approach may have indeed identified TonBs in the Roseobacters, further direct experimentation will be needed to ratify this (for example, by examining the iron uptake abilities of strains with mutations in these genes).

However, several Roseobacters did not contain a gene homologous to more than two of the probe sequences, and therefore **may** not possess a copy of TonB. These were: *Octadecabacter antarcticus* 238, *Oceanibulbus indolifex* HEL-45, *Rhodobacterales bacterium* HTCC2255, *Roseobacter* sp. AzWK3b, *Rhodobacterales bacterium* HTCC2083, *Rhodobacterales bacterium* HTCC2150, *Roseobacter* sp. CCS2, *Roseobacter denitrificans* Och114, *Roseobacter litoralis* Och 149, *Loktanella vestfoldensis* SKA53 and *Ruegeria lacuscaerulensis* ITI-1157.

Crucially, of these **eleven** strains that lack TonB, **five** did not have not appear to have any TBDR polypeptides (underlined above and shown in Table 2.1). Two of the other strains that had no detectable TBDR polypeptides (*Ruegeria pomeroyi* DSS-3 and *Oceanicola granulosus* HTCC2516) also had very poor homologues of TonB, which were of questionable validity (E values > 5E⁻¹⁰). Therefore, there is some correlation between the lack of TonB and the absence of a TBDR in the same strain. This observation warrants further investigation.

The concept of bacterial species lacking TonB has received some attention - *Francisella tularensis* imports a rhizoferrin-like carboxylate siderophore via the outer membrane receptor FslE, albeit still in an energy dependent process (Ramakrishnan *et al.* 2008; 2012). *Legionella pneumophila* produces a siderophore (legiobactin) which is imported via a receptor termed LbtU, which is also supposedly TonB independent. The authors report that LbtU is a 16 stranded β -barrel, distinct from 22-stranded normal TBDRs (Chatfield *et al.* 2011).

Of course, there were also strains which do have homologues of TBDRs, and yet do not appear to have TonB. Again, without further work these questions remain unanswered, but fascinating.

Table 2.3 Presence of TonB Homologues in Genome-Sequenced Strains of the Roseobacter Clade

Gene Tag	Genome	Percentage ID	Expect value
<u>CH4B_21510</u>	<i>Ruegeria</i> sp. Trich CH4B	38	4.00E ⁻⁴⁷
<u>CH4B_21510</u>	<i>Ruegeria</i> sp. Trich CH4B	27	1.00E ⁻²⁰
<u>CH4B_21510</u>	<i>Ruegeria</i> sp. Trich CH4B	24	1.00E ⁻¹³
<u>CH4B_45730</u>	<i>Ruegeria</i> sp. Trich CH4B	36	8.00E ⁻²⁸
<u>CH4B_45730</u>	<i>Ruegeria</i> sp. Trich CH4B	30	5.00E ⁻¹⁶
<u>CH4B_45730</u>	<i>Ruegeria</i> sp. Trich CH4B	27	3.00E ⁻¹³
<u>CH4B_45730</u>	<i>Ruegeria</i> sp. Trich CH4B	26	3.00E ⁻⁰⁸
<u>Dshi_0567</u>	<i>Dinoroseobacter shibae</i> DFL12	38	7.00E ⁻²⁴
<u>Dshi_0567</u>	<i>Dinoroseobacter shibae</i> DFL12	29	3.00E ⁻¹³
<u>Dshi_0567</u>	<i>Dinoroseobacter shibae</i> DFL12	28	6.00E ⁻¹²
<u>Dshi_1110</u>	<i>Dinoroseobacter shibae</i> DFL12	34	1.00E ⁻¹³
<u>Dshi_1110</u>	<i>Dinoroseobacter shibae</i> DFL12	37	3.00E ⁻¹⁰
<u>Dshi_1110</u>	<i>Dinoroseobacter shibae</i> DFL12	26	3.00E ⁻⁰⁷
<u>Dshi_2367</u>	<i>Dinoroseobacter shibae</i> DFL12	29	2.00E ⁻⁰⁶
<u>Dshi_2725</u>	<i>Dinoroseobacter shibae</i> DFL12	29	8.00E ⁻⁰⁹
<u>EE36_09740</u>	<i>Sulfitobacter</i> sp. EE-36	31	2.00E ⁻⁰⁹
<u>EE36_09740</u>	<i>Sulfitobacter</i> sp. EE-36	32	3.00E ⁻⁰⁹
<u>EE36_09740</u>	<i>Sulfitobacter</i> sp. EE-36	26	6.00E ⁻⁰⁷
<u>EE36_10430</u>	<i>Sulfitobacter</i> sp. EE-36	29	3.00E ⁻¹⁰
<u>EE36_13013</u>	<i>Sulfitobacter</i> sp. EE-36	42	3.00E ⁻⁵³
<u>EE36_13013</u>	<i>Sulfitobacter</i> sp. EE-36	29	5.00E ⁻²⁵
<u>EE36_13013</u>	<i>Sulfitobacter</i> sp. EE-36	28	5.00E ⁻¹⁴
<u>EE36_15637</u>	<i>Sulfitobacter</i> sp. EE-36	32	3.00E ⁻⁰⁹
<u>EE36_15637</u>	<i>Sulfitobacter</i> sp. EE-36	30	2.00E ⁻⁰⁷
<u>ISM_03305</u>	<i>Roseovarius nubinhibens</i> ISM	27	4.00E ⁻⁰⁷

<u>ISM_04245</u>	<i>Roseovarius nubinhibens</i> ISM	100	1.00E ⁻¹⁷⁴
<u>ISM_04245</u>	<i>Roseovarius nubinhibens</i> ISM	30	4.00E ⁻²⁴
<u>ISM_04245</u>	<i>Roseovarius nubinhibens</i> ISM	28	3.00E ⁻¹⁶
<u>ISM_06055</u>	<i>Roseovarius nubinhibens</i> ISM	34	1.00E ⁻¹³
<u>ISM_06055</u>	<i>Roseovarius nubinhibens</i> ISM	29	6.00E ⁻⁰⁶
<u>ISM_16395</u>	<i>Roseovarius nubinhibens</i> ISM	32	4.00E ⁻¹⁰
<u>ISM_16395</u>	<i>Roseovarius nubinhibens</i> ISM	32	8.00E ⁻⁰⁷
<u>Jann_0972</u>	<i>Jannaschia</i> sp. CCS1	28	1.00E ⁻⁰⁶
<u>Jann_1616</u>	<i>Jannaschia</i> sp. CCS1	32	2.00E ⁻⁰⁶
<u>Jann_2127</u>	<i>Jannaschia</i> sp. CCS1	36	2.00E ⁻⁴¹
<u>Jann_2127</u>	<i>Jannaschia</i> sp. CCS1	29	4.00E ⁻²⁰
<u>Jann_2127</u>	<i>Jannaschia</i> sp. CCS1	28	4.00E ⁻¹³
<u>KLH11_10350</u>	<i>Rhodobacterales bacterium</i> KLH11	27	6.00E ⁻⁰⁶
<u>KLH11_13530</u>	<i>Rhodobacterales bacterium</i> KLH11	26	2.00E ⁻⁰⁹
<u>KLH11_14940</u>	<i>Rhodobacterales bacterium</i> KLH11	30	2.00E ⁻²²
<u>KLH11_14940</u>	<i>Rhodobacterales bacterium</i> KLH11	27	6.00E ⁻¹⁷
<u>KLH11_14940</u>	<i>Rhodobacterales bacterium</i> KLH11	24	7.00E ⁻¹⁰
<u>MED193_17529</u>	<i>Roseobacter</i> sp MED193	35	6.00E ⁻⁴²
<u>MED193_17529</u>	<i>Roseobacter</i> sp MED193	30	3.00E ⁻²³
<u>MED193_17529</u>	<i>Roseobacter</i> sp MED193	26	3.00E ⁻¹⁷
<u>MED193_22036</u>	<i>Roseobacter</i> sp MED193	38	5.00E ⁻²⁹
<u>MED193_22036</u>	<i>Roseobacter</i> sp MED193	31	2.00E ⁻¹⁹
<u>MED193_22036</u>	<i>Roseobacter</i> sp MED193	27	7.00E ⁻¹⁶
<u>MED193_22036</u>	<i>Roseobacter</i> sp MED193	27	3.00E ⁻¹¹
<u>NAS141_05758</u>	<i>Sulfitobacter</i> sp. NAS-14.1	31	8.00E ⁻⁰⁸
<u>NAS141_06398</u>	<i>Sulfitobacter</i> sp. NAS-14.1	29	1.00E ⁻⁰⁶
<u>NAS141_06398</u>	<i>Sulfitobacter</i> sp. NAS-14.1	30	3.00E ⁻⁰⁶

<u>NAS141_14753</u>	<i>Sulfitobacter</i> sp. NAS-14.1	31	8.00E ⁻¹⁰
<u>NAS141_14753</u>	<i>Sulfitobacter</i> sp. NAS-14.1	25	6.00E ⁻⁰⁹
<u>NAS141_14753</u>	<i>Sulfitobacter</i> sp. NAS-14.1	26	1.00E ⁻⁰⁶
<u>NAS141_15333</u>	<i>Sulfitobacter</i> sp. NAS-14.1	29	3.00E ⁻¹⁰
<u>NAS141_18179</u>	<i>Sulfitobacter</i> sp. NAS-14.1	43	9.00E ⁻⁵⁴
<u>NAS141_18179</u>	<i>Sulfitobacter</i> sp. NAS-14.1	31	6.00E ⁻²³
<u>NAS141_18179</u>	<i>Sulfitobacter</i> sp. NAS-14.1	28	1.00E ⁻¹³
<u>NAS141_18179</u>	<i>Sulfitobacter</i> sp. NAS-14.1	23	2.00E ⁻⁰⁷
<u>OA238_811</u>	<i>Octadecabacter antarcticus</i> 238	29	3.00E ⁻⁰⁹
<u>OA307_2153</u>	<i>Octadecabacter antarcticus</i> 307	32	9.00E ⁻³²
<u>OA307_2153</u>	<i>Octadecabacter antarcticus</i> 307	25	1.00E ⁻¹⁶
<u>OA307_2153</u>	<i>Octadecabacter antarcticus</i> 307	26	2.00E ⁻¹¹
<u>OB2597_05450</u>	<i>Oceanicola batsensis</i> HTCC2597	36	2.00E ⁻⁵⁰
<u>OB2597_05450</u>	<i>Oceanicola batsensis</i> HTCC2597	29	6.00E ⁻¹⁸
<u>OB2597_05450</u>	<i>Oceanicola batsensis</i> HTCC2597	28	4.00E ⁻¹⁵
<u>OB2597_05450</u>	<i>Oceanicola batsensis</i> HTCC2597	24	3.00E ⁻⁰⁶
<u>OB2597_15655</u>	<i>Oceanicola batsensis</i> HTCC2597	24	1.00E ⁻⁰⁶
<u>OB2597_15655</u>	<i>Oceanicola batsensis</i> HTCC2597	26	2.00E ⁻⁰⁶
<u>OG2516_01015</u>	<i>Oceanicola granulosus</i> HTCC2516	30	5.00E ⁻⁰⁶
<u>OG2516_12444</u>	<i>Oceanicola granulosus</i> HTCC2516	32	5.00E ⁻¹⁰
<u>OG2516_12444</u>	<i>Oceanicola granulosus</i> HTCC2516	23	2.00E ⁻⁰⁷
<u>OG2516_12444</u>	<i>Oceanicola granulosus</i> HTCC2516	24	5.00E ⁻⁰⁷
<u>OIH45_09568</u>	<i>Oceanibulbus indolifex</i> HEL-45	25	2.00E ⁻¹⁰
<u>OIH45_09568</u>	<i>Oceanibulbus indolifex</i> HEL-45	31	5.00E ⁻⁰⁷
<u>OIH45_15869</u>	<i>Oceanibulbus indolifex</i> HEL-45	25	7.00E ⁻¹⁰
<u>OIH45_15869</u>	<i>Oceanibulbus indolifex</i> HEL-45	24	8.00E ⁻⁰⁷
<u>OM2255_13534</u>	<i>Rhodobacterales bacterium</i> HTCC2255	38	6.00E ⁻¹²

<u>OM2255_13534</u>	<i>Rhodobacterales bacterium</i> HTCC2255	37	7.00E ⁻¹²
<u>R2601_11699</u>	<i>Pelagibaca bermudensis</i> HTCC2601	25	1.00E ⁻⁰⁶
<u>R2601_12453</u>	<i>Pelagibaca bermudensis</i> HTCC2601	29	4.00E ⁻¹¹
<u>R2601_12453</u>	<i>Pelagibaca bermudensis</i> HTCC2601	38	2.00E ⁻¹⁰
<u>R2601_12453</u>	<i>Pelagibaca bermudensis</i> HTCC2601	23	2.00E ⁻⁰⁹
<u>R2601_12453</u>	<i>Pelagibaca bermudensis</i> HTCC2601	25	3.00E ⁻⁰⁷
<u>R2601_21051</u>	<i>Pelagibaca bermudensis</i> HTCC2601	33	8.00E ⁻¹¹
<u>R2601_26191</u>	<i>Pelagibaca bermudensis</i> HTCC2601	25	9.00E ⁻⁰⁸
<u>R2601_27243</u>	<i>Pelagibaca bermudensis</i> HTCC2601	42	1.00E ⁻⁶⁵
<u>R2601_27243</u>	<i>Pelagibaca bermudensis</i> HTCC2601	31	3.00E ⁻²⁹
<u>R2601_27243</u>	<i>Pelagibaca bermudensis</i> HTCC2601	31	6.00E ⁻²²
<u>R2A62_18510</u>	<i>Thalassiobium</i> sp. R2A62	26	4.00E ⁻⁰⁶
<u>R2A62_19050</u>	<i>Thalassiobium</i> sp. R2A62	32	3.00E ⁻³⁵
<u>R2A62_19050</u>	<i>Thalassiobium</i> sp. R2A62	28	3.00E ⁻¹⁹
<u>R2A62_19050</u>	<i>Thalassiobium</i> sp. R2A62	27	3.00E ⁻¹⁵
<u>R2A62_29000</u>	<i>Thalassiobium</i> sp. R2A62	21	3.00E ⁻⁰⁶
<u>RAZWK3B_06677</u>	<i>Roseobacter</i> sp. AzwK3b	26	5.00E ⁻¹¹
<u>RAZWK3B_20566</u>	<i>Roseobacter</i> sp. AzwK3b	42	2.00E ⁻⁰⁹
<u>RB2083_2039</u>	<i>Rhodobacterales bacterium</i> HTCC2083	35	7.00E ⁻⁰⁷
<u>RB2150_04948</u>	<i>Rhodobacterales bacterium</i> HTCC2150	26	2.00E ⁻⁰⁸
<u>RB2150_05338</u>	<i>Rhodobacterales bacterium</i> HTCC2150	36	8.00E ⁻¹¹
<u>RB2654_05647</u>	<i>Maritimibacter alkaliphilus</i> HTCC2654	31	1.00E ⁻¹⁰
<u>RB2654_05647</u>	<i>Maritimibacter alkaliphilus</i> HTCC2654	27	1.00E ⁻⁰⁷
<u>RB2654_05647</u>	<i>Maritimibacter alkaliphilus</i> HTCC2654	28	5.00E ⁻⁰⁷
<u>RB2654_15821</u>	<i>Maritimibacter alkaliphilus</i> HTCC2654	35	3.00E ⁻²⁷
<u>RB2654_15821</u>	<i>Maritimibacter alkaliphilus</i> HTCC2654	29	5.00E ⁻¹⁹
<u>RB2654_15821</u>	<i>Maritimibacter alkaliphilus</i> HTCC2654	26	4.00E ⁻¹²

<u>RB2654_18448</u>	<i>Maritimibacter alkaliphilus</i> HTCC2654	28	2.00E ⁻⁰⁶
<u>RB2654_19658</u>	<i>Maritimibacter alkaliphilus</i> HTCC2654	33	2.00E ⁻¹²
<u>RB4I_2464</u>	<i>Phaeobacter</i> sp. Y4I	31	2.00E ⁻⁰⁹
<u>RB4I_2464</u>	<i>Phaeobacter</i> sp. Y4I	25	1.00E ⁻⁰⁶
<u>RB4I_2464</u>	<i>Phaeobacter</i> sp. Y4I	34	3.00E ⁻⁰⁶
<u>RB4I_4149</u>	<i>Phaeobacter</i> sp. Y4I	34	1.00E ⁻²⁶
<u>RB4I_4149</u>	<i>Phaeobacter</i> sp. Y4I	30	6.00E ⁻¹⁸
<u>RB4I_4149</u>	<i>Phaeobacter</i> sp. Y4I	28	2.00E ⁻¹³
<u>RCCS2_05544</u>	<i>Roseobacter</i> sp. CCS2	24	4.00E ⁻⁰⁷
<u>RCCS2_05544</u>	<i>Roseobacter</i> sp. CCS2	25	2.00E ⁻⁰⁶
<u>RD1_1932</u>	<i>Roseobacter denitrificans</i> Och114	34	2.00E ⁻¹²
<u>RD1_1932</u>	<i>Roseobacter denitrificans</i> Och114	31	2.00E ⁻¹⁰
<u>RD1_3158</u>	<i>Roseobacter denitrificans</i> Och114	33	3.00E ⁻¹²
<u>RD1_4199</u>	<i>Roseobacter denitrificans</i> Och114	37	2.00E ⁻³⁸
<u>RD1_4199</u>	<i>Roseobacter denitrificans</i> Och114	30	4.00E ⁻²¹
<u>RG210_03453</u>	<i>Phaeobacter gallaeciensis</i> 2.10	22	2.00E ⁻⁰⁶
<u>RG210_11773</u>	<i>Phaeobacter gallaeciensis</i> 2.10	37	7.00E ⁻³¹
<u>RG210_11773</u>	<i>Phaeobacter gallaeciensis</i> 2.10	28	3.00E ⁻¹⁸
<u>RG210_11773</u>	<i>Phaeobacter gallaeciensis</i> 2.10	26	3.00E ⁻¹⁰
<u>RG210_11773</u>	<i>Phaeobacter gallaeciensis</i> 2.10	24	8.00E ⁻⁰⁸
<u>RGAI101_1183</u>	<i>Roseobacter</i> sp. GAI101	31	1.00E ⁻⁰⁹
<u>RGAI101_1183</u>	<i>Roseobacter</i> sp. GAI101	35	1.00E ⁻⁰⁹
<u>RGAI101_1183</u>	<i>Roseobacter</i> sp. GAI101	32	3.00E ⁻⁰⁷
<u>RGAI101_1183</u>	<i>Roseobacter</i> sp. GAI101	26	2.00E ⁻⁰⁶
<u>RGAI101_2719</u>	<i>Roseobacter</i> sp. GAI101	30	3.00E ⁻²¹
<u>RGAI101_2719</u>	<i>Roseobacter</i> sp. GAI101	31	1.00E ⁻¹⁶
<u>RGAI101_2719</u>	<i>Roseobacter</i> sp. GAI101	28	2.00E ⁻¹³

<u>RGAI101_3387</u>	<i>Roseobacter</i> sp. GAI101	28	1.00E ⁻⁰⁶
<u>RGAI101_4137</u>	<i>Roseobacter</i> sp. GAI101	29	2.00E ⁻¹¹
<u>RGBS107_01618</u>	<i>Phaeobacter gallaeciensis</i> BS107	36	3.00E ⁻³⁰
<u>RGBS107_01618</u>	<i>Phaeobacter gallaeciensis</i> BS107	28	6.00E ⁻¹⁸
<u>RGBS107_01618</u>	<i>Phaeobacter gallaeciensis</i> BS107	27	7.00E ⁻¹³
<u>RGBS107_01618</u>	<i>Phaeobacter gallaeciensis</i> BS107	25	3.00E ⁻⁰⁶
<u>RLO149_00770</u>	<i>Roseobacter litoralis</i> Och 149	30	1.00E ⁻⁰⁶
<u>RLO149_16723</u>	<i>Roseobacter litoralis</i> Och 149	36	5.00E ⁻⁰⁸
<u>RLO149_22885</u>	<i>Roseobacter litoralis</i> Och 149	28	3.00E ⁻⁰⁷
<u>ROS217_05079</u>	<i>Roseovarius</i> sp 217	34	1.00E ⁻¹¹
<u>ROS217_08174</u>	<i>Roseovarius</i> sp 217	28	2.00E ⁻⁰⁷
<u>ROS217_17015</u>	<i>Roseovarius</i> sp 217	30	5.00E ⁻⁰⁶
<u>ROS217_22847</u>	<i>Roseovarius</i> sp 217	43	1.00E ⁻⁵³
<u>ROS217_22847</u>	<i>Roseovarius</i> sp 217	28	9.00E ⁻¹⁹
<u>ROS217_22847</u>	<i>Roseovarius</i> sp 217	29	6.00E ⁻¹⁷
<u>RR11_3124</u>	<i>Ruegeria</i> sp. R11	27	2.00E ⁻⁰⁶
<u>RR11_420</u>	<i>Ruegeria</i> sp. R11	28	1.00E ⁻⁰⁶
<u>RR11_420</u>	<i>Ruegeria</i> sp. R11	24	1.00E ⁻⁰⁶
<u>RR11_420</u>	<i>Ruegeria</i> sp. R11	27	3.00E ⁻⁰⁶
<u>RR11_89</u>	<i>Ruegeria</i> sp. R11	38	6.00E ⁻⁴⁴
<u>RR11_89</u>	<i>Ruegeria</i> sp. R11	34	5.00E ⁻¹⁵
<u>RR11_89</u>	<i>Ruegeria</i> sp. R11	26	1.00E ⁻¹⁰
<u>RSK20926_04157</u>	<i>Roseobacter</i> sp. SK20926	26	1.00E ⁻⁰⁷
<u>RSK20926_04157</u>	<i>Roseobacter</i> sp. SK20926	37	5.00E ⁻⁰⁶
<u>RSK20926_10619</u>	<i>Roseobacter</i> sp. SK20926	35	2.00E ⁻³⁷
<u>RSK20926_10619</u>	<i>Roseobacter</i> sp. SK20926	26	7.00E ⁻²²
<u>RSK20926_10619</u>	<i>Roseobacter</i> sp. SK20926	27	1.00E ⁻¹³

<u>RSK20926_15376</u>	<i>Roseobacter</i> sp. SK20926	35	4.00E ⁻²⁹
<u>RSK20926_15376</u>	<i>Roseobacter</i> sp. SK20926	31	2.00E ⁻¹⁷
<u>RSK20926_15376</u>	<i>Roseobacter</i> sp. SK20926	26	1.00E ⁻¹⁴
<u>RSK20926_15376</u>	<i>Roseobacter</i> sp. SK20926	26	9.00E ⁻¹⁰
<u>RSK20926_17927</u>	<i>Roseobacter</i> sp. SK20926	32	5.00E ⁻⁰⁷
<u>RTM1035_05560</u>	<i>Roseovarius</i> sp. TM1035	41	4.00E ⁻⁵¹
<u>RTM1035_05560</u>	<i>Roseovarius</i> sp. TM1035	26	4.00E ⁻¹⁷
<u>RTM1035_05560</u>	<i>Roseovarius</i> sp. TM1035	24	2.00E ⁻¹²
<u>RTM1035_06468</u>	<i>Roseovarius</i> sp. TM1035	27	5.00E ⁻⁰⁶
<u>RTM1035_18951</u>	<i>Roseovarius</i> sp. TM1035	30	1.00E ⁻¹⁰
<u>RTM1035_18951</u>	<i>Roseovarius</i> sp. TM1035	26	8.00E ⁻⁰⁷
<u>SE45_29970</u>	<i>Citricella</i> sp. SE45	29	5.00E ⁻⁰⁹
<u>SE45_44320</u>	<i>Citricella</i> sp. SE45	28	3.00E ⁻⁰⁷
<u>SE45_44420</u>	<i>Citricella</i> sp. SE45	45	1.00E ⁻⁶⁵
<u>SE45_44420</u>	<i>Citricella</i> sp. SE45	34	8.00E ⁻²⁷
<u>SE45_44420</u>	<i>Citricella</i> sp. SE45	30	2.00E ⁻²⁴
<u>SE45_44420</u>	<i>Citricella</i> sp. SE45	21	6.00E ⁻⁰⁶
<u>SE45_53730</u>	<i>Citricella</i> sp. SE45	29	2.00E ⁻⁰⁹
<u>SE45_53730</u>	<i>Citricella</i> sp. SE45	22	3.00E ⁻⁰⁶
<u>SKA53_03031</u>	<i>Loktanella vestfoldensis</i> SKA53	31	7.00E ⁻¹⁰
<u>SKA53_05955</u>	<i>Loktanella vestfoldensis</i> SKA53	43	4.00E ⁻⁰⁷
<u>SKA53_06392</u>	<i>Loktanella vestfoldensis</i> SKA53	33	4.00E ⁻³¹
<u>SKA53_06392</u>	<i>Loktanella vestfoldensis</i> SKA53	31	6.00E ⁻¹⁹
<u>SKA53_06392</u>	<i>Loktanella vestfoldensis</i> SKA53	31	9.00E ⁻¹⁶
<u>SKA53_08576</u>	<i>Loktanella vestfoldensis</i> SKA53	28	5.00E ⁻⁰⁸
<u>SL1157_14710</u>	<i>Ruegeria lacuscaerulensis</i> ITI-1157	33	3.00E ⁻⁰⁹
<u>SPO0227</u>	<i>Ruegeria pomeroyi</i> DSS-3	38	7.00E ⁻¹²

<u>SPO2336</u>	<i>Ruegeria pomeroyi</i> DSS-3	28	2.00E ⁻⁰⁶
<u>SPO3110</u>	<i>Ruegeria pomeroyi</i> DSS-3	32	3.00E ⁻¹²
<u>SPO3110</u>	<i>Ruegeria pomeroyi</i> DSS-3	32	2.00E ⁻¹¹
<u>SPO3110</u>	<i>Ruegeria pomeroyi</i> DSS-3	28	8.00E ⁻⁰⁷
<u>SSE37_01135</u>	<i>Sagittula stellata</i> E-37	25	3.00E ⁻¹⁰
<u>SSE37_01135</u>	<i>Sagittula stellata</i> E-37	27	1.00E ⁻⁰⁶
<u>SSE37_20382</u>	<i>Sagittula stellata</i> E-37	34	3.00E ⁻⁰⁹
<u>SSE37_20382</u>	<i>Sagittula stellata</i> E-37	29	3.00E ⁻⁰⁷
<u>SSE37_20382</u>	<i>Sagittula stellata</i> E-37	23	8.00E ⁻⁰⁷
<u>TM1040_0352</u>	<i>Ruegeria</i> sp. TM1040	41	4.00E ⁻⁵²
<u>TM1040_0352</u>	<i>Ruegeria</i> sp. TM1040	27	5.00E ⁻²⁰
<u>TM1040_0352</u>	<i>Ruegeria</i> sp. TM1040	26	2.00E ⁻¹³
<u>TM1040_0352</u>	<i>Ruegeria</i> sp. TM1040	22	5.00E ⁻⁰⁶

Four probe sequences corresponding to TonB polypeptides were used to interrogate the sequenced *Roseobacter* genomes. The probes were from *E. coli* (Orange), *Rhizobium leguminosarum* (Green), *Roseovarius nubinhibens* (Yellow) and *Rhodobacter sphaeroides* (Blue). For each of the *Roseobacter* clade gene locus tags, the target with the closest similarity is colour coded and the similarity is indicated by the %age identities of the polypeptides and the Expect values.

2.1.4 Haeme and Ferrous iron ABC-class transporters are poorly conserved in the *Roseobacters*

Most of the known TBDRs have cognate ABC transporters that comprise the corresponding periplasmic binding protein that receive, (for example) the Fe-hydroxamate complex that has been transported through the FhuA surface-membrane receptor, which is then transported through the inner membrane via a transporter polypeptide, with the energy being delivered via the ATPase polypeptide component of the FbpABC transporter. Furthermore, there is at least one system variously known as Fbp (and there are many others in, for example, *Yersinia* and *Vibrio*) in which the ABC transporter may deliver the Fe³⁺ without the need of a corresponding OM receptor.

Table 2.1 shows that the different *Roseobacters* contain a variety of combinations of these types of ABC transporter, but mostly, there are no very close homologues.

The four main ABC-class transporters tested in this section of table 2.1 were Fep, the ferrienterobactin transporter from *E. coli*, Fbp and YfuA, both ferric iron specific from *E. coli* and *Yersinia pestis* respectively, and HmuT a periplasmic haemin binding-domain also of *Y. pestis*.

None of the Roseobacters has a homologue of FepB, the periplasmic binding-protein for enterobactin, but 11 species have homologues of FepC and FepD, the ATPase and permease components of this ABC-class transporter. Interestingly, *Pelagibaca bermudensis* HTCC2601 has a good homologue of FepA, the only member of the Roseobacters to possess this protein.

FbpA and FbpB were poorly conserved in the Roseobacters, with just 6 species containing a homologue of these particular proteins. However the ATPase, FbpC was well conserved with 25 of the 37 Roseobacters having at least one homologue with an E-value $> 1E^{-69}$. It is likely that just the conservation of peptide sequence of FbpA and FbpB is poor, and may not be representative of the actual conservation of function throughout the Roseobacters.

None of the Roseobacter strains had a peptide in their deduced proteome homologous to YfuA, although most (29 out of the 37 sequenced strains) had a weaker homologue (shown as yellow in Table 2.1).

Finally, the most common ABC-class transporter homologue shown in this table was HmuT; there are 18 strains which possess a homologue (E-value of between $1E^{-70}$ and $1E^{-158}$).

This list is far from exhaustive in terms of potential iron specific ABC transporters found in bacteria, but an in-depth study into the full range found in the Roseobacters was outside the scope of this work.

2.2 Siderophore biosynthetic genes in the Roseobacters

There is remarkably little known about the genes encoding siderophores synthesised by marine bacteria. To our knowledge, there are no studies, of any type, on the biosynthesis of siderophores in the marine Roseobacters. This made the prediction of any possible siderophore biosynthetic genes in these bacteria tenuous at best.

Known genes from biosynthetic pathways for both catecholate- and hydroxamate-type siderophores were used to interrogate the products of the all the sequenced genomes of the Roseobacters, these are detailed in Table 2.2.

2.2.1 Homologues of vicibactin and aerobactin biosynthesis genes in the Roseobacters

Vicibactin of *Rhizobium leguminosarum* is a hydroxamate-type siderophore, and is synthesised from ornithine in a pathway of dedicated enzymatic steps (Heemstra *et al.* 2009). The translated protein products of the genes *vbsC*, *vbsG* and *vbsA* of *Rhizobium*, were each used to interrogate the Roseobacters, but no species contained even a moderate ($<E^{-25}$) homologue. Similarly, aerobactin synthetic enzymes (encoded by the genes *iucABCD*) from *Shigella boydii* yielded no homologues in the Roseobacters, with the exception of *Phaeobacter gallaeciensis* BS107, which had moderate homologues ($2e^{-48}$ and $4e^{-48}$) to *lucA* and *lucC* respectively. A single homologue ($3e^{-38}$) of *Shigella boydii* *lucC* was present in a different strain (*P. gallaeciensis* 2.10) of the same species.

2.2.2 Vibriobactin biosynthetic genes in the Roseobacters

Vibriobactin is produced by *Vibrio cholerae* during iron deficiency. Mutants in the biosynthetic pathway can no longer produce vibriobactin and show increased sensitivity to EDDA, as it removes any available iron from the growth medium (Wyckoff *et al.* 1997). The first dedicated step in vibriobactin biosynthesis in *V. cholerae* is the catalysis of 2,3-dihydro-2,3-dihydroxybenzoate to 2,3-dihydroxybenzoate by a vibriobactin-specific 2,3-dihydro-2,3-dihydroxybenzoate dehydrogenase, VibA. The final step in the vibriobactin biosynthetic pathway is catalysed by a non-ribosomal peptide synthetase, VibF. This step forms the complete vibriobactin from dihydroxyphenyl-5-methyloxazoline-norspermidine-2,3-dihydroxybenzoate and dihydroxyphenyl-5-methyloxazoline bound to VibF (Crosa and Walsh 2002). The protein sequences encoded by genes *vibA* and *vibF* of *V. cholerae* 0395 were used to interrogate all Roseobacter genomes as before, refer to Table 2.1.

The closest homologue of *V. cholerae* 0395 VibF in the Rhodobacteraceae ($4e^{-53}$) was the *Citricella* SE45 gene CSE45_4536, which is annotated as being 'enterobactin synthetase component-F'. A good homologue of this gene is found in four other Roseobacter genomes - *Phaeobacter gallaeciensis* 2.10 ($1E^{-91}$), *Phaeobacter gallaeciensis* BS107 ($2E^{-90}$), *Phaeobacter* sp. Y4I ($6E^{-69}$) and *Roseobacter* sp. MED193, which has two good homologues ($2E^{-91}$ and E^{-79}). There are 19 other Roseobacters genomes which encode moderate ($1E^{-30}$ – $1E^{-60}$) homologues of VibF of *Citricella* SE45 (refer to Table 2.1).

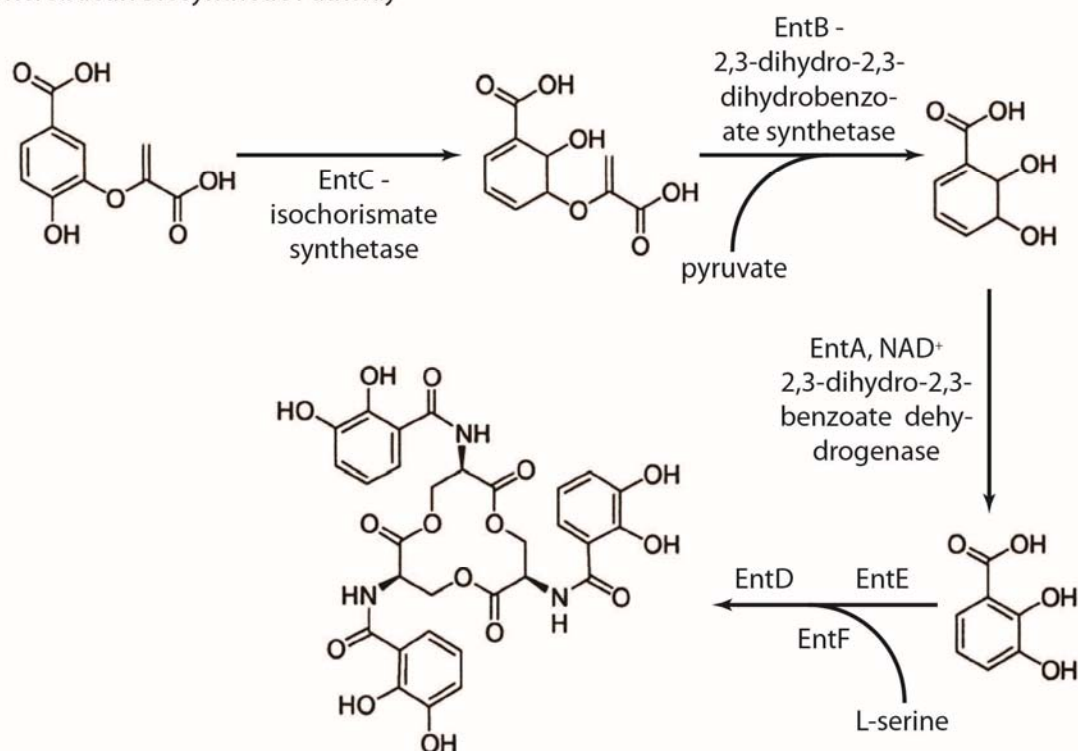
Furthermore, the closest homologue of *V. cholerae* 0395 VibA in the Rhodobacteraceae was found in *Roseovarius nubinhibens* ISM ($1e^{-44}$), and is indeed predicted to be a 2,3-dihydro-2,3-dihydroxybenzoate dehydrogenase as expected. The Roseobacters were found to have 16 members which encode homologues of this gene, although not particularly well conserved – all were between $1E^{-25}$ and $1E^{-29}$. Crucially, of those 16 Roseobacters which have a homologue of VibA, 15 also had VibF, perhaps validating the presence of this, or at least a related, biosynthetic pathway in those strains.

2.2.3 Enterobactin biosynthesis genes in the Roseobacters

The iron-scavenging siderophore produced by *E. coli* and *Salmonella* is the catecholate enterobactin, also called enterochelin (O'Brien and Gibson 1970; Pollack and Neilands 1970). The biosynthesis requires several steps, beginning with the aromatic amino acid precursor chorismic acid (see Figure 2.2). This is converted to isochorismate by EntC, and then into 2,3-dihydro-2,3-dihydroxybenzoate by EntB, and finally into 2,3-dihydroxybenzoic acid (DHB) by EntA. A DHB moiety is joined with an amide linkage to a serine molecule by EntD, EntE, EntF and EntB, then three DHB-lysine molecules cyclise to form *iso*-enterobactin (Raymond *et al.* 2003).

Figure 2.2 The enterochelin biosynthetic pathway

Enterobactin Biosynthetic Pathway



The biosynthetic pathway of enterobactin, adapted from (Raymond et al. 2003).

The protein sequences of EntA, EntB, EntC, EntD, EntE and EntF of *E. coli* K-12 were used to interrogate the Rhodobacteriaceae, and the sequence of the most similar protein was used as a query in the Roseobacter genomes.

There is a homologue of EntA in *Paracoccus* sp. TRP ($9e^{-59}$), and when this was used, in turn, as a probe, homologues were found in 23 different strains of the Roseobacters, the most similar being in *Roseovarius nubinhibens* ISM ($1E^{-42}$). There were no homologues of EntB or EntC found in any of the Roseobacters, when searched either directly, or using *Paracoccus* species homologues as queries. In contrast, the presence of an EntD homologue was shown in several Roseobacters.

The putative translated products of both *entE* and *entF* were extremely well conserved in the Rhodobacteraceae, with the genome of *Paracoccus denitrificans* PD1222 encoding an EntE homologue (E-value of 0, gene locus: Pden_2386), and *Paracoccus* sp. TRP encoding an EntF homologue (E-value of 0, gene locus: PaTRP_010100004572). Given the conservation of these *E. coli* protein-coding genes in the Rhodobacteraceae, the resultant data from homology based searches of the Roseobacters was unparalleled when compared to the rest of this bioinformatic study. The

genome of *Citricella* sp. SE45 has good homologues to both *entE* ($1E^{-133}$) and *entF* (E-value of 0) and also contains a homologue of *entA*, but lacks homologues to the *entB*, *entC* and *entD*.

2.3 Siderophore export and uptake in the Roseobacters

2.3.1 Enterobactin export genes in the Roseobacters

Export of enterobactin into the periplasm is facilitated by the protein EntS, which is a member of the major facilitator superfamily (MFS) of transporters. The closest homologue of this gene product in the Rhodobacteraceae is in *Jannaschia* sp. CCS1 ($3e^{-14}$), which although poorly conserved, is predicted to be a MFS-family protein. Homologues to this peptide sequence are only found in few Roseobacters - *Maritimibacter alkaliphilus* HTCC2654 ($5E^{-63}$), *Rhodobacterales bacterium* HTCC2255 ($2E^{-74}$), *Roseobacter denitrificans* OCh 114 ($2E^{-31}$), *Roseovarius* sp. 217 ($1E^{-30}$) and *Roseovarius* sp. TM1035 ($1E^{-26}$) – and it is certainly not impossible that these MFS polypeptides have function(s) other than siderophore export.

2.3.2 Aerobactin uptake genes in the Roseobacters

The uptake of iron-bound aerobactin, and indeed other hydroxamate-type siderophores by *E. coli* is mediated by a TonB dependent outer membrane receptor – FhuA, and then by the cognate ABC-type transporter FhuCDB (Forman *et al.* 2007). The translated products of the permease gene *fhuB* and ATPase gene *fhuC* have ‘moderate’ homologues ($1E^{-31}$ - $1E^{-60}$) in 21 of the Roseobacter strains, and indeed many of these strains (12) have multiple homologues to each of these genes (refer to Table 2.1). Four Roseobacter strains have ‘good’ homologues ($>1E^{-60}$) to both FhuB and FhuC, namely *Roseovarius* sp. 217, *Sulfitobacter* NAS-14.1, *Sulfitobacter* EE36 and *Pelagibaca bermudensis* HTCC2601, the latter of which is the only Roseobacter to also have a copy of the periplasmic binding protein gene *fhuD* ($6E^{-31}$).

2.3.3 Rhodochellin uptake genes in the Roseobacters

The Actinomycete *Rhodococcus jostii* RHA1 is known to synthesise a mixed catecholate-hydroxamate siderophore, rhodochellin. The biosynthetic genes for this siderophore have been described by Bosello *et al.* (2011). The first step from l-ornithine into l- δ -N-hydroxyornithine is catalysed by the monooxygenase, Rmo (Bosello *et al.* 2012), and a secondary structural pathway mediated by RhcB later adds the final module to complete the siderophore molecule (Bosello *et al.* 2011). The products of each of these two genes, *rmo*, and *rhcB*, were used to interrogate the Roseobacter genome sequences. Only homologues to RhcB were found in the Roseobacters, with 19 species having moderate ($1E^{-30}$ – $1E^{-60}$) homologues, and 6 species, namely, *Citricella* SE45, *Phaeobacter gallaeciensis* 2.10, *Phaeobacter gallaeciensis* BS107, *Roseobacter* sp. GAI101, *Roseobacter* sp. MED193 and *Roseovarius* sp. TM1035, having good homologues ($7E^{-63}$ – $1E^{-135}$). *Roseobacter* sp. MED193 was found to have two well conserved homologues of RhcB ($1E^{-82}$ and $1E^{-67}$), although the best conservation was that observed for *Citricella* SE45, with an E value of $1E^{-135}$.

2.4 Iron responsive regulators in the Roseobacters

To examine the presence of *known* iron-responsive transcriptional regulators in the Roseobacters, several, well characterised examples were used as queries.

2.4.1 Mur

Fur is the global Ferric uptake regulator originally identified in *E. coli* (Hantke 1981), and since shown to control iron homeostasis in a wide range of bacterial phyla. However, in the rhizobiales, Fur has become a “Mur”, and regulates genes in response to Mn availability (see Introduction).

Two well-studied Mur peptides are those of *Bradyrhizobium japonicum*, and of *Rhizobium leguminosarum*. These probes revealed the presence of convincing Mur homologues in the great majority of Roseobacter strains (Table 2.1). These are considered in more detail in Chapter 6, as are those (which are of more interest) that *lack* a Mur-like regulator.

2.4.2 *Irr and RirA*

Rhizobium does regulate ferric iron and haem uptake, and to do so, it uses the antagonistic action of two transcriptional regulators; the Fur-family Iron responsive regulator, *Irr* and the RRF-2 family Rhizobial iron regulator, *RirA* (Todd *et al.* 2002). *Irr* represses genes in Fe-depleted conditions and, conversely, *RirA* negatively regulates genes in the presence of iron (again, refer to Introduction). Consequently, the amino acid sequences of both *RirA* of *R. leguminosarum*, and *Irr* of *B. japonicum* were each used to search for homologues in the Roseobacters.

No Roseobacter genome contains a homologue of the protein coding sequence of *Rhizobium rirA* with a cut-off value $< E^{-27}$. In contrast, all but three of the Roseobacter genomes had a close homologue of *Irr*, these being *Phaeobacter* sp. Y41, *Rhodobacterales bacterium* HTCC2083 and *Rhodobacterales bacterium* KLH11, the last of which also lacked a homologue of *Fur/Mur* and *RirA*.

2.4.3 *IscR*

The final Fe-responsive regulator examined in Table 2.1 was the Iron sulphur cluster Regulator, *IscR*, which regulates the biosynthesis of iron sulphur cluster in *E. coli* (Schwartz *et al.* 2001), and whose encoding gene is found directly 5' of the Fe-S biosynthesis *suf* genes in the α -proteobacteria - refer to the Introduction for more detail.

However, *IscR* has been lost in the Rhizobiales (Rodionov *et al.* 2006), and although the *suf* genes remain, these are regulated by *RirA* and *Irr* (Todd *et al.* 2005). When the translated peptide sequence of *iscR* of *E. coli* O104:H4 was used to interrogate the *Rhodobacteraceae* proteomes, the closest homologue was found in *Rhodobacteraceae bacterium* KLH11 ($9E^{-39}$). This protein was found to be well conserved in the Roseobacters, and most homologues were annotated as *IscR*, and were found upstream of the *suf* genes, as occurs in other bacteria. All the sequenced Roseobacters had a homologue of *IscR* of *Rhodobacteraceae bacterium* KLH11 at an E-value of between $1E^{-50}$ and $1E^{-75}$.

2.4.4 *The Roseobacters likely do not use ferric reductases*

There were no homologues found in any Roseobacter genome to any known characterised ferric reductase (the products of the *ferA*, *ferB* / *mtrA* and *mtrB* genes of *Paracoccus denitrificans*

/Shewanella oneidensis). However, YqjH, a possible ferric reductase from *E. coli* - see Miethke *et al.* (Miethke *et al.* 2011), was found in only one Roseobacter genome - *Oceanicola granulosus* HTCC2516 (gene locus OG2516_12819, 38% ID to YqjH). However, even using this *Oceanicola* polypeptide as a probe, no other convincing homologues were found in the Roseobacters.

2.4.5 The Roseobacters may not import ferrous iron

Table 2.1 also includes two characterised ferrous iron transporter genes, *feoA* and *feoB* from *E. coli* K-12. Ferrous iron transport in *E. coli* is switched on in response to anaerobic growth, to facilitate iron uptake during infection (Cartron *et al.* 2006). Strikingly, there were no close homologues of the FeoA and FeoB gene products in any sequenced Roseobacter genome. This may indicate that the Roseobacters always live aerobically and do not have access to ferrous iron; indeed, there are no reports of anaerobic growth of Roseobacters.

2.4.6 Other genes linked to iron

Also shown in table 2.1 are the genes *irpA* and *irpB* of *R. pomeroyi* DSS-3 (refer to Chapter 3 for a detailed discussion of these genes). Both appear to be under the control of a strongly iron repressed promoter in *R. pomeroyi* and so their distribution among the Roseobacters was of interest. As table 2.1 shows, the IrpA polypeptide exhibited a clear “present or absent” pattern, with 30 strains having very close homologues ($<1e^{-150}$) to IrpA of *R. pomeroyi* (SPO0086), with the remaining 7 strains lacking a polypeptide with a detectable IrpA-like polypeptide. The *irpB* (SPO0087) gene of *R. pomeroyi* encodes a putative membrane protein. Homologues to this peptide were found only in *Sulfitobacter* sp. EE-36 ($2E^{-56}$), *Roseovarius* sp. 217 ($6E^{-48}$), *Roseovarius* sp. TM1035 ($3E^{-49}$), *Roseobacter* sp. GAI101 ($8E^{-56}$), *Roseobacter* sp. MED193 ($7E^{-85}$) and *Roseobacter* sp. SK209-2-6 ($2E^{-86}$), and in all cases the corresponding gene was very close to the *irpA* gene.

2.7 Discussion

This bioinformatic study of the iron homeostasis genes in the Roseobacters has revealed both the diversity of genes present, and the striking differences between species.

The Roseobacters are a taxonomically distinct group of the Rhodobacteraceae, so it may be expected that they share some features in their ability to acquire and respond to iron. However, this survey has shown that different strains and species may use very distinct portfolios of genes for the import of this metal, probably as a result of repeated acquisition of genes by horizontal gene transfer and/or loss of genes, and crucially demonstrates that the Roseobacters are a collection of very different bacteria, from many different genera.

The distribution of the TBDR proteins with specificity for iron-bound molecules appears to reveal three evolutionary strategies within the Roseobacters, the generalist strategy, where some species have many TBDR homologues; the specialist strategy, where only one or two TBDR homologues are present; and the “unknown strategy” group, which appear to lack any TBDR homologues. These organisms may have iron receptors which fall into a yet uncharacterised class of TBDR proteins, or simply lack TonB-mediated transport, and therefore use an entirely new method of outer membrane translocation of iron. It would be of great interest to study the function of TonB homologues in the Roseobacters to help identify these proteins definitively. Furthermore, those strains which appear to not have TonB could use a novel TonB independent iron import system.

Synthesis of siderophores is an expensive process for bacteria, especially so if they do not recover these siderophores. However, if enough marine bacteria synthesise these molecules, and indeed enough iron-bound chelating molecules leach into the oceans from the land, then a strategy of having receptors for a wide range of these iron-chelators would be advantageous; just as having a receptor with high promiscuity for various iron-chelates would be advantageous.

However, if a bacterium were to remove iron from a chelator at the outer membrane, then transport the iron in a ferrous form, this would negate the requirement for a complex and presumably substrate limiting receptor. We see such a ‘reduction linked uptake strategy’ in *Synechocystis* sp. PCC 6803, where Fe-siderophore complexes are reduced at the outer membrane interface, allowing uptake of biologically available iron into the cell (Kranzler *et al.* 2011). Nevertheless, we do see several genes that may encode siderophore biosynthesis and indeed uptake in the Roseobacters, but the lack of functionally verified genes from marine bacteria, for either uptake or biosynthesis of siderophores demonstrates the clear gap in knowledge here which unfortunately limits this analysis.

The distribution of RirA and Irr is interesting, and may be indicative of the loss of function of RirA in particular within most Roseobacters – indeed this gene is not conserved across the α -proteobacteria. Irr was conserved in nearly all Roseobacters, and indeed the function of this peptide is examined directly in *R. pomeroyi* in Chapter 5.

IscR is highly conserved throughout the Roseobacters, and is likely the functional regulator of iron-sulfur clusters across this group –always being found upstream of the *suf* genes.

It is very clear that all bioinformatic predictions here will require direct work to validate them. The following chapters do go some way towards this, with regards to Fe and Mn uptake in *R. pomeroyi*, and indeed go further afield to the Roseobacters and beyond when looking at Mn uptake systems (see Chapter 6).

Chapter 3 - *in silico* study of putative iron regulated genes of *R. pomeroyi*

3.0 Introduction

The previous chapter described an *in silico* survey of all the genome-sequenced strains of the Roseobacter clade for their types of iron uptake systems, as deduced by the presence of genes whose products were known to be involved in Fe homeostasis in other types of bacteria.

In this chapter, and in those that follow, attention is focussed on one particular strain of the Roseobacters, namely *Ruegeria pomeroyi* DSS-3 (see Introduction). From the survey conducted above, *R. pomeroyi* DSS-3 was one of the unusual strains in that it lacked any discernible siderophore production systems and also had no genes that were predicted to encode an outer-membrane TonB-dependent receptor. Indeed, this was one of those 30 Roseobacter strains that appeared to lack a version of TonB itself. Therefore, it was of interest to determine how this strain obtained its iron.

Before embarking on direct experimental work on this topic in *R. pomeroyi* DSS-3, its genome was subjected to another round of *in silico* analyses, but this time with the focus being on *cis*-acting regulatory sequences which by comparison with known regulatory motifs, were likely to be the binding sites for iron-responsive transcriptional regulators.

As before, Rodionov *et al.* (2006) set the stage for these studies, having already predicted some of these motifs and their downstream target genes. As described in the Introduction, the mechanisms of iron homeostasis in the alpha proteobacteria are very different from those in many other bacterial phyla, including those that harbour such model bacteria as *E. coli*, *Bacillus*, *Pseudomonas* and many others, in which the Ferric uptake Regulator, Fur, is the pivotal global Fe-responsive transcriptional regulator (Stojiljkovic *et al.* 1994; Vassinova and Kozyrev 2000). Instead a limited number of lab-based studies, mainly on the Rhizobia, *Agrobacterium* and *Brucella* coupled with the *ab initio* bioinformatic predictions have shown the one of the key Fe-responsive regulators in the α -proteobacteria is Irr, which, although a member of the Fur super-family, is very different from Fur, *sensu stricto*, refer to the Introduction and (Hamza *et al.* 1998). In addition, some of the Rhizobia and their close relatives also have the transcriptional regulator RirA, which is a member of the Rrf2-

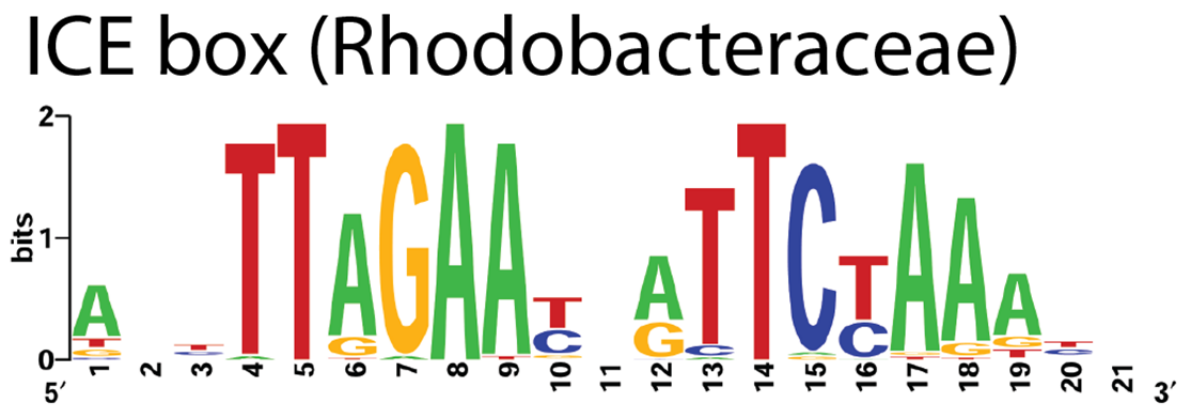
superfamily of regulators, very different in all ways from Fur, except in its overall role, which is to repress several genes involved in Fe acquisition in Fe-replete conditions (Todd *et al.* 2002).

Here we describe the distribution of two of these predicted regulatory, *cis* acting sequences in *Ruegeria pomeroyi*. These are (a) the ICE motifs, recognised by the Irr regulator and (b) the Iron-Rhodo (IR) boxes, whose corresponding transcriptional regulator has not been identified.

3.1.1 Irr and its target ICE sequences and genes in *Ruegeria pomeroyi*

Under Fe-depleted conditions (usually) the Irr polypeptide of several α -proteobacteria has been shown to bind to “iron control elements”, repressing transcription of the downstream genes. These ICE boxes have a canonical sequence whose particular version in the Rhodobacteraceae is shown in Figure 3.1.

Figure 3.1 Logos of iron responsive regulator binding sites in *Ruegeria pomeroyi*



Logo of predicted iron responsive regulator binding motif, the ICE box. Reproduced from Rodoionov et al. (2006).

Inspection of the genome of *R. pomeroyi* DSS-3 revealed four convincing ICE motifs, situated near the predicted promoters of the genes that would be regulated by Irr (summarized in table 3.1). Significantly, several of these resemble those that have been shown to be Fe/Irr-regulated in other bacteria and are as follows.

Table 3.1 Genes with ICE boxes

Those genes with a predicted ICE motif are shown. Detailed are their predicted function, locus and name. The sequence and position relative to the translational start codon of each ICE motif are also shown.

Gene locus / name	Predicted function	ICE box sequence	Position
<i>SPO3842 mbfA</i>	membrane-bound ferritin	AtcTTgGAATCATTCATAAAcT	-33 bp
<i>SPO0382 fssA</i>	hypothetical Fe-S scaffold protein	t cTTTAGAAcCgTTCcAAAgt	-75 bp
<i>SPO2025 iscR-sufSBCD</i>	Fe-S cluster assembly	AtcTTAGAATGgTTCCTAAgtc	-102 bp
<i>SPO0330 ccpA</i>	cytochrome c peroxidase	AtgTTAGAATGATTCTAAcCg	-73 bp

3.1.2 *SPO3842, MbfA*

This 324 amino acid polypeptide is ~70% identical to the corresponding gene product in the rhizobia, where it was first identified (Rudolph *et al.* 2006; Todd *et al.* 2005). The *mbfA* gene has been shown to be expressed at higher level in Fe-replete conditions, under the control of *Irr* in *Rhizobium*, *Brucella*, *Bradyrhizobium* and, very recently, in *Rhodobacter sphaeroides*, the first published example in the Rhodobacterales (Peuser *et al.* 2012). MbfA has an unusual domain constitution – an N-terminal half with a ferritin-like fold within a domain that resembles a Rubrerythrin electron transporter and a C-terminal half that is strongly predicted to be in the inner membrane – hence the term membrane-bound ferritin. A similar C-terminal domain is found in the CCC1 protein of yeast, where it also has a link with iron, being a trans-membrane protein that is required to accumulate manganese and iron in the vacuole of this fungus (Li *et al.* 2001).

MbfA is very much a signature polypeptide for the α -proteobacteria, being found in nearly all genome-sequenced strains of this sub-phylum, but only very rarely in other clades.

3.1.3 SPO0382 *FssA*

A second *Ruegeria pomeroyi* gene that has an ICE box in its promoter region is *SPO0382*, whose product is 63% identical to *FssA* (iron sulfur scaffold) of *Rhizobium leguminosarum*. This was first described by Todd *et al.* (Todd *et al.* 2006) who noted that it is very similar (48% identical) to a eukaryotic protein, which is termed Nfu1 in yeast and HIRIP5 (HIRA-interacting protein 5, the HirA protein being a transcriptional regulator of histone gene transcription) in mammals. These two eukaryotic proteins HIRIP5 act as scaffolds to transfer FeS clusters to different acceptor proteins (Lorain *et al.* 2001). As with MbfA, predicted orthologues of *FssA* protein are confined to the α -proteobacteria, although there is lower-level sequence similarity to parts of the NifU protein, another scaffold protein that delivers FeS clusters to nitrogenase (Agar *et al.* 2000).

3.1.4 SPO0330; *CcpA*

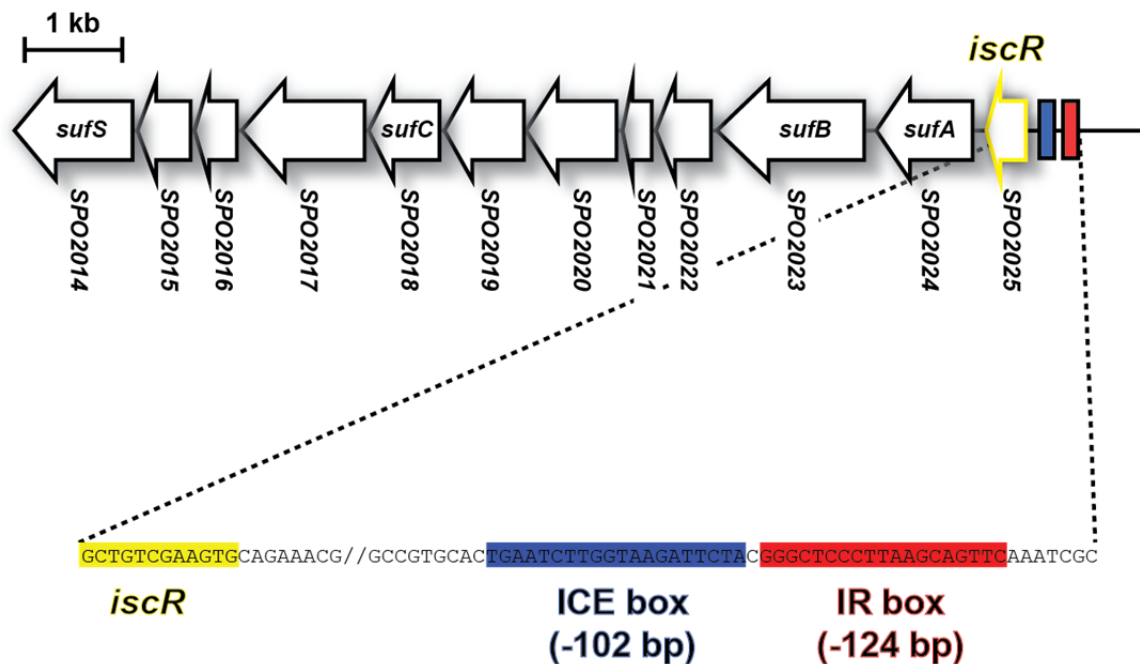
CcpA is a widely distributed cytochrome-c peroxidase enzyme (pfam03150), which contains two haem groups, using the iron centres as cofactors to reduce H_2O_2 to water (reviewed by Torres and Ayala, 2010). Predicted orthologues (at least 70% identical) occur in a wide range of Proteobacteria, and in some cases, the regulation of the corresponding gene has been studied. For example, *ccpA* of *Pseudomonas stutzeri*, it was found to be under the control of Fnr, an O_2 -sensing transcriptional regulator (Vollack *et al.* 1999). Homologues of *ccpA* in the Rhizobiaceae and Rhodobacteraceae were shown to likely be under the control of Irr (Rodionov *et al.* 2006).

3.1.5 SPO2025–SPO2014; – *the iscR-suf operon*

As shown in Figure 3.2, the *Ruegeria pomeroyi* genome has a group of 12 contiguous genes that are preceded by an ICE motif. Based on detailed studies in several other bacteria, these are the *suf* genes, which are responsible for the synthesis of FeS clusters, plus the promoter-proximal gene, *iscR*, which encodes a transcriptional regulator of the Rrf2 family that regulates this operon in response to iron availability (Bandyopadhyay *et al.* 2008). The *suf* operon of several α -proteobacteria have ICE boxes in their *cis*-acting regulatory DNA (Rodionov *et al.* 2006) and it had been shown directly that the *suf* operon of *Rhizobium leguminosarum* is regulated by Irr, in response to Fe availability.

It was noted by Rodionov *et al.* (2006) that there was another potential regulatory motif, termed an IR box, which was predicted to be the site at which the IscR regulator bound. Interestingly the *suf* operon of *Rhizobium* is also under dual control, being repressed under Fe-depleted conditions, but, when the cells were grown with Fe sufficiency, the RirA regulator exerted a level of repression, due to its interaction with its cognate binding (IRO) motif that was immediately downstream of the ICE box (Todd *et al.*, 2006).

Figure 3.2 The *iscR-suf* operon of *R. pomeroyi*

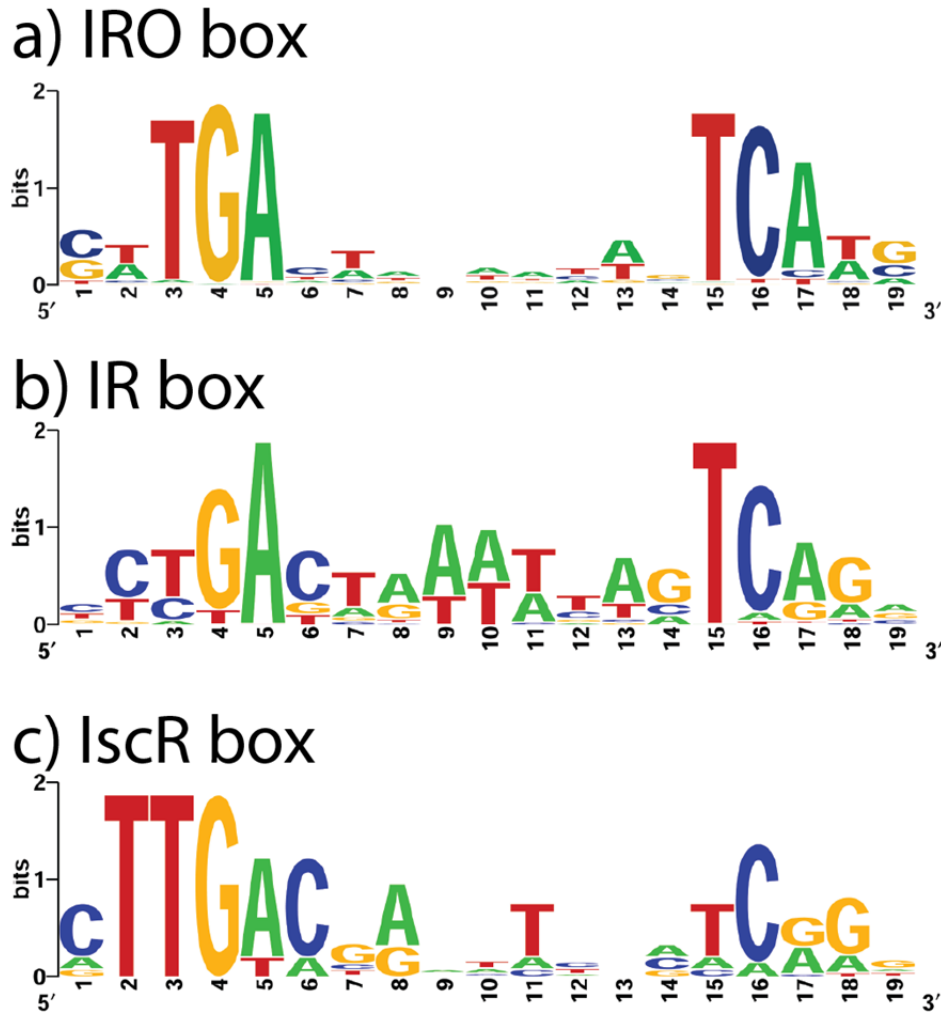


Representation of the R. pomeroyi iscR-suf genes (SPO2014-SPO2025). Zoomed region shows position of IR (red) and ICE (blue) boxes 5' of iscR, whose 5' coding sequence is shown in yellow.

3.2.1 Iron-Rhodo (IR) boxes

The second set of conserved, potential *cis* acting regulatory sequences that might respond to Fe availability were termed Iron-Rhodo (IR) boxes by Rodionov *et al.* (2006). The consensus IR box had some similarity to that of the IRO box recognition site of the previously identified RirA transcriptional regulator in the rhizobia and, to a lesser extent, to the motif termed IscR^α-box-I, which is the predicted IscR-binding site for the IscR of the Rhodobacterales (see Figure 3.3).

Figure 3.3 Logos of iron responsive regulator binding sites in *Ruegeria pomeroyi*



Logo representations of predicted iron responsive regulator binding motifs. a) IRO box, predicted binding motif of RirA, generated from DNA loci found in four Rhizobiaceae, two Mesorhizobium species, Brucella, and Bartonella. b) Iron-Rhodo box found in the Rhodobacteraceae, and c) Iscr box from the Rhodobacteraceae. Reproduced from Rodionov et al. (2006).

A total of six transcriptional units, together with their predicted IR sequences are listed in Table 3.2, and are as follows:

Table 3.2 *Ruegeria pomeroyi* genes with predicted IR motifs

Those genes with a predicted IR motif are shown. Detailed are their predicted function, locus and name. The sequence and position relative to the translational start codon of each IR motif is also shown.

Gene locus / name	Predicted function	IR box sequence	Position
<i>SPO0086 irpA</i>	iron-regulated protein A	aCTGACaAATTTAGTCAGA	-89 bp
<i>SPO3139</i>	similar to truncated hemoglobins	TCcGACTttAacAGTCgGA	-32 bp
<i>SPO3287 fbpA</i>	periplasmic binding protein	I cCcGACTgAAaTAaTCAGt II atTGACTAtTTcAGTCgGA	-74 bp -25 bp
<i>SPO0789 hemP</i>	haemin uptake	ggcGACaAAAAaTAGTCAGg	-100 bp
* <i>SPO2025 iscR -sufSBCD</i>	Fe-S cluster assembly	ctTGACgAATTcccTCgGg	-141 bp
* <i>SPO3288 fbpB</i>	permease	TCcGACTAAAcTgGTCgat	-39 bp

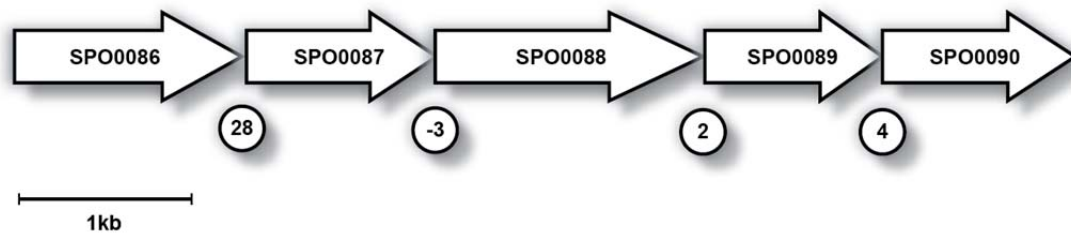
3.2.2 SPO0086 - irpA

The *SPO0086* gene is the promoter proximal gene of a strongly predicted 5 gene operon, *SPO0086* – *SPO0090* shown in Figure 3.4 below. Of the polypeptides that are similar in sequence to the *SPO0086* gene product, the one that is, *a priori*, of most interest is that of *Synechococcus elongatus* PCC6301 (previously strain PCC7942) gene locus: syc0095_d (34% identical; $1e^{-53}$). This polypeptide had been termed IrpA, because it was shown to be an iron-regulated-protein, mediated by the Fur transcriptional regulator and which was involved in iron uptake in these cyanobacteria (Reddy *et al.* 1988).

More broadly, the IrpA polypeptides are membrane-bound members of the M75 family of peptidases (Pfam cl09159), as first identified in *Pseudomonas aeruginosa* (Fricke *et al.* 1999). The IrpA-like polypeptide from *P. aeruginosa* PA4370 can cleave radiolabelled insulin, and was therefore

the founding member of the M75 family of proteins - the insulin cleaving metallopeptidases (ICMP), or imelysins, which were thought to bind to zinc. A functional and structural study of two groups of imelysin-like proteins was performed by Xu *et al.* (2011) who suggested that these proteins may act as a scaffold for iron uptake complexes to form on the outer membrane. Recently, a novel iron transporter EfeUOB was identified and characterised (Cao *et al.* 2007; Rajasekaran *et al.* 2009; Rajasekaran *et al.* 2010). Interestingly the 250 C-terminal residues of the EfeO protein was shown to contain an imelysin-like domain, the other half of this protein being a putative iron binding cupredoxin domain, which might bind iron (Rajasekaran *et al.* 2010).

Figure 3.4 SPO0086-SPO0090 Operon Map



The SPO0086-SPO0090 genes of R. pomeroyi (arrows) likely form a single transcriptional unit, with small intergenic gaps shown as circled numbers of base pairs. Scale is indicated by 1 kb bar.

Close homologues of the IrpA of *Ruegeria pomeroyi* (termed IrpA^{RP}) are found throughout all divisions of the proteobacteria, with >250 homologues with greater than 50% identity. Perhaps significantly, the first ~25 amino acids is sometimes absent from homologues of IrpA^{RP} when aligned (not shown). Indeed, when the IrpA^{RP} sequence was used as a query with SignalP [available at: <http://www.cbs.dtu.dk/services/SignalP/>] (Petersen *et al.* 2011), this program strongly predicted (90% chance) an N-terminal signal peptide that would be cleaved at position 22.

Furthermore, Irp^{RP} is strongly predicted to be localised in the outer membrane when analysed with psortb [available at: <http://www.psort.org/psortb/index.html>] (Yu *et al.* 2010), with a score of 9.93 (a value >7.5 is the cut-off value with this tool). The predicted topology was examined, using the trans-membrane domain prediction software Pred-TMBB [<http://biophysics.biol.uoa.gr/PRED-TMBB/>] (Bagos *et al.* 2004), which indicated that IrpA^{RP} has an extracellular loop, flanked by two transmembrane domains. It is unclear why a usually soluble M75 protein would be present in the outer membrane, but IrpA^{RP} may represent a significant evolution away from the canonical examples

of this peptide family. Furthermore, IrpA^{RP} does contain a putative metal binding site – HxxE, at position 182 of the amino acid sequence.

Of those imelysin-type proteins that have been functionally linked to iron uptake, the imelysin homologue in *Pseudomonas aeruginosa*, IcmP (gene locus - PA4370) was Fur-regulated (Cornelis *et al.* 2009). There is also a homologue of IrpA^{RP} in *Vibrio cholerae* VC1264, which has two Fur boxes in its promoter region, and is highly regulated by both Fur and iron (Mey *et al.* 2005). And, of course, the eponymous, original, IrpA of *Synechococcus* was identified on the basis of its response to Fe availability.

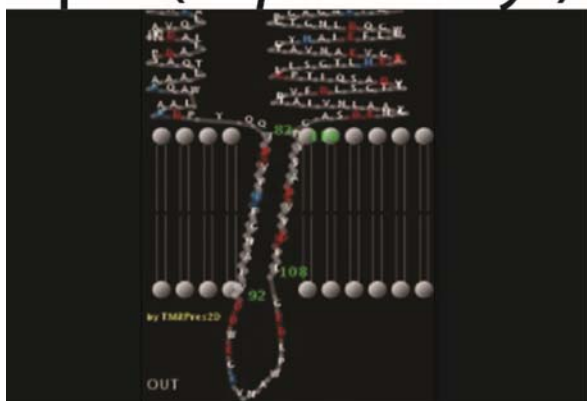
3.2.3 SPO0087 – irpB

The *SPO0087* gene product has no known domains and its function is unknown. In contrast to the very widespread range of IrpA homologues in the NCBI data base, there are very few (14) homologues of the *SPO0087* gene product, even when a relaxed threshold ($<4e^{-08}$) was used, with seven of these being in other *Roseobacter* strains. (See table 2.1). It is also extremely poorly represented in the GOS marine metagenome data base, with only 5 homologues with E values < 0.01 . It was noted, though, that the gene *MICA_2042* from the predatory ‘vampire’ bacterium *Micavibrio aeruginosavorus* ARL-13 (Wang *et al.* 2011) encodes a homologue of IrpB (30% identity, $8e^{-21}$) and that this gene may encode the periplasmic protein of a suggested manganese transporter.

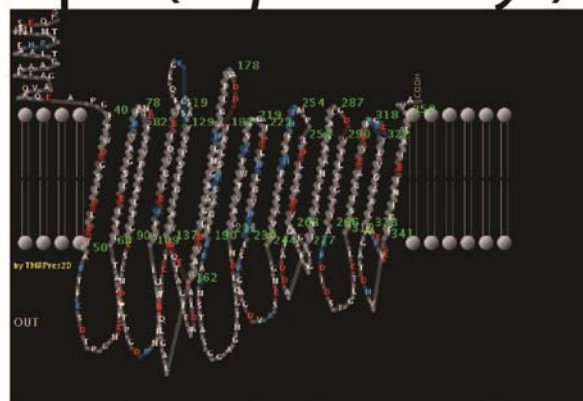
The IrpB of *R. pomeroyi* is predicted to be in the outer membrane (psortb, >7.5), and to have a signal peptide (SignalP). Furthermore, Pred-TMBB predicts 16 trans-membrane helices, and a cytoplasmic, n-terminal ‘plug’ domain as shown in Figure 3.5 below. Indeed, IrpB is not dissimilar to the classical beta-barrels of the TonB-dependent receptors (Locher *et al.* 1998) or the outer membrane porin OmpF (both shown in Figure 3.5 below). However the IrpB polypeptide has no sequence similarity to either of these types of outer membrane polypeptides, so, if this general function has any validity, IrpB would have to represent a wholly new class of porin molecules.

Figure 3.5 IrpA, IrpB, OmpF and FhuA modelled in the outer membrane

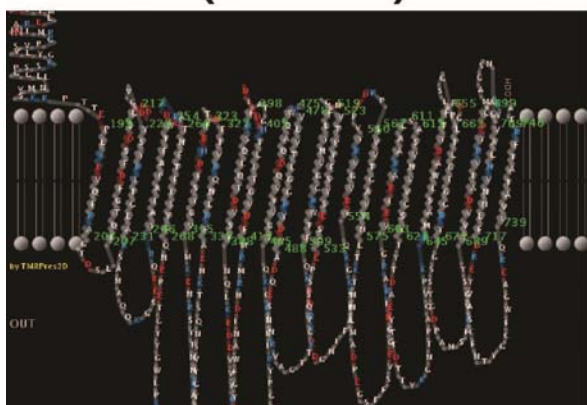
IrpA (*R. pomeroyi*)



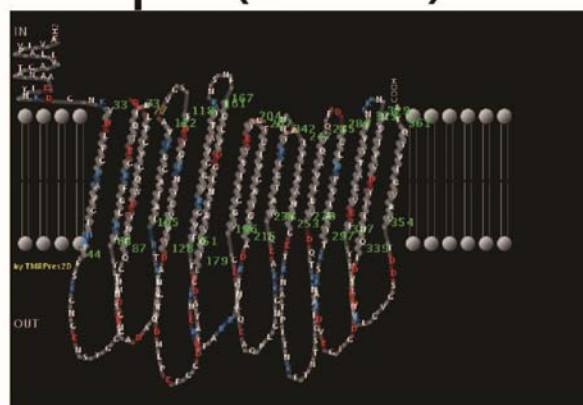
IrpB (*R. pomeroyi*)



FhuA (*E. coli*)



OmpF (*E. coli*)



The membrane architecture of IrpA and IrpB, of Ruegeria pomeroyi and FhuA and OmpF of E. coli DH1 as predicted using Pred-TMBB (Bagos et al., 2004).

3.2.4 SPO0088

This gene encodes a hypothetical protein, with 2 cytochrome C-like domains (DUF1111 [[pfam06537](#)]), but it is predicted to localise to the cytoplasmic membrane (10.0 in psortb). There are close homologues in many alpha-Proteobacteria (including 33 of the Roseobacter strains) where for example, the *RSKD131_2939* of *Rhodobacter sphaeroides* KD131 (61% identity, E-value = 0), is adjacent to 2 bacterioferritin genes and an M75 imelysin homologue of IrpA^{RP}.

3.2.5 SPO0089

The *SPO0089* gene product is also a member of the imelysin group of M75 family peptidases and, indeed, is 31% identical to the *SPO0086* product (see above) and 25% identical to the experimentally characterised IrpA of *Synechococcus*. Its closest match (56%) was to a gene (*SL1157_1932*) in *Silicibacter lacuscaerulensis* ITI-1157, and most of the genome-sequenced Roseobacter strains contain homologues with ~50% identity to the *SPO0089* gene product.

3.2.6 SPO0090

Finally, in this operon, the product of *SPO0090* is also a domain of unknown function, although it is strongly predicted {by tatP: (Bendtsen *et al.* 2005)} to contain a TAT export signal (see review by Palmer and Berks 2012), with the mature protein being located in the membrane.

When the layout of the genes in other bacteria that encoded homologues of the *Ruegeria pomeroyi* *SPO0086* – *SPO0090* was examined, it was striking how similar was their synteny, even in distantly related bacterial strains. Thus, very similar arrangements were seen in members of the Alteromonadales (28 taxa), Vibrionaceae (14 taxa), Pseudomonadales (29 taxa), Oceanospirales (4 taxa) {all gamma-proteobacteria}, Comamonadaceae (10 taxa) {betas}. And, outside the Proteobacteria, homologues of both *SPO0086* and *SPO0088* are found as adjacent genes in several strains of the Cyanobacteria (37 taxa), the Bacteroides/Chlorobi (36 taxa), the Spirochaetales (18 taxa) and finally the Chlamydiae/Verrucamicrobia (18 taxa).

It was noted that the γ -proteobacterium *Vesicomysocius okutanii*, an intracellular endosymbiont of the deep-sea clam, and which has a small (<1.1 Mb) genome, has a predicted operon that comprises, in order from the promoter: a homologue of *SPO0086*, then *SPO0088*, followed by two hypothetical genes, then a multicopper oxidase, and finally, an iron ABC transporter, including a homologue (36 % identical) of *SPO3288*; this points to a role in Fe transport for this operon.

Furthermore, all sequenced genomes of the Rhizobiales, and both *Rhodobacter sphaeroides*, and *Ruegeria* TM1040 contain all but one (*SPO0087*) of the members of the *SPO0086* - *SPO0090* operon. However, these all have one or more genes in the position occupied by *SPO0087* in *Ruegeria pomeroyi*; in the Rhizobiales there is a single gene that encodes a multicopper oxidase, and in both

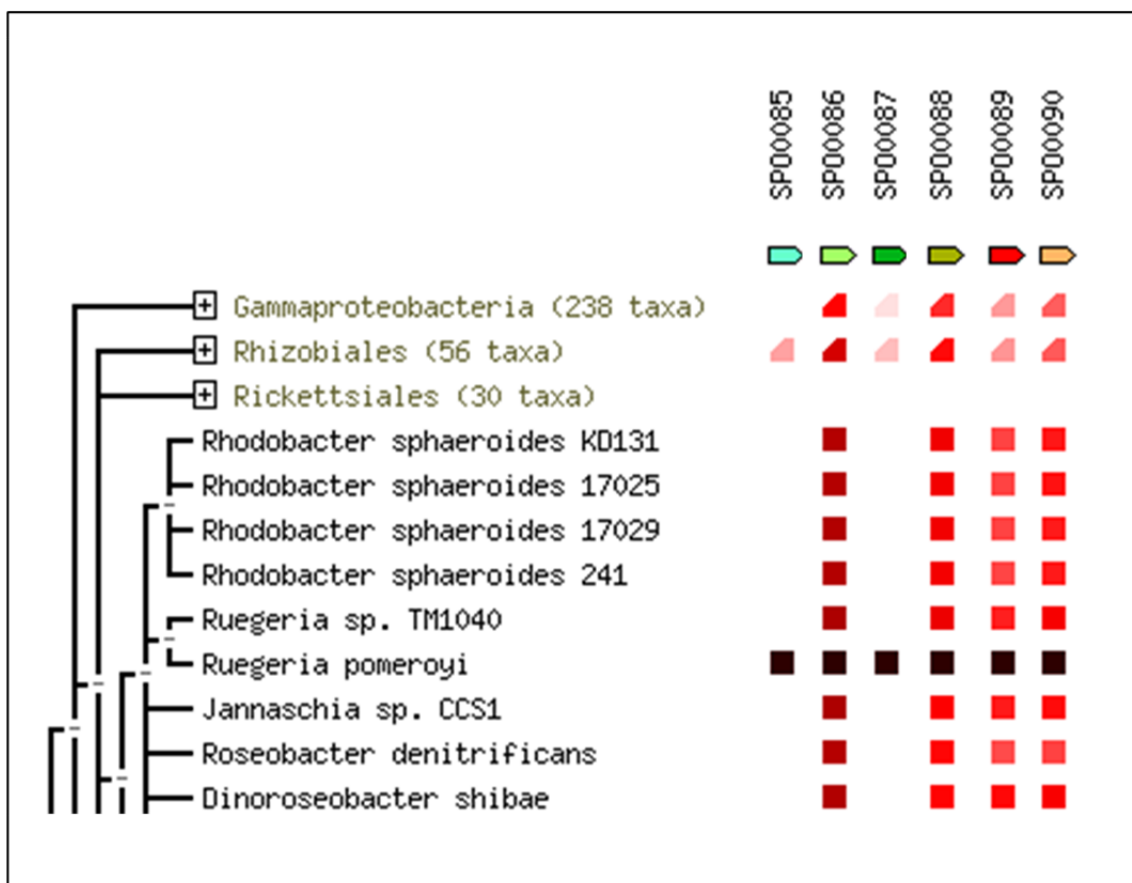
Rhodobacter and *Ruegeria* TM1040, there are two genes which encode bacterioferritin (reviewed in Andrews 1998; Carrondo 2003).

We also noted that the genome of *Roseobacter denitrificans* contains a homologue (74 % identical at the amino acid level) of *SPO0086*. Perhaps significantly, this is adjacent to a gene that encodes a predicted, FbpB-type (see below), permease of an ABC transporter for Fe uptake.

Taken together, the *SPO0086* – *SPO0090* operon of *Ruegeria* appears to have several suggested and ratified links as judged by the predicted functions of the homologues of the various gene products. It is also striking that several of the gene products are associated with the bacterial membrane(s), again pointing to a possible role in Fe transport.

The preservation of this cluster of genes in a range of bacteria suggests that their products function co-ordinately, though the role of the special case of *SPO0087* is certainly not clear.

Figure 3.6 STRING 9.0 Co-occurrence analysis of SPO0086-SPO0090



Co-occurrence analysis of SPO0086 to SPO0090 reveals the presence of a homologue of SPO0085 in those species and taxa shown. The darkness of squares indicated the quality of similarity, black being 100%, fading from dark red to light pink as similarity diminishes. Analysis was performed using STRING 9.0 [<http://www.string-db.org/>].

3.2.7 SPO3139 – A truncated haemoglobin protein

The product of the gene SPO3139 is a member of the family of O₂-binding homo-dimers that are widespread in bacteria and eukaryotes, but its function is unknown. Significant homologues (>30 % identity) are found in most other Roseobacters. The function of this gene is not known in any of the bacteria in which it has been found, though its general predicted function, as a polypeptide that binds O₂ is consistent with its being regulated in response to Fe availability.

3.2.8 SPO0789- hemP

This gene encodes a very small (50 amino acids) polypeptide, that resembles the HemP polypeptide of *Escherichia coli*, which had been shown to be required for the uptake of haeme in that species, and to be regulated by Fur, in response to Fe availability (Stojiljkovic and Hantke 1992). There is a motif homologous to an IR box located 100 bp upstream of the *hemP* translational start. The *hemP* gene in *R. pomeroyi* is found as part of a two gene (predicted) operon, the other member, *SPO0790*, encodes a hypothetical protein found in a few Roseobacter genomes. However, *hemP* is only present in *R. pomeroyi*, and not in any other Roseobacters. A close homologue of HemP was found in *Rhodobacter sphaeroides* (64 % identity), where a recent microarray study showed that this gene was ~5-fold induced by low iron, and deregulated (~15-fold) in a Fur⁻ background (Peuser *et al.* 2011). This Fur homologue is described as a Fur/Mur, regulating both Fe and Mn uptake in *Rhodobacter* (Peuser *et al.* 2011).

3.2.9 Components of an iron specific ABC-class transporter – *FbpA* and *FbpB*

There are two adjacent, convergent transcribed genes, *SPO3287* and *SPO3288*, each of which is preceded by a convincing IR sequence (Figure 3.7). These two genes are strongly predicted to encode the periplasmic binding protein and the permease of an ABC-type transporter, each of these polypeptides being particularly similar to those that are involved in iron uptake in many other bacteria – hence their names of ferrous binding proteins (Fbp). Close homologues of these two gene products not only occur in all the Roseobacters (see Table 2.1) but in a very wide range of other bacteria many different phyla (proteobacteria, Firmicutes, Cyanobacteria, for example). Not unexpectedly for Fe uptake polypeptides, the expression of the *fbp* genes has been shown to be repressed in Fe-replete bacteria (for example *Vibrio cholerae* (Mey *et al.* 2005), *Sinorhizobium meliloti* (Chao *et al.* 2005) and *Rhizobium leguminosarum* (Todd *et al.* 2005; Todd *et al.* 2002)), and this has been shown to be mediated by the Fur transcriptional regulator in *V. cholerae*, and by RirA in *Rhizobium* and *Sinorhizobium*.

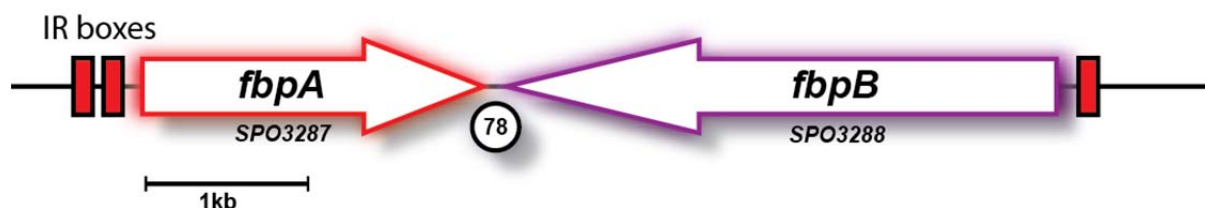
The genome of one species, *Vibrio cholerae* O1 biovar El Tor str. N16961, encodes good homologues of *fbpA* (40% identity) and *fbpB* (41% identity), plus *SPO2689* (40% identity). These three genes, *VC0608*, *VC0609* and *VC0610*, are all transcribed unidirectionally, and are identified as *fbpABC* in this strain. There is a sequence homologous to the canonical Fur box upstream of *fbpA*, and indeed this

gene has been shown to be negatively regulated by both iron, and Fur (Mey *et al.* 2005). The subsequent genes *fbpBC* must be transcribed from a second promoter, as their expression was unaffected by iron or Fur (Mey *et al.* 2005). The function of these genes were verified by Wyckoff *et al.* (2006), where they showed that cloned *V. cholerae fbpABC* is able to complement the growth defect of an iron uptake deficient strain *S. flexneri* (strain SM193w). Wyckoff and colleagues also showed that the uptake of ⁵⁹Fe into SM193w cells increased 6-fold when the cloned *fbpABC* genes were present. Intriguingly, they also show that iron deficient growth of an *E. coli* TonB⁻ EntF⁻ strain (ARM100) was enhanced when the cloned *Vibrio fbpABC* genes were introduced (Wyckoff *et al.* 2006). This is especially interesting given that another FbpA homologue in *Neisseria shayegani* 871¹ (locus *HMPREF9371_0466*, 39% identity to FbpA of *R. pomeroyi*) is possibly extracellular. Homologues of FbpA are present in all pathogenic strains of *Neisseria* (Ferreiros *et al.* 1999) and have been shown to bind to iron (Zhu *et al.* 2003). Ferreiros *et al.* (1999) also show that FbpA is antigenic and subsequently that parts of the protein have an extracellular presence through the outer membrane.

Although *R. pomeroyi* FbpA and FbpB are similar in sequence to other Fbp polypeptides, they have two rather unusual features, compared to the canonical arrangement of the *fbp* genes elsewhere. In most bacteria the genes that encode all three components of the Fbp transporter are contiguous and co-transcribed. Clearly this is not the case here, where *fbpA* and *fbpB* are both in single gene transcriptional units. Furthermore, there is no nearby gene that corresponds to *fbpC*, which encodes the ATPase cassette that is a signature of ABC transporters.

¹ misannotated as an ATPase of the FbpABC transporter. The translated product of *HMPREF9371_0466* has an E-value of 0 to the characterised FbpA of *Neisseria weaveri* ATCC51223 and *Neisseria weaveri* LMG5135.

Figure 3.7 Arrangement of *fbpA* and *fbpB* genes in *R. pomeroyi*



Arrangement of the genes SPO3287 (*fbpA*) and SPO3288 (*fbpB*) in the genome of *R. pomeroyi*; the positions of IR boxes are shown as red squares. The intergenic gap of 78 bp is indicated, and scale is shown by the bar marked 1kb.

In an attempt to identify the cognate ATPase of this transporter in *Ruegeria pomeroyi*, the amino acid sequence of a *bona fide* FbpC was used to interrogate the deduced proteome of this strain. The closest matches were to SPO2689.

Furthermore, STRING 9.0 neighbourhood analysis was performed using FbpA and FbpB of *R. pomeroyi* as query proteins. This analysis confirmed the presence of FbpAB arranged as a potential transcriptional unit in many phyla of bacteria. In many species, homologues of genes encoding FbpA and FbpB had a third gene present, *fbpC*. This gene was in the same orientation as *fbpA* and *fbpB* indicating that it may be part of the same transcriptional unit. This pattern was observed throughout the proteobacteria, and even extended further from this taxonomic group, although with decreasing certainty as the similarity between proteins decreased with evolutionary distance; this gene was always predicted to be homologous to SPO2689 of *R. pomeroyi*.

3.3.1 Concluding comments

These *in silico* searches of the *Ruegeria pomeroyi* have extended those of Rodionov et al (2006). We can conclude that many of those genes predicted to be under the control of iron responsive regulatory motifs are indeed likely to be involved in Fe uptake and/or metabolism or are at least deduced to be so. The likely iron homeostasis system of *R. pomeroyi* involves a large set of genes, including probably transporters, iron storage proteins and transcriptional regulators. However, some of the genes discussed above remain a mystery, such as the *irp* genes, and the seemingly incomplete

fbp transporter. Indeed, homologues of many of the predicted iron-regulated genes discussed above have been shown to be regulated by iron in other bacteria, either via unknown means, or by cognate iron responsive regulators such as Fur and RirA and Irr.

Although useful, bioinformatic studies need to be confirmed, or otherwise, by direct experimental work. Such is the material in the remainder of this thesis, in which the roles and regulation of some selected genes is described and, at the end, by a pan-genomic, microarray investigation of *R. pomeroyi*.

Chapter 4 - *in vivo* studies on iron uptake in *R. pomeroyi*

4.0.1 Introduction

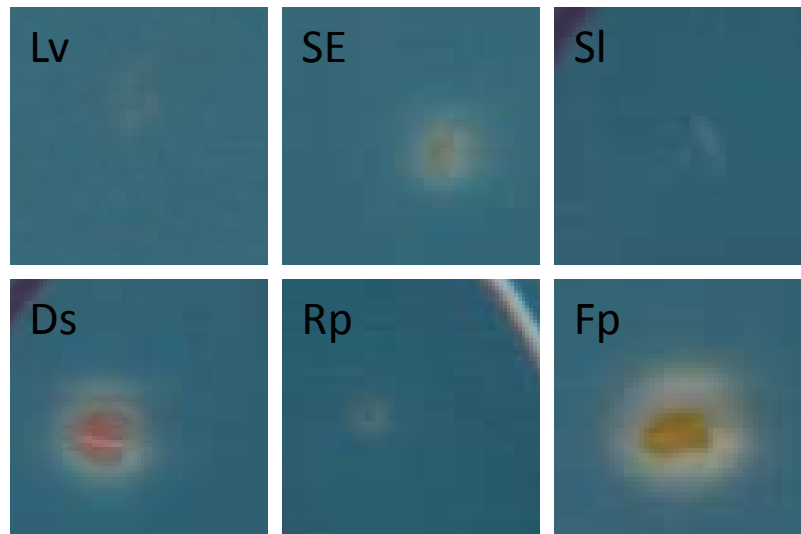
As shown previously, several potential iron homeostasis genes were identified, *in silico*, for *R. pomeroyi*. However, this strain appears to lack any known outer membrane transport system for iron, and does not appear to be able to synthesise siderophores. Also, the *fbp* genes of *R. pomeroyi* appear to be incomplete and are arranged in an unusual orientation. The following experimental work explores these facets of this marine bacterium.

4.1.1. *R. pomeroyi* does not produce siderophores

The bioinformatic interrogations in Table 2.1 predicted that *R. pomeroyi* DSS-3 does not appear to be able to synthesise siderophores, nor does it possess the necessary receptors for siderophore uptake or the energy conduit TonB. This was tested directly, using the chrome azurol sulphonate (CAS) assay for siderophore production (Schwyn and Neilands 1987). When complexed with Fe^{3+} , CAS agar is blue in colour, but this turns orange when the iron is chelated by a molecule with higher affinity than CAS, such as a siderophore. Importantly, this assay is independent of the chemical class of siderophore and can be readily adapted to microbes growing on solid media, in which case, colonies of siderophore-producing strains are surrounded by orange halos.

As seen in Figure 4.1, *Ruegeria pomeroyi* DSS-3 failed to make such an orange halo, nor did some other Roseobacter strains (Petursdottir and Kristjansson 1997; Van Trappen *et al.* 2004) that were also examined (Figure 4.1). In contrast, *Fulvimarina pelagi* strain HTCC2506, which is in the closely related Rhizobiales family of α -Proteobacteria, did make a pronounced orange halo on CAS medium. Another strain of the Rhizobiales, *Dinoroseobacter shibae* DFL-12 (Biebl *et al.* 2005) also produced a small CAS halo.

Figure 4.1 Siderophore production by different strains and species of the Roseobacter clade



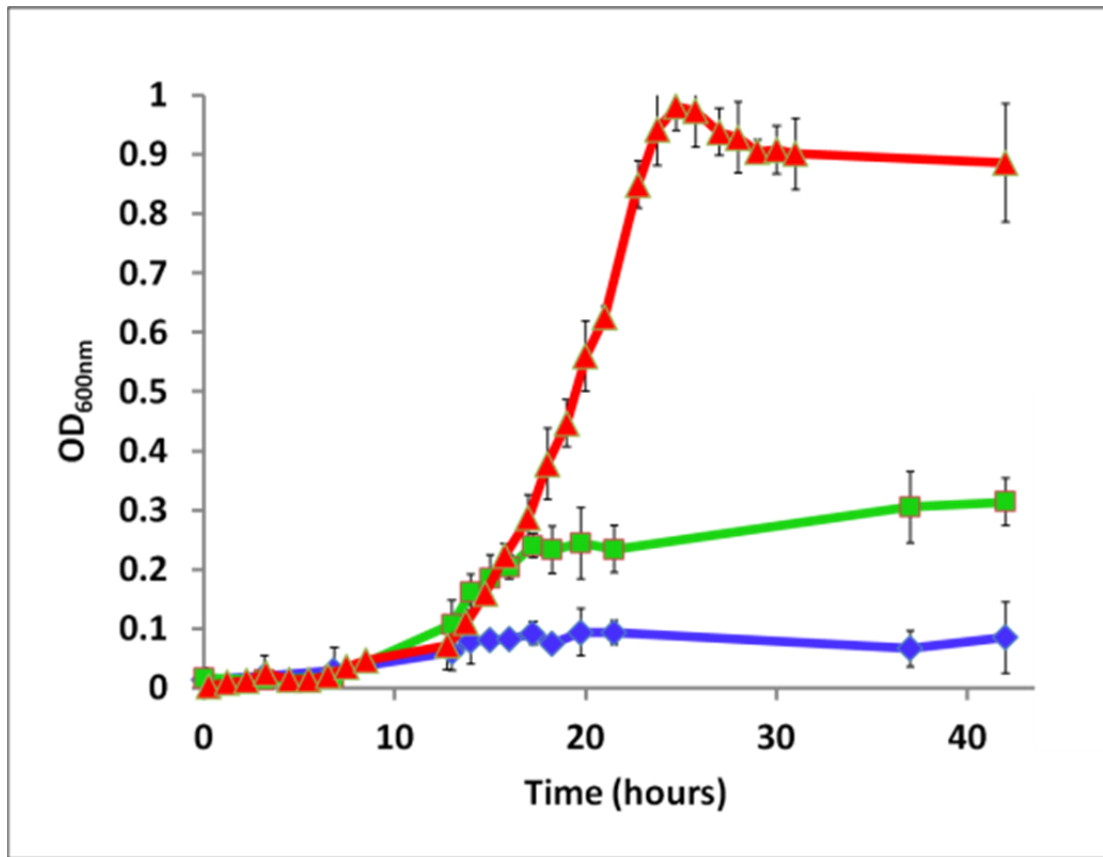
Cells from single colonies of a selection of Roseobacter strains were picked to MBM minimal medium with CAS and 5mM FeCl₃ and incubated at 28°C for 4 days before scoring for the orange halo that indicates siderophore production. Lv = Loktanella vestfoldensis SKA53, SE = Sulfitobacter EE36, SI = Silicibacter lacuscaerulensis ITI-1157, Ds = Dinoroseobacter shibae DFL-12, Rp = Ruegeria pomeroyi DSS-3, Fp = Fulvimarina pelagi.

4.1.2 Iron deficiency limits growth of R. pomeroyi

Since *R. pomeroyi* does not produce siderophores, and appears to lack an identifiable means of outer membrane iron transport, it was of interest to examine its iron requirement for growth, something that had not been previously done for *R. pomeroyi* or indeed, any strains of Roseobacters. Therefore, *R. pomeroyi* DSS-3 (a rifampicin resistant derivative of strain J470) was grown in minimal MBM media, containing 500 nM or 20 μ M FeCl₃ respectively, and in MBM with no added iron.

As shown in Figure 4.2, *R. pomeroyi* has an absolute requirement for Fe for growth and responds to levels as high as 20 μ M. Higher concentrations did not enhance growth rate or final cell density (data not shown). In comparative experiments with another bacterium, *Rhizobium leguminosarum*, whose Fe homeostasis has been studied in detail (summarised in Crosa *et al.* 2004), a similar pattern was seen. Thus, *R. pomeroyi* is not exceptional in terms of its need for a supply of Fe for its ability to grow and must therefore have an effective system for capture of this metal.

Figure 4.2 Growth of *R. pomeroyi* in MBM with iron limitation



R. pomeroyi cells were grown in MBM with no added iron (BLUE line), with 0.5 μM FeCl₃ (GREEN line) or 20 μM FeCl₃ (RED line). Triplicate cultures were incubated at 28°C, shaking at 200 rpm. OD_{600nm} values with standard errors are shown.

4.1.3 The *fbp* iron transport genes of *R. pomeroyi*

The only genes that were strongly predicted *in silico* in the *R. pomeroyi* genome sequence were the adjacent *SPO3287* and *SPO3288*, whose products were similar to two of the key components that form Fbp iron ABC-type transporters, found in many other bacteria (see Table 2.1 and Figure 3.7). The product of *SPO3287* and *SPO3288* gene products closely resemble the periplasmic binding protein and the trans-membrane transporter respectively. As mentioned above, the convergently transcribed arrangement of *fbpA* and *fbpB* is unusual, as is the lack of a nearby *fbpC* gene, encoding the ATPase.

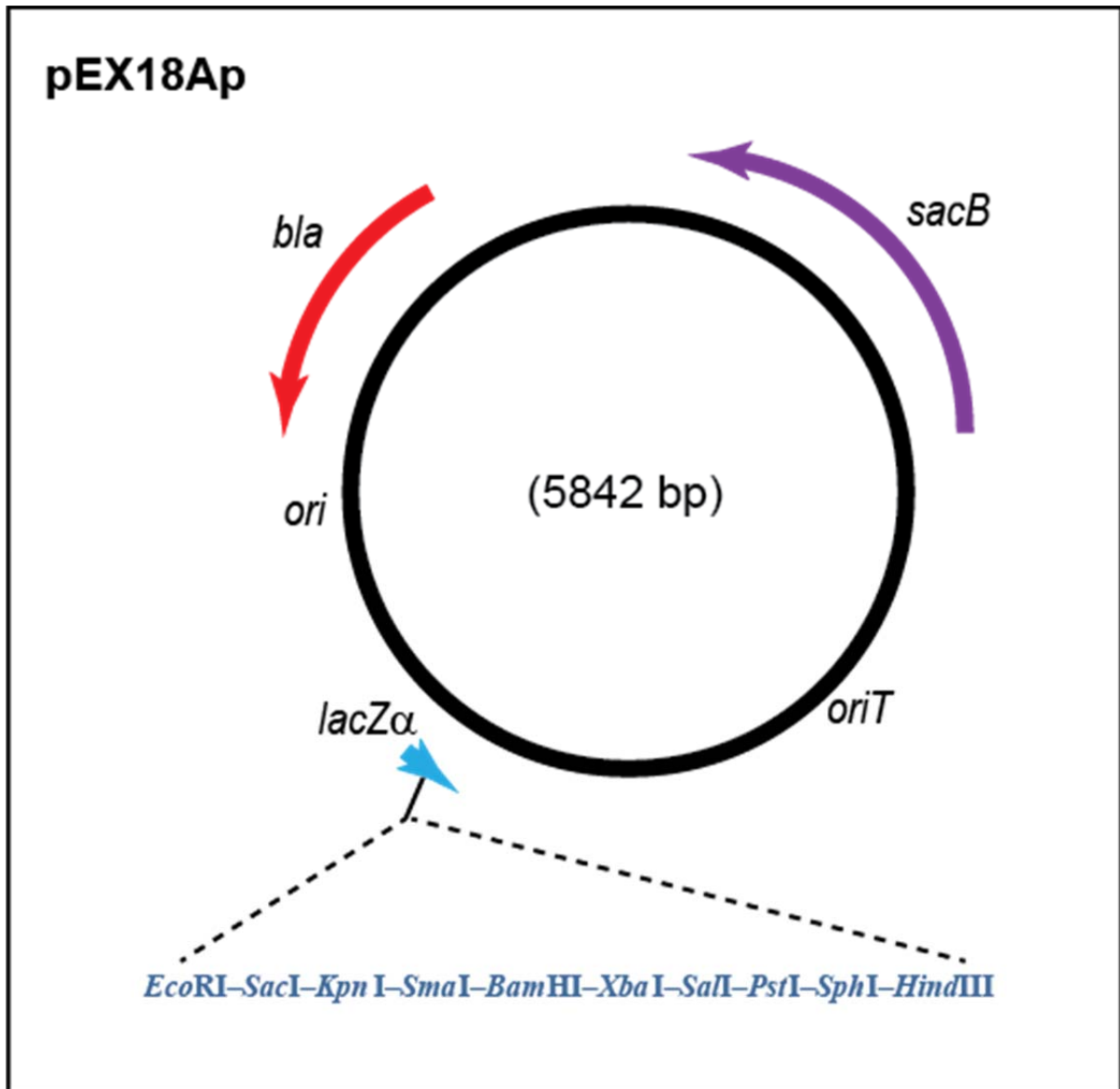
The sections below describe attempts to show if these genes do indeed, encode Fe transporters and to determine if and how they are subject to Fe-responsive regulation.

4.1.4 Disruption of the *fbpAB* genes does not affect growth of *R. pomeroyi*

To make a genomic mutation in *fbpA* and *fbpB* of *R. pomeroyi* DSS-3 (J470), most of the coding region of both genes was deleted and was replaced with a selectable marker. To do this, the “suicide” plasmid pEX18Ap (Hoang *et al.* 1998) was used. This is a wide host-range plasmid that encodes ampicillin resistance (via its *bla* gene) and can be mobilised from *E. coli* to many different proteobacteria, but it fails to replicate in such hosts (Figure 4.3 PLASMID MAP). It also contains a polylinker cloning region and a *sacB* gene, which encodes a levan-sucrase that cleaves sucrose into glucose plus fructose, the latter being polymerised to levan, a toxin for most bacteria (Bollen *et al.* 1979; Gay *et al.* 1985).

A 5011bp region of DNA that spans both *fbpA* and *fbpB* was amplified by PCR, using oligonucleotides **FbpABflankF** and **FbpABflankR** and *R. pomeroyi* genomic DNA as a template. This PCR product was cut using *EcoRI* and *HindIII* and ligated into pEX18Ap, cut with the same enzymes. The ligated products were used to transform competent *E. coli* JM101 cells (a *lacZα* $-ω+$ strain) which were spread onto LB agar plates containing ampicillin to select for transformants. The resultant colonies were screened for plasmids with the correct insert by restriction endonuclease analysis of plasmids that were isolated from a selection of these transformants (Figure 4.4). Two recombinant plasmids (pBIO2103 and pBIO2104) containing a band of the correct size - 5011bp, were confirmed by sequencing.

Figure 4.3 Map of plasmid pEX18Ap



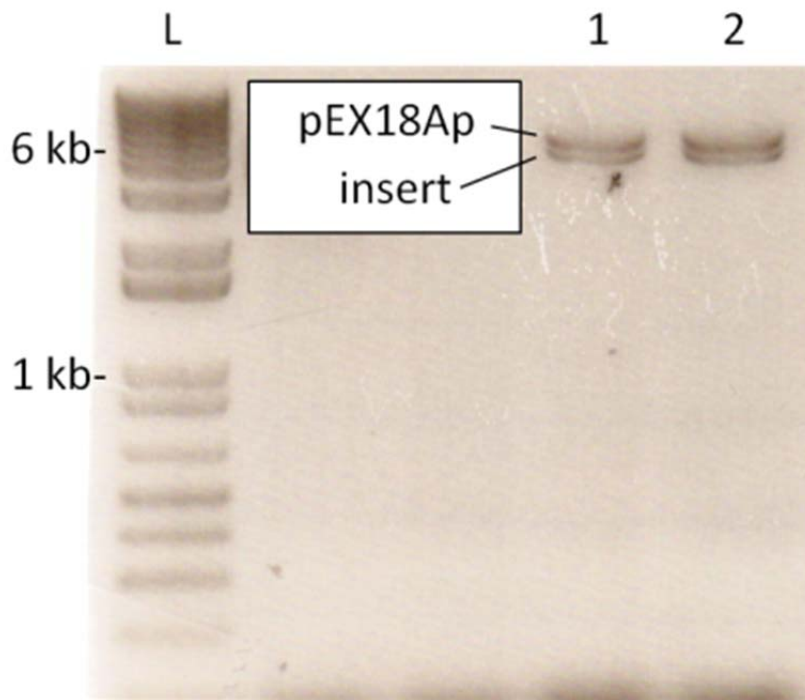
Key features of plasmid vector pEX18Ap showing positions of the origins of replication (ori), and of transfer (oriT), the sucrose inducible sacB gene, the ampicillin resistance gene (bla) and the lacZα gene, containing multiple cloning sites, indicated with dotted lines.

One of these plasmids, pBIO2103 was then used for further manipulations in which most of the *fbpA* and *fbpB* genes were removed and were replaced with a spectinomycin resistance (Spc^{R}) cassette. There are two *PstI* sites, one located within *fbpA* and one within *fbpB*, such that most of the coding sequence of the genes could be deleted by cutting with *PstI*, and replaced with the SPEC^{R} cassette which was obtained by PCR using oligonucleotides **SpecPstIF** and **SpecPstIR** on DNA of another plasmid, R100, as the template (see Figure 4.5). Both pBIO2103 and the SPEC^{R} cassette DNA were

digested with *Pst*I, ligated together, and used to transform *E. coli* JM101 as described before, selecting ampicillin and spectinomycin resistance. This resulted in pBIO2105, shown in panel 3 of Figure 4.5.

Plasmid pBIO2104 was transferred from *E. coli* to *R. pomeroyi* cells via a tri-parental conjugation, selecting for Amp^R/Spc^R transconjugants. Since pBIO2104 is a derivative of pEX18Ap, the only surviving cells should be those that had undergone a single recombination (SCO) event between the chromosome and the incoming plasmid, in the homologous region flanking *fbpA* or *fbpB* (refer to Figure 4.5 below). Cultures from three such transconjugants were grown overnight in non-selective complete HY medium, to allow for a second, intra-molecular crossover event that would remove the majority of the plasmid DNA, including the *sacB* gene, but would retain the insertion of the Spc^R cassette in the *fbpAB* genes. These were detected by examining single colonies derived from the overnight cultures for those that were Spc^R and sucrose resistant, but had lost their resistance to ampicillin; three such derivatives were retained for further study. Approximately 30% of the colonies derived from the initial cross proved to be correct as judged by their resistance patterns.

Figure 4.4 pBIO2103, and pBIO2104

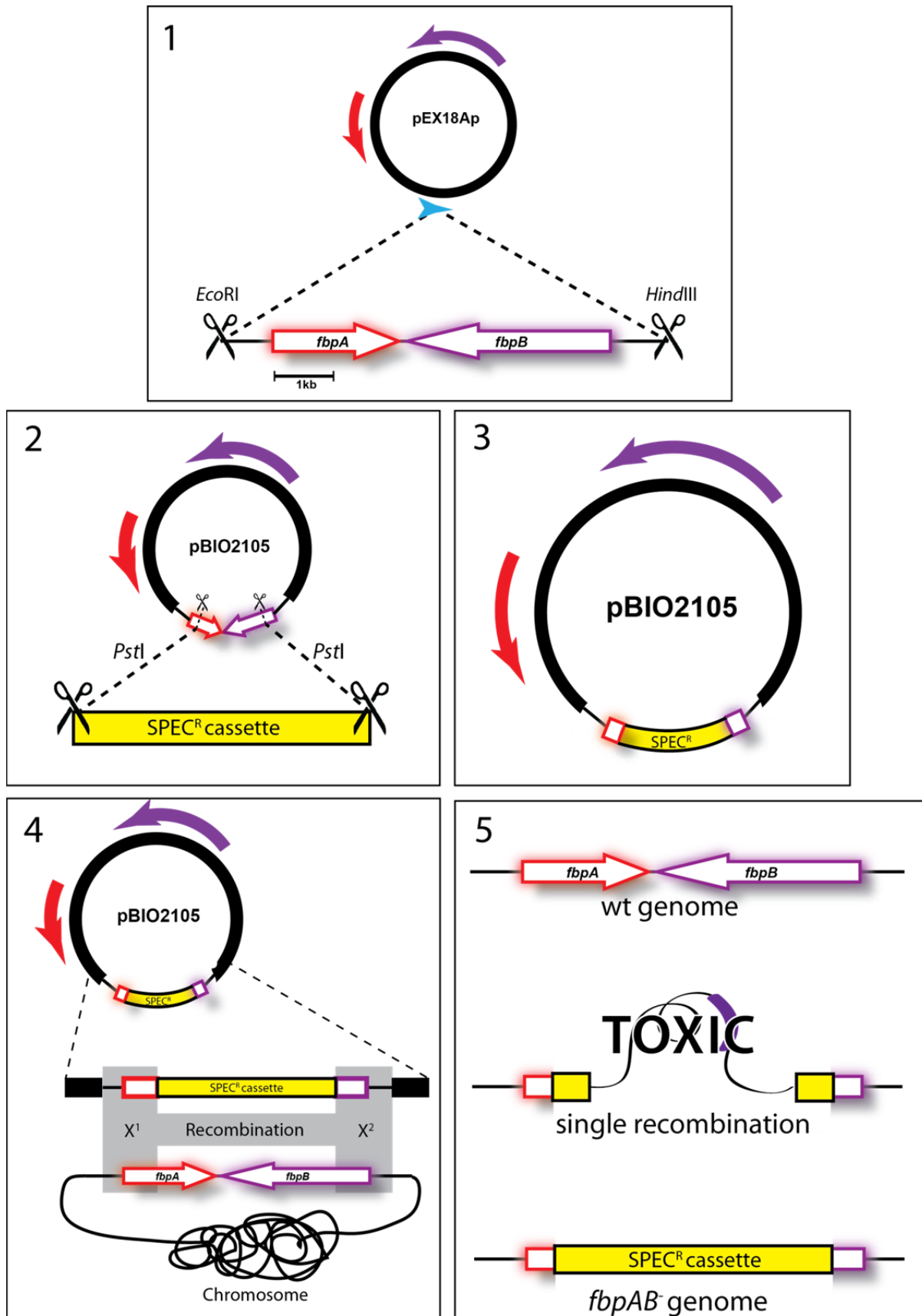


Two independent derivatives of pEX18Ap, into which a 5011bp fragment spanning fbpA and fbpB of R. pomeroyi was cloned, were digested with EcoRI and HindIII and the resultant fragments were visualised following electrophoresis on a 1% agarose gel. Lanes 1 (pBIO2103) and 2 (pBIO2104) both show two distinct bands at the appropriate size for both pEX18Ap (5842bp) and the 5011bp cloned fragment (labelled as insert). Size marker ladder (L).

To check that these were genuine replacement mutants, genomic DNA was obtained from each of these three strains and was used as template for PCR amplification using two sets of primers, whose ability to produce amplicons of particular sizes should provide diagnostic evidence for the veracity of the intended mutational events.

Thus, primers **P1** and **P2** should yield a product of 2316 bps if the SPEC^R cassette has inserted as intended but should give no product if not (e.g. if the cassette had inserted elsewhere in the genome). Primers **P1** and **P3** would show that a size difference would occur for the deletion of a 1880 bp *PstI* fragment within *fbpA* and *fbpB*, and the insertion of a 1700 bp Spc^R cassette – the wild type product was expected to be 2800 bps, and the mutant strain should yield 2620 bps. This 180 bps difference is clearly visible in the lower right panel of Figure 4.6, for samples 2 and 3 compared to the wild type. These two sample strains were renamed J531 and J532.

Figure 4.5 Creating a mutagenic pEX18Ap derivative pBIO2105



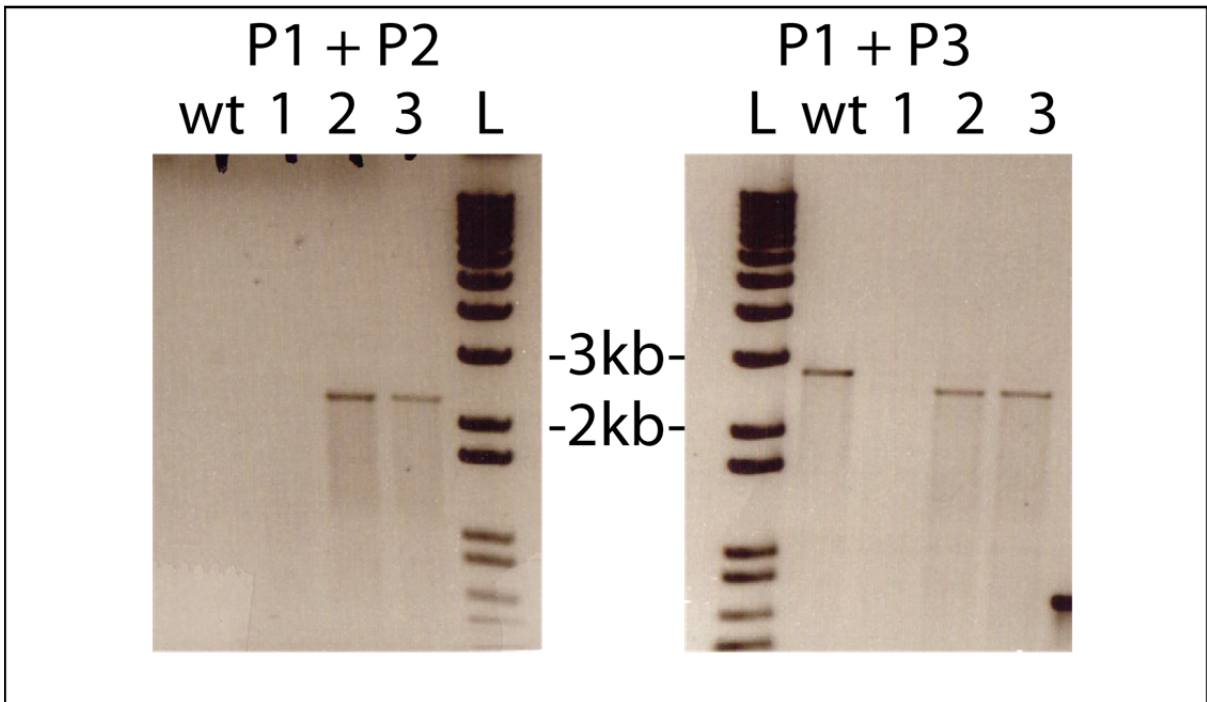
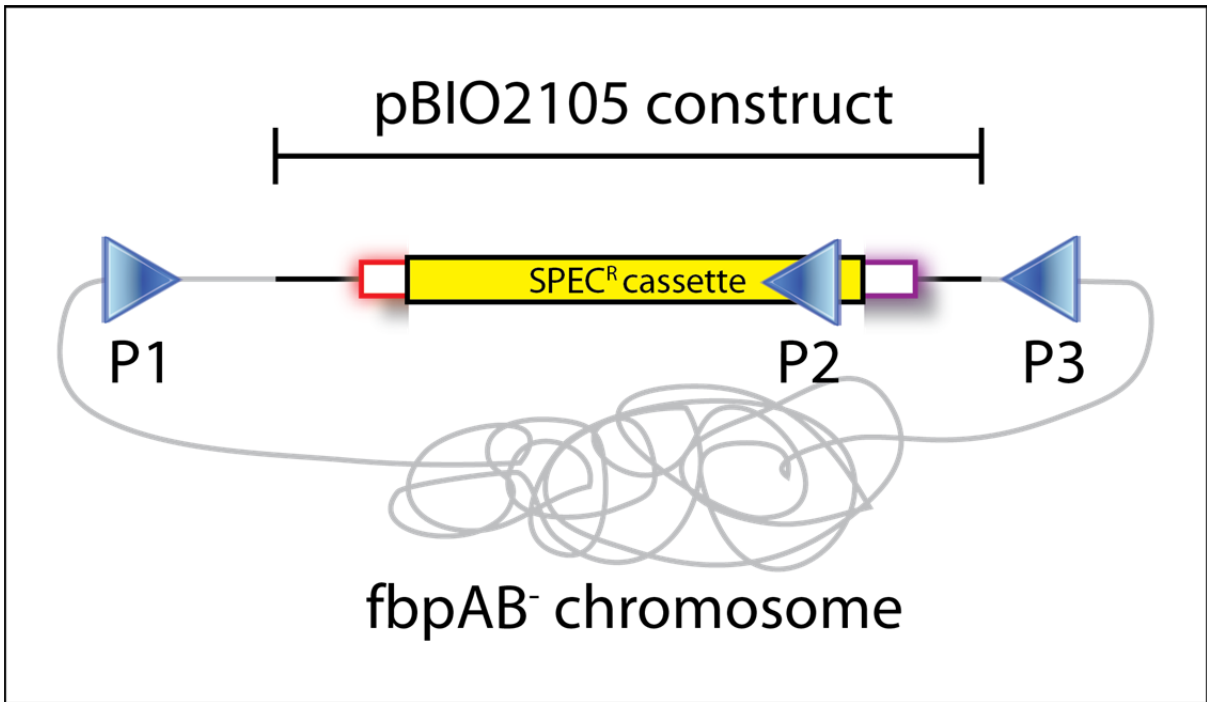
Panel 1. A 5011 bp region of *R. pomeroyi* genome was amplified and cloned into pEX18Ap using *EcoRI* and *HindIII* (panel 1), yielding pBIO2103

Panels 2 and 3. The DNA between the *PstI* sites in *fbpA* and *fbpB* was removed and was replaced with a *SPEC^R* fragment, also cleaved with *PstI*, to form plasmid pBIO2105.

Panel 4. Plasmid pBIO2105 was transferred to *R. pomeroyi* cells via conjugation, a host in which this plasmid cannot replicate. Homologous recombination events within the regions of homology between the genomic DNA and pBIO2105 occur at locations shown as X¹ and X².

Panel 5. Addition of sucrose ensures that the incoming plasmid pBIO2105 is lost, by selecting against single recombination mutants, which will express the lethal *sacB* gene expressed from the pEX18Ap plasmid DNA. The final product is a strain in which the cassette has replaced the majority of the *fbpAB* DNA.

Figure 4.6 Screening FbpAB⁻ strains of *R. pomeroiyi* using PCR

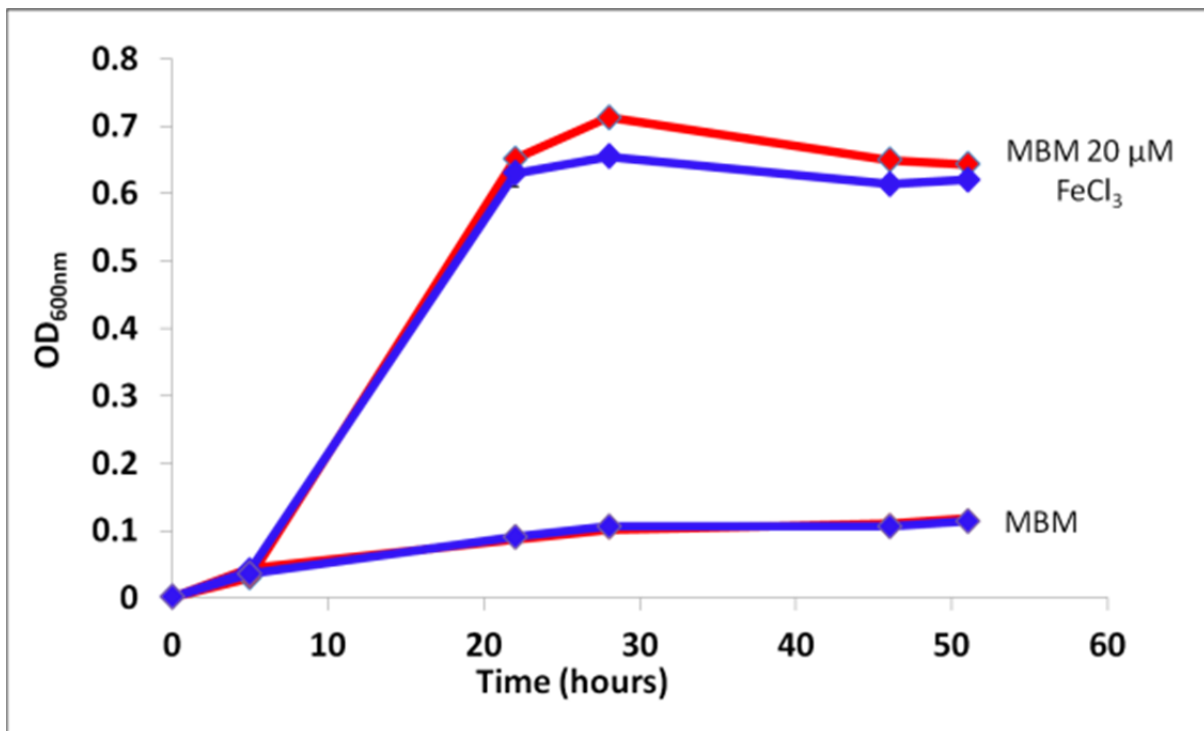


Upper panel depicts the position of oligonucleotide priming sites for screening potential *fbpAB* strains of *R. pomeroyi*. The sites are located within the *SPEC^R* cassette (P2), and upstream of the region 5' of *fbpA* used to generate pBIO2105 (P1). Used in a standard colony PCR reaction (see *Materials and Methods*) these oligonucleotides would fail to generate a product in the wt strain, but could amplify the region shown between P1 and P2 to generate a 2400bp PCR product. As shown in the lower panel, a band at 2400bp is visible for samples 2 and 3, but not in the wt, verifying the mutagenesis for samples 2 and 3. Furthermore, primers P1 and P3 used together allowed the visualisation of the change in size of the *fbp* region following the replacement of a 1880 bp *PstI* fragment by a 1700 bp *SPEC^R* cassette. Lane 1 did not produce a PCR product with either set of primers and so this strain was discarded.

4.1.5 Growth phenotype of the $\Delta FbpAB$ strain of *R. pomeroyi*

To test the effects of deleting the *fbpAB* genes in strains J531 and J532 the growth rates of these two mutants in Fe-replete and Fe-depleted MBM media were compared with the wild type. As shown in Figure 4.7, the $\Delta fbpAB$ mutation had no detectable effect on the growth either in the presence (20 μ M) or absence of added $FeCl_3$. Thus, this putative FbpAB transporter was not critical for iron uptake in *Ruegeria*. In addition to the data shown in figure 4.7 below, an intermediate level of $FeCl_3$ was tested (500 nM); however, the $FbpAB^-$ strains were unchanged in growth compared to the wt at this intermediate iron concentration and so it was omitted.

Figure 4.7 The effect of iron limitation on growth of FbpAB⁻ strains of *R. pomeroyi*



R. pomeroyi wt (red lines) and FbpAB⁻ (blue lines) were grown in MBM with no added iron (- FeCl₃) or supplemented with 20 μM FeCl₃ (+ FeCl₃). Cultures were incubated at 28°C, shaking at 200 rpm. Data shown are the mean OD_{600nm} values of three replicate cultures of each mutant strain (J531 and J532) with the standard deviation shown as error bars.

4.1.6 Analysis of fbpA-lacZ and fbpB-lacZ transcriptional fusions

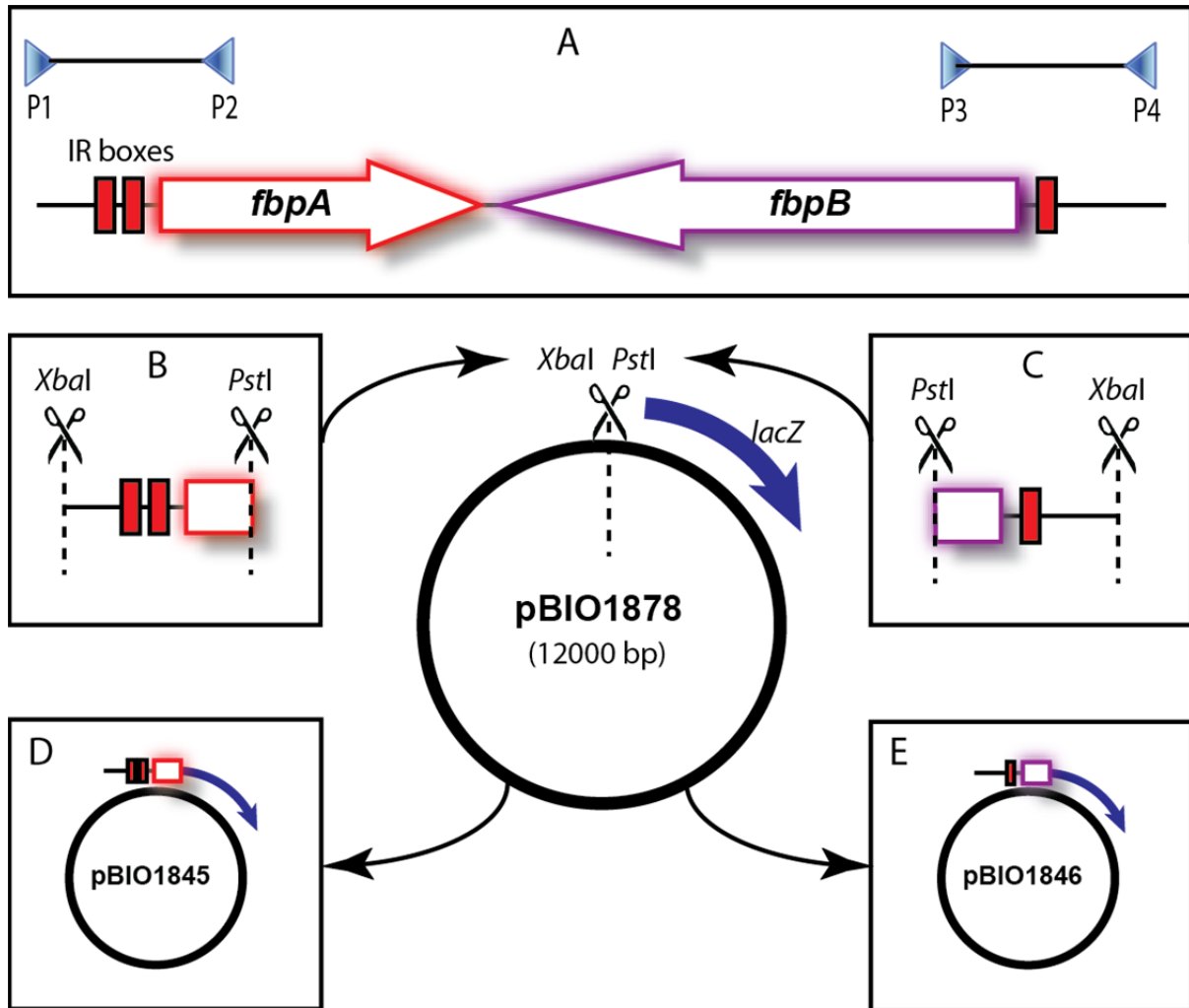
The genes *fbpA* and *fbpB* were predicted to be under the control of a putative *cis*-acting regulatory motif, the IR box (described earlier), suggesting that their transcription would vary, according to the availability of Fe in the medium, through the action of an as-yet unknown transcriptional regulator. To test directly if the expression of *fbpA* and/or *fbpB* was affected by Fe availability, transcriptional fusions to each of these genes were made, and assayed, as follows.

The transcriptional fusion vector pBIO1878 (Todd *et al.* 2011) was used as the basis for the construction of these *lac* fusions. Plasmid pBIO1878 is derived from pMP220, which has a wide host-range in gram negative bacteria, a polylinker 5' of its promoter-less *lacZ* reporter and a gene that confers tetracycline resistance (Spaink 1987). However, the Tet^R phenotype is expressed rather poorly in *Ruegeria* and other Roseobacters, so a more suitable selectable *spc* gene marker, which

confers resistance to spectinomycin, had been cloned into the *SphI* site of its poly-cloning site (Todd *et al.* 2011).

To generate the *fbpA-lacZ* and *fbpB-lacZ* fusion plasmids, their individual promoter regions were each amplified from *R. pomeroyi* genomic DNA using primers **fbpAfwd** and **fbpArev** for the *fbpA* promoter (**P1** and **P2** in Figure 4.8) and primers **fbpBfwd** and **fbpBrev**, (**P4** and **P3** in Figure 4.8) for the *fbpB* promoter. These fragments were each purified from gels, cloned into pBIO1878 such that the *lacZ* reporter would be under the control of the *fbpA* (pBIO1845) or *fbpB* (pBIO1846) promoter. The constructs were verified by sequencing. Details of the steps involved are shown in Figure 4.8.

Figure 4.8 Generation of wide host range *fbpA*- and *fbpB-lacZ* fusion plasmids pBIO1845 and pBIO1846

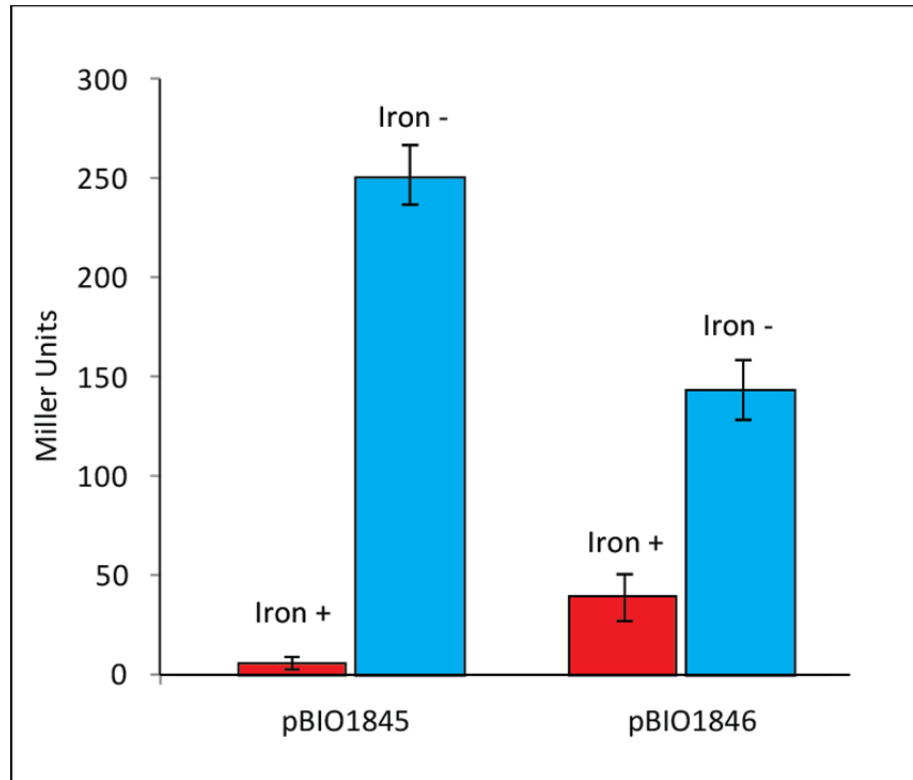


Locations of the primers used to amplify the promoter regions of fbpA (P1 and P2) and of fbpB (P3 and P4) are shown in panel A. Note that these primers contain XbaI and PstI restriction sites used for subsequent cloning steps (see Panels B and C). Each PCR fragment was cleaved with XbaI plus PstI and ligated to pBIO1878, digested with the same enzymes. These manipulations produced plasmids pBIO1845 and pBIO1846 in which the reporter lacZ would be controlled by the fbpA and fbpB promoters respectively (Panels D and E). The two IR boxes preceding fbpA gene and the one preceding fbpB are indicated.

To measure the transcription of *fbpA* and *fbpB*, plasmids pBIO1845 and pBIO1846 were each mobilised by conjugation into *R. pomeroyi* strain J470. Transconjugants were selected on HY agar plates containing 50 µg/ml rifampicin and 200 µg/ml spectinomycin. For each cross, three separate, purified transconjugants were assayed for β-galactosidase activity (detailed in Materials and

Methods) following growth in MBM minimal media that either contained (20 μ M) or lacked added FeCl_3 .

Figure 4.9 Expression of iron availability on the expression of *fbpA-lacZ* and *fbpB-lacZ* fusions.



Ruegeria pomeroyi containing either the *fbpA-lacZ* or *fbpB-lacZ* fusion plasmids (pBIO1845 and pBIO1846 respectively) were grown in minimal medium (MBM) either supplemented with 20 μ M FeCl_3 (Iron +) or not (Iron -) and assayed for β -galactosidase activity, expressed in Miller units. Error bars represent the standard deviation of 2 biological, and three technical replicates.

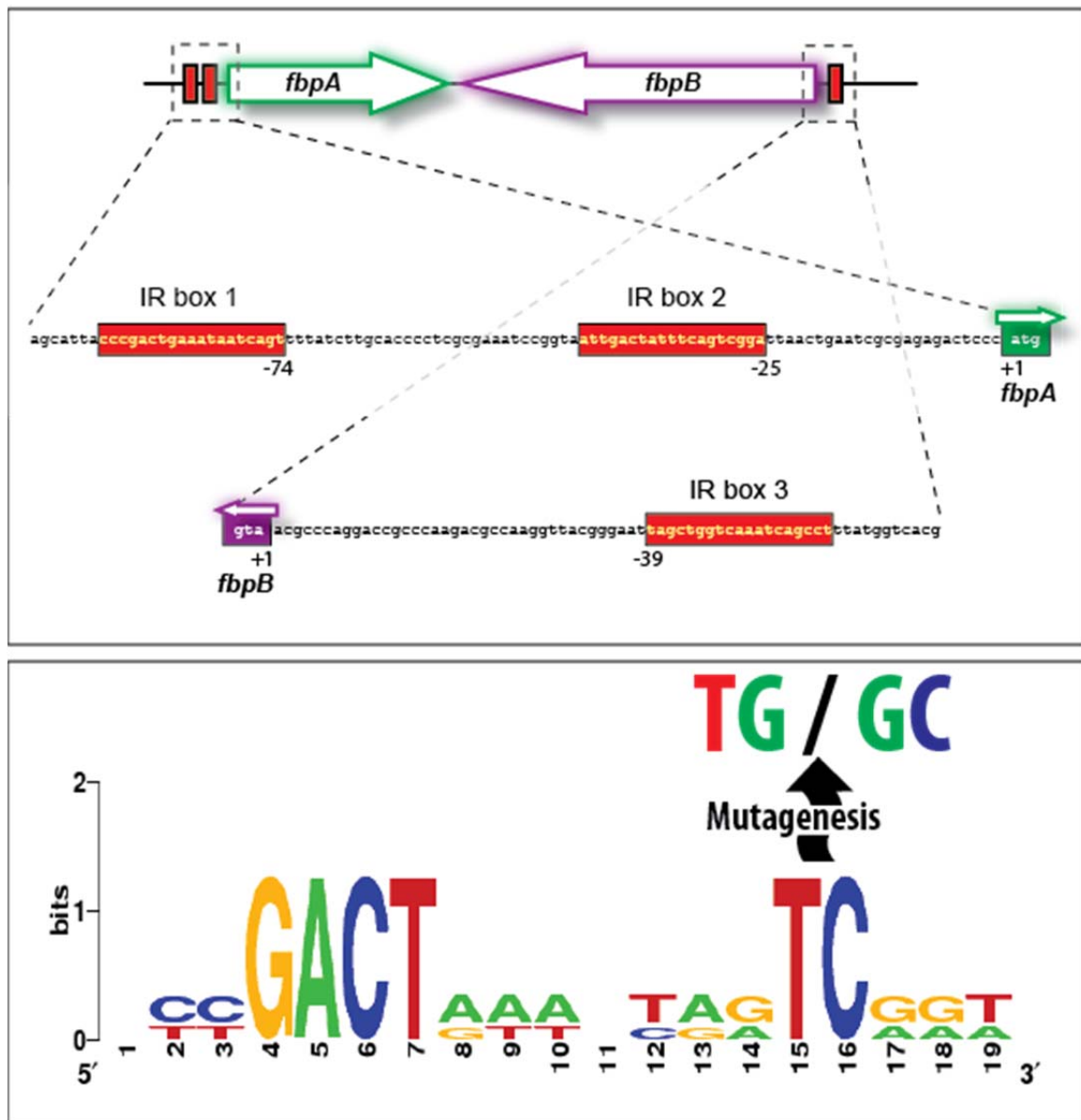
Both the *fbpA-lacZ* and *fbpB-lacZ* fusions were expressed at much higher levels in Fe-depleted than Fe-replete media, ~41-fold for *fbpA-lacZ* and rather less (3.5-fold), for *fbpB*.

4.1.7 IR motifs preceding *fbpA* and *fbpB* are important for their Fe-responsive transcription

As predicted by Rodionov and colleagues (2006), and discussed in Chapter 3, both *fbpA* and *fbpB* have regions of dyad symmetry upstream of their transcriptional start codons, which are resemble

the motifs found upstream of many putative iron-responsive genes in the Rhodobacteraceae. These “IR boxes”, their sequences and positions are shown in Figure 4.10 below.

Figure 4.10 The IR boxes upstream of *fbpA* and *fbpB* of *R. pomeroyi*



Upper panel shows the *R. pomeroyi* genomic *fbp* region, with sequences 5' of *fbpA* and *fbpB* shown in the zoomed boxes, dotted lines. The locations of the two IR motifs (boxes 1 and 2) upstream region of *fbpA* and the single IR 5' of *fbpB* (box 3) are shown in red. The numbers on the DNA sequences denote the distances from the corresponding "A" of the ATG translational starts of *fbpA* (green highlight) and *fbpB* (purple highlight).

Lower panel shows the consensus sequence for all three IR boxes generated using WEBLOGO. The conserved TC motif was used as a target for subsequent site-directed mutagenesis, and was changed to both a TG and GC motif for all three boxes.

The *lacZ*-fusion plasmids pBIO1845 and pBIO1846 contained the promoter regions of *fbpA* and *fbpB* respectively, including all perceived IR boxes, and so were used as templates to generate site directed mutations in these putative regulatory motifs. To do this, the mutagenic primers shown in Table 4.1 were used to alter the conserved TC motif shown in Figure 4.10. Both the T and C bases were mutated to a G for each of the three IR boxes (6 mutants in total). Since *fbpA* has two IR boxes, a seventh mutant was constructed, where the T nucleotide of the conserved TC motif in each IR box was changed to a G. Care was taken to not disrupt the putative -10 and -35 promoter sequences, which were predicted to overlap the 3' end of the IR boxes, hence the selection of bases at the 5' end of the IR boxes for mutagenesis.

Table 4.1 Oligonucleotide primer sequences for IR box site directed mutagenesis

Oligonucleotide primers used to mutate the bases of IR boxes 1-3 as shown in Figure 4.10, of fbpA (boxes 1 and 2) and fbpB (box 3) of R. pomeroyi. The primer names, sequence and nucleotide target for mutagenesis are shown along with the resultant mutagenised plasmid name. All bases listed as a target were mutated to a G.

Oligo Name	Sequence	Target	Plasmid
fbpA51TtoGFWD	GCGACAGCATTACCCGACTGAAATAAGCAGTTTTATCTTGC	IR box 1 'T'	pBIO2106
fbpA51TtoGREV	GCAAGATAAAAACCTGCTTATTTTCAGTCGGTAATGCTGTCCG		
fbpA51CtoGFWD	GCGACAGCATTACCCGACTGAAATAATGAGTTTTATCTTGC	IR box 1 'C'	pBIO2107
fbpA51CtoGREV	GCAAGATAAAAACCTCATTATTTTCAGTCGGTAATGCTGTCCG		
fbpA2TtoGFWD	GCGAAATCCGGTAATTGACTATTTTCAGGCGGATTAAGTGAATCG	IR box 2 'T'	pBIO2108
fbpA2TtoGREV	CGATTCAGTTAATCCGCCTGAAATAGTCAATTACCGGATTTCCG		
fbpA2CtoGFWD	GCGAAATCCGGTAATTGACTATTTTCAGTGGGATTAAGTGAATCG	IR box 2 'C'	pBIO2109
fbpA2CtoGREV	CGATTCAGTTAATCCCACTGAAATAGTCAATTACCGGATTTCCG		
fbpBTtoGFWD	TCAGGCACTGGTATTTCCGACTAAACTGGGCGATTAAGGGCATTGGAACC	IR box 3 'T'	pBIO2110
fbpBTtoGREV	GGTTCCAATGCCCTTAATCCGCCAGTTTAGTCGGAAATACCAGTGCCTGA		
fbpBCtoGFWD	TCAGGCACTGGTATTTCCGACTAAACTGGTGGATTAAGGGCATTGGAACC	IR box 3 'C'	pBIO2111
fbpBCtoGREV	GGTTCCAATGCCCTTAATCCACCAGTTTAGTCGGAAATACCAGTGCCTGA		
fbpA51TtoG	Both sets of primers used sequentially.	IR box 1 and 2 'T'	pBIO2112
fbpA2TtoG	Both sets of primers used sequentially.		

Each mutagenic reaction was performed, as detailed in Materials and Methods, and the mutated plasmid DNA was used to transform *E. coli* XL10-GOLD cells. Transformants were selected on LB agar with spectinomycin added at 200 µg/ml. Plasmids containing the correct mutations were assigned pBIO numbers shown in Table 4.1 above.

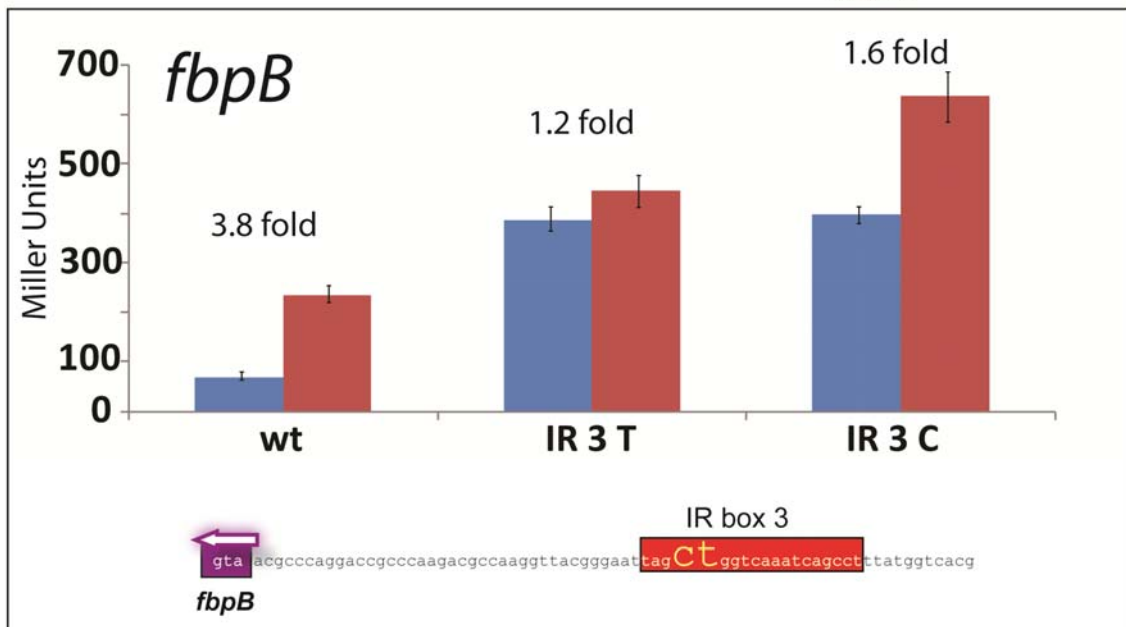
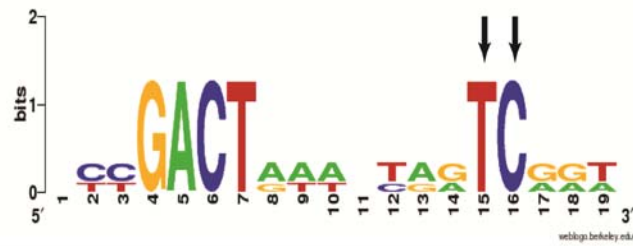
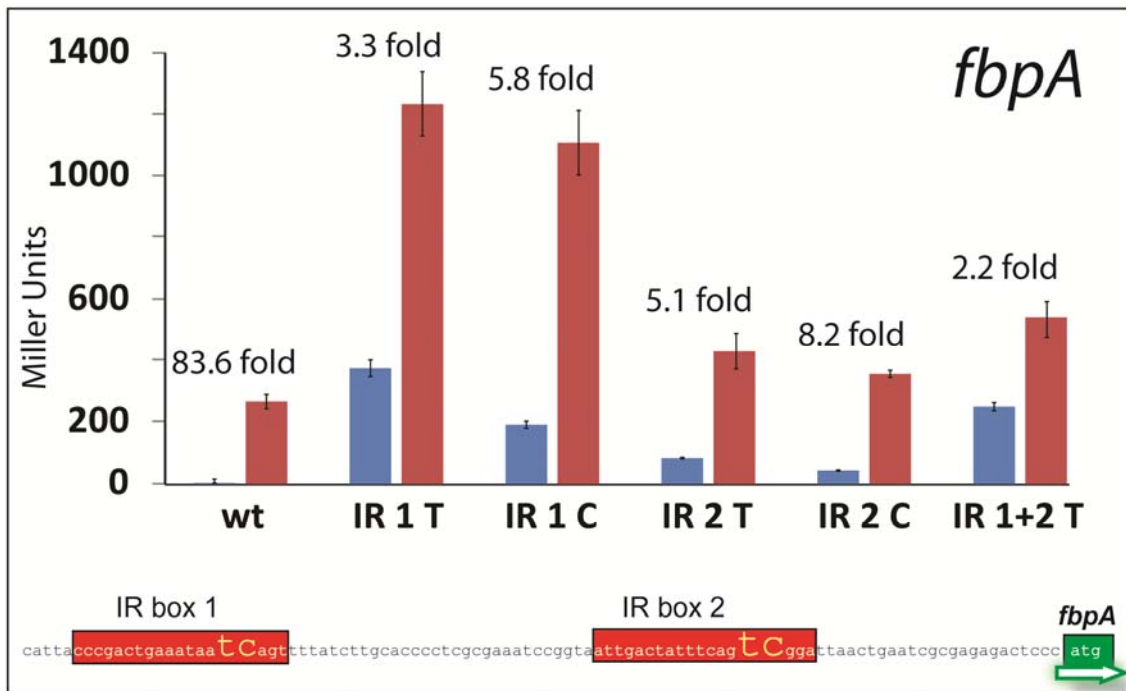
Having generated, and sequence verified, a suite of single base-pair mutations in the IR boxes of *fbpA* and *fbpB*, each of the mutant plasmids was mobilised into *R. pomeroyi* and the transconjugants were assayed for β -galactosidase activities after growth in Fe-depleted and Fe-replete conditions.

As shown in Figure 4.11, all of the mutations resulted in an increase in the level of expression of the corresponding fusion, though there were differences in the details of this deregulation in the individual mutations.

Thus for *fbpA-lacZ*, both mutations (referred to here as T and C) in IR box 1 greatly increased the expression of the fusion both in +Fe: 4.6- (T) and 4.2-fold (C) compared to wild type, and –Fe: 118- (T) and 60.1-fold (C) when compared to wild type. Mutations in IR box 2 also enhanced the transcription of *fbpA-lacZ*, in both media, though not to the same extent as those in box 1: 1.6- (T) and 1.3-fold (C) in the +Fe media, and 26.5- (T) and 13.7-fold (C) in the –Fe media, compared to the wild type. Perhaps surprisingly, the mutant plasmid pBIO2112, which had mutations in both IR box 1 and IR box 2 behaved similarly to pBIO2110, which had mutations only in IR box 2.

Turning to the *fbpB-lacZ* fusion, its expression was also enhanced by each of the mutations in the IR box 3. The “T” mutation led to an enhanced constitutive expression, in which the transcription of the fusion was similar in both –Fe and +Fe media. When the “C” was mutated, though, there was even higher expression in the –Fe than the +Fe media (Figure 4.11).

Figure 4.11 Effects of mutations in the IR boxes on the expression of *fbpA* and *fbpB*

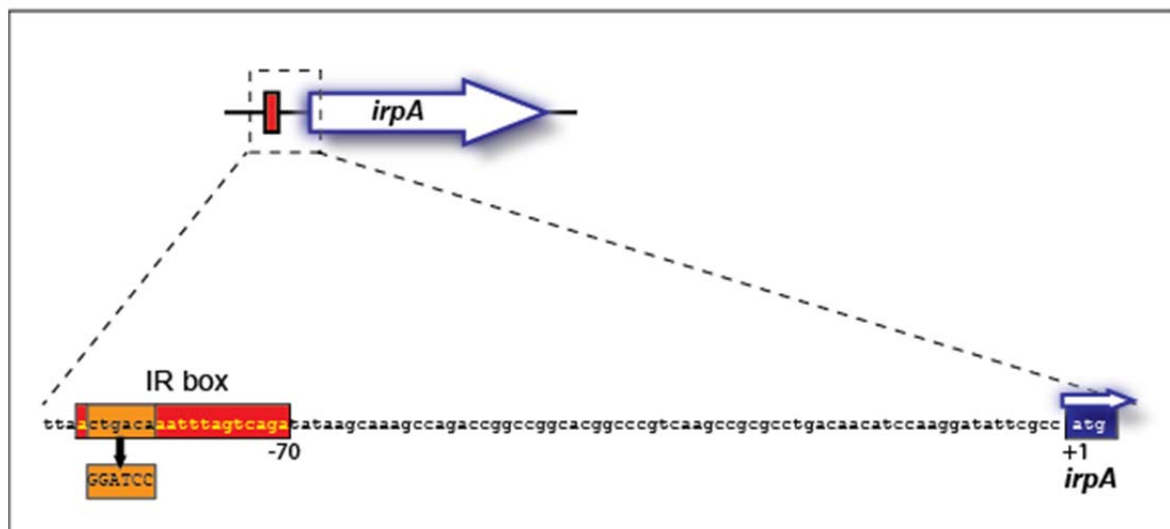


The *fbpA-lacZ* and *fbpB-lacZ* fusion plasmids pBIO1845 and pBIO1846 respectively were used to generate IR box mutants. The highly conserved TC motif in the IR boxes of *fbpA* and *fbpB* (arrowed in middle panel) was mutated, so that each base became a G nucleotide, separately, in 6 different mutant plasmids. In a seventh mutant, the conserved T bases in both *fbpA* IR boxes were mutated to G. Expression of the *lacZ* fusions in *R. pomeroyi* containing the various mutant plasmids after growth in MBM with 20 μM FeCl_3 (BLUE BARS) or none added (RED BARS) and is shown in Miller units in the upper and lower panels, for *fbpA* and *fbpB* respectively. Wild type fusion is labelled wt. All data are the average of 3 biological and two technical replicates.

4.1.8 The “Irp” operon of *Ruegeria pomeroyi*.

Of the transcriptional units that were preceded by IR motifs, located in their predicted regulatory regions, another one whose gene products were implicated in Fe uptake was the 5-gene operon comprising *SPO0086* – *SPO0090*, in which the product of the promoter-proximal gene, *SPO0086* was very similar to *IrpA* in other bacteria. The location and sequence of this IR motif is shown in Figure 4.12.

Figure 4.12 The *irpA* promoter region showing IR box location and sequence

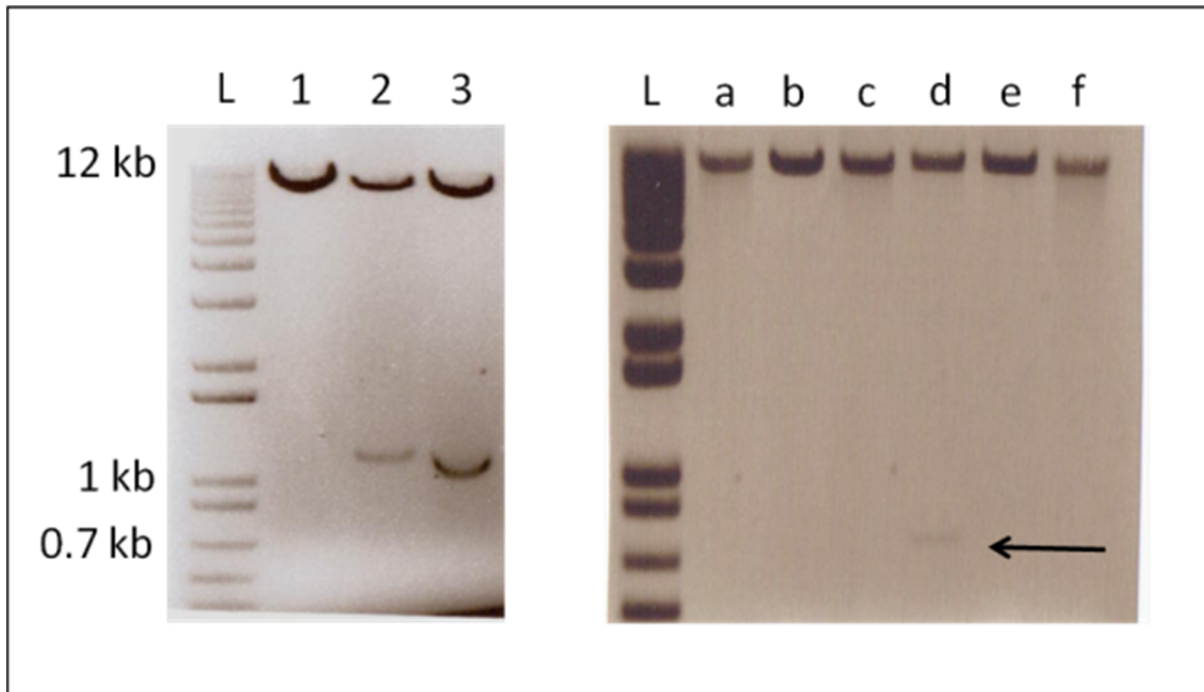


The sequence 5' of *irpA* is shown, including the IR box (red box) 70bp upstream of the ATG start of *irpA*. The sequence in orange was subject to SDM, from *ctgaca* to *ggatcc*, creating a *Bam*HI site.

4.1.9 Expression of *irpA* is repressed by iron in *R. pomeroyi*

To study the expression of the *irp* operon, a transcriptional fusion plasmid, pBIO1847, was constructed by cloning a 1016bp region spanning the 5' upstream region of *irpA* of *R. pomeroyi* into pBIO1878, following amplification by PCR using primers **irpA_{fwd}** and **irpA_{rev}** and *R. pomeroyi* genomic DNA as the template. DNA from plasmid pBIO1847 was also used as a template for site-directed mutagenesis (SDM) of the IR motif upstream region of *irpA*. Briefly, primers **IrpABamHIFWD** and **IrpABamHIREV** were used to substitute the CTGACA (which includes the adjacent, highly conserved GA – see figure 3.3b) to GGATCC, which represents a *Bam*HI site to facilitate screening of potential mutants (see Figure 4.13).

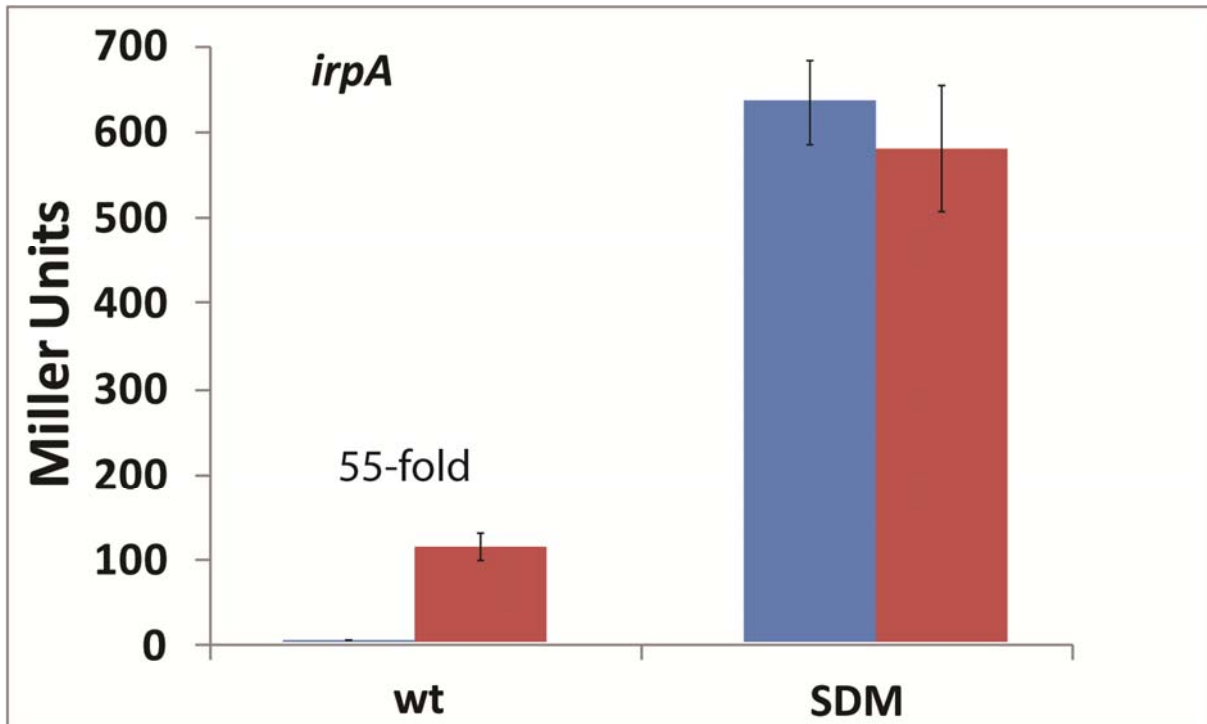
Figure 4.13 Gel photos of clone, and site-directed mutant clone, of the promoter region of *irpA* into pBIO1878



*The left panel shows the restriction digest pattern of the DNA of three potential recombinant plasmids, containing the *irpA* promoter region cloned into pBIO1878, and digested with *Xba*I plus *Pst*I, and separated on a 1% agarose gel. A fragment of the correct size (1016 bp) is seen in Lanes 1 and 2. The plasmid in Lane 2 was used as the template for SDM, where a *Bam*HI site was made in the IR motif, 744 bp downstream of the *Pst*I site. The right panel shows the DNA of 6 potential mutant derivatives of pBIO1847, digested with *Pst*I and *Bam*HI. Sample 'd' liberated a fragment of the correct size (see arrow). Following sequence verification, this mutated plasmid was named pBIO2115.*

The plasmids pBIO1847 and pBIO2115 were introduced by conjugation into *R. pomeroyi* J470. For each plasmid, three different transconjugants were grown in MBM minimal medium either containing 20 μ M FeCl₃ or with no added Fe, before assaying β -galactosidase activities.

Figure 4.14 Effects of Fe and the IR motif on the expression of *irpA-lacZ*



Plasmids pBIO1847 (wt *irpA-lacZ*) and pBIO2115 (SDM *irpA-lacZ*) in *R. pomeroyi* were assayed for β -galactosidase activity following growth in MBM either containing 20 μM FeCl₃ (blue bars) or no added iron (red bars). Data are in Miller units (y-axis) and represent the average of three biological replicates.

As shown in (Figure 4.14), the expression of the wild type version of the *irpA-lacZ* fusion (in plasmid pBIO1847) was much higher (55-fold) in the Fe-depleted than the Fe-replete media. Furthermore, the removal of the IR box in the mutated plasmid pBIO2115 resulted in greatly increased expression, both in the absence and even more dramatically (313-fold compared to the wild-type) in the presence of added Fe. Thus, the *irpA* operon is regulated in response to Fe and this requires a functional IR box motif.

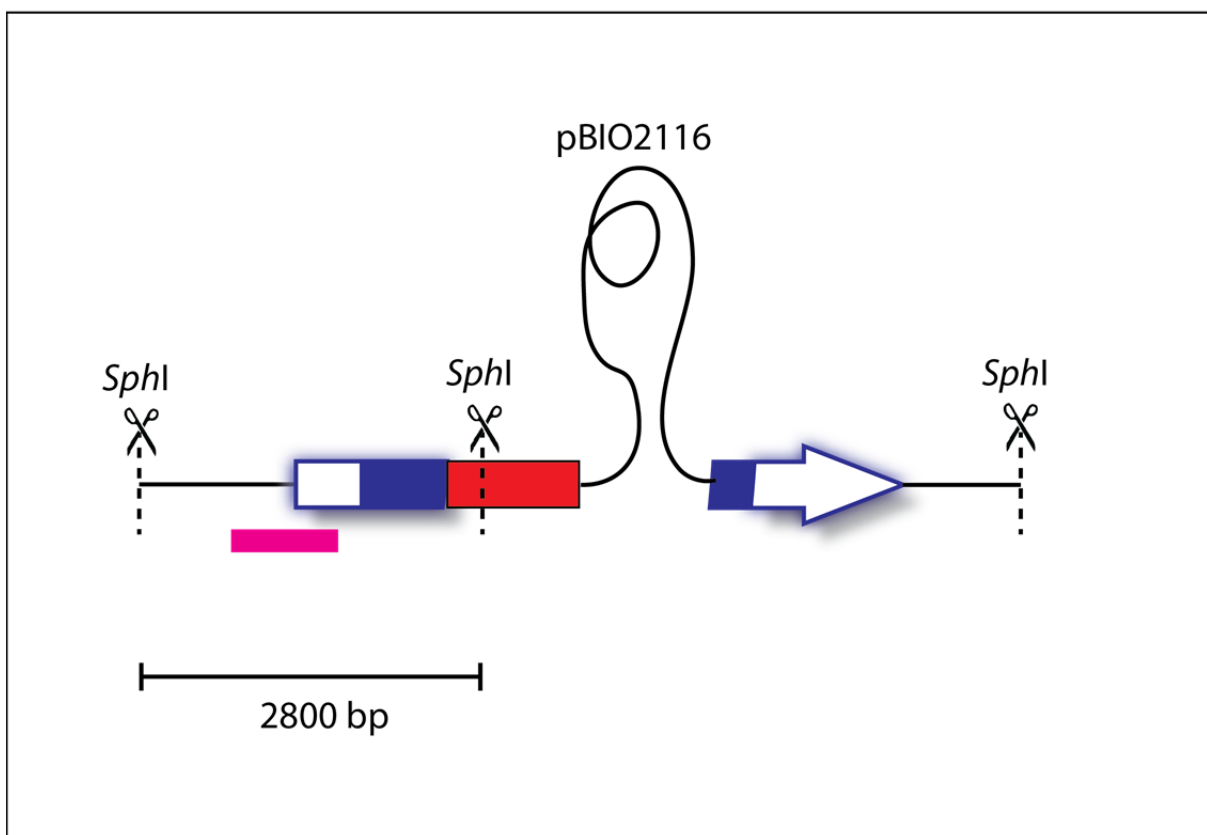
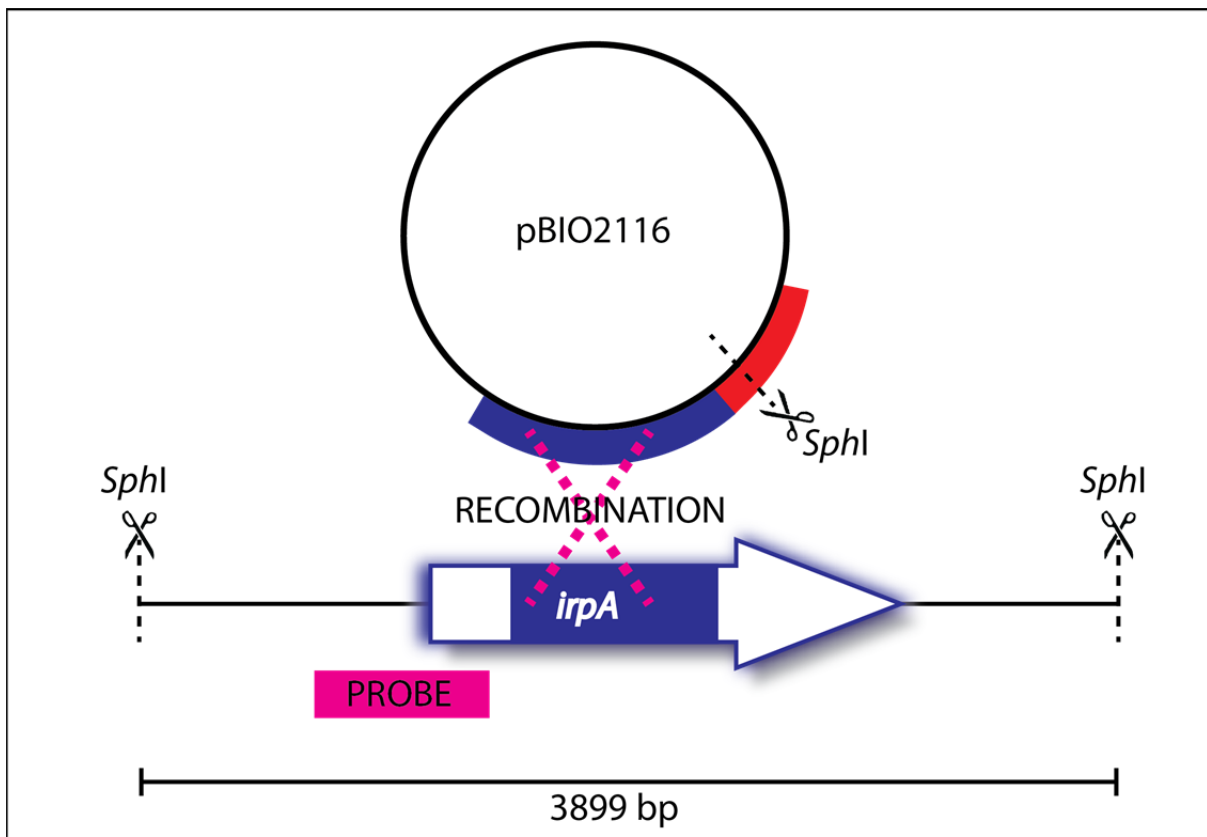
4.1.10 Construction of an *IrpA*⁻ strain of *R. pomeroyi*

Mutations in *irpA* of *Synechococcus elongatus* PCC 7942 had been shown to be deficient in their growth in low-Fe media (Reddy *et al.* 1988). To examine the effects of mutating the homologous gene in *Ruegeria*, an *IrpA*⁻ strain was made, as follows. The vector used to construct this mutant, pBIO1879, was derived from the wide host-range “suicide” plasmid pK19mob (Schafer *et al.* 1994),

and has a spectinomycin resistance cassette cloned into the PCS, and so confers resistance to both spectinomycin and kanamycin (Todd *et al.* 2011). The chosen method of mutagenesis involves the cloning of an internal fragment of the targeted gene into pBIO1879, followed by the introduction of the resulting plasmid in a recipient bacterium (in this case *Ruegeria pomeroyi*) in which it cannot replicate. Therefore, by plating on selective media containing spectinomycin plus kanamycin, insertional mutants, generated by homologous recombination between the cloned internal fragment and the target gene can be obtained (see Figure 4.15).

An internal fragment of *irpA* was amplified using PCR, using primers **IrpApk19fwd** and **IrpApk19rev**, using *R. pomeroyi* genomic DNA as a template. This 740 bp PCR product was purified and digested with *EcoRI* and *XbaI*, ligated into pBIO1879, then transformed into *E. coli*, a host species in which the plasmid can replicate normally. Plasmid DNA was isolated from a selection of the transformants and one, termed pBIO2116, that contained the correct insert (as checked by restriction digests and sequencing) was retained for further use.

Figure 4.15 Insertion and ratification of insertion mutation into *R. pomeroi irpA*

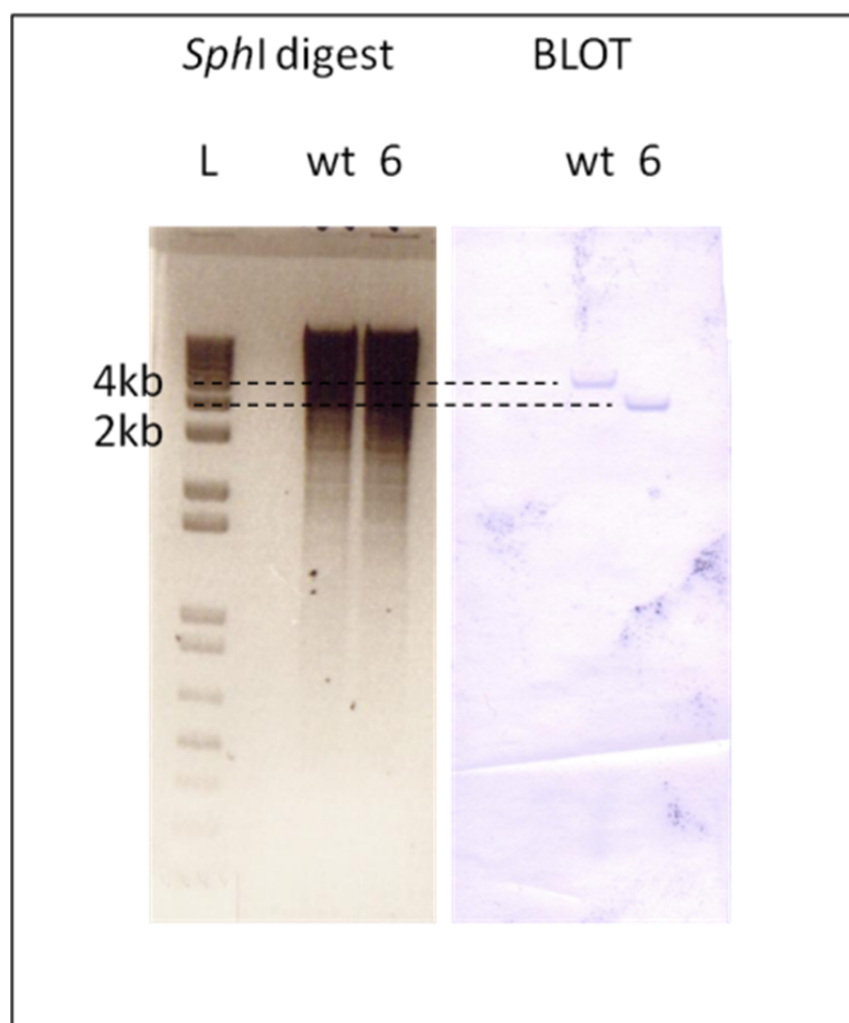


The pK19mob derived suicide vector pBIO2116 integrates into irpA of the R. pomeroyi genome, via a single recombination event with the cloned internal irpA DNA, shown in blue. The dimensions of the DNA used as the probe in the Southern blots are shown in pink. As shown, this would hybridise to a 3899 bp fragment in the wild type, and a 2,800 bp fragment if pBIO2116 has inserted into irpA.

This plasmid was then mobilised into *R. pomeroyi* J470 by conjugation, selecting transconjugants on HY medium containing rifampicin (to kill the donor *E. coli*) plus spectinomycin and kanamycin (conferred by the incoming plasmid). Colonies arose at a frequency of $\sim 10^{-2}$, and several of these were purified and checked for insertions into *irpA*, as follows.

First, a 'colony-PCR' based approach was used, with primers **irpA1F1** and **irpA2R2**, which are located to either side of the *irpA* gene. These would amplify a 1751bp region if presented with wild type template DNA, but if there was a large insertion within the gene, no PCR product would be made. Of 6 colonies that were examined, one failed to generate a PCR product, so likely contained an insertion in *irpA*. This was confirmed by a Southern blot, in which genomic DNA was isolated from this putative mutant and probed with a DIG-labelled DNA fragment that spanned the 5' end of the *irpA* gene. This would reveal a ~ 4 kb (exact size is 3899 bp) band in a Southern blot with the wild type DNA, but if the plasmid pBIO2116 had inserted into *irpA*, the predicted size of the hybridising band would be smaller, since pBIO2116 contains a *SphI* site within the spectinomycin resistance cassette. The DNA from the putative IrpA- mutant did indeed, lead to the production of a hybridising fragment of the expected size for an insertional mutation, as shown in Figure 4.16 below. This IrpA- mutant was named J533.

Figure 4.16 Verification by Southern blot of an insertional mutation into *irpA*



Genomic preps of wild type R. pomeroyi (wt) and putative IrpA⁻ strain (6) digested with SphI and separated on a 1% agarose gel (left-hand panel), were blotted and probed with DIG-labelled DNA corresponding to the 5' end of irpA. The sizes of the hybridising bands are indicated. The size marker is shown as L.

4.1.11 Phenotypic analysis of the IrpA⁻ strain of R. pomeroyi

Although the IrpA⁻ strain of *Synechococcus* grew poorly on iron deficient media compared to the wild type strain (Reddy *et al.* 1988), no such defect was seen when the IrpA⁻ mutant strain J533 of *R. pomeroyi* was cultured in MBM minimal medium to which no FeCl₃ had been added.

There was no detectable difference between the wild type and *IrpA*⁻ strain after 60 hours of growth. To see if there was an effect of residual iron from the starter culture, the MBM cultures were sub-cultured into MBM containing iron or not as before. These cultures were still identical for growth in both iron-depleted and -replete MBM after another 70 hours. It is therefore unlikely that *IrpA* alone is required for iron uptake or storage, as suggested by Reddy et al. (1988) for the *Synechococcus* *IrpA* protein.

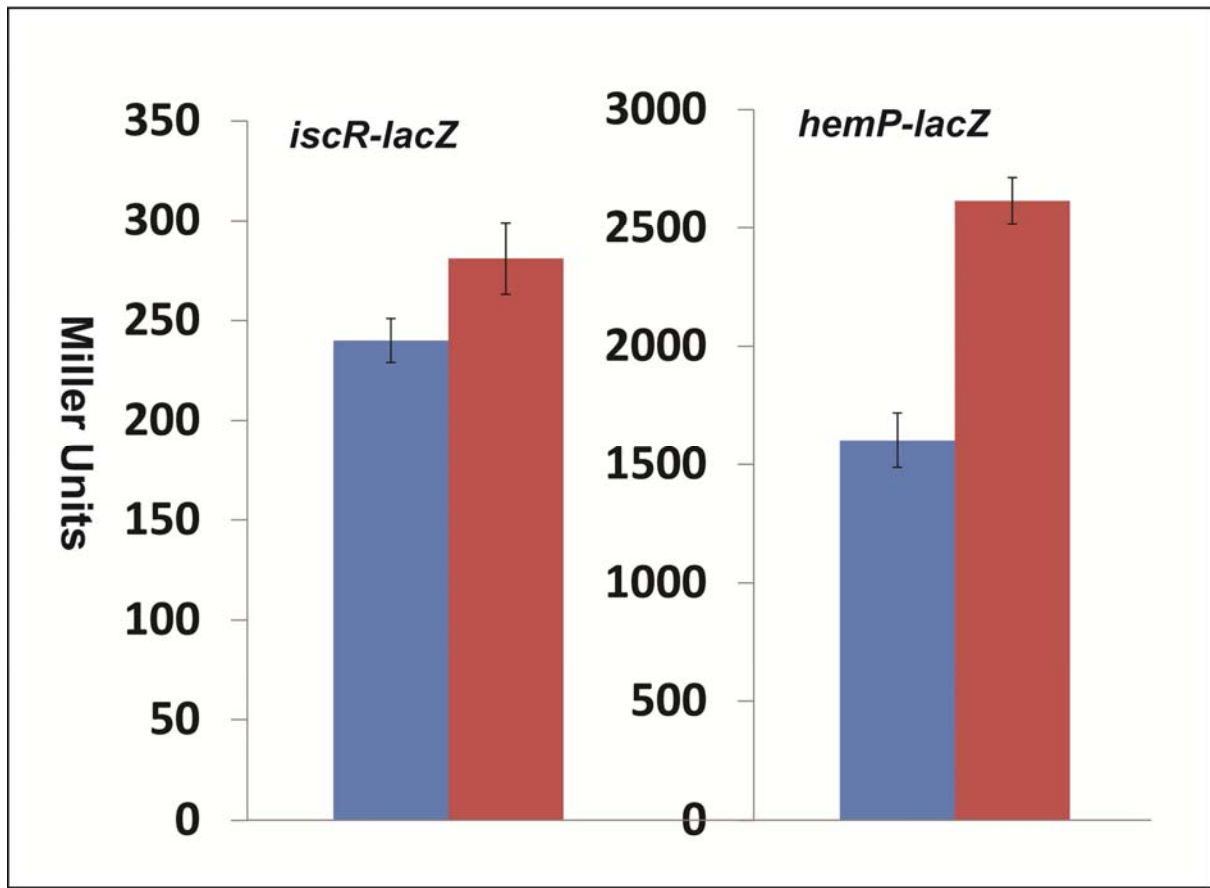
4.1.12 Iron-responsive expression of the *hemP* and *iscR* genes of *R. pomeroyi*

As described in Chapter 3, two other *Ruegeria pomeroyi* genes, namely *hemP* and *iscR* are preceded by predicted IR boxes, these two genes being predicted to encode, respectively, a polypeptide involved in haem uptake and in the regulation of the complex operon that includes *iscR* itself, plus the downstream *suf* genes (Table 3.2).

To examine the expression of *hemP* and of *iscR*, transcriptional *lacZ* fusions to each gene were constructed, using the same general approach as described above for the *fbp* genes. For *hemP*, a 546 bp spanning its promoter region was amplified, using primers **SPO0789XbaI1** and **SPO0789PstI1**. For *iscR*, an 840 bp region spanning its 5' upstream region was amplified, using primers **iscRpS4F** and **iscRpS4R**. The resultant products were each purified, digested with *XbaI* plus *PstI*, and cloned, separately, into pBIO1878. The sequence verified *hemP-lacZ* and *iscR-lacZ* fusion plasmids were named pBIO2117 and pBIO2118 respectively. These plasmids were crossed into *R. pomeroyi* by triparental conjugation as described earlier and the transconjugants were assayed for β -galactosidase after growth in Fe-depleted and Fe-replete MBM minimal medium.

As shown in Figure 4.17, both the *hemP*- and *iscR-lacZ* fusions were expressed at significantly higher level in the Fe-depleted medium than in the medium to which 20 μ M FeCl₂ had been added. However, the factors of increase were much less than had been seen with the *fbp-lacZ* fusions, especially for *hemP*, where the *hemP* fusion was expressed <2-fold more in the -Fe than in the + Fe medium. This was due, largely, to the higher expression of both these fusions in the Fe-replete medium. Note that the absolute levels of expression were considerably greater for the *hemP*- than the *iscR-lacZ* fusion.

Figure 4.17 Effect of iron limitation on expression of *hemP*- and *iscR-lacZ* fusions



Assays were performed on *R. pomeroyi* containing the *iscR-lacZ* and *hemP-lacZ* fusion plasmids *pBIO2118* and *pBIO2117* respectively, after pre-growth in MBM containing 20 μM FeCl_3 (RED BARS) or no added iron (BLUE BARS). Results are averages of three biological and two technical replicates.

4.2 Discussion

The *fbp* genes of *R. pomeroyi* are expressed separately, immediately obvious due to the convergent transcription of each gene. Although the *fbpABC* genes are arranged contiguously in *Vibrio*, the genes still have very different expression patterns, as the RNA levels of each gene differ significantly, *fbpA* is expressed at a much greater level than *fbpB* (Wyckoff *et al.* 2006). This was also clearly true of *R. pomeroyi*, shown via the expression of *lacZ*-fusions. The regulation of each of these two genes was also different, with *fbpA* far more inducible by low iron conditions than *fbpB*.

It is possible that FbpA is capable of binding to extracellular iron and facilitate transport across the outer membrane without the need for a TBDR, as the evidence of (Ferreiros *et al.* 1999) in *Neisseria* show.

However, mutations in the *fbp* genes of *R. pomeroyi* have shown that there must be at least one other system of iron uptake encoded on the *Ruegeria* genome. The bioinformatics predictions made in this work and in (Rodionov *et al.* 2006) did not give any insight into the identity of this transporter.

R. pomeroyi is predicted to lack TonB, or any TBDR. Given that FbpABC of *V. cholerae* is able to enhance growth of TonB⁻ *E. coli* in low iron conditions (Wyckoff *et al.* 2006), it is possible that iron is transported into the cell in ferrous form – possibly via a ferric reductase, where it is internalised through a porin, much like the predicted product of *irpB* (*SPO0087*). Indeed, the bioinformatics study on the *irp* operon of *R. pomeroyi* alludes to fascinating future data on the role of these genes in iron uptake and homeostasis.

The expression of several iron uptake genes - those with an IR box motif upstream, was not completely deregulated in response to site directed mutations made in these motifs. This phenotype must mean another regulator – or regulatory system is controlling these genes. Whether this is via an uncharacterised transcriptional regulator, or a small RNA such as in the case of RyhB (Massé *et al.* 2005), remains unresolved.

The expression of *fbpA* and *irpA* in particular appeared to be highly inducible by low iron, something which was not so apparent from the expression of the *lacZ*-fusions for *fbpB*, *hemP* and *iscR*, although all these genes also had an IR box motif. Perhaps the cognate regulator of these IR boxes has highly specific binding properties, and has simply lost the ability to control these boxes. Bioinformatic searches for such motifs does risk finding ‘pseudo-motifs’ - relics of iron regulation in an ancestral strain.

Chapter 5 - Iron-Responsive transcriptional regulators in *R. pomeroyi* DSS-3

5.1 Introduction

As shown in Chapter 4, two potential (though not ratified) iron uptake systems in *R. pomeroyi* are tightly controlled, and have been shown to be expressed in Fe-depleted condition. This regulation was shown to require IR boxes, as shown by the effects of disrupting these *cis*-acting sequences. As mentioned before, the canonical IR box sequences are similar to those of the “IRO box” which are the target of an Rrf2 family transcriptional regulator, RirA.

A second Fe-responsive transcriptional regulator that is characteristic of the α -Proteobacteria is Irr, which can bind to very different motifs, known as ICE boxes (see above).

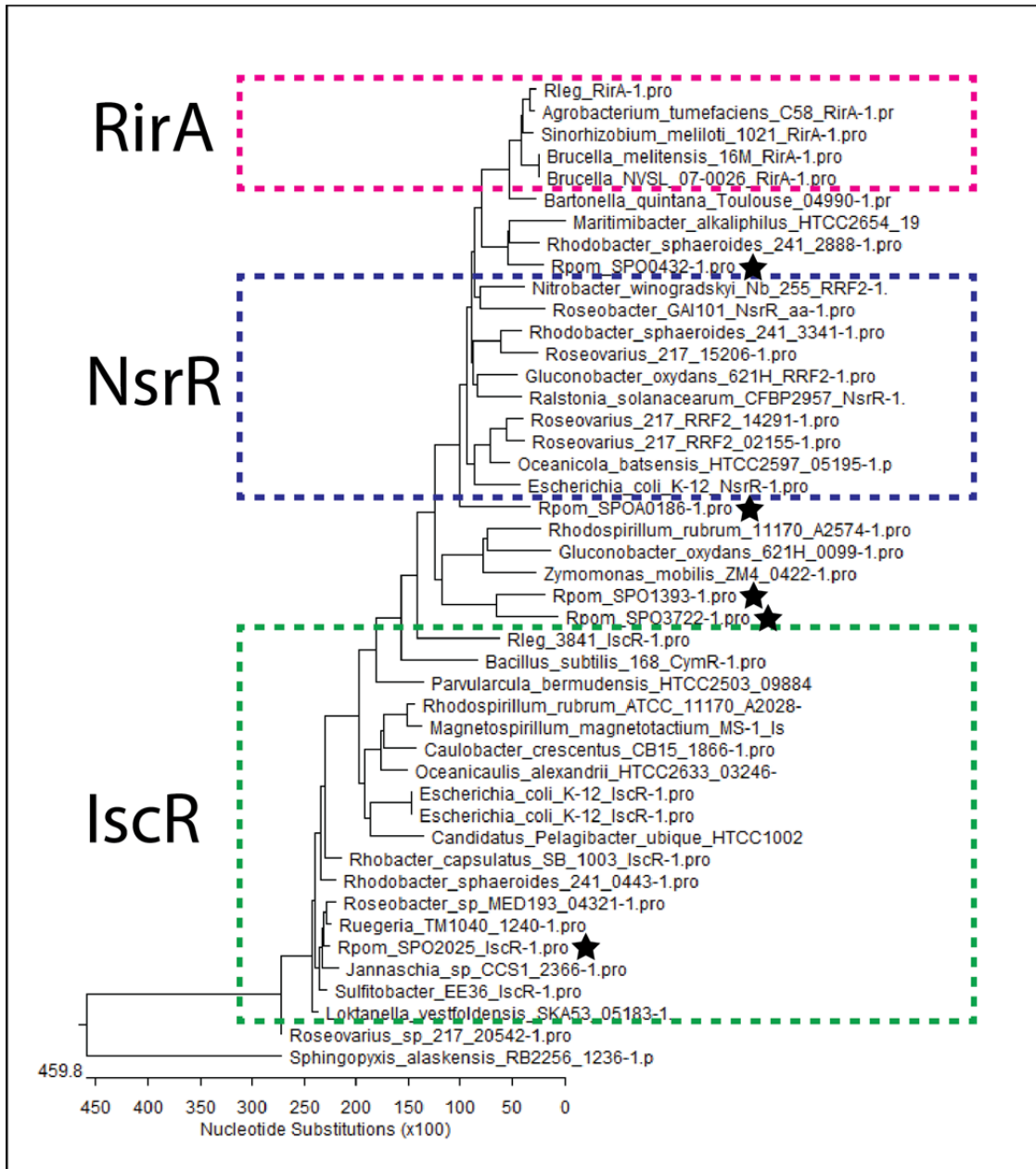
The genome of *Ruegeria pomeroyi* has several genes with products in the Rrf2 family of transcriptional regulators plus one gene that resembles *irr*. This observation, coupled with the fact that this bacterium has motifs that correspond to ICE boxes and to IR boxes, underpins the work described in this chapter, in which evidence was sought to define the roles, if any, of these regulators in iron homeostasis in *Ruegeria*.

5.2 *in vivo* analysis of iron responsive regulators of *R. pomeroyi*

5.2.1 The Rrf2 family of proteins in *Ruegeria pomeroyi* and the *Roseobacters*

A BLASTp search of the proteins encoded by the genome of *R. pomeroyi*, using the *Rhizobium leguminosarum* RirA amino acid sequence (gene locus *RL_0777*) as the probe revealed five members of the Rrf2 family proteins, encoded by the genes *SPO0432*, *SPOA0186*, *SPO1393*, *SPO3722* and *SPO2025*. To show the relationship between the five Rrf2 family proteins and several characterised examples of Rrf2 family transcriptional regulators a phylogenetic tree was made.

Figure 5.1 Phylogenetic tree of Rrf2 family transcriptional regulator peptide sequences



Phylogenetic tree generated using an alignment of peptide sequences of Rrf2 family proteins. Those with a functional annotation are labelled accordingly – RirA, IscR and NsrR (Nitrosative stress response Regulator). Marked with a star are the 5 Rrf2 peptides found in the deduced proteome of *R. pomeroyi*.

As shown in Figure 5.1 and in Rodionov *et al.*, (2006), none of these *Ruegeria* Rrf2 family proteins cluster with the characterised examples of RirA. However, there is a likely candidate for an NsrR-type regulator, the product of *SPOA0186*, and a likely candidate for an IscR-type regulator, the product of

SPO2025. Interestingly, two Rrf2 family proteins (the products of *SPO1393* and *SPO3722*) are not very similar to each other (42% identical), but form something of an out-group of the Rrf2 super-family in this bacterium.

As table 5.1 below shows, only *SPO2025* is present in all the *Roseobacter* genomes. The next most common and indeed the most similar to RirA of *Rhizobium* was *SPO0432*. Proteins homologous to both *SPO1393* and *SPO3722* were only found in *Ruegeria pomeroyi*.

Table 5.1 Prevalence of Rrf2 gene homologues of *Ruegeria* in the Roseobacters

Gene	No. of hits in Roseobacters $1E^{-20}$
SPO0432	26
SPOA0186	10
SPO1393	1
SPO3722	1
SPO2025	38

5.2.2 Construction and analysis of mutations in genes for Rrf2-family proteins in *Ruegeria*

Since there was no obvious candidate that matched RirA *sensu stricto*, it was decided to make insertional mutations in all five genes that encode Rrf2-family proteins and determine if these have any effects on the expression of one or more genes that contain IR motifs. The approach taken was the same as that used to make the *irpA* mutation, above. Thus, fragments internal to each of the five genes were cloned into the suicide plasmid pBIO1879 and these were used to generate insertional mutations into the corresponding chromosomal gene following the introduction of the various mutagenic plasmids into *Ruegeria pomeroyi* J470. The particular primers used to generate the insert fragments for this set of constructions are shown in Table 5.2 below.

Table 5.2 Primer sequences used to generate mutant strains of *R. pomeroyi*.

Primer	Sequence	Plasmid	Mutant
SPO0432EcoF	ATCGGAATTCGCATTACCAAGCGCACAAAT	pBIO2119	J534
SPO0432XbaR	ACGTTCTAGATTATCACAGACCAGCGCATC		
SPO3722F	CACCGAAGGACTGGAATGG	pBIO2120	J535
SPO3722R	ACGTTCTAGATGAGAGCTTTTCCTGAAACCA		
SPO1393F	AGTCGAATTCATTGGGTGACGGGGTAGAG	pBIO2121	J536
SPO1393R	TACGTCTAGAGCCTGGAGATTCTCAAATCC		
SPO2025F	TGACGAATTCGTCGACAAAGGGGCGCTAT	pBIO2122	J537
SPO2025R	AGTCTCTAGATCTTACCACATCCGAAAGC		
SPOA0186F	ACGTGAATTCCTCCAAGTTCTCCGACTATGC	pBIO2123	J538
SPOA0186R	GACTTCTAGACCGGATCGTATTTTGACCTG		

Each of the five recombinant plasmids was ratified by verifying the correct insert, and then crossed into *R. pomeroyi* J470 by tri-parental conjugation. Mutants were selected for using spectinomycin, kanamycin and rifampicin as detailed earlier. Each mutant was checked using Southern blots and/or PCR. The mutant strains with ratified insertions in the five *SPO* genes were named as follows: SPO1393⁻ = J536, SPO3722⁻ = J535, SPO0432⁻ = J534, SPOA0186⁻ = J538, SPO2025⁻ = J537.

Then, into each of these mutants was introduced each of the two transcriptional fusion plasmids containing *fbpA-lacZ* (pBIO1845) and *irpA-lacZ* (pBIO1847). The array of transconjugants were then grown in Fe-depleted and Fe-replete media as described above and assayed for β -galactosidase activity. In no case was the behaviour of either fusion, in either of the growth media markedly different from the case when the wild type strain harboured these plasmids (not shown). Thus, it appears that neither *irpB* nor *fbpA* is under the control of any of the Rrf2 family proteins examined here.

5.2.3 *Ruegeria pomeroyi* *Irr* – a global iron-responsive regulator in other α -proteobacteria

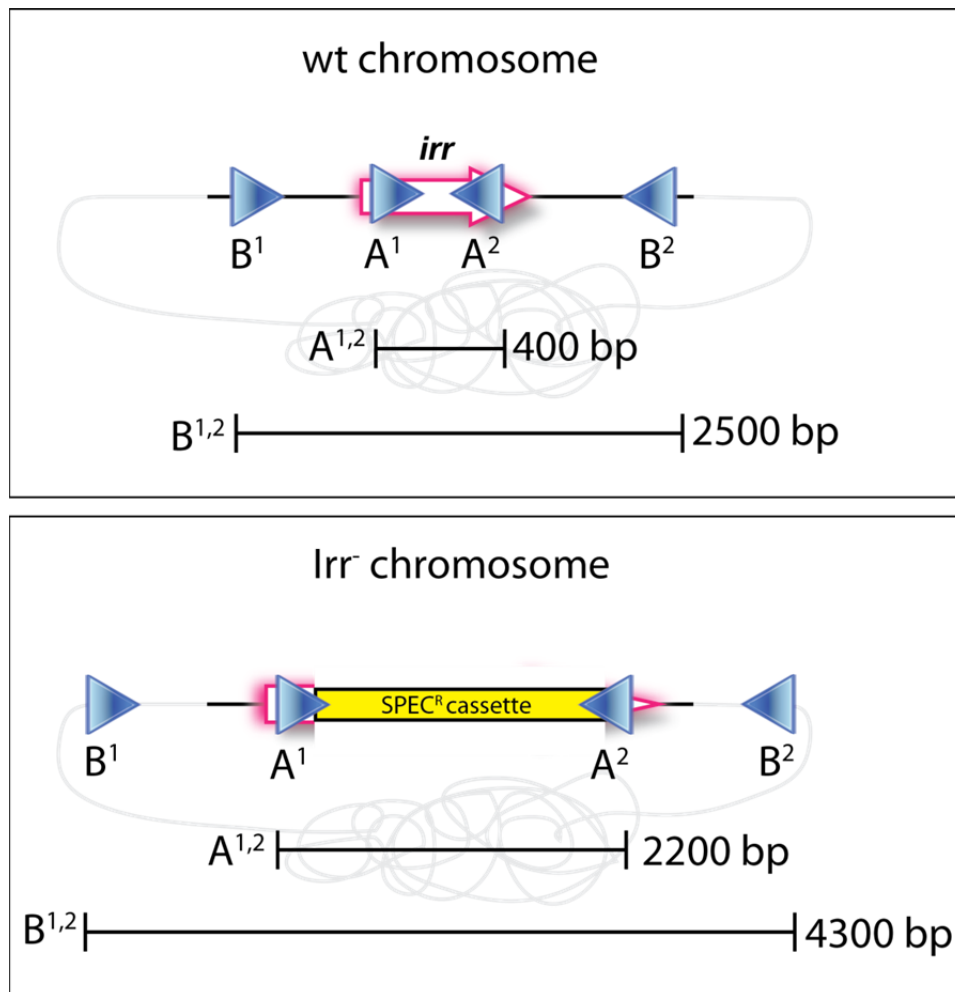
The second, “global” iron-responsive transcriptional regulator that is found in alpha-Proteobacteria is the iron responsive regulator, *Irr*. *R. pomeroyi* has a predicted *irr* gene *SPOA0445*, on its large resident plasmid whose translated product is 57% identical to *Rhizobium* *Irr*. Furthermore, there are ICE boxes in the promoter regions of several genes that are *Irr*-regulated in other bacteria. This

section examines if *SPOA0455* does indeed encode a functional *Irr* regulator that acts on these ICE boxes.

Therefore, an *Irr*⁻ mutant strain was made, using the pEX18Ap delivery system (see Chapter 4, and Material and Methods for the pEX18Ap procedure) to create an insertion into *SPOA0455*. Briefly, a 2.2 kb region that flanked the *irr* coding sequence was amplified from *R. pomeroyi* genomic DNA using standard PCR protocols, and primers **irrflankEcoFWD** and **irrflankHindIIIREV**. This product was digested with *EcoRI* and *HindIII*, and ligated into pEX18Ap, cut using the same enzymes. The ligation products were used to transform *E. coli* 803 competent cells, selecting transformants by their ampicillin resistance. After screening the plasmids from several transformants, one (termed pBIO2113) was confirmed by sequencing to have the correct insert. Into this plasmid was then introduced the 1.8 kb spectinomycin cassette (as detailed in chapter 4) cloned into a *PstI* site that is internal to *irr*, 220 bp downstream of its start codon. Following ligation, transformants of *E. coli* 803 were selected on media containing ampicillin and spectinomycin. Following the usual ratification procedures, one recombinant plasmid, named pBIO2114, was confirmed to have the correct constitution. This plasmid was then mobilised into *R. pomeroyi* and recombinants that were resistant to spectinomycin, but sensitive to ampicillin, were chosen as candidates in which the spectinomycin cassette had recombined into the genomic version of *irr*.

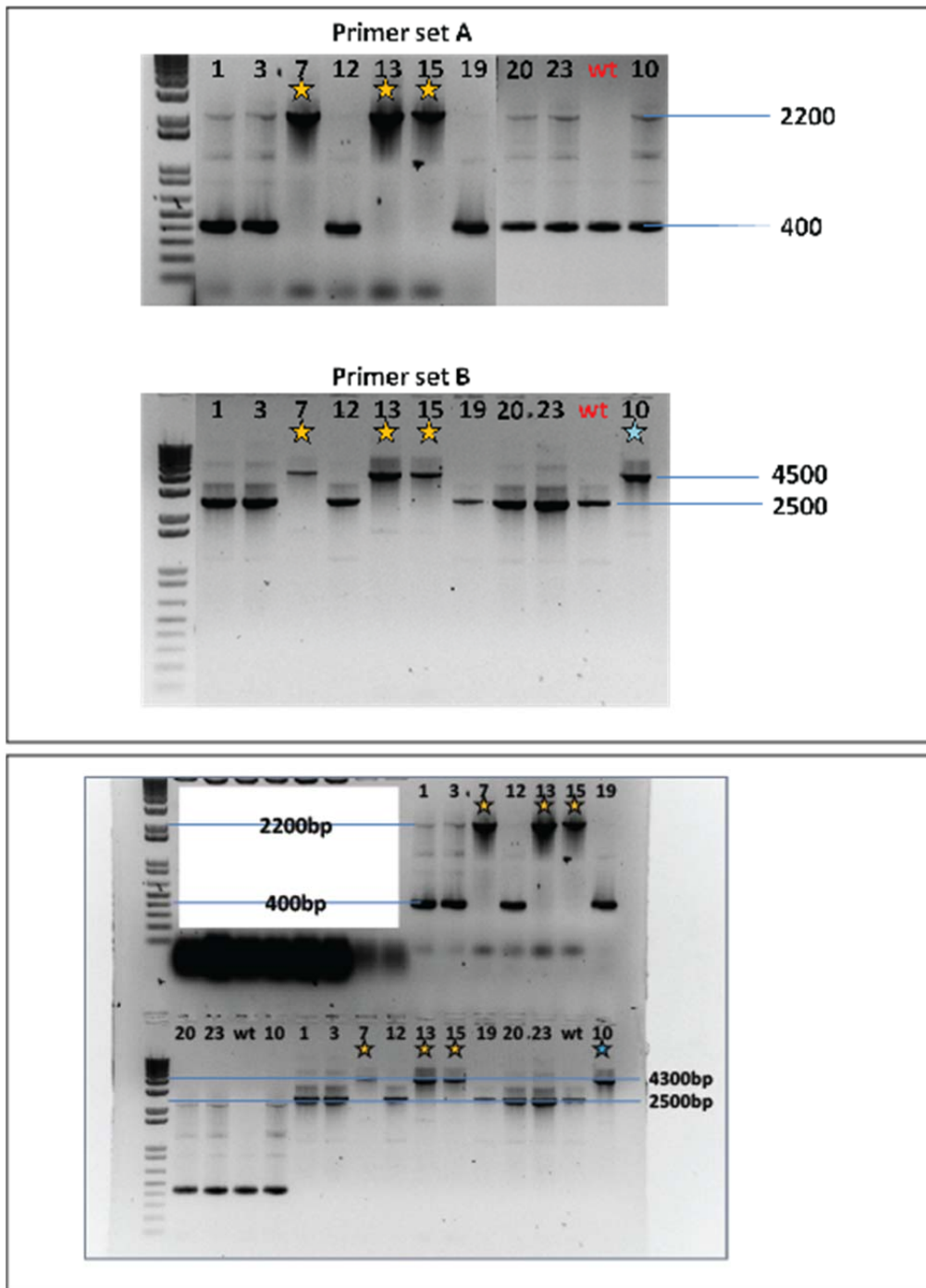
Several potential mutants were tested using two sets of primers that flanked the *irr* gene **Irrflank1F** and **Irrflank2R** (labelled primer set B in Figure 5.2, which amplify a 2.5 kb region in the wild type) and primers which flanked the *PstI* site within the *irr* gene **IrrcheckF** and **IrrcheckR** (labelled primer set A in Figure 5.2, which amplify a 400 bp region in the wild type). Of ten mutants screened, three were correct in both primer sets, and did not make any secondary products. The *Irr*⁻ discussed in this work relates to sample 13 in Figure 5.3, and was renamed J539.

Figure 5.2 Map of *Irr*^r recombinant mutant



Map of irr locus in wild type and Irr^r strain of R. pomeroi showing position of primers used to screen for successful mutation, and showing predicted sizes of amplified products using these primers.

Figure 5.3 PCR screening of potential *Irr*⁻ mutants of *R. pomeroyi*



Upper panel shows the results of electrophoretic separation (1% agarose gel) of PCR products generated using primers which flank a *Pst*I site within the *irr* gene of *R. pomeroyi* (primer set A), and primers which anneal either side of the *irr* gene (primer set B). These primers were used in colony PCR reactions on potential *Irr*⁻ mutants of *R. pomeroyi* (numbered) and the wild type *R. pomeroyi* (wt). Colonies which generated a mutant PCR product without a wild type product are shown with a gold star. The blue star indicates a colony which did not produce a mutant product with both primer sets. The lower panel shows the agarose gel photo without any editing.

5.2.4 Phenotype of *Irr*⁻ mutant of *R. pomeroyi*

It was immediately obvious that colonies and liquid cultures of the *Irr*⁻ mutant strain of *R. pomeroyi* J539 were pigmented, with a brick-red colour. This was particularly pronounced under conditions of iron deficiency, in which the chelating agent dipyriddyI (30 μ M) was added to HY rich medium and was abolished by adding extra (100 μ M) FeCl₃ into HY rich medium.

Previous work in both *Rhizobium leguminosarum* and *Bradyrhizobium japonicum* (Hamza *et al.* 1998) had shown that an *Irr*⁻ strain accumulates Protoporphyrin IX (PPIX), due to constitutive expression of HemB, likely due to an uncoupling of the haem biosynthetic pathway from iron availability.

However, in *R. pomeroyi*, the pigment produced by the *Irr*⁻ strain did not fluoresce under UV light, making it unlikely to be PPIX. Furthermore, attempts to isolate the pigment using acetone (Yeoman *et al.* 1997) were also unsuccessful. The pigment appeared to be a precipitate which was separate from the cell pellet. In support of the red pigment being unrelated to PPIX, the expression of *Rhodobacter sphaeroides hemB* was shown to be unchanged in an *Irr* mutant (Peuser *et al.* 2012). Furthermore, in a microarray study performed as part of this work (see chapter 7) expression of *hemB* of *Ruegeria* {SPO2076} was shown to be unchanged in an *Irr*⁻ strain.

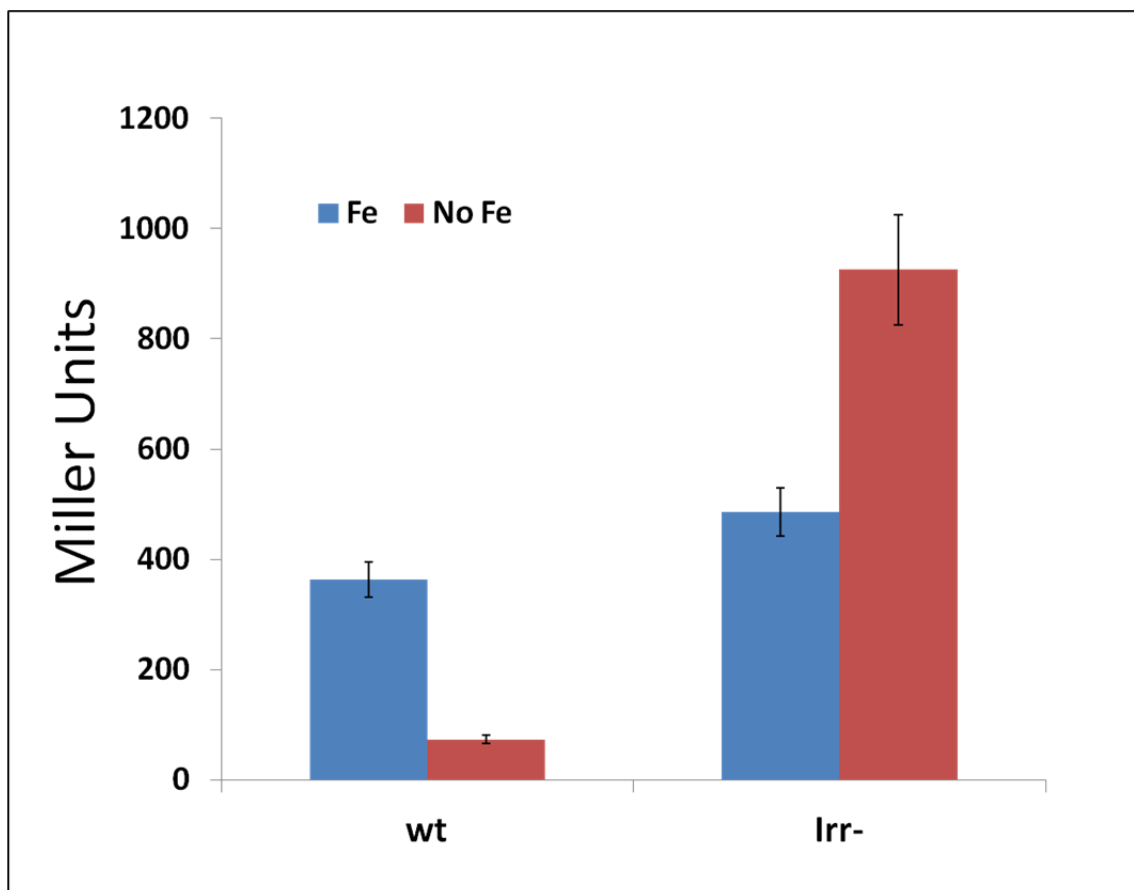
5.2.5 Expression of *mbfA* in the *Irr*⁻ strain of *R. pomeroyi*

The gene SPO0382 (*mbfA*) was predicted to be preceded with an ICE box, and, indeed, a homologue of this gene had been shown to be regulated by *Irr*, in other alpha-proteobacteria, namely *Rhizobium leguminosarum*, *Bradyrhizobium japonicum*, *Agrobacterium tumefaciens* and *Brucella abortus* in *Irr* repressed *mbfA* in Fe-depleted conditions (Martinez *et al.* 2005; Rudolph *et al.* 2006; Todd *et al.* 2006; Ruangkiattikul *et al.* 2012). Furthermore, a homologue of *mbfA* has been shown to be *Irr*-regulated in *Rhodobacter* (Peuser *et al.* 2011).

To test the expression of *mbfA* in *R. pomeroyi*, a fusion of its promoter to the *lacZ* gene in pBIO1878 was made. The primers **MbfApXba1fwd** and **MbfApPst1rev** were used to amplify a 759 bp region that spanned the upstream region of *mbfA*, this was digested with *Xba*I and *Pst*I, and cloned into pBIO1878, to generate pBIO1929. This fusion plasmid was crossed into *R. pomeroyi* by conjugation, and single colonies of purified transconjugants were used to make starter cultures for β -galactosidase assays. As shown in Figure 5.4, in the wild type background, the expression of the

mbfA-lacZ fusion is considerably higher (~5-fold) in the +Fe than the –Fe medium. Strikingly though, in the *Irr*[–] mutant, expression of the fusion was greatly enhanced in both sets of media – indeed, in the absence of *Irr*, the expression is *greater* in the Fe-depleted than the Fe-replete media. This suggests that the *mbfA* promoter is subject to another, as yet unknown, Fe-responsive regulator, whose action is normally masked by the opposing regulatory action of *Irr*.

Figure 5.4 Effect of iron limitation and *irr* on expression of *mbfA* in *R. pomeroyi*



Ruegeria pomeroyi containing the *mbfA-lacZ* fusion plasmid (pBIO1929) were grown in minimal medium (MBM) either supplemented with 20 μ M FeCl_3 (Fe) or not (No Fe) and assayed for β -galactosidase activity, expressed in Miller units. Error bars represent the standard deviation of 2 biological, and three technical replicates.

To confirm that the mutation in *irr* was indeed responsible for the altered expression of the *mbfA-lacZ* fusion, the effects of introducing a wild-type version of *irr* were determined. To do this, a fragment of DNA that contained the entire *irr* gene plus its upstream regulatory sequence was generated by PCR from genomic DNA using the primers **irrCOMPFW**D and **irrCOMPREV**. This

fragment was then cloned (using *Xba*I) into pOT2, another, wide host-range plasmid, which confers resistance to gentamicin and is compatible with pBIO1845, the *lacZ* fusion plasmid. The resulting plasmid, called pBIO1928, was mobilised into the *R. pomeroyi* *Irr*⁻ mutant that harboured the *mbfA-lacZ* fusion plasmid pBIO1929. The expression pattern of β -galactosidase activities were restored to normal, being higher in +Fe than -Fe media, conforming that the mutation in *irr* was indeed responsible for the altered expression of the *mbfA-lacZ* fusion.

5.2.6 Expression of *iscR* in the *Irr* strain of *R. pomeroyi*

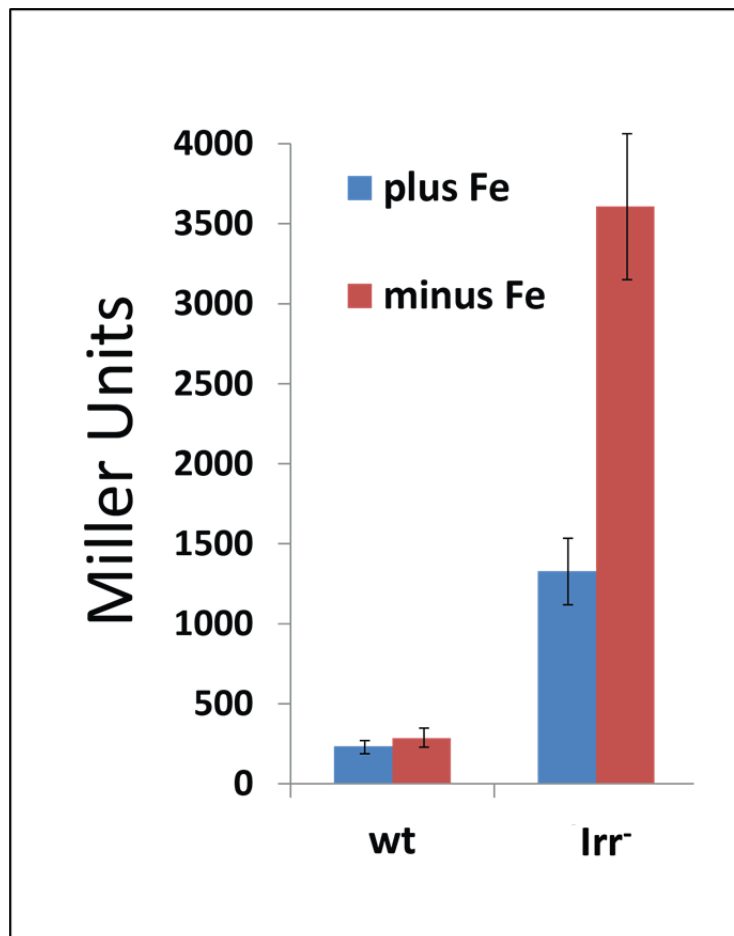
IscR is predicted to regulate the biosynthesis of Fe-S clusters, and indeed is found as part of a *suf* gene cluster in *R. pomeroyi* (see chapter 3 for details).

The potential regulation of IscR in *R. pomeroyi* is intriguing, and leads us to believe that the regulation of the Fe-S synthesis pathway in *R. pomeroyi* is of particular importance to the Fe-homeostasis in this bacterium. There is a motif homologous to the IR box, and a motif homologous to the ICE boxes discussed earlier (see Figure 3.3). This feature has been identified in several proteobacteria (Rodionov *et al.* 2006).

A fusion was made to *iscR* (*SPO2025*) of *R. pomeroyi* described in chapter 4 – pBIO2118. This fusion was crossed into the *R. pomeroyi* strain J470 and the *Irr*⁻ strain J539.

Here, shown in figure 5.5, the expression of *iscR* is clearly hugely deregulated in the *Irr*⁻ background, but is still clearly Fe regulated (~2-fold Fe-repressed).

Figure 5.5 Effect of Fe on a *iscR* fusion in both wild type, and *Irr*⁻ *R. pomeroyi*



Ruegeria pomeroyi containing either the *iscR-lacZ* fusion plasmid (pBIO2118) was grown in minimal medium (MBM) either supplemented with 20 μM FeCl_3 (Iron +) or not (Iron -) and assayed for β -galactosidase activity, expressed in Miller units. Error bars represent the standard deviation of 2 biological, and three technical replicates.

5.3 Discussion

It was clear that *Irr*, one of the recognised global Fe-responsive gene regulators in the alpha-proteobacteria behaves in a conventional way in *Ruegeria pomeroyi* as expected from the canonical systems of the rhizobiales. Further characterisation would be required to ascertain if this *Irr* behaves more like that of *Rhizobium*, or *Bradyrhizobium* in response to haem binding.

The expression of *mbfA* and *iscR* is likely controlled by the recognition of the ICE boxes that precede these genes by *Irr* in Fe-depleted conditions. It would be surprising if the other genes *fssA* and *ccpA*

(*SPO0382* and *SPO0330*) (see Table 3.1) with a conserved ICE box did not respond in a similar way, though this was not examined directly.

Peuser *et al.* (2012) performed a microarray study in the well characterised α -proteobacteria *Rhodobacter sphaeroides*, and showed that repression of *mbfA* in this strain was mediated by *Irr* under low iron conditions. Conversely, a homologue of *iscR* in *Rhodobacter* (*RSP_0443*) was not regulated by *Irr* under high or low iron conditions. This related bacterial species would likely use *Irr* in a similar way to *Ruegeria*, especially as it is likely that *Rhodobacter* was isolated from a marine environment. To further investigate the transcriptome of *Ruegeria*, a transcriptomic experiment was performed as part of this work, including the *Irr*⁻ strain, which adds to this interesting story (see chapter 7).

In contrast, the picture is much less clear concerning the identity of a regulator or regulators that repress genes under Fe-replete conditions. As shown in Chapter 4, there are at least some genes whose expression is massively increased in low-Fe media, including some of those that are predicted – though not confirmed – to be involved in the import of Fe. In most bacterial taxa, these are the types of gene that are repressed by *Fur* and, in the special case of at least some members of the alpha-proteobacteria, by a very different transcriptional regulator, *RirA*.

However, close homologues of *RirA* are confined to *Rhizobium*, and a few close relatives, namely *Sinorhizobium*, *Mesorhizobium*, *Agrobacterium*, *Brucella* and *Bartonella*, so the identity of any analogous regulator in other, alpha-proteobacteria is not immediately obvious. However, the “iron-rhodo” boxes that precede several genes that are expected, *a priori*, to be involved in iron uptake and therefore repressed under +Fe conditions has a similar sequence to that of the IRO box recognition site for the *RirA* regulator (see Figure 3.3). Given the experimentally confirmed importance (see Chapter 4) of the IR boxes, this provides circumstantial, though not cast-iron evidence that the IR boxes are also recognition sites for transcriptional regulators that are in the *Rrf2* family and so would have some similarity to *RirA*. However, this was not supported by the evidence described in this chapter; none of the mutant strains, with insertions in each of the genes that encode *Rrf2*-family proteins in *Ruegeria pomeroyi* was altered in the Fe-dependent repression of those genes (*fbpA* and *irpA*) that have IR regulatory sequences.

Taken together, these findings mean that *R. pomeroyi* may use a novel Fe-responsive transcriptional regulator to regulate genes under the control of *cis*-acting IR boxes. In time, a library of transposon mutants could be created for *R. pomeroyi*, allowing the potential identification of candidate regulators of the IR box, as was performed in *Rhizobium* to identify *RirA* (Todd *et al.* 2002). Here, the authors utilised both an iron regulated promoter-gfp fusion to identify a Tn5 mutant which was

deregulated for *gfp* expression in high iron conditions. This mutant was also shown to produce ~3-fold more vicibactin. Both phenotypes were corrected by using a gene library of *Rhizobium leguminosarum*, and the correcting clone was mapped to finally identify the RirA gene locus.

Of course, there could be functional redundancy in this regulatory network of *Ruegeria*, which would make identifying the regulator of IR boxes a lot more difficult. This may be evident in both the lack of complete deregulation of several of the site-directed mutants in IR boxes, and the lack of phenotype for any single Rrf2 family mutant in *Ruegeria*.

It would be expected that there would be reasonable conservation of the IR box-binding transcriptional regulator in those closely related marine species – the Roseobacters, so a more complete and detailed analysis of potential transcriptional regulators could provide more targets for testing.

These negative results show that the classical-type Fe-responsive transcriptional regulator(s) that represses Fe-uptake genes remain(s) elusive. It is clearly not an Rrf2-type (unless, of course there is redundancy between the five Rrf2 family proteins in *Ruegeria*). We assumed that the regulator would be an Rrf2-type given the similarity of IR and IRO boxes, but this may have been an oversight, there is great similarity between IR, IRO and IscR boxes in the α -proteobacteria, but all have very different and distinct regulons.

Furthermore, the IR boxes are not recognised by the γ -proteobacterial global iron regulator “Fur”, which is actually a Mur – see chapter 6, for Mn responsive regulation.

Without any further target genes identifiable, this work is left for future projects, and would be of great interest, potentially identifying a novel iron-responsive regulator in marine α -proteobacteria. The difference between the RirA-mediated IRO box regulation in *Rhizobium* and what we observe in *R. pomeroyi* is also very exciting. The shift away from the Fur paradigm of *E. coli*, to the Irr/RirA system of *Rhizobium* was an abrupt change in our understanding of iron uptake, and the potential for another such shift is clearly possible here in the marine α -proteobacteria.

Chapter 6_a - Manganese Uptake and Regulation in *R. pomeroyi*

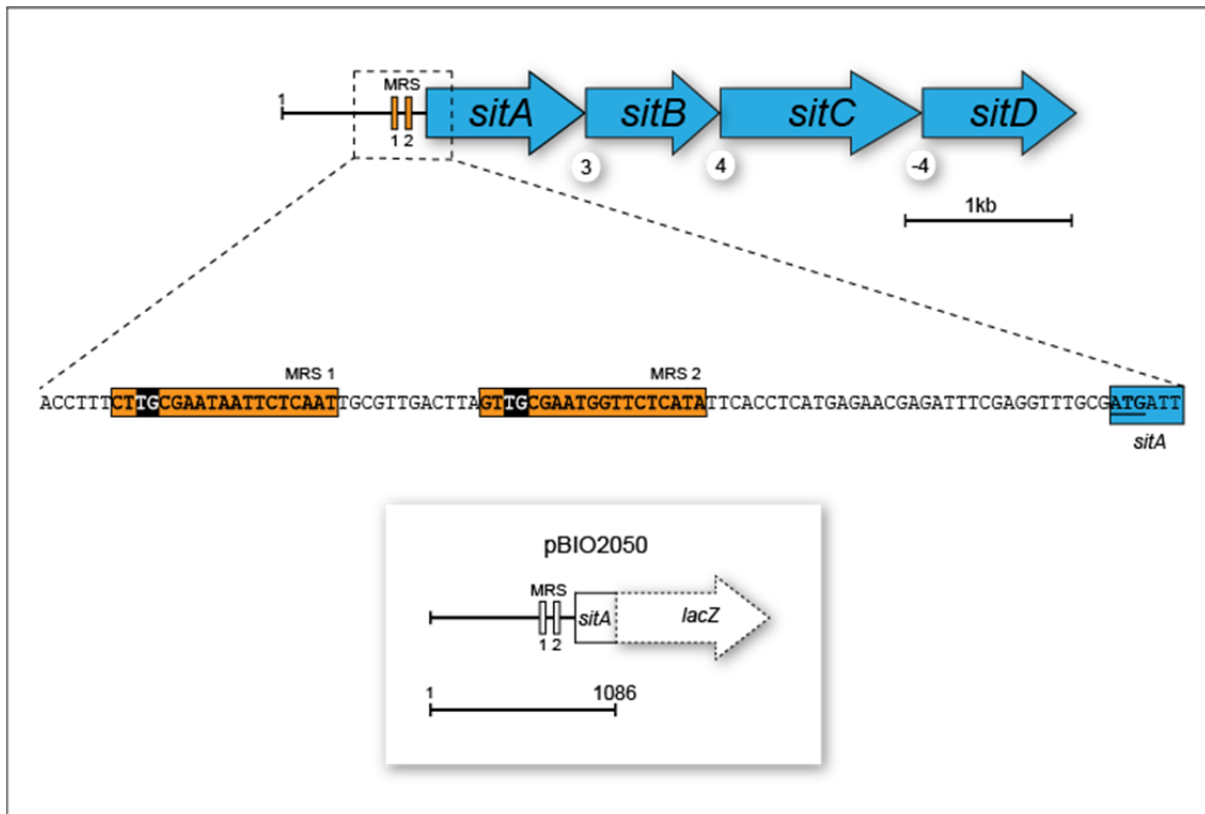
6.1 Introduction

Like iron, manganese is largely biologically unavailable in the marine environment. Bacteria have therefore evolved highly specific transport systems to import this physiologically important metal. Somewhat less studied than iron uptake systems in bacteria, Mn transport has been shown to be tightly regulated in response to both Mn availability and to oxidative stress. Here, I will examine the Mn responsive regulation and uptake of this metal in *Ruegeria*, and further afield.

6.1.1 *Ruegeria pomeroyi* has a homologue of the SitABCD manganese transporter

Inspection of the *R. pomeroyi* DSS-3 genome identified at least two sets of genes with a likely role in Mn uptake (Rodionov *et al.* 2006). One of these comprised the consecutive chromosomal genes *SPO3366*, *SPO3365*, *SPO3364* and *SPO3363*, which are predicted to encode the individual polypeptides that comprise the ABC-class Mn²⁺-transporter SitABCD (Figure 6.1) on the basis of the striking similarity with the corresponding gene products in other bacteria – see below; *sitA* encodes the periplasmic binding protein, *sitB* the ATPase and *sitC* and *sitD* the two inner membrane permease polypeptides. These genes are likely expressed as a single operon from a single promoter upstream of *sitA*. We confirmed that *Ruegeria pomeroyi* *sitABCD* are indeed involved in Mn uptake as follows.

Figure 6.1 Map of the *sit* locus of *R. pomeroyi*



The operon structure of *R. pomeroyi* *sitABCD* is shown, with the sizes of the intergenic gaps indicated, in base pairs, in circles between genes. The “-4” between *sitC* and *sitD* denotes overlap between these two genes, suggestive of translational coupling. The positions of two MRS boxes are shown upstream of *sitA*. The sequence of this upstream region is shown as the zoomed (dotted lines) region. Bases targeted for site-directed mutagenesis in the two MRS boxes are shaded black. The start codon of *sitA* is shown in blue, and underlined. The inset shows the dimensions of the 1086 bp cloned DNA in the *sitA-lacZ* fusion plasmid pBIO2050.

6.1.2 The expression of *sitABCD* responds to manganese levels

In order to study the regulation of *sitABCD*, a 1086 bp region spanning the predicted regulatory region of this operon, and extending into *sitA* itself was cloned into the wide host-range *lacZ* transcriptional fusion plasmid pBIO1878, generating pBIO2050 (Figure 6.1). To do this, oligonucleotide primers **SitAF2** and **SitAR2** were used to amplify the insert DNA, using *R. pomeroyi* gDNA as a template in a standard PCR reaction. This PCR product was purified and digested using *Xba*I and *Pst*I, as was the vector pBIO1878. These were ligated together and used to transform *E. coli* 803 competent cells. Transformants were purified on selective LB agar medium (containing

spectinomycin and tetracycline as detailed before). A single transformant was used to purify the recombinant plasmid, which was checked for the presence of an insert and sequence-verified.

The resultant plasmid, pBIO2050, was crossed into *R. pomeroyi* by conjugation and the purified transconjugant strain was used to conduct β -galactosidase assays. The cells were grown in MBM or in MBM to which extra MnCl_2 (20 μM) had been added. In both media, the fusion was expressed at barely detectable levels, which was surprising, since it had been anticipated that the *sitABCD* promoter would be expressed at higher levels in the Mn-deficient medium, not least because there were two convincing MRS regulatory sequences upstream of *sitA*.

It was then realised that a component of MBM is a proprietary blend of sea salts from Sigma, the recipe of which is unavailable. It was plausible that these sea salts contained sufficient levels of Mn to repress *sitABCD*, even with no addition of MnCl_2 . Therefore, a new, defined “sea salts” cocktail, termed Rob’s Sea Salts (RSS), was devised. It was designed to comprise a mix of magnesium, calcium, sodium and potassium that resembled those in natural seawater, with the exception of manganese, which was deliberately omitted. The constitution of RSS is shown in the Materials and Methods (Chapter 9).

The experiment above was therefore repeated, but this time using RSS as the background medium, to which extra MnCl_2 was added, or not. In this case, it was found that the expression of the *sitA-lacZ* fusion was 16-fold higher in the cultures that lacked Mn (789 Miller Units) than when 20 μM MnCl_2 was present (42 Miller Units), shown in Figure 6.4. Thus the expression of *sitABCD* was repressed in Mn-replete conditions, as expected by the precedents seen in other bacteria that contain these genes (Diaz-Mireles *et al.* 2004; Platero *et al.* 2004).

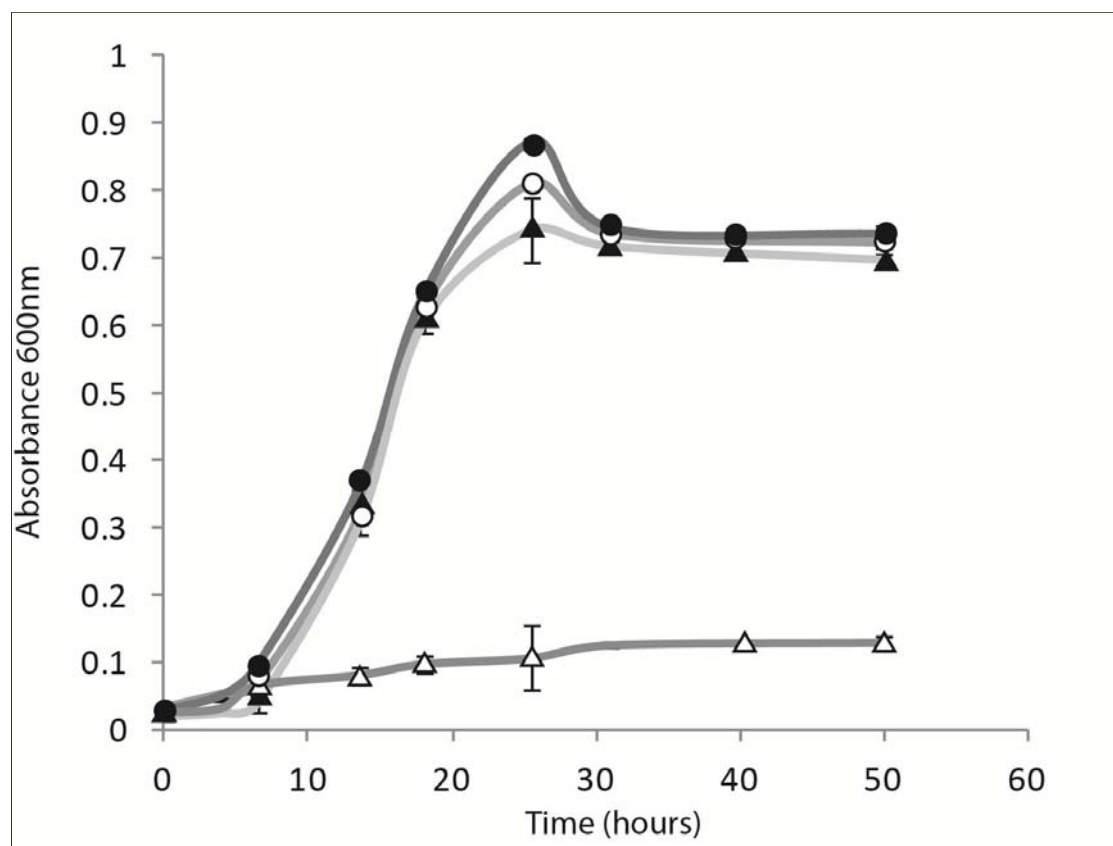
6.1.3 A *SitA* strain of *R. pomeroyi* requires manganese for growth

The wild type *R. pomeroyi* DSS-3 does not show any growth limitation when Mn is excluded from the medium, as shown in Figure 6.2. If *SitABCD* is the only Mn-specific transporter encoded by the *R. pomeroyi* genome, as predicted bioinformatically, and by Rodionov and colleagues (2006), then a deletion mutant should have a growth phenotype during Mn limitation. To test this, a *SitA* mutant was made using the pK19mob derivative pBIO1879, into which a fragment of *SitA*, >100bp from each end of the coding sequence was cloned into pBIO1879, generating pBIO2124. This was sequence verified and crossed into *R. pomeroyi* J470 by conjugation. Successful single recombinant mutants

were screened as detailed before, selecting for Spec^R and Kan^R colonies. These were purified and checked by PCR.

Cultures of wild type *R. pomeroyi* and J529 were grown at 28°C for two days before being diluted 1:100 into RSS medium with or without added Mn (as with MBM minimal medium experiments, succinate was added at 10 mM, and vitamin solution {1:1000} was added to all cultures, refer to Material and Methods, chapter 9). As shown in Figure 6.2, growth of the SitA⁻ strain J529 was deficient in growth without added Mn.

Figure 6.2 Effects of mutating *Ruegeria pomeroyi* *sitA* on growth in manganese-depleted media



Cultures of *R. pomeroyi* DSS-3 wild-type (circles) or the *SitA* mutant J529 (triangles) were diluted, in triplicate, into RSS minimal media that either lacked (open symbols) or contained (filled symbols) added 20µM MnCl₂. Growth at 28°C, with shaking, was monitored by measuring absorbance at 600nm.

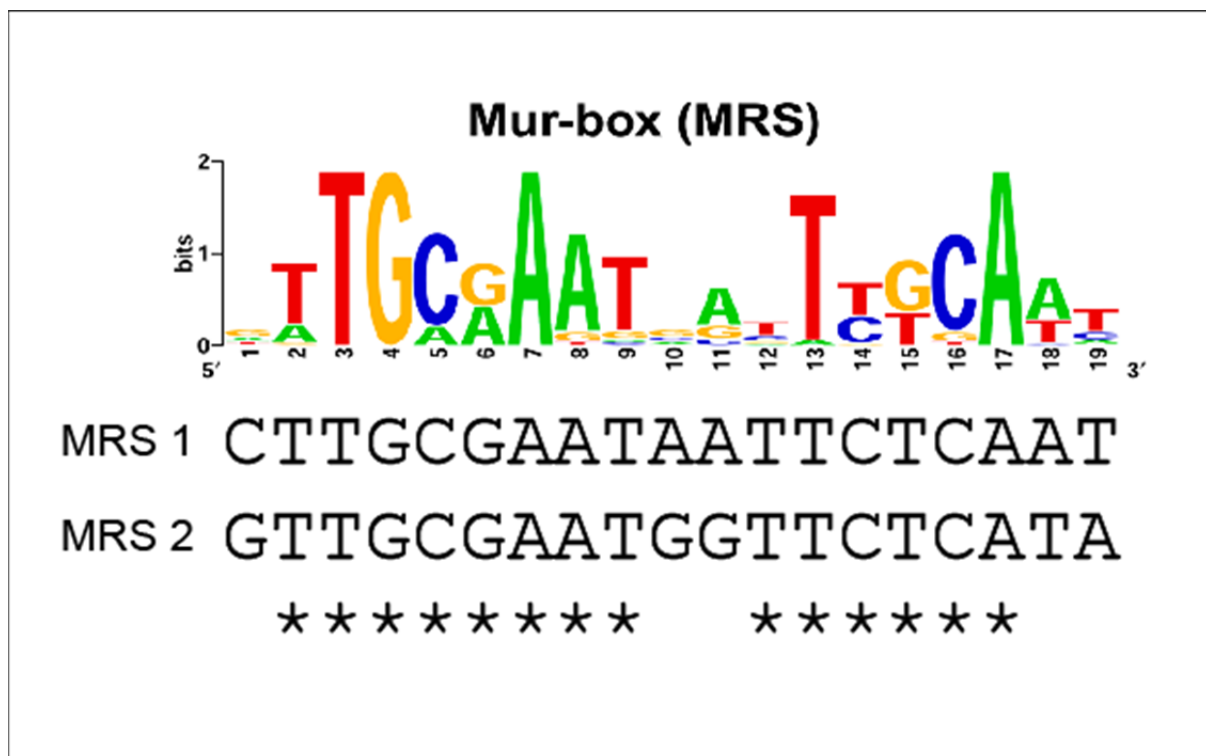
As shown in Figure 6.2 above, the SitA⁻ strain J529 was unable to grow well without added Mn, but addition of 20 µM MnCl₂ restored growth to that of the wild type, which grew well irrespective of

the addition of extra MnCl₂. Thus, the SitABCD polypeptides do indeed appear to constitute a very effective manganese import system.

6.1.4 Two cis-acting motifs regulate expression of sitABCD

Rodionov *et al.* (2006) identified canonical target sequences upstream of predicted and ratified Mn-regulated genes in various α -Proteobacteria, including several members of the Rhodobacteraceae, including *R. pomeroyi* DSS-3. These 19 bp “Mur recognition sequences” (MRS) have dyad symmetry, and are the targets for the Mn²⁺-responsive transcriptional regulator Mur (Figure 6.3).

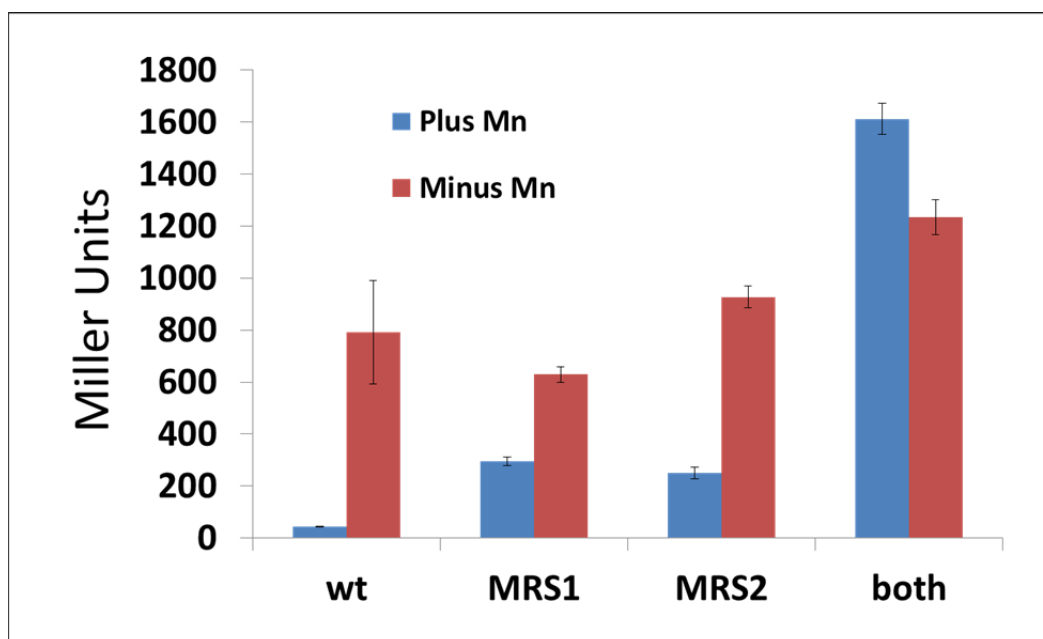
Figure 6.3 Mur-box (MRS) of the Rhodobacteraceae and an alignment of the two MRS boxes upstream of *sitA* in *R. pomeroyi*



Top: logo of the Rhodobacteraceae MRS consensus sequence (Rodionov et al., 2006). Below: sequences found 5' of sitA of R. pomeroyi. Identical bases in the two MRS motifs are marked with a star.

There are two such MRS boxes centred 75 and 45 bps upstream of the ATG translational start of *R. pomeroiyi sitA*, termed MRS1 and MRS2 respectively (Figures 6.1, and 6.3). To establish the effects (if any) of these potential *cis*-acting elements on transcription of *sitA*, site-directed mutants within each of them were constructed. To do this, the highly conserved TG motif, found at position 3 and 4 within the 19 bp MRS box, and highlighted in Figure 6.1, was replaced with AA, using the Agilent Quikchange lightning mutagenesis kit. Briefly, the plasmid pBIO2050 was used as a template for mutagenesis, and the mutagenic primers **MRS1sdmF**, **MRS1sdmR**, **MRS2sdmF** and **MRS2sdmR** were used to mutate both boxes separately, and then to create a plasmid in which both boxes contained the TG → AA mutation. Following sequence verification, three new plasmids were named: MRS1 mutant, pBIO2100, MRS2 mutant pBIO2101 and both, pBIO2102. These were each crossed into *R. pomeroiyi* J470 by conjugation and the resultant transconjugants were assayed for β-galactosidase activity in both Mn replete (20 μM) and Mn limited (no addition) conditions in RSS minimal medium. The results of these assays are shown in Figure 6.4.

Figure 6.4 β-galactosidase activity of *sitA-lacZ* fusion in *R. pomeroiyi* and the effect of mutating the MRS boxes



The wild type sitA-lacZ fusion plasmid pBIO2050, or derivatives (respectively pBIO2100, pBIO2101 and pBIO2102) containing mutations in the MRS1 or MRS2 or in both regulatory sequences were introduced into wild type R. pomeroiyi DSS-3. The transconjugants were grown in RSS minimal medium either without Mn or with 20μM MnCl₂ added. Data shown represent two biological and three technical replicates.

Compared to the wild type fusion, the mutation in the upstream MRS1 caused a ~7-fold increase in β -galactosidase activity in Mn-replete conditions, but was little changed under Mn-limitation. Similarly, the mutation in MRS2 caused a ~6-fold higher expression of β -galactosidase than the wild type in Mn-replete conditions (Figure 6.4). The fusion plasmid with mutations in both MRS1 and MRS2 was deregulated even further, under both Mn replete (38-fold) and Mn-depleted (1.5-fold) conditions. Thus, both MRS1 and MRS2 contribute to the Mn-responsive, Mur-dependent repression of the *sitABCD* operon, as had been seen in other bacteria, such as *Rhizobium leguminosarum* (Diaz-Mireles *et al.* 2004).

6.1.5 Mur regulates *sitABCD* in *Ruegeria pomeroyi*

The predicted regulator of MRS boxes is the Fur-family transcriptional regulator Mur. There is a good Mur homologue in *R. pomeroyi*, encoded by the gene *SPO2477*, whose product is 67% identical to Mur of *Rhizobium leguminosarum*, which has been shown to regulate *sitA* in that species (Diaz-Mireles *et al.* 2004; Diaz-Mireles *et al.* 2005). To demonstrate the effects of *R. pomeroyi* Mur on the expression of *sitA*, an insertion mutant in the *mur* gene was made, using single recombination of the pK19*mob*-derived pBIO1879 into the *mur* locus. Briefly (see Figure 4.15 for the procedure used), primers **FURFwd** and **FURRev** were used to generate a PCR product that was internal to the coding sequence of *mur* of *R. pomeroyi*. This 231 bp fragment was ligated into pBIO1879 following digestion with *Xba*I and *Bam*HI. The resultant recombinant plasmid was purified, sequence-verified, and named pBIO1861. This was crossed into *R. pomeroyi* J470 by conjugation, and derivatives in which pBIO1861 had inserted into *mur* via a single resultant single recombination mutant colonies were selected using rifampicin, spectinomycin and kanamycin as described earlier and in Materials and Methods. The insertion into the *mur* gene was verified by Southern blot, performed as detailed earlier and the Mur⁻ mutant strain was named J528. The *sitA-lacZ* fusion plasmid pBIO2050 was then crossed into the Mur⁻ *R. pomeroyi* strain J528 and β -galactosidase assays were performed in cultures grown in Mn, or without, as detailed earlier.

Table 6.1 The effect of a Mur⁻ mutation on the expression of a *sitA-lacZ* fusion.

	WT <i>sitA-lacZ</i>	Mur ⁻ <i>sitA-lacZ</i>
Plus Mn	42±1	1736±178
Minus Mn	791±30	1817±204

The wild type sitA-lacZ fusion plasmid pBIO2050 was introduced into wild type and Mur⁻ mutant Ruegeria pomeroyi DSS-3 recipients. Transconjugants were grown in media that either did or did not have added MnCl₂ before assaying β-galactosidase in triplicate. Activities are shown in Miller Units, with standard errors.

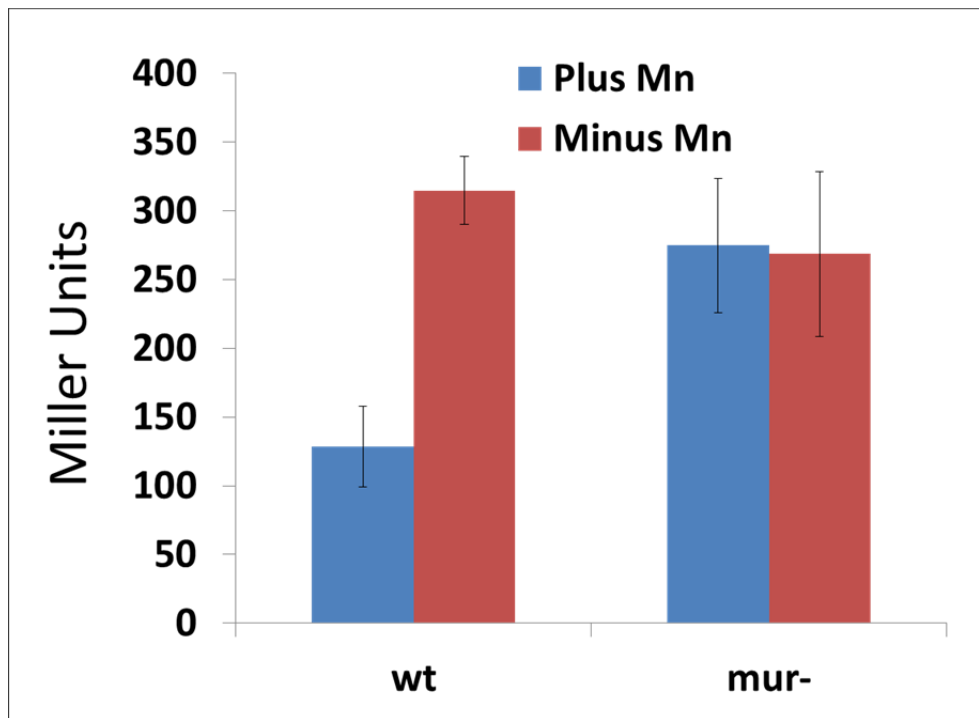
As shown in table 6.1, the Mn-dependent repression of the *sitA-lacZ* fusion was completely abolished in the Mur⁻ background, just as was noted when the two MRS boxes had been mutated, in plasmid pBIO2102 (see above). Thus, Mur is required for the Mn-dependent repression of *sitA* in *R. pomeroyi*.

6.1.6 Mur regulates another Fur-family transcriptional regulator, *irr* in *R. pomeroyi*

There is a predicted *irr* gene (*SPOA0445*) on the large plasmid of *Ruegeria pomeroyi*. Interestingly, this gene has a predicted MRS sequence (Rodionov *et al.* 2006), suggesting that it might be regulated in response to Mn²⁺ availability, via the action of the Mur regulator. Both these predictions were verified as follows. An *irr-lacZ* transcriptional fusion was made, using a 198 bps DNA fragment that spanned the predicted transcriptional start of the *irr* gene, and covered the entire intergenic region upstream of *irr*. This amplified region was cloned into the promoter-probe plasmid pBIO1878. The resultant *irr-lacZ* fusion plasmid was sequence-verified and named pBIO2125. It was then crossed into *R. pomeroyi* J470, and into the Mur⁻ strain J528 as described before, and single colonies of transconjugants were used to inoculate RSS medium either lacking Mn, or containing 20 μM as detailed earlier. These cultures were assayed for β-galactosidase activity. As shown in Figure 6.5 the *irr-lacZ* fusion is repressed ~2-fold by growth in the presence of added 20μM MnCl₂. in the wild type

background. However, this Mn-dependent repression was completely absent in the *Mur*⁻ background, with constitutive expression of *irr-lacZ* in both Mn conditions.

Figure 6.5 Effects of Mn-limitation of the expression of the *irr-lacZ* fusion



The irr-lacZ fusion plasmid pBIO2125 was crossed into both the wild type and the Mur⁻ R. pomeroyi strains. Transconjugants were grown in RSS medium with or without added 20μM MnCl₂. The β-galactosidase levels were assayed and shown as the means of two biological and three technical replicates.

Chapter 6_b - Manganese uptake in other Marine Bacteria

6.2 Diversity of *mur*, *sitABCD* and other genes involved in Mn uptake and sensing in the Roseobacters

6.2.1 *Mur*

Inspection of the genomes of 37 other Roseobacters showed that none of them contained a MntR-type transcriptional regulator, but that all of them contained at least one gene whose product was within the Mur branch of the Fur super-family. However, we discerned different sub-types of these Mur polypeptides, judged by their sequences in different strains and species (Table 6.2). In most Roseobacter strains, the Mur polypeptide closely resembles (>70% identical) that of *R. pomeroyi* DSS-3 (above). However, those of *Sulfitobacter*, *Citreicella*, *Pelagibaca*, and one strain (GAI101) of *Roseobacter* are only ~40% identical to that of *R. pomeroyi*, with those of *Sulfitobacter*, *Pelagibaca bermudensis* and *Roseobacter* GAI101 being very similar to each other. *Citreicella* Mur is very similar (65% identical) to that of *Sinorhizobium meliloti*, a ratified manganese-responsive regulator in that species (Platero *et al.* 2007). Finally, one Roseobacter strain, *Octadecabacter antarcticus* 307, had two Mur polypeptides; one resembled that in *Ruegeria pomeroyi* and the other is of the *Sulfitobacter/Roseobacter* GAI101 type. These different sub-types of Mur are seen in a relatedness tree, which also includes Mur polypeptides from other bacteria (Figure 6.6).

Figure 6.6 Phylogenetic tree of Mur peptides in the α -proteobacteria

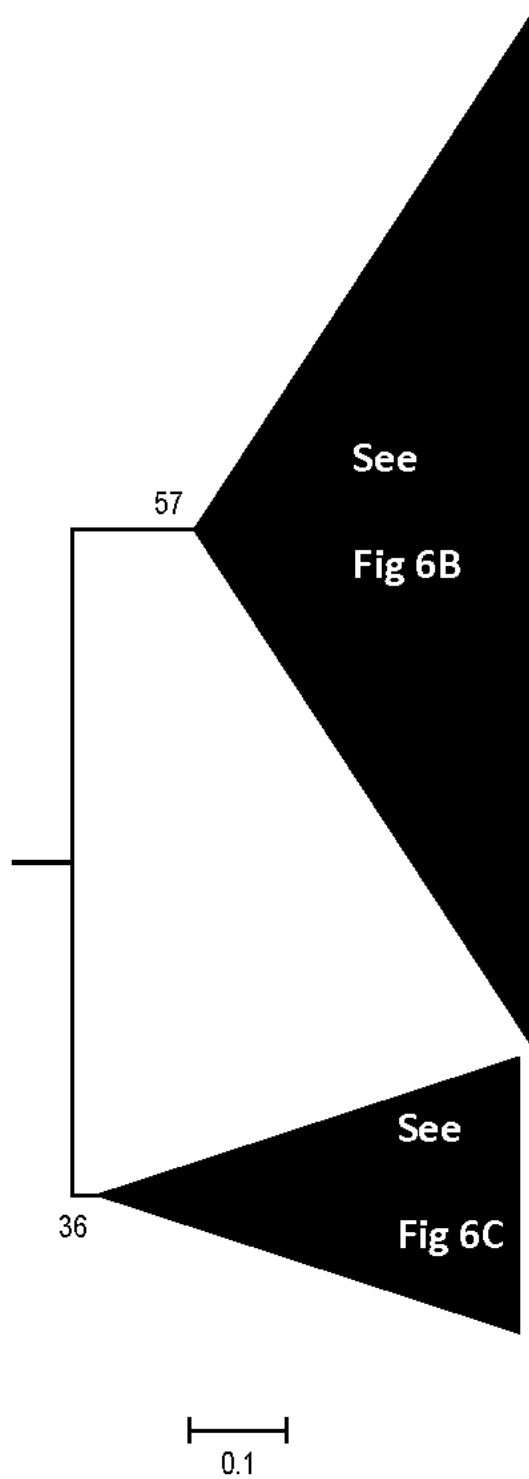


Figure 6.6B

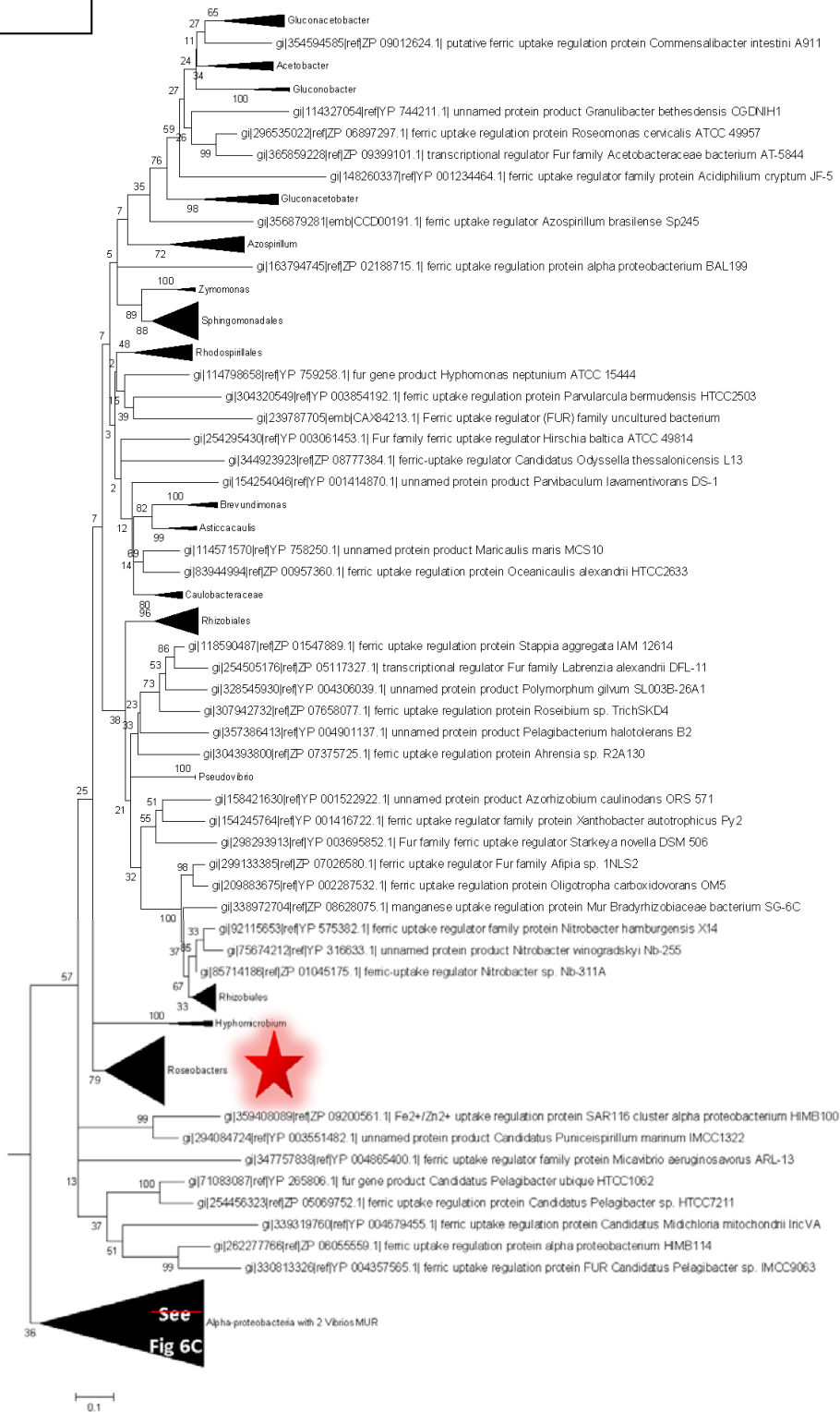
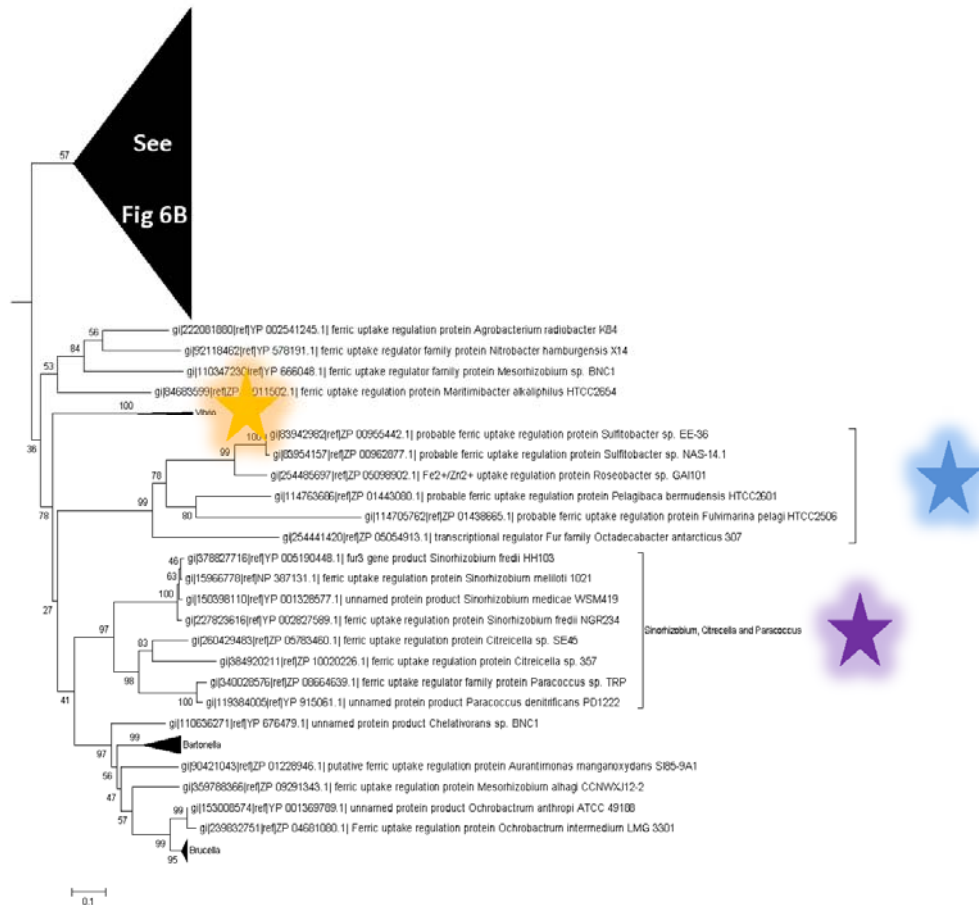


Figure 6.6C



Mega 5 was used to construct a neighbour-joining tree of the Mur polypeptides of the alpha-proteobacteria.

Figure 6a) shows that there are two sub-groups, which are shown in detail in 6b and 6c.

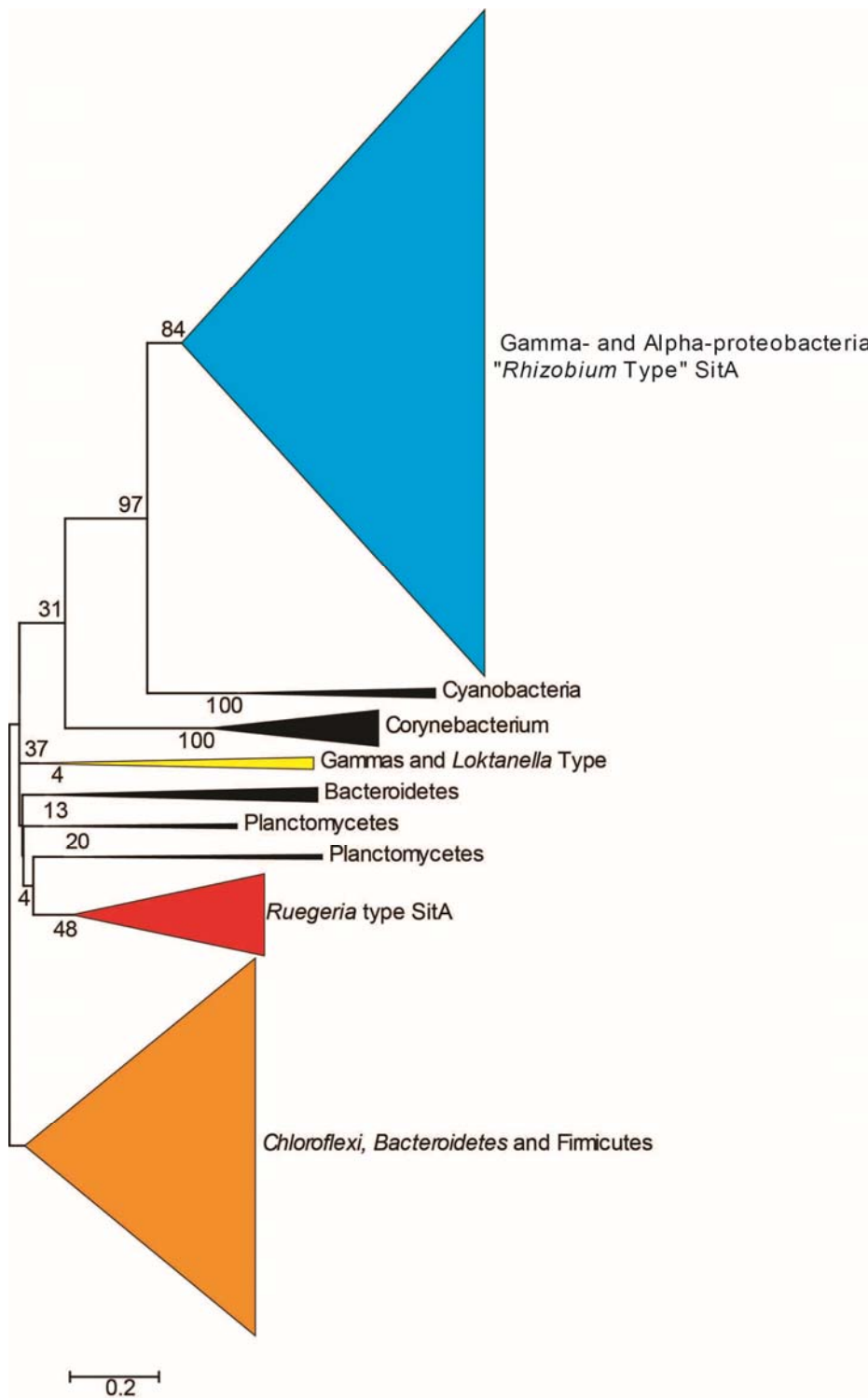
6b) the triangle marked with the red star includes Mur of Ruegeria pomeroyi and contains the other closely related polypeptides.

6c) the close relationship of the Murs of Citreicella to those of Sinorhizobium is demonstrated (purple star), these being also similar to Mur of Roseobacter sp GA101, Pelagibaca bermudensis HTCC2601, Sulfitobacter and one of those in Octadecabacter antarcticus 307 (blue stars). Note, too, the two Mur-like polypeptides in Vibrio strains Vibrio sinaloensis DSM 21326 and Vibrio caribbenthicus ATCC BAA-2122 (Orange star).

6.2.2 SitABCD

This ABC-type transporter is also widespread in the Roseobacters, with all but four strains (see below) containing the corresponding four genes, arranged contiguously (Table 6.2). Closer examination of the sequences of SitA, SitB, SitC and SitD showed that in most strains, these closely resemble (~70% identical) those in *R. pomeroyi* DSS-3 itself (Table 6.2). Several other Roseobacters contained a somewhat distinct version of the SitABCD polypeptides, which were very similar to each other in the different strains (~77% identity) but less so (40-50% identity) to those of the *R. pomeroyi* group (Table 6.2). This second sub-class of Roseobacter SitABCD polypeptides closely resembled (~75% identical) those of various strains of *Rhizobium*, *Sinorhizobium* and *Agrobacterium*, and other bacteria, whose function as manganese transporters has been ratified (Davies and Walker 2007; Diaz-Mireles *et al.* 2004). Finally, the SitABCD polypeptides of *Loktanella vestfoldensis* SKA53 are somewhat divergent from those homologues in all the other Roseobacters and more closely resembles deduced SitA-like polypeptides in two other species of marine bacteria, *Halomonas elongata* and *Pelagibacterium halotolerans*. A phylogenetic tree was drawn, using an alignment of SitA peptides closely homologous to both the *Rhizobium* type, and the *Ruegeria* type, and is shown in Figure 6.7. Peptide sequences homologous to SitB, SitC and SitD always showed very similar phylogenetic relationships.

Figure 6.7 Phylogenetic tree of SitA-like peptides



Using Mega5, a tree of SitA peptides, identified due to their homology to peptides from Ruegeria pomeroyi and from Rhizobium leguminosarum was constructed using the neighbour-joining method, bootstrap values are shown for 500 replicates performed.

It was noted that all those *Roseobacter* strains that had a form of the Mur polypeptide that did not closely resemble that of *Ruegeria pomeroyi* (see above) also had SitABCD polypeptides that were somewhat divergent from those in that species (Table 6.2). However, some strains with the “non-*R. pomeroyi*” version of SitABCD (e.g. *Dinoroseobacter shibae*) did have the “conventional” form of Mur that resembles that of *R. pomeroyi* (Table 6.2).

Although the SitA polypeptides may be of different sub-classes, all the corresponding *sitA* genes are preceded by sequences that strongly resemble MRS motifs, indicating that they are regulated in a similar fashion, via the Mur transcriptional regulator (Figure 6.8).

Figure 6.8 Comparison of MRS sequences that precede the *sitA* and *mntX* genes of selected *Roseobacter* strains

<i>Ruegeria pomeroyi</i> DSS-3	<i>sitA</i> MRS1	-35 bp	TCACCTTT	CTT*G*CG*AA*TA*AT*TC*CA*AT	TGC GTTGA
	<i>sitA</i> MRS2	-66 bp	TTGACTTA	GTT*G*CG*AA*TG*GT*TC*CA*TA	TTCACCTC
<i>Citricella</i> SE45	<i>sitA</i> MRS1	-119 bp	CACATCGA	AA*T*G*CG*AA*CT*G*AG*TT*G*CA*AT	TGTCAACT
	<i>sitA</i> MRS2	-148 bp	TCAACTCA	CTT*G*CG*AA*GT*CA*TT*G*CA*AC	AGGACCTT
<i>Roseobacter denitrificans</i> OCh 114	<i>sitA</i> MRS1	-56 bp	GAACTTTT	AT*G*CG*AA*TG*CT*TC*G*CA*AC	TGCATTGA
	<i>sitA</i> MRS2	-84 bp	GCATTGAC	CTT*G*CG*AA*CG*AT*TC*CA*AT	ATCAATCT
<i>Loktanella vestfoldensis</i> SKA53	<i>sitA</i> MRS	-137 bp	TAAAAACA	GTT*G*CG*AA*CG*CT*TC*CA*AT	TGCATATA
<i>Roseovarius nubinhibens</i> ISM	<i>mntX</i> MRS	-46 bp	TTCCTGCA	AT*G*CG*AA*TT*AT*TC*CA*AT	TGCACCTC
<i>Oceanicola granulosis</i> HTCC2516	<i>mntX</i> MRS	-43 bp	TATGTGCA	AT*G*CG*AA*TT*AT*TC*G*CA*AT	TGCATCGG
<i>Rhodobacterales bacterium</i> HTCC2255	<i>mntX</i> MRS	-37 bp	AATTTCTA	CTT*G*CG*AA*TAG*TT*TC*CA*AT	TGCATTAG

The sequences of the ratified MRS1 and MRS2 motifs of *Ruegeria pomeroyi* were compared, using MEME (Bailey and Elkan 1994), with those that preceded different sub-classes (see Table 6.2) of the *sitA* and *mntX* genes in a selection of *Roseobacter* strains. Conserved bases in these motifs are denoted by asterisks. Distances, in base pairs, from the gene-proximal end of the MRS box to the corresponding ATG start codons are shown.

6.2.3 The Mn^{2+} specific transporter *MnH* is also found in the *Roseobacters*

Two *Roseobacter* strains, *Ruegeria* sp. TrichCH4B and *Citricella* sp. 357, contain a gene (SCH4B_0376 and C357_18417 respectively) whose product resembles MntH, a very different Mn^{2+} transporter, being ~50% (E value $1e^{-120}$) identical to *E. coli* MntH. These two *mntH* genes were both preceded by convincing MRS boxes, strongly suggesting that they, too, are regulated by Mur, in response to Mn^{2+} availability (Figure 6.8). Note that *Ruegeria* sp. TrichCH4B contains both MntH and

SitABCD, whereas in *Citricella* sp. 357, MntH is its *only* recognisable manganese transporter (Table 6.2).

Table 6.2 Distribution of sub-types of the SitA, MntX, MntH and Mur polypeptides in genome-sequenced Roseobacter strains

In-fills with the same colours represent polypeptides that closely resemble each other. In the case of the SitA, B, C and D polypeptides, all four components of this transport system showed a coherent relatedness pattern; thus all four polypeptides of (e.g.) Sulfitobacter were most similar to those in strains (e.g. Octadecabacter) with the same in-fill pattern. Empty boxes represent absence of the corresponding polypeptide. Note that Octadecabacter antarcticus 307 has two Mur sequences, one resembling that in most of the Roseobacters (Including Ruegeria pomeroyi) and one that is similar to those in Sulfitobacter, Pelagibaca and Roseobacter GAI101.

Gene Name Species	<i>sit</i> ABCD	<i>mnt</i> X	<i>mnt</i> H	<i>mur</i>
<i>Citricella</i> SE45				
<i>Citricella</i> sp. 357				
<i>Dinoroseobacter shibae</i> DFL 12				
<i>Jannaschia</i> sp. CCS1				
<i>Loktanella vestfoldensis</i> SKA53				
<i>Maritimibacter alkaliphilus</i> HTCC2654				
<i>Oceanibulbus indolifex</i> HEL45				
<i>Oceanicola batsensis</i> HTCC2597				
<i>Oceanicola granulosus</i> HTCC2516				
<i>Octadecabacter antarcticus</i> 307				
<i>Octadecabacter arcticus</i> 238				
<i>Pelagibaca bermudensis</i> HTCC2601				
<i>Phaeobacter gallaeciensis</i> 2.10				
<i>Phaeobacter gallaeciensis</i> BS107				
<i>Phaeobacter</i> sp. Y4I				
<i>Rhodobacterales bacterium</i> HTCC2083				
<i>Rhodobacterales bacterium</i> HTCC2150				
<i>Rhodobacterales bacterium</i> HTCC2255				
<i>Rhodobacterales bacterium</i> KLH11				
<i>Roseobacter denitrificans</i> OCh 114				
<i>Roseobacter litoralis</i> Och 149				
<i>Roseobacter</i> sp. AzwK-3b				
<i>Roseobacter</i> sp. CCS2				
<i>Roseobacter</i> sp. GAI101				
<i>Roseobacter</i> sp. MED193				
<i>Roseobacter</i> sp. SK209-2-6				
<i>Roseovarius nubinihibens</i> ISM				
<i>Roseovarius</i> sp. 217				
<i>Roseovarius</i> sp. TM1035				
<i>Ruegeria lacuscaerulensis</i> ITI-1157				
<i>Ruegeria pomeroyi</i> DSS-3				
<i>Ruegeria</i> sp. R11				
<i>Ruegeria</i> sp. TM1040				
<i>Ruegeria</i> sp. Trich CH4B				
<i>Sagittula stellata</i> E-37				
<i>Sulfitobacter</i> NAS-14.1				
<i>Sulfitobacter</i> sp. EE-36				
<i>Thalassiobium</i> R2A62				

6.2.4 A novel class of Marine Mn uptake systems, *MntX*

We noted that three members, namely *Roseovarius nubinhibens* ISM, *Oceanicola granulosus* HTCC2516 and *Rhodobacterales* strain HTCC22 of the Roseobacter group lack homologues of both MntH and SitABCD and contained no known manganese transporter. However, these three strains, and *only* these three were found to have a predicted MRS motif that preceded a gene whose product was likely to be an inner membrane polypeptide, and therefore was a possible candidate to be a novel Mn²⁺ transporter. This MRS motif was first noted by Rodionov *et al.* (2006) in *Roseovarius nubinhibens* ISM and *Oceanicola granulosus* HTCC2516, who termed the corresponding gene *mntX*. The MntX polypeptides are ~400 amino acids in length (e.g. 387 for *Roseovarius nubinhibens* ISM_02005 gene product) and are categorised as “function unknown”, with their C-terminal 300 amino acids corresponding to a domain of unknown function (DUF2899 [pfam11449]). They have predicted trans-membrane helices, as shown in Figure 6.10. {This MntX has no similarity to a hydrophobic Mn exporter, also termed MntX, described in *Neisseria meningitides* by Veyrier *et al.* (2011).}

Confirmation of that MntX is indeed a Mn²⁺ transporter and that *mntX* is regulated by Mur in response to Mn availability forms the subject matter of the following sections.

6.2.5 Expression of *mntX* of *Roseovarius nubinhibens* is regulated by Mn levels via the Mur transcriptional regulator

To study the regulation of *mntX* of *Roseovarius nubinhibens* ISM, a *lacZ* transcriptional fusion to this gene was made. This comprised a 569 bp fragment that spanned its predicted promoter, plus its predicted MRS *cis*-acting regulatory sequence, and extended into the first 180 bps of the *mntX* structural gene, cloned into the promoter-probe plasmid pBIO1628, forming pBIO2067. This plasmid was mobilised by conjugation into wild type *Roseovarius nubinhibens* and into two strains of *Ruegeria pomeroyi*, namely the wild type J470 and the Mur⁻ mutant J528. For both wild type versions of these two species, the β-galactosidase activities were ~16-fold greater when transconjugants were grown in Mn-depleted than in Mn-replete medium, with respectively, 1607 and 94 Miller Units. However, in the Mur⁻ mutant of *Ruegeria pomeroyi*, the fusion was expressed at high level in both +Mn and -Mn media (1861 and 1889 Miller Units respectively). Thus, the *mntX* gene of one Roseobacter strain (*Roseovarius nubinhibens*) is indeed regulated by Mur in response to

Mn²⁺, even if the regulatory gene is supplied by a different species (namely *Ruegeria pomeroyi*). This is consistent with the similarity of the MRS box sequences in the different Roseobacters, as shown in Figure 6.8.

6.2.6 Cloning and complementation of *mntX* of *R. nubinhibens*

To confirm that this predicted transporter gene really is involved in Mn transport, a functional complementation test was used, in an attempt to restore the mutant phenotype of the SitA⁻ mutant of *Ruegeria pomeroyi*. This was done, initially, with the *mntX* gene of *Roseovarius nubinhibens*, from whose genomic DNA a 1574 bp fragment that included the *mntX* gene (*ISM_02005*) plus upstream regulatory sequences was amplified and cloned into the wide host-range vector pOT2, forming the recombinant plasmid pBIO2066. This was mobilised into the SitA⁻ strain J529 of *R. pomeroyi* by conjugation. The growth of J529 with pBIO2066 was restored to wild type levels without added Mn – refer to Figure 6.11 below. Thus, MntX of *Roseovarius nubinhibens* is able to complement the growth of a Mn transporter mutant, in a heterologous bacterial strain.

6.2.7 The distribution of MntX in other bacteria

We found that there are many significant MntX homologues, in addition to those in the three Roseobacter strains. These homologues were restricted to a few genera in the Orders Vibrionales, Altermonadales and Oceanospirillales of γ -proteobacteria and in two α -proteobacterial clades, namely SAR11 and SAR116. Significantly, all these taxa are sea-dwelling and are considered individually as follows.

6.2.8 The γ -proteobacterial MntX

Vibrionales

Among this Order of marine bacteria, there are genome-sequenced strains in the genera *Aliivibrio* (*A. salmonicida*), *Photobacterium* (five species, six strains) and *Vibrio* itself (20 species, 99 strains). The single *Aliivibrio*, and three *Photobacterium* strains contain MntX homologues (E values <e⁻⁷⁵) as do all

but four of the total of the 99 sequenced strains of *Vibrio* itself, the exceptions being the strains of *V. campbellii*, *V. caribbenthicus*, *V. nigripulchritudo* and *V. sinaloensis*. Strikingly, all these strains that lacked *mntX* contained at least one other known Mn²⁺ transporter, either SitABCD alone (*V. caribbenthicus*, *V. sinaloensis*, *V. nigripulchritudo*) or both SitABCD plus MntH (three *Photobacterium* strains and *V. campbellii* DS40M4). Furthermore, the *sitABCD* operon of *V. caribbenthicus* and *V. sinaloensis* about a gene that encodes a Mur-like polypeptide whose sequence resembled those of *Citreicella*, *Sulfitobacter* and a few other Roseobacters (Figure 6.6). Finally, some *Vibrio* and *Photobacterium* strains contain MntH and MntX, but no SitABCD transporters (Table 6.3). (The available genomes of all those strains that had no known Mn transporters and were in draft form were not included here.)

Altermonadales

MntX homologues occur in some strains of *Colwellia*, *Alteromonas*, *Pseudoalteromonas*, all of which are in the Altermonadales Order of γ -proteobacteria. As in other clades, there is diversity even within a single genus; thus, *Alteromonas macleodii* ATCC 27126 contains *mntX* but strain “Deep ecotype” does not (Table 6.3).

Oceanospirillales

Within the Order Oceanospirillales, too, some strains of a given genus, namely *Marinomonas*, harbour *mntX* (*M. mediterranea* MMB-1 and *M. posidonica* IVIA-Po-181), but strain MWYL1 lacks the gene (Table 6.3).

Table 6.3 Distribution of manganese transporters in α -proteobacterial genera that have at least one strain with a homologue of MntX

Names of the genome-sequenced strains in those genera with at least one MntX homologue are shown in the left-hand column. The presence of a close homologue of the Mn²⁺ transporters MntX, SitA or MntH is denoted by a coloured box, containing the E value in comparison to the corresponding polypeptide in Roseovarius nubinhibens (MntX), Ruegeria pomeroyi (SitA) or E. coli (MntH). Those strains whose deduced proteomes lacked any of these polypeptides, and whose genome was only available in draft form are not included.

Genome-sequenced strains in genera with at least one MntX homologue	MntX	SitA	MntH
<i>Aliivibrio salmonicida</i> LFI1238	1.00E-74		
<i>Alteromonadales bacterium</i> TW7	2.00E-83		
<i>Alteromonas madeodii</i> ATCC 27126	4.00E-75		
<i>Alteromonas madeodii</i> str. 'Deep ecotype'			
<i>Colwellia psychrerythraea</i> 34H	2.00E-71		
<i>Marinomonas mediterranea</i> MMB-1	2.00E-73	2E-35 ¹	
<i>Marinomonas</i> sp. MWYL1			
<i>Marinomonas posidonica</i> IVIA-Po-181	5.00E-78	3E-48 ¹	
<i>Photobacterium angustum</i> S14		2.00E-154	3.00E-169
<i>Photobacterium damsela</i> subsp. <i>damsela</i> CIP 102761	6.00E-76		0
<i>Photobacterium leiognathi</i> subsp. <i>mandapamensis</i> svers.1.1		8.00E-153	5.00E-167
<i>Photobacterium profundum</i> 3TCK	4.00E-80		
<i>Photobacterium profundum</i> SS9	3.00E-78		
<i>Photobacterium</i> sp. SKA34		4.00E-154	3.00E-168
<i>Pseudoalteromonas atlantica</i> T6c			
<i>Pseudoalteromonas haloplanktis</i> TAC125	3.00E-84		
<i>Pseudoalteromonas</i> sp BSi20311	7.00E-82		
<i>Pseudoalteromonas</i> sp BSi20429	4.00E-87		
<i>Pseudoalteromonas</i> sp BSi20439	7.00E-82		
<i>Pseudoalteromonas</i> sp BSi20480	1.00E-82		
<i>Pseudoalteromonas</i> sp BSi20495	4.00E-84		
<i>Pseudoalteromonas</i> sp BSi20652	2.00E-83		
<i>Pseudoalteromonas</i> sp SM9913	3.00E-84		
<i>Pseudoalteromonas tunicata</i> D2	1.00E-78		
<i>Vibrio alginolyticus</i> 12G01	2.00E-76		
<i>Vibrio alginolyticus</i> 40B	1.00E-76		
<i>Vibrio brasiliensis</i> LMG	3.00E-77		
<i>Vibrio campbellii</i> DS40M4		2.00E-159	6.00E-178
<i>Vibrio caribbenthicus</i> ATCC BAA-2122		2.00E-137	

Genome-sequenced strains in genera with at least one MntX homologue	MntX	SitA	MntH
<i>Vibrio cholerae</i> 12129(1)	3.00E-75		
<i>Vibrio cholerae</i> 1587	7.00E-76		
<i>Vibrio cholerae</i> 2740-80	5.00E-76		
<i>Vibrio cholerae</i> 623-39	7.00E-76		
<i>Vibrio cholerae</i> AM-19226	7.00E-76		
<i>Vibrio cholerae</i> B33	5.00E-76		
<i>Vibrio cholerae</i> BJG-01	7.00E-76		
<i>Vibrio cholerae</i> bv. <i>albensis</i> VL426	4.00E-76		
<i>Vibrio cholerae</i> BX 330286	5.00E-76		
<i>Vibrio cholerae</i> CIRS101	3.00E-76		
<i>Vibrio cholerae</i> CT 5369-93	7.00E-76		
<i>Vibrio cholerae</i> HC-02A1	1.00E-73		
<i>Vibrio cholerae</i> HC-06A1	3.00E-76		
<i>Vibrio cholerae</i> HC-19A1	5.00E-76		
<i>Vibrio cholerae</i> HC-21A1	3.00E-76		
<i>Vibrio cholerae</i> HC-22A1	3.00E-76		
<i>Vibrio cholerae</i> HC-23A1	3.00E-76		
<i>Vibrio cholerae</i> HC-28A1	3.00E-76		
<i>Vibrio cholerae</i> HC-32A1	3.00E-76		
<i>Vibrio cholerae</i> HC-33A2	3.00E-76		
<i>Vibrio cholerae</i> HC-38A1	3.00E-76		
<i>Vibrio cholerae</i> HC-40A1	5.00E-76		
<i>Vibrio cholerae</i> HC-43A1	3.00E-76		
<i>Vibrio cholerae</i> HC-48A1	3.00E-76		
<i>Vibrio cholerae</i> HC-48B2	5.00E-76		
<i>Vibrio cholerae</i> HC-49A2	5.00E-76		
<i>Vibrio cholerae</i> HC-61A1	3.00E-76		
<i>Vibrio cholerae</i> HC-70A1	3.00E-76		
<i>Vibrio cholerae</i> HCUF01	3.00E-76		
<i>Vibrio cholerae</i> HE-09	6.00E-76		
<i>Vibrio cholerae</i> HE39	1.00E-74		
<i>Vibrio cholerae</i> HE48	1.00E-74		
<i>Vibrio cholerae</i> HFU-02	5.00E-76		
<i>Vibrio cholerae</i> IEC224	3.00E-76		
<i>Vibrio cholerae</i> INDRE 91/1	5.00E-76		

Genome-sequenced strains in genera with at least one MntX homologue	MntX	SitA	MntH
<i>Vibrio cholerae</i> M66-2	5.00E-76		
<i>Vibrio cholerae</i> MAK 757	5.00E-76		
<i>Vibrio cholerae</i> MJ-1236	5.00E-76		
<i>Vibrio cholerae</i> MO10	5.00E-76		
<i>Vibrio cholerae</i> MZO-2	3.00E-75		
<i>Vibrio cholerae</i> MZO-3	6.00E-76		
<i>Vibrio cholerae</i> NCTC 8457	5.00E-76		
<i>Vibrio cholerae</i> O1 biovar El Tor str. N16961	5.00E-76		
<i>Vibrio cholerae</i> O1 str. 2010EL-1786	5.00E-76		
<i>Vibrio cholerae</i> O395	4.00E-76		
<i>Vibrio cholerae</i> RC27	4.00E-76		
<i>Vibrio cholerae</i> RC385	6.00E-76		
<i>Vibrio cholerae</i> RC9	5.00E-76		
<i>Vibrio cholerae</i> TM 11079-80	1.00E-75		
<i>Vibrio cholerae</i> TMA 21	6.00E-76		
<i>Vibrio cholerae</i> V51	7.00E-76		
<i>Vibrio cholerae</i> V52	7.00E-76		
<i>Vibrio coralliilyticus</i> ATCC BAA450	4.00E-70		
<i>Vibrio fischeri</i> ES114	5.00E-77		
<i>Vibrio fischeri</i> MJ11	2.00E-77		
<i>Vibrio fischeri</i> SR5	1.00E-77		
<i>Vibrio furnissii</i> CIP 102972	1.00E-72		5.00E-164
<i>Vibrio furnissii</i> NCTC 11218	4.00E-73		6.00E-164
<i>Vibrio harveyi</i> 1DA3	2.00E-76		1.00E-178
<i>Vibrio harveyi</i> ATCC BAA1116	4.00E-79		1.00E-178
<i>Vibrio harveyi</i> HY01	2.00E-79		2.00E-179
<i>Vibrio ichthyoenteri</i> ATCC 700023	1.00E-77		
<i>Vibrio mimicus</i> MB451	3.00E-76		
<i>Vibrio mimicus</i> SX4	5.00E-76		
<i>Vibrio mimicus</i> VM223	1.00E-76		
<i>Vibrio mimicus</i> VM573	2.00E-75		
<i>Vibrio mimicus</i> VM603	3.00E-76		
<i>Vibrio nigripulchritudo</i> ATCC 27043		6.00E-146	
<i>Vibrio orientalis</i> CIP 102891	4.00E-78		

Genome-sequenced strains in genera with at least one MntX homologue	MntX	SitA	MntH
<i>Vibrio parahaemolyticus</i> 10329	5.00E-79		
<i>Vibrio parahaemolyticus</i> 16	4.00E-81		
<i>Vibrio parahaemolyticus</i> AN5034	4.00E-80		
<i>Vibrio parahaemolyticus</i> AQ3810	1.00E-80		
<i>Vibrio parahaemolyticus</i> AQ4037	1.00E-80		
<i>Vibrio parahaemolyticus</i> K5030	4.00E-80		
<i>Vibrio parahaemolyticus</i> Peru466	4.00E-80		
<i>Vibrio parahaemolyticus</i> RIMD 2210633	4.00E-80		
<i>Vibrio rotiferianus</i> DAT722	3.00E-80		8.00E-178
<i>Vibrio scophthalmi</i> LMG 19158	5.00E-78		
<i>Vibrio shilonii</i> AK1	2.00E-63		7.00E-178
<i>Vibrio sinaloensis</i> DSM 21326		3.00E-139	
<i>Vibrio</i> sp AND4	4.00E-81		
<i>Vibrio</i> sp EY3	3.00E-76		
<i>Vibrio</i> sp Ex25	2.00E-75		
<i>Vibrio</i> sp MED222	6.00E-71		
<i>Vibrio</i> sp N418	1.00E-74		1.00E-163
<i>Vibrio splendidus</i> 12B01	1.00E-73		
<i>Vibrio splendidus</i> ATCC 33789	2.00E-70		
<i>Vibrio splendidus</i> LGP32	6.00E-71		
<i>Vibrio tubiashii</i> ATCC 19109	5.00E-76		
<i>Vibrio vulnificus</i> CMCP6	8.00E-73		
<i>Vibrio vulnificus</i> MO624/O	9.00E-73		
<i>Vibrio vulnificus</i> YJ016	7.00E-72		

¹These genes are similar to Zn and Mn periplasmic binding proteins from ABC-class transporters, including RL1049 from *R. leguminosarum*.

6.2.9 The α -proteobacterial MntX

In addition to the few Roseobacter strains described above, two other taxa of important marine α -Proteobacteria contain *mntX* genes. These two clades, SAR11 (*Candidatus* Pelagibacter ubique) and SAR116 (*Candidatus* Puniceispirillum marinum) were initially detected by culture-independent analysis of bacterial DNA sequence samples from the Sargasso Sea (Rappe *et al.* 2002; Stingl *et al.* 2007), but both were subsequently grown in pure culture and some strains have been genome-sequenced.

SAR11

These bacteria are the most abundant on Earth (Morris *et al.* 2002). Of four sequenced strains, one, *Candidatus* Pelagibacter sp. IMCC9063, encodes a homologue of MntX (gene tag SAR11G3_00277), which is 39% identical to that of *R. nubinhibens*. Interestingly, this *mntX*-like gene is adjacent to a divergently transcribed gene (SAR11G3_00278) whose product is predicted to be in the MntR family, being 50% identical to the *E. coli* version of this manganese-responsive transcriptional repressor. Strain IMCC9063 is in *Pelagibacter* subgroup 3, rather distantly related to other genome-sequenced strains (HTCC7211, HTCC1062 and HTCC1002) (Oh *et al.* 2011), all of which lack MntX. Indeed, these three strains lack genes for any known Mn²⁺ transporters.

SAR116

SAR116 bacteria are also widespread throughout the oceans, although they are not as abundant as the SAR11 group (Morris *et al.* 2012). The only genome-sequenced SAR116 strain, *Candidatus* Puniceispirillum marinum IMCC1322 (Oh *et al.* 2010) contains a gene, SAR116_1166, whose product is 46% identical to MntX of *R. nubinhibens*. The draft genome sequence of the SAR116 cluster alpha proteobacterium sp. HIMB100 also has a gene (HIMB100_00004540), whose product is 44% identical to MntX of *R. nubinhibens*.

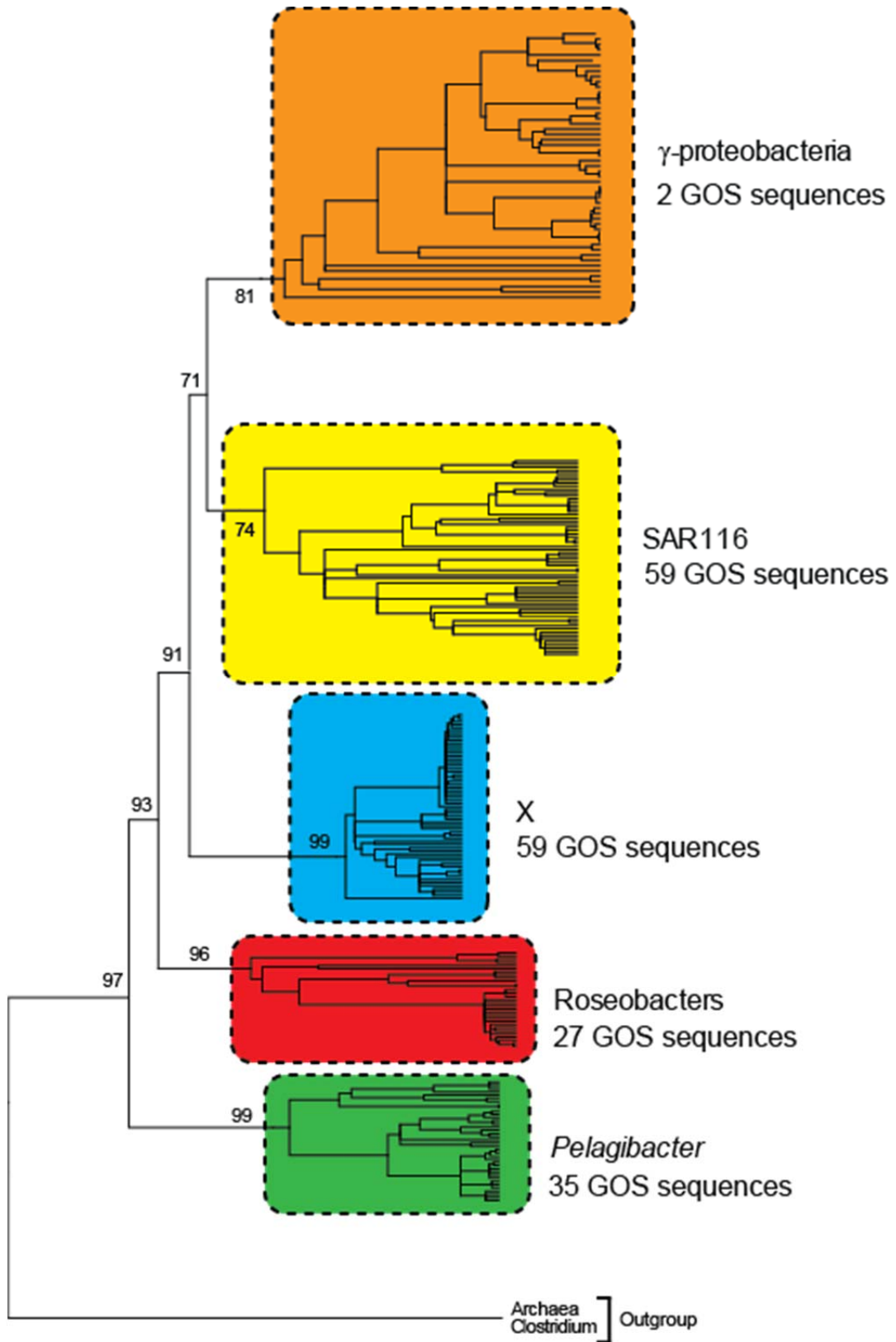
6.2.10 MntX in the GOS

To identify all the MntX peptides possible, we interrogated the CAMERA database for the Global Oceanic Survey (GOS) in addition to the NCBI peptide records using *R. nubinhibens* MntX as a query sequence.

All resulting MntX polypeptides fell into 6 sub-classes, each being associated with one the above

bacterial lineages (Figure 6.9), as described below. One set of sequences did not cluster with any described taxonomic group. Closer examination of these peptide sequences revealed that they had a very low GC content; often below 30% (refer to Appendix 2). This unidentified clade of sequences, and presumably strains which harbour these peptides was named clade X in figure 6.9. These peptides could be indicative of a novel, and widespread new clade of bacteria, analogous to SAR11. Individual phylogenetic trees were constructed for each of the 5 distinct groups of MntX peptides shown in Figure 6.9 and these are included as Appendix 1. In addition, some basic information about each of the MntX peptides shown in figure 6.9 is included as Appendix 2.

Figure 6.9 Phylogenetic tree of all MntX peptides

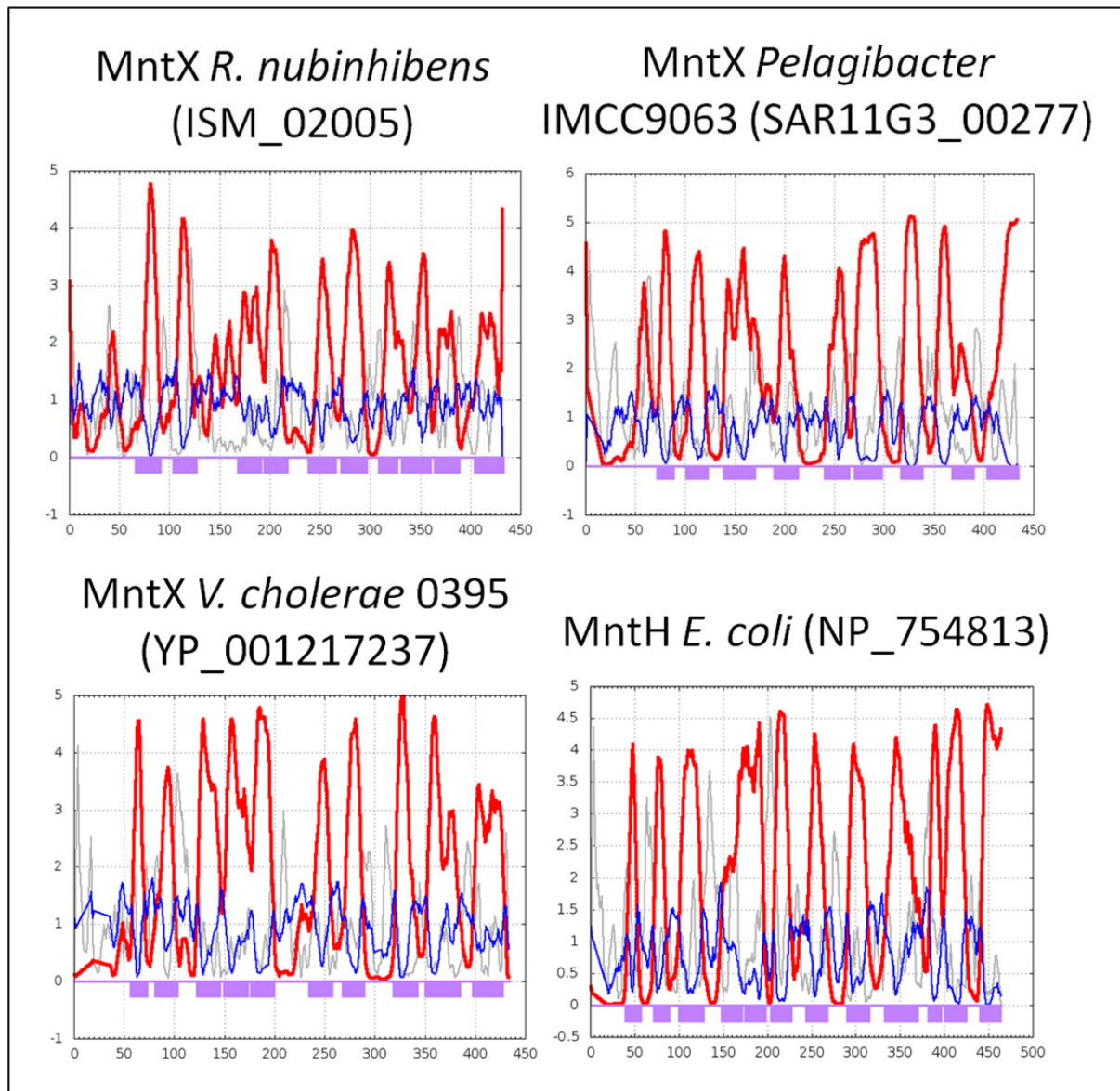


Using Mega5, a tree of the MntX homologues in the bacteria described in the text and in the GOS marine metagenome was constructed using the neighbour-joining method; bootstrap values are shown for 500 replicates performed. The MntX homologues were of five sub-classes as indicated, each corresponding to those found in the bacterial clade that is shown. Group “X”, shown in blue, corresponds to those in the GOS that were not close homologues of a polypeptide in any known bacterium. The numbers of GOS sequences found in each of the five groups are indicated. Accession numbers of the individual GOS sequences are in Appendix 2.

6.2.11 Structural predictions for *mntX*

The translated products of *mntX* from *R. nubinhibens*, *Vibrio cholerae*, and from *Pelagibacter* IMCC9063 are predicted to be localised in the cytoplasmic membrane, as judged by the program pSORTB 3.0 (Yu *et al.* 2010). It was also possible to predict the presence of hydrophobic regions of these polypeptide sequences, which may indicate the trans-membrane (TM) parts of the protein that are embedded in the membrane *in vivo*. The presence of possible TM domains in any given peptide sequence can be evaluated using SPLIT4 {<http://split4.pmfst.hr/split/4/>} (Juretic *et al.* 2002)}, which predicted that MntX of *R. nubinhibens*, *V. cholerae*, and *Pelagibacter* all have ~10 TM domains, with a similar overall profile to that of another Mn²⁺ transporter, namely MntH of *E. coli* (Figure 6.10).

Figure 6.10 Prediction of TM domains in MntX proteins, with MntH for reference



SPLIT4 (Juretic et al. 2002) output for three MntX peptide sequences show the presence of hydrophobic regions of the peptide sequence (red lines). These are used to predict possible TM regions (purple boxes). The peptide sequence of *E. coli* MntH was included for reference.

6.2.12 Correction of the *SitA* mutant of *Ruegeria pomeroyi* DSS-3 with the cloned *mntX* genes of *Candidatus Pelagibacter* sp. IMCC9063 and of *Vibrio cholerae*

Although the MntX homologues were very similar to those in the various bacterial clades described above, it was important to confirm that these were functional Mn transporters by direct experimentation. It was decided to do this for two examples, namely *Candidatus Pelagibacter* sp.

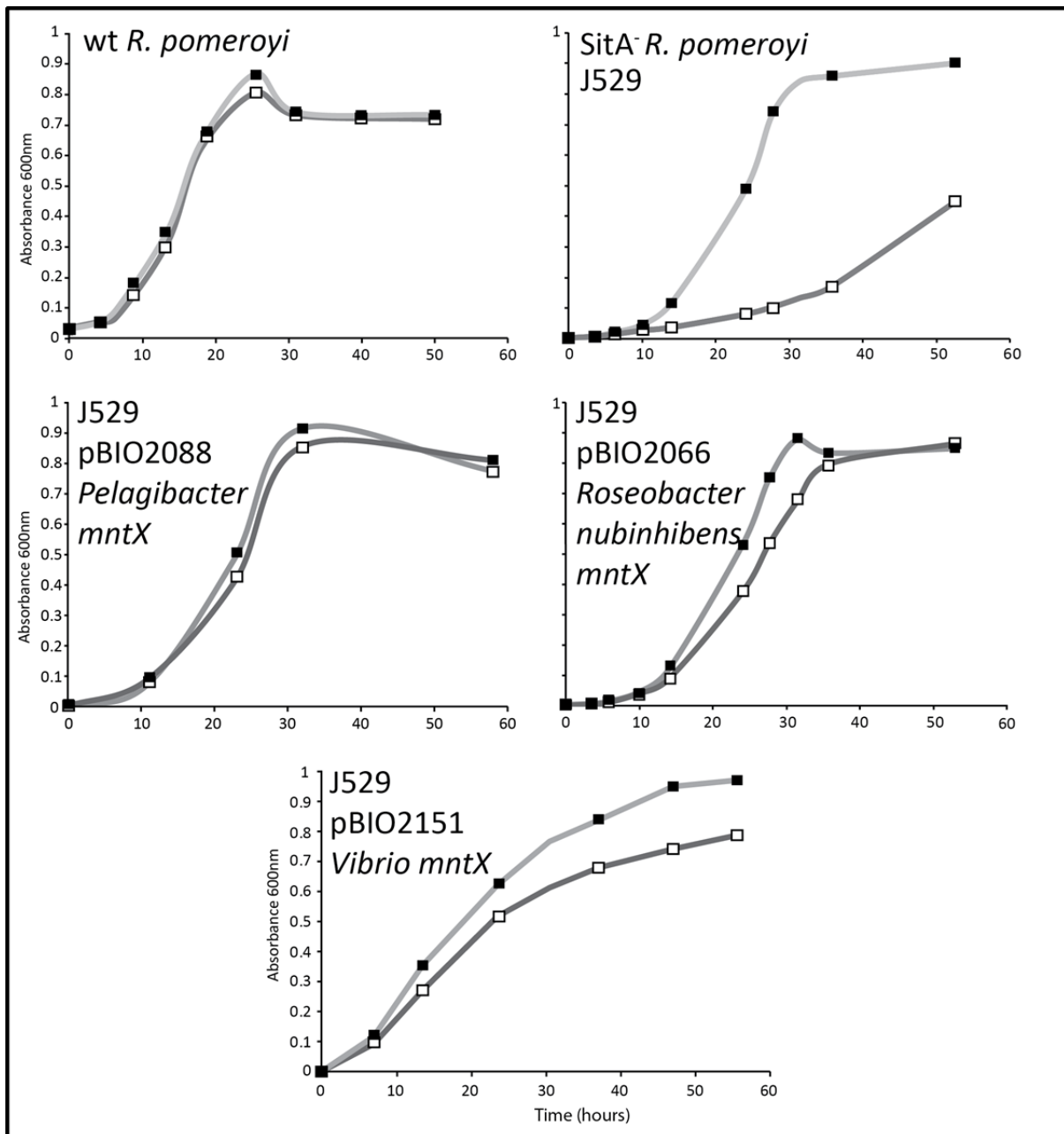
IMCC9063 and *Vibrio cholerae*, because these are (a) in different sub-phyla of the Proteobacteria and (b) because, in their different ways, they are very important bacteria, at a global level.

For *Candidatus Pelagibacter* sp. IMCC9063 we purchased (from GenScript) a 1345 bp fragment that contained its intact *mntX* gene (*SAR11G3_00277*), in a form whose codon usage was optimised {using OPTIMIZER (Puigbo *et al.* 2007)} for expression in the Roseobacters (whose GC content is ~60%, compared to ~30% in Pelagibacter). This *mntX*-like gene was sub-cloned into pRK415 (Keen *et al.* 1988) and the resulting plasmid (pBIO2088) was conjugated into the *Ruegeria pomeroyi* DSS-3 SitA⁻ mutant J529.

For *Vibrio cholerae*, we obtained a plasmid, VcCD00018495, from the DNASU Plasmid Repository. This plasmid contains the *mntX* gene (*VC1688*) of *Vibrio cholerae* O1 biovar ElTor str. N16961, cloned in the vector pDONR221 (Nakagawa *et al.* 2008). Using primers **VcXbamp1** and **VcXecop2**, this *mntX* gene was then amplified and ligated to pRK415 that had been cut with *Bam*HI and *Eco*RI, forming pBIO2150. This plasmid was conjugated into the *Ruegeria pomeroyi* DSS-3 SitA⁻ mutant J529.

As shown in Figure 6.11, the cloned genes of both *V. cholera* and of Pelagibacter could complement the growth defect of the SitA mutant in Mn-depleted media, just as had been shown for the cloned *mntX* of *Roseovarius nubinhibens*.

Figure 6.11 Growth defect of the *R. pomeroyi* SitA⁻ strain J529 is corrected by the cloned *mntX* genes of *Pelagibacter*, *Roseovarius nubinhibens* and *Vibrio cholerae*.



Cultures of Ruegeria pomeroyi wild type, or the SitA⁻ mutant J529 or J529 corrected with cloned *mntX* of *Roseovarius nubinhibens* (pBIO2066), *Candidatus Pelagibacter ubique* (pBIO2088) or *Vibrio cholerae* (pBIO2151) were diluted into RSS minimal medium either lacking any added MnCl₂ (white squares), or supplemented with 10 μM MnCl₂ (black squares). Cultures were grown, with shaking, at 28°C, and growth was measured by absorbance at 600 nm.

6.3 Discussion

To date there has been no research into manganese uptake and regulation in marine bacteria.

The work described here initially generated a series of conventional results, relating to Mn homeostasis in *Ruegeria pomeroyi*, but more novelty emerged from a comparative study of the portfolio of the relevant genes in the different strains of Roseobacters (Table 6.2).

- All contained Mur and no other known, dedicated Mn-responsive transcriptional regulator.
- There were two distinct families of SitA peptides
- Three strains lacked any known Mn uptake genes – SitA or MntH
- These three strains all had a homologue of MntX – a novel Mn transporter

It was fascinating to see that SitABCD was not well conserved across the Roseobacters, the distribution of this Mn transporter was clearly divided into three separate groups, that of *R. pomeroyi*, a group homologous to the Rhizobial SitA, and another group, most similar to *Loktanella vesfoldensis*. This was surprising and perhaps highlights the potential for diversity in this group of taxonomically distinct bacteria; applied to the wider marine community, diversity of metal transporters within taxonomic groups may be the rule rather than the exception.

From this analysis of the diversity of Mn transporters in the Roseobacters came the identification of MntX. Only those Roseobacter strains which lacked homologues of either SitABCD or MntH contained a homologue of MntX. One strain, *Ruegeria* sp. Trich CH4B had a homologue of MntH and SitABCD, it would be interesting to see the effect of mutations in each Mn-uptake system of this strain.

In the Roseobacters, the *mntX* gene was always preceded by a MRS box; both protein and MRS box were well conserved between *Roseovarius nubinhibens* ISM, *Oceanicola granulosus* HTCC2516 and *Rhodobacterales* strain HTCC22. The MntX protein is structurally predicted to be similar to MntH, and is located in the inner membrane making a good candidate for being a functional Mn transporter. Indeed, we were able to show that the *R. nubinhibens mntX* gene encodes a functional Mn transporter, and that regulation of *mntX* is via Mur.

The MntX peptide is found in a limited number of orders of the Proteobacteria, namely in the Oceanospirillales, the Altermonadales, the Vibrionales, all in the γ -subphylum, and in the SAR11, SAR116 and Roseobacter clades of α -proteobacteria. MntX is not distributed throughout each genus which has a homologue to this Mn transporter, indicating that MntX may have been acquired by

horizontal gene transfer (HGT). Also, since none of the Roseobacters which have SitABCD or MntH also had MntX it may be that this system is more beneficial in the marine habitat.

It must be noted that nearly all sequenced strains of the Vibrionales contained MntX, and indeed all *Vibrio cholerae* strains have a homologue of MntX. This may either mean that these bacteria acquired *mntX* early in their evolution, or that it originated from these bacteria. The function of one of the *Vibrio cholerae mntX* genes was demonstrated, in the complementation of the SitA⁻ strain of *R. pomeroyi*. This gene is also likely regulated by MntR, and not Mur, since the γ -proteobacteria use MntR to regulate Mn homeostasis. Unfortunately, I was unable to identify any potential *cis*-acting motifs homologous to MntH-boxes upstream of the *Vibrio mntX* gene. It is of course pertinent to mention the potential for MntX to be a target for therapeutic research. *Vibrio cholerae* is still a very dangerous pathogen where water sanitation is insufficient, and since MntX is likely an inner membrane protein, it could represent a potential vaccine antigen.

MntX was also found in the abundant α -proteobacterial SAR11 and SAR116 groups, of which Candidatus Pelagibacter sp. IMCC9063 encoded another functional MntX protein, capable of complementing the SitA⁻ strain of *R. pomeroyi*.

Given the abundance of the Roseobacters, Vibrios and SAR11/116 in the oceans, it was unsurprising to find that MntX was 82% as abundant in the GOS samples as SitA, and ~4-fold more abundant than MntH. This surely makes MntX a hugely important component of the marine Mn cycle and indeed for the bioavailability of Mn globally.

Fascinatingly, the analysis of MntX peptides found in the GOS survey revealed the presence of an as-yet unidentified group of bacteria, which harbour MntX (group X in the MntX phylogenetic tree, Figure 6.9). These bacteria likely have a very low genomic GC content, with all homologues of MntX being between 28 and 33% GC in this group. This is very comparable to the GC content of SAR11 bacteria, and perhaps is the first identification of a new large and abundant clade of bacteria related to SAR11. Further study into these bacteria would be extremely rewarding, perhaps using the novel group X MntX homologues as DNA probes to identify these previously uncharacterised bacteria.

Since MntX appears to be a solely marine Mn transporter, it would be of interest to perform biochemical studies on this transporter to show if the saline environment is of benefit to this transporter system, or perhaps it functions better than SitABCD/MntH when there is very low Mn concentration, as found in the oceans.

Finally, the fact that both SitA and MntX have been shown to be Mn-repressed means that these transporters are not always required either due to high levels of available Mn, such as in marine

sediments or algal blooms, or simply that these bacteria can simply shut down a lot of gene expression and wait for a better environment for growth. We already know that there are many strategies for survival in the oceans, such as the extreme minimalism of SAR11, and the extreme levels of iron uptake systems shown by some Roseobacters. All those in between can alter gene expression to suit a variety of conditions experienced by these bacteria in the variable habitat of the ocean.

Finally, this study identified bacterial strains which had no characterised systems for Mn uptake – most noteworthy in the SAR11 clade. These must have yet another novel Mn transporter, or could even have lost their requirement for this metal, in both cases; this would be an interesting study.

Chapter 7 - Microarray study of the Fe- and Mn-responsive transcriptome of *Ruegeria pomeroyi*

7.1 Introduction

The volume of data generated from a transcriptomics experiment is vast. The transcription of each of the >4000 genes of *R. pomeroyi* was measured using two conditions, and in two different mutant strains, so to go through all those genes whose expression went up or down in response to one or more of these parameters is not practical. Instead, only those genes of particular interest or whose on/off ratio in response to one or more of the conditions was truly out of the ordinary will be discussed here; also, this chapter will be presented with discussion forming part of the main text. The full data set is available at Appendix 3.

7.1.1 Methodology

A microarray chip was designed for *Ruegeria pomeroyi* DSS-3 using ArrayDesigner (Premier Biosoft). Here, each gene on both the main chromosome and the megaplasmid had a minimum of three oligonucleotides, each 60 nucleotides in length, designed, and randomised, before being printed in single spots on a glass slide by Agilent. Each array was printed eight separate times on a single glass slide. These eight arrays allowed the comparison of eight pairs of fluorescently labelled populations of cDNA, synthesised using total RNA extractions from different genotypes of *R. pomeroyi* cells that had been grown in our chosen conditions. The cDNA copies of a given gene would be labelled with two fluorescent dyes, which competitively bind to the oligonucleotide spot printed on the slide. If the gene is differentially expressed in one of the conditions, then the relative fluorescence will be higher for one colour than the other. The array is also, to a degree, quantitative, in that highly expressed genes will have a high level of fluorescence due to the higher level of cDNA copies of the mRNA; this does of course depend on the binding affinity of the individual oligo probes, and so is not truly quantitative.

I chose to use type I arrays (DeRisi *et al.* 1997), where RNA from two different conditions are compared on a single array. For example, two cultures of *R. pomeroyi*, one grown with added FeCl₃, and one without, would be used to prepare total RNA, which could then be compared on a single array. (In contrast, Type II arrays use labelled genomic DNA as a control on each array, to which RNA from a single condition can be compared.) Type II arrays can be compared to each other, but are less economical. For this work, we intended the arrays to be provide an overview of the transcriptional changes which occur during Fe and Mn limitation, hence our choice of type I arrays.

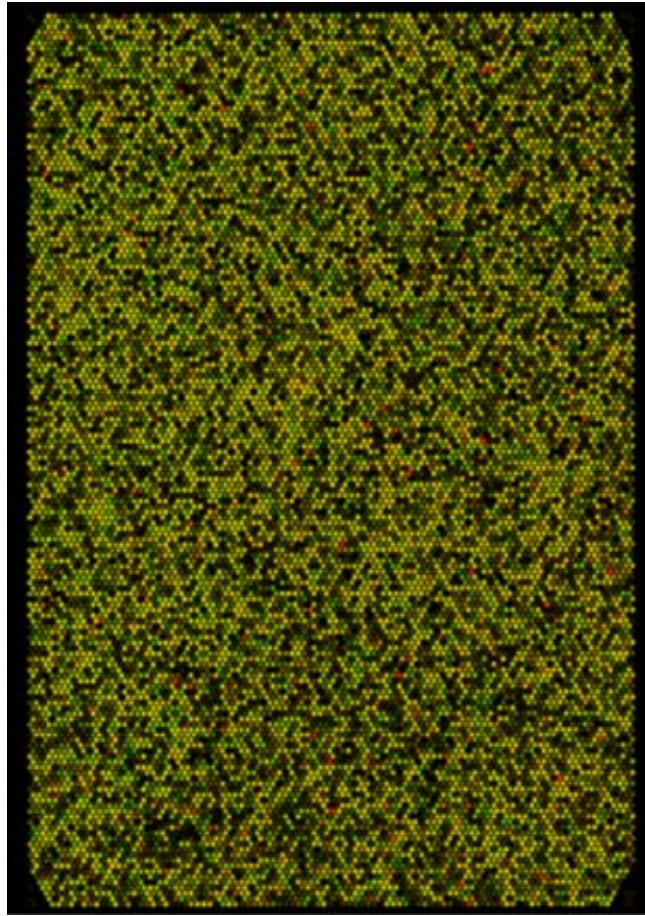
7.1.2 Performing the microarray

My array experiments consisted of the following comparisons:

1. Wild type *R. pomeroyi* grown in MBM with, or without extra, 20µM, FeCl₃.
2. Wild type *R. pomeroyi* grown in RSS with, or without extra, 20µM, MnCl₂.
3. Wild type *R. pomeroyi* and the Mur⁻ strain J528, both grown in RSS with 20µM FeCl₃ plus 20µM MnCl₂ added.
4. Wild type *R. pomeroyi* and the Irr⁻ strain J539 grown in MBM with 20µM FeCl₃ added.

Each comparison was performed in duplicate on cultures derived from single colonies of each of the strains that were used. The RNA was extracted from 100 ml cultures grown to early exponential phase (the RNA extraction and labelling method is detailed in Materials and Methods), which equated to around 14 hours of growth in each condition. At this point, the cultures in all the conditions tested were at a similar growth phase and optical densities (OD_{600nm} = 0.15). Total RNA was checked for quality and quantity and was labelled during reverse transcription using either Cy3 (green) or Cy5 (red) fluorescent residues. The cDNA samples were purified and hybridised to the array slide. Where RNA from each condition was in equal concentration, the hybridised probe would fluoresce yellow, and where either Cy3 or Cy5 labelled RNA proliferated, the probe would fluoresce red or green (see Figure 7.1).

Figure 7.1 Scanned microarray slide from this work



Scanned array showing both fluorescent channels together. Green or red spots indicate where a gene was expressed at different levels in the two conditions. Yellow spots indicated equal levels of binding of both fluorescently labelled cDNA samples.

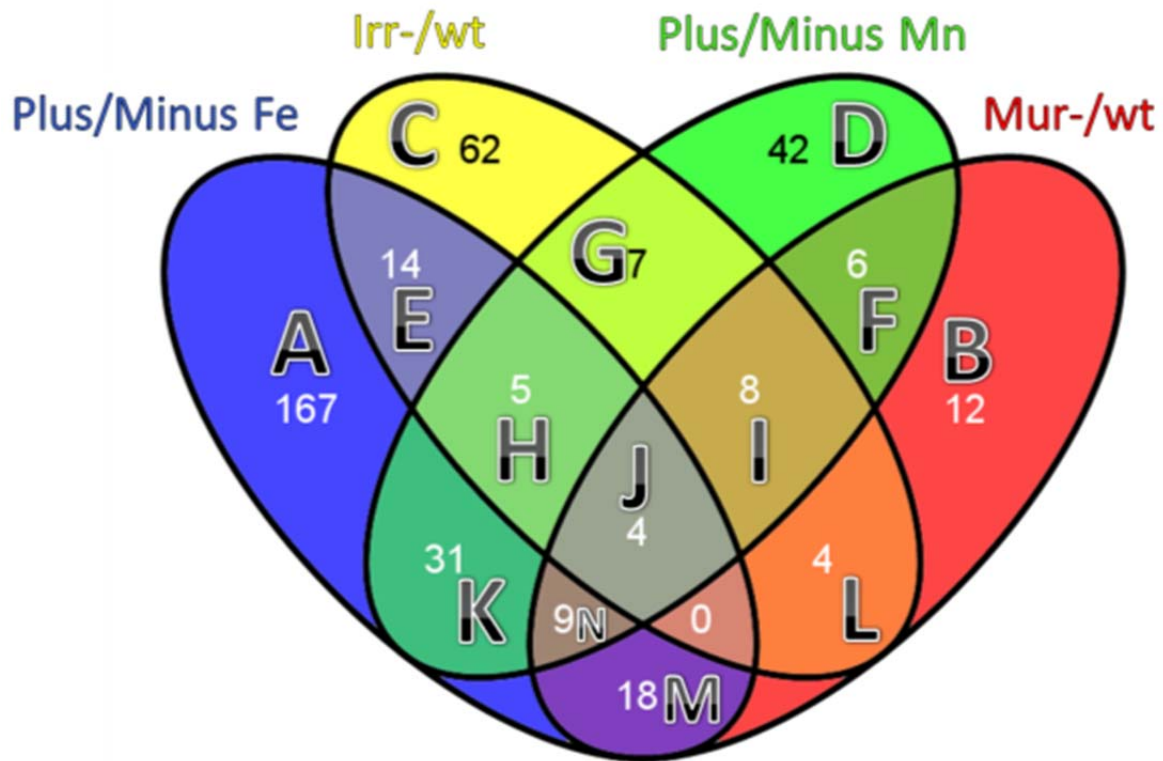
The relative fluorescence of each spot on each array was measured, and these data were normalised to eliminate any bias of the total fluorescence of each dye. These values of relative fluorescence were used to calculate a ratio for each probe, which could then be used to calculate the relative fold-change in expression for each gene, based on the three technical replicates of the three separate probes to each gene, and the two biological replicates of the two separate arrays. These values could then be assigned significance, to establish if they were statistically similar between all replicates, based on their p-value in a t-test of normalised values.

Large scale, batch analysis of groups of similarly behaving genes was performed first, to obtain a sense of the overall changes occurring across all arrays. These analyses are detailed in the following sections.

7.2.1 Venn diagrams of gene expression patterns

A selection of the genes whose expression changed in each condition was used to populate lists, as shown below. Only those genes that (a) behaved in a similar way in all the replicates (and which therefore had small errors associated with the measurements) and (b) had a significant-fold difference greater expression than the control condition, were used (see Figure 7.2 for different fold-change cut-off values used). These lists were compared using Venn diagrams, to see if any genes were co-regulated by the environmental conditions (+/- Mn and/or Fe), or genotype (Mur⁻, Irr⁻, wild type) wild type/mutant) as shown in Figure 7.2.

Figure 7.2 Venn diagram showing numbers of genes that were differentially expressed depending on availability of Mn and/or Fe and/or the *mur* or *irr* genotype



Venn diagram produced using Venny (Oliveros 2007). The integers in each of the areas represent the numbers of genes whose expression was affected (either positively or negatively) by the particular environmental and genetic variables. Thus, for example, the expression of 42 genes (in Box D) was affected by the *mur* genotype but not by that of *irr* or the presence of added Mn or Fe. In contrast, expression of the 4 genes in Box J was affected by all four of these variables. The cut off values of the -fold differences were; 3-fold for Fe limitation, 1.5-fold for *Irr* vs. wild type, and 2-fold for both Mn limitation and for *Mur* vs. wild type. The letters A-N correspond to those used in the gene list in Table 7.1.

Table 7.1 Lists of *Ruegeria pomeroyi* genes in the categories in the Venn diagram in Figure 7.2

A				B		C		D		
SPO0021	SPO0432	SPO1409	SPO2370	SPO3230	SPO3770	SPO1139	SPO0185	SPO2014	SPO0162	SPO2994
SPO0045	SPO0692	SPO1419	SPO2450	SPO3275	SPO3882	SPO1533	SPO0186	SPO2015	SPO0351	SPO3161
SPO0050	SPO0759	SPO1548	SPO2508	SPO3288	SPOA0037	SPO2093	SPO0274	SPO2016	SPO0459	SPO3284
SPO0051	SPO0789	SPO1557	SPO2516	SPO3329	SPOA0056	SPO2432	SPO0323	SPO2017	SPO0537	SPO3509
SPO0052	SPO0858	SPO1587	SPO2567	SPO3354	SPOA0057	SPO2717	SPO0328	SPO2020	SPO0761	SPO3513
SPO0071	SPO0909	SPO1689	SPO2580	SPO3355	SPOA0059	SPO2721	SPO0330	SPO2021	SPO0886	SPO3540
SPO0088	SPO0930	SPO1780	SPO2614	SPO3381	SPOA0061	SPO3364	SPO0608	SPO2022	SPO1226	SPO3671
SPO0090	SPO0937	SPO1794	SPO2615	SPO3409	SPOA0186	SPO3596	SPO0609	SPO2025	SPO1317	SPO3823
SPO0112	SPO0943	SPO1796	SPO2619	SPO3410	SPOA0289	SPO3597	SPO0610	SPO2159	SPO1500	SPOA0337
SPO0115	SPO1017	SPO1799	SPO2631	SPO3457	SPOA0315	SPO3615	SPO0611	SPO2163	SPO1507	SPOA0349
SPO0175	SPO1018	SPO1848	SPO2632	SPO3459	SPOA0321	SPOA0224	SPO0612	SPO2180	SPO1512	SPOA0410
SPO0179	SPO1019	SPO1849	SPO2633	SPO3460	SPOA0338		SPO0613	SPO2236	SPO1516	
SPO0180	SPO1020	SPO1860	SPO2635	SPO3461			SPO0614	SPO2390	SPO1518	
SPO0181	SPO1021	SPO1909	SPO2637	SPO3484			SPO0615	SPO2573	SPO1520	
SPO0192	SPO1060	SPO1938	SPO2802	SPO3523			SPO0628	SPO2645	SPO1521	
SPO0197	SPO1063	SPO1983	SPO2804	SPO3524			SPO0646	SPO3085	SPO1524	
SPO0198	SPO1064	SPO2102	SPO2817	SPO3525			SPO0662	SPO3543	SPO1564	
SPO0201	SPO1089	SPO2106	SPO2839	SPO3526			SPO0671	SPO3589	SPO1568	
SPO0202	SPO1177	SPO2130	SPO2846	SPO3527			SPO0718	SPO3685	SPO1569	
SPO0203	SPO1195	SPO2131	SPO2871	SPO3529			SPO0831	SPO3774	SPO1602	
SPO0227	SPO1236	SPO2135	SPO2872	SPO3532			SPO0855	SPO3842	SPO1798	
SPO0254	SPO1256	SPO2222	SPO2876	SPO3547			SPO1054	SPO3843	SPO1840	
SPO0255	SPO1271	SPO2240	SPO2930	SPO3604			SPO1173	SPOA0104	SPO1878	
SPO0307	SPO1281	SPO2241	SPO2932	SPO3606			SPO1405	SPOA0152	SPO1929	
SPO0313	SPO1351	SPO2242	SPO2962	SPO3613			SPO1440	SPOA0225	SPO1975	
SPO0314	SPO1366	SPO2246	SPO3032	SPO3700			SPO1478	SPOA0351	SPO2048	
SPO0363	SPO1376	SPO2247	SPO3078	SPO3701			SPO1718	SPOA0388	SPO2107	
SPO0382	SPO1387	SPO2295	SPO3095	SPO3721			SPO1957	SPOA0411	SPO2252	
SPO0388	SPO1392	SPO2324	SPO3103	SPO3722			SPO1973	SPOA0443	SPO2253	
SPO0390	SPO1393	SPO2335	SPO3118	SPO3767			SPO1978	SPOA0444	SPO2255	
SPO0404	SPO1398	SPO2346	SPO3119	SPO3768			SPO1999	SPOA0446	SPO2263	
E	F	G	H	I	J	K	L	M	N	
SPO0086	SPO0834	SPO0698	SPO0222	SPO1055	SPO1216	SPO0900	SPO0154	SPO0089	SPO0769	
SPO0087	SPO0919	SPO1217	SPO0701	SPO2576	SPO2398	SPO1502	SPO1977	SPO0157	SPO0833	
SPO0169	SPO0921	SPO1682	SPO1565	SPOA0392	SPO2399	SPO1503	SPO2018	SPO0784	SPO1555	
SPO0199	SPO1556	SPO1863	SPO1861	SPOA0393	SPOA0399	SPO1504	SPO2577	SPO0924	SPO1790	
SPO0647	SPO1789	SPO2154	SPO2264	SPOA0395		SPO1508		SPO1015	SPO1791	
SPO0790	SPO2331	SPO2396		SPOA0396		SPO1514		SPO1280	SPO3363	
SPO2023		SPO2397		SPOA0397		SPO1515		SPO1593	SPO3365	
SPO2486				SPOA0398		SPO1517		SPO1795	SPO3366	
SPO3014						SPO1847		SPO2568		
SPO3287						SPO1862		SPO2686		
SPO3359						SPO2257		SPO2706		
SPO3360						SPO2261		SPO2867		
SPO3607						SPO2262		SPO3027		
SPOA0445						SPO2289		SPO3081		
						SPO2371		SPO3445		
						SPO2628		SPO3781		
						SPO2634		SPOA0273		
						SPO2636				
						SPO3017				
						SPO3031				
						SPO3033				
						SPO3600				
						SPOA0339				
						SPOA0340				
						SPOA0341				
						SPOA0342				
						SPOA0343				
						SPOA0345				
						SPOA0346				
						SPOA0347				
						SPOA0348				
		ICE BOX								
		IR BOX								
		MUR BOX								
		Rrf-2								
		Operons								

Each set of genes shown in Figure 7.2 had an associated letter. These letters are shown here, as lists of genes which populated each section of the Venn diagram. Any gene which has a predicted regulatory motif (ICE, IR, MUR, see Chapter 3) or was a predicted Rrf-2 family transcriptional regulator (Chapter 3), or was in a predicted operon of genes, is coloured according to the key shown in column G.

This analysis revealed some expected, and also some surprising findings. As expected, there were 13 genes which were altered in expression in response to both Irr and to Fe, consistent with the known responses of the Irr regulator to Fe availability. Similarly, 27 genes responded to both the *mur* genotype and to its cognate co-regulator Mn. However, 31 genes were altered in both Fe and Mur, and 24 in both Irr and Mn. Thus, there is still considerable cross-talk in the regulatory networks for Mn and Fe homeostasis. Indeed, Mur of *R. pomeroyi* was shown to repress the *irr* locus in response to Mn levels (chapter 4). The *mur* gene is thought to have evolved from the global iron regulator gene *fur*, and clearly still has potential to be involved (directly or indirectly) in the response to Fe availability.

No genes were regulated by Mur, Irr and by Fe above the cut-off values used in this analysis, but 9 genes were shown to be regulated by Mn, Fe and Irr. This may show that Mur plays a lesser role in the homeostasis of Mn and Fe than the levels of Fe and Mn themselves, and that Irr is the more important regulator. Indeed, the fact that Mur itself is regulated by Irr makes this regulatory hierarchy more probable.

A total of 12 genes changed in response to Mn independently of Mur, or Fe, or Irr, indicating the presence of a yet unidentified Mn-responsive transcriptional regulator. Similarly, a total of 31 genes responded to Fe AND Mn limitation, but to neither Mur nor Irr.

Although not shown in the Venn diagram, it was apparent that several adjacent, contiguous genes displayed the same pattern of differential expression, consistent with their being part of the same transcriptional units (operons), and also demonstrating the robustness of the data.

In what follows, some of the more interesting of these operons are described in more detail.

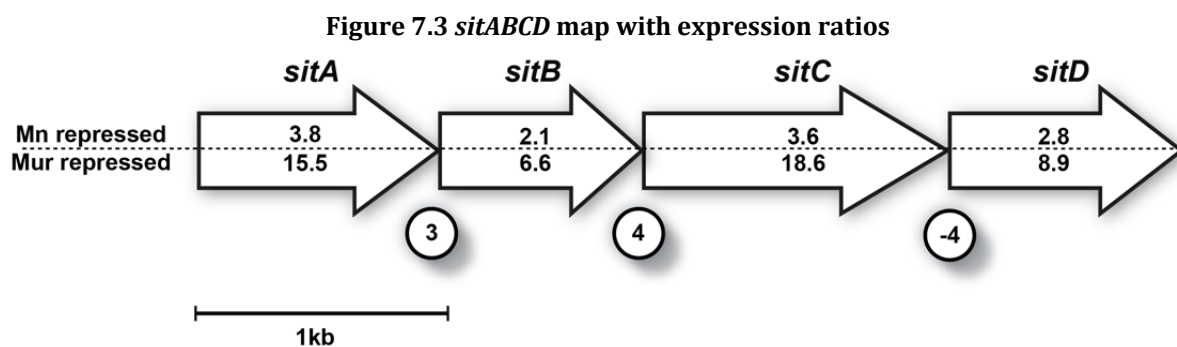
7.3.1 Effects of manganese availability and mutations in mur on the transcriptome of Ruegeria pomeroyi

The focus of this section is on those operons whose expression was markedly affected (>5-fold difference) by the *mur* genotype and/or the availability of Mn. These fell into one of four classes, depending on their response to Mn and to the *mur* genotype, as follows.

7.3.2 Class I – expression repressed in Mn-replete medium, and enhanced in Mur mutant

As shown in Table 7.1, a total of 12 genes, in just two clusters, behaved in a conventional way for those that are repressed by the Mur regulator, in cells grown in Mn-replete conditions.

SPO3366, SPO3365, SPO3364 and SPO3363 (*sitABCD*)

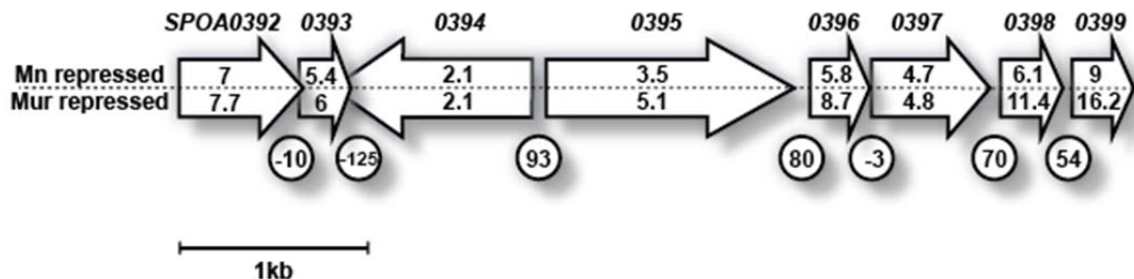


Scale map of the *sitABCD* locus of *R. pomeroyi* (SPO3363-SPO3366) including intergenic gaps (circled) and fold-change ratios for both +/- Mn and wt/mur microarray experiments (Mn repressed and Mur repressed).

Reassuringly, the *sitABCD* genes were among those whose expression was most strikingly repressed in the +Mn medium and this effect was dependent on a functional *mur* gene. The expression of *mur* itself was not affected significantly by the presence of added Mn in the medium. Here, the fold-change ratio of *sitA* expression shown in Figure 7.3 is lower (3.8-fold) to that obtained using a *sitA-lacZ* fusion (16-fold), but both show that *sitA* expression is repressed by Mn (see Chapter 6).

Interestingly, the *sit* genes appear to be induced by Fe (see Appendix 3, *sitA*, *sitC* and *sitD* all ~4-fold induced by Fe), although the mechanism of this regulation is unknown.

Figure 7.4 *SPOA0392-SPOA0399* map with expression ratios



Scale map of the *SPOA0392-SPOA0399* locus of *R. pomeroyi* including intergenic gaps (circled) and fold-change ratios for both +/- Mn and wt/mur microarray experiments (Mn repressed and Mur repressed).

R. pomeroyi DSS-3 has a resident, 491,611 bp, megaplasmid (Moran *et al.* 2004). It has a cluster of 8 contiguous genes, arranged in at least four predicted transcriptional units (Figure 7.4), whose expression was markedly reduced in cells grown in Mn-replete medium. This only occurred in the wild type strain, showing that Mur was required for this repression. The leftmost (as shown in Figure 7.4) of these genes, *SPOA0392*, encodes a polypeptide that is weakly predicted to be an RpoE-type σ -factor of RNA polymerase, but the closest homologue, Fecl of *Pseudomonas*, is only 34% identical to the *SPOA0392* gene product. So, if this *Ruegeria* gene does indeed encode a σ -factor, it must be of a rather novel type and predictions of its function are not possible. Downstream of *SPOA0392*, and in the same orientation, is *SPO0393*, which encodes a small (99 amino acid) polypeptide with significant similarity to one of the components of refractile inclusion bodies (R-bodies), which are ribbon-like polypeptides associated with the ability of some bacteria to act as killers in endosymbiotic interactions with eukaryotes (Pond *et al.* 1989). At the other end of the cluster lie the adjacent genes *SPOA0398* and *SPOA0399*, whose products are 78% identical to each other and less so (34%) to that of *SPOA0393*, with all three having significant identity to other R-body proteins in *Caedibacter taeniospiralis*, an obligate endosymbiont of *Paramecium* (Beier *et al.* 2002; Jeblick and Kusch 2005). I could find no links between manganese availability and R-bodies in the literature and the reason why the expression of these three genes should be elevated in Mn-deficient media, under the control of Mur, is unknown. Between the two sets of R-body genes are four other genes (*SPOA0394 – SPOA0397*), one of which, *SPO0394* is in the opposite orientation and shows only a modest response to Mur and to Mn availability. The genes in this cluster do not occur in any other genome-sequenced

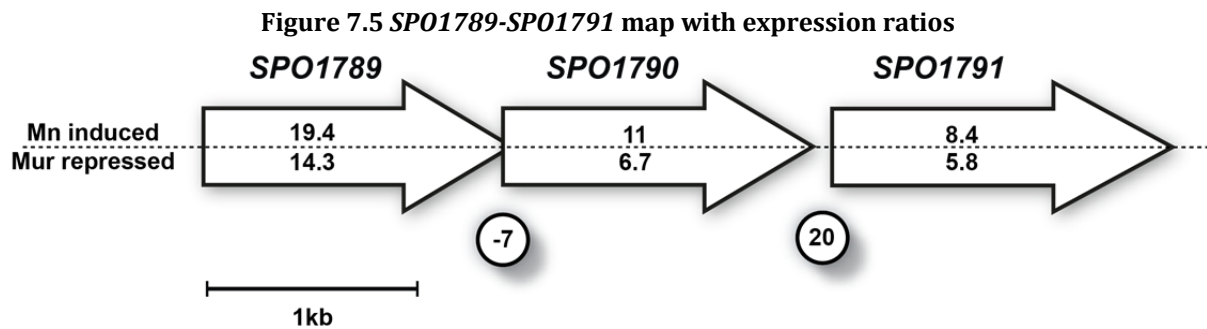
Roseobacter species, their products have no known function, and they have no homologues in any known organism. However, the SPO0397 gene product has three significant matches in the Global Ocean Sampling metagenome (Sun *et al.* 2010), pointing to the presence of the corresponding gene in (unknown) marine organisms.

The *sitABCD* operon has two MRS motifs in its promoter region (see Chapter 6), but no such sequence was seen 5' of any of the genes in the *SPOA0392* – *SPOA0399* cluster. It is not known, therefore, if Mur acts directly by binding to motifs that share only very limited similarity to the canonical MRS boxes or indirectly, perhaps by affecting the expression of another regulatory system that affects the transcription of these R-body genes.

7.3.3 Class II – expression enhanced in Mn-replete medium, and enhanced in wild type, compared to Mur⁻ mutant

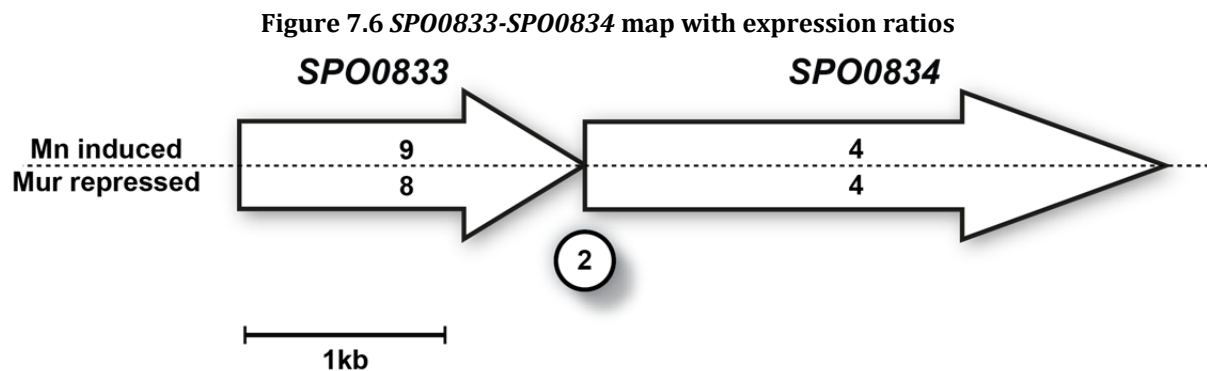
There were several groups of different genes, in four separate regions of the *R. pomeroyi* genome, whose expression was enhanced in the +Mn medium in the wild type strain, but this induction was not seen in the Mur⁻ mutant (Table 7.2).

SPO1789, SPO1790, and SPO1791.



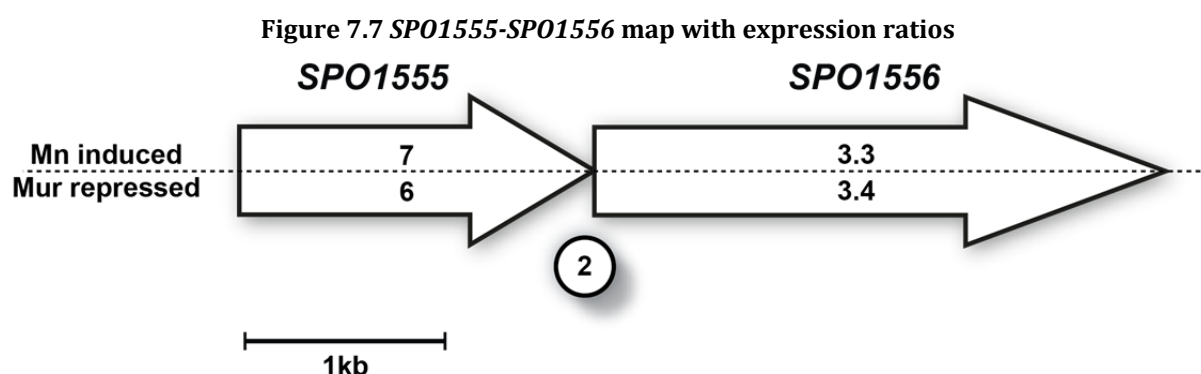
Scale map of the SPO1789-SPO1791 locus of *R. pomeroyi* including intergenic gaps (circled) and fold-change ratios for both +/- Mn and wt/mur microarray experiments (Mn induced and Mur repressed).

These three genes are strongly predicted to encode the components of an ABC transporter, respectively its permease, ATPase and periplasmic binding protein. Their expression was enhanced 19.4-, 11- and 8.4-fold respectively in the "+Mn" compared to the "-Mn" medium and by 14.3-, 6.7- and 5.8-fold respectively in the Mur⁺ wild type compared to the Mur⁻ mutant (see Figure 7.5 and Table 7.2). There are close homologues (> 60% identical) of all these gene products in many other *Roseobacter* strains, and also in bacteria in other sub-phyla of Proteobacteria. There were no close homologues to any transporter whose substrate specificity has been ratified, although the products of the *SPO1789* and *SPO1791* genes are classified as likely being involved in the import of tungstate or sulfate. However, this prediction needs to be ratified. Without knowing the identity of the substrate, and, indeed, without being certain if this transporter acts as an exporter or an importer, the adaptive advantage of its enhanced expression in Mn-rich medium is not clear.



Scale map of the SPO0833-SPO0834 locus of *R. pomeroyi* including intergenic gaps (circled) and fold-change ratios for both +/- Mn and wt/mur microarray experiments (Mn induced and Mur repressed).

The consecutive genes *SPO0833* and *SPO0834* are in a predicted two-gene operon whose expression was much enhanced (9- and 4-fold) in the +Mn media and 8- and 4-fold higher in the in wild type strain, relative to the Mur⁻ mutant. Their corresponding products are highly conserved, not only in the Roseobacters, but in a wide range of other bacterial clades and, strikingly, in the products of two other, *SPO1555* and *SPO1556*, in *R. pomeroyi* DSS-3 itself (see below). Their products are strongly predicted to encode the two polypeptides of a family of NADH:ubiquinone reductases. The predicted sub-type of this family that most closely resembled the *SPO0833* and *SPO1555* gene products are the β -subunit of a molybdopterin-containing formate dehydrogenase and those of *SPO0834* and *SPO1556* correspond to the α -polypeptide of the same enzyme.



Scale map of the SPO1555-SPO1556 locus of *R. pomeroyi* including intergenic gaps (circled) and fold-change ratios for both +/- Mn and wt/mur microarray experiments (Mn induced and Mur repressed).

As mentioned above, *SPO1555* and *SPO1556* are two contiguous genes (see Figure 7.7) that respond similarly to *SPO0833* and *SPO0834* with regard to manganese availability and to the *mur* genotype. Not only are the gene products of *SPO1555* and *SPO1556* very similar (>98% identical) to those of *SPO0833* and *SPO0834* respectively, but so too were the corresponding DNA sequences of the genes. This was the only example in which these genes had been duplicated in any of the genome-sequenced Roseobacters.

Perhaps coincidentally, at least some formate dehydrogenases contain tungsten, a metal that occurs in only a few metallo-enzymes. Furthermore, in *Desulfovibrio vulgaris* Hildenborough, the expression of the FdhAB formate dehydrogenase is induced by addition of tungstate (da Silva *et al.* 2011). Direct experiments are required to show if the purported formate dehydrogenases of *Ruegeria* (and other, related bacteria) do indeed contain tungsten. If so, it would provide a functional, though not mechanistic, explanation for the parallel induction of the two sets of genes that encode this enzyme plus a putative transport system for this metallic co-factor, encoded by the *SPO1789*, *SPO1790*, and *SPO1791* genes (see above).

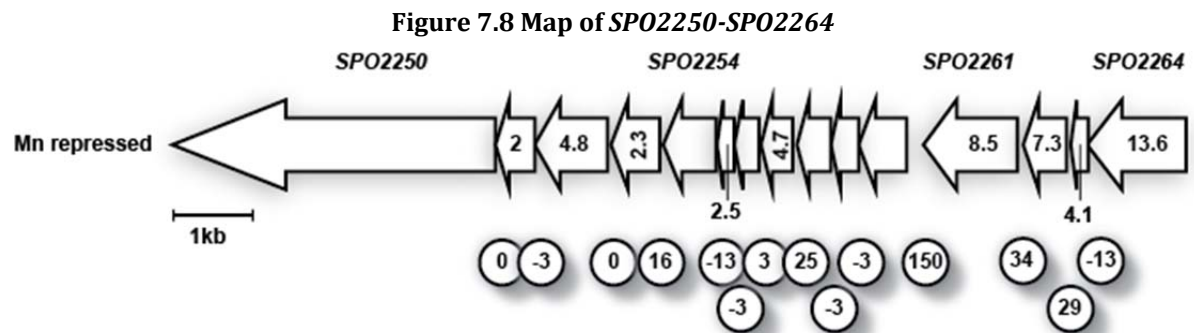
The *SPO1216* gene forms a single-gene transcriptional unit that encodes a 239 amino acid polypeptide with no domains with known function. There is a near-identical homologue in just one

other Roseobacter strain, namely *Dinoroseobacter shibae* DFL 12; other than that, there are no homologues in any known organism, or in any metagenomic data base.

These findings of genes whose expression is enhanced in Mn-replete media and which require a functional Mur regulator for this induction are novel for this particular regulator. However, other members of the Fur super-family, including Fur itself, have analogous properties. Thus, although Fur is an Fe-responsive repressor of genes involved in iron uptake, for example, it is required for the expression of some other genes (e.g., the *sdh* operon for succinate dehydrogenase in *E. coli*), giving Fur the initial appearance of acting as an activator. However, this is due to its ability to repress a repressor, in this case the small RNA *ryhB*, which can act post-transcriptionally to inhibit the expression of several target genes (including *sdH*). Since transcription of *ryhB* itself is repressed by Fur in Fe-replete media, the *sdh* (and several other) targets for the RyhB RNA will be expressed in these conditions. Conversely, in a Fur⁻ mutant, RyhB RNA is made constitutively, and so the expression of its targets will be lowered under all conditions (Massé *et al.* 2007). Since small RNAs have not (yet) been identified in Roseobacters, it is possible that an analogous mechanism exists here, but this would require further work to demonstrate a role for such molecules in this particular case. There are no conserved sequences in the vicinity of the promoters of any of the genes that displayed this form of regulation. Indeed, the regions immediately upstream of *SPO0833* and *SPO1555* had very little similarity to each other, despite the remarkable similarities of the genes themselves and their patterns of regulation (see above).

7.3.4 Class III – expression repressed in Mn-replete medium, independent of mur genotype

There was one transcriptional unit that appeared to be repressed by Mn, but, in contrast to the cases described above, this was unaffected by the genotype at the *mur* locus (Table 7.2).



Scale map of the SPO2250-SPO2264 locus of *R. pomeroyi* including intergenic gaps (circled) and fold-change ratios for +/- Mn microarray experiments (Mn repressed).

Gene Transfer Agents (GTAs) are very small, virus-like particles, first found in *Rhodobacter* (Marrs 1974), and then shown to be a feature of the Rhodobacterales family, including many strains of the Roseobacter clade (Biers *et al.* 2008). There are also homologues of the corresponding genes in other genera of alpha-proteobacteria, including *Agrobacterium*, *Brucella* and *Caulobacter*. In *R. pomeroyi* DSS-3, Biers *et al.* (2008) identified a cluster of ~15 genes whose products correspond to the various components required to make its GTA (shown Figure 7.8).

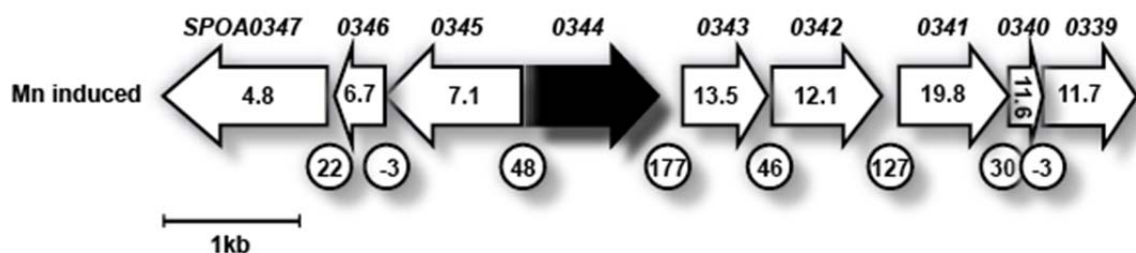
Within that cluster are four consecutive genes, SPO2264 – SPO2261, which are predicted to be in one operon. The expression of all four genes is much lower in the +Mn medium, with that of the promoter-proximal gene, SPO2264 having the highest factor of reduction (11.4-fold). The promoter-proximal gene (SPO2260) of a downstream operon is also significantly repressed by Mn, as are some of the other genes in the cluster, though to a lesser degree (Table 7.2; Figure 7.8). I am unaware of any reports that describe any biochemical or functional connections between manganese and GTAs.

7.3.5 Class IV – expression enhanced in Mn-replete medium, independent of the *mur* genotype

There were at least three other gene clusters whose expression was greater, sometimes to a remarkable extent, in the +Mn medium, irrespective of the *mur* genotype. These are as follows.

SPOA0343 –SPOA0339 and *SPOA0345-SPOA0347*

Figure 7.9 Map of *SPOA0339-SPOA0347*



Scale map of the *SPOA0339-SPOA0347* locus of *R. pomeroyi* including intergenic gaps (circled) and fold-change ratios for + Mn microarray experiments (Mn induced).

There is a cluster of nine closely linked genes, *SPOA0347 – SPOA0339* with a remarkable response to Mn availability. As shown in table 7.2, the expression of some of these was markedly *enhanced* (by factors as high as 20-fold) in Mn-replete medium, but this response was not mediated by Mur, since they displayed no differential expression in the Mur⁻ mutant and in the wild type strains. This cluster comprised two, divergently transcribed sets of genes, *SPOA0343 - SPOA0339* and *SPOA0345 - SPOA0347*, which were separated by *SPOA0344*, whose expression was unaffected by the availability of manganese or the *mur* genotype (Table 7.2; Figure 7.9).

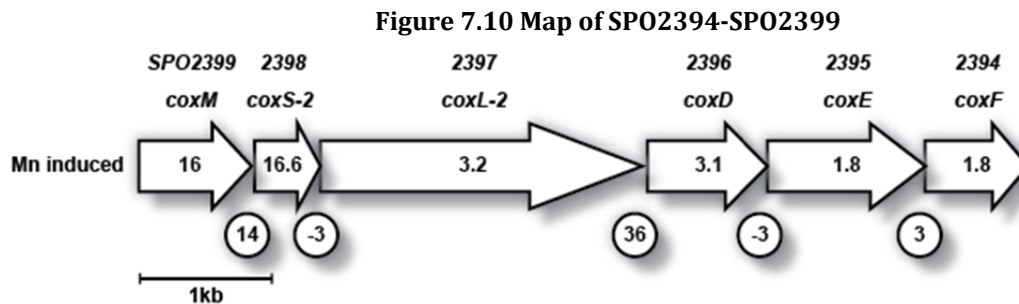
Three of these Mn-induced genes, *SPOA0345-SPOA0347*, were contiguous and are likely in a single operon. The other five may be co-transcribed, or may comprise two operons, *SPOA0343-SPOA0342* and *SPOA0341-SPOA0339*, separated by 128 bps (see Figure 7.9). None of these eight gene products

had close similarity to polypeptides of known function, although those of *SPOA0339*, *SPOA0340*, *SPOA0342*, *SPOA0345*, *SPOA0346* and *SPOA0347* could be allocated to general polypeptide families (Table 7.2). But even taking these various gene products together did not predict their overall biochemical function. However, it was noted that the closest homologues (ranging from 30% – 50% identical) of all of the gene products in this cluster occurred in a limited number of bacterial strains, namely *Erwinia tasmaniensis* Et1/99, *Acinetobacter* sp. ATCC 27244, *Photorhabdus asymbiotic*, and *Klebsiella oxytoca* KCTC 1686. And, in each of these strains, the corresponding genes that encoded the homologues were often clustered, as in *R. pomeroyi* DSS-3. Thus, even though these versions of the genes may have diverged very considerably in their sequences compared to those in *Ruegeria*, there has been long-term, concerted selection to maintain their linkage within the genomes of different bacteria, suggesting that the individual gene functions in these clusters operate co-ordinately towards similar biochemical purposes.

It is noteworthy that *SPOA0344*, which is located between the highly induced *SPOA0343* and *SPOA0345* but whose expression is not itself affected by the addition of $MnCl_2$, encodes a LysR-type regulatory (LTTR) protein. Members of this very widespread family normally activate their target gene(s) in response to a cognate small molecular weight co-inducer and are often autoregulatory, repressing their own transcription (Maddocks and Oyston 2008). There are no known members of the LTTR family that respond to Mn^{2+} , but the location of *SPOA0344*, between two sets of genes whose expression is markedly enhanced by this metal makes this gene a strong candidate for encoding a regulator that does sense manganese. In that connection, it was noted that there is a motif with dyad symmetry (5'-TTTCC-N₆-GGAAA-3'), respectively 137 and 79 bps upstream of the ATG starts of both *SPOA0343* and of *SPOA0345*, which might represent binding sites for the *SPOA0344* regulatory protein.

The *cox* genes, implicated in carbon monoxide oxidation

Cox cluster I



Scale map of the SPO2394-SPO2399 locus of *R. pomeroyi* including intergenic gaps (circled) and fold-change ratios for + Mn microarray experiments (Mn induced).

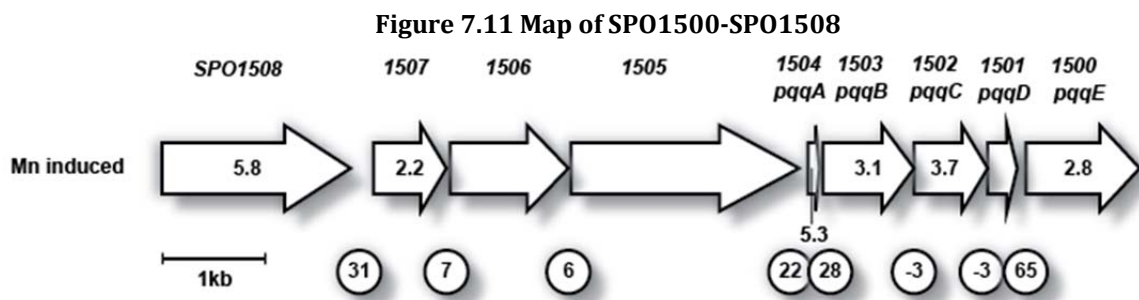
A feature of the Roseobacters is that most strains of this clade contain a group of *cox* genes (Cluster I – Figure 7.10), which are predicted to encode the enzyme carbon monoxide dehydrogenase, which catalyses the production of CO₂ from CO (Cunliffe 2011). Indeed, several strains, including *R. pomeroyi* DSS-3, have been shown to have CO oxidation activity (Cunliffe 2011), and it has very recently been shown in *Ruegeria pomeroyi* DSS-3 that these do indeed function on CO oxidation, since a mutation in one of them (*coxL-2* – SPO2397) completely abolished this ability (Simone Payne and Michael Cunliffe, personal communication) though it has not been formally shown that this is due to their annotated *cox* genes. Furthermore, some Roseobacters, including *R. pomeroyi* DSS-3, contain another cluster (Cluster II) of genes whose products have some sequence similarity to the *bona fide* Cox polypeptides, but which may not function in CO oxidation (Simone Payne and Michael Cunliffe, personal communication) (Cunliffe, 2011).

The expression of several of the genes within both the Form I cluster (SPO2394 – to SPO2499 inclusive; Figure 7.10) and in the Form II cluster (SPO1515 – SPO1521) was markedly enhanced in cells grown in +Mn medium, but that the *mur* genotype was not involved in this effect (Table 7.2). This enhanced expression is particularly pronounced with the consecutive and likely co-transcribed *coxM*, *coxS-2*, *coxL-2*, *coxD*, *coxE* and *coxG* genes in the Form I cluster; the signal for the promoter-proximal *coxM* gene is 16-fold greater in the Mn-grown cells. Several of the Form II genes show more

modestly enhanced expression in response to added Mn (Table 7.2). These include the consecutive genes *coxG*, *coxS-1*, *coxS-2* and *coxM*, plus two upstream genes *SPO1515* and *SPO1516*, which respectively encode a putative cytochrome c550 and a predicted periplasmic binding protein of an ABC transporter, though their functional link, if any, with carbon monoxide is unknown.

Although the CO dehydrogenase of *Oligotropha carboxidovorans* is a metallo-protein, with a very unusual metallo-cofactor, CuSMoO₂ (Resch *et al.* 2005), no functional links between manganese and the CO dehydrogenase enzyme have been reported in the literature.

SPO1508- SPO1500 region



Scale map of the SPO1500-SPO1508 locus of *R. pomeroyi* including intergenic gaps (circled) and fold-change ratios for + Mn microarray experiments (Mn induced).

Close to the Form II cluster of *cox* genes is another predicted operon, *SPO1504-SPO1500*, whose expression is enhanced by factors ranging from 1.6- to 5.3-fold for the different genes (Table 7.2). These five genes are predicted to encode components of the enzymes needed to make the bacterial redox active cofactor, pyrroloquinoline quinone (Puehringer *et al.* 2008). There is evidence that a quinone is used as a cofactor in Mn(II) oxidase of a strain of the alpha-proteobacterium *Erythrobacter*, a genus that is closely related to the Roseobacters (Johnson and Tebo 2008). Although several Roseobacters do have Mn(II) oxidase activity, *R. pomeroyi* DSS-3 does not (Hansel and Francis 2006), so the significance of this observation in terms of the effect of Mn on the expression of this *pqq* operon is not known.

Not far upstream of *SPO1504*, is *SPO1508* forming a predicted one gene operon that likely encodes

an ethanol dehydrogenase of a type that (perhaps significantly – see above) has PQQ as a co-factor. Though closely linked to *SPO1504-SPO1500* (Figure 7.11) it is not co-transcribed with these genes.

Table 7.2 Genes whose expression is affected by the Mur regulator and/or Mn²⁺ availability.

A. Class I genes; expression is reduced by Mn, and greater in Mur⁻ mutant than wild type.

^a Gene	^b Factor of reduction with added Mn ²⁺	^c Factor of increase in Mur ⁻ mutant	^d Predicted general function
SPO3363	3.8 ± 0.1	15.5 ± 1.1	Permease of ABC transporter; SitD
SPO3364	2.0 ± 0.3	6.6 ± 0.7	Permease ABC transporter; SitC
SPO3365	3.6 ± 0.2	18.3 ± 2.6	ATPase of ABC transporter; SitB
SPO3366	2.8 ± 0.1	8.8 ± 1.6	Periplasmic binding protein of ABC transporter; SitA
SPOA0392	6.95 ± 0.6	7.7 ± 0.4	Weak homology to RpoE-type σ-factor
SPOA0393	5.4 ± 0.6	6 ± 0	R body protein RebB-like protein
SPOA0394	2.1 ± 0.2	2.1 ± 0.3	Hypothetical; no known domains
SPOA0395	3.5 ± 0	5.1 ± 1.0	Hypothetical; no known domains
SPOA0396	5.75 ± 0.1	8.65 ± 2.2	Hypothetical; no known domains
SPOA0397	4.7 ± 0.6	4.75 ± 0.9	Hypothetical; no known domains
SPOA0398	6.1 ± 0.1	11.4 ± 0.1	R body protein RebB-like protein
SPOA0399	9.0 ± 0.5	16.2 ± 0.5	R body protein RebB-like protein

B. Class II genes; expression is enhanced by Mn, and lower in Mur⁻ mutant than wild type.

^a Gene	^b Factor of increase with added Mn ²⁺	^c Factor of reduction in Mur ⁻ mutant	^d Predicted general function
SPO1789	19.35 ± 2.7	14.25 ± 0.4	Related to permease of sulfate/tungstate ABC-type- transporter
SPO1790	10.5 ± 2.8	6.65 ± 0.9	Related to ATPase of sulfate/tungstate ABC-type- transporter
SPO1791	8.4 ± 2.4	5.75 ± 0.5	Related to periplasmic binding protein of sulfate/tungstate ABC-type-transporter
SPO0833	8.8 ± 0.2	7.9 ± 0.3	β polypeptides, molybdopterin-containing formate dehydrogenase
SPO1555	7 ± 0.1	5.95 ± 0.1	β polypeptides, molybdopterin-containing formate dehydrogenase α polypeptides, molybdopterin-containing formate dehydrogenase
SPO0834	3.9 ± 0.0	3.85 ± 0.5	
SPO1556	3.25 ± 0.2	3.4 ± 0.2	α polypeptides, molybdopterin-containing formate dehydrogenase
SPO1216	10 ± 0.1	12.55 ± 2.1	Hypothetical; no known domains

C. Class III genes; expression is reduced by Mn, and is unaffected by *mur* genotype.

^a Gene	^b Factor of reduction with added Mn ²⁺	^d Predicted general function
SPO2261	8.5 ± 1.4	GTA gene cluster; major capsid protein
SPO2262	7.3 ± 0.5	GTA gene cluster; possible peptidase
SPO2263	4.1 ± 1.0	GTA gene cluster; no known domains
SPO2264	13.6 ± 2.2	GTA gene cluster; phage portal polypeptide

D. Class IV genes; expression is enhanced by Mn, and is unaffected by *mur* genotype.

^a Gene	^b Factor of increase with added Mn ²⁺	^d Predicted general function
SPOA0339	11.7 ± 0.5	Subfamily of haloacid dehalogenase superfamily of aspartate nucleophile hydrolases
SPOA0340	11.6 ± 1.4	Related to 4-oxalocrotonate tautomerase
SPOA0341	19.8 ± 0.6	Hypothetical; no known domains
SPOA0342	12.1 ± 0.5	Related to AfsA family protein, involved in A-factor biosynthesis
SPOA0343	13.5 ± 2.0	Hypothetical; no known domains
SPOA0344	No change	LysR-type transcriptional regulator
SPOA0345	7.1 ± 0.6	In superfamily of soluble NAD(P)(H) oxidoreductases
SPOA0346	6.7 ± 0.4	Related to 4-carboxymuconolactone decarboxylase
SPOA0347	4.8 ± 0.4	Low-level similarity to major facilitator subfamily (MFS) of transporters
SPO2394	1.8 ± 0.15	Carbon monoxide dehydrogenase, CoxF subunit
SPO2395	1.8 ± 0.0	Carbon monoxide dehydrogenase, CoxE subunit
SPO2396	3.1 ± 0.1	Carbon monoxide dehydrogenase, CoxD subunit
SPO2397	3.2 ± 0.2	Carbon monoxide dehydrogenase, CoxL-2 subunit
SPO2398	16.6 ± 3.1	Carbon monoxide dehydrogenase, CoxS-2 subunit
SPO2399	16.0 ± 1.3	Carbon monoxide dehydrogenase, CoxM subunit
SPO1515	8.2 ± 0.5	Putative cytochrome <i>c550</i>
SPO1516	2.3 ± 0.1	Periplasmic-binding protein of ABC transporter; substrate unknown
SPO1517	6.5 ± 0.5	Membrane attachment for CoxG subunit (Form II) of CO dehydrogenase

SPO1518	2.5 ± 0.4	S-I subunit of CO dehydrogenase
SPO1519	No change	L-I subunit of CO dehydrogenase
SPO1520	2.1 ± 0.1	Medium sub-unit CO dehydrogenase
SPO1504	5.3 ± 0.1	PqqA-like; coenzyme PQQ synthesis protein A
SPO1503	3.1 ± 0.0	PqqB-like; coenzyme PQQ synthesis protein B
SPO1502	3.7 ± 0.1	PqqC-like; coenzyme PQQ synthesis protein C
SPO1501	No change	PqqD-like; coenzyme PQQ synthesis protein D
SPO1500	2.8 ± 0.4	PqqE-like; coenzyme PQQ synthesis protein E
SPO1508	5.8 ± 0.1	Strongly predicted quinoprotein (PQQ-dependent type I alcohol dehydrogenase)

*Tables 7.2: A, B, C and D respectively show the gene numbers in Classes I, II, III and IV, described in text. Column ^a; Clusters of genes whose levels of expression are affected by Mn availability and/or mur genotype are grouped. Column ^b; Mean ratios plus standard errors of increase or decrease in the microarray signals in "+" and "-" manganese media. Column ^c; Mean ratios plus standard errors of increase or decrease in the microarray signals in wild type compared to the Mur⁻ mutant in Mn-replete medium. Column ^d; Polypeptide family of gene product, where known, is indicated **Bold typeface** indicates RNA levels significantly reduced/increased ($p < 0.05$).*

7.4.1 Genes regulated by iron in *Ruegeria pomeroyi*

The expression of many *Ruegeria pomeroyi* genes was affected by the availability of Fe. In some cases, this appeared to be mediated by (or implicated) Irr or the Mur (or both) transcriptional regulators, but in other cases, neither of these was involved. Some examples of such genes are presented in the following section, note that these are given in much more abridged style than the Mn-regulated genes. The data generated in this experiment presented literally dozens of different combinations. So, I will restrict myself to those in which there is a really big difference irrespective of Irr and Mur and Mn.

7.4.2 Effects of iron availability and mutations in irr on the transcriptome of Ruegeria pomeroyi

There were 23 genes that were altered above the chosen cut-off points in their expression in both Fe limitation and in the *Irr*⁻ mutant (refer to Table 7.3). Of these, 10 had similar responses; repressed by Fe, and were expressed higher in the *Irr*⁻ background (see Table 7.1, sections E, H and J in Figure 7.2).

Table 7.3 Genes affected by both Fe limitation and the *irr* mutation

Venn box ^a	Gene ^b	result in Fe ^c	result in Irr ^d
E	<i>SPO0086</i>	49.7 ± 9.1	3.83 ± 0.15
E	<i>SPO0087</i>	56.25 ± 0.04	4.135 ± 0.4
E	<i>SPO0169</i>	4.53 ± 1.4	3.71 ± 1.4
E	<i>SPO0199</i>	5.96 ± 0.5	1.615 ± 0.06
E	<i>SPO0647</i>	3.08 ± 0.02	1.56 ± 0.03
E	<i>SPO0790</i>	28 ± 0.4	2.31 ± 0.03
E	<i>SPO2023</i>	4.42 ± 0.2	2.3 ± 0
E	<i>SPO2486</i>	2.975 ± 0.4	3.04 ± 0.2
E	<i>SPO3014</i>	6.69 ± 0.4	2.235 ± 0.1
E	<i>SPO3287</i>	45.85 ± 5.1	1.995 ± 0.01
E	<i>SPO3359</i>	16 ± 0.5	1.96 ± 0.03
E	<i>SPO3360</i>	13.25 ± 0.1	1.985 ± 0.04
E	<i>SPO3607</i>	4.095 ± 0.03	1.7 ± 0.05
E	<i>SPOA0445</i>	3.52 ± 0.04	n/a
H	<i>SPO0222</i>	32.15 ± 1.2	5.8 ± 0.5
H	<i>SPO0701</i>	13.85 ± 0.1	2.105 ± 0.02
H	<i>SPO1565</i>	4.125 ± 0.2	1.55 ± 0.01
H	<i>SPO1861</i>	3.085 ± 0.02	1.545 ± 0.04
H	<i>SPO2264</i>	8.8 ± 0.4	2.145 ± 0.2
J	<i>SPO1216</i>	6.655 ± 0.4	13.7 ± 1
J	<i>SPO2398</i>	6.36 ± 0.6	3.38 ± 0.09
J	<i>SPO2399</i>	7.87 ± 0.3	3.44 ± 0.2
J	<i>SPOA0399</i>	3.205 ± 0.2	15.7 ± 1.2

(Column a) shows those genes from sections E and H and J of Venn diagram, Figure 7.2, their resultant expression (in fold change, ± the standard deviation {Column b}). Red indicates that the gene was expressed higher in the absence of Fe than its presence (Column c) or that expression was higher in the *Irr*-mutant than in the wild type (Column d). The green boxes indicate the opposite ratio of expression.

Six genes had the opposite phenotype, being induced by iron, but expressed at lower levels in the *Irr*⁻ mutant than in the wild type. These genes include the *cox* genes *SPO2398* and *SPO2399* which are discussed above in relation to their responses to manganese. Another gene that displayed this pattern was *SPO1216*, which was expressed 6.6-fold higher when Fe was present in the medium, and 13.7-fold less in the *Irr*⁻ strain compared to the wild type. The translated product of *SPO1216* does not have any predicted function, and there is only one other homologous peptide found in the ncbi database – in *Dinoroseobacter shibae* DFL-12.

Finally, there were six genes that were shown to be repressed by Fe, and were expressed at higher levels in the *Irr⁻* background. These genes may be under the control of a repressor in the *Irr* regulatory hierarchy, and would be good targets for further experiments to elucidate the Fe-regulatory networks in *R. pomeroyi*.

Four of these genes have predicted function, and two were adjacent to each other in the genome. These two genes, *SPO3359* and *SPO3360*, were closely linked to the *sitABCD* operon, and were ~14-fold repressed by the added FeCl₃, and were 2-fold lower in the *Irr⁻* background compared to the wild type. These two genes are predicted to encode an L-threonine 3-dehydrogenase and a 2-amino-3-ketobutyrate coenzyme A ligase respectively; these are both well conserved in the Roseobacters, and are closely related to peptides found in both α - and γ -proteobacteria.

Two other, unlinked genes, *SPO0222* and *SPO0701*, were significantly Fe repressed, 32- and 14-fold respectively, and were 5.8- and 2.1-fold lower in the *Irr⁻* background. The translated product of *SPO0222* is predicted to be an alanine dehydrogenase, which is well conserved in the Roseobacters and indeed throughout the proteobacteria.

Finally, *SPO0701* is predicted to encode a Type 1 glyceraldehyde-3-phosphate dehydrogenase. It is difficult to assign any likely link to iron for these genes, other than these preliminary transcriptomic data.

In summary, there are clearly some interesting target genes here for further study into the role *Irr* plays in regulated iron uptake and usage in *R. pomeroyi*. Given that the genes presented in table 7.2 exhibit differential regulation in response to both Fe, and *Irr*, there must be other transcriptional regulatory elements which mediate this, and indeed this précis of the *R. pomeroyi* transcriptional response to Fe should allow a focussed approach into this future work. Note that 12 out of the 23 genes shown in table have no predicted function; there is therefore still much to learn about the “iron-ome” in this bacterium.

7.5.1 Genes that enhance the story already told in this thesis – regulation and uptake of Mn and Fe

So far, we have defined the system for Mn uptake, via *SitABCD*, and the regulation of this process, via *Mur* in *R. pomeroyi*, and this microarray analysis has verified our findings. However, the same cannot be said for Fe; an *FbpAB⁻* strain of *R. pomeroyi* did not have a growth deficiency on low iron,

meaning there must be functional redundancy for inner membrane iron transport, or that these genes do not encode an iron-specific transporter. Also, Fe-responsive regulation has been demonstrated for *Irr* of *R. pomeroyi*, but the regulator of other iron-responsive genes – those with an IR box has not been identified. The following provides a walk-through of the transcriptional responses of genes already studied in this work, and provides further insight into the ‘unknown’ aspects of *Ruegeria* iron metabolism.

7.5.2 *Irr*

The transcription of *Irr* was *induced* ~3.5-fold by Fe. This agrees with findings in *Rhizobium* (Todd *et al.* 2002), but in *Brucella abortis*, *Bradyrhizobium japonicum* and *Rhodobacter sphaeroides*, *Irr* was not Fe-regulated at a transcriptional level (Martinez *et al.* 2005; Peuser *et al.* 2012; Qi *et al.* 1999). In these organisms, *Irr* is regulated at a post-transcriptional level. It would be of interest to study the effect of high/low Fe on *Irr* protein levels in *R. pomeroyi*, and also whether this protein has a haem binding capacity. As shown above, several genes were altered in expression in the *Irr*⁻ strain of *R. pomeroyi*.

7.5.3 *MbfA*

The expression of *mbfA* homologues have been shown to be regulated by *Irr* in *Rhizobium*, *Bradyrhizobium* and *Brucella* (Martinez *et al.* 2005; Qi *et al.* 1999; Todd *et al.* 2002).

In *Ruegeria*, *mbfA* expression was Fe induced, as shown by both *lacZ* fusion, and in the microarray study. This regulation is likely due to *Irr*, via an ICE box motif, as *mbfA* expression was significantly higher in the *Irr*⁻ background than in the wild type (13.5-fold), also in agreement with *lacZ* fusion data.

7.5.4 IscR

Another gene with a conserved ICE motif was the regulator of [Fe-S] biosynthesis, *iscR*. Indeed, it is likely that this gene forms part of a single transcriptional unit with the downstream *suf* genes. The expression of *iscR* was only significantly differently (2.5-fold) regulated in the *Irr* mutant compared to the wild type, and not by Fe levels. Furthermore, the downstream *suf* genes showed little regulation in response to either *Irr*, or Fe (all <2-fold). A *lacZ* fusion to *iscR* showed considerable deregulation in the *Irr*- strain, which is not apparent in the microarray data. It is clear that further work on the regulation of both *iscR* and the *suf* genes is required.

7.5.5 RRF-2 family proteins

It was hypothesised that the regulator of the IR boxes of *R. pomeroyi* may be an Rrf2 family protein, similar to RirA found in the rhizobiales. However, mutant strains lacking each individual Rrf2 family protein found in *R. pomeroyi* were not deregulated in expression of genes under the control of IR boxes (see Chapter 4). It was of interest to observe the transcriptional response of each Rrf2 gene in *R. pomeroyi*, to both Fe, and to *Irr* since RirA has been shown to be *Irr* and Fe regulated in *Rhizobium* (Todd *et al.* 2006; Todd *et al.* 2002).

Interestingly, four of the Rrf2 family genes were iron regulated:

SPO0432 – 7.8-fold Fe induced

SPO3722 – 5.4-fold Fe repressed

SPO1393 – 3.9-fold Fe repressed

SPOA0186 – 3.4-fold Fe repressed

And, as discussed, the fifth Rrf2 family gene, *iscR* (*SPO2025*) was not Fe regulated, but was *Irr* repressed.

This result would appear to show that there may well be functional redundancy between these regulators, and it is possible that multiple, clearly Fe-responsive regulators are responsible for the repression of genes under the control of IR boxes. Crucially, none of the Rrf2 family genes were altered in expression by either Mn or Mur.

7.5.6 The *fbpAB* genes

As shown in Chapter 4, the expression of *fbpA* and *fbpB* is Fe-repressed, mediated by IR boxes of which *fbpA* has two and *fbpB* just one. As discussed earlier, there is a lack of a cognate ATPase gene for this putative iron transporter, FbpAB, and it was proposed that *SPO2689* may encode a likely candidate (refer to Chapter 4).

The microarray data confirm that *fbpA* is highly Fe-repressed; indeed it is one of the most Fe-repressed genes in the array data (~45-fold). However, and in agreement with *lacZ* fusion data, expression of *fbpB* is far less Fe-repressed (3.9-fold).

The expression of any potential ATPase peptide is less clear, the hypothesised *SPO2689* is poorly induced in low Fe conditions (<2-fold), and is unlikely to be the ATPase for the FbpAB transporter. Indeed, this transporter may not be required at all by *R. pomeroyi* as a functional mutant was unaffected in growth (Chapter 4). Furthermore, as shown in Table 7.4, there were no other ABC-class transporter genes induced >5-fold by Fe limitation in this microarray experiment.

7.5.7 The *irp* genes

The *irp* locus of *R. pomeroyi* is a fascinating prospect for a novel iron uptake mechanism (see Chapter 3). Here, the microarray study further emphasised this potential: As shown in Table 7.4, the genes *SPO0086-SPO0090* were all hugely Fe-repressed, and are therefore very likely to form a single transcriptional unit. Indeed *SPO0086* (*irpA*) was the single highest iron regulated gene in all replicates of these conditions. Furthermore, there were strong predictions of signal peptides, and localisation to the outer membrane for *SPO0086*, and other genes in this operon (Table 7.4).

In Chapter 4, *irpA* was shown to be Fe-repressed, and that this was mediated by a copy of an IR box.

The expression of both *SPO0086* and *SPO0087* were also shown to be Irr repressed, albeit by a low level compared to the level of Fe-repression (Appendix 3). This could be an artefact of the Fe status of an Irr⁻ strain compared to the wild type, or may represent a cross-over in regulation from Irr to the transcriptional regulator of IR boxes.

7.6.1 Genes highly regulated by iron and manganese limitation

A detailed predictive functional analysis was performed on all those genes whose expression was altered, >5-fold in the iron limitation experiment. This list of 98 genes was analysed using a variety of online predictive programs to gain an insight into the putative function, location and structure of all 98 proteins.

Table 7.4 *Ruegeria pomeroyi* genes whose expression was altered >5-fold in response to iron limitation; predicted function, cellular location, structural prediction and prevalence in the Roseobacters

Gene ID - operons shaded	Iron Array Result	Manganese Array Result	Function (if known)	Accession number	Localisation (pSORTB)	Signal Peptide (SIGNALP)	TAT signal (TATP)	Beta Barrel (MCMBB)	Pred TMBB	Presence in other Roseobacters (max 150)
SPO0086	56.3	1.48	lipoprotein, putative	YP_165360	OuterMembrane 9.93	YES		0.014	YES	33
SPO0087	58.8	1.245	hypothetical	YP_165361	Unknown	YES		0.052	YES	8
SPO0088	29.7	1.11	thiol oxidoreductase	YP_165362	CytoplasmicMembrane 9.82			-0.042	YES	33
SPO0089	11	1.9	Imelysin, Peptidase_M75	YP_165363	Unknown	YES		-0.018	YES	30
SPO0090	14.8	1.13	hypothetical	YP_165364	Unknown		YES	0.003	YES	32
SPO0181	7.66	1.0375	Flagella rod protein FlIC	YP_165451	Unknown MLS		YES (But no TA)	0.009	NO	30
SPO0197	6.37	1.24	flagellar motor switch protein FlIN	YP_165467	Extracellular 2.00			-0.004		20
SPO0198	6.2	1.08	ABC transporter ATP-binding protein, flagellar	YP_165468	Extracellular 0.26			-0.031		18
SPO0199	5.45	1.15	Flagella MS-ring protein	YP_165469	Extracellular 0.00			0.008	Possible	32
SPO0222	33.3	4.025	Alanine dehydrogenase [Amino acid transport and metabolism]	YP_165491	Periplasmic 0.01			-0.024		78
SPO0227	5.28	1.51	Peptidase M10 serralyisin C terminal	YP_165496	Extracellular MLS* 10.00			-0.067		100
SPO0254	6.01	1.72	organic hydroperoxide resistance protein OsmC	YP_165518	Cytoplasmic 9.26			-0.001		11
SPO0313	9.97	1.425	Glyoxalase/Bleomycin resistance protein	YP_165576	Unknown			0.001	NO	23
SPO0390	5.5	1.23	glutamate/leucine/phenylalanine/valine dehydrogenase	YP_165653	Cytoplasmic 9.97			0		17
SPO0432	7.42	1.775	rirA' RRF-2 family transcriptional regulator	YP_165695	Cytoplasmic 8.96			-0.069		28
SPO0692	9.04	1.0005	Cytochrome C oxidase subunit II, periplasmic	YP_165947	Periplasmic 9.76		YES	-0.032		49
SPO0701	13.7	4.02	glyceraldehyde-3-phosphate dehydrogenase	YP_165955	Cytoplasmic 9.97			-0.013		121
SPO0759	9.11	1.11	hypothetical	YP_166012	Unknown			-0.01		1
SPO0784	12.8	1.585	chloramphenicol acetyltransferase	YP_166037	Unknown			-0.044		26
SPO0789	18.8	1.0045	Hemin uptake protein hemP	YP_166042	Unknown			-0.024		1
SPO0790	28.4	1.0605	hypothetical	YP_166043	Unknown			-0.087		21
SPO0858	13.9	1.155	MauG methylamine utilisation protein	YP_166111	Periplasmic 9.76	YES		-0.028		49
SPO0900	5.5	2.465	bifunctional sulfate adenylyltransferase 'sat'	YP_166153	Cytoplasmic 9.97			-0.058		38
SPO1018	5.93	1.535	branched-chain amino acid ABC transporter ATPase	YP_166270	Cytoplasmic MLS 9.12			-0.039		150
SPO1019	8.37	1.355	branched-chain amino acid ABC transporter permease	YP_166271	CytoplasmicMembrane 10.00			-0.023		150
SPO1020	7.33	1.385	branched-chain amino acid ABC transporter permease	YP_166272	CytoplasmicMembrane 10.00			-0.051		150
SPO1021	7.58	1.62	branched-chain amino acid ABC transporter substrate binding	YP_166273	Unknown	YES	YES	-0.002		39
SPO1177	9.85	1.06	hypothetical	YP_166424	Unknown			-0.006		1
SPO1216	7.05	9.985	hypothetical	YP_166463	CytoplasmicMembrane 10.00			-0.026		2
SPO1280	5.48	1.635	hypothetical	YP_166525	Cytoplasmic 8.96			-0.052		33
SPO1351	8.23	1.65	MetZ - O-succinylhomoserine sulphydrylase - Methionine biosynthesis	YP_166593	Cytoplasmic 9.97			-0.01		135
SPO1366	5.41	1.11	ilvC ketol-acid reductoisomerase Isoleucine biosynthesis	YP_166608	Cytoplasmic 9.97			-0.064		37
SPO1387	7.65	1.215	cation efflux system protein	YP_166629	CytoplasmicMembrane 10.00			-0.075		40
SPO1409	5.28	1.265	rpoH heat shock sigma factor	YP_166650	Cytoplasmic 9.97			-0.023		112
SPO1515	9.3	8.165	cytochrome c550	YP_166756	Unknown MLS	YES		-0.011		8
SPO1517	5.76	6.49	coxG carbon monoxide dehydrogenase operon G protein	YP_166758	Unknown			-0.034		52
SPO1593	5.49	1.82	zinc-dependent alcohol dehydrogenase	YP_166834	CytoplasmicMembrane 9.82			-0.022		100
SPO1689	12.1	1.0225	hypothetical	YP_166928	Unknown	YES		-0.018		3
SPO1795	12.6	1.15	HybA - formate dehydrogenase, iron-sulfur subunit	YP_167032	Cytoplasmic 9.97			-0.132		31
SPO1796	24.8	1.07	formate dehydrogenase subunit alpha	YP_167033	Periplasmic 9.76			-0.041		97
SPO1847	5.24	2.29	Long-chain acyl-CoA synthetases	YP_167084	CytoplasmicMembrane 7.88			-0.049		150
SPO1909	8.03	1.07	NTF2_like domain, hypothetical protein	YP_167145	Cytoplasmic 8.96			-0.03		8
SPO2130	6.47	1.755	alpha-isopropylmalate/homocitrate synthase	YP_167358	Cytoplasmic 9.97			-0.008		75
SPO2131	8.54	1.045	cysS - cysteinyl-tRNA synthetase	YP_167359	Cytoplasmic 10.00			-0.039		36
SPO2135	5.86	1.205	Hypothetical	YP_167363	Unknown	YES		0.004	Possible	2
SPO2222	5.51	1.055	dihydrolipoamide dehydrogenase	YP_167448	Cytoplasmic 9.97			-0.039		150
SPO2246	9.66	1.305	CysK - cysteine synthase A	YP_167472	Cytoplasmic 9.26			-0.008		56
SPO2261	10.8	8.44	HK97 family major capsid protein	YP_167486	Unknown			0.008	YES	34

Gene ID - operons shaded	Iron Array Result	Manganese Array Result	Function (if known)	Accession number	Localisation (pSORTB)	Signal Peptide (SIGNALP)	TAT signal (TATP)	Beta Barrel (MCMBB)	Pred TMBB	Presence in other Roseobacters (max 150)
SPO2262	7.83	7.23	HK97 family phage prohead protease	YP_167487	Unknown			0.02	YES	36
SPO2264	8.4	13.6	HK97 family portal protein	YP_167489	Unknown		YES	-0.011		33
SPO2398	5.74	16.55	coxS carbon monoxide dehydrogenase, small subunit	YP_167617	Cytoplasmic 9.97			-0.121		150
SPO2399	8.18	16	coxM carbon monoxide dehydrogenase, medium subunit	YP_167618	Cytoplasmic 9.97			-0.027		80
SPO2508	10.5	1.54	hypothetical	YP_167723	Unknown			-0.005		1
SPO2614	17.7	1.105	hypothetical	YP_167824	Cytoplasmic 8.96			-0.06		1
SPO2615	18.5	1.15	Oye family NADH-dependent flavin oxidoreductase	YP_167825	Cytoplasmic 9.97			0.017	YES	96
SPO2632	9.08	1.925	CobJ type uroporphyrin-III C-methyltransferase	YP_167842	Cytoplasmic 9.26			-0.01		100
SPO2633	8.67	1.675	hypothetical	YP_167843	Unknown			-0.011		33
SPO2634	10.8	2.43	CysI - sulfite reductase	YP_167844	Cytoplasmic 9.97			-0.031		37
SPO2636	8.25	2.225	hypothetical	YP_167846	Unknown			0.013	NO	37
SPO2637	5.43	1.565	ferredoxin-NADP reductase	YP_167847	Cytoplasmic 9.97			-0.049		46
SPO2686	5.84	1.515	LysM/M23/M37 peptidase	YP_167896	OuterMembrane 9.92	YES		0.016	YES	38
SPO2706	14.5	1.845	caiD-1 carnitiny-CoA dehydratase	YP_167916	Cytoplasmic 9.97			-0.057		150
SPO2839	5.05	1.64	GlcB - malate synthase G	YP_168047	Cytoplasmic 9.97			-0.053		35
SPO2867	6.69	1.21	CobJ type precorrin-3B C(17)-methyltransferase	YP_168075	Cytoplasmic 9.97			-0.031		36
SPO2962	10.8	1.93	hypothetical	YP_168170	Unknown			-0.058		1
SPO3014	7.04	1.56	hypothetical	YP_168218	Unknown			-0.097		2
SPO3027	7.61	1.28	HisC - histidinol-phosphate aminotransferase	YP_168231	Periplasmic 9.80			-0.025		77
SPO3118	6.09	1.06	hypothetical	YP_168321	Unknown		YES	0.043	Possible	1
SPO3287	50.9	1.155	FbpA - ferric iron ABC transporter periplasmic binding protein	YP_168483	Periplasmic 9.76			0.01	YES	41
SPO3355	5.34	1.93	SerA - serine biosynthesis D-3-phosphoglycerate dehydrogenase	YP_168551	Cytoplasmic 9.97			-0.02		150
SPO3359	15.5	1.3	L-threonine 3-dehydrogenase	YP_168555	Cytoplasmic 9.97			-0.035		57
SPO3360	13.2	1.695	2-amino-3-ketobutyrate CoA ligase	YP_168556	Cytoplasmic 9.97			-0.008		92
SPO3409	5.32	1.37	anti-anti-sigma factor	YP_168605	Unknown			0.01	NO	30
SPO3445	7.42	1.255	IpxK tetraacyldisaccharide 4'-kinase	YP_168641	Unknown			-0.016		37
SPO3523	5.68	1.18	CcoP cytochrome c oxidase, cbb3-type subunit III	YP_168718	Unknown			-0.01		37
SPO3524	6.68	1.3	CcoQ cytochrome c oxidase, cbb3-type subunit IV	YP_168719	CytoplasmicMembrane 9.82			-0.015		8
SPO3525	8.25	1.36	CcoO-1 cbb3-type cytochrome c oxidase subunit II	YP_168720	Unknown			-0.029		37
SPO3526	6.66	1.27	CcoN-1 cbb3-type cytochrome c oxidase subunit I	YP_168721	CytoplasmicMembrane 10.00			-0.04		39
SPO3529	5.97	1.155	serine hydroxymethyltransferase	YP_168724	Cytoplasmic 9.97			-0.022		61
SPO3547	8.45	1.89	hypothetical	YP_168742	Unknown			-0.074		6
SPO3606	5.28	1.215	mandelate racemase	YP_168801	Periplasmic 9.51			-0.026		37
SPO3613	5.7	1.1	LysE - amino acid transporter	YP_168808	CytoplasmicMembrane 10.00			-0.026		59
SPO3721	7.17	1.46	hypothetical	YP_168915	CytoplasmicMembrane 10.00			-0.058		1
SPO3722	5.33	1.145	RRF2 family transcriptional regulator	YP_168916	Unknown			-0.053		2
SPO3770	5.24	1.585	GlhD type oxidoreductase	YP_168965	Cytoplasmic 9.97			-0.039		73
SPOA0061	6.16	1.83	KatG - catalase/peroxidase HPI (heme binding site)	YP_164892	Cytoplasmic 9.26			-0.02		39
SPOA0273	8	1.355	PuuR - transcriptional repressor, putrescine degradation	YP_165102	Cytoplasmic 9.97			-0.017		11
SPOA0321	6.05	1.05	glyoxalase family protein	YP_165148	Unknown			-0.05		7
SPOA0339	149	11.65	HAD family hydrolase	YP_165166	Cytoplasmic 9.97			-0.015		1
SPOA0340	109	11.6	4-Oxalocrotonate Tautomerase	YP_165167	Unknown			-0.032		1
SPOA0341	164	19.8	hypothetical	YP_165168	Cytoplasmic 8.96			-0.05		1
SPOA0342	47.4	12.05	hypothetical	YP_165169	Cytoplasmic 8.96			-0.071		1
SPOA0343	86.5	13.5	hypothetical	YP_165170	Cytoplasmic 8.96			-0.002		1
SPOA0345	79.8	7.125	aldo/keto reductase family oxidoreductase	YP_165172	Cytoplasmic 9.97			-0.04		57
SPOA0346	91.2	6.665	carboxymuconolactone decarboxylase family protein	YP_165173	Unknown			-0.031		4
SPOA0347	29.8	4.745	MFS - secondary transporter superfamily	YP_165174	CytoplasmicMembrane 10.00			0.011	YES	13
SPOA0348	10.4	3.35	hypothetical	YP_165175	Unknown			-0.031		13

*MLS means this protein may have multiple localisation sites.

The 97 genes with >5-fold difference in expression are listed in column 1, and the relative fold change in expression is shown for Fe limitation in column 2, and for Mn in column 3. The accession number of each protein is shown in column 4, and the predicted subcellular location as given by pSORTB (Yu et al. 2010) in column 5. Column 6 contains the prediction of a SEC signal peptide {SignalP, (Petersen et al. 2011)}, and column 7 contains a TAT signal peptide prediction {TATP, (Bendtsen et al. 2005)}. Columns 8 and 9 contain predictions for beta-barrel structure, and transmembrane beta-barrel structure respectively {PredTMBB, (Bagos et al. 2004)}. Each peptide sequence was used to interrogate the Roseobase database, and the relative numbers of homologues found were converted into a scale from 1, where there was only one homologue, to 150, where there were multiple homologues in many of the Roseobacter strains. These data are shown in column 10.

There are a few intriguing genes which were highly regulated by Fe limitation, referring to table 7.4. Given that the only homologue for an Fe-specific ABC-class transporter is incomplete (*fbpA* and *fbpB*), it was of interest to see that *SPO1018-SPO0121* were all induced >6-fold in the absence of iron. These genes encode a complete ABC-class transporter, an ATPase, 2 permease proteins and a substrate binding protein (respectively, *SPO1018-SPO1021*). These genes are annotated as a branched –chain amino acid transporter, but are <10% ID to FbpAB or SitABCD. However, given their induction by iron limitation, further work on these genes would be useful for our understanding of their possible role in Fe uptake.

The two genes of the transcriptional unit *SPO0789-SPO0790* were both highly induced (19- and 28-fold respectively) in the absence of Fe. Interestingly, the former is predicted to be a haemin uptake protein, HemP (pfam10636), but the *SPO0790* product has no predicted function. HemP has been shown to be required for haem uptake in *Yersinia enterocolitica*, where it serves as a haemin uptake system, and is Fur regulated (Stojiljkovic and Hantke 1992). *R. pomeroyi* is the only genome-sequenced Roseobacter that contains such a *hemP* like gene, unlike *SPO0790* which is present in >20 Roseobacter genomes.

A suite of cytochrome genes (*SPO3523-SPO3526*) were shown to be repressed in low Fe (5 to 8-fold). These four genes encode all four subunits of a Cbb3-class cytochrome C oxidase. This family of cytochromes are haem-copper oxidases, and catalyse the final step in aerobic respiration of dioxygen to water. It is interesting to see that a haem containing protein complex is repressed in low

Fe conditions, and could be an example of bacterial adaptation to a low Fe environment, conserving the demand for the metal by down-regulating gene products which require Fe.

The Cox genes introduced above for their Mn-responsive expression also show a significant increase in expression by Fe, and that this is likely mediated by Irr. The expression of *coxL-2* (*SPO2399*) is ~5-fold induced by iron, and shows a ~3-fold induction by Irr.

Finally, and of note, a gene encoding a predicted anti-anti sigma factor (*SPO3409*) was 5.3-fold Fe-repressed. The deduced protein of this gene is in the STAS and SulP families (pfam01740) which are proposed to be regulatory over anion transport – including sulphur, from where the SulP name is derived. Given that *SPO3409* was Fe-repressed, this gene product would therefore be in a higher concentration during Fe-limitation, and would be predicted to increase its binding to its cognate anti sigma factor, releasing the sigma factor which would, in turn, allow the expression of a suite of genes. Further microarray analysis of a mutant in this gene might be instructive in the analysis of such a regulatory circuit.

Chapter 8 - General Discussion

The work described in this thesis represents the first sortie into the genetics and genomics of manganese and of iron homeostasis in the Roseobacters and is one of very few studies on this subject in any marine bacteria. The recent work on *Rhodobacter* and *Pelagibacter* only appeared well into the project (Peuser *et al.*, 2011; Smith *et al.*, 2010).

In what follows, I summarise the major outcomes of the work in the form of a series of questions that address future challenges in these topics, and outline the sorts of experiments that could be used to answer these. The discussion deals separately with the two metals.

8.1 Iron - Bioinformatically based outcomes

8.1.1 Paucity of ferrous iron and Fe-reductase genes

One consistent observation of the deduced proteomes of the Roseobacters was that they lack the FeoA/B ferrous iron uptake system, although the *feoAB* genes are commonly found in other alpha-proteobacteria, such as *Rhodobacter sphaeroides* and *Caulobacter crescentus*. This suggests that the Roseobacters may not use this reduced form of the metal, consistent with the fact that the surface waters of the oceans are fully oxygenated. Furthermore, there were no examples of any enzyme that resembled a flavo-reductase in the deduced proteomes of any Roseobacters. However, given that UV light has been shown to reduce Fe(II), the Roseobacters may simply not require a cognate reductase (Butler and Theisen 2010).

However, Roseobacters are also found in marine sediments (Wagner-Döbler and Biebl, 2006), where the O₂ tension would be lower, so the Roseobacters may be able to import Fe(II), but via an uncharacterised transporter. FeoAB mutants are deficient in Fe(II) uptake, shown by growth, and by final Fe content of cells. For growth experiments, Fe(II) can be produced by the addition of ascorbate to FeCl₃ (Kammler *et al.* 1993). To identify a potential Fe(II) uptake system, a Tn5 mutant library could be screened for increased expression of an iron-repressed reporter fusion during growth on Fe(II) supplemented media.

All Roseobacters lacked any known ferric reductases that correspond to the *ferAB* or *mtrAB* gene products. However, *Oceanicola granulosus* HTCC2516 was unusual in that it encodes a protein (*OG2516_12819*) that is 34% identical to YqjH of *E. coli* – a polypeptide that is implicated in ferric iron reduction from siderophores (Miethke *et al.* 2011). Indeed, the *Oceanicola* gene product is annotated as a siderophore-interacting protein. It would be interesting to see if *Oceanicola* can grow with only reduced Fe, and if so, to examine the effect of a mutation in the *OG2516_12819* gene.

It is possible that Roseobacters simply have no need to reduce Fe (III) and instead entirely rely on the uptake of Fe-chelates. It has been shown that Fe-siderophore complexes can be reduced by sunlight, which causes an increase in Fe uptake by marine microorganisms (Amin *et al.* 2009). This may make ferric reductases redundant in the case of the Roseobacters.

The status of Fe in the oxygenated open water is likely to be mostly fully oxidised. However, within other marine environments, such as marine snow, sediment and in large clusters of bacteria, it would be possible for areas of reduced Fe to exist, and would likely be a target for uptake by bacteria inhabiting such places.

To further study the Fe status of different habitats, and how this relates to the types of bacteria Fe uptake systems would require careful sampling of bacteria from such habitats, and then to study the presence of Fe(II) uptake genes in these strains. Currently, the Roseobacter strains that have available genome sequences were not sampled precisely from specific marine habitats. Although demanding, it might be instructive to examine the expression of genes, and indeed, genomes of the Roseobacters in more precisely defined niches, in which, for example, the O₂ levels were much lower than in the surface waters of the oceans. This might be done by high throughput metatranscriptomics, for example.

Another major outcome of the work in this thesis was the demonstration of the diversity of the predicted systems for the uptake of iron. There is a bewildering variety in the numbers and identities of the different, predicted mechanisms for the acquisition of this metal, with some strains being predicted to have multiple (the maximum predicted number, In *Ruegeria* sp. Trich CH4B, was ten) TonB-dependent receptors and others with none (see Chapters 2 and 6).

8.1.2 Marine siderophore production and uptake

Several strains of *Roseobacter* that contain TBDRs lack predicted siderophore synthesis genes (see Chapter 2). These strains are most probably siderophore ‘pirates’, being able to use siderophores that are made by other strains. This phenomenon is not unique to the *Roseobacters* and has been reported in many bacteria (Traxler *et al.* 2012).

However, this strategy may be expected to be more prevalent in marine bacteria since unattached siderophores will drift away from the bacterial cell that produced them. Alison Butler and colleagues have shown that marine bacteria can produce lipid-bound, amphiphilic siderophores that can form micelles, as described in Butler and Theisen (2010). However, there is no evidence that any *Roseobacter* siderophores have these properties, as there is no information about the siderophore biosynthetic genes for those molecules identified by Alison Butler’s lab.

It was noted that several strains of *Roseobacters* have genes that are predicted to be involved in siderophore production – and other genes involved in uptake (see Chapter 2). This raises a pertinent question: Is it beneficial to synthesise a siderophore in a marine environment? The likelihood of a single cell ever synthesising, exporting and then recovering a siderophore seems highly unlikely.

Since very little is known about the biosynthetic genes of marine siderophores, bioinformatic predictions about the presence of siderophores in any *Roseobacter* should be treated with caution. The logical next step in this area of my work would be to screen all of the *Roseobacter* strains for siderophore production using CAS plate, or other assays (see Chapter 4). Those strains which do produce siderophores would be used to construct mutant libraries, and screened again for a CAS phenotype. This would function two-fold, firstly in the identification of any potential negative regulators of siderophore production (a larger CAS halo) and secondly to identify siderophore biosynthetic genes (no CAS halo). This would represent the first example of siderophore biosynthetic gene identification in marine bacteria.

Furthermore, and importantly to supplement the data generated in Chapter 2, would be to identify the cognate molecules taken up by each TBDR. One approach to achieve this would be to take those *Roseobacters* with a single, or small number of receptor genes, and to perform metabolic arrays, for growth on many different Fe-ligand sources. Once a potential Fe-ligand has been identified, the

cognate outer membrane receptors can be systematically mutated until the strain no-longer grows on that Fe source.

Since there is no exact information about the siderophores that may be produced by members of the Roseobacter clade, it would also be pertinent to perform siderophore purification, and structural analysis on these molecules. These novel siderophores could be used to identify their cognate receptors using metabolomics if a high enough concentration can be purified. This strategy would be particularly useful in those strains which appear to have both siderophore synthesis and uptake systems in their genome.

8.1.3 *TonB*

TonB is required for outer membrane transport of several Fe-bound compounds: siderophores, haem and vitamin B₁₂, for example. It was therefore surprising to find that TonB was missing from many Roseobacter strains, as had been noted by Rodionov *et al.* (2006.) However, given the significant variation of TonB peptides (*E. coli* TonB is only ~30% identical to TonB of *Rhizobium* for example), it could be that a gene performing the function of TonB is present in these genomes, but is unidentifiable by means of homology-based searches. Importantly, some Roseobacters *do* have siderophore biosynthetic genes, and yet do not appear to have TonB.

It was also apparent that several Roseobacters lacked both a copy of TonB, and any identifiable TBDR's, and these species could indeed represent a class of bacteria which use a novel means of outer membrane iron transport. This may be via Fbp class transporters which can span the periplasm – such as may occur in *Vibrio* (Wyckoff *et al.* 2006), or even via the IrpA system, as described in chapter 3. In both cases, TonB-independent outer membrane Fe transport could be possible, and would be a significant change in our understanding of iron uptake by gram negative bacteria.

TonB functions to energise outer membrane transport with two other proteins – ExbB and ExbD. It should be noted that *R. pomeroyi* likely does not have functional ExbBD proteins. Indeed, the presence of *exbBD* genes in the Roseobacters is unresolved – there were no proteins with greater than 50 % identity to either ExbB or ExbD from *E. coli* K-12 encoded in any Roseobacter genome.

The lack of knowledge in marine metal uptake systems is exemplified by our observations in *R. pomeroyi*, a strain that apparently lacks any known TBDR, lacks TonB itself (see Chapter 2), does not require its FbpABC-type transporter for iron uptake, does not use RirA to regulate Fe uptake and yet

does regulate this process using motifs homologous to IRO boxes of *Rhizobium*. There are therefore some major unanswered questions even in this one “model” strain:

How does *Ruegeria pomeroyi* import iron complexes through the outer membrane?

Does *R. pomeroyi* really lack a TonB-type system and, if so, what, if anything, does it use in its place?

How does *R. pomeroyi* import iron from the periplasm to the cytoplasm?

What transcriptional regulator binds to IR boxes?

These questions extend further than just this species, as similar portfolios of genes exist in other Roseobacters. Indeed, the IR box may be present in many of the Rhodobacteraceae, as identified in Rodionov *et al.* (2006).

To answer these questions will take some careful and thorough experiments, as detailed below.

8.1.4 Iron transporters in *R. pomeroyi*

Fbp

Although a clear objective of this work was to identify the transporters responsible for Fe uptake in *R. pomeroyi*, this was unsuccessful, despite identifying a likely *a priori* candidate pair of genes, *fbpA* and *fbpB*, whose expression was markedly induced in lo-Fe and whose products comprised two of the polypeptide components of an ABC transporter that closely resembled those involved in Fe import in other bacteria. There were also no clear indications of a TonB-dependent uptake system for Fe-ligands, and indeed no alternative identified for the inner membrane transport of Fe. All we know is that growth of *R. pomeroyi* is limited when Fe is at, or < 0.5 μM . There was an indication that another ABC-class transporter, encoded by the *SPO1018-SPO1021* genes, might be involved, since its expression was induced by Fe limitation. It would be interesting to mutate these genes, either alone, or in combination with a mutation in *fbpA* and examine its Fe uptake phenotype.

It would be expected that the further microarray experiments may generate more potential target genes for investigation. The regulon of the IR box regulator may indeed include the entire range of iron uptake genes, which our bioinformatic predictions are currently missing.

IrpA

A second set of gene products whose initial properties made them promising candidates for *the*, or at least “*a*” set of Fe transporters were those encoded by an operon that included the *irpA* gene plus *SPO0087-SPO0090*. However, this too did not come to fruition. Even though the IrpA is known in other bacteria to be an Fe transporter, and indeed this study confirmed that it was markedly induced in Fe-depleted conditions, it was a big disappointment when a mutation in the *irpA* gene was not deficient in growth on Fe limited media. Furthermore, the predictions made for IrpB were tantalising, but experimental work failed to produce any meaningful results.

The range of metal uptake strategies used by the Roseobacters could well reflect the niches that these bacteria occupy. Very little is known of the various strains that have been studied in the laboratory, which have been obtained almost randomly by sampling various coastal and far-ocean sites. Although some strains (e.g. *Dinoroseobacter shibae* DFL 12) were obtained from blooms of dinoflagellates (e.g. *Prorocentrum lima*) this does not necessarily mean that the particular isolate that was cultivated on a Petri dish in Georgia or in Braunschweig was necessarily adapted to life in association with that species of marine plankton. It may be, therefore, that a particular strategy for the acquisition of iron and/or manganese is linked to a particular lifestyle, but our lack of knowledge of their precise niches precludes such a judgment. And, of course, the bioinformatic insights presented the predicted functions of any given set of genes also pose many unanswered questions. Most notably, just because a strain has a TBDR that resembles (say) FhuA, this only suggests but does not prove that its function is to recognise hydroxamate-type siderophores and it certainly does not reveal the exact chemical structure of such a molecule. Similarly with manganese, the each of the different Mnt systems may be more suited to particular lifestyles.

And, as if the complexity revealed already were not enough, the few genome-sequenced strains of Roseobacters are but a tiny fraction of those that are in the oceans and even more diversity is yet to be uncovered.

8.2 Iron - Experimentally based outcomes

8.2.1 Regulation of the *fbpAB* genes of *R. pomeroyi*

Unusually, the *fbpA* and *fbpB* genes were not co-transcribed and were not near *fbpC*. This is not unique, though, where the transcription of *fbpA* of *Vibrio cholerae* is different from *fbpBC* (Mey *et al.* 2005).

A potential candidate for a complete Fe-ABC transporter in *R. pomeroyi* may be *SPO1018-SPO1021* predicted to be an ABC-class transporter, with binding protein, two permease proteins, and an ATPase; which were all ~7-fold Fe-repressed (Chapter 7). These genes are annotated as a branched chain amino acid transporter, but lack any functional characterisation.

Crucially, given the phenotype of the FbpAB⁻ strain, there must be another high-affinity Fe-specific, inner-membrane transport system in *R. pomeroyi*.

8.2.2 The IR box cognate regulator

The work on the IR box-containing promoters of *irpA*, *fbpA* and *fbpB* in Chapter 4 showed that these motifs are responsible for (or at least contribute to) the Fe-responsive regulation of these genes. Point mutations in the most conserved bases in the IR boxes caused deregulation of *lacZ* fusions, under Fe-repressed conditions. It should be noted that there is significant homology between IR boxes and IRO boxes of *Rhizobium*, as shown in Rodionov *et al.* (2006), and that the predicted IscR box and IR box of *Ruegeria* is actually the same motif. Given this similarity, it was anticipated that an Rrf2 family transcriptional repressor might be responsible for the regulation of IR boxes in *R. pomeroyi*. This was not the case, as shown in Chapter 5.

Perhaps this was to be not wholly unexpected, since none of the Rrf2 family proteins of *R. pomeroyi* closely resembled the RirA sub-group of this family (Chapter 5), the closest homologue to RirA of *Rhizobium* being just 30% identical to *SPO0432* of *Ruegeria*. Despite this, four of the five Rrf2 genes in *R. pomeroyi* were shown to be significantly regulated by Fe, but not at all by Mn (Chapter 7). Furthermore, the expression of the fifth Rrf2 gene, *iscR*, was confirmed, by the use of a *lacZ* fusion, to be Fe-regulated, and affected by the *irr* genotype. Given the differences we observe between *E.*

coli, *Bradyrhizobium* and *Rhizobium*, in terms of Fur, Irr and RirA mediated regulation, it is possible that their distant marine cousins use a wholly new, or significantly adapted system of Fe-regulation.

By far the most important missing detail in this work is the identity of the regulator which binds to IR boxes in *R. pomeroyi*. To this end, the first future project would entail the construction of a Tn5 mutant library of *R. pomeroyi*, with complete genome coverage. This could be achieved using the E-Z-Tn5 kit from Illumina, for example. Having generated such a library, the potential regulator of both *fbpA*, and *irpA* could be found. These genes both showed large induction by Fe-limitation, enough that a fluorescent fusion could be shown to be differentially expressed on an agar plate with varied Fe levels. Here, a *gfp*, or other fluorescent reporter gene could be fused to the promoter of either *fbpA* or *irpA*, and crossed into the complete set of the *R. pomeroyi* mutant library. The library could then be plated onto Fe-replete medium, to obtain many single colonies. Those that were deregulated in expression of the fusion should fluoresce brightly. These colonies may well have a mutation in the IR box regulator. By simply mapping the location of Tn5 in these strains, the identity of the regulator should be apparent.

8.2.3 The marine Irr story

The global Fe-responsive regulator Irr has been shown to be a repressor of iron storage and iron utilisation genes in *Rhizobium leguminosarum*, and as a repressor and activator of such genes in *Bradyrhizobium japonicum*. Irr binds to motifs known as ICE boxes, and these are well conserved in several α -proteobacteria (Rodionov *et al.*, 2006). Several ICE box-like motifs were identified in the genome of *R. pomeroyi*, upstream of genes known to be Fe-regulated in other α -proteobacteria – *mbfA*, *iscR*, *fssA* and *ccpA*. However, when analysing the transcriptional response of these genes, we found that *fssA* (*SPO0382*) was Fe-repressed, but was unchanged in expression in the Irr mutant. However, the converse was true for *mbfA*, *iscR* and *ccpA*, all were repressed by Irr, and not shown to be significantly Fe-regulated.

It should be said here, that the microarray conditions used to study Irr were not complete – Irr represses genes in low Fe conditions, and yet the mutant transcriptome was produced from high Fe cultures, where it was compared to the wild type, also from high Fe cultures. It was hoped that many genes would be significantly deregulated by the lack of Irr peptide, even in this Fe-replete state.

Therefore, it is possible that we are yet to show the full extent of the Irr-regulon in *R. pomeroyi*, or the extent to which the genes mentioned above are regulated.

Nevertheless, it is likely that Irr does function as a regulator of Fe storage in *R. pomeroyi*, as demonstrated by the expression of *mbfA*. Whether this is in tandem with another RirA-type repressor or not, remains to be shown.

It is interesting to note that some genes were shown to be positively regulated by Irr, such as *SPO1957*, which was ~16-fold higher in the wild type than in the Irr mutant, and that again, as with *mbfA* and friends, this was not mediated by Fe. Clearly, more work needs to be done to verify these results, and to study the Irr regulator in detail.

Finally, it would be of interest to observe if Irr binds to haem, as has been shown for other Irr peptides, and indeed if a haem-Irr complex is stable or degraded.

8.2.4 Pigment production by Irr- *R. pomeroyi*

Another 'loose-end' in this study is the red pigment produced by the Irr mutant strain of *R. pomeroyi*. Although the Irr mutants of *Rhizobium* and *Bradyrhizobium* have a coloured phenotype, due to protoporphyrin IX (PPIX) over-production, the pigment in the Irr⁻ *R. pomeroyi* mutant did not fluoresce under UV light, which is a property of PPIX. Attempts to isolate the pigment were unsuccessful (see Chapter 5), but it was noted that it was extracellular, because it formed a particulate layer on top of the pellet when cells were centrifuged. Finally, the red pigment was dark, brick red, not the light pink of PPIX.

Taken together, these observations suggest that Irr of *R. pomeroyi* represses the production of a highly pigmented, extracellular particle, or at least a particle that can be separated from the cells when grown in culture. The identity of this pigmented substance could be identified by careful physical separation and then further characterisation. Also, the identity of the genes responsible for the production of the substance in the Irr⁻ strain could become evident once more is known about the pigment itself, and once further microarrays are performed – see below.

8.3 Manganese - Bioinformatically based outcomes

8.3.1 MntX

Possibly the most surprising, and potentially the most important outcome of the work on manganese was the identification of a novel Mn-specific transporter, MntX. This peptide was found to in three Roseobacter species, namely *Oceanicola granulosus* HTCC2516, *Rhodobacterales bacterium* HTCC2255 and *Roseovarius nubinhibens* ISM, but was far more widespread than that, being present in several gamma proteobacterial genera, many other α -proteobacteria, and potentially in the Firmicutes and Archaea too (see Chapter 6). The MntX polypeptide was also present at every sampling site present in the GOS data, at a frequency similar to that of the SitABCD transporter, but was not represented in any other metagenomic data base. It is therefore a very important player in manganese uptake in the oceans, but it is not clear why it should be confined to bacteria, even very distantly related ones, that are mainly (e.g. *Vibrio*) or exclusively (e.g. the SAR11 and SAR116 clades, *Alteromonas*, and the Roseobacters) marine in origin.

8.3.2 Manganese uptake and regulation in the Roseobacters

In *Ruegeria pomeroyi* the primary means of Mn uptake is via SitABCD. The expression of the *sit* genes is repressed by Mn, via the Mur transcriptional regulator, which likely binds to two MRS-like motifs found upstream of *sitA*. However, not all Roseobacters have the *sit* genes, and indeed those that do, are in two subclasses of peptides, one being similar to the version in *R. pomeroyi*, and the other closer to the Sit polypeptides in *Rhizobium* SitABCD – furthermore, it was shown that a third type was present, but found only in *Loktanella*. Thus the *sitABCD* genes were likely acquired, on more than one occasion by the different Roseobacter species. Either the acquisition of SitABCD in the Roseobacters happened on two separate occasions, or that significant evolution away from the Rhizobial type peptides has occurred.

Furthermore, one Roseobacter, *Ruegeria* sp. Trich CH4B lacked SitABCD altogether, and had a copy of MntH, and *Citricella* sp. 357 had both SitABCD and MntH. These species clearly have either acquired these genes separately, or all the other Roseobacters have lost MntH during their evolution.

A final point of interest in this Mn-uptake story is that the hugely abundant SAR11 bacteria still do not appear to have a known Mn-specific transporter. Only one member of this clade was found to have MntX, the others lacked SitABCD, MntH and MntX. This either means that the non-MntX SAR11 strains do not have a requirement for Mn, or that they use another novel Mn transporter.

These data could be obtained by testing the Mn-requirement of the SAR11 strains, and then performing a full bioinformatic search of the genome sequences for potential MRS, or MntR regulatory motifs. It is expected that genes involved in uptake of Mn by these strains would be regulated by one of these Mn-responsive regulators, since they are the only two we have observed in the α -proteobacteria. Any potential transporter genes could be cloned, or synthesised and tested in the SitA⁻ strain of *R. pomeroyi*, as demonstrated for MntX in chapter 6.

8.4 Manganese - Experimentally based outcomes

8.4.1 SitABCD

The function and regulation of the ABC-class transporter SitABCD in *R. pomeroyi* was similar to that which had been found in other alpha-proteobacteria, notably the Rhizobia. It is the main Mn transporter of *R. pomeroyi*, as a mutant strain was unable to grow well without the addition of exogenous MnCl₂. There may be other non-specific, and/or low affinity transporters that import Mn when present at higher levels in the medium. The expression of *sitA* was shown to be repressed by Mn, most likely by the binding of Mur to the MRS motifs found upstream of *sitA*. Further, confirmatory work could include the exact mapping of the transcript start site(s) by 5' RACE, or by 5' transcriptome sequencing. Also, direct foot-printing of Mur protein to the MRS sequences would confirm the direct interaction between these two regulatory components.

8.4.2 MntX is a functional Mn transporter

The three strains of Roseobacters that lacked SitABCD led me to investigate the function of MntX, which was thought to be a likely Mn transporter because (a) it only occurred in the three strains of Roseobacter that lacked any known Mn transporters; (b) the *mntX* gene is preceded by a MRS motif

in all three strains of *Roseobacter*, and (c) MntX is predicted to be a membrane-spanning protein. This work showed that MntX of *Roseovarius nubinhibens* is indeed a functional Mn transporter, that can correct the Mn-deficient growth phenotype of a *Ruegeria pomeroyi* SitA⁻ mutant. Furthermore, this MntX was also regulated by Mur of *Ruegeria*, when a transcriptional fusion to *mntX* from *Roseovarius* was expressed in both the wild type and Mur⁻ *Ruegeria* strains.

One strain of *Roseobacter*, *Ruegeria* sp. Trich CH4B has both SitABCD and MntH Mn transporters, and it would be very interesting to make mutants in each gene to observe the relative importance of each system in this strain. Perhaps this strain uses each transporter in quite different environmental conditions – such as in different oxygen concentrations for example. This may show that this strain is adapted to take up Mn in different environmental niches within the ocean, or, it may just happen to have two Mn specific transporters.

Moving away from the *Roseobacters*, the MntX transporter was found in several orders of the Proteobacteria. Specifically, these are the Vibrionales, Oceanospirillales and Alteromonadales, all in the γ -proteobacteria; and in the SAR11, SAR116 and *Roseobacter* clades of the α -proteobacteria, and in two cases, namely *Vibrio cholera* El Tor and of *Candidatus Pelagibacter* sp. IMCC9063, the MntX was shown directly to be a functional Mn transporter. Strikingly, all these bacteria live in marine or brackish habitats, showing that MntX is clearly an important Mn transporter in this habitat.

Cholera is a major disease, with 3–5 million cases and 100,000–120,000 deaths worldwide each year, and every single sequenced strain of *V. cholerae* encodes *mntX* in their genome. This makes MntX a potentially important component of *Vibrio* pathogenesis.

MntX occurs in several bacterial clades that are abundant in the oceans – namely SAR11, SAR116 and the *Roseobacters*. Subsequently it was not surprising to see large numbers of homologues in the GOS marine metagenome database. Furthermore, MntX homologues in the GOS metagenome were found to be 82% as abundant as SitABCD, and 373% compared to MntH (Green et al, 2012, in press). Of great interest was the group of bacteria which did not cluster with peptides from any known genus, when MntX was used to construct a neighbour-joining tree (see Chapter 6). This group of bacteria was shown to have ~30% GC content of the region surrounding, and including MntX, which is similar to the GC content of SAR11 strains. However, these MntX homologues may well be in a novel group of abundant and low GC organisms. It would be of great interest to attempt to culture these strains, or at least prove their existence by probing seawater samples using the identified *mntX* genes from this group.

Finally, these observations on MntX distribution have provided another interesting observation. Several strains of bacteria, including *Pelagibacter ubique*, lack SitABCD, MntH and MntX, and must therefore either not require Mn for growth, or must possess another novel Mn transporter.

8.5 The transcriptome of *R. pomeroyi* – some conclusions

An interesting aspect of the effects of the environment (high and low Fe; high and low Mn) or genotype (wild type, Mur-, Irr-) on the *R. pomeroyi* transcriptome was that the expression of many genes was affected by more than one of these parameters, and in some cases, by as many as 4. Thus, the transcriptional responses of *R. pomeroyi* to both Fe and Mn limitation are linked to some degree.

Regulatory interplay between these two metals has been seen in other alpha-proteobacteria. For example, Mn deficiency in *Bradyrhizobium japonicum* caused cells to be Fe deficient (Puri *et al.* 2010). This was likely due to a lack of Mn binding to Irr, which normally inhibits Irr-haem binding. Therefore in the absence of Mn, more Irr protein was degraded, thus affecting the global Fe status of the cell (Puri *et al.* 2010).

There were several very interesting clusters of genes that were significantly regulated in the microarray data, the importance of these will be discussed in the following:

Firstly, a completely uncharacterised gene cluster, likely comprising two separate operons – *SPOA0339-SPOA0347* was highly induced by both Fe and Mn. These genes had very little functional predictions available in the NCBI databases, but their regulation does present an interesting prospect. The gene product of *SPOA0344* encodes a LysR-type transcriptional regulator, not known for their metal responsive regulation. Additionally, a conserved, 16 bp motif was found upstream of both *SPOA0343* and *SPOA0345*, which could be the cognate binding site for this LysR regulator. Pending further investigation, this regulator may be a novel, and highly Fe- and Mn-responsive transcriptional regulator.

The *cox* cluster genes of *R. pomeroyi* also showed significant Mn- and Fe-responsive regulation, and this was independent of Mur, but not Irr. This could be a good example of the regulation of Fe-responsive genes by Irr, which can be also mediated by a Mn deficiency.

Also, and very interestingly, a cluster of genes which encode components of GTAs, capable of disseminating genetic material of *R. pomeroyi*, possibly as a means of propagating beneficial traits to other *Ruegeria* cells. The exact cause and function of GTAs are not fully understood, but the idea that extreme stress, such as metal deficiency, could induce their production, in an attempt to form a natural 'library' of the genome, is an attractive thought. If such a strategy gave a selective advantage to the species as a whole, then it could certainly have been selected for in the evolution of *R. pomeroyi*, and indeed other bacteria that harbour GTA-like genes.

8.5.1 Future microarray studies

The microarrays performed as part of this study were always intended to be 'a first pass' at the transcriptional response of *R. pomeroyi* to Mn and Fe limitation, and the role that Irr and Mur played in this. As such, an important extension of this study has to be further microarray experiments. It would be immediately important to perform some Type II arrays, where all results can be compared between experiments, allowing more analysis of the transcriptional regulatory networks to be performed. Here, both Fe- and Mn-limited cultures would be used on arrays with a labelled gDNA sample as the control.

In addition, I would perform arrays on the Irr mutant, in both high and low Fe and Mn, to fully characterise the Irr-ome already alluded to in this study. Similarly, once the regulator of IR boxes was identified, microarray analysis of a mutant strain in this regulator would be fascinating – and would be performed in the same conditions used to analyse the response of the Irr⁻ strain, again using type II arrays.

Having completed these new transcriptomics experiments, there should be further scope for future work on the nature of iron uptake and regulation in *R. pomeroyi*.

8.5.2 Other targets for study

The array data already collected have provided numerous targets for further study, all of which would make very interesting, small projects. These include:

- The mechanisms and the functions of the metal-dependent regulation of the *cox* genes.
- The production of GTAs in response to metal (and other) limitations
- The potential predicted LysR transcriptional regulator SPOA0344 and its interactions with Fe and/or Mn.
- Finally, a study of the effects on the *R. pomeroyi* transcriptome of a mutation in the predicted anti-anti sigma factor gene – *SPO3409*.

Chapter 9 - Materials and Methods

9.0 Media and General Growth Conditions

9.0.1 *Luria-Bertani (LB) medium*

Luria-Bertani (LB) medium (Maniatis *et al.* 1982) was used to maintain *E. coli* and comprises, per litre ddH₂O:

10 g Tryptone

5 g Yeast extract

5 g NaCl

1.5 g D-glucose

Adjusted to pH 7.2 using 1M HCl or 1M NaOH.

E. coli strains were routinely grown at 37°C with 200 rpm agitation.

9.0.2 *Half-YTSS (HY) Medium*

R. pomeroyi strains were maintained on half strength YTSS medium (Gonzalez *et al.* 1997) which comprises, per litre ddH₂O:

2 g Yeast extract

1.25 g Tryptone

20 g Sea salts (Sigma)

9.0.3 Marine Basal Medium (MBM)

R. pomeroyi was grown in defined medium MBM (Baumann and Baumann 1981) to analyse growth and gene expression during iron limitation. It comprises per litre of ddH₂O:

75 ml 1M Tris HCl pH 7.5

43 mg K₂HPO₄

0.75 g NH₄Cl

20 g Sea salts (Sigma)

Supplemented 1:1000 with vitamins solution from (Gonzalez *et al.* 1997) which comprises, per 100 ml of ddH₂O:

2 mg Biotin

2 mg Folic acid

10 mg Pyridoxine-HCl

5 mg Riboflavin

5 mg Thiamine

5 mg Nicotinic acid

5 mg Pantothenic acid

5 mg Cyanocobalamin

5 mg of p-Aminobenzoic acid

The pH was adjusted to 7.

9.0.4 Rob's Sea Salts (RSS) Medium

R. pomeroyi was grown in RSS to analyse growth and gene expression during manganese limitation using succinate at 10mM as carbon source, and vitamin solution added. RSS comprises per litre of ddH₂O:

75 ml 1M Tris HCl pH 7.5

43 mg K₂HPO₄

0.75 g NH₄Cl

17 g NaCl

1.5 g MgCl₂

0.75 g CaCl₂

0.75 g KCl

9.0.5 Growth experiments

All *R. pomeroyi* experiments were performed at 28°C, with 180 rpm of agitation. For all growth experiments, a starter culture in complete HY media with selective antibiotic(s) was inoculated using a single colony of the desired strain. This was incubated for two days, or until in stationary phase. This culture was diluted 1 in 200 into minimal medium: MBM for Fe limitation and RSS for Mn limitation. As appropriate, FeCl₃ or MnCl₂ was added to the media, along with vitamin solution and succinate as detailed above. Growth was measured as optical density at 600nm wavelength in a spectrophotometer.

9.1 Strain storage

9.1.1 Glycerol storage

Strains of *E. coli* were grown overnight at 28°C in LB with antibiotics. An aliquot (1 ml) of overnight culture was mixed with the same volume of 50% glycerol solution and frozen at -80°C.

9.1.2 DMSO storage

Cultures of *R. pomeroyi* strains were grown to stationary phase, then stored in 15% glycerol plus 15% DMSO at -80°C.

9.2 *in vivo* genetic manipulations

9.2.1 Bacterial Conjugations

Plasmids were transferred by conjugation from *E. coli* strains JM101 or 803 to *R. pomeroyi* strains using patch crosses (Johnston *et al.* 1978) or filter crosses (Beringer and Hopwood 1976) in tri-parental matings with *E. coli* 803 containing helper plasmid pRK2013 to mobilise the transfer of plasmids between strains.

9.2.2 Conjugation via patch crosses

R. pomeroyi and *E. coli* strains were cultured on HY and LB agar medium, respectively, prior to patch crossing. A sterile loop was used to transfer approximately a 3:1:1 ratio of donor:helper:recipient bacteria where they were mixed in a patch on an HY agar medium plate and incubated for 48 hours at 28°C. These patches were then streaked onto selective HY agar plates containing the appropriate antibiotics, incubated at 28°C for ~4 days, allowing single colony transconjugants to form.

9.2.3 Conjugation via filter crosses

Filter crosses were used when selecting for low frequency events, such as insertional mutations with pEX18Ap. *R. pomeroyi* strains were grown in HY medium overnight at 28°C, and the *E. coli* donor and helper strains were grown overnight at 37°C in LB medium, all **without** antibiotics. A 3:1:1 ratio of donor:helper:recipient was used, with 1.5 ml of the donor, and 0.5 ml of the other cultures mixed

and pelleted via centrifugation. These were resuspended in 200µl of HY and spread onto a sterile nitrocellulose filter (Whatman) positioned on a HY plate without any selective antibiotics. This was incubated for 48 hours at 28°C, after which the cells were washed off the filters using MBM medium and diluted sufficiently to obtain single colonies when 200 µl of the diluted cells were spread onto selective HY agar medium. The selective plates were incubated for around 4 days.

9.3 Methods of Nucleic Acid Purification

9.3.1 Purification of plasmid DNA using QIAGEN Miniprep kit

For small-scale (< 5 µg), high purity isolation of plasmids from *E. coli*, to use for restriction digest analyses, transformation, sequencing, and as PCR templates, Plasmid Miniprep kits (Qiagen) were used, which employ a protocol optimised from Birnboim and Doly (1979). Cells are lysed using an alkaline buffer and a silica gel column facilitates the purification of plasmid DNA. This was done (see below) according to manufacturer's specifications, using all the reagents supplied with the kit. All centrifugation steps, were performed at 16,000 x g in a 5415 D Microcentrifuge (Eppendorf).

1. A single colony of *E. coli* containing the required plasmid was inoculated into 5 ml LB liquid, containing the appropriate antibiotics, and incubated at 37 °C overnight.
2. Cells were pelleted (1.5 ml culture for high copy number plasmids; 3 ml for low copy number plasmids) by centrifugation in 1.5 ml microfuge tubes; the supernatant was removed.
3. Pelleted cells were resuspended in 250 µl P1 resuspension buffer, containing 100 µg ml⁻¹ RNase A to remove RNA, and incubated at room temperature for 5 minutes.
4. 250 µl P2 lysis buffer was added and mixed well by inversion. Samples were then incubated at room temperature for no more than 5 minutes.
5. 350 µl P3 (stored at 4 °C) neutralisation buffer was added and mixed well by inversion. Samples were then incubated on ice for 5 minutes to precipitate protein, genomic DNA and cell debris.
6. Each tube was centrifuged for 15 minutes to clear precipitate.

7. The resultant supernatant was applied to a Qiaprep spin column and centrifuged for 1 minute. The pelleted precipitate was discarded.
8. The eluate was discarded and 500 µl PB binding buffer was applied to the column and centrifuged for 1 minute. This step removes excess nuclease activity and high carbohydrate content from *endA* mutant strains such as JM101.
9. The eluate was discarded and 750 µl PE wash buffer was applied to the column and centrifuged for 1 minute.
10. The eluate was discarded and the column and collection tube was centrifuged again for 1 minute to remove residual wash buffer from the column matrix.
11. Spin columns were transferred to clean, labelled 1.5 ml microfuge tubes and DNA was eluted by pipetting 50 µl dH₂O onto the matrix and allowed to stand for 1 minute. This was then centrifuged for 1 minute; the spin column was discarded and the eluted DNA stored at -20 °C.

9.3.2 Mini-preparation of plasmid DNA by alkaline lysis and phenol-chloroform purification

To isolate and purify DNA of plasmids > 10 kb in size the following method was used, as the QIAGEN Miniprep spin column did not yield sufficient DNA. Buffers used here were from this kit however, as they still provided means of cell lysis. All centrifugation steps were performed at 16,000 x g in a 5415 D Microcentrifuge (Eppendorf).

1. A single colony of *E. coli* containing the required plasmid was inoculated into 5 ml LB liquid, containing the appropriate antibiotics, and incubated at 37 °C overnight.
2. Cells were pelleted (total of 3 ml) by centrifugation in 1.5 ml microfuge tubes; the supernatant was completely removed.
3. Pelleted cells were resuspended in 250 µl P1 resuspension buffer, containing 100 µg ml⁻¹ RNase A to remove RNA, and incubated at room temperature for 5 minutes.
4. 250 µl P2 lysis buffer was added and mixed well by inversion. Samples were then incubated at room temperature for no more than 5 minutes.

5. 350 µl P3 (stored at 4 °C) neutralisation buffer was added and mixed well by inversion. Samples were then incubated on ice for 5 minutes to precipitate protein, genomic DNA and cell debris.
6. Each tube was centrifuged for 15 minutes to clear precipitate.
7. The resultant supernatant was transferred to a clean 1.5 ml microfuge tube to which 400 µl of phenol-chloroform (phenol:chloroform:isoamyl alcohol 25:24:1, Sigma) were added and mixed by vortexing for 10 seconds. Samples were then centrifuged for 2 minutes.
8. The upper aqueous layer was transferred to a clean 1.5 ml microfuge tube containing 700 µl room temperature 100% ethanol to precipitate plasmid DNA. Samples were then centrifuged for 15 minutes.
9. The supernatant was then discarded and the resultant DNA pellet was washed in 500 µl 70% (v/v) ethanol and centrifuged for 2 minutes.
10. The supernatant was then completely removed using a micropipette, and the DNA pellet was air-dried for 10 minutes.
11. The pelleted DNA was resuspended in 30 µl dH₂O and stored at -20 °C.

9.3.3 Purification of plasmid DNA using QIAGEN Midi kit

The QIAGEN plasmid Midi Kit was used to purify high quality plasmid DNA in large quantities (~100 µg). This DNA was of sufficient quality for sequencing, cloning and site-directed mutagenesis.

The QIAGEN kit used alkaline lysis, optimised from Birnboim and Doly (1979), followed by column-based purification of plasmid DNA, and precipitation of the DNA using isopropanol. The procedure was performed according to manufacturer's specifications, using all the reagents supplied with the kit:

1. A single colony of *E. coli* containing the required plasmid was inoculated into 100 ml LB media, containing the appropriate antibiotic(s), and incubated at 37 °C, with 200 rpm of shaking for 16 hours.

2. The culture was used to fill a 50 ml centrifuge tube (Corning), and centrifuged to produce a pellet (9000 x g for 10 minutes in an Eppendorf Centrifuge, model 5804R).
3. This pellet was resuspended in 4 ml of P1 buffer (stored at 4 °C), containing 100 µg ml⁻¹ RNase A to remove RNA.
4. Then, 4 ml of P2 lysis buffer was added and inverted until a blue colour appeared (indicating alkaline pH); this was incubated at room temperature for 5 minutes.
5. To precipitate all cellular debris, 4 ml of neutralisation buffer N3 was added, mixed well by inversion and incubated on ice for 15 minutes.
6. Precipitates were pelleted by centrifugation for 15 minutes.
7. A column (supplied with the kit) was equilibrated by adding 4 ml QBT equilibration buffer, which was discarded after passing through the column by gravity.
8. The supernatant from Step 6 was applied to the column, allowing it to enter the column matrix by gravity flow. The eluate was discarded.
9. The DNA bound to the column matrix was washed by two separate additions of 10 ml of QC buffer to the column; again, the eluate was discarded.
10. Plasmid DNA was eluted from the matrix by adding 5 ml QF elution buffer, and the eluate was collected in a sterile 50 ml Falcon tube (Corning).
11. Eluted plasmid DNA was precipitated by adding 3.5 ml of 100% isopropanol, mixed by inversion and centrifuged at 9000 x g for 30 minutes to pellet precipitated plasmid DNA.
12. The DNA pellet was washed by adding 1 ml 70% ethanol and centrifuged as before for 2 minutes. The resultant supernatant was removed completely using a micropipette, and the DNA pellet was air-dried for 10 minutes.
13. The dried pellet was rehydrated in 80 µl of Ultra-pure water (Sigma).

9.3.4 Purification of genomic DNA

A Wizard genomic DNA purification kit (Promega) was used to purify genomic DNA from *Ruegeria pomeroyi* strains and from *Roseovarius nubinhibens* ISM. This genomic DNA (gDNA) was used for PCR amplifications and Southern blot analyses.

1. A single colony of either *Ruegeria* or *Roseovarius* was inoculated into 5 ml HY media and grown for 2 days at 28°C.
2. Using a benchtop Eppendorf centrifuge, 1.5 ml of each culture was pelleted at 13,000 x g.
3. The supernatant was removed, and 600 µl Nuclei lysis solution was added and used to resuspend the pellet. Cells were lysed by incubating at 80 °C for 5 minutes before cooling to room temperature.
4. To remove RNA from the samples, 3 µl of RNase solution were added and mixed into the lysate; this was incubated at 37 °C for 1 hour.
5. To this, 200 µl of Protein precipitation solution was added and mixed well; this mixture was incubated on ice for 5 minutes to precipitate all cellular debris.
6. The precipitate was removed by centrifugation for 3 minutes.
7. The DNA was precipitated from the supernatant using 600 µl of isopropanol. This was collected by centrifugation for 2 minutes; the supernatant was discarded.
8. The pelleted DNA was washed with 600 µl room temperature 70% ethanol (v/v) and mixed by inversion. DNA was again pelleted by centrifugation for 2 minutes and the supernatant was removed carefully.
9. The DNA pellet was air-dried for 10 minutes.
10. Dried DNA pellets were then resuspended in 100 µl Ultra-pure water (Sigma) and incubated for 1 hour at 65 °C. Genomic DNA preparations were always stored at -20 °C.

9.3.5 RNA purification for microarrays

The extraction of RNA from bacteria requires careful measures to ensure there is no degradation. A clean space was used, where all equipment was treated with RNaseZAP® (Ambion) and all plastics were autoclaved prior to use to ensure no contamination with RNase enzymes. TipOne® RNase-free filter tips (*StarLab*) were used when pipetting.

Firstly, a single colony of *Ruegeria pomeroyi* Rif^R strain J470 was used to inoculate HY broth with 20 µg/ml rifampicin; this was grown for 48 hours at 28°C with shaking.

For the experiments in which the effects of Fe were measured, this starter culture was diluted 1 in 200 into 100ml of MBM minimal medium, pre-warmed to 28°C and with vitamin solution added (1 in 1000 dilution) and succinate at 10 mM. In total 2 biological replicates were performed, with either 20 µM FeCl₃ or no iron added to each flask.

For Mn limitation experiments the cultures were diluted 1 in 200 into RSS media, pre-warmed to 28°C with 20 µM FeCl₃, vitamins and succinate as in MBM. Here, 2 replicates were performed with 20 µM MnCl₂ or no manganese added to each flask.

For the “Irr⁻ vs. wild type” microarray comparison experiment, both cultures were grown in 20 µM FeCl₃ in MBM as detailed above.

For the “Mur⁻ vs. wild type” experiment, two replicates were performed, where both cultures were grown in RSS with 20 µM MnCl₂ and 20 µM FeCl₃ as detailed above.

To grow the cells and stabilise the RNA the following steps were performed:

1. All cultures were incubated in 250 ml conical flasks for exactly 16 hours at 28°C, with 180 rpm shaking.
2. Following growth, the cells were killed and their RNA was stabilised using a 1 in 5 addition of 10 % Phenol:Ethanol solution (Sigma), before being put on ice for 1 hour.

3. The cells were harvested by centrifugation (3200 x g at 4 °C for 10 minutes in an Eppendorf Centrifuge, model 5804R); then, the supernatant was removed, and the cell pellet was resuspended in the residual liquid.
4. This was centrifuged again at 13000 x g for 30 seconds, and all residual supernatant was removed.
5. Each sample was frozen in dry ice pellets and stored overnight at -80°C.

To extract and purify the RNA, three cell lysis steps were used, since *R. pomeroi* cells grown in minimal medium gave poor RNA yield when any of these three steps was omitted.

1. Treatment with lysozyme: 100 µl RNase-free TE buffer (10 mM Tris, 1 mM EDTA, pH 8.0) containing 100 mg ml⁻¹ chicken egg white lysozyme (Sigma) was added to each sample, which was then incubated at 37°C for 30 minutes.
2. Five successive freeze-thaw cycles using dry ice were performed on each sample.
3. Mechanical shearing: 1 g of 0.1 µm acid-washed glass beads (Sigma) were added to each sample, and were agitated in an MP Biomedicals FastPrep24 machine, on setting 6, for 40 seconds. Samples were all immediately cooled on ice. The resultant supernatant was removed following centrifugation (2 minutes at 13,200 x g).

Total RNA was purified from the resultant lysates using the Promega SV total RNA kit as per the manufacturer's protocol, as follows.

1. 75 µl Lysis Reagent were added and mixed by inversion.
2. 350 µl RNA dilution buffer were then added and mixed by inversion, and samples were incubated for 3 minutes at 70 °C, before being centrifuged for 10 minutes at 13000 x g at 4 °C.
3. 200 µl 100% ethanol were added and mixed by pipette.
4. A spin column was used to bind and clean the RNA, here, each sample was added to a column and centrifuged for 30 s at 13000 x g at 4 °C, the flow through was discarded.

5. The RNA, bound to the column matrix, was washed using 600 µl Wash buffer) and centrifuged for 30 s at 13000 x g at 4 °C, the flow through was discarded.

6. A DNase mix (see below) was prepared, and 50 µl was added to the RNA in the each column. These were incubated at 37 °C for 40 minutes to remove any DNA contamination.

DNase mix comprised (all supplied with kit):

a. 5 µl 90 mM MnCl₂

b. 40 µl DNase core buffer

c. 5 µl DNase solution

7. To inactivate the DNase, 200 µl of DNase stop mix was added to each column and then removed by centrifugation for 30 s at 13000 x g at 4 °C. The flow through was discarded.

8. The RNA sample bound to the matrix in each spin column was washed twice by adding 600 µl Wash Buffer and centrifuging for 30 s at 13000 x g at 4 °C. After each wash, the flow through was discarded.

9. The RNA was eluted into a clean microfuge tube by applying 80 µl of Ultra-pure water (Sigma), incubating for 2 minutes at room temperature before being centrifuged for 2 minutes at 4500 x g.

10. To ensure there was no DNA in any sample, TURBO DNA-free (Ambion) was used, according to the protocol supplied, as follows:

a. To each RNA sample, 0.1 volumes of 10 x Turbo buffer, and 1 µl of Turbo DNase enzyme was added and incubated at 37 °C for 30 minutes.

b. Following incubation, 0.1 volumes of DNase inactivation reagent were added, mixed well and incubated for 5 minutes at room temperature.

c. This mixture was then centrifuged for 90 s at 13000 x g at 4°C to pellet any precipitate, and the supernatant was harvested into a clean microfuge tube.

The RNA was assayed for purity and lack of degradation using a Bioanalyser chip (Agilent 2100). Here, the appearance of 16S and 23S ribosome bands were required to be bright and sharp, with no smearing, as this would indicate RNA degradation.

The concentration of the RNA was determined using a Nanodrop Spectrophotometer NS-1000 (Thermo Scientific) and it was ensured that both the 260/280 and 260/230nm ratios were >2. All RNA samples were stored at -80°C until required.

9.4 Microarrays

9.4.1 Performing microarray experiments

An 8 × 15K microarray slide (Agilent) specific for the genome of *R. pomeroiy* DSS-3 was used to visualise relative mRNA levels between samples. An Affinity Script kit (GE Healthcare) was used to produce cDNA, from each RNA sample, which was then labelled with single-stranded DNA containing the Cy3 or Cy5 fluorescence marker as follows:

10 µg of RNA dried using a rotary vacuum, then resuspended in 7.7 µl of RNase free water.

Random priming reactions set up with:

7.7 µl of RNA sample (10 µg)

5 µg (1.7 µl) of random hexamers (Invitrogen)

These were incubated at 70°C for 5 mins then placed on ice for 10 mins before being briefly centrifuged to collect any evaporated liquid.

To each tube, the following were added:

- a. 2 μ l of 10 x RT buffer
- b. 2 μ l of 0.1 M DTT
- c. 0.6 μ l of 50 x dNTPs (25 mM of dATP, dGTP, dTTP and 10 mM of dCTP, which was 25 μ l of dA, dG, dT and 10 μ l of dCTP from Amersham Pharmacia 100 mM stock dNTP kit.
- d. 2 μ l of Cy3 or Cy5-dCTP (1 mM stock from Amersham Pharmacia) and 4 μ l of reverse transcriptase (AffinityScript, Stratagene), total volume is 20 μ l.

These were pipette mixed, and incubated at 25°C for 10 mins, before being incubated overnight at 42°C.

In the morning, the RNA was degraded to leave only the labelled cDNA as follows:

- a. 15 μ l of freshly made 0.1 M NaOH, to hydrolyse RNA. This was incubated at 70°C for 10 mins
- b. To this, 15 μ l of 0.1 M HCl was added to neutralise the NaOH.

Clean up (Invitrogen PureLink PCR Purification Kit):

1. 50 μ l of labelled RNA/gDNA reactions were added to 200 μ l of PureLink binding buffer B2 and mixed well by inversion.
2. Sample was added to a spin column and centrifuged at 10,000 x g in a microcentrifuge for 1 minute.
3. The flow through was discarded, and column washed with 650 μ l of Wash Buffer, then spun as before.
4. The flow through discarded again, and the empty spin column was spun at full speed for 3 mins to remove all traces of wash buffer.

4. DNA was eluted using 50 μ L DEPC-treated water and spun after incubating for 1 min at room temperature, elution was performed by centrifugation into a clean eppendorf for 2 minutes at maximum speed.

The labelled cDNA was mixed as per the design of experiments and hybridised to the microarray slide using the Agilent Hi-RPM Gene Expression Hybridization Kit according to the manufacturer's instructions, as follows:

1. Both conditions for each array were dried in a rotary vacuum, then resuspended in 10 μ L of DEPC-treated water, before being mixed.
2. To this 20 μ L sample, 25 μ L of hybridisation buffer (Agilent) and 5 μ L of blocking reagent (Agilent) were added, and boiled for 3 minutes before being cooled to room temperature.
3. 40 μ L of each sample was applied to a well on an Agilent hybridisation chamber, held in a clamp (Agilent). The array was carefully applied on top of the chamber, and clamped down firmly. This was incubated in a hybridisation oven at 65°C overnight.

Washing the hybridised arrays:

1. The hybridisation chamber and microarray, held in the clamp was disassembled in wash buffer 1 (Agilent) away from bright light.
2. The array was loaded into a foil covered 50 ml falcon tube filled with wash buffer 1 and rotated gently for 1 minute at room temperature.
3. The array slide was transferred to another falcon tube containing wash buffer 2, prewarmed to 37°C and rotated again for 2 minutes.
4. Finally, the array slide was dried by placing in acetonitrile and removing, then into stabilisation buffer, air dried and then stored in the dark before scanning.

Scanning:

The array slide was scanned using a GenePix 4000B scanner, and data acquired using GenePix 6.0 software.

9.4.2 Microarray analysis

DNA microarrays were scanned using an Axon GenePix 4000A microarray laser scanner (Axon Instruments) and the data from detected features were initially processed using the GenePix 3.0 software. Statistical analysis of the data was performed with Marray as described in Holmes *et al.* (2005).

All data were deposited in a large file (Appendix 3) where for each gene, the relative expression change was shown as a ratio for the pair of conditions under comparison, and the P-value for each gene is shown.

9.5 Manipulation and in vitro analysis of nucleic acids – DNA amplification and plasmid construction

9.5.1 Design of oligonucleotides used for PCR and SDM

DNA oligonucleotide primers were ordered from MWG Biotech, and designed using Primer3Plus (Untergasser *et al.* 2007) and ARTEMIS (Rutherford *et al.* 2000). Where appropriate, they had a GC content <60%, a melting temperature (T_m) of ~60 °C and a length of 18-22 base pairs. For those that incorporated a restriction site, this was placed to the 5' end of the primer, with a further 4 bases added upstream to ensure that the enzyme could clamp the DNA. Sequences and use of primers are listed in Table 10.1.

9.5.2 Polymerase chain reaction (PCR) amplification of DNA

A TC-512 Thermal cycler machine (Techne) was used to perform PCR to amplify fragments from genomic or plasmid DNA. Typically, Taq master mix (Roche) was used according to specifications of the manufacturer. Unless otherwise stated, standard PCR reactions were set up as follows:

1 μ l genomic DNA template (~ 50 ng / μ l)

22 μ l dH₂O

1 μ l Forward primer (20 pmol μ l⁻¹)

1 μ l Reverse primer (20 pmol μ l⁻¹)

25 μ l Taq Master Mix

Thermal cycling was always performed as follows: (30 cycles)

1. Denaturation was performed at 95°C for 2 minutes
2. Primer annealing was at 2°C below the melting temperature of the primer pair used.
3. Extension was at 72°C for 30 seconds per kb of DNA to be amplified, so for a 2 kb amplicon, a one minute extension time was used.
4. Finally, a 5 minute extension was performed, and this was quickly cooled to 10°C.

9.5.3 Colony PCR

A single colony was picked to a small PCR tube using a toothpick, with just enough cell material to see a trace on the side of the tube. These cells were mixed with 10 μ l of Ultra-pure water (Sigma), and vortexed to mix. The tube was heated to 99°C for 10 minutes in a TC-512 Thermal cycler machine (Techne) to lyse the cells. To use the released plasmid DNA as a template in a PCR reaction, the cell debris was pelleted by centrifugation at 13,000 x g for 2 minutes, and 1 μ l of the supernatant

was carefully transferred from the top of the 10 µl sample to a fresh PCR tube. A normal PCR reaction (see above) was then performed, using the 1 µl of the colony preparation as the template.

9.5.4 Southern blot

Before the lab-based work, a virtual digest of the relevant DNA was performed using NEBcutter (<http://tools.neb.com/NEBcutter2/index.php>). Here, the sites of restriction endonuclease cleavage were visualised, to select an enzyme which would cut the genome either side of the target gene, generating a genomic fragment that would be easily visualised on a gel (ideally, 3 - 10 kb).

The genomic DNA to be tested was purified using the Promega Wizard genomic DNA kit (see above) and the resultant fragments were electrophoretically separated on a 1% agarose gel.

The agarose gel was treated using the following solutions, to allow DNA transfer onto a nitrocellulose membrane:

Denaturation Solution (500ml)

0.5M NaOH (10g)

1.5M NaCl (43.75g)

Neutralising Solution (500ml)

1M Tris-HCl pH 8 (60.55g)

1.5M NaCl (45.75g)

Depurination Solution (500ml)

0.2M HCl (4.55ml)

20x SSC (in 2L)

346.6g NaCl

176.4g Tri Sodium Citrate pH 7

Method

1. A photo of the finished gel was produced with a ruler alongside to allow measurement of the migration of each band relative to the size marker (1kb Plus, Roche). The gel was carefully placed in a plastic box for subsequent treatment:
2. The gel was depurinated by soaking for 20 mins in Depurination Solution before being washed with dH₂O.
3. Next, the gel was immersed in Denaturation Solution for 20 minutes before being washed with dH₂O.
4. Finally, the gel was neutralised by immersion in Neutralising Solution for 20 mins, before a final wash with dH₂O.

The DNA could then be transferred from the gel to a nylon membrane (Hybond-N+, Amersham) by upward capillary action as in Sambrook *et al.* (1989). Once transferred, the DNA was fixed to the membrane by cross-linking using UV light (254nm wavelength for 20 seconds, using a UV Stratalinker 2400, Stratagene).

To label and hybridise a probe to the DNA on the nylon membrane, the following steps were performed, using reagents and protocols from the (Roche) DIG High Prime DNA Labelling and Detection kit:

1. To make the probe, 4 µl of reagent 1 was added to 20 µl of purified PCR product, and incubated at 37°C overnight.

(This procedure attaches a steroid isolated from digitalis plants, dixoxigenin (DIG), to the DNA probe. A PCR product was used that would bind within the digested genomic DNA fragment containing the suspected mutation).

2. The nylon filter was incubated in 20ml DIG-easy hybridisation solution (Roche) at 42°C, for 30 minutes (prehybridisation).

3. 5 µl of the DIG-labelled probe was heat denatured at 95°C for 10 minutes and added to 5ml of DIG-easy hybridisation solution.

4. The nylon filter was removed from the prehybridisation solution and the probe-containing hybridisation solution was added at a volume of 2.5 ml per 100cm² of membrane. This was incubated overnight at 42°C, with gentle agitation.

5. The filter was washed to remove all remaining unbound probe, and the hybridisation solution:

a. 2 x 5 minutes with 50 ml of solution 1 (2x SSC, 0.1% SDS) at room temperature.

Then,

b. 2 x 15 minutes with solution 2 (0.1x SSC, 0.1% SDS) at 68°C.

The targeted genomic fragments were now bound by many copies of probe, which had DIG steroid attached. To visualise the probe signals an anti-DIG antibody was bound to the membrane. This required the following reagents:

Maleic Acid Buffer

0.1 M Maleic acid

0.15 M NaCl;

Adjusted to pH 7.5 with NaOH.

Blocking Solution (500 ml)

50 ml Blocking reagent (Roche)

450 ml Maleic Acid Buffer.

Detection Buffer

0.1 M Tris-HCl

0.1 M NaCl

50 mM MgCl₂

Adjusted to pH 9.5.

Method:

1. The membrane was immersed in Maleic Acid Buffer for 5 minutes, before being removed.
2. The membrane was incubated for 30 min in 100 ml of Blocking Solution at room temperature.
3. The Anti-DIG-AP-conjugate (Alkaline Phosphatase conjugated to the anti-DIG antibody) was diluted 1 in 10,000 in 5 ml of Blocking Solution and added to the membrane, this was incubated for 30 minutes at room temperature.
4. The membrane was washed for 15 minutes in 100 ml of Maleic Acid Buffer, then removed, and repeated with fresh buffer.
5. Following washing, the membrane was equilibrated for 5 minutes by incubation in Detection Buffer at room temperature.
6. Finally, 5 ml of a solution of 5-Bromo-4-chloro-3-indolyl phosphate, toluidine salt [BCIP] and Nitro blue tetrazolium chloride [NBT] (Roche) was added to the membrane. Briefly, BCIP is dephosphorylated by the alkaline phosphatase enzyme, and then oxidised by NBT.

Dephosphorylated and oxidised BCIP is dark blue in colour, as is reduced NBT, providing an intense coloured band at the site of the probe.

9.5.5 Purification of PCR-amplified DNA

Following PCR amplification, DNA was purified using a High-Pure PCR purification kit (*Roche*) according to the supplied protocol as follows. All centrifugation steps were performed at 16,000 x g in a 5415 D Microcentrifuge (Eppendorf).

1. For each 50 µl PCR reaction, 500 µl Binding buffer was added and mixed using a pipette.
2. This was applied to a High Pure filter column and centrifuged for 1 minute; the eluate was discarded.
3. To the column, 500 µl of Wash buffer was added, centrifuged for 1 minute and the eluate was discarded.
4. Here, 200 µl of Wash buffer was added, and again centrifuged for 1 minute, discarding the eluate.
5. To collect the purified PCR product, the column was transferred to a 1.5 ml microfuge tube and 30 µl of Ultra-pure water (Sigma) was added, allowed to stand for 2 minutes and then centrifuged for 1 minute. The resultant PCR products were routinely stored at -20°C.

9.5.6 Restriction enzyme digestion

DNA digestions were carried out using restriction enzymes supplied by *Roche* with their supplied buffers. Here, around 300 ng of plasmid DNA was cut in a 20 µl reaction as follows:

2 µl of appropriate buffer solution

17 µl of Ultra-pure water containing 300 ng of plasmid DNA

1 µl (10 units) of the appropriate enzyme(s)

These reactions were always incubated at 37°C for 4 hours to ensure all DNA was cut. To inactivate the enzymes, samples were heated to 65°C for 10 minutes.

9.5.7 Dephosphorylation of plasmid DNA

To prevent religation of plasmid DNA when only cut with one enzyme, rAPID Alkaline Phosphatase (Roche) was used to dephosphorylate the 5' ends. To a typical 20 µl digest reaction, 10 units of rAPID Alkaline Phosphatase was added, without any extra buffer or water. Reactions were incubated for 30 minutes at 37 °C, and were stopped by heating at 75 °C for 2 minutes.

9.5.8 Ligation of DNA fragments

Concentrations of vector and insert DNA were determined using a nanodrop spectrophotometer (Agilent), before being mixed in a 1:3 molar ratio of vector:insert, calculated using a ligation calculator (http://www.insilico.uni-duesseldorf.de/Lig_Input.html). The insert DNA was ligated to the vector using Roche T4 DNA ligase overnight at 11°C in a 10 µl reaction, containing 0.5 µl of enzyme, 1 µl of 10 x ligase buffer (Roche), and the correct molar ratio of DNA in 8.5 µl of Ultra-pure water (Sigma).

9.5.9 DNA gel electrophoresis

All separations of DNA performed used 1 % agarose dissolved in TBE buffer (45 mM Tris-borate, 1 mM EDTA, pH 8.0) containing ethidium bromide (500 ng /ml) to stain the DNA. Samples (5 µl) were mixed with loading buffer containing 0.25% bromophenol blue and 30% glycerol (v/v). Gels were run in SCIE-PLAS mini or midi horizontal gel tanks, with 1x TBE as running buffer, at 70-100 mV until desired separation had occurred. To measure the sizes of DNA fragments, a lane loaded with 1 kb+ DNA ladder (Invitrogen) was added to each gel prior to running.

9.5.10 Extraction of DNA from agarose gels

To extract digested DNA from agarose gels, a QIAquick Gel Extraction kit (Qiagen) was used, as per the supplied protocol.

1. A sterile scalpel was used to cut around and remove the desired DNA fragment.
2. To this, 300 µl of QG buffer was added in a 1.5 ml microfuge tube. This was incubated for 10 minutes at 50 °C to melt the agarose.
3. This sample was decanted into a QIAquick spin column and centrifuged for 1 minute. The eluate was discarded.
4. The column was washed by adding 750 µl PE buffer before centrifuging for 1 minute. The eluate was discarded.
5. The column was transferred to a clean 1.5 ml microfuge tube, and the DNA was eluted by adding 30 µl of Ultra-pure water (Sigma).

9.5.11 Site-directed mutagenesis (SDM)

Site directed mutagenesis was performed using an Agilent Quikchange Lightning kit. Mutagenesis of plasmids was achieved by using two primers, which are the reverse complement of each other, which span the region targeted for mutagenesis. The nucleotides to be mutated are altered within the primer sequences, which are then used in a PCR reaction, with a long elongation cycle time to allow replication of the entire plasmid. New copies of the plasmid will contain the mutated bases, due to the incorporation of the primers into the PCR products. The newly synthesised DNA from a PCR reaction is not methylated, so the restriction endonuclease *DpnI* is used to cut the methylated template plasmids into small pieces (*DpnI* cuts at 5'-GATC-3' sites). The linear PCR products that contain the mutations are used to transform a strain of *E. coli* (XL10-GOLD) which can repair the nicked-DNA plasmids to generate functionally replicating mutated versions of the original template plasmid.

Reactions were set up as follows, using reagents supplied with the Agilent kit:

2.5 µl Reaction Buffer

62.5 ng of each oligonucleotide primer

25 ng of template plasmid DNA

0.5 µl of dNTP mix

0.75 µl of Quik Solution

0.5 µl Quikchange Enzyme

20.25 µl of Ultra Pure H₂O

The thermal cycles used to generate the site-directed mutants in this work were as follows:

2 minutes at 95°C, 1 cycle.

18 cycles of:

20 seconds at 95°C

10 seconds at 60°C

5 minutes at 68°C

Followed by:

5 minutes at 68°C

1. To each reaction, 2 µl of *DpnI* was added, and incubated for 2 hours at 37°C.

2. 1 µl of *DpnI* treated sample was used to transform *E. coli* XL10-Gold (Agilent) according to the manufacturer's specification.

3. Transformed XL10-Gold cells were selected by plating on LB containing the appropriate antibiotics.

9.6 Generation of genomic insertion mutants of *R. pomeroyi*

9.6.1 pK19 derivatives

Several of the insertional mutations that were made in this study were based on a suicide plasmid, pBIO1879 (Todd *et al.* 2011), which is a derivative of pK19*mob* (Schafer *et al.* 1994) into which a spectinomycin resistance (Spc^{R}) cassette was cloned into the polycloning site, and so confers resistance to both spectinomycin in addition to kanamycin, present on pK19*mob*.

Firstly, a fragment internal to the targeted gene was ligated into pBIO1879. The newly formed recombinant plasmid was then introduced into *Ruegeria* by tri-parental conjugation (see above). Since pK19*mob* and its derivatives cannot replicate outside the enteric bacteria, selection for Spc^{R} / Kan^{R} transconjugants can yield recombinants between the cloned internal fragment and the target gene, generating a targeted, insertional mutation. See Figure 4.15 in Chapter 4 for an illustration of this procedure.

9.6.2 pEX18Ap derivatives

pEX18Ap (Hoang *et al.* 1998) is a wide host range plasmid that encodes ampicillin resistance (via its *bla* gene) and can be mobilised from *E. coli* to many different proteobacteria, but it fails to replicate in such hosts. It also contains a polylinker cloning region and a *sacB* gene, which encodes a levansucrase that cleaves sucrose into glucose plus fructose, the latter being polymerised to levan, a toxin for most bacteria (Merlin *et al.* 2002). pEX18Ap is therefore a selectable, suicide vector that can be used to generate genomic mutants. This can be achieved by cloning a selectable marker between two regions of DNA that flank the gene that is targeted for mutagenesis, crossing this construct into the target strain, and then selecting for the cloned marker, usually spectinomycin resistance (200 μg /ml), making sure that the resultant transconjugants are sucrose resistant and have therefore lost the pEX18Ap derivative.

9.7 Transformation of *E. coli* with plasmid DNA

9.7.1 Preparation of competent cells

Recipient *E. coli* cells for transformations were made competent using ice-cold CaCl_2 (Sambrook *et al.* 1989), as follows:

1. A single colony of the required *E. coli* strain was used to inoculate 5 ml LB media. This was incubated overnight at 37°C with 200 rpm of shaking.
2. This culture was then diluted 1 in 100 into 100 ml of LB media and incubated for ~1.5 hours until the $\text{OD}_{600\text{nm}}$ value reached ~0.4.
3. The cultures were cooled on ice for 10 minutes, before harvesting the cells in two 50 ml centrifuge tubes (Corning) at 4500 x g for 10 minutes at 4 °C using an Eppendorf centrifuge, model 5804R.
4. The supernatant was quickly removed and the cells were resuspended in 15 ml of ice-cold 0.1M CaCl_2 and incubated for 30 minutes on ice.
5. The cells were pelleted by centrifugation as before, the supernatant discarded, and the cell pellet was resuspended, in 2 ml of ice-cold 0.1M CaCl_2 . This was incubated on ice for at least 2 hours.
6. The now competent cells were used immediately or within 24 hours, if stored on ice.

9.7.2 Transformation of competent cells

1. Either 5 μl of a ligation reaction, or 0.5 μl of a plasmid preparation was added to 100 μl of competent *E. coli* cells in an ice-cold microfuge tube.
2. These were incubated for 30 minutes on ice.
3. The tubes were transferred to a water bath at 42°C for 1 minute, and returned to ice for a further 2 minutes.
4. Then, 500 μl pre-warmed LB broth (42°C) was added to each tube and incubated at 37°C for one hour, to allow expression of the introduced selectable marker..

5. Cells were plated onto selective LB medium containing the appropriate antibiotic(s) using a sterile spreader. Transformants were screened following overnight incubation at 37°C.

9.7.3 DNA sequencing

Sequencing was carried out by Genome Enterprise Ltd., (John Innes Centre, UK) using an AbiPrism 3730 capillary sequencer. Plasmid DNA that was to be used as template for sequencing reactions was isolated using the Qiagen Midiprep method as detailed earlier. For each sample, 5 µg of template DNA was sent to be sequenced, using primers specific to the cloned fragment, or to the vector, where appropriate, at a concentration of 1.5 pmol / µl.

9.7.4 β-Galactosidase assays

The plasmid pBIO1878 is a derivative of the wide host-range promoter-probe plasmid vector pMP220 derivative (Spaink 1987). It has an additional Spc^R cassette, cloned into the *SphI* site of pMP220 in order to facilitate counter-selection when the plasmid was to be introduced into strains of *Ruegeria*. The cloning sites in pBIO1878 are upstream of a *lacZ* gene, which has a ribosome binding site derived from the chloramphenicol acetyl transferase gene of *E. coli*, but lacks any promoter or operator sequence. Thus, a promoter from a gene of choice, cloned in the correct orientation into the PCS of pBIO1878 will control the expression of β-galactosidase encoded by the reporter *lacZ*.

The assay for β-galactosidase involves the cleavage of o-nitrophenyl-β-D-galactoside (ONPG) to o-nitrophenol a yellow product that absorbs at 420nm and is measured in a spectrophotometer (Genova spectrophotometer {Jenway}).

Reagents required:

Z-buffer - in 50 ml of dH₂O

1 ml 3M Na₂HPO₄·7H₂O

0.5 ml 4M NaHPO₄·7H₂O

0.5 ml 1M KCl

0.5 ml MgSO₄·7H₂O

175 µl β-mercaptoethanol

ONPG solution – per ml of dH₂O

4 mg O-nitrophenyl-β-D-galactopyranoside

1. *R. pomeroyi* strains were inoculated from single colonies into 5 ml HY medium containing appropriate antibiotics and grown for 2 days at 28°C.
2. These starter cultures were used to inoculate either MBM (for Fe limitation experiments) or RSS (for Mn limitation) containing 10 mM succinate and vitamin solution as described earlier.
3. These cultures were grown for ~15 hours or until the OD_{600nm} had reached at least 0.1. The cultures which lacked iron rarely grew above an OD_{600nm} value of 0.15.
4. From each culture, 500 µl aliquots were added to a 2 ml microfuge tube containing 500 µl Z-buffer.
5. Using a Pasteur pipette, 2 drops of chloroform and 1 drop of 0.1% SDS (w/v) were added to each microfuge tube and vortexed for 10 seconds. These were then incubated at 28° C for 5 minutes.
6. To each tube, 200 µl ONPG solution was added, before returning the tubes to 28°C.
7. When sufficient yellow colour had developed, the reactions were stopped using 500 µl 1M sodium bicarbonate, and the length of incubation was recorded.
8. All tubes were centrifuged for 3 minutes at 13,200 x g to clear the cell debris.
9. A 1 ml aliquot from each tube was transferred to a 2 ml cuvette and the OD_{420nm} was recorded.
10. β-galactosidase activities, in Miller Units, were calculated using the following equation:

$$\text{Miller Units} = \frac{1000 \times \text{OD}_{420\text{nm}}}{t \times V \times \text{OD}_{600\text{nm}}}$$

Where,

t = time in minutes, and V = volume of culture

9.7.5 CAS assay plates

Chrome azural sulfonate (CAS) solution was made as follows:

60.5 mg CAS, dissolved in 50 ml dH₂O

10 ml 1 mM FeCl₃·6H₂O in 10 mM HCl

72.9 mg HDTMA (Hexadecyltrimethylammonium bromide) in 40 ml dH₂O.

These constituents were mixed and autoclaved. Then 20 ml of this CAS solution was added per 200 ml of MBM agar to make CAS plates.

9.8 *in silico* analyses

9.8.1 DNA sequence analysis

DNA sequences returned from TGAC were analysed using *BioEdit*. Sequences were compared to genomic and protein sequences available from the National Centre for Biotechnology Information (NCBI - www.ncbi.nlm.nih.gov) using the Basic Local Alignment Search Tool, BLAST (Altschul *et al.* 1997).

DNA sequence motifs were discovered, and logo graphics of these motifs generated using MEME (Bailey and Elkan 1994).

9.8.2 Sequence alignments and phylogenetic trees

Evolutionary analyses were conducted in MEGA5 (Tamura *et al.* 2011). Alignments were performed using the Neighbor-Joining method (Saitou and Nei 1987). Bootstrap consensus trees were inferred from 500 replicates and are taken to represent the evolutionary history of the taxa analyzed (Felsenstein 1985). Branches corresponding to partitions reproduced in fewer than 50% bootstrap replicates are collapsed. The percentages of replicate trees in which the associated taxa clustered together in the bootstrap test (500 replicates) are shown next to the branches (Felsenstein 1985). The trees are drawn to scale, with branch lengths in the same units as those of the evolutionary distances used to infer the phylogenetic tree. The evolutionary distances were computed using the JTT matrix-based method (Jones *et al.* 1992) and are in the units of the number of amino acid substitutions per site.

9.8.3 Database searches

Searches for homologous protein sequences in the NCBI non-redundant protein database were done using BLAST. Metagenomic databases were interrogated using BLAST, with input sequences obtained from NCBI, using the Community Cyberinfrastructure for Advanced Microbial Ecology Research and Analysis (CAMERA), described by Sun *et al.* (2010).

9.8.4 Other bioinformatic tools

Several online programmes were used to analyse peptide sequences where indicated in the text. They are available at the following websites:

- SignalP (Petersen *et al.* 2011) – used to predict the presence of a SEC-signal peptide.
- TatP (Bendtsen *et al.* 2005) – used to predict the presence of a TAT-signal peptide.
- iMembrane (Kelm *et al.* 2009) – predicts putative tertiary / membrane structure of a protein based on closest homologue within the iMembrane database.
- String 9.0 (Szklarczyk *et al.* 2011) – functional prediction / neighbourhood / co-occurrence analysis of genes.

- PredTM-BB (Bagos *et al.* 2004) – predicts whether a protein is likely found within a bacterial membrane, and can be used to draw the secondary structure of a protein integrated in a membrane.

Table 9.1 Details of Strains, Plasmids and Oligonucleotide primers used in this work

STRAINS

Strain	Description	Source
<i>Escherichia coli</i> 803	Met ^r ; used as host for transformation with large plasmids	Wood (1966)
<i>E. coli</i> XL10-Gold	High transformation rate, used for site directed mutagenesis	Stratagene
<i>E. coli</i> JM101	Used as host for pUC18-based plasmids	Messing (1979)
<i>Dinoroseobacter shibae</i> DFL-12	Lab strain	Biebl <i>et al.</i> (2005)
<i>Sulfitobacter</i> EE36	Lab strain	Gonzalez <i>et al.</i> (1996)
<i>Silicibacter lacuscaerulensis</i> ITI-1157	Lab strain	Petersdottir and Kristjansson (1997)
<i>Fulvimarina pelagi</i> HTCC2506	Lab strain	Cho and Giovannoni (2003)
<i>Loktanella vestfoldensis</i> SKA53	Lab strain	Van Trappen <i>et al.</i> (2004)
J469	<i>R. pomeroyi</i> wild type strain	González (2003)
J470	J469, Rif ^r	Todd <i>et al.</i> (2011)
J528	Mur ^r strain of <i>R. pomeroyi</i> , generated using pBIO1861. Spec ^r Rif ^r Kan ^r	This Work
J529	SitA ^r strain of <i>R. pomeroyi</i> , generated using pBIO2124. Spec ^r Rif ^r Kan ^r	This Work
J531	FbpAB ^r strain of <i>R. pomeroyi</i> , generated using pBIO2104. Spec ^r Rif ^r	This Work
J532	FbpAB ^r strain of <i>R. pomeroyi</i> , generated using pBIO2104. Spec ^r Rif ^r	This Work
J533	IrpA ^r strain of <i>R. pomeroyi</i> , generated using pBIO2116. Spec ^r Rif ^r Kan ^r	This Work
J534	SPO0432 ^r strain of <i>R. pomeroyi</i> , generated using pBIO2119. Spec ^r Rif ^r Kan ^r	This Work
J535	SPO3722 ^r strain of <i>R. pomeroyi</i> , generated using pBIO2120. Spec ^r Rif ^r Kan ^r	This Work
J536	SPO1393 ^r strain of <i>R. pomeroyi</i> , generated using pBIO2121. Spec ^r Rif ^r Kan ^r	This Work
J537	SPO2025 ^r strain of <i>R. pomeroyi</i> , generated using pBIO2122. Spec ^r Rif ^r Kan ^r	This Work
J538	SPOA0186 ^r strain of <i>R. pomeroyi</i> , generated using pBIO2123. Spec ^r Rif ^r Kan ^r	This Work
J539	Irr ^r -strain of <i>R. pomeroyi</i> , generated using pBIO2114. Rif ^r Amp ^r Spec ^r	This Work

PRIMERS

Oligo Name	Sequence	Restriction site / Function	Plasmid
fbpA fwd:	GCTTAGAGCAATACGTGACGAGGGC	PstI / XbaI	
fbpA rev:	CGCTGCTCTGCGAGTTGGCGGAATGC	PstI / XbaI	
fbpB fwd:	CGCGTTTGCTGACGAGGAGCCCGCCGCG	PstI / XbaI	
fbpB rev:	CGCTTAGACACCAAGATCAAGGCG	PstI / XbaI	
irpA fwd:	GCTTAGACGCGATCGATCGCTCGCCG	PstI / XbaI	
irpA rev:	CGGTGCGCGCTCGAGTAGGCGCC	PstI / XbaI	
IrpApk19FWD	GGTGAATCTCTGCGCGCTGAGG	EcoRI	
IrpApk19REV	CCATCTAGACGTTCCGGATACC	XbaI	
mbfApXba1FWD	CGCGCTTAGACCGCTCGCGCTCGGCGAGGC	Amplifies <i>mbfA</i> promoter	
mbfApPst1REV	CGCGCTGACGCGTTCATCGAGCGGATCAG	Amplifies <i>mbfA</i> promoter	
irrCOMPFW	CGCGCTTAGAGTCTTCTGTCAAAGCTCG	Amplifies <i>irr</i> and its promoter	
irrCOMPREV	CGCGCTTAGACCGCGCGGCGCACAGGTC	Amplifies <i>irr</i> and its promoter	
fbpA51ToGFWD	CGGACAGCAATACCCGACTGAAATAAGCAGTTTATCTTGC		
fbpA51ToGREV	GCAAGATAAAAGTCTTATTCAGTGGGTAATGCTGTGCG	Mutagenesis of IR box 1 'T'	pBIO2106
fbpA51CtoGFWD	CGGACAGCAATACCCGACTGAAATAAGTATTTATCTTGC		
fbpA51CtoGREV	GCAAGATAAAAGTCTTATTCAGTGGGTAATGCTGTGCG	Mutagenesis of IR box 1 'C'	pBIO2107
fbpA2ToGFWD	CGGAAATCCGGTAATGACTATTCAGTGGGTAATGACTGATCG		
fbpA2ToGREV	CGATTCAGTTAATCCGCTGAAATAGTCAATACCGGATTTGCG	Mutagenesis of IR box 2 'T'	pBIO2108
fbpA2CtoGFWD	CGGAAATCCGGTAATGACTATTCAGTGGGTAATGACTGATCG		
fbpA2CtoGREV	CGATTCAGTTAATCCGCTGAAATAGTCAATACCGGATTTGCG	Mutagenesis of IR box 2 'C'	pBIO2109
fbpBToGFWD	TCAGGCGTGGTATTTCCGACTAAACTGGGCGATTAAAGGCAATTGGAACC		
fbpBToGREV	GGTTCGAATGCCCTAATCGCCCGATTTAGTCGGAATACCGGTCCTGA	Mutagenesis of IR box 3 'T'	pBIO2110
fbpBCToGFWD	TCAGGCGTGGTATTTCCGACTAAACTGGGCGATTAAAGGCAATTGGAACC		
fbpBCToGREV	GGTTCGAATGCCCTAATCGCCCGATTTAGTCGGAATACCGGTCCTGA	Mutagenesis of IR box 3 'C'	pBIO2111
IrpABamH1FWD	ATCGGTGTGATCGGGGTGTGACTTAAGGATCCAAATTTAGTCAGATATAAGCAAGCCAG		
IrpABamH1REV	CTGGCTTTCCTTATCTGACTAAATGATCTTAACTCAAGCCCGATCACCCGAT	Mutagenesis of IR box upstream of <i>irpA</i>	pBIO2115
SpecPstIR	GGCGCTGACGATCGTGGCGTATCGAAAT	spec cassette amplification Pst I	
SpecPstIR	GGCGCTGACGATCGTGGCGTATCGAAAT	spec cassette amplification Pst I	
P1	CGTGGTCTGCGCTGGCG	fbpAB mutant check primers	
P2	AGATCGCTTGGCTGCGCG	fbpAB mutant check primers	
P3	CACCTCGCCATCGCCGAGG	fbpAB mutant check primers	
irpA1F1	GCATGATCCCGTCGACGCGCTGGTGCAGCA	irpA mutant check primers	
irpA2R2	GCTGAAAGTATCGTTGAAC	irpA mutant check primers	
SPO0789Xba1F1	GCACCTAGACCTCGCTGTCATCAGTGTG	SPO0789 promoter cloning	
SPO0789Pst1R1	CGATCTGACGCAAGATTGCGCCCTTGGT	SPO0789 promoter cloning	
iscRpS4F	TGCATCTAGAGTTCCTATGCTGGTCTCTG	iscR promoter cloning	
iscRpS4R	GCATCTGACGTCGACGCGATATCGGTCAG	iscR promoter cloning	
SPO0432EcoF	ATCGGAATTCGCAATACCAACGCGCAAAAT	pBIO1879 cloning to create mutagenic suicide plasmid	
SPO0432XbaR	ACGTCTAGATTATACAGACCCAGCCGATC	pBIO1879 cloning to create mutagenic suicide plasmid	
SPO3722F	CACCGAAGGACTGGAATGG	pBIO1879 cloning to create mutagenic suicide plasmid	
SPO3722R	ACGTCTAGAGTGGAGCTTTCTCGAAACCA	pBIO1879 cloning to create mutagenic suicide plasmid	
SPO1393F	AGTCGAATTCATGGGTGACGGGTGAGAG	pBIO1879 cloning to create mutagenic suicide plasmid	
SPO1393R	TACGCTAGAGCTGGAGATCTCAAATCC	pBIO1879 cloning to create mutagenic suicide plasmid	
SPO2025F	TBACGAAATTCCTGACAAAGGGGCGCTAT	pBIO1879 cloning to create mutagenic suicide plasmid	
SPO2025R	AGTCTTAGATCTTACACCATCCGAAAGC	pBIO1879 cloning to create mutagenic suicide plasmid	
SPOA0186F	ACGTGAATTCCTCAAGTCTCCGACTATGC	pBIO1879 cloning to create mutagenic suicide plasmid	
SPOA0186R	GACTCTAGACCGGATCGTATTTGACCTG	pBIO1879 cloning to create mutagenic suicide plasmid	
irrfankEcoFWD	CACATGCCGAGAGACGGAAT	irr flanking region amplification for pEX18Ap cloning	
irrfankHindIIIREV	CGCAAGCTTGCAGGCTCTGTCAAATCA	irr flanking region amplification for pEX18Ap cloning	
irrfank1F	CACATGCCGAGAGACGGAAT	irr mutant screening	
irrfank2R	CGCAAGCTTGCAGGCTCTGTCAAATCA	irr mutant screening	
IrrcheckF	CAGGAAATCGCCACCGATTG	irr mutant screening	
IrrcheckR	CUTTGGCGGACGCGGATC	irr mutant screening	
SitAF2	CGCGCTTAGAGCGCGGAGATCACGATGCG	sitA promoter cloning	
SitAR2	CGACTGACGCAACTGTGCGCATAATCG	sitA promoter cloning	
MRS1sdmF	TTTACTTTCCGACAAAATTCACCTTTCTACGAAATATTCTCAATTGCGGT	MRS box mutagenesis upstream of <i>sitA</i>	
MRS1sdmR	AACGCAATGAGAAATATTCTGTAGAAAGGTAAATTTCCGAAAGGTAAA	MRS box mutagenesis upstream of <i>sitA</i>	
MRS2sdmF	CTGCGAAATTAATCTCAATTCGTTGACTTATGAAAGCAATGGTCTCATATT	MRS box mutagenesis upstream of <i>sitA</i>	
MRS2sdmR	AATATGAAACCAATCGTACTAAGTCAACGCAATGAGAAATATTCCGCAAG	MRS box mutagenesis upstream of <i>sitA</i>	
FURFwd	GCTTAGACGGGTGCGAGAACTCG	internal fragment of Mur for cloning into pBIO1879	
FURRev	CGGATCCCGATGTGAGGAGCTGTATGC	internal fragment of Mur for cloning into pBIO1879	
Irrpromfwd	CTGTCAAAGCTGCTCGGT	Irr promoter cloning	
Irrpromrev	CGGATTTCTGAGAAATTTGGCGT	Irr promoter cloning	
VcXbamp1	CGGATCCGAAAGGATATACATATGTCGATAAATTTCTCAATCA	cloning Vibrio mntX into pRK415	
VcXecop2	CGGATTTCTGATTTCAATTAACCAAGT	cloning Vibrio mntX into pRK415	
SitApk19F	ACTGGAATTCGCGATGGTGGTATGTGT	internal fragment of <i>sitA</i> of <i>R. pomeroyi</i>	
SitApk19R	ATCGTCTAGAGTGGCAACCCCGGTATG	internal fragment of <i>sitA</i> of <i>R. pomeroyi</i>	
MntXpF	ACGTCTAGAGTGGATCACCCCGTTC	mntX of <i>R. rubinihibens</i> promoter fusion	
MntXpR	GCATCTGACGACATAGGCATCGACCAATCA	mntX of <i>R. rubinihibens</i> promoter fusion	
MntXF	ACGTCTAGAGTGGATCACCCCGTTC	mntX of <i>R. rubinihibens</i> cloning	
MntXR	CGATCTGACGACCCCGCTAGTTCATAAGC	mntX of <i>R. rubinihibens</i> cloning	

PLASMIDS

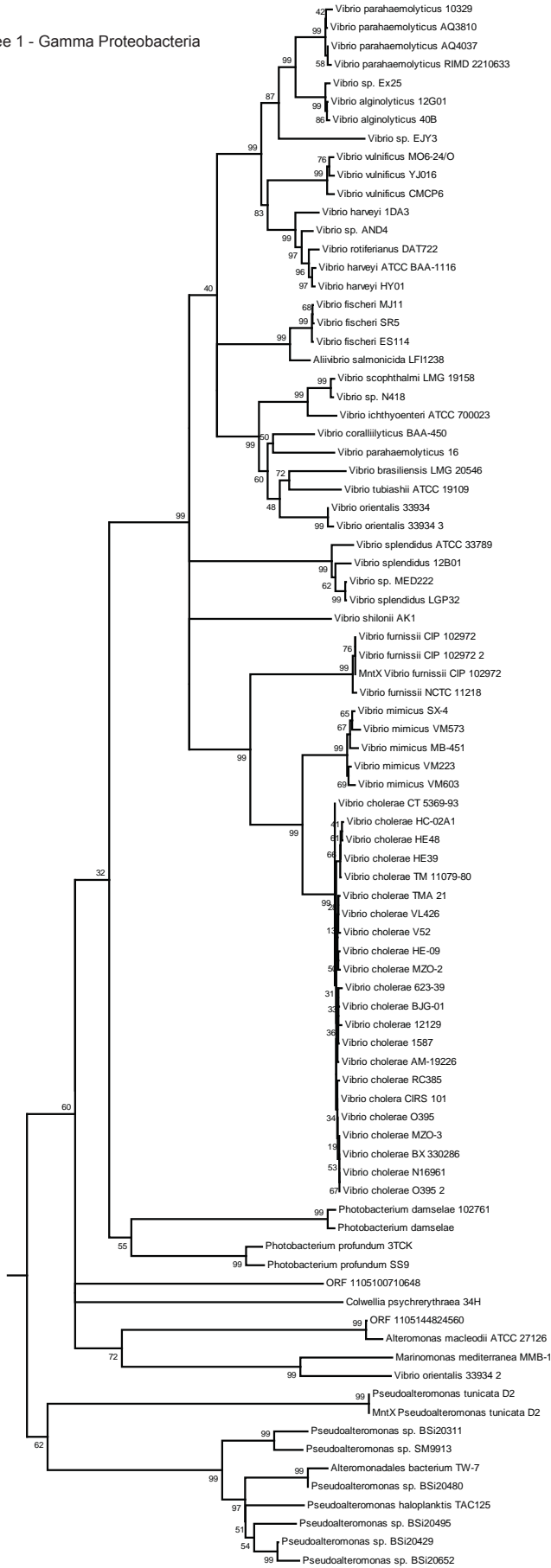
Vector	Function	Source	Marker Selection
pRK2013	Used as mobilising plasmid in tri-parental crosses	Figurski and Helinski (1979)	Kan ^R
pμP220	Wide host-range lacZ promoter probe vector	Spaink <i>et al.</i> (1987)	Tet ^R
pOT2	Broad host-range promoter probe vector with promoterless <i>gfp</i> gene	Allaway <i>et al.</i> (2001)	Gent ^R
pBIO1879	pK19mob::spec, Suicide insertion plasmid with a spectinomycin resistance cassette	Todd <i>et al.</i> (2011)	Spec ^R , Kan ^R
pRK415	Broad host-range expression vector	Keen <i>et al.</i> (1988)	Tet ^R
pDONR221	pUC origin Gateway vector	Nakagawa <i>et al.</i> (2008)	Kan ^R
pBIO1845	pBIO1878 with <i>fbpA</i> promoter from <i>R. pomeroyi</i> cloned in using <i>Xba</i> I and <i>Bam</i> HI	This Work	Spec ^R , Tet ^R
pBIO1846	pBIO1878 with <i>fbpB</i> promoter from <i>R. pomeroyi</i> cloned in using <i>Xba</i> I and <i>Bam</i> HI	This Work	Spec ^R , Tet ^R
pBIO1847	pBIO1878 with <i>irpA</i> promoter from <i>R. pomeroyi</i> cloned in using <i>Xba</i> I and <i>Bam</i> HI	This Work	Spec ^R , Tet ^R
pBIO1861	pBIO1879 with internal fragment of <i>mur</i> cloned in using <i>Xba</i> I and <i>Bam</i> HI	This Work	Spec ^R , Kan ^R
pBIO1863	pBIO1879 with internal fragment of <i>iscR</i> cloned in using <i>Xba</i> I and <i>Eco</i> RI	This Work	Spec ^R , Kan ^R
pBIO1864	pBIO1879 with internal fragment of <i>rirA</i> cloned in using <i>Xba</i> I and <i>Eco</i> RI	This Work	Spec ^R , Kan ^R
pBIO1928	Contains <i>irr</i> plus promoter of J470 in pOT2	This Work	Gent ^R
pBIO1929	Contains J470 <i>mbfA</i> promoter- <i>LacZ</i> fusion in pS4	This Work	Spec ^R , Tet ^R
pBIO2088	<i>Candidatus</i> Pelagibacter sp. IMCC9063 <i>mntX</i> gene cloned into pRK415	This Work	
pBIO2050	1086 bp promoter region of <i>sitA</i> cloned into pBIO1878	This Work	Spec ^R , Tet ^R
pBIO2100	MRS1 box mutation in pBIO2050	This Work	Spec ^R , Tet ^R
pBIO2101	MRS2 box mutation in pBIO2050	This Work	Spec ^R , Tet ^R
pBIO2102	MRS1 and MRS2 box mutation in pBIO2050	This Work	Spec ^R , Tet ^R
pBIO2103	5011bp region flanking <i>fbpAB</i> of <i>R. pomeroyi</i> in pEX18Ap	This Work	Amp ^R
pBIO2104	5011bp region flanking <i>fbpAB</i> of <i>R. pomeroyi</i> in pEX18Ap	This Work	Amp ^R
pBIO2105	pBIO2104 with a 1.8 kb Spec ^R cassette cloned into <i>Pst</i> I	This Work	Amp ^R , Spec ^R
pBIO2106	pBIO2104 with a 1.8 kb Spec ^R cassette cloned into <i>Pst</i> I	This Work	Amp ^R , Spec ^R
pBIO2107	pBIO1878 with mutation in IR box 1 T	This Work	Spec ^R , Tet ^R
pBIO2108	pBIO1878 with mutation in IR box 1 C	This Work	Spec ^R , Tet ^R
pBIO2109	pBIO1878 with mutation in IR box 2 T	This Work	Spec ^R , Tet ^R
pBIO2110	pBIO1878 with mutation in IR box 2 C	This Work	Spec ^R , Tet ^R
pBIO2111	pBIO1879 with mutation in IR box 3 T	This Work	Spec ^R , Tet ^R
pBIO2112	pBIO1879 with mutation in IR box 3 C	This Work	Spec ^R , Tet ^R
pBIO2113	<i>irr</i> flanking region cloned into pEX18Ap	This Work	Amp ^R
pBIO2114	pBIO2113 with a 1.8 kb Spec ^R cassette cloned into <i>Pst</i> I	This Work	Amp ^R , Spec ^R
pBIO2115	pBIO1847 with mutation, IR box changed to <i>Bam</i> HI site	This Work	Spec ^R , Tet ^R
pBIO2116	<i>irpA</i> internal fragment cloned into pBIO1879	This Work	Spec ^R , Kan ^R
pBIO2117	SPO0789 promoter cloned into pBIO1878	This Work	Spec ^R , Tet ^R
pBIO2118	<i>iscR</i> promoter cloned into pBIO1878	This Work	Spec ^R , Tet ^R
pBIO2119	SPO0432 internal fragment cloned into pBIO1879	This Work	Spec ^R , Kan ^R
pBIO2120	SPO3722 internal fragment cloned into pBIO1879	This Work	Spec ^R , Kan ^R
pBIO2121	SPO1393 internal fragment cloned into pBIO1879	This Work	Spec ^R , Kan ^R
pBIO2122	SPO2025 internal fragment cloned into pBIO1879	This Work	Spec ^R , Kan ^R
pBIO2123	SPOA0186 internal fragment cloned into pBIO1879	This Work	Spec ^R , Kan ^R
pBIO2124	<i>sitA</i> internal fragment cloned into pBIO1879	This Work	Spec ^R , Kan ^R
pBIO2125	<i>irr</i> promoter fusion cloned into pBIO1878	This Work	Spec ^R , Tet ^R

Appendix

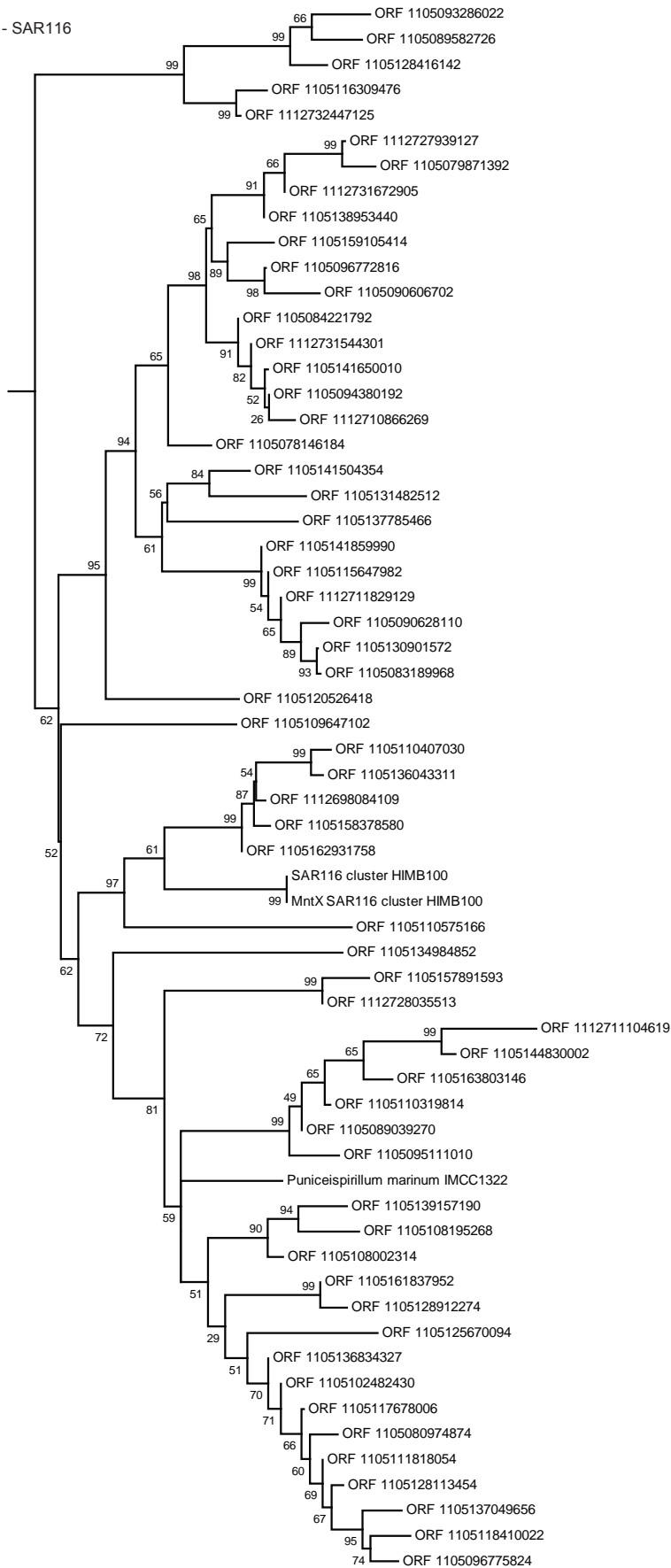
Appendix Figure 1. Blow-up of relatedness tree of MntX polypeptides

The individual sequences in each of the five sub-groups of MntX polypeptides in the relatedness tree in Figure 6.9 are shown in higher magnification. Those with the prefix “ORF” are from the GOS data base and are described further in Appendix Table 1. The MntX subtrees 1-5 contain the MntX sequences of the γ -proteobacterial, SAR116, Class X, Roseobacter and Pelagibacter types, respectively.

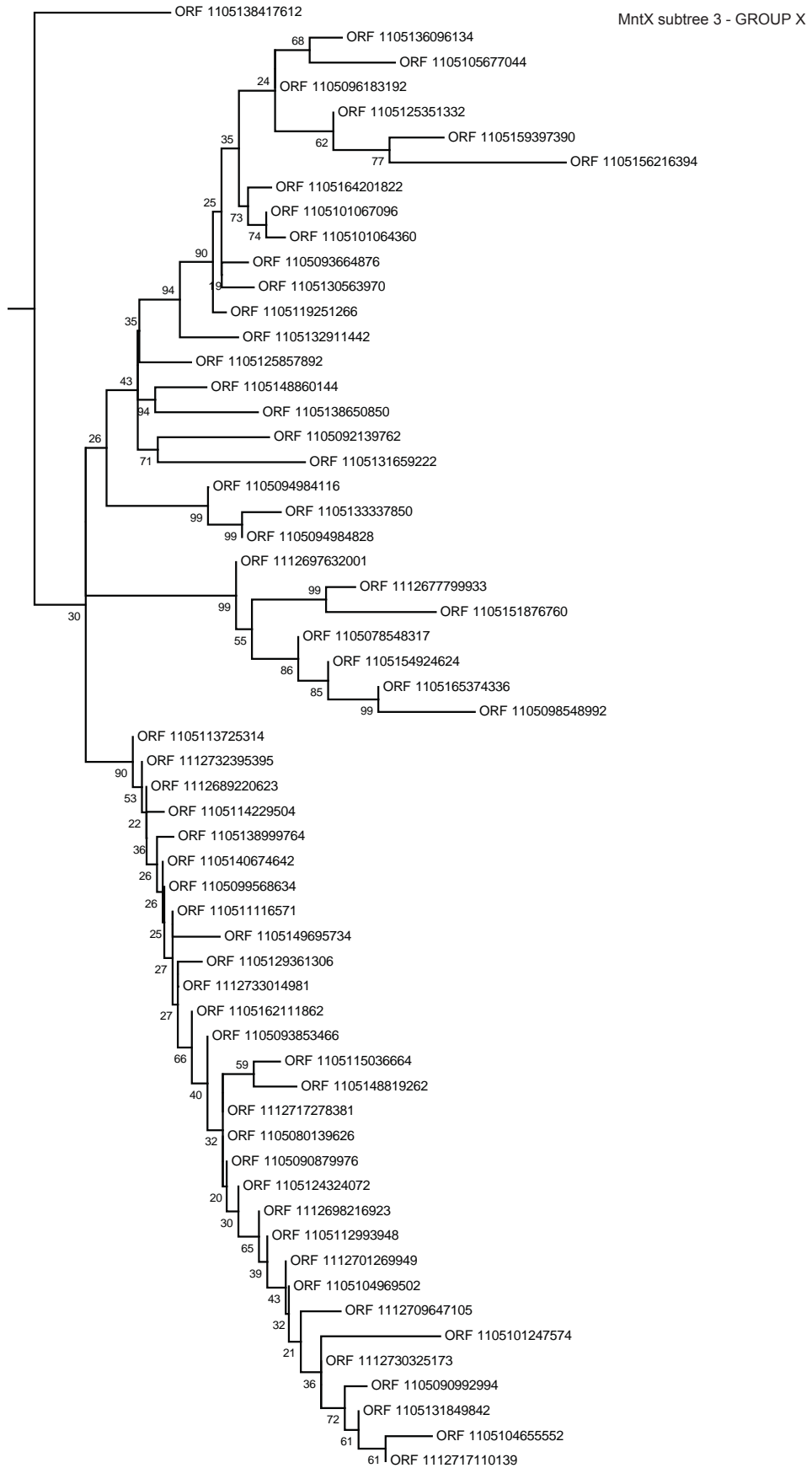
MntX subtree 1 - Gamma Proteobacteria



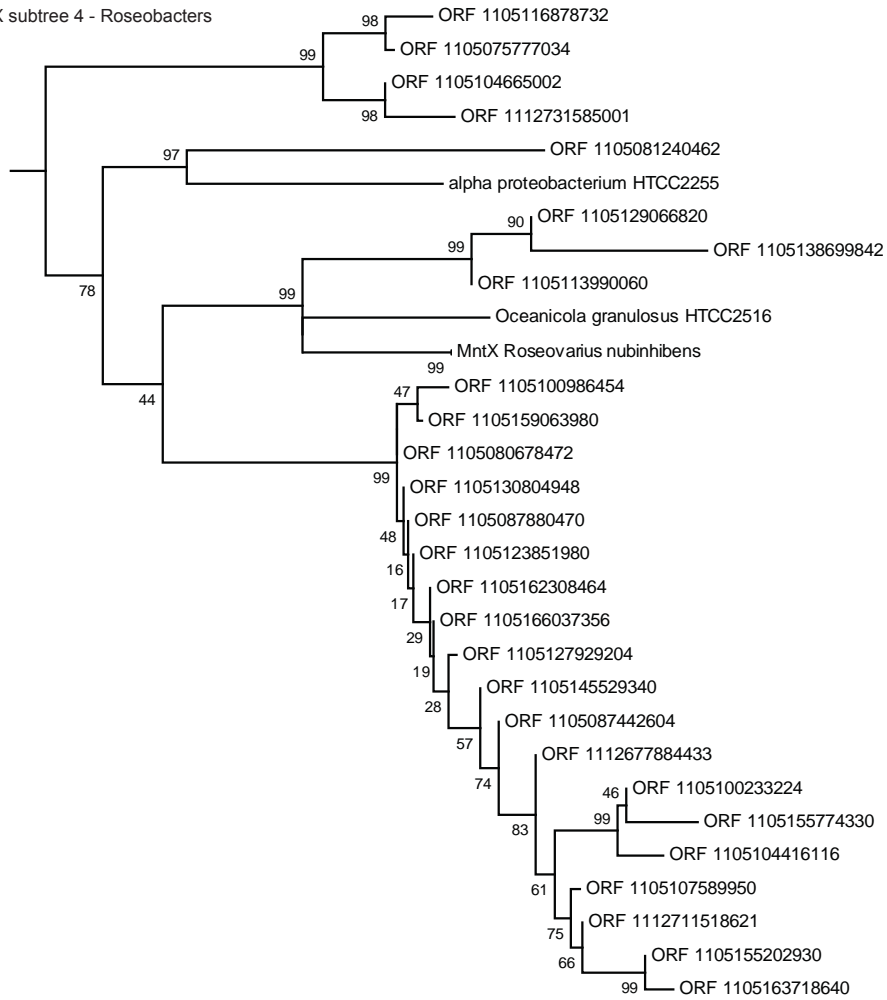
MntX subtree 2 - SAR116



0.1

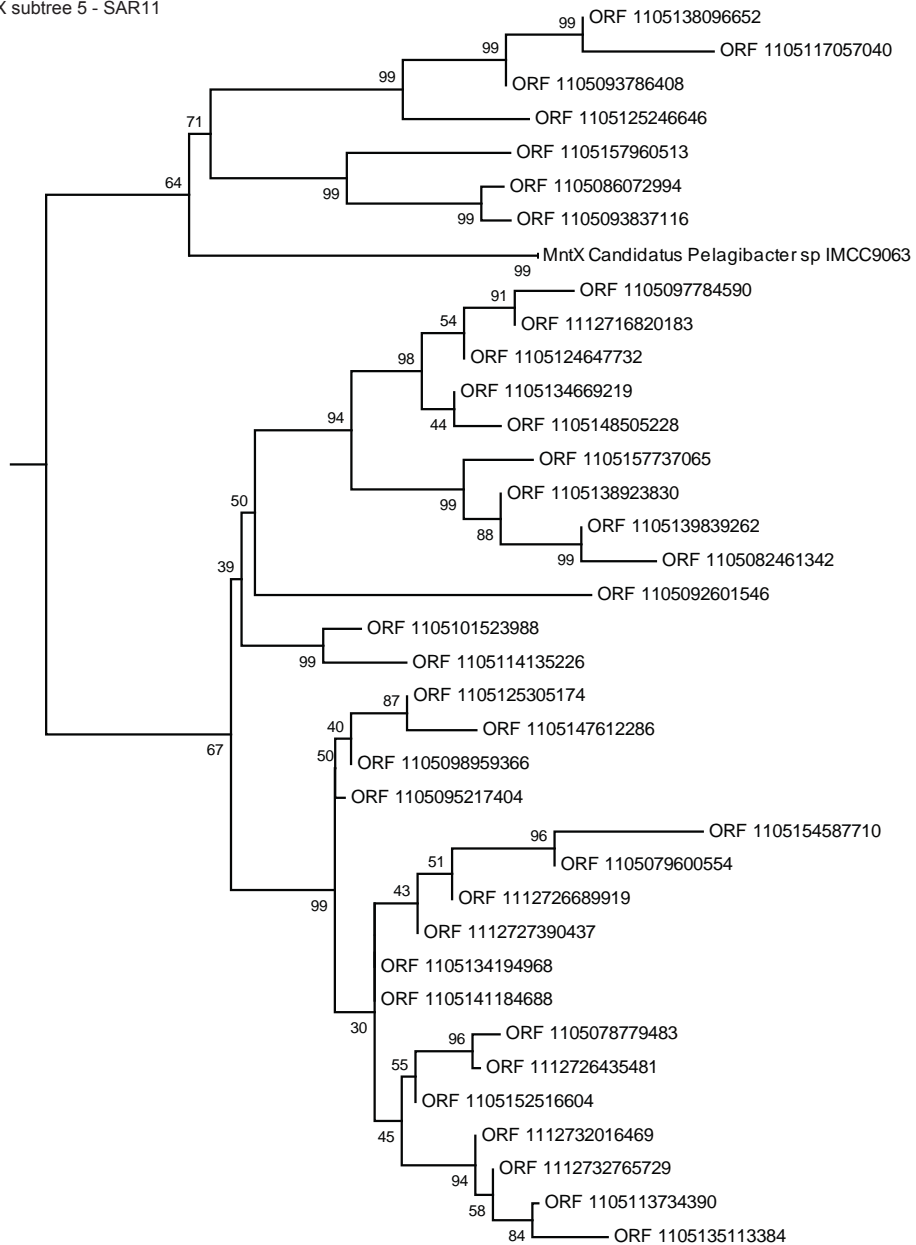


MntX subtree 4 - Roseobacters



0.1

MntX subtree 5 - SAR11



0.1

Appendix Table 1. Details of the MntX homologues in the GOS data base

The CAMERA data set “GOS: All ORF Peptides” was interrogated using MntX of *Roseovarius nubinhibens* (locus: *ISM_02005*). All GOS homologous sequences (in column ^a) with E-values $<1E^{-20}$, (values in column ^b) are shown, together with their geographic origin (column ^c) and habitat (column ^d). Column ^e lists the GOS homologues on the bases of the clusters shown in Figure 6.9 and Appendix Figure 1, using abbreviations: “116” = SAR116 group; “G” = gamma-proteobacteria; “P” = *Pelagibacter*; “R” = Roseobacters; “X” = the cluster that contains only GOS sequences. Those GOS homologues with insufficient coverage of the MntX polypeptide to be included in the neighbor-joining trees are shown as “not used” in column ^e.

Subject Name ^a	E-Value ^b	Sample Position ^c	Habitat ^d	Cluster ^e
JCVI_PEP_1105136834328	1.13E-52	Cape May, NJ	Coastal	116
JCVI_PEP_1105111818055	2.45E-50	Newport Harbor, RI	Coastal	116
JCVI_PEP_1105117678007	1.68E-49	Block Island, NY	Coastal	116
JCVI_PEP_1105102482431	1.03E-47	Block Island, NY	Coastal	116
JCVI_PEP_1105138953441	8.65E-47	250 miles from Panama City	Open Ocean	116
JCVI_PEP_1105078146185	2.08E-46	Upwelling, Fernandina Island	Coastal	116
JCVI_PEP_1105159105415	2.69E-46	Off Nags Head, NC	upwelling	116
JCVI_PEP_1105141859991	1.31E-45	Rangirora Atoll	Coastal	116
JCVI_PEP_1105162931759	7.76E-45	Wolf Island	Atoll	116
JCVI_PEP_1105115647983	6.74E-45	Hydrostation S	Coastal	116
JCVI_PEP_1105158378581	6.68E-44	Devil's Crown, Floreana Island	Open Ocean	116
JCVI_PEP_1105084221793	5.61E-44	Rangirora Atoll	Coastal	116
JCVI_PEP_1105128416143	2.10E-42	Upwelling, Fernandina Island	Atoll	116
JCVI_PEP_1105120526419	4.05E-42	Upwelling, Fernandina Island	upwelling	116
JCVI_PEP_1112711829130	1.85E-41	International water between Madagascar and South Africa	Coastal	116
JCVI_PEP_1105116309477	2.56E-41	Sargasso Station 13	Open Ocean	116
JCVI_PEP_1105095111011	1.16E-40	Cabo Marshall, Isabella Island	Open Ocean	116
JCVI_PEP_1105128113455	9.03E-40	Off Nags Head, NC	Coastal	116
JCVI_PEP_1105089039271	2.13E-39	Rangirora Atoll	Coastal	116
JCVI_PEP_1105109647103	2.79E-39	Hydrostation S	Atoll	116
JCVI_PEP_1105096772817	9.66E-39	Gulf of Maine	Open Ocean	116
JCVI_PEP_1112732447126	2.54E-38	Moorea, Outside Cooks Bay	Coastal	116
JCVI_PEP_1105094380193	2.50E-38	Devil's Crown, Floreana Island	Coastal	116
JCVI_PEP_1105141650011	4.27E-38	Coastal Floreana	Coastal	116
JCVI_PEP_1105093286023	6.98E-38	Coastal Floreana	Coastal	116
JCVI_PEP_1105161837953	1.98E-37	250 miles from Panama City	Coastal	116
JCVI_PEP_1105157891594	2.86E-37	Yucatan Channel	Open Ocean	116
JCVI_PEP_1112731544302	5.13E-37	St. Anne Island, Seychelles	Coastal	116
JCVI_PEP_1105110407031	8.46E-37	Wolf Island	sample	116
JCVI_PEP_1105080974875	7.40E-37	Off Nags Head, NC	Coastal	116
JCVI_PEP_1105128912275	1.13E-36	Northeast of Colon	Coastal	116
JCVI_PEP_1105130901573	2.19E-36	North James Bay, Santiago Island	Coastal	116
JCVI_PEP_1105083189969	3.67E-36	North James Bay, Santiago Island	Coastal	116
JCVI_PEP_1105136043312	2.38E-35	Wolf Island	Coastal	116
JCVI_PEP_1105139157191	2.93E-35	134 miles NE of Galapagos	Coastal	116
JCVI_PEP_1105110319815	2.28E-34	Upwelling, Fernandina Island	Open Ocean	116
JCVI_PEP_1112728035514	1.81E-33	Outside Seychelles, Indian Ocean	upwelling	116
JCVI_PEP_1105110575167	2.19E-33	Gulf of Panama	Open Ocean	116
			Coastal	116

JCVI_PEP_1105141504355	1.16E-32	Rosario Bank	Open Ocean	116
JCVI_PEP_1105108002315	1.16E-31	Devil's Crown, Floreana Island	Coastal	116
JCVI_PEP_1105131482513	1.93E-31	Sargasso Station 13	Open Ocean	116
JCVI_PEP_1112698084110	2.72E-31	Coccos Keeling, Inside Lagoon	Lagoon Reef	116
JCVI_PEP_1105090606703	4.61E-31	Devil's Crown, Floreana Island	Coastal	116
JCVI_PEP_1105137785467	1.77E-30	Sargasso Station 13	Open Ocean	116
JCVI_PEP_1105118410023	2.47E-30	Gulf of Maine	Coastal	116
JCVI_PEP_1105137049657	4.77E-30	Newport Harbor, RI	Coastal	116
JCVI_PEP_1105089582727	7.18E-29	Upwelling, Fernandina Island	Coastal	116
JCVI_PEP_1105125670095	4.21E-28	250 miles from Panama City	upwelling	116
JCVI_PEP_1105096775825	5.63E-28	Gulf of Maine	Open Ocean	116
JCVI_PEP_1105108195269	3.04E-27	Rangirora Atoll	Coastal	116
JCVI_PEP_1112731672906	2.68E-26	St. Anne Island, Seychelles	Coral Reef	116
JCVI_PEP_1105163803147	2.71E-26	Upwelling, Fernandina Island	Atoll	116
JCVI_PEP_1105134984853	5.41E-26	Hydrostation S	Coastal	116
JCVI_PEP_1112711104620	5.41E-26	Indian Ocean	sample	116
JCVI_PEP_1112727939128	2.89E-25	Outside Seychelles, Indian Ocean	Coastal	116
JCVI_PEP_1105079871393	1.42E-23	Northeast of Colon	upwelling	116
JCVI_PEP_1105144830003	4.54E-23	Sargasso Station 13	Open Ocean	116
JCVI_PEP_1105090628111	5.50E-22	Sargasso Station 13	Open Ocean	116
JCVI_PEP_1112710866270	1.17E-20	Indian Ocean	Open Ocean	116
JCVI_PEP_1105100710649	5.03E-42	Upwelling, Fernandina Island	Coastal	116
JCVI_PEP_1105144824561	3.79E-41	Sargasso Station 13	upwelling	G
JCVI_PEP_1105086072995	7.77E-44	Delaware Bay, NJ	Open Ocean	G
JCVI_PEP_1105093837117	1.40E-43	Delaware Bay, NJ	Estuary	P
JCVI_PEP_1105095217405	1.85E-42	Warm seep, Roca Redonda	Estuary	P
JCVI_PEP_1105101523989	2.69E-42	Newport Harbor, RI	Warm Seep	P
JCVI_PEP_1105152516605	3.67E-42	Warm seep, Roca Redonda	Coastal	P
JCVI_PEP_1105134669220	3.24E-41	Sargasso Station 13	Warm Seep	P
JCVI_PEP_1105124647733	1.66E-39	Devil's Crown, Floreana Island	Open Ocean	P
JCVI_PEP_1105114135227	2.03E-39	Off Nags Head, NC	Coastal	P
JCVI_PEP_1105078779484	4.26E-39	Warm seep, Roca Redonda	Coastal	P
JCVI_PEP_1105134194969	6.31E-39	North James Bay, Santiago Island	Warm Seep	P
JCVI_PEP_1105093786409	3.73E-38	Off Nags Head, NC	Coastal	P
JCVI_PEP_1105125305175	2.17E-37	Warm seep, Roca Redonda	Coastal	P
JCVI_PEP_1105125246647	2.26E-37	Gulf of Maine	Warm Seep	P
JCVI_PEP_1105157960514	3.35E-37	Chesapeake Bay, MD	Coastal	P
JCVI_PEP_1105154587711	4.34E-37	Warm seep, Roca Redonda	Estuary	P
JCVI_PEP_1105098959367	6.70E-37	Warm seep, Roca Redonda	Warm Seep	P
JCVI_PEP_1105079600555	6.64E-37	Warm seep, Roca Redonda	Warm Seep	P
JCVI_PEP_1112727390438	1.73E-36	East coast Zanzibar (Tanzania), offshore Paje lagoon	Warm Seep	P
JCVI_PEP_1105147612287	2.32E-36	Warm seep, Roca Redonda	Fringing Reef	P
			Warm Seep	P

JCVI_PEP_1105141184689	3.64E-35	North James Bay, Santiago Island West coast Zanzibar (Tanzania), harbour region	Coastal	P
JCVI_PEP_1112726689920	2.25E-34		Harbor	P
JCVI_PEP_1105113734391	4.34E-33	Warm seep, Roca Redonda	Warm Seep	P
JCVI_PEP_1105138923831	2.66E-32	Wolf Island	Coastal	P
JCVI_PEP_1112732765730	9.44E-32	St. Anne Island, Seychelles	Coastal sample	P
JCVI_PEP_1105138096653	5.68E-31	Chesapeake Bay, MD	Estuary	P
JCVI_PEP_1105157737066	3.44E-30	Warm seep, Roca Redonda	Warm Seep	P
JCVI_PEP_1105139839263	2.94E-28	Warm seep, Roca Redonda	Warm Seep	P
JCVI_PEP_1105117057041	3.45E-27	Chesapeake Bay, MD	Estuary	P
JCVI_PEP_1105092601547	9.86E-27	Coastal Floreana West coast Zanzibar (Tanzania), harbour region	Coastal	P
JCVI_PEP_1112726435482	6.13E-26		Harbor	P
JCVI_PEP_1105097784591	3.53E-25	201 miles from F. Polynesia	Open Ocean	P
JCVI_PEP_1105082461343	1.17E-23	Warm seep, Roca Redonda	Warm Seep Coastal	p
JCVI_PEP_1112732016470	1.64E-23	St. Anne Island, Seychelles	sample	P
JCVI_PEP_1105135113385	2.78E-23	North James Bay, Santiago Island	Coastal	P
JCVI_PEP_1105148505229	2.62E-23	Sargasso Station 13	Open Ocean	P
JCVI_PEP_1112716820184	6.14E-22	Indian Ocean	Open Ocean	P
JCVI_PEP_1105113990061	5.79E-105	Bedford Basin, Nova Scotia	Embayment	R
JCVI_PEP_1105129066821	2.56E-95	Cape May, NJ	Coastal	R
JCVI_PEP_1105100986455	5.74E-82	Yucatan Channel	Open Ocean	R
JCVI_PEP_1105162308465	5.28E-79	North James Bay, Santiago Island	Coastal	R
JCVI_PEP_1105116878733	1.58E-78	134 miles NE of Galapagos	Open Ocean	R
JCVI_PEP_1105123851981	8.58E-73	Warm seep, Roca Redonda	Warm Seep	R
JCVI_PEP_1105087880471	2.24E-72	Warm seep, Roca Redonda	Warm Seep	R
JCVI_PEP_1105087442605	1.09E-68	Northeast of Colon	Coastal	R
JCVI_PEP_1105159063981	2.34E-68	Northeast of Colon	Coastal	R
JCVI_PEP_1105104665003	3.06E-66	134 miles NE of Galapagos	Open Ocean	R
JCVI_PEP_1105080678473	4.38E-65	Rosario Bank	Open Ocean	R
JCVI_PEP_1105075777035	6.43E-64	Yucatan Channel	Open Ocean	R
JCVI_PEP_1105127929205	6.37E-64	Warm seep, Roca Redonda	Warm Seep	R
JCVI_PEP_1105130804949	2.63E-63	Hydrostation S	Open Ocean	R
JCVI_PEP_1105138699843	5.86E-63	Newport Harbor, RI	Coastal	R
JCVI_PEP_1105145529341	3.65E-59	Warm seep, Roca Redonda	Warm Seep Coastal	R
JCVI_PEP_1105081240463	2.49E-56	Upwelling, Fernandina Island	upwelling	R
JCVI_PEP_1105104416117	3.62E-56	Wolf Island	Coastal	R
JCVI_PEP_1105166037357	4.07E-56	201 miles from F. Polynesia	Open Ocean	R
JCVI_PEP_1105107589951	7.48E-56	Yucatan Channel	Open Ocean	R
JCVI_PEP_1105100233225	9.00E-55	Coastal Floreana	Coastal	R
JCVI_PEP_1112711518622	1.05E-51	International water between Madagascar and South Africa 500 Miles west of the Seychelles in the Indian Ocean	Open Ocean	R
JCVI_PEP_1112677884434	4.66E-48		Open Ocean	R
JCVI_PEP_1105155202931	8.65E-47	Off Key West, FL	Coastal	R

JCVI_PEP_1105163718641	1.19E-46	South of Charleston, SC	Coastal	R
JCVI_PEP_1105155774331	6.15E-43	North James Bay, Santiago Island	Coastal	R
JCVI_PEP_1112731585002	6.63E-43	St. Anne Island, Seychelles	Coastal sample	R
JCVI_PEP_1105119251267	1.41E-58	Sargasso Stations 3	Open Ocean	X
JCVI_PEP_1105090879977	2.23E-56	Warm seep, Roca Redonda	Warm Seep	X
JCVI_PEP_1105148860145	8.20E-56	Yucatan Channel	Open Ocean	X
JCVI_PEP_1105154924625	1.95E-54	Off Key West, FL	Coastal	X
JCVI_PEP_1105162111863	3.25E-54	Yucatan Channel	Open Ocean	X
JCVI_PEP_1105096183193	2.49E-53	Mangrove on Isabella Island	Mangrove Coastal	X
JCVI_PEP_1105132911443	1.02E-52	Upwelling, Fernandina Island	upwelling	X
JCVI_PEP_1105093664877	3.20E-52	Sargasso Stations 3	Open Ocean	X
JCVI_PEP_1105101067097	9.79E-50	Sargasso Station 13	Open Ocean	X
JCVI_PEP_1105129361307	1.09E-47	Warm seep, Roca Redonda	Warm Seep	X
JCVI_PEP_1105111165715	1.09E-47	Sargasso Station 13	Open Ocean	X
JCVI_PEP_1105099568635	1.63E-47	Sargasso Station 13	Open Ocean	X
JCVI_PEP_1105124324073	1.70E-47	Sargasso Stations 3	Open Ocean	X
JCVI_PEP_1105112993949	6.51E-47	Off Key West, FL	Coastal	X
JCVI_PEP_1105138999765	9.32E-47	Warm seep, Roca Redonda	Warm Seep	X
JCVI_PEP_1105092139763	5.33E-46	Sargasso Stations 3	Open Ocean	X
JCVI_PEP_1112732395396	9.89E-46	Moorea, Outside Cooks Bay	Coastal	X
JCVI_PEP_1105093853467	1.24E-45	Off Key West, FL	Coastal	X
JCVI_PEP_1105130563971	2.58E-45	Sargasso Stations 3	Open Ocean	X
JCVI_PEP_1105094984117	4.22E-45	Block Island, NY	Coastal	X
JCVI_PEP_1112689220624	4.40E-45	500 Miles west of the Seychelles in the Indian Ocean	Open Ocean	X
JCVI_PEP_1105140674643	6.91E-45	Warm seep, Roca Redonda	Warm Seep	X
JCVI_PEP_1105113725315	1.07E-44	30 miles from Cocos Island	Open Ocean	X
JCVI_PEP_1105114229505	9.33E-44	Sargasso Station 13	Open Ocean	X
JCVI_PEP_1105115036665	9.81E-44	Warm seep, Roca Redonda	Warm Seep Coastal	X
JCVI_PEP_1105138417613	1.36E-43	Upwelling, Fernandina Island	upwelling	X
JCVI_PEP_1105133337851	1.80E-43	Gulf of Maine	Coastal	X
JCVI_PEP_1105101064361	1.36E-41	Sargasso Station 13	Open Ocean	X
JCVI_PEP_1105149695735	1.61E-41	Sargasso Station 13	Open Ocean	X
JCVI_PEP_1105136096135	1.14E-40	Cabo Marshall, Isabella Island	Coastal	X
JCVI_PEP_1105148819263	1.48E-40	Warm seep, Roca Redonda	Warm Seep	X
JCVI_PEP_1112697632002	1.98E-40	Moorea, Cooks Bay	Coral Reef	X
JCVI_PEP_1105078548318	2.05E-39	Sargasso Station 13	Open Ocean	X
JCVI_PEP_1105165374337	1.93E-39	Rosario Bank	Open Ocean	X
JCVI_PEP_1105104969503	2.91E-39	Warm seep, Roca Redonda	Warm Seep	X
JCVI_PEP_1105138650851	8.31E-39	North Seamore Island	Coastal	X
JCVI_PEP_1105125351333	1.20E-37	Sargasso Station 13	Open Ocean	X
JCVI_PEP_1105094984829	3.52E-37	Block Island, NY	Coastal	X
JCVI_PEP_1112701269950	1.25E-36	Indian Ocean	Open Ocean	X
JCVI_PEP_1105131659223	1.14E-36	Sargasso Stations 3	Open Ocean	X
JCVI_PEP_1105125857893	1.24E-36	Upwelling, Fernandina Island	Coastal	X

JCVI_PEP_1105159397391	2.15E-36	Sargasso Stations 3	upwelling Open Ocean	X
JCVI_PEP_1112698216924	2.54E-36	Coccos Keeling, Inside Lagoon	Lagoon Reef	X
JCVI_PEP_1105164201823	3.01E-36	Sargasso Station 13	Open Ocean	X
JCVI_PEP_1112733014982	2.70E-35	Moorea, Outside Cooks Bay	Coastal	X
JCVI_PEP_1112717278382	2.44E-34	Indian Ocean	Open Ocean	X
JCVI_PEP_1105080139627	1.51E-32	Devil's Crown, Floreana Island	Coastal	X
JCVI_PEP_1105156216395	2.82E-32	Mangrove on Isabella Island	Mangrove	X
JCVI_PEP_1105104655553	3.68E-32	Northeast of Colon	Coastal	X
JCVI_PEP_1105131849843	1.08E-30	Warm seep, Roca Redonda	Warm Seep	X
JCVI_PEP_1112717110140	1.71E-30	Indian Ocean	Open Ocean	X
JCVI_PEP_1105098548993	9.29E-30	250 miles from Panama City 500 Miles west of the Seychelles in the Indian Ocean	Open Ocean	X
JCVI_PEP_1112677799934	1.16E-29	Sargasso Station 13	Open Ocean	X
JCVI_PEP_1105101247575	1.65E-29	North Seamore Island	Coastal	X
JCVI_PEP_1105090992995	4.07E-28	International Water Outside of Reunion Island	Open Ocean	X
JCVI_PEP_1112709647106	3.56E-28	St. Anne Island, Seychelles	Coastal sample	X
JCVI_PEP_1112730325174	2.00E-27	30 miles from Cocos Island	Open Ocean	X
JCVI_PEP_1105151876761	3.72E-22	Sargasso Stations 3	Open Ocean	X
JCVI_PEP_1105105677045	2.39E-21	Off Nags Head, NC	Coastal	Not used
JCVI_PEP_1105107514191	1.28E-15	Off Key West, FL	Coastal	Not used
JCVI_PEP_1105099089301	7.07E-52	134 miles NE of Galapagos	Open Ocean	Not used
JCVI_PEP_1105136338456	3.10E-50	500 Miles west of the Seychelles in the Indian Ocean	Open Ocean	Not used
JCVI_PEP_1112690003418	8.93E-50	134 miles NE of Galapagos	Open Ocean	Not used
JCVI_PEP_1105116878665	6.45E-49	Newport Harbor, RI	Coastal	Not used
JCVI_PEP_1105143559379	2.97E-47	Indian Ocean	Open Ocean	Not used
JCVI_PEP_1112700253728	2.76E-44	Outside Seychelles, Indian Ocean	Open Ocean	Not used
JCVI_PEP_1112727904146	3.73E-44	Browns Bank, Gulf of Maine	Coastal	Not used
JCVI_PEP_1105114026345	2.98E-42	St. Anne Island, Seychelles	Coastal sample	Not used
JCVI_PEP_1112731465778	5.21E-42	Upwelling, Fernandina Island	upwelling	Not used
JCVI_PEP_1105113025343	1.04E-39	Hydrostation S	Open Ocean	Not used
JCVI_PEP_1105159847901	1.32E-39	South of Charleston, SC	Coastal	Not used
JCVI_PEP_1105110435823	7.84E-39	Outside Seychelles, Indian Ocean	Open Ocean	Not used
JCVI_PEP_1112727988980	8.67E-39	South of Charleston, SC	Coastal	Not used
JCVI_PEP_1105135357286	1.12E-38	500 Miles west of the Seychelles in the Indian Ocean	Open Ocean	Not used
JCVI_PEP_1112689810654	1.28E-38	Sargasso Stations 3	Open Ocean	Not used
JCVI_PEP_1105083323561	3.58E-38	Moorea, Outside Cooks Bay	Coastal	Not used
JCVI_PEP_1112732711068	3.61E-38	Indian Ocean	Open Ocean	Not used
JCVI_PEP_1112700904284	6.81E-38	North Seamore Island	Coastal	Not used
JCVI_PEP_1105089169351	6.58E-38	Hydrostation S	Open Ocean	Not used
JCVI_PEP_1105147669289	1.30E-37	Sargasso Station 13	Open Ocean	Not used
JCVI_PEP_1105096718169	5.08E-37	Sargasso Station 13	Open Ocean	Not used
JCVI_PEP_1105106372949	7.04E-37	Sargasso Station 13	Open Ocean	Not used

JCVI_PEP_1112715377066	1.07E-36	International waters between Madagascar and South Africa	Open Ocean Coastal sample	Not used
JCVI_PEP_1112732036080	1.15E-36	St. Anne Island, Seychelles	Open Ocean	Not used
JCVI_PEP_1105113364519	1.01E-35	Warm seep, Roca Redonda	Warm Seep	Not used
JCVI_PEP_1112736930156	1.53E-35	International water between Madagascar and South Africa	Open Ocean	Not used
JCVI_PEP_1105114415063	8.61E-35	134 miles NE of Galapagos	Open Ocean	Not used
JCVI_PEP_1105111010569	1.69E-33	Sargasso Station 13	Open Ocean	Not used
JCVI_PEP_1105113630737	2.48E-33	Hydrostation S	Open Ocean	Not used
JCVI_PEP_1105104989057	3.01E-33	Hydrostation S	Open Ocean	Not used
JCVI_PEP_1105141522597	5.44E-33	Off Key West, FL	Coastal	Not used
JCVI_PEP_1105154687927	8.12E-33	Wolf Island	Coastal	Not used
JCVI_PEP_1112716329812	1.61E-32	Indian Ocean	Open Ocean	Not used
JCVI_PEP_1105106556727	1.43E-32	Northeast of Colon	Coastal	Not used
JCVI_PEP_1105113595619	1.39E-32	Sargasso Station 13	Open Ocean	Not used
JCVI_PEP_1105164191053	1.93E-32	Sargasso Stations 3	Open Ocean	Not used
JCVI_PEP_1105105072647	1.78E-32	Sargasso Stations 3	Open Ocean	Not used
JCVI_PEP_1105109654545	2.00E-32	Sargasso Station 13	Open Ocean	Not used
JCVI_PEP_1105086669349	1.97E-32	Cabo Marshall, Isabella Island	Coastal	Not used
JCVI_PEP_1112740668362	1.95E-32	Indian Ocean	Open Ocean	Not used
JCVI_PEP_1105154381661	2.40E-32	30 miles from Cocos Island	Open Ocean	Not used
JCVI_PEP_1105116215075	2.84E-32	Sargasso Station 13	Open Ocean	Not used
JCVI_PEP_1112717206458	3.68E-32	Indian Ocean	Open Ocean	Not used
JCVI_PEP_1105095036641	3.24E-32	Off Key West, FL	Coastal	Not used
JCVI_PEP_1105119379713	2.96E-32	North Seamore Island	Coastal	Not used
JCVI_PEP_1105097618317	4.35E-32	Tropical South Pacific	Open Ocean	Not used
JCVI_PEP_1105145646771	4.13E-32	Rosario Bank	Open Ocean	Not used
JCVI_PEP_1105120406825	6.22E-32	Rosario Bank	Open Ocean Coastal	Not used
JCVI_PEP_1112732355738	5.87E-32	St. Anne Island, Seychelles	sample	Not used
JCVI_PEP_1105166013885	5.97E-32	250 miles from Panama City	Open Ocean	Not used
JCVI_PEP_1112677954140	5.97E-32	500 Miles west of the Seychelles in the Indian Ocean	Open Ocean	Not used
JCVI_PEP_1112736829988	5.92E-32	International water between Madagascar and South Africa	Open Ocean	Not used
JCVI_PEP_1105155324503	1.12E-31	Sargasso Station 13	Open Ocean	Not used
JCVI_PEP_1105091666459	1.24E-31	Sargasso Station 13	Open Ocean	Not used
JCVI_PEP_1112701697274	1.32E-31	500 Miles west of the Seychelles in the Indian Ocean	Open Ocean	Not used
JCVI_PEP_1112678137292	1.67E-31	500 Miles west of the Seychelles in the Indian Ocean	Open Ocean	Not used
JCVI_PEP_1105096964981	1.61E-31	Coastal Floreana	Coastal	Not used
JCVI_PEP_1105165869551	2.27E-31	North James Bay, Santigo Island	Coastal	Not used
JCVI_PEP_1105082141787	1.87E-31	Hydrostation S	Open Ocean Coastal	Not used
JCVI_PEP_1105091831231	2.10E-31	Upwelling, Fernandina Island	upwelling	Not used
JCVI_PEP_1105110024891	1.92E-31	Sargasso Stations 3	Open Ocean	Not used
JCVI_PEP_1112697730458	2.68E-31	Moorea, Cooks Bay	Coral Reef	Not used

JCVI_PEP_1105117775409	2.79E-31	North James Bay, Santigo Island 500 Miles west of the Seychelles in	Coastal	Not used
JCVI_PEP_1112700762872	4.13E-31	the Indian Ocean	Open Ocean	Not used
JCVI_PEP_1112711565750	5.40E-31	International water between Madagascar and South Africa	Open Ocean	Not used
JCVI_PEP_1112730419344	5.58E-31	St. Anne Island, Seychelles	Coastal sample	Not used
JCVI_PEP_1105085284613	5.49E-31	Upwelling, Fernandina Island	upwelling	Not used
JCVI_PEP_1105103638901	1.10E-30	Sargasso Station 13	Open Ocean	Not used
JCVI_PEP_1105158948811	1.43E-30	Newport Harbor, RI	Coastal	Not used
JCVI_PEP_1105118294623	1.89E-30	Sargasso Station 13	Open Ocean	Not used
JCVI_PEP_1112732506124	2.64E-30	St. Anne Island, Seychelles	Coastal sample	Not used
JCVI_PEP_1105132253699	2.53E-30	Upwelling, Fernandina Island	upwelling	Not used
JCVI_PEP_1105145195751	3.30E-30	Northern Gulf of Maine	Coastal	Not used
JCVI_PEP_1112710545372	2.96E-30	Indian Ocean	Open Ocean	Not used
JCVI_PEP_1112736597466	3.04E-30	International water between Madagascar and South Africa	Open Ocean	Not used
JCVI_PEP_1105115884603	4.21E-30	Coastal Floreana	Coastal	Not used
JCVI_PEP_1105104491509	5.49E-30	Coastal Floreana	Coastal	Not used
JCVI_PEP_1105144133381	4.69E-30	Wolf Island	Coastal	Not used
JCVI_PEP_1112689265682	6.94E-30	500 Miles west of the Seychelles in the Indian Ocean	Open Ocean	Not used
JCVI_PEP_1105150593617	7.17E-30	North James Bay, Santigo Island	Coastal	Not used
JCVI_PEP_1105084814695	8.99E-30	Devil's Crown, Floreana Island	Coastal	Not used
JCVI_PEP_1105118423279	1.08E-29	Gulf of Maine	Coastal	Not used
JCVI_PEP_1105085958526	1.47E-29	Sargasso Station 13	Open Ocean	Not used
JCVI_PEP_1105102055405	1.72E-29	Block Island, NY	Coastal	Not used
JCVI_PEP_1105143160005	1.40E-29	Browns Bank, Gulf of Maine	Coastal Coastal	Not used
JCVI_PEP_1112731010420	1.86E-29	St. Anne Island, Seychelles	sample	Not used
JCVI_PEP_1105117204245	2.23E-29	North James Bay, Santigo Island 500 Miles west of the Seychelles in	Coastal	Not used
JCVI_PEP_1112677871538	2.73E-29	the Indian Ocean	Open Ocean	Not used
JCVI_PEP_1105163551669	2.75E-29	Yucatan Channel	Open Ocean	Not used
JCVI_PEP_1105105202075	2.82E-29	Sargasso Stations 3	Open Ocean	Not used
JCVI_PEP_1105098197629	2.39E-29	North James Bay, Santigo Island	Coastal	Not used
JCVI_PEP_1105135289252	3.39E-29	Yucatan Channel	Open Ocean	Not used
JCVI_PEP_1105146897813	3.06E-29	Yucatan Channel	Open Ocean	Not used
JCVI_PEP_1105127980721	3.09E-29	201 miles from F. Polynesia	Open Ocean	Not used
JCVI_PEP_1105103115679	3.36E-29	Bay of Fundy, Nova Scotia	Estuary	Not used
JCVI_PEP_1105138603371	4.24E-29	Block Island, NY	Coastal	Not used
JCVI_PEP_1112701310826	4.24E-29	Indian Ocean	Open Ocean	Not used
JCVI_PEP_1105091541629	4.73E-29	Sargasso Station 13	Open Ocean	Not used
JCVI_PEP_1105124799295	5.97E-29	Bay of Fundy, Nova Scotia	Estuary	Not used
JCVI_PEP_1105126693923	8.00E-29	134 miles NE of Galapagos	Open Ocean	Not used
JCVI_PEP_1105129750425	6.88E-29	North Seamore Island	Coastal	Not used
JCVI_PEP_1105108274835	1.36E-28	Warm seep, Roca Redonda	Warm Seep	Not used

JCVI_PEP_1105158222097	1.77E-28	Northeast of Colon	Coastal	Not used
JCVI_PEP_1105147549529	1.55E-28	Sargasso Station 13	Open Ocean Coral Reef	Not used
JCVI_PEP_1105136237363	1.65E-28	Rangirora Atoll	Atoll	Not used
JCVI_PEP_1105140117765	1.48E-28	Sargasso Station 13	Open Ocean	Not used
JCVI_PEP_1105122641279	1.68E-28	Sargasso Station 13	Open Ocean	Not used
JCVI_PEP_1105125171135	1.59E-28	134 miles NE of Galapagos	Open Ocean	Not used
JCVI_PEP_1105143074023	2.12E-28	Upwelling, Fernandina Island	Coastal upwelling	Not used
JCVI_PEP_1105119959175	2.47E-28	Sargasso Station 13	Open Ocean	Not used
JCVI_PEP_1105146457801	2.41E-28	30 miles from Cocos Island	Open Ocean	Not used
JCVI_PEP_1105087623455	2.31E-28	Off Key West, FL	Coastal	Not used
JCVI_PEP_1105116097393	2.91E-28	Devil's Crown, Floreana Island	Coastal	Not used
JCVI_PEP_1105119057297	3.25E-28	Sargasso Station 13	Open Ocean	Not used
JCVI_PEP_1105126224171	2.51E-28	Wolf Island	Coastal	Not used
JCVI_PEP_1105158569931	2.53E-28	Warm seep, Roca Redonda	Warm Seep	Not used
JCVI_PEP_1105105227201	3.90E-28	Warm seep, Roca Redonda	Warm Seep	Not used
JCVI_PEP_1105113173947	3.30E-28	Warm seep, Roca Redonda	Warm Seep	Not used
JCVI_PEP_1112700650814	3.68E-28	Indian Ocean	Open Ocean	Not used
JCVI_PEP_1105098554789	3.65E-28	250 miles from Panama City	Open Ocean	Not used
JCVI_PEP_1105092898513	3.59E-28	Cabo Marshall, Isabella Island	Coastal Coral Reef	Not used
JCVI_PEP_1105118401697	5.14E-28	Rangirora Atoll	Atoll	Not used
JCVI_PEP_1105092561319	6.55E-28	Mangrove on Isabella Island	Mangrove	Not used
JCVI_PEP_1105125434021	9.14E-28	Off Nags Head, NC	Coastal Coral Reef	Not used
JCVI_PEP_1105156491461	9.53E-28	Rangirora Atoll	Atoll	Not used
JCVI_PEP_1105092387615	1.18E-27	Sargasso Stations 3	Open Ocean	Not used
JCVI_PEP_1105162749005	1.59E-27	30 miles from Cocos Island	Open Ocean	Not used
JCVI_PEP_1112715898796	1.47E-27	International waters between Madagascar and South Africa	Open Ocean	Not used
JCVI_PEP_1112736927170	1.64E-27	International water between Madagascar and South Africa	Open Ocean	Not used
JCVI_PEP_1105105125543	1.77E-27	Upwelling, Fernandina Island	Coastal upwelling	Not used
JCVI_PEP_1105165471345	3.39E-27	North Seamore Island	Coastal	Not used
JCVI_PEP_1112710779374	3.28E-27	Indian Ocean	Open Ocean	Not used
JCVI_PEP_1105114874431	3.14E-27	Hydrostation S	Open Ocean	Not used
JCVI_PEP_1112731646012	3.84E-27	St. Anne Island, Seychelles	Coastal sample	Not used
JCVI_PEP_1105080855761	6.08E-27	30 miles from Cocos Island	Open Ocean	Not used
JCVI_PEP_1105106333735	5.68E-27	Sargasso Station 13	Open Ocean	Not used
JCVI_PEP_1105141696121	5.59E-27	Devil's Crown, Floreana Island	Coastal	Not used
JCVI_PEP_1105120443141	7.74E-27	Delaware Bay, NJ	Estuary	Not used
JCVI_PEP_1105097461657	8.92E-27	Sargasso Station 13	Open Ocean	Not used
JCVI_PEP_1105081307505	8.70E-27	Yucatan Channel	Open Ocean	Not used
JCVI_PEP_1112736226318	8.92E-27	International water between Madagascar and South Africa	Open Ocean	Not used
JCVI_PEP_1105088248059	8.48E-27	Sargasso Station 13	Open Ocean	Not used

JCVI_PEP_1105165585411	9.38E-27	Delaware Bay, NJ	Estuary	Not used
JCVI_PEP_1105106739435	1.03E-26	Delaware Bay, NJ	Estuary Coastal	Not used
JCVI_PEP_1105152531997	1.25E-26	Upwelling, Fernandina Island	upwelling	Not used
JCVI_PEP_1105102340705	1.30E-26	Sargasso Station 13	Open Ocean	Not used
JCVI_PEP_1112736547410	1.46E-26	International water between Madagascar and South Africa	Open Ocean	Not used
JCVI_PEP_1112715632406	2.16E-26	International waters between Madagascar and South Africa	Open Ocean	Not used
JCVI_PEP_1105108895531	2.33E-26	Sargasso Station 13	Open Ocean	Not used
JCVI_PEP_1105110703857	1.89E-26	Sargasso Station 13	Open Ocean	Not used
JCVI_PEP_1105100445535	3.09E-26	Sargasso Stations 3	Open Ocean	Not used
JCVI_PEP_1112697484856	4.58E-26	Moorea, Cooks Bay	Coral Reef	Not used
JCVI_PEP_1105139830403	5.64E-26	Off Key West, FL	Coastal	Not used
JCVI_PEP_1105162291717	8.41E-26	Newport Harbor, RI	Coastal	Not used
JCVI_PEP_1105095790659	1.16E-25	Bay of Fundy, Nova Scotia	Estuary	Not used
JCVI_PEP_1105161697585	1.18E-25	Chesapeake Bay, MD	Estuary	Not used
JCVI_PEP_1105133358451	1.86E-25	Yucatan Channel	Open Ocean	Not used
JCVI_PEP_1105157143905	2.00E-25	Chesapeake Bay, MD	Estuary Coral Reef	Not used
JCVI_PEP_1105135428984	2.55E-25	Rangirora Atoll	Atoll	Not used
JCVI_PEP_1105107383401	2.62E-25	Sargasso Stations 3	Open Ocean	Not used
JCVI_PEP_1105151220301	2.68E-25	Chesapeake Bay, MD	Estuary	Not used
JCVI_PEP_1105093949197	3.81E-25	Gulf of Panama	Coastal	Not used
JCVI_PEP_1105139459569	4.98E-25	Newport Harbor, RI	Coastal	Not used
JCVI_PEP_1112689421410	7.43E-25	500 Miles west of the Seychelles in the Indian Ocean	Open Ocean	Not used
JCVI_PEP_1112726506970	7.68E-25	West coast Zanzibar (Tanzania), harbour region	Harbor	Not used
JCVI_PEP_1105145927877	9.54E-25	Sargasso Station 13	Open Ocean	Not used
JCVI_PEP_1105141881745	7.62E-25	Coastal Floreana	Coastal	Not used
JCVI_PEP_1105118643945	1.59E-24	Sargasso Station 13	Open Ocean	Not used
JCVI_PEP_1112736431814	1.45E-24	International water between Madagascar and South Africa	Open Ocean	Not used
JCVI_PEP_1105139672153	1.53E-24	Warm seep, Roca Redonda	Warm Seep	Not used
JCVI_PEP_1105143724721	2.18E-24	Warm seep, Roca Redonda	Warm Seep Coastal	Not used
JCVI_PEP_1112730289950	2.13E-24	St. Anne Island, Seychelles	sample	Not used
JCVI_PEP_1112732611676	2.53E-24	Moorea, Outside Cooks Bay	Coastal	Not used
JCVI_PEP_1105095212519	3.25E-24	Warm seep, Roca Redonda	Warm Seep	Not used
JCVI_PEP_1105142526283	4.50E-24	Sargasso Station 13	Open Ocean	Not used
JCVI_PEP_1112711765764	4.32E-24	International water between Madagascar and South Africa	Open Ocean Coastal	Not used
JCVI_PEP_1112730564854	4.81E-24	St. Anne Island, Seychelles	sample	Not used
JCVI_PEP_1105159007305	4.28E-24	134 miles NE of Galapagos	Open Ocean	Not used
JCVI_PEP_1112701681448	4.01E-24	500 Miles west of the Seychelles in the Indian Ocean	Open Ocean	Not used
JCVI_PEP_1105091810867	6.08E-24	Warm seep, Roca Redonda	Warm Seep	Not used
JCVI_PEP_1105124126853	5.46E-24	Newport Harbor, RI	Coastal	Not used

JCVI_PEP_1105141429891	8.08E-24	Off Key West, FL	Coastal	Not used
JCVI_PEP_1105125820711	7.94E-24	Northeast of Colon	Coastal	Not used
JCVI_PEP_1105125216765	8.71E-24	134 miles NE of Galapagos	Open Ocean	Not used
JCVI_PEP_1105119376039	1.18E-23	North Seamore Island	Coastal	Not used
JCVI_PEP_1105099708065	1.68E-23	Coastal Floreana	Coastal	Not used
JCVI_PEP_1105113485987	2.92E-23	Yucatan Channel	Open Ocean	Not used
JCVI_PEP_1105124122977	2.60E-23	Newport Harbor, RI	Coastal	Not used
JCVI_PEP_1105128061417	3.15E-23	250 miles from Panama City	Open Ocean	Not used
JCVI_PEP_1105127055507	2.69E-23	Sargasso Station 13	Open Ocean	Not used
JCVI_PEP_1105093675327	2.75E-23	Warm seep, Roca Redonda	Warm Seep	Not used
JCVI_PEP_1105165959985	3.88E-23	Sargasso Station 13	Open Ocean	Not used
JCVI_PEP_1105126736045	6.89E-23	Gulf of Panama	Coastal	Not used
JCVI_PEP_1105122405441	5.41E-23	134 miles NE of Galapagos	Open Ocean	Not used
JCVI_PEP_1112716859452	8.35E-23	Indian Ocean	Open Ocean	Not used
JCVI_PEP_1112700318142	9.31E-23	Indian Ocean	Open Ocean	Not used
JCVI_PEP_1105106811677	1.39E-22	Cape May, NJ	Coastal	Not used
JCVI_PEP_1105147329807	1.83E-22	Sargasso Stations 3	Open Ocean	Not used
JCVI_PEP_1105127299435	1.74E-22	Yucatan Channel	Open Ocean	Not used
JCVI_PEP_1112730859118	1.86E-22	St. Anne Island, Seychelles	Coastal sample	Not used
JCVI_PEP_1105098531181	2.14E-22	Gulf of Panama	Coastal	Not used
JCVI_PEP_1105142526493	2.09E-22	Sargasso Station 13	Open Ocean	Not used
JCVI_PEP_1105100740193	2.51E-22	Hydrostation S	Open Ocean	Not used
JCVI_PEP_1105140347375	3.12E-22	Coastal Floreana	Coastal	Not used
JCVI_PEP_1105155289873	2.85E-22	North Seamore Island	Coastal	Not used
JCVI_PEP_1112716468310	3.17E-22	Indian Ocean	Open Ocean	Not used
JCVI_PEP_1105135987488	2.99E-22	Sargasso Station 13	Open Ocean	Not used
JCVI_PEP_1105149886963	3.12E-22	134 miles NE of Galapagos	Open Ocean	Not used
JCVI_PEP_1105080298835	3.54E-22	Upwelling, Fernandina Island	Coastal upwelling	Not used
JCVI_PEP_1105091051111	5.41E-22	Warm seep, Roca Redonda	Warm Seep	Not used
JCVI_PEP_1105146303567	5.50E-22	Cabo Marshall, Isabella Island	Coastal	Not used
JCVI_PEP_1105086989417	4.86E-22	Gulf of Maine	Coastal	Not used
JCVI_PEP_1105131426975	6.90E-22	Sargasso Station 13	Open Ocean	Not used
JCVI_PEP_1105100950699	8.42E-22	Off Nags Head, NC	Coastal	Not used
JCVI_PEP_1105151211469	8.50E-22	Chesapeake Bay, MD	Estuary	Not used
JCVI_PEP_1105160660249	1.21E-21	Upwelling, Fernandina Island	Coastal upwelling	Not used
JCVI_PEP_1105129908865	1.28E-21	250 miles from Panama City	Open Ocean	Not used
JCVI_PEP_1105091806945	1.14E-21	Sargasso Station 13	Open Ocean	Not used
JCVI_PEP_1112707080748	1.31E-21	West coast Zanzibar (Tanzania), harbour region	Harbor	Not used
JCVI_PEP_1105083202315	1.66E-21	Devil's Crown, Floreana Island	Coastal	Not used
JCVI_PEP_1105093948591	1.60E-21	Gulf of Panama	Coastal	Not used
JCVI_PEP_1105149813711	1.54E-21	Chesapeake Bay, MD	Estuary	Not used
JCVI_PEP_1105112940361	1.71E-21	Sargasso Station 13	Open Ocean	Not used
JCVI_PEP_1112736667600	1.64E-21	International water between Madagascar and South Africa	Open Ocean	Not used

JCVI_PEP_1112701128738	1.96E-21	Indian Ocean	Open Ocean	Not used
JCVI_PEP_1105100457189	2.16E-21	Bay of Fundy, Nova Scotia	Estuary	Not used
JCVI_PEP_1112726649886	1.74E-21	West coast Zanzibar (Tanzania), harbour region	Harbor	Not used
JCVI_PEP_1105134931704	1.83E-21	Sargasso Station 13	Open Ocean	Not used
JCVI_PEP_1112728035934	2.53E-21	Outside Seychelles, Indian Ocean	Open Ocean	Not used
JCVI_PEP_1105117730315	2.92E-21	North James Bay, Santigo Island	Coastal	Not used
JCVI_PEP_1105150508493	2.69E-21	Chesapeake Bay, MD	Estuary	Not used
JCVI_PEP_1112689973594	3.81E-21	500 Miles west of the Seychelles in the Indian Ocean	Open Ocean	Not used
JCVI_PEP_1105130457819	3.75E-21	Sargasso Station 13	Open Ocean	Not used
JCVI_PEP_1112701696480	3.75E-21	500 Miles west of the Seychelles in the Indian Ocean	Open Ocean	Not used
JCVI_PEP_1105092807081	3.60E-21	Sargasso Station 13	Open Ocean	Not used
JCVI_PEP_1105139938083	3.78E-21	Sargasso Station 13	Open Ocean	Not used
JCVI_PEP_1105156577609	3.81E-21	Chesapeake Bay, MD	Estuary	Not used
JCVI_PEP_1105081942563	3.15E-21	Sargasso Stations 3	Open Ocean	Not used
JCVI_PEP_1112708273324	4.47E-21	West coast Zanzibar (Tanzania), harbour region	Harbor	Not used
JCVI_PEP_1105127048611	4.58E-21	Chesapeake Bay, MD	Estuary	Not used
JCVI_PEP_1112731372198	4.62E-21	St. Anne Island, Seychelles	Coastal sample	Not used
JCVI_PEP_1112697229568	4.94E-21	Madagascar Waters	Open Ocean	Not used
JCVI_PEP_1112710167110	4.43E-21	Indian Ocean	Open Ocean Coastal	Not used
JCVI_PEP_1112731662020	4.01E-21	St. Anne Island, Seychelles	sample	Not used
JCVI_PEP_1105096213641	6.45E-21	Sargasso Station 13	Open Ocean	Not used
JCVI_PEP_1105146521897	5.84E-21	Warm seep, Roca Redonda	Warm Seep Coral Reef	Not used
JCVI_PEP_1105104110707	5.15E-21	Rangirora Atoll	Atoll	Not used
JCVI_PEP_1105100076867	5.42E-21	Warm seep, Roca Redonda	Warm Seep	Not used
JCVI_PEP_1105158351529	5.65E-21	Sargasso Station 13	Open Ocean	Not used
JCVI_PEP_1105104652049	5.84E-21	Northeast of Colon	Coastal	Not used
JCVI_PEP_1105111584485	7.44E-21	Bay of Fundy, Nova Scotia	Estuary	Not used
JCVI_PEP_1105097457325	7.88E-21	Sargasso Station 13	Open Ocean	Not used
JCVI_PEP_1112700722492	1.11E-20	Indian Ocean	Open Ocean	Not used
JCVI_PEP_1105154510997	9.63E-21	Warm seep, Roca Redonda	Warm Seep Coastal	Not used
JCVI_PEP_1105161925515	1.04E-20	Upwelling, Fernandina Island	upwelling	Not used
JCVI_PEP_1105108169439	1.02E-20	Coastal Floreana	Coastal	Not used
JCVI_PEP_1105160085301	9.71E-21	Sargasso Station 13	Open Ocean	Not used
JCVI_PEP_1112736817690	1.43E-20	International water between Madagascar and South Africa	Open Ocean	Not used
JCVI_PEP_1105134803719	1.24E-20	30 miles from Cocos Island	Open Ocean	Not used
JCVI_PEP_1105161199357	1.17E-20	Off Key West, FL	Coastal	Not used
JCVI_PEP_1105141830183	1.51E-20	Equatorial Pacific TAO Buoy	Open Ocean	Not used
JCVI_PEP_1112709099426	1.77E-20	East coast Zanzibar (Tanzania), offshore Paje lagoon	Fringing Reef	Not used
JCVI_PEP_1112711357040	1.59E-20	International water between Madagascar and South Africa	Open Ocean	Not used

JCVI_PEP_1112729206852	1.76E-20	St. Anne Island, Seychelles	Coastal sample	Not used
JCVI_PEP_1112710886578	1.74E-20	Indian Ocean	Open Ocean	Not used
JCVI_PEP_1112700685818	1.86E-20	Indian Ocean	Open Ocean	Not used
JCVI_PEP_1105156079629	1.64E-20	Sargasso Station 13	Open Ocean	Not used
JCVI_PEP_1105115760905	2.08E-20	North James Bay, Santiago Island	Coastal	Not used
JCVI_PEP_1105161930303	2.13E-20	Upwelling, Fernandina Island	Coastal upwelling	Not used
JCVI_PEP_1105157010119	2.20E-20	Upwelling, Fernandina Island	Coastal upwelling	Not used
JCVI_PEP_1112709338490	3.00E-20	Madagascar Waters	Open Ocean	Not used
JCVI_PEP_1105075560255	2.92E-20	North James Bay, Santiago Island	Coastal	Not used
JCVI_PEP_1105158717777	3.26E-20	Warm seep, Roca Redonda	Warm Seep	Not used
JCVI_PEP_1105125545815	2.67E-20	Rosario Bank	Open Ocean	Not used
JCVI_PEP_1105108872723	2.87E-20	Coastal Floreana	Coastal	Not used
JCVI_PEP_1105122486497	3.69E-20	Rosario Bank	Open Ocean	Not used
JCVI_PEP_1105124317113	3.95E-20	Yucatan Channel	Open Ocean	Not used
JCVI_PEP_1105083261181	3.75E-20	Delaware Bay, NJ	Estuary	Not used
JCVI_PEP_1105149163675	4.82E-20	Cape May, NJ	Coastal Coral Reef	Not used
JCVI_PEP_1105164402459	4.78E-20	Rangirora Atoll	Atoll	Not used
JCVI_PEP_1105086250205	4.58E-20	Newport Harbor, RI	Coastal	Not used
JCVI_PEP_1105097981111	8.36E-20	Sargasso Station 13	Open Ocean	Not used
JCVI_PEP_1105138279939	9.40E-20	Wolf Island	Coastal	Not used
JCVI_PEP_1105075079390	8.94E-20	30 miles from Cocos Island	Open Ocean	Not used
JCVI_PEP_1105127489175	8.36E-20	North Seamore Island	Coastal	Not used

Appendix Table 2. Full microarray dataset discussed in this work

Mn 1			Mn 2			Mur 1			Mur 2			F 1			F 2			Irr 1			Irr 2		
Gene ID	Ratio of Mn vs - Mn	p-value	Gene ID	Ratio of Mn vs - Mn	p-value	Gene ID	Ratio of Mur vs Mur	p-value	Gene ID	Ratio of Mur vs Mur	p-value	Gene ID	Ratio of F vs - F	p-value	Gene ID	Ratio of F vs - F	p-value	Gene ID	Ratio of Irr vs - Irr	p-value	Gene ID	Ratio of Irr vs - Irr	p-value
SP00001	1.16	0.051	SP00001	1.23	0.106	SP00001	0.92	0.645	SP00001	0.85	0.509	SP00001	1.86	0.000	SP00001	2.03	0.000	SP00001	1.09	0.416	SP00001	1.11	0.339
SP00002	1.49	0.0	SP00002	1.38	0.0	SP00002	0.89	0.111	SP00002	0.91	0.253	SP00002	2.09	0.001	SP00002	2.09	0.000	SP00002	1.29	0.118	SP00002	1.08	0.437
SP00003	0.94	0.512	SP00003	1.01	0.71	SP00003	0.93	0.368	SP00003	0.89	0.947	SP00003	1.32	0.019	SP00003	1.27	0.054	SP00003	0.86	0.365	SP00003	0.92	0.516
SP00004	0.91	0.22	SP00004	0.97	0.78	SP00004	0.75	0.596	SP00004	0.76	0.78	SP00004	1.44	0.002	SP00004	1.47	0.001	SP00004	1.01	0.866	SP00004	1.04	0.504
SP00005	1.32	0.000	SP00005	1.37	0.000	SP00005	0.76	0.206	SP00005	0.76	0.206	SP00005	0.96	0.005	SP00005	0.98	0.005	SP00005	1.12	0.066	SP00005	1.03	0.605
SP00006	1.18	0.143	SP00006	1.27	0.009	SP00006	0.93	0.614	SP00006	0.93	0.337	SP00006	1.41	0.022	SP00006	1.45	0.076	SP00006	1.12	0.466	SP00006	1.23	0.058
SP00007	1.33	0.359	SP00007	1.35	0.219	SP00007	0.85	0.287	SP00007	0.88	0.177	SP00007	1.62	0.063	SP00007	1.59	0.023	SP00007	1.43	0.235	SP00007	1.37	0.354
SP00008	1.02	0.762	SP00008	1.02	0.423	SP00008	0.99	0.006	SP00008	0.87	0.031	SP00008	1.42	0.005	SP00008	1.48	0.001	SP00008	1.17	0.123	SP00008	1.21	0.120
SP00009	0.9	0.509	SP00009	0.95	0.976	SP00009	0.91	0.043	SP00009	0.96	0.049	SP00009	0.89	0.463	SP00009	0.96	0.763	SP00009	0.95	0.449	SP00009	0.95	0.608
SP00010	1.28	0.052	SP00010	1.15	0.038	SP00010	0.74	0.741	SP00010	0.65	0.459	SP00010	0.84	0.429	SP00010	0.89	0.321	SP00010	1.20	0.356	SP00010	1.14	0.477
SP00011	1.33	0.001	SP00011	1.19	0.024	SP00011	0.98	0.082	SP00011	1.23	0.135	SP00011	1.23	0.135	SP00011	1.24	0.009	SP00011	0.99	0.805	SP00011	1.01	0.000
SP00012	1.83	0.002	SP00012	1.52	0.001	SP00012	0.97	0.704	SP00012	0.96	0.325	SP00012	0.82	0.370	SP00012	0.79	0.000	SP00012	1.26	0.249	SP00012	1.21	0.028
SP00013	1.01	0.375	SP00013	1.41	0.253	SP00013	0.98	0.583	SP00013	1.01	0.709	SP00013	1.22	0.354	SP00013	1.19	0.559	SP00013	1.06	0.863	SP00013	1.11	0.778
SP00014	0.74	0.018	SP00014	0.77	0.037	SP00014	0.99	0.989	SP00014	0.9	0.198	SP00014	0.95	0.009	SP00014	0.95	0.000	SP00014	1.01	0.863	SP00014	0.95	0.517
SP00015	1.18	0.24	SP00015	1.03	0.116	SP00015	0.93	0.623	SP00015	0.82	0.482	SP00015	0.93	0.350	SP00015	1.06	0.782	SP00015	1.06	0.388	SP00015	1.04	0.772
SP00016	1.33	0.009	SP00016	1.07	0.068	SP00016	0.88	0.347	SP00016	0.96	0.001	SP00016	0.88	0.608	SP00016	0.64	0.003	SP00016	0.80	0.307	SP00016	0.77	0.076
SP00017	1.47	0.1	SP00017	1.47	0.022	SP00017	0.93	0.53	SP00017	0.79	0.562	SP00017	1.06	0.677	SP00017	0.96	0.934	SP00017	0.99	0.947	SP00017	1.05	0.824
SP00018	1.32	0.032	SP00018	1.37	0.001	SP00018	0.81	0.146	SP00018	0.75	0.107	SP00018	1.11	0.027	SP00018	1.08	0.079	SP00018	1.02	0.669	SP00018	1.01	0.715
SP00019	1.37	0.034	SP00019	1.16	0.02	SP00019	0.9	0.046	SP00019	0.8	0.096	SP00019	0.43	0.000	SP00019	0.45	0.000	SP00019	0.96	0.653	SP00019	0.94	0.666
SP00020	0.52	0.006	SP00020	0.58	0.054	SP00020	0.86	0.599	SP00020	0.74	0.883	SP00020	1.95	0.032	SP00020	1.88	0.068	SP00020	1.26	0.106	SP00020	1.23	0.129
SP00021	1.01	0.693	SP00021	1.11	0.224	SP00021	0.97	0.893	SP00021	0.96	0.896	SP00021	0.96	0.896	SP00021	0.96	0.896	SP00021	1.21	0.617	SP00021	1.05	0.529
SP00022	0.74	0.129	SP00022	0.74	0.129	SP00022	0.77	0.109	SP00022	0.97	0.044	SP00022	0.61	0.008	SP00022	0.69	0.068	SP00022	1.21	0.668	SP00022	1.06	0.884
SP00023	1.11	0.112	SP00023	1.18	0.097	SP00023	0.92	0.947	SP00023	0.97	0.947	SP00023	1.13	0.296	SP00023	1.15	0.302	SP00023	1.20	0.222	SP00023	1.22	0.201
SP00024	1.17	0.116	SP00024	1.22	0.115	SP00024	0.89	0.058	SP00024	0.99	0.158	SP00024	1.26	0.015	SP00024	1.25	0.005	SP00024	1.26	0.106	SP00024	1.20	0.210
SP00025	1.88	0.003	SP00025	1.62	0.011	SP00025	0.85	0.064	SP00025	0.85	0.02	SP00025	1.33	0.053	SP00025	1.51	0.000	SP00025	1.46	0.008	SP00025	1.32	0.046
SP00026	1.41	0.157	SP00026	1.48	0.182	SP00026	0.78	0.533	SP00026	0.79	0.54	SP00026	1.08	0.802	SP00026	1.07	0.821	SP00026	1.06	0.913	SP00026	1.10	0.776
SP00027	1.14	0.482	SP00027	1.07	0.716	SP00027	0.74	0.236	SP00027	0.7	0.616	SP00027	0.79	0.284	SP00027	0.80	0.504	SP00027	0.96	0.813	SP00027	0.95	0.856
SP00028	0.96	0.996	SP00028	1.02	0.757	SP00028	0.92	0.738	SP00028	0.94	0.703	SP00028	1.07	0.756	SP00028	1.02	0.923	SP00028	0.93	0.614	SP00028	0.91	0.752
SP00029	1.69	0.001	SP00029	1.59	0.002	SP00029	0.85	0.889	SP00029	0.95	0.56	SP00029	1.04	0.806	SP00029	1.06	0.509	SP00029	1.03	0.867	SP00029	1.03	0.773
SP00030	1.81	0.018	SP00030	1.44	0.034	SP00030	0.96	0.168	SP00030	0.96	0.168	SP00030	0.76	0.299	SP00030	0.89	0.356	SP00030	1.21	0.347	SP00030	1.12	0.263
SP00031	1.11	0.621	SP00031	1.09	0.624	SP00031	0.98	0.869	SP00031	0.99	0.825	SP00031	1.28	0.214	SP00031	1.25	0.265	SP00031	1.02	0.876	SP00031	1.03	0.833
SP00032	0.88	0.656	SP00032	0.93	0.913	SP00032	0.97	0.908	SP00032	0.92	0.704	SP00032	0.91	0.676	SP00032	0.79	0.325	SP00032	0.91	0.754	SP00032	1.01	0.988
SP00033	1.08	0.181	SP00033	1.08	0.055	SP00033	0.93	0.523	SP00033	0.96	0.742	SP00033	1.41	0.016	SP00033	1.57	0.002	SP00033	0.94	0.329	SP00033	1.00	0.778
SP00034	0.95	0.711	SP00034	0.96	0.683	SP00034	0.8	0.811	SP00034	0.94	0.297	SP00034	1.02	0.325	SP00034	1.06	0.641	SP00034	0.95	0.786	SP00034	0.97	0.807
SP00035	1.07	0.606	SP00035	1.07	0.066	SP00035	0.9	0.155	SP00035	0.93	0.037	SP00035	1.02	0.755	SP00035	1.08	0.065	SP00035	1.07	0.530	SP00035	1.05	0.455
SP00036	0.87	0.493	SP00036	0.93	0.796	SP00036	0.95	0.882	SP00036	0.83	0.655	SP00036	1.11	0.415	SP00036	1.08	0.389	SP00036	1.00	0.985	SP00036	0.98	0.941
SP00037	0.97	0.799	SP00037	1.01	0.444	SP00037	0.96	0.681	SP00037	0.99	0.335	SP00037	1.29	0.074	SP00037	1.16	0.303	SP00037	1.34	0.077	SP00037	1.03	0.881
SP00038	1.81	0.215	SP00038	1.24	0.034	SP00038	0.99	0.344	SP00038	0.92	0.226	SP00038	0.86	0.376	SP00038	0.89	0.356	SP00038	1.05	0.603	SP00038	1.06	0.235
SP00039	1.17	0.001	SP00039	1.24	0.011	SP00039	0.93	0.471	SP00039	0.92	0.494	SP00039	1.09	0.068	SP00039	1.06	0.016	SP00039	1.05	0.376	SP00039	1.06	0.437
SP00040	1.07	0.303	SP00040	1.04	0.643	SP00040	0.93	0.781	SP00040	0.93	0.187	SP00040	0.60	0.001	SP00040	0.56	0.001	SP00040	0.82	0.220	SP00040	0.79	0.070
SP00041	1.27	0.42	SP00041	1.12	0.176	SP00041	0.89	0.579	SP00041	0.86	0.579	SP00041	0.58	0.212	SP00041	0.57	0.278	SP00041	0.88	0.720	SP00041	0.90	0.795
SP00042	1.49	0.427	SP00042	1.26	0.69	SP00042	0.93	0.875	SP00042	0.91	0.861	SP00042	0.81	0.782	SP00042	0.78	0.727	SP00042	0.94	0.891	SP00042	0.94	0.904
SP00043	0.94	0.772	SP00043	0.9	0.704	SP00043	0.95	0.971	SP00043	0.94	0.835	SP00043	0.93	0.714	SP00043	0.94	0.608	SP00043	1.03	0.834	SP00043	1.03	0.800
SP00044	1.66	0.043	SP00044	1.38	0.178	SP00044	0.95	0.342	SP00044	0.98	0.512	SP00044	0.64	0.149	SP00044	0.65	0.155	SP00044	0.97	0.856	SP00044	1.06	0.742
SP00045	1.09	0.22	SP00045	1.04	0.539	SP00045	0.83	0.47	SP00045	0.96	0.597	SP00045	0.90	0.001	SP00045	0.90	0.000	SP00045	1.04	0.826	SP00045	1.09	0.606
SP00046	0.93	0.356	SP00046	0.83	0.253	SP00046	0.88	0.219	SP00046	0.93	0.143	SP00046	0.97	0.001	SP00046	0.93	0.009	SP00046	0.93	0.692	SP00046	0.97	0.787
SP00047	0.98	0.967	SP00047	1.01	0.892	SP00047	0.83	0.856	SP00047	0.85	0.941	SP00047	0.93	0.032	SP00047	0.93	0.021	SP00047	1.01	0.992	SP00047	1.02	0.982
SP00048	0.96	0.858	SP00048	0.96	0.853	SP00048	0.97	0.035	SP00048	0.97	0.000	SP00048	0.97	0.000	SP00048	0.97	0.000	SP00048	1.43	0.017	SP00048	1.30	0.038
SP00049	0.56	0.003	SP00049	0.65	0.04	SP00049	0.92	0.252	SP00049	1.01	0.051	SP00049	0.96	0.000	SP00049	0.96	0.000	SP00049	1.10	0.698	SP00049	1.11	0.495
SP00050	0.66	0.154	SP																				

SP00137	1.02	0.816	SP00137	1.01	0.566	SP00137	0.88	0.892	SP00137	0.81	0.843	SP00137	1.11	0.461	SP00137	1.10	0.255	SP00137	1.27	0.159	SP00137	1.16	0.133
SP00138	1.07	0.311	SP00138	1.04	0.248	SP00138	0.93	0.513	SP00138	0.95	0.609	SP00138	1.09	0.116	SP00138	1.13	0.047	SP00138	0.98	0.856	SP00138	1.01	0.778
SP00139	0.68		SP00139	0.74	0.001	SP00139	0.93	0.151	SP00139	0.93	0.671	SP00139	0.97	0.116	SP00139	0.95	0.007	SP00139	0.83	0.011	SP00139	0.87	0.028
SP00140	1.16	0.079	SP00140	1.23	0.021	SP00140	0.93	0.152	SP00140	0.94	0.341	SP00140	0.98	0.003	SP00140	0.76	0.021	SP00140	1.03	0.021	SP00140	1.03	0.833
SP00141	0.85	0.19	SP00141	0.88	0.443	SP00141	0.81	0.547	SP00141	0.95	0.995	SP00141	0.97	0.007	SP00141	0.65	0.028	SP00141	0.85	0.862	SP00141	1.02	0.839
SP00142	1.04	0.259	SP00142	0.81	0.031	SP00142	0.93	0.547	SP00142	0.68	0.18	SP00142	1.98	0.000	SP00142	1.92	0.000	SP00142	1.20	0.103	SP00142	1.16	0.054
SP00143	0.68	0.047	SP00143	0.77	0.033	SP00143	0.97	0.804	SP00143	0.9	0.665	SP00143	1.18	0.140	SP00143	1.18	0.265	SP00143	1.01	0.978	SP00143	1.04	0.852
SP00144	1.49	0.011	SP00144	1.34	0.016	SP00144	0.99	0.231	SP00144	1.01	0.233	SP00144	0.63	0.003	SP00144	0.54	0.001	SP00144	0.98	0.847	SP00144	0.93	0.690
SP00145	0.88	0.479	SP00145	0.98	0.719	SP00145	0.78	0.009	SP00145	0.88	0.016	SP00145	1.53	0.003	SP00145	1.58	0.000	SP00145	1.28	0.404	SP00145	1.25	0.155
SP00146	0.78	0.034	SP00146	0.81	0.129	SP00146	0.59	0.932	SP00146	0.94	0.055	SP00146	1.06	0.318	SP00146	1.22	0.171	SP00146	1.17	0.075	SP00146	1.19	0.188
SP00147	1.5	0.005	SP00147	1.37	0.013	SP00147	0.74	0.524	SP00147	0.84	0.321	SP00147	0.72	0.037	SP00147	0.76	0.052	SP00147	1.03	0.698	SP00147	0.88	0.338
SP00148	1.16	0.309	SP00148	1.23	0.021	SP00148	0.98	0.823	SP00148	0.93	0.541	SP00148	1.15	0.020	SP00148	1.04	0.026	SP00148	1.07	0.593	SP00148	1.07	0.633
SP00149	1.05	0.813	SP00149	0.95	0.006	SP00149	0.93	0.916	SP00149	0.78	0.821	SP00149	0.99	0.034	SP00149	1.88	0.014	SP00149	1.12	0.571	SP00149	1.10	0.633
SP00150	1.7	0.002	SP00150	1.41	0.028	SP00150	0.87	0.025	SP00150	0.98	0.108	SP00150	0.72	0.080	SP00150	0.66	0.019	SP00150	1.19	0.101	SP00150	1.01	0.807
SP00151	1.35	0.292	SP00151	1.26	0.015	SP00151	0.85	0.286	SP00151	0.98	0.114	SP00151	1.28	0.017	SP00151	1.39	0.001	SP00151	1.15	0.277	SP00151	1.12	0.300
SP00152	1.28	0.392	SP00152	1.24	0.485	SP00152	0.92	0.533	SP00152	0.97	0.525	SP00152	0.88	0.807	SP00152	0.92	0.822	SP00152	0.81	0.519	SP00152	0.80	0.308
SP00153	1.32	0.144	SP00153	1.39	0.004	SP00153	0.9	0.001	SP00153	0.74	0.001	SP00153	0.83	0.088	SP00153	0.78	0.004	SP00153	0.71	0.011	SP00153	0.68	0.023
SP00154	1.25	0.058	SP00154	1.26	0.043	SP00154	0.99	0.002	SP00154	0.56	0.001	SP00154	1.34	0.019	SP00154	1.41	0.000	SP00154	0.4	0.000	SP00154	0.46	0.000
SP00155	1.06	0.02	SP00155	1.09	0.06	SP00155	0.99	0.906	SP00155	0.76	0.198	SP00155	1.43	0.007	SP00155	1.48	0.000	SP00155	0.87	0.280	SP00155	0.95	0.765
SP00156	1.12	0.437	SP00156	1.08	0.328	SP00156	0.87	0.574	SP00156	0.92	0.924	SP00156	1.25	0.412	SP00156	1.59	0.104	SP00156	1.31	0.651	SP00156	1.10	0.784
SP00157	1.23	0.038	SP00157	1.2	0.008	SP00157	0.9	0.1	SP00157	0.95	0.1	SP00157	0.98	0.000	SP00157	0.98	0.000	SP00157	1.21	0.042	SP00157	1.39	0.001
SP00160	1.28	0.017	SP00160	1.27		SP00160	0.53	0.004	SP00160	0.83	0.001	SP00160	0.64	0.000	SP00160	0.71	0.000	SP00160	1.07	0.694	SP00160	1.04	0.659
SP00161	0.83	0.15	SP00161	0.88	0.525	SP00161	0.99	0.066	SP00161	0.98	0.151	SP00161	1.05	0.228	SP00161	0.94	0.836	SP00161	1.16	0.140	SP00161	1.14	0.108
SP00162	0.23	0.015	SP00162	0.28	0.0	SP00162	0.96	0.199	SP00162	0.89	0.285	SP00162	1.64	0.002	SP00162	1.64	0.002	SP00162	1.20	0.159	SP00162	1.12	0.319
SP00163	0.75	0.203	SP00163	0.76	0.185	SP00163	0.95	0.44	SP00163	0.96	0.793	SP00163	0.99	0.900	SP00163	1.07	0.529	SP00163	1.30	0.403	SP00163	1.28	0.505
SP00164	0.97	0.866	SP00164	1.03	0.093	SP00164	0.89	0.71	SP00164	0.91	0.536	SP00164	1.63	0.020	SP00164	1.70	0.020	SP00164	1.09	0.679	SP00164	0.97	0.608
SP00165	1.13	0.192	SP00165	1.11	0.081	SP00165	0.81	0.683	SP00165	0.85	0.394	SP00165	1.59	0.003	SP00165	1.61	0.003	SP00165	0.95	0.612	SP00165	0.88	0.258
SP00166	0.85	0.193	SP00166	0.89	0.255	SP00166	0.87	0.198	SP00166	0.95	0.284	SP00166	1.75	0.000	SP00166	1.63	0.000	SP00166	0.84	0.058	SP00166	0.82	0.119
SP00167	1.23	0.038	SP00167	1.2	0.008	SP00167	0.91	0.034	SP00167	0.95	0.034	SP00167	0.98	0.001	SP00167	0.98	0.001	SP00167	0.82	0.044	SP00167	0.85	0.064
SP00168	1.17	0.008	SP00168	1.2		SP00168	0.95	0.23	SP00168	0.98	0.383	SP00168	1.77	0.004	SP00168	1.82	0.002	SP00168	0.94	0.549	SP00168	0.91	0.255
SP00169	1.02	0.463	SP00169	1.13	0.173	SP00169	0.98	0.933	SP00169	0.88	0.92	SP00169	0.17	0.016	SP00169	0.33	0.000	SP00169	1.23	0.031	SP00169	0.43	0.004
SP00170	1.08	0.697	SP00170	1.19	0.279	SP00170	0.97	0.86	SP00170	0.85	0.32	SP00170	0.71	0.068	SP00170	0.76	0.013	SP00170	1.09	0.807	SP00170	1.06	0.916
SP00171	1.16	0.045	SP00171	1.24	0.011	SP00171	0.71	0.032	SP00171	0.82	0.002	SP00171	0.75	0.017	SP00171	0.98	0.106	SP00171	0.93	0.405	SP00171	0.83	0.016
SP00172	0.99	0.523	SP00172	0.78	0.082	SP00172	0.69	0.904	SP00172	0.88	0.577	SP00172	1.05	0.583	SP00172	1.00	0.371	SP00172	1.02	0.894	SP00172	0.93	0.552
SP00173	1.04	0.324	SP00173	1.05	0.018	SP00173	0.96	0.246	SP00173	0.95	0.243	SP00173	0.89	0.503	SP00173	0.88	0.112	SP00173	1.01	0.888	SP00173	1.09	0.617
SP00174	1.21	0.067	SP00174	1.19	0.003	SP00174	0.97	0.981	SP00174	0.97	0.842	SP00174	0.92	0.002	SP00174	0.98	0.000	SP00174	1.01	0.912	SP00174	0.96	0.670
SP00175	1.28	0.015	SP00175	1.28	0.001	SP00175	0.98	0.132	SP00175	0.91	0.071	SP00175	0.95	0.003	SP00175	0.95	0.003	SP00175	1.01	0.972	SP00175	0.95	0.670
SP00176	0.93	0.956	SP00176	0.88	0.362	SP00176	0.96	0.881	SP00176	0.69	0.861	SP00176	0.67	0.000	SP00176	0.33	0.000	SP00176	1.02	0.954	SP00176	0.96	0.701
SP00177	0.89	0.19	SP00177	1.02	0.63	SP00177	0.72	0.914	SP00177	0.81	0.964	SP00177	0.58	0.011	SP00177	0.61	0.014	SP00177	0.81	0.615	SP00177	0.95	0.699
SP00178	1.1	0.885	SP00178	1.12	0.884	SP00178	0.75	0.033	SP00178	0.88	0.002	SP00178	0.36	0.342	SP00178	0.42	0.404	SP00178	0.81	0.300	SP00178	1.05	0.974
SP00179	0.81	0.192	SP00179	0.85	0.347	SP00179	0.93	0.060	SP00179	0.67	0.29	SP00179	0.23	0.000	SP00179	0.27	0.000	SP00179	1.15	0.579	SP00179	1.12	0.446
SP00180	0.85	0.659	SP00180	0.92	0.843	SP00180	0.94	0.576	SP00180	0.97	0.886	SP00180	0.22	0.000	SP00180	0.28	0.000	SP00180	1.00	0.714	SP00180	1.13	0.250
SP00181	0.92	0.941	SP00181	1.02	0.412	SP00181	0.93	0.012	SP00181	0.94	0.109	SP00181	0.14	0.000	SP00181	0.13	0.000	SP00181	1.03	0.941	SP00181	0.93	0.429
SP00182	0.8	0.346	SP00182	0.65	0.013	SP00182	0.99	0.868	SP00182	0.98	0.513	SP00182	0.68	0.000	SP00182	0.68	0.000	SP00182	1.05	0.924	SP00182	1.08	0.805
SP00183	1.06	0.851	SP00183	1.06	0.828	SP00183	0.96	0.834	SP00183	0.94	0.94	SP00183	0.61	0.221	SP00183	0.61	0.221	SP00183	0.77	0.523	SP00183	0.83	0.640
SP00184	1.14	0.596	SP00184	1.17	0.471	SP00184	0.89	0.252	SP00184	0.74	0.196	SP00184	0.78	0.411	SP00184	0.77	0.311	SP00184	1.20	0.492	SP00184	1.22	0.346
SP00185	1.34	0.065	SP00185	1.13	0.546	SP00185	0.94	0.011	SP00185	0.79	0.087	SP00185	0.93	0.738	SP00185	1.04	0.743	SP00185	1.50	0.046	SP00185	1.56	0.022
SP00186	0.95	0.803	SP00186	0.89	0.239	SP00186	0.95	0.425	SP00186	0.88	0.482	SP00186	0.68	0.009	SP00186	0.70	0.020	SP00186	1.51	0.000	SP00186	1.54	0.026
SP00187	0.8	0.259	SP00187	0.99	0.933	SP00187	1	0.058	SP00187	0.93	0.089	SP00187	0.56	0.050	SP00187	0.63	0.291	SP00187	0.72	0.227	SP00187	0.78	0.280
SP00188	1.22	0.026	SP00188	1.16	0.047	SP00188	0.98	0.566	SP00188	0.94	0.366	SP00188	0.62	0.005	SP00188	0.63	0.000	SP00188	0.97	0.221	SP00188	0.95	0.565
SP00189	1.02	0.684	SP00189	0.95	0.946	SP00189	0.99	0.125	SP00189	0.97	0.239	SP00189	0.79	0.183</									

SPO0285	1.13	0.011	SPO0285	1.18	0.019	SPO0286	0.93	0.445	SPO0286	0.92	0.162	SPO0285	1.23	0.061	SPO0285	1.32	0.015	SPO0285	1.03	0.749	SPO0285	1.01	0.918
SPO0286	1.82	0.001	SPO0286	1.63	0.008	SPO0287	0.83	0.519	SPO0287	0.74	0.524	SPO0286	1.00	0.282	SPO0286	0.86	0.171	SPO0286	0.96	0.788	SPO0286	0.97	0.818
SPO0287	1.62	0.001	SPO0287	1.58	0.002	SPO0288	0.94	0.619	SPO0288	0.93	0.557	SPO0287	1.00	0.747	SPO0287	1.04	0.523	SPO0287	1.09	0.512	SPO0287	1.05	0.686
SPO0288	1.17	0.314	SPO0288	1.13	0.340	SPO0289	0.79	0.973	SPO0289	0.83	0.993	SPO0288	0.79	0.959	SPO0288	0.81	0.964	SPO0288	0.89	0.931	SPO0288	0.99	0.929
SPO0289	1.04	0.838	SPO0289	1.04	0.816	SPO0290	0.75	0.662	SPO0290	0.79	0.507	SPO0289	0.57	0.515	SPO0289	0.59	0.513	SPO0289	0.89	0.828	SPO0289	0.83	0.756
SPO0290	0.98	0.04	SPO0290	0.91	0.081	SPO0291	0.88	0.006	SPO0291	0.84	0.020	SPO0290	0.63	0.004	SPO0290	0.67	0.006	SPO0290	1.02	0.734	SPO0290	1.06	0.381
SPO0291	0.74	0.004	SPO0291	0.72	0.015	SPO0292	0.98	0.53	SPO0292	0.98	0.47	SPO0291	0.93	0.351	SPO0291	0.93	0.683	SPO0291	1.01	0.890	SPO0291	1.05	0.639
SPO0292	1.09	0.510	SPO0292	0.97	0.971	SPO0293	0.76	0.007	SPO0293	0.81	0.012	SPO0292	1.12	0.596	SPO0292	1.15	0.526	SPO0292	0.96	0.863	SPO0292	1.01	0.962
SPO0293	1.61	0.005	SPO0293	1.42	0.008	SPO0294	0.71	0.606	SPO0294	0.93	0.763	SPO0293	0.54	0.000	SPO0293	0.51	0.012	SPO0293	1.04	0.811	SPO0293	1.02	0.942
SPO0294	1.29	0.024	SPO0294	1.28	0.299	SPO0295	0.75	0.507	SPO0295	0.85	0.17	SPO0294	0.89	0.295	SPO0294	0.91	0.412	SPO0294	1.01	0.987	SPO0294	1.10	0.152
SPO0295	1.23	0.038	SPO0295	1.25	0.038	SPO0296	0.71	0.367	SPO0296	0.97	0.372	SPO0295	0.61	0.002	SPO0295	0.60	0.000	SPO0295	1.01	0.697	SPO0295	0.98	0.997
SPO0296	1.19	0.314	SPO0296	1.13	0.420	SPO0297	0.85	0.979	SPO0297	0.79	0.973	SPO0296	0.81	0.176	SPO0296	0.81	0.655	SPO0296	0.75	0.711	SPO0296	0.72	0.325
SPO0297	1.06	0.896	SPO0297	1.05	0.922	SPO0298	0.79	0.8	SPO0298	0.86	0.864	SPO0297	0.99	0.879	SPO0297	0.99	0.859	SPO0297	0.96	0.989	SPO0297	1.00	0.961
SPO0298	1.2	0.197	SPO0298	1.23	0.096	SPO0299	0.96	0.707	SPO0299	0.95	0.748	SPO0298	0.68	0.040	SPO0298	0.70	0.022	SPO0298	0.90	0.480	SPO0298	0.88	0.384
SPO0299	1.3	0.098	SPO0299	1.14	0.051	SPO0300	0.89	0.078	SPO0300	1.01	0.118	SPO0299	1.11	0.812	SPO0299	1.21	0.452	SPO0299	1.13	0.613	SPO0299	1.00	0.932
SPO0300	1.28	0.014	SPO0300	1.08	0.225	SPO0301	0.76	0.936	SPO0301	1.01	0.786	SPO0300	0.51	0.001	SPO0300	0.50	0.000	SPO0300	1.01	0.966	SPO0300	0.97	0.467
SPO0301	0.77	0.166	SPO0301	0.78	0.437	SPO0302	0.83	0.879	SPO0302	0.94	0.896	SPO0301	0.81	0.351	SPO0301	0.85	0.544	SPO0301	1.01	0.905	SPO0301	1.00	0.960
SPO0302	0.79	0.603	SPO0302	0.81	0.533	SPO0303	0.71	0.132	SPO0303	0.81	0.266	SPO0302	0.92	0.754	SPO0302	0.93	0.738	SPO0302	1.03	0.939	SPO0302	1.12	0.764
SPO0303	1.46	0.001	SPO0303	1.4	0.001	SPO0304	0.82	0.653	SPO0304	0.98	0.786	SPO0303	0.48	0.000	SPO0303	0.47	0.000	SPO0303	1.03	0.161	SPO0303	1.04	0.133
SPO0304	1.18	0.491	SPO0304	1.1	0.54	SPO0305	0.88	0.839	SPO0305	0.7	0.809	SPO0304	0.90	0.321	SPO0304	0.93	0.752	SPO0304	0.87	0.986	SPO0304	1.02	0.875
SPO0305	1.16	0.369	SPO0305	0.95	0.812	SPO0306	0.86	0.788	SPO0306	0.8	0.791	SPO0305	1.07	0.886	SPO0305	1.23	0.323	SPO0305	0.98	0.923	SPO0305	0.99	0.974
SPO0306	0.92	0.428	SPO0306	0.96	0.907	SPO0307	0.67	0.238	SPO0307	0.67	0.238	SPO0306	0.75	0.029	SPO0306	0.78	0.010	SPO0306	0.94	0.410	SPO0306	1.01	0.813
SPO0307	0.81	0.731	SPO0307	0.88	0.844	SPO0308	0.9	0.577	SPO0308	0.83	0.268	SPO0307	1.07	0.008	SPO0307	1.08	0.026	SPO0307	0.88	0.881	SPO0307	0.91	0.899
SPO0308	1.15	0.09	SPO0308	1.09	0.105	SPO0309	0.79	0.784	SPO0309	0.79	0.876	SPO0308	1.23	0.003	SPO0308	1.39	0.003	SPO0308	1.10	0.374	SPO0308	1.08	0.367
SPO0309	1.12	0.513	SPO0309	1.11	0.54	SPO0310	0.85	0.976	SPO0310	0.93	0.895	SPO0309	0.92	0.848	SPO0309	0.97	0.934	SPO0309	0.99	0.947	SPO0309	1.02	0.870
SPO0310	1.15	0.255	SPO0310	0.99	0.882	SPO0311	0.94	0.199	SPO0311	0.83	0.293	SPO0310	0.74	0.236	SPO0310	0.73	0.147	SPO0310	0.81	0.924	SPO0310	0.83	1.040
SPO0311	1.27	0.089	SPO0311	1.23	0.14	SPO0312	0.85	0.768	SPO0312	0.75	0.911	SPO0311	1.12	0.397	SPO0311	1.12	0.370	SPO0311	1.01	0.967	SPO0311	1.03	0.865
SPO0312	0.75	0.234	SPO0312	0.81	0.295	SPO0313	0.9	0.277	SPO0313	0.98	0.008	SPO0312	1.28	0.054	SPO0312	1.12	0.197	SPO0312	1.01	0.763	SPO0312	1.04	0.990
SPO0313	1.07	0.399	SPO0313	0.7	0.029	SPO0314	0.96	0.044	SPO0314	0.83	0.000	SPO0313	0.41	0.000	SPO0313	0.39	0.000	SPO0313	1.23	0.219	SPO0313	1.26	0.048
SPO0314	1.3	0.023	SPO0314	1.37	0.322	SPO0315	0.88	0.906	SPO0315	0.7	0.823	SPO0314	0.41	0.000	SPO0314	0.39	0.000	SPO0314	0.90	0.621	SPO0314	0.87	0.361
SPO0315	0.61	0.004	SPO0315	0.67	0.001	SPO0316	0.95	0.478	SPO0316	0.78	0.623	SPO0315	0.72	0.031	SPO0315	0.73	0.016	SPO0315	0.96	0.808	SPO0315	0.93	0.514
SPO0316	1.07	0.462	SPO0316	1.05	0.561	SPO0317	0.86	0.223	SPO0317	0.72	0.4	SPO0316	1.34	0.076	SPO0316	1.27	0.033	SPO0316	0.91	0.718	SPO0316	0.93	0.738
SPO0317	1.22	0.019	SPO0317	1.1	0.006	SPO0318	0.87	0.204	SPO0318	0.79	0.088	SPO0317	0.84	0.103	SPO0317	0.82	0.106	SPO0317	0.97	0.975	SPO0317	0.98	0.931
SPO0318	1.3	0.0	SPO0318	1.28	0.001	SPO0319	0.97	0.064	SPO0319	0.93	0.17	SPO0318	1.13	0.019	SPO0318	1.13	0.052	SPO0318	0.92	0.402	SPO0318	0.90	0.289
SPO0319	1.44	0.003	SPO0319	1.47	0.9	SPO0320	0.94	0.903	SPO0320	0.91	0.899	SPO0319	1.28	0.018	SPO0319	1.21	0.012	SPO0319	1.10	0.365	SPO0319	1.12	0.255
SPO0320	0.99	0.896	SPO0320	0.99	0.822	SPO0321	0.9	0.447	SPO0321	0.95	0.943	SPO0320	1.02	0.553	SPO0320	1.01	0.704	SPO0320	1.14	0.409	SPO0320	1.12	0.590
SPO0321	0.97	0.902	SPO0321	0.91	0.182	SPO0322	0.91	0.182	SPO0322	0.91	0.182	SPO0321	1.09	0.001	SPO0321	1.03	0.001	SPO0321	0.97	0.981	SPO0321	1.01	0.921
SPO0322	0.75	0.024	SPO0322	0.73	0.019	SPO0323	0.85	0.229	SPO0323	0.91	0.242	SPO0322	1.02	0.322	SPO0322	1.02	0.322	SPO0322	0.95	0.987	SPO0322	0.76	0.100
SPO0323	1.44	0.039	SPO0323	1.74	0.001	SPO0324	0.92	0.442	SPO0324	0.99	0.853	SPO0323	0.54	0.003	SPO0323	0.66	0.006	SPO0323	1.81	0.005	SPO0323	1.63	0.005
SPO0324	1.2	0.014	SPO0324	1.16	0.006	SPO0325	0.83	0.192	SPO0325	0.94	0.116	SPO0324	1.12	0.171	SPO0324	1.14	0.111	SPO0324	1.04	0.705	SPO0324	1.06	0.257
SPO0325	0.77	0.068	SPO0325	0.75	0.018	SPO0326	0.85	0.289	SPO0326	0.81	0.308	SPO0325	1.07	0.052	SPO0325	1.00	0.088	SPO0325	0.97	0.959	SPO0325	1.00	0.767
SPO0326	0.7	0.001	SPO0326	0.67	0.002	SPO0327	0.97	0.978	SPO0327	0.94	0.567	SPO0326	0.67	0.003	SPO0326	0.66	0.026	SPO0326	0.99	0.513	SPO0326	1.07	0.001
SPO0327	0.88	0.804	SPO0327	0.89	0.737	SPO0328	0.78	0.003	SPO0328	0.9	0.002	SPO0327	1.47	0.015	SPO0327	1.61	0.01	SPO0327	0.61	0.006	SPO0327	0.92	0.560
SPO0328	1.17	0.121	SPO0328	1.2	0.008	SPO0329	0.9	0.002	SPO0329	0.88	0.016	SPO0328	1.04	0.988	SPO0328	1.12	0.356	SPO0328	0.65	0.077	SPO0328	0.63	0.044
SPO0329	0.97	0.399	SPO0329	0.78	0.01	SPO0330	0.95	0.407	SPO0330	0.85	0.333	SPO0329	1.23	0.014	SPO0329	1.37	0.009	SPO0329	1.10	0.217	SPO0329	0.68	0.016
SPO0330	1.28	1.109	SPO0330	1.22	0.285	SPO0331	0.92	0.447	SPO0331	0.79	0.096	SPO0330	1.19	0.301	SPO0330	1.29	0.165	SPO0330	0.67	0.000	SPO0330	0.67	0.004
SPO0331	1.07	0.138	SPO0331	1.04	0.381	SPO0332	0.88	0.699	SPO0332	0.96	0.433	SPO0331	0.72	0.012	SPO0331	0.74	0.010	SPO0331	1.12	0.230	SPO0331	1.12	0.106
SPO0332	1.31	0.021	SPO0332	1.29	0.051	SPO0333	0.79	0.789	SPO0333	0.81	0.661	SPO0332	0.95	0.789	SPO0332	0.95	0.678	SPO0332	1.03	0.716	SPO0332	1.04	0.497
SPO0333	1.32	0.187	SPO0333	1.18	0.224	SPO0334	0.85	0.239	SPO0334	0.9	0.182	SPO0333	0.59	0.441	SPO0333	0.55	0.011	SPO0333	0.86	0.710	SPO0333	0.86	0.596
SPO0334	1.23	0.044	SPO0334	1.2	0.132	SPO0335	0.79	0.466	SPO0335	0.95	0.54	SPO0334	1.59	0.002	SPO0334	1.63	0.002	SPO0334	1.19	0.065	SPO0334	1.26	0.032
SPO0335	0.57	0.017	SPO0335	0.63	0.001	SPO0336	0.99	0.021	SPO0336	0.84	0.028	SPO0335	0.83	0.104	SPO0335	0.85	0.335	SPO0335	1.02	0.833	SPO0335	0.97	0.913
SPO0336	1.06	0.142	SPO0336	1.05	0.296	SPO0337	0.81	0.447	SPO0337	0.95	0.877	SPO0336	0.89	0.643	SPO0336	0.88	0.575	SPO0336	1.00	0.691	SPO0336	1.03	0.663
SPO0337	1.37	0.001	SPO0337	1.24	0.101	SPO																	

SPO0424	1.05	0.160	SPO0424	0.83	0.183	SPO0425	0.62	0.701	SPO0425	0.33	0.256	SPO0424	1.35	0.087	SPO0424	1.21	0.047	SPO0424	1.02	0.896	SPO0424	0.99	0.766
SPO0425	0.82	0.041	SPO0425	0.91	0.44	SPO0426	0.72	0.4	SPO0426	0.97	0.206	SPO0425	1.12	0.017	SPO0425	1.18	0.016	SPO0425	0.80	0.128	SPO0425	0.84	0.297
SPO0426	1.11	0.042	SPO0426	1.15	0.08	SPO0427	0.78	0.052	SPO0427	0.86	0.004	SPO0426	0.76	0.037	SPO0426	0.85	0.238	SPO0426	1.12	0.100	SPO0426	1.06	0.203
SPO0427	1.37	0.13	SPO0427	1.32	0.093	SPO0428	0.96	0.873	SPO0427	0.97	0.873	SPO0427	0.58	0.039	SPO0427	0.94	0.039	SPO0427	0.94	0.039	SPO0427	0.94	0.039
SPO0428	1.05	0.312	SPO0428	0.98	0.923	SPO0429	0.5	0.383	SPO0428	0.97	0.072	SPO0428	1.11	0.540	SPO0428	1.00	0.922	SPO0428	0.94	0.743	SPO0428	0.95	0.876
SPO0429	0.81	0.03	SPO0429	0.75	0.084	SPO0430	0.84	0.422	SPO0429	0.99	0.328	SPO0429	0.72	0.003	SPO0429	0.77	0.003	SPO0429	1.20	0.064	SPO0429	1.14	0.362
SPO0430	1.45	0.001	SPO0430	1.33	0.001	SPO0431	0.94	0.83	SPO0431	0.96	0.717	SPO0430	1.03	0.137	SPO0430	1.08	0.052	SPO0430	1.10	0.292	SPO0430	1.07	0.271
SPO0431	1.37	0.536	SPO0431	1.4	0.468	SPO0432	0.93	0.04	SPO0432	0.94	0.001	SPO0431	0.86	0.704	SPO0431	0.90	0.763	SPO0431	1.04	0.982	SPO0431	0.88	0.787
SPO0432	0.57	0.004	SPO0432	0.55	0.007	SPO0433	0.98	0.559	SPO0433	0.89	0.497	SPO0432	8.18	0.000	SPO0432	7.92	0.000	SPO0432	1.30	0.030	SPO0432	1.39	0.010
SPO0433	1.25	0.604	SPO0433	1.24	0.388	SPO0434	0.97	0.003	SPO0434	0.95	0.007	SPO0433	0.92	0.669	SPO0433	0.93	0.703	SPO0433	1.22	0.549	SPO0433	1.20	0.375
SPO0434	1.01	0.945	SPO0434	1.08	0.114	SPO0435	0.86	0.007	SPO0435	0.75	0.633	SPO0434	0.69	0.030	SPO0434	0.69	0.030	SPO0434	0.99	0.921	SPO0434	0.99	0.869
SPO0435	1.37	0.13	SPO0435	1.32	0.093	SPO0436	0.96	0.028	SPO0436	0.61	0.074	SPO0435	0.95	0.559	SPO0435	1.03	0.441	SPO0435	0.95	0.983	SPO0435	0.95	0.634
SPO0436	1.03	0.370	SPO0436	1.05	0.130	SPO0437	0.93	0.602	SPO0437	0.71	0.409	SPO0436	0.05	0.476	SPO0436	1.07	0.147	SPO0436	0.98	0.735	SPO0436	0.99	0.719
SPO0437	1.16	0.326	SPO0437	0.99	0.976	SPO0438	0.94	0.053	SPO0438	0.71	0.069	SPO0437	0.93	0.453	SPO0437	0.90	0.344	SPO0437	0.85	0.415	SPO0437	0.98	0.804
SPO0438	0.76	0.028	SPO0438	0.78	0.109	SPO0439	0.96	0.917	SPO0439	0.93	0.93	SPO0438	1.13	0.077	SPO0438	1.11	0.005	SPO0438	0.75	0.062	SPO0438	0.83	0.062
SPO0439	0.83	0.373	SPO0439	0.96	0.939	SPO0440	0.81	0.74	SPO0440	0.98	0.663	SPO0439	0.83	0.387	SPO0439	0.76	0.319	SPO0439	1.02	0.947	SPO0439	1.03	0.882
SPO0440	1.01	0.461	SPO0440	0.97	0.827	SPO0441	0.84	0.288	SPO0441	0.99	0.023	SPO0440	0.94	0.421	SPO0440	0.92	0.402	SPO0440	1.25	0.318	SPO0440	1.27	0.067
SPO0441	0.83	0.73	SPO0441	0.95	0.721	SPO0442	0.76	0.019	SPO0442	0.93	0.005	SPO0441	1.08	0.641	SPO0441	0.95	0.532	SPO0441	1.12	0.839	SPO0441	1.17	0.528
SPO0442	1.28	0.029	SPO0442	1.21	0.029	SPO0443	0.62	0.038	SPO0443	0.81	0.026	SPO0442	0.60	0.000	SPO0442	0.62	0.000	SPO0442	0.98	0.010	SPO0442	1.05	0.560
SPO0443	1.09	0.528	SPO0443	1.11	0.155	SPO0444	0.89	0.44	SPO0444	0.85	0.463	SPO0443	0.58	0.066	SPO0443	0.56	0.054	SPO0443	0.90	0.741	SPO0443	0.87	0.318
SPO0444	0.89	0.614	SPO0444	0.85	0.670	SPO0445	0.79	0.8	SPO0445	0.99	0.889	SPO0444	1.39	0.234	SPO0444	1.29	0.289	SPO0444	0.99	0.999	SPO0444	0.93	0.776
SPO0445	1.14	0.644	SPO0445	1.51	0.546	SPO0446	0.81	0.25	SPO0446	0.93	0.35	SPO0445	3.19	0.019	SPO0445	0.52	0.006	SPO0445	0.83	0.482	SPO0445	0.89	0.782
SPO0446	0.95	0.642	SPO0446	1.02	0.469	SPO0447	0.74	0.633	SPO0447	0.93	0.326	SPO0446	1.11	0.027	SPO0446	1.16	0.007	SPO0446	1.01	0.882	SPO0446	1.03	0.806
SPO0447	0.88	0.582	SPO0447	0.98	0.175	SPO0448	0.72	0.922	SPO0448	0.87	0.929	SPO0447	2.22	0.000	SPO0447	2.25	0.000	SPO0447	1.27	0.809	SPO0447	1.31	0.012
SPO0448	1	0.98	SPO0448	0.97	0.959	SPO0449	0.83	0.628	SPO0449	0.9	0.645	SPO0448	0.71	0.769	SPO0448	0.74	0.832	SPO0448	0.81	0.809	SPO0448	0.88	0.876
SPO0449	1.51	0.381	SPO0449	1.31	0.524	SPO0450	0.89	0.508	SPO0450	0.93	0.541	SPO0449	0.74	0.636	SPO0449	0.79	0.747	SPO0449	0.93	0.907	SPO0449	0.98	0.987
SPO0450	1.62	0.064	SPO0450	1.43	0.123	SPO0451	0.71	0.159	SPO0451	0.93	0.144	SPO0450	0.68	0.056	SPO0450	0.73	0.156	SPO0450	1.07	0.834	SPO0450	1.18	0.442
SPO0451	0.98	0.993	SPO0451	0.93	0.733	SPO0452	0.91	0.785	SPO0452	0.19	0.818	SPO0451	0.70	0.122	SPO0451	0.70	0.122	SPO0451	0.87	0.675	SPO0451	0.83	0.439
SPO0452	1.11	0.011	SPO0452	1.19	0.011	SPO0453	0.81	0.016	SPO0453	0.81	0.016	SPO0452	0.80	0.013	SPO0452	0.81	0.013	SPO0452	0.93	0.529	SPO0452	0.93	0.529
SPO0453	1.17	0.174	SPO0453	1.18	0.016	SPO0454	0.92	0.995	SPO0454	0.98	0.744	SPO0453	0.83	0.170	SPO0453	0.96	0.021	SPO0453	1.23	0.334	SPO0453	1.18	0.422
SPO0454	1.04	0.647	SPO0454	1.02	0.612	SPO0455	0.78	0.891	SPO0455	0.75	0.998	SPO0454	0.89	0.572	SPO0454	0.95	0.775	SPO0454	0.90	0.417	SPO0454	0.88	0.384
SPO0455	1.2	0.446	SPO0455	1.16	0.694	SPO0456	0.83	0.39	SPO0456	0.91	0.458	SPO0455	1.32	0.291	SPO0455	1.44	0.291	SPO0455	1.18	0.679	SPO0455	1.12	0.700
SPO0456	0.9	0.703	SPO0456	0.85	0.057	SPO0457	0.97	0.927	SPO0457	0.72	0.953	SPO0456	1.79	0.028	SPO0456	0.82	0.108	SPO0456	0.93	0.359	SPO0456	0.92	0.504
SPO0457	0.88	0.334	SPO0457	1.01	0.668	SPO0458	0.91	0.227	SPO0458	0.65	0.469	SPO0457	0.87	0.800	SPO0457	0.87	0.800	SPO0457	1.16	0.296	SPO0457	1.13	0.280
SPO0458	1.14	0.52	SPO0458	1.23	0.423	SPO0459	0.69	0.596	SPO0459	0.89	0.605	SPO0458	0.82	0.260	SPO0458	0.75	0.221	SPO0458	0.94	0.682	SPO0458	0.81	0.443
SPO0459	0.95	0.001	SPO0459	0.95	0.001	SPO0460	0.54	0.269	SPO0460	0.76	0.244	SPO0459	0.39	0.009	SPO0459	0.43	0.011	SPO0459	0.83	0.375	SPO0459	0.84	0.547
SPO0460	1.30	0.011	SPO0460	1.19	0.011	SPO0461	0.81	0.016	SPO0461	0.81	0.016	SPO0460	0.80	0.013	SPO0460	0.81	0.013	SPO0460	0.98	0.914	SPO0460	0.99	0.923
SPO0461	0.73	0.011	SPO0461	0.81	0.033	SPO0462	0.86	0.99	SPO0462	0.71	0.289	SPO0461	1.59	0.002	SPO0461	1.68	0.000	SPO0461	0.98	0.656	SPO0461	0.88	0.022
SPO0462	0.91	0.168	SPO0462	0.91	0.617	SPO0463	0.96	0.089	SPO0463	0.64	0.064	SPO0462	3.17	0.000	SPO0462	3.15	0.000	SPO0462	0.95	0.252	SPO0462	0.92	0.370
SPO0463	0.82	0.038	SPO0463	0.83	0.007	SPO0464	0.93	0.467	SPO0464	0.83	0.044	SPO0463	1.29	0.002	SPO0463	1.34	0.000	SPO0463	1.14	0.090	SPO0463	1.12	0.093
SPO0464	0.78	0.052	SPO0464	0.82	0.022	SPO0465	0.83	0.661	SPO0465	0.85	0.888	SPO0464	0.86	0.652	SPO0464	0.96	0.699	SPO0464	0.93	0.730	SPO0464	0.92	0.483
SPO0465	1.02	0.12	SPO0465	0.98	0.661	SPO0466	0.69	0.999	SPO0466	0.68	0.791	SPO0465	1.10	0.891	SPO0465	1.30	0.064	SPO0465	1.14	0.525	SPO0465	1.07	0.322
SPO0466	1.03	0.84	SPO0466	0.96	0.927	SPO0467	0.83	0.847	SPO0467	0.91	0.847	SPO0466	0.96	0.860	SPO0466	1.06	0.990	SPO0466	1.06	0.990	SPO0466	1.06	0.990
SPO0467	1.1	0.676	SPO0467	1.01	0.827	SPO0468	0.56	0.928	SPO0468	0.99	0.847	SPO0467	1.11	0.888	SPO0467	1.13	0.850	SPO0467	0.85	0.683	SPO0467	0.85	0.716
SPO0468	0.98	0.064	SPO0468	0.98	0.978	SPO0469	0.86	0.933	SPO0469	0.86	0.977	SPO0468	0.91	0.554	SPO0468	0.95	0.922	SPO0468	0.99	0.914	SPO0468	0.99	0.923
SPO0469	0.76	0.129	SPO0469	0.75	0.105	SPO0470	0.68	0.988	SPO0470	0.92	0.383	SPO0469	1.06	0.797	SPO0469	0.93	0.544	SPO0469	0.94	0.745	SPO0469	0.96	0.790
SPO0470	0.69	0.008	SPO0470	0.84	0.229	SPO0471	0.97	0.778	SPO0471	0.99	0.881	SPO0470	1.75	0.050	SPO0470	2.14	0.000	SPO0470	1.17	0.583	SPO0470	1.20	0.434
SPO0471	0.93	0.844	SPO0471	0.98	0.854	SPO0472	0.85	0.777	SPO0472	0.71	0.799	SPO0471	0.95	0.711	SPO0471	0.88	0.496	SPO0471	0.89	0.426	SPO0471	0.94	0.805
SPO0472	0.93	0.801	SPO0472	0.89	0.295	SPO0473	0.72	0.569	SPO0473	0.83	0.37	SPO0472	1.20	0.263	SPO0472	1.01	0.059	SPO0472	1.01	0.944	SPO0472	1.07	0.635
SPO0473	1.14	0.107	SPO0473	1.04	0.253	SPO0474	0.92	0.669	SPO0474	0.85	0.547	SPO0473	1.19	0.390	SPO0473	1.44	0.024	SPO0473	0.99	0.583	SPO0473	1.07	0.583
SPO0474	1.13	0.527	SPO0474	1.06	0.653	SPO0475	0.97	0.646	SPO0475	1.02	0.575	SPO0474	0.83	0.555	SPO0474	0.88	0.584	SPO0474	0.87	0.686	SPO0474	0.88	0.703
SPO0475	1.21	0.203	SPO0475	1.25	0.052	SPO0476	0.86	0.85	SPO0476	0.78	0.789	SPO0475	1.06	0.703	SPO0475	1.21	0.137	SPO0475	1.25	0.116	SPO0475	1.25	0.063
SPO0476	1.19	0.056	SPO0476	1.12	0.11																		

SPO0566	0.75	0.017	SPO0566	0.81	0.06	SPO0567	0.8	0.346	SPO0567	0.65	0.558	SPO0566	0.78	0.078	SPO0566	0.76	0.013	SPO0566	0.98	0.829	SPO0566	0.99	0.889
SPO0567	1.26	0.326	SPO0567	1.14	0.072	SPO0568	0.81	0.245	SPO0568	0.74	0.227	SPO0567	0.88	0.268	SPO0567	1.03	0.840	SPO0567	1.05	0.907	SPO0567	0.99	0.816
SPO0568	1.12	0.326	SPO0568	0.95	0.852	SPO0569	0.95	0.728	SPO0569	0.88	0.327	SPO0568	0.81	0.030	SPO0568	0.72	0.099	SPO0568	1.06	0.953	SPO0568	0.86	0.605
SPO0569	0.98	0.137	SPO0570	0.98	0.137	SPO0570	0.98	0.137	SPO0570	0.98	0.137	SPO0569	0.98	0.137	SPO0569	0.98	0.137	SPO0569	0.98	0.137	SPO0569	0.98	0.137
SPO0570	0.98	0.784	SPO0570	1.07	0.317	SPO0571	0.92	0.368	SPO0571	0.94	0.305	SPO0570	0.98	0.615	SPO0570	1.04	0.979	SPO0570	1.25	0.585	SPO0570	1.11	0.759
SPO0571	0.66	0.456	SPO0571	0.63	0.491	SPO0572	0.93	0.711	SPO0572	0.78	0.711	SPO0571	3.38	0.015	SPO0571	2.37	0.133	SPO0571	1.19	0.748	SPO0571	1.23	0.711
SPO0572	1.26	0.014	SPO0572	1.07	0.477	SPO0573	0.85	0.069	SPO0573	0.82	0.015	SPO0572	0.87	0.335	SPO0572	0.80	0.156	SPO0572	0.93	0.556	SPO0572	0.96	0.818
SPO0573	2.13	0.011	SPO0573	1.93	0.009	SPO0574	0.82	0.72	SPO0574	0.82	0.014	SPO0573	0.41	0.003	SPO0573	0.40	0.003	SPO0573	1.17	0.323	SPO0573	1.06	0.568
SPO0574	0.81	0.259	SPO0574	0.83	0.296	SPO0575	0.74	0.162	SPO0575	0.75	0.256	SPO0574	0.88	0.742	SPO0574	0.99	0.729	SPO0574	0.97	0.879	SPO0574	0.88	0.381
SPO0575	1.03	0.666	SPO0575	1.06	0.728	SPO0576	0.85	0.124	SPO0576	0.87	0.038	SPO0575	0.68	0.153	SPO0575	0.61	0.077	SPO0575	0.76	0.262	SPO0575	0.74	0.160
SPO0576	0.66	0.008	SPO0576	0.73	0.009	SPO0577	0.93	0.721	SPO0577	0.95	0.527	SPO0576	1.30	0.079	SPO0576	1.33	0.083	SPO0576	0.98	0.859	SPO0576	0.99	0.951
SPO0577	0.98	0.773	SPO0577	1.01	0.559	SPO0578	0.78	0.303	SPO0578	0.96	0.258	SPO0577	1.00	0.794	SPO0577	0.98	0.204	SPO0577	1.04	0.991	SPO0577	1.01	0.694
SPO0578	1.15	0.006	SPO0578	1.13	0.061	SPO0579	0.88	0.904	SPO0579	0.93	0.826	SPO0578	0.95	0.054	SPO0578	0.96	0.380	SPO0578	0.96	0.384	SPO0578	0.96	0.223
SPO0579	1.17	0.736	SPO0579	1.17	0.775	SPO0580	0.89	0.823	SPO0580	1.02	0.966	SPO0579	0.90	0.911	SPO0579	0.88	0.906	SPO0579	0.98	0.976	SPO0579	1.01	0.981
SPO0580	0.76	0.324	SPO0580	0.81	0.664	SPO0581	0.91	0.391	SPO0581	0.81	0.557	SPO0580	0.67	0.386	SPO0580	0.57	0.212	SPO0580	0.79	0.336	SPO0580	0.89	0.731
SPO0581	0.75	0.205	SPO0581	0.78	0.408	SPO0582	0.81	0.295	SPO0582	0.81	0.446	SPO0581	1.14	0.181	SPO0581	1.09	0.301	SPO0581	0.88	0.332	SPO0581	0.91	0.625
SPO0582	0.8	0.153	SPO0582	0.88	0.74	SPO0583	0.95	0.364	SPO0583	0.85	0.486	SPO0582	0.68	0.034	SPO0582	0.75	0.207	SPO0582	0.78	0.086	SPO0582	0.83	0.241
SPO0583	0.77	0.298	SPO0583	0.72	0.294	SPO0584	0.78	0.413	SPO0584	0.87	0.18	SPO0583	0.97	0.945	SPO0583	0.89	0.631	SPO0583	0.97	0.810	SPO0583	0.98	0.892
SPO0584	1.15	0.089	SPO0584	1.16	0.072	SPO0585	0.74	0.937	SPO0585	0.69	0.863	SPO0584	0.70	0.025	SPO0584	0.64	0.017	SPO0584	0.97	0.321	SPO0584	0.79	0.070
SPO0585	1.19	0.32	SPO0585	1.17	0.461	SPO0586	0.95	0.011	SPO0586	0.85	0.036	SPO0585	0.79	0.443	SPO0585	0.88	0.605	SPO0585	1.12	0.753	SPO0585	0.98	0.872
SPO0586	0.77	0.063	SPO0586	0.83	0.028	SPO0587	0.73	0.028	SPO0587	0.99	0.016	SPO0586	1.64	0.008	SPO0586	1.63	0.002	SPO0586	0.88	0.429	SPO0586	1.05	0.691
SPO0587	0.87	0.538	SPO0587	0.78	0.028	SPO0588	0.93	0.98	SPO0588	0.98	0.969	SPO0587	1.31	0.214	SPO0587	1.58	0.006	SPO0587	0.88	0.714	SPO0587	0.93	0.742
SPO0588	0.78	0.71	SPO0588	0.83	0.862	SPO0589	0.83	0.92	SPO0589	0.87	0.821	SPO0588	1.46	0.544	SPO0588	1.32	0.667	SPO0588	1.04	0.973	SPO0588	1.02	0.991
SPO0589	0.81	0.554	SPO0589	0.86	0.784	SPO0590	0.93	0.055	SPO0590	0.86	0.387	SPO0589	0.93	0.762	SPO0589	0.89	0.676	SPO0589	0.98	0.839	SPO0589	0.94	0.465
SPO0590	1.55	0.049	SPO0590	1.55	0.013	SPO0591	0.93	0.011	SPO0591	0.98	0.025	SPO0590	1.05	0.093	SPO0590	1.11	0.823	SPO0590	1.17	0.385	SPO0590	1.03	0.984
SPO0591	1.08	0.262	SPO0591	1.05	0.101	SPO0592	0.74	0.627	SPO0592	0.69	0.161	SPO0591	1.85	0.006	SPO0591	1.96	0.000	SPO0591	1.96	0.000	SPO0591	0.91	0.141
SPO0592	0.92	0.883	SPO0592	0.98	0.881	SPO0593	0.72	0.934	SPO0593	0.84	0.971	SPO0592	0.93	0.885	SPO0592	0.88	0.587	SPO0592	1.01	0.932	SPO0592	1.05	0.821
SPO0593	0.99	0.813	SPO0593	0.98	0.918	SPO0594	0.99	0.188	SPO0594	0.97	0.024	SPO0593	1.18	0.555	SPO0593	1.12	0.790	SPO0593	0.88	0.366	SPO0593	0.84	0.044
SPO0594	0.81	0.034	SPO0594	0.81	0.034	SPO0595	0.94	0.541	SPO0595	0.94	0.541	SPO0594	1.17	0.004	SPO0594	1.17	0.004	SPO0594	1.14	0.781	SPO0594	1.01	0.716
SPO0595	1.09	0.168	SPO0595	1.09	0.025	SPO0596	0.85	0.204	SPO0596	0.74	0.002	SPO0595	1.55	0.243	SPO0595	1.60	0.011	SPO0595	0.92	0.402	SPO0595	0.88	0.223
SPO0596	0.85	0.387	SPO0596	0.95	0.815	SPO0597	0.99	0.678	SPO0597	0.86	0.807	SPO0596	1.96	0.001	SPO0596	1.99	0.000	SPO0596	1.14	0.554	SPO0596	1.10	0.448
SPO0597	0.78	0.354	SPO0597	0.8	0.378	SPO0598	0.94	0.384	SPO0598	0.95	0.087	SPO0597	1.13	0.611	SPO0597	0.87	0.509	SPO0597	0.92	0.430	SPO0597	0.93	0.748
SPO0598	0.75	0.186	SPO0598	0.87	0.691	SPO0599	0.97	0.459	SPO0599	0.89	1.02	SPO0598	0.86	0.955	SPO0598	0.83	0.893	SPO0598	0.93	0.928	SPO0598	1.03	0.768
SPO0599	1.06	0.512	SPO0599	1.1	0.24	SPO0600	0.98	0.178	SPO0600	0.78	0.121	SPO0599	1.06	0.499	SPO0599	1.11	0.262	SPO0599	1.14	0.582	SPO0599	1.15	0.207
SPO0600	0.62	0.038	SPO0600	0.53	0.037	SPO0601	0.98	0.035	SPO0601	0.76	0.071	SPO0600	2.38	0.036	SPO0600	2.38	0.036	SPO0600	1.13	0.727	SPO0600	1.16	0.674
SPO0601	0.85	0.016	SPO0601	0.88	0.138	SPO0602	0.9	0.172	SPO0602	0.88	0.028	SPO0601	1.09	0.51	SPO0601	1.10	0.209	SPO0601	1.10	0.420	SPO0601	1.10	0.188
SPO0602	0.95	0.028	SPO0602	0.92	0.066	SPO0603	0.96	0.688	SPO0603	0.96	0.688	SPO0602	1.02	0.202	SPO0602	1.02	0.202	SPO0602	1.15	0.253	SPO0602	1.15	0.253
SPO0603	0.75	0.136	SPO0603	0.83	0.445	SPO0604	0.83	0.4	SPO0604	0.97	0.097	SPO0603	1.77	0.035	SPO0603	2.14	0.015	SPO0603	1.12	0.425	SPO0603	1.13	0.750
SPO0604	0.68	0.001	SPO0604	0.67	0.001	SPO0605	0.96	0.067	SPO0605	0.75	0.177	SPO0604	1.48	0.002	SPO0604	1.58	0.000	SPO0604	0.89	0.328	SPO0604	0.98	0.822
SPO0605	0.75	0.048	SPO0605	0.85	0.12	SPO0606	0.96	0.653	SPO0606	0.87	0.873	SPO0605	1.98	0.003	SPO0605	1.71	0.001	SPO0605	0.90	0.328	SPO0605	0.97	0.627
SPO0606	0.7	0.045	SPO0606	0.76	0.233	SPO0607	0.93	0.87	SPO0607	0.83	0.764	SPO0606	1.22	0.205	SPO0606	1.31	0.244	SPO0606	0.99	0.879	SPO0606	0.97	0.755
SPO0607	0.85	0.742	SPO0607	0.76	0.176	SPO0608	0.97	0.896	SPO0608	0.92	0.797	SPO0607	0.94	0.979	SPO0607	0.99	0.955	SPO0607	0.94	0.882	SPO0607	1.00	0.996
SPO0608	0.94	0.985	SPO0608	0.86	0.74	SPO0609	0.98	0.725	SPO0609	0.9	0.983	SPO0608	3.01	0.002	SPO0608	2.78	0.000	SPO0608	0.13	0.002	SPO0608	0.15	0.000
SPO0609	0.97	0.815	SPO0609	0.96	0.882	SPO0610	0.95	0.957	SPO0610	0.72	0.538	SPO0609	1.06	0.976	SPO0609	1.21	0.476	SPO0609	0.99	0.900	SPO0609	0.92	0.001
SPO0610	1.11	0.78	SPO0610	1.12	0.443	SPO0611	0.93	0.275	SPO0611	0.76	0.344	SPO0610	0.96	0.808	SPO0610	0.97	0.664	SPO0610	0.98	0.863	SPO0610	0.95	0.825
SPO0611	0.81	0.643	SPO0611	0.84	0.577	SPO0612	0.87	0.934	SPO0612	0.96	0.721	SPO0611	1.13	0.587	SPO0611	1.07	0.970	SPO0611	1.07	0.970	SPO0611	1.07	0.970
SPO0612	0.9	0.62	SPO0612	0.9	0.621	SPO0613	0.81	0.204	SPO0613	0.88	0.415	SPO0612	1.02	0.882	SPO0612	0.94	0.193	SPO0612	0.92	0.009	SPO0612	0.92	0.001
SPO0613	1.06	0.356	SPO0613	1.03	0.498	SPO0614	0.63	0.027	SPO0614	0.87	0.035	SPO0613	0.96	0.280	SPO0613	0.95	0.292	SPO0613	0.95	0.292	SPO0613	0.95	0.292
SPO0614	0.88	0.15	SPO0614	0.84	0.224	SPO0615	0.92	0.001	SPO0615	0.95	0.002	SPO0614	0.56	0.001	SPO0614	0.53	0.001	SPO0614	0.57	0.001	SPO0614	0.57	0.000
SPO0615	1.14	0.022	SPO0615	0.99	0.734	SPO0616	0.88	0.873	SPO0616	0.9	0.505	SPO0615	0.54	0.001	SPO0615	0.56	0.000	SPO0615	0.61	0.003	SPO0615	0.61	0.001
SPO0616	1.25	0.006	SPO0616	1.06	0.045	SPO0617	0.76	0.415	SPO0617	0.96	0.608	SPO0616	0.56	0.002	SPO0616	0.56	0.000	SPO0616	1.00	0.830	SPO0616	1.00	0.958
SPO0617	0.67	0.264	SPO0617	0.72	0.259	SPO0618	0.98	0.691	SPO0618	0.97	0.548	SPO0617	0.79	0.351	SPO0617	0.77	0.383	SPO0617	0.81	0.256	SPO0617	0.83	0.610
SPO0618	0.91	0.408	SPO0618	0.91																			

SPO0711	1.15	0.14	SPO0711	1.13	0.573	SPO0712	0.78	0.592	SPO0712	0.84	0.897	SPO0711	0.86	0.804	SPO0711	0.91	0.934	SPO0711	0.90	0.421	SPO0711	0.86	0.567
SPO0712	0.84	0.536	SPO0712	0.9	0.874	SPO0713	0.89	0.723	SPO0713	0.96	0.801	SPO0712	1.40	0.253	SPO0712	1.40	0.422	SPO0712	0.95	0.875	SPO0712	1.03	0.958
SPO0713	1.17	0.36	SPO0713	1.2	0.215	SPO0714	0.93	0.51	SPO0714	0.84	0.024	SPO0713	1.24	0.155	SPO0713	1.31	0.094	SPO0713	1.15	0.500	SPO0713	1.14	0.840
SPO0714	0.54	0.98	SPO0714	0.66	0.208	SPO0715	0.79	0.343	SPO0715	0.78	0.411	SPO0714	1.01	0.334	SPO0714	1.39	0.044	SPO0714	0.95	0.943	SPO0714	1.06	0.943
SPO0715	0.89	0.129	SPO0715	0.96	0.81	SPO0716	0.86	0.862	SPO0716	0.93	0.865	SPO0715	1.07	0.167	SPO0715	1.04	0.155	SPO0715	1.02	0.695	SPO0715	1.05	0.952
SPO0716	1.27	0.277	SPO0716	1.29	0.277	SPO0717	0.17	0.232	SPO0717	0.96	0.284	SPO0716	1.02	0.706	SPO0716	0.98	0.719	SPO0716	1.06	0.842	SPO0716	1.04	0.878
SPO0717	0.96	0.309	SPO0717	0.88	0.278	SPO0718	0.53	0.996	SPO0718	0.93	0.789	SPO0717	0.95	0.647	SPO0717	1.03	0.241	SPO0717	0.97	0.845	SPO0717	0.98	0.923
SPO0718	0.96	0.955	SPO0718	1.1	0.911	SPO0719	0.71	0.175	SPO0719	0.69	0.853	SPO0718	0.56	0.306	SPO0718	0.48	0.125	SPO0718	0.53	0.204	SPO0718	0.57	0.908
SPO0719	2.06	0	SPO0719	1.74	0	SPO0720	0.93	0.08	SPO0720	0.99	0.031	SPO0719	0.87	0.864	SPO0719	0.85	0.444	SPO0719	1.16	0.235	SPO0719	1.07	0.329
SPO0720	1.06	0.607	SPO0720	1.07	0.217	SPO0721	0.75	0.206	SPO0721	1.01	0.26	SPO0720	1.18	0.001	SPO0720	1.27	0.001	SPO0720	1.11	0.036	SPO0720	1.09	0.039
SPO0721	1.26	0.095	SPO0721	1.13	0.013	SPO0722	0.88	0.49	SPO0722	0.95	0.461	SPO0721	0.89	0.260	SPO0721	0.96	0.324	SPO0721	1.08	0.819	SPO0721	1.14	0.025
SPO0722	1.59	0.023	SPO0722	1.5	0.023	SPO0723	0.94	0.733	SPO0723	0.94	0.584	SPO0722	0.74	0.536	SPO0722	0.74	0.511	SPO0722	1.03	0.943	SPO0722	1.06	0.942
SPO0723	1.01	0.97	SPO0723	0.88	0.833	SPO0724	0.97	0.917	SPO0724	0.9	0.823	SPO0723	1.28	0.340	SPO0723	1.38	0.282	SPO0723	0.97	0.984	SPO0723	0.97	0.999
SPO0724	0.94	0.901	SPO0724	0.98	0.931	SPO0725	0.96	0.824	SPO0725	0.93	0.3	SPO0724	1.14	0.509	SPO0724	1.15	0.482	SPO0724	1.07	0.831	SPO0724	1.01	0.959
SPO0725	0.78	0.398	SPO0725	0.78	0.991	SPO0726	0.99	0.559	SPO0726	0.92	0.151	SPO0725	1.27	0.639	SPO0725	1.42	0.294	SPO0725	1.32	0.367	SPO0725	1.05	0.935
SPO0726	1.1	0.949	SPO0726	0.99	0.812	SPO0727	0.9	0.03	SPO0727	0.99	0.535	SPO0726	1.50	0.051	SPO0726	1.47	0.000	SPO0726	1.10	0.657	SPO0726	1.07	0.405
SPO0727	1.08	1.91	SPO0727	1.05	0.642	SPO0728	0.92	0.079	SPO0728	0.97	0.117	SPO0727	1.83	0.000	SPO0727	2.03	0.000	SPO0727	1.06	0.375	SPO0727	1.06	0.626
SPO0728	1.13	0.621	SPO0728	0.99	0.801	SPO0729	0.72	0.584	SPO0729	1	0.937	SPO0728	1.02	0.031	SPO0728	1.00	0.042	SPO0728	1.10	0.384	SPO0728	1.19	0.000
SPO0729	1.58	0.000	SPO0729	1.37	0.003	SPO0731	0.8	0.289	SPO0731	0.98	0.747	SPO0729	1.07	0.244	SPO0729	1.08	0.124	SPO0729	0.83	0.040	SPO0729	0.93	0.555
SPO0731	1.23	0.081	SPO0731	1.27	0.002	SPO0732	0.93	0.466	SPO0732	0.81	0.413	SPO0731	1.83	0.003	SPO0731	1.20	0.031	SPO0731	1.10	0.743	SPO0731	1.00	0.931
SPO0732	1.1	0.829	SPO0732	1.04	0.446	SPO0733	0.75	0.132	SPO0733	0.78	0.067	SPO0732	1.10	0.596	SPO0732	1.09	0.029	SPO0732	0.89	0.245	SPO0732	0.94	0.078
SPO0733	1.08	0.437	SPO0733	1.04	0.149	SPO0734	0.83	0.748	SPO0734	0.85	0.794	SPO0733	0.64	0.010	SPO0733	0.69	0.004	SPO0733	1.01	0.884	SPO0733	1.05	0.543
SPO0734	0.93	0.621	SPO0734	0.93	0.719	SPO0735	0.67	0.115	SPO0735	1.01	0.443	SPO0734	0.72	0.120	SPO0734	0.77	0.109	SPO0734	1.04	0.827	SPO0734	1.02	0.843
SPO0735	0.78	0.129	SPO0735	0.81	0.378	SPO0736	0.67	0.877	SPO0736	0.71	0.832	SPO0735	1.13	0.627	SPO0735	0.98	0.561	SPO0735	1.02	0.996	SPO0735	1.10	0.573
SPO0736	0.97	0.988	SPO0736	0.89	0.956	SPO0737	0.76	0.953	SPO0737	0.78	0.477	SPO0736	0.89	0.919	SPO0736	0.80	0.825	SPO0736	0.77	0.796	SPO0736	0.80	0.827
SPO0737	1.09	0.395	SPO0737	1	0.541	SPO0738	0.8	0.41	SPO0738	0.96	1.229	SPO0737	1.22	0.491	SPO0737	0.98	0.233	SPO0737	0.98	0.783	SPO0737	0.93	0.565
SPO0738	0.79	0.256	SPO0738	0.82	0.09	SPO0739	0.89	0.787	SPO0739	0.7	0.479	SPO0738	1.70	0.057	SPO0738	1.57	0.015	SPO0738	1.08	0.696	SPO0738	1.11	0.512
SPO0739	0.7	0.032	SPO0739	0.81	0.593	SPO0740	0.93	0.736	SPO0740	0.97	0.906	SPO0739	1.20	0.753	SPO0739	0.98	0.849	SPO0739	0.87	0.596	SPO0739	0.96	0.879
SPO0740	0.83	0.03	SPO0740	0.81	0.819	SPO0741	0.72	0.72	SPO0741	0.81	0.378	SPO0740	0.74	0.533	SPO0740	0.75	0.448	SPO0740	1.12	0.581	SPO0740	1.11	0.913
SPO0741	0.62	0.015	SPO0741	0.74	0.493	SPO0742	0.85	0.236	SPO0742	0.91	0.096	SPO0741	0.88	0.498	SPO0741	0.88	0.608	SPO0741	0.77	0.055	SPO0741	0.79	0.022
SPO0742	0.67	0.013	SPO0742	0.72	0.039	SPO0743	0.91	0.025	SPO0743	0.75	0.274	SPO0742	0.93	0.806	SPO0742	1.05	0.162	SPO0742	1.05	0.797	SPO0742	1.07	0.540
SPO0743	0.99	0.849	SPO0743	1.02	0.425	SPO0744	0.77	0.109	SPO0744	0.96	0.315	SPO0743	1.27	0.003	SPO0743	1.39	0.027	SPO0743	1.17	0.523	SPO0743	1.13	0.576
SPO0744	0.73	0.316	SPO0744	0.78	0.147	SPO0745	0.91	0.158	SPO0745	0.94	0.199	SPO0744	1.03	0.979	SPO0744	1.14	0.450	SPO0744	1.24	0.441	SPO0744	1.17	0.529
SPO0745	0.64	0.078	SPO0745	0.68	0.019	SPO0746	0.88	0.019	SPO0746	0.94	0.044	SPO0745	1.30	0.077	SPO0745	1.37	0.047	SPO0745	1.15	0.339	SPO0745	1.14	0.471
SPO0746	0.6	0.014	SPO0746	0.66	0.001	SPO0747	0.94	0.27	SPO0747	0.82	0.143	SPO0746	1.23	0.082	SPO0746	1.26	0.011	SPO0746	0.95	0.010	SPO0746	1.05	0.733
SPO0747	0.81	0.69	SPO0747	0.9	0.676	SPO0748	0.61	0.855	SPO0748	0.93	0.787	SPO0747	0.88	0.95	SPO0747	0.97	0.451	SPO0747	0.91	0.455	SPO0747	0.93	0.431
SPO0748	0.93	0.951	SPO0748	0.81	0.818	SPO0749	0.78	0.78	SPO0749	0.85	0.85	SPO0748	0.85	0.85	SPO0748	0.85	0.85	SPO0748	0.85	0.85	SPO0748	0.85	0.85
SPO0749	1.05	0.548	SPO0749	0.8	0.064	SPO0750	0.98	0.827	SPO0750	0.7	0.957	SPO0749	1.14	0.832	SPO0749	1.08	0.547	SPO0749	1.34	0.116	SPO0749	0.96	0.699
SPO0750	0.99	0.97	SPO0750	0.92	0.962	SPO0751	0.86	0.585	SPO0751	0.78	0.628	SPO0750	0.66	0.701	SPO0750	0.60	0.630	SPO0750	0.86	0.877	SPO0750	0.87	0.862
SPO0751	1.28	0.418	SPO0751	1.03	0.827	SPO0752	0.98	0.304	SPO0752	0.97	0.278	SPO0751	1.17	0.516	SPO0751	1.07	0.718	SPO0751	1.12	0.804	SPO0751	1.08	0.821
SPO0752	1.01	0.903	SPO0752	0.99	0.955	SPO0753	0.85	0.371	SPO0753	0.76	0.397	SPO0752	0.90	0.892	SPO0752	0.89	0.889	SPO0752	1.26	0.416	SPO0752	1.26	0.476
SPO0753	0.76	0.518	SPO0753	0.75	0.458	SPO0754	0.93	0.009	SPO0754	0.83	0.009	SPO0753	0.75	0.466	SPO0753	0.74	0.392	SPO0753	0.98	0.946	SPO0753	1.07	0.817
SPO0754	0.6	0.006	SPO0754	0.68	0.01	SPO0755	0.76	0.616	SPO0755	0.7	0.662	SPO0754	1.04	0.761	SPO0754	1.13	0.259	SPO0754	1.23	0.109	SPO0754	1.23	0.183
SPO0755	0.75	0.531	SPO0755	0.78	0.728	SPO0756	0.85	0.072	SPO0756	0.64	0.033	SPO0755	0.88	0.894	SPO0755	0.81	0.771	SPO0755	1.13	0.817	SPO0755	1.18	0.706
SPO0756	0.82	0.03	SPO0756	0.81	0.711	SPO0757	1	0.171	SPO0757	0.81	0.171	SPO0756	0.98	0.516	SPO0756	0.85	0.341	SPO0756	1.12	0.581	SPO0756	1.11	0.913
SPO0757	0.62	0.005	SPO0757	0.67	0.008	SPO0758	0.95	0.722	SPO0758	0.99	0.782	SPO0757	0.85	0.324	SPO0757	0.81	0.191	SPO0757	0.56	0.902	SPO0757	1.06	0.484
SPO0758	0.93	0.913	SPO0758	0.94	0.939	SPO0759	0.85	0.004	SPO0759	0.96	0.402	SPO0758	0.58	0.033	SPO0758	0.65	0.028	SPO0758	0.65	0.468	SPO0758	0.88	0.388
SPO0759	1.13	0.308	SPO0759	1.09	0.213	SPO0760	0.92	0.689	SPO0760	0.8	0.534	SPO0759	1.12	0.000	SPO0759	1.11	0.000	SPO0759	1.23	0.016	SPO0759	1.15	0.163
SPO0760	0.83	0.557	SPO0760	0.86	0.621	SPO0761	0.84	0.51	SPO0761	0.93	0.004	SPO0760	1.77	0.027	SPO0760	1.14	0.080	SPO0760	1.14	0.542	SPO0760	1.07	0.772
SPO0761	0.41	0	SPO0761	0.45	0	SPO0762	0.99	0.134	SPO0762	0.87	0.118	SPO0761	2.31	0.000	SPO0761	2.35	0.000	SPO0761	1.04	0.423	SPO0761	1.16	0.005
SPO0762	1.16	0.09	SPO0762	1.11	0.028	SPO0763	0.85	0.249	SPO0763	0.81	0.25	SPO0762	0.76	0.017	SPO0762	0.80	0.048	SPO0762	0.98	0.774	SPO0762	0.93	0.328
SPO0763	0.76	0.117	SPO0763	0.87	0.598	SPO0764	0.91	0.157	SPO0764	0.85	0.345	SPO0763	1.40	0.102	SPO0763	1.43	0.083	SPO0763	1.29	0.324	SPO0763	1.15	0.641
SPO0764	0.93	0.951	SPO0764	0.91	0.587	SPO0765	0.93	0.071	SPO0765														

SPO0851	1.63	0.334	SPO0851	1.46	0.375	SPO0852	0.88	0.391	SPO0852	0.9	0.41	SPO0851	0.80	0.714	SPO0851	0.79	0.614	SPO0851	0.91	0.861	SPO0851	0.92	0.891	
SPO0852	1.05	0.663	SPO0852	1.03	0.63	SPO0853	0.91	0.23	SPO0853	0.94	0.998	SPO0852	1.13	0.474	SPO0852	1.19	0.249	SPO0852	1.07	0.732	SPO0852	1.16	0.286	
SPO0853	0.81	0.017	SPO0853	0.83	0.603	SPO0854	0.37	0.146	SPO0854	0.98	0.446	SPO0853	1.58	0.066	SPO0853	1.47	0.064	SPO0853	1.10	0.541	SPO0853	1.04	0.880	
SPO0854	0.97	0.1	SPO0854	0.7	0.72	SPO0855	0.98	0.38	SPO0855	0.94	0.938	SPO0854	1.1	0.713	SPO0854	1.2	0.45	SPO0854	1.24	0.05	SPO0854	1.24	0.05	
SPO0855	0.74	0.54	SPO0855	0.9	0.844	SPO0856	0.91	0.703	SPO0856	0.73	0.712	SPO0855	0.90	0.02	SPO0855	0.78	0.502	SPO0855	0.59	0.035	SPO0855	0.53	0.122	
SPO0856	0.86	0.875	SPO0856	0.9	0.934	SPO0857	0.97	0.804	SPO0857	0.97	0.808	SPO0856	0.98	0.780	SPO0856	0.93	0.731	SPO0856	0.63	0.236	SPO0856	0.67	0.334	
SPO0857	1.02	0.562	SPO0857	0.93	0.811	SPO0858	0.56	0.59	SPO0858	0.74	0.888	SPO0857	0.97	0.400	SPO0857	0.83	0.219	SPO0857	0.95	0.814	SPO0857	0.85	0.490	
SPO0858	0.84	0.709	SPO0858	0.89	0.585	SPO0859	0.91	0.825	SPO0859	0.81	0.545	SPO0858	0.98	0.005	SPO0858	0.97	0.001	SPO0858	1.11	0.674	SPO0858	1.16	0.572	
SPO0859	0.85	0.186	SPO0859	0.89	0.527	SPO0860	0.81	0.974	SPO0860	0.76	0.734	SPO0859	1.45	0.018	SPO0859	1.53	0.005	SPO0859	1.19	0.449	SPO0859	1.12	0.406	
SPO0860	0.99	0.982	SPO0860	0.96	0.991	SPO0861	0.83	0.184	SPO0861	0.99	0.149	SPO0860	0.98	0.782	SPO0860	0.97	0.796	SPO0860	0.99	0.983	SPO0860	0.98	0.987	
SPO0861	0.9	0.879	SPO0861	0.85	0.116	SPO0862	0.94	0.393	SPO0862	0.79	0.045	SPO0861	1.73	0.009	SPO0861	1.72	0.009	SPO0861	0.93	0.734	SPO0861	0.81	0.151	
SPO0862	0.97	0.229	SPO0862	0.74	0.07	SPO0863	0.98	0.873	SPO0863	0.94	0.938	SPO0862	0.79	0.714	SPO0862	0.90	0.447	SPO0862	0.87	0.585	SPO0862	0.87	0.585	
SPO0863	1.15	0.407	SPO0863	1.08	0.539	SPO0864	0.93	0.981	SPO0864	0.76	0.896	SPO0863	1.17	0.409	SPO0863	1.21	0.417	SPO0863	0.92	0.686	SPO0863	0.96	0.619	
SPO0864	1.38	0.802	SPO0864	1.32	0.815	SPO0865	0.97	0.933	SPO0865	0.85	0.855	SPO0864	1.45	0.760	SPO0864	1.44	0.751	SPO0864	1.10	0.963	SPO0864	1.19	0.909	
SPO0865	1.31	0.568	SPO0865	1.14	0.7	SPO0866	0.9	0.27	SPO0866	0.98	0.382	SPO0865	0.84	0.753	SPO0865	0.94	0.888	SPO0865	0.84	0.714	SPO0865	0.86	0.696	
SPO0866	1.25	0.123	SPO0866	1.26	0.157	SPO0867	0.96	0.024	SPO0867	0.82	0.308	SPO0866	1.11	0.367	SPO0866	1.31	0.036	SPO0866	1.23	0.355	SPO0866	1.09	0.615	
SPO0867	1.04	0.729	SPO0867	1.09	0.405	SPO0868	0.74	0.34	SPO0868	0.85	0.89	SPO0867	0.97	0.880	SPO0867	0.98	0.299	SPO0867	1.14	0.033	SPO0867	1.08	0.661	
SPO0868	1.2	0.164	SPO0868	1.06	0.486	SPO0869	0.86	0.883	SPO0869	0.57	0.903	SPO0868	0.84	0.457	SPO0868	0.83	0.087	SPO0868	1.01	0.944	SPO0868	0.97	0.861	
SPO0869	0.85	0.907	SPO0869	0.85	0.873	SPO0870	0.93	0.538	SPO0870	0.93	0.538	SPO0869	0.86	0.891	SPO0869	0.87	0.997	SPO0869	0.91	0.997	SPO0869	1.00	0.997	
SPO0870	1.2	0.871	SPO0870	1.13	0.174	SPO0871	0.85	0.976	SPO0871	0.83	0.852	SPO0870	0.97	0.967	SPO0870	0.95	0.992	SPO0870	0.81	0.662	SPO0870	0.97	0.857	
SPO0871	0.88	0.754	SPO0871	0.9	0.006	SPO0872	0.83	0.95	SPO0872	0.85	0.895	SPO0871	1.09	0.775	SPO0871	1.12	0.770	SPO0871	1.02	0.862	SPO0871	1.00	0.866	
SPO0872	1.11	0.201	SPO0872	1.1	0.094	SPO0873	0.61	0.899	SPO0873	0.95	0.81	SPO0872	1.15	0.612	SPO0872	1.23	0.226	SPO0872	1.12	0.396	SPO0872	0.99	0.939	
SPO0873	1.05	0.848	SPO0873	1.1	0.741	SPO0874	0.68	0.902	SPO0874	0.97	0.252	SPO0873	1.40	0.422	SPO0873	1.49	0.389	SPO0873	0.97	0.907	SPO0873	0.89	0.761	
SPO0874	1.17	0.319	SPO0874	1.25	0.003	SPO0875	0.79	0.051	SPO0875	0.17	0.068	SPO0874	1.37	0.146	SPO0874	1.16	0.301	SPO0874	0.97	0.935	SPO0874	0.96	0.834	
SPO0875	0.85	0.162	SPO0875	0.85	0.048	SPO0876	0.82	0.14	SPO0876	0.19	0.16	SPO0875	1.22	0.020	SPO0875	1.26	0.023	SPO0875	1.17	0.030	SPO0875	1.22	0.098	
SPO0876	0.91	0.623	SPO0876	1.03	0.408	SPO0877	0.9	0.371	SPO0877	0.89	0.488	SPO0876	0.76	0.041	SPO0876	0.75	0.072	SPO0876	1.18	0.134	SPO0876	1.22	0.113	
SPO0877	1.18	0.552	SPO0877	1.09	0.59	SPO0878	0.93	0.989	SPO0878	0.98	0.975	SPO0877	0.74	0.377	SPO0877	0.81	0.423	SPO0877	0.92	0.716	SPO0877	0.88	0.649	
SPO0878	0.75	0.639	SPO0878	0.75	0.477	SPO0879	0.88	0.154	SPO0879	0.99	0.169	SPO0878	0.61	0.423	SPO0878	0.59	0.376	SPO0878	0.91	0.894	SPO0878	0.97	0.997	
SPO0879	0.82	0.225	SPO0879	0.9	0.906	SPO0880	0.87	0.404	SPO0880	0.87	0.404	SPO0879	0.74	0.144	SPO0879	0.81	0.491	SPO0879	0.90	0.491	SPO0879	0.90	0.491	
SPO0880	0.76	0.343	SPO0880	0.86	0.522	SPO0881	0.63	0.057	SPO0881	0.75	0.396	SPO0880	1.43	0.062	SPO0880	1.38	0.079	SPO0880	1.14	0.311	SPO0880	1.06	0.605	
SPO0881	0.77	0.02	SPO0881	0.76	0.025	SPO0882	0.59	0.642	SPO0882	0.87	0.708	SPO0881	1.77	0.014	SPO0881	1.75	0.040	SPO0881	0.91	0.402	SPO0881	0.88	0.657	
SPO0882	1.02	0.908	SPO0882	0.91	0.961	SPO0883	0.91	0.596	SPO0883	0.77	0.253	SPO0882	0.97	0.853	SPO0882	0.96	0.840	SPO0882	1.25	0.789	SPO0882	1.14	0.849	
SPO0883	1.18	0.507	SPO0883	1.06	0.322	SPO0884	0.96	0.627	SPO0884	0.89	0.519	SPO0883	1.01	0.733	SPO0883	1.02	0.171	SPO0883	0.87	0.739	SPO0883	0.85	0.065	
SPO0884	1.14	0.588	SPO0884	1.08	0.572	SPO0885	0.95	0.945	SPO0885	0.87	0.979	SPO0884	1.16	0.439	SPO0884	1.08	0.222	SPO0884	0.96	0.959	SPO0884	0.93	0.646	
SPO0885	0.97	0.985	SPO0885	0.97	0.843	SPO0886	0.94	0.016	SPO0886	0.93	0.038	SPO0885	0.83	0.788	SPO0885	0.77	0.653	SPO0885	0.96	0.950	SPO0885	0.90	0.865	
SPO0886	0.73	0.493	SPO0886	0.85	0.669	SPO0887	0.98	0.14	SPO0887	0.98	0.14	SPO0886	0.98	0.013	SPO0886	0.98	0.013	SPO0886	1.23	0.054	SPO0886	1.44	0.070	
SPO0887	1.61	0.065	SPO0887	1.45	0.065	SPO0888	0.95	0.94	SPO0888	0.94	0.988	SPO0887	1.39	0.046	SPO0887	1.44	0.028	SPO0887	0.93	0.553	SPO0887	0.93	0.727	
SPO0888	1.06	0.889	SPO0888	0.99	0.989	SPO0889	0.98	0.942	SPO0889	0.95	0.794	SPO0888	0.83	0.920	SPO0888	0.76	0.918	SPO0888	0.85	0.853	SPO0888	0.88	0.923	
SPO0889	1.61	0.017	SPO0889	1.77	0.014	SPO0890	0.88	0.339	SPO0890	0.91	0.371	SPO0889	1.10	0.689	SPO0889	1.13	0.119	SPO0889	1.00	0.883	SPO0889	0.94	0.711	
SPO0890	1.6	0.064	SPO0890	1.64	0.012	SPO0891	0.89	0.409	SPO0891	0.96	0.234	SPO0890	1.57	0.028	SPO0890	1.53	0.006	SPO0890	1.43	0.099	SPO0890	1.26	0.192	
SPO0891	1.11	0.452	SPO0891	1.12	0.466	SPO0892	0.84	0.125	SPO0892	0.89	0.677	SPO0891	1.22	0.020	SPO0891	1.24	0.106	SPO0891	1.04	0.037	SPO0891	1.10	0.187	
SPO0892	1.59	0.006	SPO0892	1.54	0.003	SPO0893	0.88	0.6	SPO0893	0.93	0.231	SPO0892	1.31	0.026	SPO0892	1.17	0.013	SPO0892	1.31	0.177	SPO0892	1.17	0.365	
SPO0893	1.15	0.426	SPO0893	1.13	0.291	SPO0894	0.97	0.236	SPO0894	0.89	0.109	SPO0893	0.77	0.188	SPO0893	0.73	0.056	SPO0893	1.06	0.612	SPO0893	1.04	0.722	
SPO0894	1.29	0.25	SPO0894	1.29	0.223	SPO0895	0.98	0.72	SPO0895	0.94	0.689	SPO0894	0.99	0.59	SPO0894	0.99	0.59	SPO0894	1.16	0.412	SPO0894	1.16	0.216	
SPO0895	1.25	0.169	SPO0895	1.01	0.866	SPO0896	0.97	0.279	SPO0896	0.81	0.145	SPO0895	0.79	0.388	SPO0895	0.83	0.629	SPO0895	1.02	0.681	SPO0895	1.10	0.202	
SPO0896	1.55	0.079	SPO0896	1.37	0.048	SPO0897	0.97	0.578	SPO0897	0.93	0.6	SPO0896	0.78	0.512	SPO0896	0.80	0.272	SPO0896	0.97	1.18	0.086	SPO0896	1.13	0.656
SPO0897	1.17	0.711	SPO0897	1.19	0.608	SPO0898	0.91	0.542	SPO0898	0.74	0.263	SPO0897	0.76	0.400	SPO0897	0.60	0.329	SPO0897	0.96	0.961	SPO0897	0.93	0.827	
SPO0898	0.81	0.675	SPO0898	0.78	0.596	SPO0899	0.93	0.523	SPO0899	0.85	0.691	SPO0898	0.76	0.448	SPO0898	0.92	0.638	SPO0898	0.92	0.852	SPO0898	0.88	0.753	
SPO0900	2.64	0.025	SPO0900	2.37	0.031	SPO0901	0.83	0.039	SPO0901	0.98	0.411	SPO0900	0.18	0.023	SPO0900	0.14	0.009	SPO0900	0.97	0.988	SPO0900	0.92	0.811	
SPO0901	0.92	0.502	SPO0901	0.88	0.121	SPO0902	0.88	0.819	SPO0902	0.86	0.831	SPO0901	0.65	0.013	SPO0901	0.71	0.066	SPO0901	1.00	0.945	SPO0901	0.97	0.732	
SPO0902	1.36	0.523	SPO0902	1.32	0.571	SPO0903	0.8	0.422	SPO0903	0.93	0.215	SPO0902	0.82	0.856	SPO0902	0.77	0.866	SPO0902	1.18	0.772	SPO0902	1.08	0.909	
SPO0903	1.22	0.461	SPO0903	1.26	0.72	SPO0904	0.96	0.869	SPO0904	0.95	0.491	SPO0903	0.68	0.221	SPO0903	0.68	0.101	SPO0903	1.00	0.962	SPO0903	1.05	0.710	
SPO0904	1.59	0.065	SPO0904	1.51	0.07	SPO0905</																		

SPO0992	0.53	0.050	SPO0991	0.79	0.633	SPO0992	0.92	0.229	SPO0993	0.79	0.053	SPO0991	0.64	0.399	SPO0991	0.57	0.424	SPO0991	0.66	0.465	SPO0991	0.79	0.699
SPO0993	0.67	0.392	SPO0992	0.57	0.062	SPO0993	0.93	0.097	SPO0994	0.99	0.765	SPO0992	1.65	0.172	SPO0992	1.75	0.037	SPO0992	1.13	0.743	SPO0992	1.17	0.672
SPO0994	0.79	0.572	SPO0993	0.74	0.086	SPO0994	0.84	0.735	SPO0995	0.92	0.193	SPO0993	2.72	0.157	SPO0993	2.87	0.083	SPO0993	1.13	0.743	SPO0993	1.22	0.557
SPO0995	0.94	0.039	SPO0994	0.95	0.263	SPO0995	0.94	0.509	SPO0996	0.94	0.302	SPO0994	1.34	0.311	SPO0994	1.21	0.540	SPO0994	0.93	0.631	SPO0994	1.08	0.689
SPO0996	0.89	0.339	SPO0995	0.76	0.509	SPO0996	0.94	0.097	SPO0997	0.75	0.308	SPO0995	2.51	0.010	SPO0995	2.11	0.012	SPO0995	1.03	0.891	SPO0995	1.11	0.531
SPO0997	0.66	0.072	SPO0996	0.91	0.309	SPO0997	0.97	0.155	SPO0998	0.99	0.132	SPO0996	2.56	0.005	SPO0996	2.37	0.002	SPO0996	1.09	0.428	SPO0996	1.09	0.163
SPO0998	0.64	0.157	SPO0997	0.65	0.214	SPO0998	0.98	0.506	SPO0999	0.76	0.7	SPO0997	2.29	0.147	SPO0997	2.29	0.109	SPO0997	1.12	0.645	SPO0997	1.10	0.792
SPO0999	0.88	0.488	SPO0998	0.65	0.064	SPO0999	0.79	0.324	SPO1000	0.75	0.264	SPO0998	1.92	0.041	SPO0998	1.75	0.068	SPO0998	1.09	0.450	SPO0998	1.16	0.506
SPO1000	0.79	0.046	SPO0999	0.92	0.911	SPO1000	0.82	0.052	SPO1001	0.63	0.028	SPO0999	1.52	0.048	SPO0999	1.63	0.274	SPO0999	1.07	0.889	SPO0999	1.07	0.690
SPO1001	1.18	0.048	SPO1000	0.81	0.106	SPO1001	0.81	0.093	SPO1002	0.55	0.923	SPO1000	1.53	0.057	SPO1000	1.65	0.018	SPO1000	0.98	0.719	SPO1000	1.03	0.769
SPO1002	0.86	0.856	SPO1001	1.11	0.307	SPO1002	0.83	0.837	SPO1003	0.98	0.28	SPO1001	2.26	0.011	SPO1001	2.26	0.006	SPO1001	1.06	0.789	SPO1001	1.14	0.275
SPO1003	0.65	0.039	SPO1002	0.92	0.227	SPO1003	0.92	0.227	SPO1004	0.92	0.166	SPO1002	0.94	0.171	SPO1002	1.10	0.026	SPO1002	1.01	0.989	SPO1002	1.01	0.689
SPO1004	1.18	0.33	SPO1003	0.66	0.040	SPO1004	0.79	0.197	SPO1005	0.67	0.107	SPO1003	0.93	0.077	SPO1003	0.93	0.077	SPO1003	0.93	0.828	SPO1003	0.92	0.702
SPO1005	0.88	0.231	SPO1004	1.11	0.367	SPO1005	0.92	0.182	SPO1006	0.82	0.05	SPO1004	3.16	0.028	SPO1004	0.93	0.027	SPO1004	0.93	0.828	SPO1004	0.85	0.248
SPO1006	1.22	0.028	SPO1005	0.88	0.361	SPO1006	0.98	0.015	SPO1007	0.74	0.107	SPO1005	1.13	0.125	SPO1005	1.15	0.034	SPO1005	0.97	0.91	SPO1005	1.01	0.692
SPO1007	1.4	0.066	SPO1006	1.18	0.052	SPO1007	0.87	0.09	SPO1008	0.66	0.124	SPO1006	0.84	0.415	SPO1006	0.88	0.473	SPO1006	0.98	0.890	SPO1006	0.93	0.713
SPO1008	1.74	0.03	SPO1007	1.28	0.1	SPO1008	0.91	0.101	SPO1009	0.65	0.385	SPO1007	0.82	0.343	SPO1007	0.81	0.681	SPO1007	1.05	0.219	SPO1007	0.97	0.934
SPO1009	1.56	0.062	SPO1008	1.64	0.032	SPO1009	0.86	0.901	SPO1010	0.86	0.985	SPO1008	0.68	0.172	SPO1008	0.67	0.219	SPO1008	0.89	0.498	SPO1008	0.88	0.452
SPO1010	1.83	0.016	SPO1009	1.58	0.023	SPO1010	0.93	0.997	SPO1011	0.86	0.961	SPO1009	1.24	0.301	SPO1009	1.18	0.255	SPO1009	1.05	0.743	SPO1009	0.98	0.889
SPO1011	0.92	0.606	SPO1010	1.56	0.023	SPO1011	0.93	0.997	SPO1012	0.84	0.961	SPO1010	1.07	0.176	SPO1010	1.15	0.037	SPO1010	1.01	0.442	SPO1010	0.95	0.788
SPO1012	0.77	0.549	SPO1011	0.98	0.497	SPO1012	0.94	0.913	SPO1013	0.96	0.798	SPO1011	1.29	0.060	SPO1011	1.24	0.020	SPO1011	1.06	0.786	SPO1011	1.13	0.223
SPO1013	0.97	0.008	SPO1012	0.79	0.372	SPO1013	0.87	0.931	SPO1014	0.84	0.456	SPO1012	0.83	0.805	SPO1012	0.86	0.753	SPO1012	0.91	0.322	SPO1012	0.93	0.834
SPO1014	0.47	0.043	SPO1013	0.52	0.202	SPO1014	1.32	0.808	SPO1015	0.81	0.285	SPO1013	1.16	0.313	SPO1013	1.28	0.048	SPO1013	1.24	0.235	SPO1013	1.27	0.170
SPO1015	0.46	0.456	SPO1014	0.52	0.136	SPO1015	0.96	0.046	SPO1016	0.95	0.063	SPO1014	1.72	0.029	SPO1014	1.74	0.021	SPO1014	1.39	0.244	SPO1014	1.36	0.162
SPO1016	1.01	0.654	SPO1015	0.58	0.17	SPO1016	0.97	0.188	SPO1017	0.82	0.539	SPO1015	6.02	0.020	SPO1015	4.91	0.046	SPO1015	1.15	0.887	SPO1015	1.17	0.877
SPO1017	0.71	0.017	SPO1016	1.01	0.471	SPO1017	0.96	0.287	SPO1018	0.84	0.636	SPO1016	0.74	0.042	SPO1016	0.72	0.060	SPO1016	0.88	0.285	SPO1016	0.89	0.350
SPO1018	0.62	0.41	SPO1017	0.71	0.138	SPO1018	0.93	0.812	SPO1019	0.8	0.28	SPO1017	0.22	0.002	SPO1017	0.24	0.006	SPO1017	1.16	0.006	SPO1017	1.28	0.065
SPO1019	0.76	0.524	SPO1018	0.69	0.475	SPO1019	0.96	0.62	SPO1020	0.91	0.684	SPO1018	0.17	0.017	SPO1018	0.17	0.011	SPO1018	0.93	0.605	SPO1018	0.89	0.735
SPO1020	0.63	0.142	SPO1019	0.98	0.403	SPO1020	0.91	0.84	SPO1021	0.91	0.84	SPO1019	0.21	0.004	SPO1019	0.21	0.004	SPO1019	1.07	0.395	SPO1019	1.07	0.412
SPO1021	0.63	0.142	SPO1020	0.74	0.573	SPO1021	0.76	0.738	SPO1022	0.98	0.129	SPO1020	0.14	0.019	SPO1020	0.14	0.022	SPO1020	0.84	0.623	SPO1020	0.86	0.710
SPO1022	1.34	0.129	SPO1021	0.6	0.156	SPO1022	0.72	0.246	SPO1023	0.93	0.725	SPO1021	0.13	0.003	SPO1021	0.13	0.012	SPO1021	1.00	0.955	SPO1021	1.05	0.780
SPO1023	1.1	0.875	SPO1022	1.37	0.056	SPO1023	0.87	0.88	SPO1024	0.93	0.305	SPO1022	0.32	0.004	SPO1022	0.36	0.016	SPO1022	0.97	0.471	SPO1022	0.93	0.637
SPO1024	1.31	0.653	SPO1023	1.05	0.924	SPO1024	0.84	0.153	SPO1025	0.69	0.816	SPO1023	0.69	0.672	SPO1023	0.62	0.579	SPO1023	0.97	0.993	SPO1023	0.94	0.926
SPO1025	1.07	0.53	SPO1024	1.27	0.083	SPO1025	0.88	0.72	SPO1026	0.91	0.484	SPO1024	0.63	0.092	SPO1024	0.68	0.114	SPO1024	0.88	0.226	SPO1024	0.97	0.885
SPO1026	1.1	0.349	SPO1025	1.1	0.691	SPO1026	0.81	0.417	SPO1027	0.93	0.957	SPO1025	0.89	0.295	SPO1025	1.32	0.515	SPO1025	0.97	0.97	SPO1025	0.87	0.360
SPO1027	1.11	0.41	SPO1026	1.13	0.488	SPO1027	0.79	0.528	SPO1028	0.96	0.953	SPO1026	0.92	0.070	SPO1026	0.94	0.009	SPO1026	0.79	0.239	SPO1026	0.85	0.168
SPO1028	1.11	0.468	SPO1027	0.91	0.34	SPO1028	0.91	0.34	SPO1029	0.91	0.34	SPO1027	0.92	0.373	SPO1027	0.92	0.373	SPO1027	1.02	0.771	SPO1027	1.01	0.412
SPO1029	1.11	0.468	SPO1028	0.93	0.97	SPO1029	0.91	0.73	SPO1030	0.71	0.517	SPO1028	0.83	0.963	SPO1028	0.83	0.963	SPO1028	0.89	0.808	SPO1028	0.81	0.878
SPO1030	0.8	0.612	SPO1029	1.01	0.538	SPO1030	0.93	0.613	SPO1031	0.79	0.315	SPO1029	0.76	0.412	SPO1029	0.76	0.412	SPO1029	1.00	0.994	SPO1029	0.96	0.885
SPO1031	0.48	0.152	SPO1030	0.83	0.407	SPO1031	0.86	0.456	SPO1032	0.83	0.761	SPO1030	1.00	0.836	SPO1030	0.94	0.940	SPO1030	0.88	0.329	SPO1030	0.93	0.585
SPO1032	1.69	0.003	SPO1031	0.9	0.148	SPO1032	0.85	0.625	SPO1033	0.78	0.609	SPO1031	2.22	0.082	SPO1031	2.17	0.074	SPO1031	1.03	0.887	SPO1031	1.17	0.566
SPO1033	1.73	0.414	SPO1032	1.42	0.062	SPO1033	0.88	0.634	SPO1034	0.91	0.369	SPO1032	0.94	0.894	SPO1032	0.93	0.489	SPO1032	1.16	0.084	SPO1032	1.12	0.540
SPO1034	1.25	0.371	SPO1033	1.65	0.23	SPO1034	0.97	0.357	SPO1035	0.92	0.823	SPO1033	0.72	0.562	SPO1033	0.74	0.681	SPO1033	1.02	0.903	SPO1033	0.88	0.797
SPO1035	0.73	0.702	SPO1034	1.27	0.305	SPO1035	0.63	0.821	SPO1036	0.76	0.221	SPO1034	0.84	0.620	SPO1034	0.81	0.571	SPO1034	0.87	0.400	SPO1034	0.85	0.246
SPO1036	0.67	0.143	SPO1035	0.78	0.817	SPO1036	0.55	0.421	SPO1037	0.96	0.84	SPO1035	1.38	0.088	SPO1035	1.23	0.156	SPO1035	1.02	0.96	SPO1035	1.07	0.911
SPO1037	1.07	0.574	SPO1036	0.68	0.06	SPO1037	0.85	0.648	SPO1038	0.98	0.723	SPO1037	1.20	0.239	SPO1037	1.20	0.063	SPO1037	1.08	0.628	SPO1037	1.08	0.485
SPO1038	0.74	0.653	SPO1037	0.89	0.279	SPO1038	0.87	0.598	SPO1039	0.98	0.615	SPO1038	0.83	0.316	SPO1038	0.96	0.262	SPO1038	1.18	0.071	SPO1038	1.15	0.606
SPO1039	0.76	0.269	SPO1038	0.98	0.944	SPO1040	0.89	0.036	SPO1041	0.83	0.975	SPO1039	1.22	0.662	SPO1039	1.21	0.844	SPO1039	1.58	0.594	SPO1039	1.30	0.700
SPO1040	0.7	0.771	SPO1039	0.59	0.264	SPO1041	0.97	0.855	SPO1042	0.94	0.057	SPO1040	1.65	0.609	SPO1040	1.32	0.684	SPO1040	1.20	0.603	SPO1040	1.19	0.792
SPO1041	0.6	0.014	SPO1040	0.84	0.033	SPO1042	0.9	0.515	SPO1043	0.91	0.911	SPO1041	1.03	0.982	SPO1041	1.06	0.966	SPO1041	0.88	0.864	SPO1041	0.93	0.899
SPO1042	1.13	0.423	SPO1041	0.64	0.032	SPO1043	0.91	0.945	SPO1044	0.93	0.376	SPO1042	1.87	0.123	SPO1042	1.67	0.054	SPO1042	1.24	0.727	SPO1042	1.27	0.520
SPO1043	0.85	0.804	SPO1042	0.97	0.764	SPO1044	0.89	0.864	SPO1045	0.89	1	SPO1043	1.35	0.140	SPO1043	0.92	0.416	SPO1043	1.13	0.832	SPO1043	1.25	0.633
SPO1044	0.91	0.33	SPO1043	0.76	0.391	SPO1045</																	

SPO1133	1.23	0.070	SPO1132	1.02	0.619	SPO1133	0.87	0.174	SPO1134	1.02	0.857	SPO1131	1.29	0.062	SPO1131	1.34	0.010	SPO1131	1.04	0.564	SPO1131	1.02	0.406
SPO1134	1	0.966	SPO1133	1.21	0.123	SPO1134	0.96	0.989	SPO1135	0.82	0.917	SPO1132	2.33	0.000	SPO1132	2.75	0.008	SPO1132	1.05	0.679	SPO1132	1.03	0.464
SPO1135	1.27	0.25	SPO1134	1.05	0.935	SPO1135	0.93	0.965	SPO1136	0.76	0.472	SPO1133	1.17	0.080	SPO1133	1.23	0.055	SPO1133	1.05	0.530	SPO1133	1.08	0.345
SPO1136	0.98	0.539	SPO1135	1.11	0.423	SPO1136	0.89	0.794	SPO1137	0.92	0.493	SPO1134	1.04	0.024	SPO1134	0.99	0.592	SPO1134	0.94	0.824	SPO1134	0.85	0.272
SPO1137	0.89	0.889	SPO1136	0.83	0.234	SPO1137	0.63	0.022	SPO1138	0.97	0.142	SPO1135	0.77	0.649	SPO1135	0.72	0.389	SPO1135	0.89	0.789	SPO1135	0.85	0.626
SPO1138	1.19	0.367	SPO1137	0.83	0.277	SPO1138	0.88	0.298	SPO1139	0.81	0.221	SPO1136	1.19	0.143	SPO1136	1.36	0.068	SPO1136	1.07	0.803	SPO1136	1.10	0.577
SPO1139	0.43	0.408	SPO1138	1.26	0.099	SPO1139	0.92	0.207	SPO1140	0.88	0.8	SPO1137	1.02	0.908	SPO1137	1.26	0.330	SPO1137	1.00	0.893	SPO1137	1.04	0.912
SPO1140	0.89	0.918	SPO1139	0.51	0.443	SPO1140	0.95	0.766	SPO1141	0.56	0.622	SPO1138	1.21	0.670	SPO1138	1.06	0.671	SPO1138	1.08	0.676	SPO1138	0.94	0.756
SPO1141	0.82	0.594	SPO1140	0.83	0.568	SPO1141	0.6	0.084	SPO1142	0.68	0.383	SPO1139	2.67	0.034	SPO1139	2.55	0.098	SPO1139	1.46	1.096	SPO1139	1.66	0.452
SPO1142	0.76	0.07	SPO1141	0.76	0.659	SPO1142	0.93	0.443	SPO1143	0.91	0.338	SPO1140	0.83	0.700	SPO1140	0.89	0.667	SPO1140	1.17	0.808	SPO1140	1.05	0.880
SPO1143	0.81	0.764	SPO1142	0.83	0.579	SPO1143	0.89	0.772	SPO1144	0.93	0.348	SPO1141	1.08	0.540	SPO1141	1.08	0.520	SPO1141	1.02	0.993	SPO1141	0.99	0.957
SPO1144	0.76	0.59	SPO1143	0.85	0.625	SPO1144	0.95	0.275	SPO1145	0.99	0.468	SPO1142	1.13	0.414	SPO1142	1.10	0.268	SPO1142	1.05	0.769	SPO1142	1.02	0.827
SPO1145	1.06	0.321	SPO1144	0.76	0.254	SPO1145	0.95	0.774	SPO1146	0.75	0.667	SPO1143	1.10	0.850	SPO1143	1.10	0.766	SPO1143	1.12	0.929	SPO1143	1.02	0.776
SPO1146	0.85	0.817	SPO1145	1.05	0.736	SPO1146	0.73	0.48	SPO1147	0.75	0.91	SPO1144	1.44	0.074	SPO1144	1.05	0.727	SPO1144	0.95	0.894	SPO1144	1.21	0.568
SPO1147	0.82	0.835	SPO1146	0.85	0.425	SPO1147	0.91	0.924	SPO1148	0.92	0.898	SPO1145	0.76	0.570	SPO1145	0.80	0.372	SPO1145	0.84	1.066	SPO1145	0.92	0.500
SPO1148	0.68	0.249	SPO1147	0.88	0.948	SPO1148	0.97	0.844	SPO1149	0.94	0.802	SPO1146	1.39	0.519	SPO1146	1.89	0.095	SPO1146	1.13	0.753	SPO1146	1.16	0.900
SPO1149	1.13	0.332	SPO1148	0.71	0.417	SPO1149	0.93	0.863	SPO1150	0.85	0.395	SPO1147	1.66	0.683	SPO1147	1.44	0.725	SPO1147	0.93	0.929	SPO1147	0.95	0.945
SPO1150	1.56	0.066	SPO1150	1.08	0.644	SPO1151	0.9	0.743	SPO1152	0.84	0.075	SPO1148	1.19	0.748	SPO1148	1.32	0.613	SPO1148	1.32	0.811	SPO1148	0.98	0.930
SPO1151	1.04	0.7	SPO1151	1.25	0.068	SPO1152	0.96	0.439	SPO1153	0.83	0.877	SPO1150	0.83	0.643	SPO1150	0.79	0.474	SPO1150	0.88	0.551	SPO1150	0.90	0.145
SPO1152	1.13	0.686	SPO1152	0.92	0.822	SPO1153	0.96	0.913	SPO1154	0.83	0.771	SPO1151	0.96	0.066	SPO1151	0.86	0.056	SPO1151	1.12	0.639	SPO1151	1.08	0.534
SPO1153	1.18	0.59	SPO1153	1.14	0.542	SPO1154	0.85	0.665	SPO1155	0.84	0.642	SPO1152	0.74	0.250	SPO1152	0.78	0.134	SPO1152	0.97	0.805	SPO1152	1.01	0.696
SPO1154	1.18	0.126	SPO1154	0.83	0.416	SPO1155	0.97	0.924	SPO1156	0.95	0.279	SPO1153	0.90	0.819	SPO1153	0.93	0.940	SPO1153	1.00	0.998	SPO1153	0.99	0.978
SPO1155	1.16	0.336	SPO1155	1.12	0.263	SPO1156	0.95	0.324	SPO1157	0.99	0.788	SPO1154	0.86	0.812	SPO1154	0.95	0.375	SPO1154	0.94	0.852	SPO1154	0.94	0.774
SPO1156	0.83	0.03	SPO1156	1.3	0.444	SPO1157	0.93	0.041	SPO1158	0.97	0.988	SPO1155	0.78	0.453	SPO1155	0.80	0.260	SPO1155	0.93	0.837	SPO1155	0.92	0.629
SPO1157	1.38	0.495	SPO1157	1.03	0.723	SPO1158	0.93	0.89	SPO1159	0.68	0.428	SPO1156	0.89	0.726	SPO1156	0.79	0.637	SPO1156	0.91	0.280	SPO1156	0.84	0.285
SPO1158	0.84	0.323	SPO1158	1.43	0.535	SPO1159	0.92	0.179	SPO1160	0.93	0.107	SPO1157	0.81	0.251	SPO1157	0.76	0.456	SPO1157	1.37	0.409	SPO1157	1.31	0.693
SPO1159	0.75	0.273	SPO1159	0.78	0.242	SPO1160	0.93	0.664	SPO1161	1	0.204	SPO1158	1.22	0.500	SPO1158	1.27	0.459	SPO1158	1.10	0.871	SPO1158	1.04	0.908
SPO1160	1.09	0.248	SPO1160	0.79	0.466	SPO1161	0.91	0.194	SPO1162	0.96	0.651	SPO1159	1.61	0.053	SPO1159	1.82	0.015	SPO1159	0.80	0.154	SPO1159	0.85	0.237
SPO1161	1.26	0.881	SPO1161	1.1	0.529	SPO1162	0.96	0.34	SPO1163	0.96	0.334	SPO1160	1.16	0.549	SPO1160	1.17	0.549	SPO1160	1.03	0.885	SPO1160	1.18	0.459
SPO1162	1.1	0.651	SPO1162	1.32	0.104	SPO1163	0.96	0.995	SPO1164	1.08	0.66	SPO1161	0.94	0.878	SPO1161	0.95	0.991	SPO1161	0.93	0.658	SPO1161	0.93	0.408
SPO1163	1.1	0.97	SPO1163	1.08	0.54	SPO1164	0.86	0.815	SPO1165	1.02	0.838	SPO1162	1.91	0.029	SPO1162	1.97	0.003	SPO1162	0.93	0.511	SPO1162	1.03	0.761
SPO1164	0.68	0.549	SPO1164	0.92	0.809	SPO1165	0.95	0.584	SPO1166	0.72	0.718	SPO1163	1.97	0.030	SPO1163	2.01	0.015	SPO1163	1.08	0.687	SPO1163	1.04	0.712
SPO1165	0.94	0.847	SPO1165	0.78	0.202	SPO1166	0.92	0.705	SPO1167	0.89	0.251	SPO1164	0.80	0.406	SPO1164	0.81	0.234	SPO1164	0.96	0.894	SPO1164	0.88	0.578
SPO1166	0.84	0.336	SPO1166	0.85	0.86	SPO1167	0.77	0.977	SPO1171	0.84	0.621	SPO1165	0.82	0.791	SPO1165	0.65	0.334	SPO1165	0.93	0.894	SPO1165	0.95	0.926
SPO1167	1.16	0.236	SPO1166	0.83	0.501	SPO1171	0.8	0.771	SPO1172	0.81	0.431	SPO1166	0.60	0.116	SPO1166	0.61	0.324	SPO1166	1.05	0.646	SPO1166	1.06	0.925
SPO1172	0.88	0.254	SPO1171	0.99	0.929	SPO1172	0.75	0.233	SPO1173	0.9	0.949	SPO1168	0.56	0.029	SPO1168	0.52	0.005	SPO1168	1.00	0.883	SPO1168	1.00	0.946
SPO1173	1.26	0.382	SPO1172	1.01	0.919	SPO1173	0.9	0.919	SPO1174	0.94	0.701	SPO1169	1.16	0.514	SPO1169	1.17	0.549	SPO1169	1.09	0.888	SPO1169	1.01	0.971
SPO1174	0.73	0.126	SPO1173	1.01	0.919	SPO1174	0.94	0.701	SPO1175	1.24	0.004	SPO1172	1.46	0.004	SPO1172	1.46	0.004	SPO1172	1.05	0.893	SPO1172	0.93	0.798
SPO1175	1.5	0.178	SPO1174	0.77	0.122	SPO1175	0.79	0.03	SPO1176	0.65	0.214	SPO1173	0.54	0.687	SPO1173	0.53	0.644	SPO1173	0.94	0.873	SPO1173	0.58	0.746
SPO1176	0.93	0.938	SPO1175	1.34	0.011	SPO1176	0.96	0.703	SPO1177	0.62	0.268	SPO1174	1.26	0.911	SPO1174	1.24	0.118	SPO1174	1.29	0.403	SPO1174	1.18	0.545
SPO1177	1.07	0.857	SPO1176	0.88	0.292	SPO1177	0.96	0.146	SPO1178	0.9	0.412	SPO1175	0.74	0.191	SPO1175	0.85	0.213	SPO1175	1.09	0.708	SPO1175	1.10	0.660
SPO1178	1.03	0.811	SPO1177	0.95	0.916	SPO1178	0.7	0.288	SPO1179	0.91	0.097	SPO1176	0.87	0.718	SPO1176	1.38	0.686	SPO1176	1.25	0.719	SPO1176	1.06	0.931
SPO1179	1.16	0.706	SPO1178	1.1	0.722	SPO1179	0.93	0.064	SPO1180	0.87	0.039	SPO1177	1.10	0.017	SPO1177	1.10	0.017	SPO1177	0.77	0.768	SPO1177	0.67	0.597
SPO1180	1.01	0.86	SPO1179	1.07	0.72	SPO1180	0.79	0.053	SPO1181	0.51	0.033	SPO1178	2.97	0.009	SPO1178	2.98	0.006	SPO1178	0.81	0.428	SPO1178	0.78	0.501
SPO1181	0.73	0.365	SPO1180	0.98	0.949	SPO1181	0.89	0.918	SPO1182	0.96	0.927	SPO1179	1.94	0.035	SPO1179	1.94	0.035	SPO1179	0.95	0.805	SPO1179	0.87	0.577
SPO1182	1.14	0.247	SPO1181	0.93	0.885	SPO1182	0.83	0.055	SPO1183	0.8	0.034	SPO1180	1.95	0.014	SPO1180	1.95	0.014	SPO1180	0.96	0.860	SPO1180	0.97	0.928
SPO1183	0.89	0.284	SPO1182	1.14	0.268	SPO1183	0.88	0.054	SPO1184	0.94	0.782	SPO1181	2.45	0.016	SPO1181	2.45	0.008	SPO1181	1.10	0.296	SPO1181	1.02	0.418
SPO1184	1.09	0.793	SPO1183	1.02	0.617	SPO1184	0.98	0.284	SPO1185	0.96	0.403	SPO1182	2.40	0.011	SPO1182	2.40	0.002	SPO1182	1.05	0.719	SPO1182	1.00	0.772
SPO1185	0.66	0.02	SPO1184	0.97	0.972	SPO1185	0.79	0.262	SPO1186	0.72	0.215	SPO1183	1.88	0.020	SPO1183	2.18	0.022	SPO1183	0.98	0.973	SPO1183	0.94	0.410
SPO1186	0.8	0.187	SPO1185	0.76	0.204	SPO1186	0.89	0.163	SPO1187	0.91	0.781	SPO1184	1.21	0.368	SPO1184	1.06	0.408	SPO1184	0.81	0.809	SPO1184	0.84	0.279
SPO1187	1.31	0.332	SPO1186	0.87	0.26	SPO1187	0.95	0.684	SPO1188	0.89	0.322	SPO1185	0.88	0.110	SPO1185	0.81	0.277	SPO1185	0.87	1.020	SPO1185	0.88	0.395
SPO1188	1.27	0.452	SPO1187	1.1	0.287	SPO1188	0.98	0.768	SPO1189	0.91	0.963	SPO1186	0.85	0.566	SPO1186	0.85	0.394	SPO1186	0.91	0.741	SPO1186	0.90	0.642
SPO1189	1.03	0.881	SPO1188	1.17	0.178	SPO118																	

SPO1279	0.41	0.003	SPO1278	0.85	0.59	SPO1278	0.87	0.467	SPO1280	0.65	0.06	SPO1277	0.63	0.098	SPO1277	0.59	0.071	SPO1277	1.07	0.555	SPO1276	1.11	0.395
SPO1280	0.59	0.104	SPO1279	0.51	0.01	SPO1279	0.93	0.053	SPO1281	1.20	0.707	SPO1278	0.36	0.002	SPO1278	0.97	0.873	SPO1277	1.00	0.832	SPO1276	1.00	0.437
SPO1281	0.77	0.510	SPO1280	0.63	0.37	SPO1280	0.83	0.007	SPO1282	0.89	0.732	SPO1279	0.76	0.009	SPO1279	0.76	0.183	SPO1279	1.09	0.346	SPO1278	0.90	0.437
SPO1282	0.96	0.808	SPO1281	0.71	0.274	SPO1281	0.76	0.367	SPO1283	0.96	0.42	SPO1280	0.96	0.016	SPO1280	0.83	0.047	SPO1280	0.83	0.047	SPO1280	0.83	0.047
SPO1283	0.86	0.227	SPO1282	1.19	0.246	SPO1282	0.75	0.967	SPO1284	0.97	0.623	SPO1281	0.27	0.039	SPO1281	0.36	0.043	SPO1281	1.01	0.834	SPO1280	1.09	0.648
SPO1284	0.54	0.054	SPO1283	0.88	0.343	SPO1283	0.85	0.363	SPO1285	0.98	0.684	SPO1282	0.92	0.958	SPO1282	0.86	0.221	SPO1282	1.11	0.782	SPO1281	0.88	0.757
SPO1285	0.85	0.785	SPO1284	0.63	0.029	SPO1284	0.82	0.19	SPO1286	0.78	0.615	SPO1283	1.01	0.642	SPO1283	1.00	0.444	SPO1283	0.99	0.979	SPO1282	1.10	0.554
SPO1286	0.99	0.947	SPO1285	0.91	0.779	SPO1285	0.57	0.53	SPO1287	0.93	0.403	SPO1284	1.85	0.022	SPO1284	1.76	0.001	SPO1284	1.07	0.551	SPO1283	1.00	0.946
SPO1287	0.84	0.283	SPO1286	0.93	0.944	SPO1286	0.83	0.695	SPO1288	0.93	0.541	SPO1285	0.77	0.713	SPO1285	0.71	0.372	SPO1285	0.94	0.930	SPO1284	1.11	0.316
SPO1288	0.61	0.055	SPO1287	0.83	0.25	SPO1287	0.95	0.308	SPO1289	0.67	0.748	SPO1286	0.72	0.488	SPO1286	0.78	0.507	SPO1286	0.87	0.630	SPO1285	1.00	0.987
SPO1289	1.41	0.616	SPO1288	0.68	0.058	SPO1288	0.93	0.61	SPO1290	0.83	0.684	SPO1287	0.83	0.336	SPO1287	0.81	0.140	SPO1287	0.93	0.485	SPO1286	0.89	0.614
SPO1290	0.85	0.948	SPO1289	1.23	0.729	SPO1289	0.84	0.758	SPO1291	0.61	0.28	SPO1288	1.32	0.337	SPO1288	1.34	0.016	SPO1288	1.10	0.365	SPO1288	0.87	0.635
SPO1291	0.81	0.155	SPO1290	0.85	0.051	SPO1290	0.86	0.78	SPO1292	0.76	0.125	SPO1289	0.59	0.457	SPO1289	0.56	0.150	SPO1289	0.96	0.985	SPO1288	1.02	0.909
SPO1292	0.63	0.048	SPO1291	0.75	0.067	SPO1291	0.95	0.067	SPO1293	0.92	0.004	SPO1290	0.90	0.967	SPO1290	0.90	0.991	SPO1290	0.81	0.755	SPO1289	0.87	0.849
SPO1293	0.5	0.011	SPO1292	0.65	0.055	SPO1292	0.74	0.252	SPO1294	0.93	0.219	SPO1291	0.56	0.050	SPO1291	0.59	0.024	SPO1291	0.91	0.427	SPO1290	0.70	0.574
SPO1294	0.98	0.962	SPO1293	0.62	0.063	SPO1293	0.81	0.02	SPO1295	0.9	0.973	SPO1292	1.88	0.054	SPO1292	2.02	0.003	SPO1292	1.02	0.805	SPO1291	0.93	0.580
SPO1295	0.96	0.36	SPO1294	1.04	0.109	SPO1294	0.74	0.235	SPO1296	0.93	0.514	SPO1293	1.41	0.023	SPO1293	1.25	0.032	SPO1293	0.92	0.637	SPO1292	1.07	0.342
SPO1296	0.65	0.322	SPO1295	1	0.956	SPO1295	0.96	0.971	SPO1299	0.85	0.854	SPO1294	0.83	0.484	SPO1294	0.87	0.599	SPO1294	1.06	0.749	SPO1293	0.89	0.428
SPO1299	0.93	0.871	SPO1298	0.93	0.841	SPO1298	0.8	0.559	SPO1300	0.83	0.508	SPO1295	0.73	0.640	SPO1295	0.68	0.469	SPO1295	1.04	0.927	SPO1294	0.95	0.874
SPO1300	1.09	0.354	SPO1299	0.97	0.623	SPO1299	0.86	0.213	SPO1301	0.87	0.664	SPO1296	0.88	0.620	SPO1296	0.99	0.725	SPO1296	0.99	0.612	SPO1295	1.14	0.804
SPO1301	0.54	0.006	SPO1300	1.05	0.516	SPO1300	0.95	0.516	SPO1302	0.93	0.008	SPO1299	1.92	0.079	SPO1299	0.008	0.008	SPO1299	1.26	0.276	SPO1298	0.99	0.920
SPO1302	0.64	0.158	SPO1301	0.58	0.033	SPO1301	0.91	0.106	SPO1303	0.83	0.614	SPO1300	1.06	0.428	SPO1300	1.04	0.640	SPO1300	1.11	0.612	SPO1299	1.25	0.354
SPO1303	1.15	0.261	SPO1302	0.7	0.027	SPO1302	0.86	0.045	SPO1304	0.7	0.12	SPO1301	1.70	0.001	SPO1301	1.65	0.003	SPO1301	1.29	0.133	SPO1300	1.05	0.685
SPO1304	0.9	0.514	SPO1303	1.11	0.027	SPO1303	1	0.93	SPO1305	0.77	0.887	SPO1302	2.05	0.002	SPO1302	2.05	0.011	SPO1302	1.14	0.123	SPO1301	1.36	0.073
SPO1305	1.15	0.182	SPO1304	0.93	0.743	SPO1304	0.85	0.627	SPO1306	0.69	0.207	SPO1303	1.43	0.069	SPO1303	1.49	0.018	SPO1303	1.19	0.288	SPO1302	1.24	0.509
SPO1306	0.51	0.177	SPO1305	1.09	0.381	SPO1305	0.97	0.969	SPO1307	0.91	0.895	SPO1304	1.39	0.051	SPO1304	1.36	0.008	SPO1304	1.00	0.896	SPO1303	1.11	0.439
SPO1307	1.03	0.736	SPO1306	0.55	0.101	SPO1306	0.69	0.423	SPO1308	0.82	0.731	SPO1305	1.49	0.080	SPO1305	1.36	0.042	SPO1305	0.98	0.981	SPO1304	1.12	0.423
SPO1308	0.97	0.999	SPO1307	1.01	0.815	SPO1307	0.93	0.78	SPO1309	0.93	0.978	SPO1306	1.13	0.088	SPO1306	1.13	0.088	SPO1306	1.05	0.747	SPO1305	0.94	0.764
SPO1309	1.09	0.887	SPO1308	0.89	0.869	SPO1308	0.97	0.961	SPO1310	0.96	0.987	SPO1307	1.24	0.250	SPO1307	1.21	0.276	SPO1307	0.83	0.684	SPO1306	1.14	0.698
SPO1310	1.09	0.105	SPO1309	1.11	0.827	SPO1309	0.93	0.981	SPO1311	0.79	0.293	SPO1308	1.33	0.510	SPO1308	1.23	0.428	SPO1308	1.09	0.862	SPO1307	0.93	0.762
SPO1311	1.1	0.216	SPO1310	1.03	0.293	SPO1310	0.95	0.18	SPO1312	0.82	0.527	SPO1309	0.97	0.884	SPO1309	1.03	0.768	SPO1309	0.96	0.974	SPO1308	1.07	0.814
SPO1312	1.25	0.232	SPO1311	1.02	0.8	SPO1311	0.93	0.208	SPO1313	0.95	0.19	SPO1310	0.82	0.707	SPO1310	0.85	0.956	SPO1310	1.03	0.729	SPO1309	0.97	0.991
SPO1313	1.59	0.088	SPO1312	1.33	0.151	SPO1312	0.84	0.783	SPO1314	0.87	0.96	SPO1311	0.53	0.005	SPO1311	0.57	0.011	SPO1311	0.88	1.185	SPO1310	0.99	0.886
SPO1314	0.9	0.699	SPO1313	1.66	0.022	SPO1313	0.7	0.192	SPO1315	0.85	0.916	SPO1312	1.23	0.192	SPO1312	1.18	0.245	SPO1312	1.17	0.271	SPO1311	0.85	0.196
SPO1315	1.06	0.74	SPO1314	1.03	0.856	SPO1314	0.92	0.928	SPO1316	0.65	0.896	SPO1313	0.72	0.233	SPO1313	0.68	0.282	SPO1313	0.97	0.940	SPO1312	1.04	0.751
SPO1316	1.17	0.206	SPO1315	1.02	0.813	SPO1315	0.97	0.836	SPO1317	0.85	0.509	SPO1314	0.61	0.267	SPO1314	0.46	0.227	SPO1314	0.92	0.852	SPO1313	0.85	0.404
SPO1317	0.96	0.34	SPO1316	0.95	0.81	SPO1316	0.95	0.561	SPO1318	0.91	0.109	SPO1315	0.98	0.316	SPO1315	0.98	0.316	SPO1315	0.91	0.51	SPO1314	0.83	0.626
SPO1318	1.36	0.217	SPO1317	0.9	0.028	SPO1317	0.81	0.63	SPO1319	0.59	0.033	SPO1316	0.79	0.127	SPO1316	0.77	0.142	SPO1316	1.04	0.267	SPO1315	0.93	0.710
SPO1319	1.29	0.016	SPO1318	1.46	0.121	SPO1318	0.93	0.767	SPO1320	0.83	0.671	SPO1317	0.65	0.340	SPO1317	0.75	0.505	SPO1317	1.14	0.799	SPO1316	0.99	0.985
SPO1320	0.93	0.751	SPO1319	1.27	0.006	SPO1319	0.56	0.832	SPO1321	0.94	0.555	SPO1318	0.98	0.279	SPO1318	0.81	0.258	SPO1318	0.99	0.968	SPO1317	1.12	0.792
SPO1321	1.13	0.092	SPO1320	0.92	0.586	SPO1320	0.68	0.408	SPO1322	0.92	0.938	SPO1319	1.32	0.012	SPO1319	1.23	0.013	SPO1319	1.01	0.549	SPO1318	0.96	0.898
SPO1322	0.9	0.889	SPO1321	1.17	0.166	SPO1321	0.98	0.916	SPO1323	0.84	0.132	SPO1320	0.85	0.801	SPO1320	0.82	0.650	SPO1320	0.85	1.060	SPO1319	0.93	0.884
SPO1323	1.32	0.048	SPO1322	0.91	0.847	SPO1322	0.91	0.92	SPO1324	0.98	0.942	SPO1321	1.04	0.808	SPO1321	1.06	0.719	SPO1321	1.09	0.494	SPO1320	0.84	0.271
SPO1324	1.07	0.74	SPO1323	1.37	0.002	SPO1323	0.98	0.045	SPO1325	0.73	0.577	SPO1322	1.02	0.913	SPO1322	1.04	0.835	SPO1322	0.97	0.989	SPO1321	1.08	0.627
SPO1325	0.95	0.88	SPO1324	1.12	0.833	SPO1324	0.89	0.967	SPO1326	0.86	0.918	SPO1323	1.08	0.446	SPO1323	1.09	0.446	SPO1323	1.26	0.431	SPO1322	1.08	0.666
SPO1326	0.95	0.949	SPO1325	0.94	0.954	SPO1325	1	0.865	SPO1327	0.84	0.742	SPO1324	0.78	0.834	SPO1324	0.85	0.896	SPO1324	1.08	0.921	SPO1323	1.19	0.305
SPO1327	0.93	0.645	SPO1326	1.05	0.147	SPO1326	0.86	0.033	SPO1328	1.01	0.819	SPO1325	0.85	0.414	SPO1325	0.82	0.504	SPO1325	0.88	0.504	SPO1324	1.10	0.878
SPO1328	0.81	0.429	SPO1327	0.92	0.453	SPO1327	0.36	0.88	SPO1329	0.78	0.087	SPO1326	1.05	0.023	SPO1326	1.71	0.038	SPO1326	0.93	0.480	SPO1325	0.87	0.365
SPO1329	1.03	0.753	SPO1328	0.88	0.148	SPO1328	0.66	0.578	SPO1330	0.85	0.003	SPO1327	1.07	0.309	SPO1327	1.09	0.161	SPO1327	1.10	0.132	SPO1326	1.02	0.866
SPO1330	0.68	0.032	SPO1329	1	0.907	SPO1329	0.85	0.428	SPO1331	0.99	0.024	SPO1328	0.71	0.168	SPO1328	0.68	0.217	SPO1328	1.11	0.520	SPO1327	1.20	0.391
SPO1331	0.85	0.07	SPO1330	1.77	0.081	SPO1330	0.94	0.396	SPO1332	0.97	0.191	SPO1329	0.61	0.029	SPO1329	0.62	0.104	SPO1329	1.24	0.171	SPO1328	1.14	0.047
SPO1332	1.04	0.346	SPO1331	0.83	0.031	SPO1331	0.97	0.232	SPO1333	0.79	0.156	SPO1330	0.44	0.037	SPO1330	0.98	0.001	SPO1330	1.30	0.342	SPO1329	1.20	0.092
SPO1333	0.98	0.332	SPO1332	0.98	0.288	SPO1332	0.9																

SPO1422	1.49	0.018	SPO1422	1.34	0.01	SPO1422	0.79	0.538	SPO1424	0.81	0.632	SPO1421	0.97	0.808	SPO1420	0.74	0.476	SPO1420	0.93	0.722	SPO1419	0.81	0.103
SPO1423	1.94	0.11	SPO1423	1.81	0.07	SPO1423	0.76	0.731	SPO1425	0.56	0.984	SPO1422	1.04	0.664	SPO1421	0.93	0.965	SPO1421	1.05	0.957	SPO1420	0.89	0.509
SPO1424	0.97	0.994	SPO1424	1.05	0.707	SPO1424	0.97	0.834	SPO1426	0.79	0.408	SPO1423	1.07	0.881	SPO1422	1.10	0.216	SPO1422	1.22	1.188	SPO1421	1.03	0.967
SPO1425	0.78	0.339	SPO1425	0.95	0.947	SPO1425	0.96	0.947	SPO1426	0.98	0.864	SPO1424	1.33	0.369	SPO1423	1.61	0.347	SPO1423	1.21	0.482	SPO1422	1.21	0.842
SPO1426	0.52	0.076	SPO1426	0.66	0.039	SPO1426	0.87	0.25	SPO1428	0.84	0.401	SPO1425	1.56	0.349	SPO1424	1.34	0.031	SPO1424	1.11	0.843	SPO1423	1.34	0.080
SPO1427	1.14	0.06	SPO1427	1.11	0.234	SPO1427	0.75	0.154	SPO1429	0.76	0.802	SPO1426	1.41	0.124	SPO1425	1.48	0.355	SPO1426	0.94	0.897	SPO1424	1.06	0.311
SPO1428	1.07	0.719	SPO1428	1.2	0.495	SPO1428	0.87	0.186	SPO1430	0.83	0.785	SPO1427	0.90	0.785	SPO1426	1.31	0.090	SPO1426	1.09	0.708	SPO1425	0.89	0.812
SPO1429	0.83	0.019	SPO1429	0.93	0.124	SPO1429	0.91	0.431	SPO1431	0.91	0.112	SPO1428	1.08	0.937	SPO1427	1.03	0.345	SPO1427	0.83	0.080	SPO1426	1.13	0.586
SPO1430	1.16	0.052	SPO1430	1.02	0.866	SPO1430	0.75	0.56	SPO1432	0.99	0.842	SPO1429	1.04	0.021	SPO1428	1.07	0.981	SPO1428	1.17	0.674	SPO1427	0.83	0.460
SPO1431	0.89	0.679	SPO1431	0.81	0.365	SPO1431	0.76	0.236	SPO1433	0.96	0.59	SPO1430	0.52	0.019	SPO1429	0.93	0.251	SPO1429	1.11	1.073	SPO1428	1.20	0.648
SPO1432	0.75	0.392	SPO1432	0.74	0.271	SPO1432	0.74	0.939	SPO1434	0.94	0.478	SPO1431	1.12	0.534	SPO1430	0.51	0.089	SPO1430	0.91	0.696	SPO1429	1.06	0.149
SPO1433	0.78	0.339	SPO1433	0.95	0.123	SPO1433	0.56	0.703	SPO1434	0.93	0.805	SPO1432	0.81	0.626	SPO1431	1.13	0.332	SPO1431	1.17	0.331	SPO1430	1.06	0.855
SPO1434	0.88	0.575	SPO1434	0.89	0.263	SPO1434	0.97	0.201	SPO1436	0.79	0.403	SPO1433	0.84	0.514	SPO1432	0.81	0.465	SPO1432	1.00	0.860	SPO1431	1.25	0.311
SPO1435	1.22	0.154	SPO1435	1.16	0.292	SPO1435	0.95	0.672	SPO1437	0.71	0.511	SPO1434	1.68	0.123	SPO1433	0.78	0.076	SPO1433	1.00	0.932	SPO1432	1.02	0.820
SPO1436	1.01	0.634	SPO1436	1.09	0.146	SPO1436	0.96	0.439	SPO1438	0.68	0.889	SPO1435	0.61	0.088	SPO1434	1.74	0.008	SPO1434	1.06	0.707	SPO1433	1.05	0.794
SPO1437	1.29	0.362	SPO1437	1.37	0.371	SPO1437	0.89	0.7	SPO1439	0.67	0.972	SPO1436	0.85	0.284	SPO1435	0.62	0.032	SPO1435	0.93	0.714	SPO1434	1.13	0.122
SPO1438	0.61	0.013	SPO1438	0.67	0.021	SPO1438	0.97	0.176	SPO1440	0.40	0.407	SPO1437	0.40	0.162	SPO1436	0.86	0.076	SPO1436	1.31	0.075	SPO1435	1.01	0.999
SPO1439	1.06	0.918	SPO1439	1.04	0.939	SPO1439	0.97	0.958	SPO1441	0.92	0.994	SPO1438	0.74	0.272	SPO1437	0.59	0.163	SPO1437	0.93	0.819	SPO1436	1.16	0.064
SPO1440	1.19	0.511	SPO1440	1.15	0.568	SPO1440	0.86	0.718	SPO1442	0.76	0.441	SPO1439	1.11	0.903	SPO1438	0.72	0.037	SPO1438	0.83	0.159	SPO1437	0.95	0.832
SPO1441	0.95	0.365	SPO1441	0.58	0.074	SPO1441	0.94	0.724	SPO1443	0.67	0.141	SPO1440	0.69	0.074	SPO1439	1.16	0.858	SPO1439	1.05	0.864	SPO1438	0.76	0.018
SPO1442	1.73	0.001	SPO1442	1.54	0.006	SPO1442	0.91	0.141	SPO1444	0.63	0.759	SPO1441	0.82	0.110	SPO1440	0.60	0.282	SPO1440	0.57	0.393	SPO1439	0.97	0.979
SPO1443	0.75	0.18	SPO1443	0.86	0.11	SPO1443	0.98	0.008	SPO1445	0.89	0.088	SPO1442	1.48	0.626	SPO1441	1.77	0.023	SPO1441	0.95	0.372	SPO1440	0.54	0.085
SPO1444	0.69	0.064	SPO1444	0.83	0.23	SPO1444	0.91	0.791	SPO1446	0.66	0.714	SPO1443	2.07	0.007	SPO1442	0.91	0.886	SPO1442	1.34	0.079	SPO1441	1.04	0.808
SPO1445	0.85	0.488	SPO1445	0.86	0.331	SPO1445	0.74	0.667	SPO1447	0.85	0.714	SPO1444	1.46	0.034	SPO1443	1.81	0.008	SPO1443	1.11	0.423	SPO1442	1.12	0.175
SPO1446	0.98	0.84	SPO1446	0.94	0.484	SPO1446	0.87	0.472	SPO1448	0.93	0.397	SPO1445	1.34	0.040	SPO1444	1.28	0.147	SPO1444	1.15	0.340	SPO1443	1.05	0.323
SPO1447	1.11	0.765	SPO1447	0.93	0.958	SPO1447	0.93	0.728	SPO1449	0.83	0.647	SPO1446	1.16	0.225	SPO1445	1.47	0.023	SPO1445	1.08	0.244	SPO1444	1.01	0.988
SPO1448	1.01	0.42	SPO1448	1.06	0.331	SPO1448	0.88	0.5	SPO1450	0.92	0.327	SPO1447	1.01	0.959	SPO1446	1.14	0.291	SPO1446	0.93	0.433	SPO1445	1.16	0.031
SPO1449	0.74	0.06	SPO1449	0.86	0.392	SPO1449	0.88	0.585	SPO1451	0.88	0.475	SPO1448	1.50	0.088	SPO1447	1.13	0.734	SPO1447	1.08	0.890	SPO1446	1.04	0.737
SPO1450	1.12	0.369	SPO1450	1.07	0.649	SPO1450	0.96	0.246	SPO1452	0.85	0.381	SPO1449	1.48	0.058	SPO1448	1.41	0.026	SPO1448	1.08	0.577	SPO1447	1.05	0.833
SPO1451	0.67	0.611	SPO1451	0.72	0.116	SPO1451	0.53	0.982	SPO1453	0.72	0.757	SPO1450	1.21	0.542	SPO1449	1.44	0.103	SPO1449	0.95	0.346	SPO1448	1.14	0.358
SPO1452	0.85	0.509	SPO1452	0.94	0.953	SPO1452	0.92	0.86	SPO1454	0.77	0.631	SPO1451	1.28	0.657	SPO1450	1.17	0.552	SPO1450	1.03	0.901	SPO1449	1.05	0.799
SPO1453	0.86	0.798	SPO1453	0.82	0.759	SPO1453	0.92	0.998	SPO1455	0.78	0.623	SPO1452	1.34	0.304	SPO1451	1.41	0.016	SPO1451	1.01	1.000	SPO1450	1.04	0.808
SPO1454	0.94	0.731	SPO1454	0.91	0.851	SPO1454	0.95	0.656	SPO1456	0.96	0.653	SPO1453	0.98	0.994	SPO1452	1.36	0.261	SPO1452	0.87	0.400	SPO1451	1.05	0.410
SPO1455	1.3	0.054	SPO1455	1.18	0.034	SPO1455	0.9	0.505	SPO1457	0.87	0.591	SPO1454	0.70	0.242	SPO1453	1.02	0.921	SPO1453	1.13	0.759	SPO1452	0.88	0.569
SPO1456	1.11	0.893	SPO1456	0.96	0.999	SPO1456	0.56	0.132	SPO1458	0.9	0.999	SPO1455	0.76	0.232	SPO1454	0.71	0.253	SPO1454	0.88	0.378	SPO1453	1.14	0.814
SPO1457	1.44	0.069	SPO1457	1.26	0.092	SPO1457	0.98	0.396	SPO1459	0.93	0.38	SPO1456	1.03	0.809	SPO1455	0.71	0.089	SPO1455	1.00	0.828	SPO1454	0.91	0.527
SPO1458	1.09	0.369	SPO1458	0.96	0.92	SPO1458	0.93	0.867	SPO1461	0.86	0.943	SPO1457	0.81	0.946	SPO1456	1.02	0.93	SPO1456	1.02	0.863	SPO1455	0.88	0.391
SPO1459	1.09	0.57	SPO1459	0.96	0.92	SPO1459	0.96	0.943	SPO1461	0.86	0.888	SPO1458	0.74	0.808	SPO1457	0.92	0.796	SPO1457	1.09	0.160	SPO1456	0.94	0.431
SPO1460	1.3	0.462	SPO1460	1.22	0.567	SPO1460	0.99	0.991	SPO1462	0.98	0.991	SPO1459	1.48	0.083	SPO1458	0.71	0.765	SPO1458	0.91	0.912	SPO1457	1.11	0.258
SPO1461	1.07	0.633	SPO1461	1.05	0.685	SPO1461	0.92	0.514	SPO1463	0.98	0.041	SPO1460	1.12	0.867	SPO1459	1.45	0.086	SPO1459	1.03	0.937	SPO1458	0.95	0.930
SPO1462	0.95	0.939	SPO1462	0.93	0.692	SPO1462	0.56	0.618	SPO1464	0.79	0.009	SPO1461	1.09	0.547	SPO1460	1.23	0.669	SPO1460	1.37	0.727	SPO1459	1.08	0.745
SPO1463	0.97	0.887	SPO1463	1.07	0.129	SPO1463	0.86	0.058	SPO1465	0.98	0.584	SPO1462	0.85	0.280	SPO1461	1.09	0.648	SPO1461	0.95	0.732	SPO1460	1.24	0.750
SPO1464	0.72	0.017	SPO1464	0.83	0.272	SPO1464	0.93	0.133	SPO1466	0.97	0.289	SPO1463	0.60	0.003	SPO1462	0.93	0.903	SPO1462	1.18	0.311	SPO1461	0.93	0.709
SPO1465	0.62	0.314	SPO1465	0.69	0.32	SPO1465	0.59	0.503	SPO1467	0.88	0.512	SPO1464	0.66	0.010	SPO1463	0.57	0.006	SPO1463	0.90	0.329	SPO1462	1.11	0.203
SPO1466	1.41	0.748	SPO1466	1.22	0.423	SPO1466	0.88	0.381	SPO1468	0.88	0.348	SPO1465	0.95	0.789	SPO1464	0.58	0.442	SPO1464	0.74	0.026	SPO1463	0.88	0.391
SPO1467	1.09	0.323	SPO1467	0.93	0.961	SPO1467	0.94	0.582	SPO1469	0.73	0.826	SPO1466	0.5	0.106	SPO1465	0.82	0.731	SPO1465	0.83	0.551	SPO1464	0.83	0.230
SPO1468	0.93	0.972	SPO1468	0.84	0.309	SPO1468	0.96	0.041	SPO1470	0.76	0.18	SPO1467	0.51	0.055	SPO1466	0.54	0.007	SPO1466	0.83	0.497	SPO1465	0.85	0.636
SPO1469	1.38	0.146	SPO1469	1.4	0.031	SPO1469	0.88	0.811	SPO1471	1	0.614	SPO1468	1.06	0.533	SPO1467	0.72	0.157	SPO1467	0.92	0.708	SPO1466	0.88	0.512
SPO1470	0.72	0.21	SPO1470	0.78	0.24	SPO1470	0.42	0.453	SPO1472	0.78	0.667	SPO1469	1.18	0.778	SPO1468	1.23	0.049	SPO1468	1.28	0.096	SPO1467	0.83	0.62
SPO1471	0.82	0.055	SPO1471	0.83	0.358	SPO1471	1	0.625	SPO1473	0.78	0.84	SPO1470	1.54	0.063	SPO1469	1.26	0.190	SPO1469	1.06	0.930	SPO1468	1.25	0.208
SPO1472	0.72	0.019	SPO1472	0.79	0.014	SPO1472	0.95	0.049	SPO1474	0.76	0.646	SPO1471	1.58	0.069	SPO1470	1.84	0.047	SPO1470	1.04	0.964	SPO1469	1.00	0.940
SPO1473	0.79	0.446	SPO1473	0.92	0.868	SPO1473	0.91	0.263	SPO1475	0.6	0.805	SPO1472	1.71	0.707	SPO1471	1.53	0.081	SPO1471	0.98	0.771	SPO1470	1.02	0.942
SPO1474	0.84	0.356	SPO1474	0.88	0.146	SPO14																	

SPO1561	1.07	0.146	SPO1561	1.04	0.722	SPO1561	0.82	0.619	SPO1563	0.97	0.176	SPO1560	1.25	0.025	SPO1559	0.98	0.058	SPO1559	1.09	0.666	SPO1558	0.97	0.944
SPO1562	0.71	0.081	SPO1562	0.73	0.057	SPO1562	0.55	0.74	SPO1564	0.96	0.268	SPO1561	0.95	0.848	SPO1560	1.16	0.145	SPO1560	1.00	0.943	SPO1559	1.11	0.744
SPO1563	0.83	0.10	SPO1563	0.93	0.07	SPO1563	0.95	0.905	SPO1565	0.69	0.365	SPO1562	0.87	0.016	SPO1561	0.97	0.709	SPO1561	1.12	0.711	SPO1560	1.14	0.638
SPO1564	0.94	0.021	SPO1564	0.78	0.024	SPO1564	0.78	0.024	SPO1566	0.99	0.342	SPO1563	1.14	0.003	SPO1562	0.93	0.035	SPO1562	1.23	0.461	SPO1560	1.03	0.559
SPO1565	0.78	0.001	SPO1565	0.53	0.006	SPO1565	0.91	0.015	SPO1567	0.78	0.532	SPO1564	0.27	0.003	SPO1563	0.93	0.339	SPO1563	1.15	0.179	SPO1562	0.93	0.599
SPO1566	0.83	0.174	SPO1566	0.85	0.066	SPO1566	0.73	0.918	SPO1568	0.96	0.209	SPO1565	4.37	0.003	SPO1564	2.38	0.146	SPO1564	1.35	0.251	SPO1563	1.22	0.055
SPO1567	0.42	0.123	SPO1567	0.51	0.028	SPO1567	0.85	0.604	SPO1569	0.78	0.123	SPO1566	1.12	0.675	SPO1565	3.98	0.006	SPO1565	1.56	0.022	SPO1564	1.32	0.363
SPO1568	0.42	0.004	SPO1568	0.44	0.004	SPO1568	0.81	0.668	SPO1570	0.98	0.048	SPO1567	1.19	0.292	SPO1566	0.93	0.719	SPO1566	0.92	0.562	SPO1565	1.54	0.093
SPO1569	0.31	0.023	SPO1569	0.35	0.021	SPO1569	0.75	0.231	SPO1571	0.66	0.793	SPO1568	1.70	0.664	SPO1567	1.14	0.575	SPO1567	1.04	0.747	SPO1566	0.90	0.630
SPO1570	0.94	0.022	SPO1570	0.53	0.012	SPO1570	0.92	0.172	SPO1572	0.98	0.1	SPO1569	2.22	0.035	SPO1568	1.80	0.013	SPO1568	1.22	0.349	SPO1567	1.18	0.213
SPO1571	0.96	0.795	SPO1571	0.83	0.075	SPO1571	0.95	0.904	SPO1573	0.95	0.033	SPO1570	2.59	0.007	SPO1569	2.74	0.020	SPO1569	1.31	0.172	SPO1568	1.34	0.102
SPO1572	0.93	0.822	SPO1572	0.85	0.245	SPO1572	0.98	0.222	SPO1574	0.96	0.342	SPO1571	1.27	0.168	SPO1570	2.59	0.007	SPO1570	1.22	0.461	SPO1569	1.23	0.058
SPO1573	1.11	0.1615	SPO1573	1.28	0.033	SPO1573	0.91	0.16	SPO1575	0.78	0.032	SPO1572	0.74	0.154	SPO1571	1.47	0.400	SPO1571	1.14	0.309	SPO1570	1.38	0.038
SPO1574	0.65	0.033	SPO1574	0.71	0.086	SPO1574	0.88	0.031	SPO1576	0.84	0.892	SPO1573	1.81	0.006	SPO1572	0.70	0.059	SPO1572	1.36	0.069	SPO1571	1.16	0.190
SPO1575	0.53	0.259	SPO1575	0.57	0.038	SPO1575	0.95	0.018	SPO1577	0.82	0.997	SPO1574	1.16	0.165	SPO1573	1.70	0.005	SPO1573	1.25	0.284	SPO1572	1.26	0.076
SPO1576	0.67	0.774	SPO1576	0.73	0.863	SPO1576	0.95	0.814	SPO1578	0.88	0.949	SPO1575	1.85	0.046	SPO1574	1.10	0.075	SPO1574	0.93	0.359	SPO1573	1.08	0.670
SPO1577	0.93	0.313	SPO1577	0.85	0.44	SPO1577	0.98	0.698	SPO1579	0.95	0.382	SPO1576	1.24	0.859	SPO1575	1.84	0.031	SPO1575	1.07	0.740	SPO1574	1.01	0.953
SPO1578	1	0.78	SPO1578	1.04	0.734	SPO1578	0.83	0.937	SPO1580	0.89	0.717	SPO1577	1.30	0.069	SPO1576	1.29	0.745	SPO1576	0.98	0.989	SPO1575	1.16	0.218
SPO1579	0.52	0.40	SPO1579	0.55	0.17	SPO1579	0.77	0.442	SPO1581	0.96	0.324	SPO1578	1.04	0.917	SPO1577	1.63	0.068	SPO1577	1.28	0.258	SPO1576	1.01	0.989
SPO1580	0.61	0.097	SPO1580	0.88	0.037	SPO1580	0.71	0.693	SPO1582	0.96	0.864	SPO1579	1.32	0.265	SPO1578	1.03	0.832	SPO1578	1.07	0.800	SPO1577	1.15	0.626
SPO1581	0.79	0.321	SPO1581	0.75	0.044	SPO1581	0.79	0.688	SPO1583	0.99	0.819	SPO1580	1.12	0.150	SPO1579	1.29	0.257	SPO1579	0.94	0.800	SPO1578	0.89	0.584
SPO1582	0.79	0.723	SPO1582	0.84	0.078	SPO1582	0.85	0.861	SPO1584	0.88	0.804	SPO1581	1.26	0.248	SPO1580	1.05	0.710	SPO1580	0.99	0.910	SPO1579	0.98	0.937
SPO1583	1.47	0.343	SPO1583	1.41	0.274	SPO1583	0.93	0.675	SPO1585	0.98	0.956	SPO1582	0.88	0.805	SPO1581	1.44	0.213	SPO1581	1.03	0.959	SPO1580	0.98	0.775
SPO1584	0.79	0.889	SPO1584	0.84	0.398	SPO1584	0.79	0.925	SPO1586	0.99	0.554	SPO1583	0.98	0.929	SPO1582	0.86	0.608	SPO1583	1.00	0.827	SPO1581	1.00	0.828
SPO1585	1.14	0.908	SPO1585	1.06	0.924	SPO1585	0.89	0.966	SPO1587	0.97	0.428	SPO1584	1.26	0.844	SPO1583	0.92	0.910	SPO1583	1.03	0.951	SPO1582	0.90	0.741
SPO1586	0.9	0.62	SPO1586	0.89	0.83	SPO1586	0.92	0.676	SPO1588	0.96	0.177	SPO1585	0.86	0.935	SPO1584	1.66	0.716	SPO1584	0.91	0.966	SPO1583	0.95	0.929
SPO1587	0.93	0.984	SPO1587	0.9	0.905	SPO1587	0.83	0.623	SPO1589	0.99	0.489	SPO1586	1.02	0.835	SPO1585	0.85	0.939	SPO1585	0.88	0.921	SPO1584	0.92	0.969
SPO1588	1.14	0.273	SPO1588	1.21	0.062	SPO1588	0.75	0.245	SPO1590	0.67	0.386	SPO1587	0.92	0.087	SPO1586	1.13	0.631	SPO1586	0.96	0.274	SPO1585	0.87	0.943
SPO1589	0.75	0.253	SPO1589	0.74	0.163	SPO1589	0.69	0.198	SPO1591	0.79	0.455	SPO1588	1.14	0.421	SPO1587	1.06	0.312	SPO1587	1.06	0.988	SPO1586	1.08	0.429
SPO1590	1.11	0.487	SPO1590	1.06	0.316	SPO1590	0.92	0.948	SPO1592	1	0.545	SPO1589	1.10	0.360	SPO1588	1.84	0.257	SPO1588	1.18	0.710	SPO1587	0.98	0.965
SPO1591	0.92	0.323	SPO1591	0.94	0.917	SPO1591	0.88	0.607	SPO1593	0.89	1.18	SPO1590	1.23	0.474	SPO1589	1.12	0.190	SPO1589	0.95	0.565	SPO1588	1.13	0.325
SPO1592	0.88	0.919	SPO1592	0.89	0.719	SPO1592	0.94	0.781	SPO1594	0.92	0.957	SPO1591	1.36	0.216	SPO1590	1.18	0.136	SPO1590	0.89	0.561	SPO1589	0.93	0.745
SPO1593	0.53	0.159	SPO1593	0.57	0.245	SPO1593	0.96	0.057	SPO1595	0.94	0.352	SPO1592	1.00	0.903	SPO1591	1.23	0.042	SPO1591	1.01	0.943	SPO1590	0.89	0.534
SPO1594	1.19	0.711	SPO1594	1.14	0.812	SPO1594	0.9	0.939	SPO1596	0.97	0.727	SPO1593	0.62	0.028	SPO1592	0.94	0.722	SPO1592	0.89	0.828	SPO1591	1.05	0.734
SPO1595	0.69	0.438	SPO1595	0.64	0.475	SPO1595	0.93	0.14	SPO1597	0.77	0.406	SPO1594	1.14	0.907	SPO1593	0.98	0.085	SPO1593	1.18	0.807	SPO1592	0.92	0.690
SPO1596	0.75	0.528	SPO1596	0.71	0.584	SPO1596	0.83	0.662	SPO1598	0.96	0.518	SPO1595	1.64	0.322	SPO1594	1.21	0.867	SPO1594	0.83	0.809	SPO1593	1.14	0.874
SPO1597	0.79	0.353	SPO1597	0.87	0.161	SPO1597	0.81	0.731	SPO1599	0.91	0.811	SPO1596	1.34	0.701	SPO1595	1.32	0.701	SPO1595	1.32	0.701	SPO1594	0.84	0.824
SPO1598	1.03	0.795	SPO1598	1.06	0.804	SPO1598	0.86	0.916	SPO1600	0.89	0.875	SPO1597	0.78	0.184	SPO1596	1.57	0.319	SPO1596	1.12	0.402	SPO1595	1.17	0.837
SPO1599	0.69	0.135	SPO1599	0.99	0.969	SPO1599	0.71	0.778	SPO1601	0.93	0.256	SPO1598	0.93	0.830	SPO1597	0.84	0.152	SPO1597	0.89	0.515	SPO1596	0.99	0.884
SPO1600	1.14	0.431	SPO1600	1.05	0.339	SPO1600	0.67	0.855	SPO1602	0.95	0.995	SPO1599	0.73	0.739	SPO1598	0.99	0.851	SPO1598	1.01	0.999	SPO1597	0.94	0.360
SPO1601	1.12	0.688	SPO1601	1.04	0.490	SPO1601	0.59	0.604	SPO1603	0.55	0.481	SPO1600	0.86	0.306	SPO1599	0.57	0.325	SPO1599	0.89	0.417	SPO1598	0.96	0.833
SPO1602	0.9	0.203	SPO1602	0.96	0.907	SPO1602	0.96	0.797	SPO1604	0.75	0.81	SPO1601	0.83	0.184	SPO1600	0.96	0.698	SPO1600	1.11	0.779	SPO1599	0.91	0.765
SPO1603	0.73	0.452	SPO1603	0.79	0.883	SPO1603	0.88	0.828	SPO1605	0.92	0.036	SPO1602	0.96	0.798	SPO1601	0.67	0.063	SPO1601	1.03	0.963	SPO1600	1.07	0.904
SPO1604	1.03	0.924	SPO1604	0.99	0.959	SPO1604	0.86	0.99	SPO1606	0.99	0.387	SPO1603	0.99	0.778	SPO1602	0.97	0.517	SPO1602	0.95	0.747	SPO1601	1.02	0.998
SPO1605	0.89	0.329	SPO1605	0.74	0.038	SPO1605	0.88	0.98	SPO1607	0.89	0.245	SPO1604	0.98	0.426	SPO1603	0.99	0.282	SPO1603	0.96	0.688	SPO1602	0.98	0.911
SPO1606	0.68	0.161	SPO1606	0.74	0.275	SPO1606	0.9	0.731	SPO1608	0.8	0.827	SPO1605	1.46	0.033	SPO1604	0.347	0.047	SPO1604	0.85	0.859	SPO1603	1.01	0.525
SPO1607	0.38	0.008	SPO1607	0.52	0.039	SPO1607	0.78	0.185	SPO1609	0.84	0.001	SPO1606	1.09	0.183	SPO1605	1.49	0.004	SPO1605	1.30	0.217	SPO1604	0.91	0.907
SPO1608	1.09	0.824	SPO1608	0.94	0.998	SPO1608	0.95	0.955	SPO1610	0.7	0.105	SPO1607	1.91	0.092	SPO1606	0.98	0.702	SPO1606	0.99	0.915	SPO1605	1.23	0.092
SPO1609	0.62	0.615	SPO1609	0.64	0.706	SPO1609	0.91	0.993	SPO1611	1	0.961	SPO1608	1.02	0.968	SPO1607	1.90	0.077	SPO1607	1.19	0.482	SPO1606	1.00	0.572
SPO1610	1.16	0.069	SPO1610	1.11	0.128	SPO1610	0.96	0.586	SPO1612	0.97	0.653	SPO1609	1.48	0.426	SPO1608	0.93	0.746	SPO1608	0.98	0.928	SPO1607	1.14	0.327
SPO1611	0.98	0.992	SPO1611	0.98	0.992	SPO1611	0.81	0.938	SPO1613	0.86	0.89	SPO1610	1.19	0.296	SPO1609	1.77	0.461	SPO1609	0.90	0.758	SPO1608	1.01	0.994
SPO1612	0.95	0.825	SPO1612	1.06	0.679	SPO1612	0.66	0.955	SPO1614	0.92	0.978	SPO1611	0.91	0.989	SPO1610	1.50	0.029	SPO1610	1.10	0.793	SPO1609	0.95	0.954
SPO1613	1.28	0.135	SPO1613	1.11	0.																		

SPO1703	0.77	0.715	SPO1702	0.98	0.682	SPO1702	0.85	0.138	SPO1704	0.99	0.957	SPO1701	1.21	0.229	SPO1700	1.19	0.137	SPO1701	1.06	0.757	SPO1699	1.15	0.284
SPO1704	1.05	0.868	SPO1703	0.79	0.674	SPO1703	0.86	0.899	SPO1705	0.68	0.824	SPO1702	0.98	0.590	SPO1701	1.07	0.700	SPO1702	1.10	0.781	SPO1700	1.08	0.817
SPO1705	0.59	0.528	SPO1704	0.94	0.904	SPO1704	0.93	0.776	SPO1707	0.92	0.834	SPO1703	1.41	0.591	SPO1702	1.06	0.940	SPO1703	0.99	0.962	SPO1701	1.03	0.858
SPO1707	0.63	0.759	SPO1705	0.67	0.85	SPO1705	0.85	0.625	SPO1708	0.98	0.166	SPO1704	1.10	0.37	SPO1702	1.31	0.625	SPO1704	1.04	0.93	SPO1703	1.02	0.689
SPO1708	0.69	0.325	SPO1707	0.5	0.873	SPO1707	0.9	0.908	SPO1709	0.94	0.997	SPO1705	1.35	0.641	SPO1704	1.06	0.995	SPO1705	1.1	0.881	SPO1703	1.19	0.855
SPO1709	0.92	0.977	SPO1708	0.52	0.828	SPO1708	0.94	0.426	SPO1711	0.68	0.43	SPO1707	0.80	0.509	SPO1705	1.19	0.808	SPO1707	0.86	0.645	SPO1704	0.94	0.910
SPO1711	1.03	0	SPO1709	0.94	0.995	SPO1709	0.98	0.951	SPO1712	0.99	0.569	SPO1708	1.54	0.189	SPO1707	0.74	0.345	SPO1708	1.17	0.634	SPO1705	1.13	0.891
SPO1712	0.83	0.094	SPO1710	0.97	0.842	SPO1711	0.93	0.651	SPO1713	0.98	0.262	SPO1709	0.67	0.861	SPO1708	1.47	0.060	SPO1709	0.52	0.700	SPO1707	0.84	0.515
SPO1713	0.74	0.609	SPO1712	0.96	0.907	SPO1712	0.97	0.617	SPO1714	0.66	0.34	SPO1711	0.57	0.243	SPO1709	0.77	0.851	SPO1710	2.33	0.88	SPO1708	1.23	0.501
SPO1714	0.77	0.547	SPO1713	0.83	0.825	SPO1713	0.92	0.671	SPO1715	0.69	0.808	SPO1712	0.88	0.183	SPO1710	1.07	0.851	SPO1711	0.86	0.695	SPO1709	0.78	0.792
SPO1715	0.85	0.94	SPO1714	0.93	0.985	SPO1714	0.95	0.892	SPO1716	0.89	0.333	SPO1713	0.66	0.548	SPO1711	0.65	0.185	SPO1712	1.15	0.616	SPO1710	1.28	0.630
SPO1716	0.93	0.236	SPO1715	0.81	0.973	SPO1715	0.98	0.979	SPO1717	0.96	0.166	SPO1714	0.97	0.828	SPO1712	0.94	0.445	SPO1713	0.99	0.975	SPO1713	0.99	0.712
SPO1717	1.01	0.652	SPO1716	0.68	0.947	SPO1716	0.98	0.943	SPO1718	0.82	0.128	SPO1715	0.83	0.712	SPO1713	0.83	0.325	SPO1714	1.13	0.932	SPO1712	1.08	0.627
SPO1718	0.71	0.102	SPO1717	0.97	0.334	SPO1717	1.01	0.398	SPO1719	0.78	0.953	SPO1716	1.72	0.191	SPO1714	0.81	0.704	SPO1715	0.99	0.904	SPO1713	1.05	0.841
SPO1719	1.15	0.666	SPO1718	0.75	0.912	SPO1718	0.74	0.036	SPO1720	0.92	0.965	SPO1717	0.95	0.676	SPO1715	0.76	0.415	SPO1716	1.24	0.475	SPO1714	1.03	0.993
SPO1720	1.13	0.849	SPO1719	1.18	0.634	SPO1719	0.93	0.621	SPO1721	0.89	0.401	SPO1716	3.35	0.010	SPO1716	1.47	0.079	SPO1717	1.05	0.988	SPO1715	1.03	0.992
SPO1721	0.83	0.65	SPO1720	1.07	0.898	SPO1720	0.73	0.981	SPO1722	0.92	0.224	SPO1719	1.08	0.970	SPO1717	1.11	0.832	SPO1718	2.06	0.100	SPO1716	1.22	0.601
SPO1722	0.83	0.496	SPO1721	0.86	0.776	SPO1721	0.88	0.453	SPO1723	0.83	0.298	SPO1720	0.96	1.000	SPO1716	2.38	0.022	SPO1719	1.14	0.725	SPO1717	1.15	0.459
SPO1723	0.94	0.816	SPO1722	0.86	0.42	SPO1722	0.99	0.199	SPO1724	0.96	0.38	SPO1721	1.80	0.173	SPO1719	1.18	0.826	SPO1720	0.88	0.890	SPO1718	1.74	0.044
SPO1724	1.11	0.971	SPO1723	0.93	0.832	SPO1723	0.97	0.129	SPO1725	0.98	0.832	SPO1722	2.16	0.003	SPO1720	0.93	0.978	SPO1721	1.01	0.970	SPO1719	1.24	0.785
SPO1725	0.86	0.522	SPO1724	1.19	0.701	SPO1724	0.86	0.935	SPO1727	0.99	0.95	SPO1723	2.49	0.015	SPO1721	1.68	0.212	SPO1722	1.24	0.186	SPO1720	0.98	0.978
SPO1727	0.93	0.643	SPO1725	0.91	0.587	SPO1725	0.63	0.98	SPO1728	0.64	0.724	SPO1724	0.79	0.873	SPO1722	2.14	0.013	SPO1723	1.02	0.746	SPO1721	1.00	0.978
SPO1728	1.2	0.142	SPO1727	0.93	0.661	SPO1727	0.91	0.997	SPO1729	0.85	0.184	SPO1725	1.04	0.267	SPO1723	2.08	0.124	SPO1724	0.89	0.906	SPO1722	1.16	0.551
SPO1729	0.75	0.028	SPO1728	1.19	0.84	SPO1728	0.94	0.774	SPO1732	0.98	0.43	SPO1727	0.98	0.618	SPO1725	1.00	0.569	SPO1723	1.00	0.955	SPO1723	0.98	0.979
SPO1732	1.42	0.022	SPO1729	0.81	0.202	SPO1729	0.87	0.262	SPO1733	0.76	0.652	SPO1728	1.05	0.368	SPO1725	0.99	0.627	SPO1727	1.03	0.608	SPO1724	0.84	0.518
SPO1733	1.66	0.064	SPO1732	1.39	0.071	SPO1732	0.87	0.25	SPO1734	0.77	0.62	SPO1729	1.14	0.169	SPO1727	0.96	0.438	SPO1728	1.09	0.081	SPO1725	0.96	0.939
SPO1734	1.37	0.112	SPO1733	1.35	0.116	SPO1733	0.72	0.046	SPO1735	0.72	0.046	SPO1732	0.95	0.866	SPO1728	1.02	0.481	SPO1729	1.04	0.842	SPO1727	1.07	0.491
SPO1735	0.78	0.27	SPO1734	1.28	0.056	SPO1734	0.86	0.52	SPO1736	0.85	0.099	SPO1733	0.65	0.012	SPO1729	1.16	0.056	SPO1732	1.14	0.702	SPO1728	1.05	0.378
SPO1736	0.93	0.93	SPO1735	0.81	0.87	SPO1735	0.96	0.817	SPO1737	0.96	0.198	SPO1734	1.03	0.92	SPO1732	0.95	0.338	SPO1749	1.15	0.532	SPO1729	1.09	0.520
SPO1737	1.05	0.532	SPO1736	1.19	0.388	SPO1736	0.79	0.541	SPO1738	0.97	0.867	SPO1735	1.01	0.558	SPO1733	0.68	0.101	SPO1734	1.10	0.719	SPO1732	1.09	0.761
SPO1738	0.93	0.93	SPO1737	0.94	0.837	SPO1737	0.76	0.885	SPO1739	0.6	0.018	SPO1736	1.23	0.298	SPO1734	1.06	0.238	SPO1735	1.03	0.879	SPO1733	1.14	0.277
SPO1739	0.8	0.037	SPO1738	0.83	0.775	SPO1738	0.81	0.332	SPO1740	0.89	0.418	SPO1737	1.03	0.579	SPO1735	0.95	0.468	SPO1736	0.81	0.405	SPO1734	1.07	0.726
SPO1740	1.14	0.366	SPO1739	0.85	0.129	SPO1739	0.75	0.02	SPO1741	0.97	0.82	SPO1738	1.01	0.942	SPO1736	1.18	0.132	SPO1737	1.00	0.962	SPO1735	1.11	0.327
SPO1741	0.89	0.724	SPO1740	1.09	0.923	SPO1740	0.67	0.199	SPO1742	0.88	0.361	SPO1739	1.04	0.165	SPO1737	0.99	0.838	SPO1738	1.08	0.865	SPO1736	0.82	0.335
SPO1742	0.66	0.596	SPO1741	0.94	0.029	SPO1741	0.69	0.847	SPO1743	0.74	0.526	SPO1740	0.79	0.194	SPO1738	1.11	0.780	SPO1739	1.40	0.004	SPO1737	1.02	0.620
SPO1743	0.93	0.368	SPO1742	0.71	0.047	SPO1742	0.91	0.32	SPO1744	0.78	0.95	SPO1741	0.70	0.325	SPO1739	0.93	0.267	SPO1740	1.04	0.607	SPO1738	1.21	0.662
SPO1744	1.04	0.921	SPO1743	0.82	0.885	SPO1743	0.97	0.812	SPO1745	0.96	0.939	SPO1742	0.91	0.701	SPO1740	0.94	0.701	SPO1741	0.94	0.974	SPO1740	1.31	0.823
SPO1745	1.04	0.921	SPO1744	0.82	0.885	SPO1744	0.96	0.939	SPO1746	0.94	0.935	SPO1743	0.57	0.067	SPO1741	0.65	0.348	SPO1742	0.98	0.997	SPO1740	0.94	0.785
SPO1746	0.89	0.674	SPO1745	0.91	0.922	SPO1745	0.98	0.951	SPO1747	0.84	0.768	SPO1744	0.74	0.837	SPO1742	0.95	0.339	SPO1743	0.97	0.675	SPO1741	0.87	0.747
SPO1747	1.14	0.403	SPO1746	0.93	0.668	SPO1746	0.97	0.95	SPO1748	0.98	0.718	SPO1745	0.67	0.492	SPO1743	0.55	0.108	SPO1744	0.80	0.735	SPO1742	0.94	0.390
SPO1748	1.1	0.156	SPO1747	1.08	0.595	SPO1747	0.95	0.533	SPO1749	0.95	0.304	SPO1746	0.76	0.135	SPO1744	0.75	0.882	SPO1745	0.95	0.945	SPO1743	0.88	0.435
SPO1749	0.7	0.034	SPO1748	1.06	0.246	SPO1748	0.95	0.896	SPO1750	0.99	0.012	SPO1747	0.63	0.068	SPO1745	0.66	0.580	SPO1746	0.91	0.668	SPO1744	0.88	0.470
SPO1750	0.73	0.028	SPO1749	0.76	0.206	SPO1749	0.83	0.564	SPO1751	0.96	0.403	SPO1748	0.93	0.705	SPO1746	0.76	0.015	SPO1747	0.99	0.783	SPO1745	0.96	0.964
SPO1751	1.01	0.939	SPO1750	0.9	0.614	SPO1750	0.96	0.088	SPO1752	0.97	0.867	SPO1749	1.47	0.051	SPO1747	0.63	0.278	SPO1748	0.88	0.306	SPO1746	0.93	0.566
SPO1752	0.87	0.85	SPO1751	0.83	0.103	SPO1751	0.85	0.475	SPO1753	0.96	0.198	SPO1752	1.35	0.022	SPO1748	0.99	0.633	SPO1749	1.15	0.244	SPO1747	1.09	0.916
SPO1753	0.97	0.875	SPO1752	0.98	0.442	SPO1752	0.83	0.929	SPO1754	0.93	0.837	SPO1753	0.53	0.140	SPO1749	1.59	0.005	SPO1750	1.12	0.411	SPO1748	0.83	0.804
SPO1754	1.47	0.521	SPO1753	1.06	0.487	SPO1753	0.96	0.174	SPO1755	0.96	0.341	SPO1752	0.69	0.147	SPO1750	1.20	0.010	SPO1751	1.11	0.698	SPO1749	1.34	0.080
SPO1755	0.96	0.974	SPO1754	1.25	0.759	SPO1754	0.96	0.865	SPO1756	0.83	0.038	SPO1753	1.01	0.098	SPO1751	0.52	0.060	SPO1752	1.07	0.802	SPO1750	1.26	0.186
SPO1756	0.79	0.504	SPO1755	1	0.589	SPO1755	0.89	0.692	SPO1757	0.98	0.516	SPO1754	0.88	0.958	SPO1752	0.64	0.028	SPO1753	0.87	0.206	SPO1751	1.04	0.383
SPO1757	1.08	0.375	SPO1756	0.88	0.322	SPO1756	0.9	0.228	SPO1758	0.7	0.538	SPO1755	2.88	0.090	SPO1753	0.84	0.322	SPO1754	0.97	0.985	SPO1752	1.02	0.837
SPO1758	0.93	0.949	SPO1757	1.01	0.568	SPO1757	0.97	0.163	SPO1759	0.93	0.899	SPO1756	1.37	0.019	SPO1754	0.88	0.968	SPO1755	1.21	0.500	SPO1753	0.91	0.625
SPO1759	1.2	0.303	SPO1758	1.15	0.419	SPO1758	0.74	0.885	SPO1760	0.75	0.957	SPO1757	1.41	0.144	SPO1755	2.99	0.001	SPO1756	0.77	0.166	SPO1754	0.92	0.934
SPO1760	1.23	0.365	SPO1759	1.23	0.163	SPO1759																	

SPO1850	0.69	0.445	SPO1848	0.68	0.049	SPO1849	0.94	0.646	SPO1851	0.73	0.201	SPO1847	5.16	0.012	SPO1845	2.09	0.116	SPO1846	0.94	0.895	SPO1843	0.94	0.797
SPO1851	0.93	0.482	SPO1849	0.79	0.682	SPO1850	0.98	0.524	SPO1852	0.96	0.18	SPO1848	4.12	0.016	SPO1846	2.04	0.018	SPO1846	0.97	0.990	SPO1844	0.81	0.774
SPO1852	0.61	0.000	SPO1850	0.68	0.582	SPO1851	0.59	0.026	SPO1853	0.91	0.73	SPO1849	3.10	0.183	SPO1847	5.24	0.001	SPO1847	1.03	0.575	SPO1845	0.91	0.798
SPO1853	0.94	0.054	SPO1851	0.74	0.541	SPO1852	0.93	0.581	SPO1854	0.95	0.362	SPO1850	2.23	0.335	SPO1846	1.03	0.444	SPO1846	0.98	0.863	SPO1846	0.98	0.861
SPO1854	1.07	0.835	SPO1852	0.68	0.058	SPO1853	0.89	0.772	SPO1855	0.81	0.137	SPO1851	3.24	0.000	SPO1849	3.29	0.077	SPO1849	1.09	0.910	SPO1847	1.11	0.306
SPO1855	1.35	0.06	SPO1853	0.57	0.138	SPO1854	1.01	0.648	SPO1856	0.82	0.21	SPO1852	1.54	0.035	SPO1850	2.29	0.388	SPO1850	1.02	0.921	SPO1848	1.06	0.553
SPO1856	1.07	0.97	SPO1854	0.96	0.997	SPO1855	0.88	0.037	SPO1858	0.9	0.833	SPO1853	1.57	0.144	SPO1851	2.79	0.007	SPO1851	1.03	0.535	SPO1849	1.05	0.915
SPO1857	1.5	0.266	SPO1855	1.25	0.011	SPO1856	0.97	0.308	SPO1859	0.66	0.841	SPO1854	1.56	0.160	SPO1852	1.40	0.002	SPO1852	0.95	0.924	SPO1850	1.07	0.839
SPO1859	1.31	0.521	SPO1856	0.95	0.866	SPO1858	0.85	0.801	SPO1860	0.88	0.573	SPO1855	1.13	0.041	SPO1853	1.63	0.085	SPO1853	1.02	0.941	SPO1851	0.98	0.850
SPO1860	0.88	0.696	SPO1858	1.4	0.179	SPO1859	0.97	0.84	SPO1861	0.85	0.011	SPO1856	0.53	0.239	SPO1854	0.61	0.284	SPO1854	0.99	0.962	SPO1852	0.89	0.566
SPO1861	1.39	0.005	SPO1859	1.19	0.679	SPO1860	0.98	0.957	SPO1862	0.94	0.013	SPO1858	0.64	0.850	SPO1855	1.25	0.003	SPO1855	1.12	0.077	SPO1853	0.99	0.997
SPO1862	0.98	0.067	SPO1860	0.85	0.671	SPO1861	0.93	0.893	SPO1863	0.98	0.068	SPO1860	0.64	0.496	SPO1856	0.94	0.559	SPO1856	0.70	0.397	SPO1854	0.99	0.861
SPO1863	0.76	0.018	SPO1861	0.71	0.001	SPO1862	0.93	0.073	SPO1864	0.95	0.162	SPO1860	0.76	0.031	SPO1858	0.94	0.909	SPO1858	1.12	0.077	SPO1855	1.01	0.969
SPO1864	1.45	0.06	SPO1862	0.37	0.020	SPO1863	0.93	0.026	SPO1865	0.79	0.844	SPO1861	3.06	0.040	SPO1859	0.65	0.335	SPO1859	0.95	0.890	SPO1856	0.76	0.513
SPO1865	1.56	0.505	SPO1863	0.47	0.026	SPO1864	0.98	0.94	SPO1866	0.92	0.293	SPO1862	3.17	0.002	SPO1860	3.92	0.004	SPO1860	1.03	0.755	SPO1858	0.98	0.939
SPO1866	0.85	0.299	SPO1864	1.42	0.047	SPO1865	0.56	0.833	SPO1867	0.94	0.527	SPO1863	2.30	0.010	SPO1861	3.11	0.001	SPO1861	1.51	0.042	SPO1859	0.92	0.807
SPO1867	0.98	0.483	SPO1865	1.48	0.418	SPO1866	0.9	0.621	SPO1868	0.95	0.483	SPO1864	1.27	0.040	SPO1862	3.09	0.004	SPO1862	1.29	0.107	SPO1860	1.09	0.565
SPO1868	1.01	0.993	SPO1866	0.87	0.259	SPO1867	0.86	0.828	SPO1869	0.92	0.213	SPO1865	0.99	0.835	SPO1863	2.74	0.015	SPO1863	1.56	0.033	SPO1861	1.58	0.003
SPO1869	0.9	0.007	SPO1867	1.08	0.793	SPO1868	1	0.623	SPO1870	0.92	0.188	SPO1866	0.81	0.607	SPO1864	1.30	0.011	SPO1864	1.12	0.281	SPO1862	1.42	0.086
SPO1870	0.93	0.783	SPO1868	1.05	0.335	SPO1869	0.87	0.335	SPO1871	0.77	0.285	SPO1867	0.61	0.027	SPO1865	0.97	0.860	SPO1865	1.02	0.844	SPO1863	1.54	0.067
SPO1871	0.66	0.067	SPO1869	0.85	0.179	SPO1870	0.83	0.583	SPO1872	0.94	0.72	SPO1868	0.64	0.155	SPO1866	0.77	0.212	SPO1866	0.90	0.823	SPO1864	1.10	0.225
SPO1872	1.25	0.684	SPO1870	1.09	0.296	SPO1871	0.95	0.609	SPO1873	0.74	0.377	SPO1869	1.02	0.216	SPO1867	0.56	0.243	SPO1867	0.83	0.337	SPO1865	1.01	0.967
SPO1873	1.23	0.335	SPO1871	0.76	0.192	SPO1872	0.99	0.901	SPO1874	0.9	0.967	SPO1870	1.57	0.010	SPO1868	0.65	0.077	SPO1868	1.02	0.827	SPO1866	0.92	0.838
SPO1874	1.4	0.141	SPO1872	1.24	0.525	SPO1873	0.86	0.402	SPO1875	0.82	0.251	SPO1871	0.99	0.511	SPO1869	1.07	0.024	SPO1869	1.05	0.494	SPO1867	0.84	0.341
SPO1875	1.7	0.059	SPO1873	1.13	0.249	SPO1874	1	0.908	SPO1876	0.97	0.185	SPO1872	1.34	0.448	SPO1870	1.56	0.011	SPO1870	1.01	0.764	SPO1868	0.99	0.757
SPO1876	1	0.972	SPO1874	1.25	0.296	SPO1875	0.88	0.625	SPO1877	0.95	0.798	SPO1873	0.42	0.026	SPO1871	1.00	0.110	SPO1871	1.06	0.201	SPO1869	1.10	0.203
SPO1877	1	0.963	SPO1875	1.51	0.065	SPO1876	0.96	0.069	SPO1878	0.92	0.977	SPO1874	1.58	0.150	SPO1872	1.29	0.224	SPO1872	0.95	0.902	SPO1870	1.05	0.516
SPO1878	0.92	0.025	SPO1876	1.04	0.384	SPO1877	0.96	0.866	SPO1879	0.76	0.394	SPO1875	1.14	0.147	SPO1873	0.95	0.024	SPO1873	1.09	0.649	SPO1871	1.06	0.018
SPO1879	1.03	0.067	SPO1877	0.96	0.936	SPO1878	0.94	0.777	SPO1880	0.98	0.445	SPO1876	0.98	0.116	SPO1874	1.83	0.046	SPO1874	1.13	0.552	SPO1870	1.15	0.447
SPO1880	1.48	0.088	SPO1878	2.53	0.027	SPO1879	0.96	0.871	SPO1881	0.97	0.833	SPO1877	0.71	0.183	SPO1875	1.20	0.170	SPO1875	1.08	0.622	SPO1873	1.01	0.958
SPO1881	1.21	0.066	SPO1879	1.05	0.914	SPO1880	0.87	0.759	SPO1882	0.91	0.773	SPO1878	0.50	0.076	SPO1876	0.67	0.026	SPO1876	0.89	0.379	SPO1874	1.08	0.346
SPO1882	1.01	0.952	SPO1880	1.3	0.095	SPO1881	0.92	0.215	SPO1883	0.99	0.071	SPO1879	0.76	0.691	SPO1877	0.71	0.012	SPO1877	1.10	0.336	SPO1875	1.02	0.699
SPO1883	1.4	0.017	SPO1881	1.21	0.154	SPO1882	0.94	0.726	SPO1884	0.94	0.829	SPO1880	0.64	0.126	SPO1878	0.63	0.066	SPO1878	1.05	0.992	SPO1876	0.93	0.300
SPO1884	0.75	0.079	SPO1882	0.88	0.482	SPO1883	0.88	0.296	SPO1886	0.92	0.853	SPO1881	0.90	0.790	SPO1879	0.75	0.656	SPO1879	0.74	0.728	SPO1877	1.11	0.150
SPO1886	1.07	0.306	SPO1883	1.43	0.031	SPO1884	0.98	0.714	SPO1887	0.92	0.221	SPO1882	0.91	0.913	SPO1880	0.88	0.185	SPO1880	1.03	0.886	SPO1878	1.08	0.855
SPO1887	1.04	0.637	SPO1884	0.76	0.089	SPO1885	0.91	0.991	SPO1888	0.97	0.441	SPO1883	0.68	0.060	SPO1881	0.95	0.807	SPO1881	1.13	0.048	SPO1879	0.75	0.744
SPO1888	0.96	0.969	SPO1885	0.98	0.337	SPO1886	0.93	0.693	SPO1889	0.88	0.337	SPO1884	0.98	0.398	SPO1882	0.98	0.039	SPO1882	1.02	0.893	SPO1880	0.92	0.856
SPO1889	1.30	0.041	SPO1887	1.11	0.545	SPO1888	0.8	0.051	SPO1890	0.88	0.609	SPO1885	0.54	0.237	SPO1883	0.76	0.028	SPO1883	1.07	0.724	SPO1881	1.10	0.577
SPO1890	0.86	0.12	SPO1888	1.91	0.009	SPO1889	0.88	0.013	SPO1891	0.95	0.657	SPO1886	3.50	0.012	SPO1884	1.89	0.007	SPO1884	1.20	0.050	SPO1882	1.00	0.975
SPO1891	0.74	0.127	SPO1889	1.48	0.017	SPO1890	0.63	0.29	SPO1892	0.87	0.306	SPO1887	1.27	0.016	SPO1885	0.51	0.005	SPO1885	0.92	0.821	SPO1883	1.02	0.943
SPO1892	1.09	0.142	SPO1890	0.94	0.743	SPO1891	0.69	0.881	SPO1893	0.93	0.529	SPO1888	0.94	0.514	SPO1886	0.53	0.006	SPO1886	1.09	0.243	SPO1884	1.17	0.068
SPO1893	0.96	0.651	SPO1891	0.78	0.23	SPO1892	0.95	0.23	SPO1895	0.98	0.46	SPO1889	1.67	0.005	SPO1887	1.15	0.128	SPO1887	1.08	0.371	SPO1885	0.84	0.788
SPO1895	1.37	0.1	SPO1892	1.1	0.16	SPO1893	0.68	0.775	SPO1896	0.98	0.434	SPO1890	1.40	0.007	SPO1888	0.87	0.403	SPO1888	1.25	0.192	SPO1886	1.05	0.727
SPO1896	1.02	0.896	SPO1893	1.01	0.422	SPO1894	0.97	0.897	SPO1897	0.74	0.578	SPO1891	0.79	0.585	SPO1889	1.81	0.022	SPO1889	1.17	0.024	SPO1887	1.14	0.123
SPO1897	0.83	0.067	SPO1895	1.12	0.276	SPO1904	0.99	0.895	SPO1906	0.97	0.652	SPO1901	1.16	0.110	SPO1889	1.64	0.022	SPO1889	1.12	0.083	SPO1887	0.97	0.856
SPO1898	1.06	0.438	SPO1896	1.09	0.978	SPO1897	0.74	0.331	SPO1899	0.94	0.32	SPO1893	1.78	0.000	SPO1891	0.79	0.640	SPO1891	0.95	0.932	SPO1889	1.15	0.413
SPO1899	1.11	0.232	SPO1897	0.81	0.304	SPO1898	0.81	0.071	SPO1900	0.93	0.511	SPO1895	1.07	0.766	SPO1892	0.97	0.053	SPO1892	0.85	0.125	SPO1890	1.12	0.675
SPO1900	1.32	0.163	SPO1898	0.97	0.902	SPO1899	0.89	0.511	SPO1901	0.76	0.522	SPO1896	0.60	0.077	SPO1893	1.78	0.001	SPO1893	0.99	0.881	SPO1891	1.01	0.826
SPO1901	0.88	0.162	SPO1899	0.95	0.791	SPO1900	0.92	0.348	SPO1902	0.91	0.533	SPO1897	0.98	0.966	SPO1895	1.17	0.221	SPO1895	1.25	0.234	SPO1892	0.88	0.207
SPO1902	0.73	0.321	SPO1900	1.18	0.086	SPO1901	0.79	0.206	SPO1903	0.97	0.354	SPO1898	1.07	0.605	SPO1896	0.66	0.316	SPO1896	0.90	0.894	SPO1893	1.06	0.071
SPO1903	0.7	0.147	SPO1901	0.92	0.319	SPO1902	0.98	0.171	SPO1904	0.79	0.571	SPO1899	1.70	0.009	SPO1897	1.05	0.190	SPO1897	0.93	0.700	SPO1895	1.22	0.108
SPO1904	0.81	0.591	SPO1902	0.83	0.605	SPO1903	0.97	0.39	SPO1905	1.01	0.127	SPO1900	1.34	0.022	SPO1898	1.08	0.505	SPO1898	0.97	0.797	SPO1896	0.95	0.944
SPO1905	0.98	0.014	SPO1903	0.77	0.276	SPO190																	

SPO1995	0.82	0.021	SPO1992	0.96	0.833	SPO1994	0.78	0.929	SPO1996	0.91	0.048	SPO1990	1.29	0.031	SPO1988	1.01	0.554	SPO1987	1.11	0.653	SPO1986	1.27	0.292
SPO1996	0.58	0.002	SPO1994	0.96	0.993	SPO1995	0.84	0.25	SPO1997	0.36	0.874	SPO1991	1.18	0.256	SPO1989	0.77	0.666	SPO1988	1.12	0.280	SPO1987	1.19	0.172
SPO1997	0.68	0.150	SPO1995	0.74	0.201	SPO1996	0.88	0.016	SPO1998	0.86	0.082	SPO1992	0.83	0.167	SPO1990	1.30	0.066	SPO1989	0.98	0.873	SPO1988	1.12	0.566
SPO1998	0.99	0.43	SPO1996	0.58	0.030	SPO1997	0.89	0.72	SPO1999	0.94	0.391	SPO1994	0.86	0.560	SPO1991	1.28	0.122	SPO1990	1.13	0.348	SPO1989	1.15	0.243
SPO1999	0.83	0.609	SPO1997	0.66	0.217	SPO1998	0.93	0.17	SPO2000	0.85	0.832	SPO1995	1.04	0.583	SPO1992	0.89	0.715	SPO1992	0.81	0.065	SPO1990	1.01	0.211
SPO2000	1.22	0.512	SPO1998	0.74	0.071	SPO1999	0.95	0.134	SPO2001	0.85	0.268	SPO1996	1.05	0.032	SPO1994	0.80	0.185	SPO1994	1.31	0.175	SPO1991	1.01	0.940
SPO2001	0.63	0.294	SPO1999	0.8	0.628	SPO2000	0.86	0.765	SPO2002	0.67	0.998	SPO1997	0.79	0.525	SPO1995	1.10	0.321	SPO1995	1.36	0.464	SPO1992	0.83	0.212
SPO2002	0.96	0.98	SPO2000	1.04	0.855	SPO2001	0.73	0.653	SPO2003	0.59	0.553	SPO1998	1.42	0.131	SPO1996	1.08	0.107	SPO1996	1.26	0.068	SPO1994	1.17	0.300
SPO2003	0.83	0.694	SPO2001	0.61	0.026	SPO2002	0.66	0.937	SPO2004	0.74	0.857	SPO1999	1.71	0.371	SPO1997	0.76	0.597	SPO1997	0.95	0.773	SPO1995	1.43	0.421
SPO2004	1.06	0.283	SPO2002	0.95	0.993	SPO2003	0.78	0.267	SPO2005	0.6	0.11	SPO2000	0.72	0.560	SPO1998	1.56	0.059	SPO1998	1.20	0.648	SPO1996	1.35	0.043
SPO2005	1.04	0.212	SPO2003	0.88	0.715	SPO2004	0.95	0.468	SPO2006	0.99	0.844	SPO2001	1.44	0.262	SPO1999	1.80	0.148	SPO1999	0.97	0.040	SPO1997	1.00	0.910
SPO2006	0.79	0.45	SPO2004	1.11	0.329	SPO2005	0.99	0.043	SPO2007	0.94	0.897	SPO1998	0.93	0.326	SPO2000	0.91	0.34	SPO2000	0.85	0.981	SPO1998	1.31	0.253
SPO2007	0.6	0.24	SPO2005	1.11	0.238	SPO2006	0.93	0.852	SPO2008	0.91	0.613	SPO2003	0.01	0.919	SPO2001	1.20	0.332	SPO2001	0.85	0.686	SPO1999	1.81	0.027
SPO2008	1.09	0.514	SPO2006	0.85	0.854	SPO2007	1.11	0.395	SPO2009	0.93	0.063	SPO2004	0.97	0.846	SPO2002	0.89	0.880	SPO2002	0.72	0.927	SPO2000	0.95	0.936
SPO2009	1.19	0.3	SPO2007	0.68	0.118	SPO2008	1.04	0.836	SPO2010	0.87	0.113	SPO2005	0.95	0.652	SPO2003	1.30	0.414	SPO2003	0.99	0.924	SPO2001	0.89	0.817
SPO2010	0.55	0.001	SPO2008	0.95	0.878	SPO2009	1.16	0.296	SPO2013	0.99	0.985	SPO2006	1.11	0.498	SPO2004	1.24	0.445	SPO2004	0.97	0.585	SPO2002	0.82	0.746
SPO2013	0.99	0.888	SPO2009	1.04	0.548	SPO2010	1.23	0.023	SPO2014	0.74	0.174	SPO2007	1.23	0.470	SPO2005	0.81	0.192	SPO2005	0.97	0.556	SPO2003	0.82	0.695
SPO2014	1.28	0.06	SPO2010	0.6	0.136	SPO2013	1.03	0.839	SPO2015	0.91	0.115	SPO2009	1.01	0.788	SPO2006	1.31	0.637	SPO2006	0.97	0.753	SPO2004	0.84	0.302
SPO2015	1.32	0.224	SPO2013	1.12	0.347	SPO2014	1.14	0.118	SPO2016	0.9	0.019	SPO2008	1.04	0.968	SPO2007	1.22	0.263	SPO2007	0.83	0.536	SPO2005	0.87	0.276
SPO2016	1.51	0.096	SPO2014	1.15	0.769	SPO2015	1.06	0.245	SPO2017	1.01	0.57	SPO2010	1.85	0.038	SPO2008	0.95	0.423	SPO2008	1.02	0.960	SPO2006	0.88	0.741
SPO2017	1.23	0.405	SPO2015	1.41	0.034	SPO2016	1.11	0.099	SPO2018	0.78	0.009	SPO2013	0.83	0.279	SPO2009	0.95	0.373	SPO2009	0.84	0.452	SPO2007	0.86	0.553
SPO2018	0.9	0.16	SPO2016	1.63	0.039	SPO2017	1.1	0.348	SPO2019	0.7	0.759	SPO2014	0.64	0.074	SPO2010	2.18	0.008	SPO2010	1.23	0.216	SPO2008	0.97	0.552
SPO2019	0.89	0.34	SPO2017	1.25	0.387	SPO2018	1.17	0.007	SPO2020	0.91	0.221	SPO2015	0.84	0.569	SPO2013	0.85	0.279	SPO2013	0.98	0.747	SPO2009	0.93	0.531
SPO2020	1.55	0.434	SPO2018	1.92	0.316	SPO2019	1.07	0.548	SPO2021	0.62	0.178	SPO2016	0.63	0.020	SPO2014	0.63	0.062	SPO2014	0.65	0.118	SPO2010	1.27	0.136
SPO2021	1.31	0.106	SPO2019	0.73	0.127	SPO2020	1.02	0.087	SPO2022	0.86	0.209	SPO2017	0.56	0.257	SPO2015	0.82	0.466	SPO2015	0.62	0.027	SPO2013	1.00	0.989
SPO2022	1.49	0.044	SPO2020	1.44	0.165	SPO2021	1.19	0.243	SPO2023	0.85	0.108	SPO2018	0.53	0.008	SPO2016	0.61	0.054	SPO2016	0.53	0.017	SPO2014	0.64	0.112
SPO2023	1.32	0.175	SPO2021	1.26	0.097	SPO2022	1.33	0.028	SPO2025	0.83	0.114	SPO2019	1.08	0.309	SPO2017	0.50	0.042	SPO2017	0.41	0.013	SPO2015	0.62	0.058
SPO2025	1.47	0.06	SPO2022	1.45	0.027	SPO2023	1.17	0.157	SPO2026	0.73	0.852	SPO2020	0.42	0.039	SPO2018	0.53	0.004	SPO2018	0.06	0.006	SPO2016	0.52	0.004
SPO2026	1.36	0.083	SPO2023	1.26	0.041	SPO2024	1.04	0.087	SPO2027	0.84	0.087	SPO2021	0.94	0.193	SPO2021	0.99	0.115	SPO2019	0.63	0.149	SPO2017	0.84	0.024
SPO2027	1.36	0.083	SPO2025	1.23	0.03	SPO2026	1.08	0.992	SPO2028	0.79	0.946	SPO2022	0.33	0.005	SPO2020	0.1	0.070	SPO2020	0.53	0.073	SPO2018	0.44	0.002
SPO2028	1.35	0.017	SPO2026	1.01	0.872	SPO2027	1.01	0.872	SPO2029	0.93	0.809	SPO2023	0.22	0.005	SPO2021	0.34	0.010	SPO2021	0.42	0.003	SPO2019	0.71	0.100
SPO2029	0.82	0.689	SPO2027	1.36	0.024	SPO2028	1.2	0.898	SPO2030	0.97	0.883	SPO2025	1.34	0.216	SPO2022	0.34	0.005	SPO2022	0.42	0.017	SPO2020	0.58	0.290
SPO2030	0.88	0.597	SPO2028	1.26	0.341	SPO2029	1.06	0.662	SPO2031	0.92	0.013	SPO2026	0.73	0.277	SPO2023	0.24	0.013	SPO2023	0.43	0.024	SPO2021	0.44	0.004
SPO2031	1.08	0.64	SPO2029	0.77	0.563	SPO2030	1.19	0.062	SPO2032	1	0.766	SPO2027	0.23	0.084	SPO2025	1.48	0.059	SPO2025	0.38	0.021	SPO2022	0.45	0.006
SPO2032	1.17	0.268	SPO2030	0.95	0.957	SPO2031	1.03	0.653	SPO2033	0.75	0.769	SPO2028	1.03	0.783	SPO2026	0.72	0.416	SPO2026	0.97	0.915	SPO2023	0.44	0.034
SPO2033	1.1	0.854	SPO2031	1.2	0.047	SPO2032	1.04	0.845	SPO2034	0.95	0.558	SPO2029	1.75	0.248	SPO2027	0.80	0.343	SPO2027	1.07	0.448	SPO2025	0.87	0.017
SPO2034	0.85	0.826	SPO2033	1.18	0.219	SPO2034	1.16	0.138	SPO2036	0.95	0.933	SPO2031	1.63	0.006	SPO2029	1.78	0.140	SPO2029	1.05	0.901	SPO2027	1.07	0.272
SPO2035	1.15	0.591	SPO2034	0.83	0.541	SPO2035	1.21	0.802	SPO2037	0.99	0.128	SPO2032	0.98	0.425	SPO2030	1.07	0.643	SPO2030	0.96	0.909	SPO2028	1.07	0.814
SPO2037	1.16	0.042	SPO2035	0.84	0.801	SPO2036	1.12	0.98	SPO2038	0.93	0.878	SPO2033	1.06	0.040	SPO2031	1.66	0.007	SPO2031	1.16	0.747	SPO2029	1.03	0.912
SPO2038	1.46	0.561	SPO2036	1.09	0.714	SPO2037	1.01	0.416	SPO2039	0.95	0.235	SPO2034	0.56	0.180	SPO2032	0.98	0.571	SPO2032	1.03	0.741	SPO2030	0.98	0.932
SPO2039	1.52	0.005	SPO2037	1.32	0.006	SPO2038	1.32	0.828	SPO2040	0.95	0.412	SPO2035	1.29	0.615	SPO2033	1.08	0.020	SPO2033	0.96	0.979	SPO2031	1.07	0.790
SPO2040	0.75	0.023	SPO2038	1.42	0.465	SPO2039	1.16	0.913	SPO2041	0.9	0.298	SPO2036	0.64	0.138	SPO2034	0.56	0.206	SPO2034	1.62	0.362	SPO2032	1.02	0.854
SPO2041	1.12	0.198	SPO2039	1.45	0.157	SPO2040	1.06	0.236	SPO2042	0.96	0.212	SPO2037	1.46	0.070	SPO2035	1.30	0.533	SPO2035	1.20	0.745	SPO2033	1.00	0.486
SPO2042	0.79	0.307	SPO2040	0.78	0.319	SPO2041	1.04	0.752	SPO2044	0.95	0.913	SPO2034	1.32	0.038	SPO2038	0.83	0.151	SPO2038	0.88	0.219	SPO2034	1.37	0.542
SPO2044	0.79	0.373	SPO2041	1.02	0.135	SPO2042	1.06	0.687	SPO2045	0.6	0.888	SPO2039	0.79	0.133	SPO2037	1.54	0.011	SPO2037	1.22	0.331	SPO2035	1.22	0.170
SPO2045	1.07	0.778	SPO2042	0.76	0.083	SPO2044	0.87	0.962	SPO2046	0.63	0.623	SPO2040	1.38	0.277	SPO2038	1.04	0.844	SPO2038	1.16	0.698	SPO2036	0.83	0.158
SPO2046	2.24	0.016	SPO2044	0.99	0.888	SPO2045	0.98	0.594	SPO2047	0.92	0.744	SPO2041	1.01	0.221	SPO2039	0.82	0.144	SPO2039	1.05	0.434	SPO2037	1.23	0.244
SPO2047	1.50	0.067	SPO2045	0.97	0.96	SPO2046	1.08	0.334	SPO2048	0.96	0.852	SPO2042	1.11	0.270	SPO2040	1.45	0.062	SPO2040	0.97	0.848	SPO2038	1.16	0.697
SPO2048	2.15	0.007	SPO2046	1.85	0.07	SPO2047	1	0.484	SPO2049	0.77	0.154	SPO2044	0.76	0.215	SPO2041	1.01	0.327	SPO2041	1.04	0.506	SPO2039	1.00	0.865
SPO2049	0.83	0.527	SPO2047	1.51	0.079	SPO2048	1.16	0.876	SPO2050	0.87	0.254	SPO2045	0.92	0.997	SPO2042	1.16	0.061	SPO2042	0.99	0.977	SPO2040	1.01	0.999
SPO2050	0.98	0.842	SPO2048	0.97	0.018	SPO2049	1.11	0.358	SPO2051	0.92	0.867	SPO2046	0.46	0.018	SPO2044	0.63	0.226	SPO2044	0.99	0.978	SPO2041	1.08	0.176
SPO2051	1.44	0.07	SPO2049	0.71	0.205	SPO2050	0.99	0.863	SPO2052	0.77	0.727	SPO2047	0.54	0.070	SPO2045	0.90	0.835	SPO2045	0.98	0.912	SPO2042	1.06	0.225
SPO2052	1.01	0.633	SPO2050	1.1	0.51	SPO205																	

SPO2141	1.1	0.528	SPO2139	0.98	0.839	SPO2140	1	0.252	SPO2142	1.03	0.349	SPO2136	2.46	0.008	SPO2134	1.97	0.012	SPO2134	1.57	0.365	SPO2132	1.13	0.453
SPO2142	0.95	0.848	SPO2140	1.2	0.93	SPO2141	1.13	0.058	SPO2143	1.26	0.742	SPO2137	0.86	0.717	SPO2135	5.95	0.004	SPO2135	1.06	0.117	SPO2133	0.79	0.190
SPO2143	1.01	0.992	SPO2141	0.97	0.992	SPO2142	1.09	0.568	SPO2144	1.12	0.040	SPO2139	1.42	0.214	SPO2136	2.95	0.004	SPO2136	0.96	0.981	SPO2134	1.32	0.118
SPO2144	1.38	0.028	SPO2140	0.97	0.874	SPO2141	1.04	0.874	SPO2145	1.02	0.551	SPO2146	1.17	0.365	SPO2137	0.85	0.205	SPO2137	0.88	0.747	SPO2135	0.83	0.405
SPO2145	0.96	0.766	SPO2143	1.05	0.81	SPO2144	1.02	0.201	SPO2146	1.04	0.296	SPO2141	0.62	0.156	SPO2139	1.42	0.033	SPO2139	0.96	0.911	SPO2136	0.90	0.463
SPO2146	1.11	0.376	SPO2144	1.29	0.67	SPO2145	1.01	0.04	SPO2147	1.04	0.409	SPO2142	1.10	0.260	SPO2140	1.20	0.100	SPO2140	1.06	0.847	SPO2137	0.92	0.612
SPO2147	1.32	0.022	SPO2145	1.03	0.723	SPO2146	1.29	0.379	SPO2148	1.24	0.914	SPO2143	1.07	0.546	SPO2141	0.65	0.416	SPO2141	0.83	0.493	SPO2139	0.94	0.827
SPO2148	1.04	0.375	SPO2146	1.13	0.99	SPO2147	1.03	0.102	SPO2149	1.1	0.394	SPO2144	1.12	0.042	SPO2142	1.10	0.353	SPO2142	1.11	0.468	SPO2140	1.03	0.853
SPO2149	0.97	0.916	SPO2147	1.33	0.079	SPO2148	1.02	0.906	SPO2150	1.05	0.554	SPO2145	0.92	0.782	SPO2143	1.12	0.409	SPO2143	1.06	0.731	SPO2141	0.87	0.668
SPO2150	1	0.712	SPO2148	1.1	0.891	SPO2149	1.11	0.266	SPO2151	1.16	0.049	SPO2146	1.37	0.196	SPO2144	1.14	0.011	SPO2144	1.13	0.190	SPO2142	1.14	0.339
SPO2151	0.6	0.007	SPO2149	1.02	0.255	SPO2150	0.99	0.079	SPO2152	1.11	0.053	SPO2147	1.71	0.054	SPO2145	0.89	0.442	SPO2145	1.04	0.676	SPO2143	1.14	0.559
SPO2152	1.14	0.319	SPO2150	0.97	0.871	SPO2151	1.02	0.653	SPO2153	0.96	0.545	SPO2148	1.09	0.319	SPO2146	1.38	0.019	SPO2146	1.15	0.469	SPO2144	1.05	0.611
SPO2153	1.15	0.555	SPO2151	0.68	0.038	SPO2152	1.11	0.223	SPO2154	1.48	0.348	SPO2149	0.78	0.307	SPO2147	1.59	0.020	SPO2147	1.11	0.402	SPO2145	1.00	0.437
SPO2154	0.73	0.196	SPO2152	1.02	0.736	SPO2153	1.12	0.264	SPO2155	1.16	0.489	SPO2150	0.85	0.283	SPO2148	0.94	0.813	SPO2148	0.94	0.380	SPO2146	1.14	0.172
SPO2155	0.95	0.824	SPO2153	1.08	0.228	SPO2154	1.07	0.953	SPO2156	1.22	0.93	SPO2151	1.54	0.008	SPO2149	0.76	0.057	SPO2149	0.93	0.645	SPO2147	1.23	0.195
SPO2156	1.55	0.558	SPO2154	0.41	0.144	SPO2155	1.11	0.772	SPO2157	1.76	0.466	SPO2152	1.08	0.115	SPO2150	0.91	0.981	SPO2150	0.89	0.577	SPO2148	0.95	0.245
SPO2157	1.65	0.027	SPO2155	0.99	0.579	SPO2156	1.04	0.823	SPO2158	3.83	0.046	SPO2153	1.32	0.309	SPO2151	1.52	0.016	SPO2151	1.06	0.447	SPO2149	0.91	0.664
SPO2158	1.47	0.155	SPO2156	1.43	0.603	SPO2157	1.13	0.39	SPO2159	2.89	0.08	SPO2154	2.45	0.158	SPO2152	1.06	0.071	SPO2152	1.05	0.570	SPO2150	0.89	0.228
SPO2159	0.6	0.127	SPO2157	1.54	0.037	SPO2158	1.08	0.092	SPO2160	1.59	0.254	SPO2155	0.83	0.466	SPO2153	1.47	0.037	SPO2153	1.19	0.696	SPO2151	1.11	0.093
SPO2160	0.52	0.289	SPO2158	1.32	0.072	SPO2159	1.12	0.245	SPO2161	1.97	0.269	SPO2156	0.63	0.674	SPO2154	2.94	0.066	SPO2154	0.88	0.197	SPO2152	1.05	0.528
SPO2161	0.79	0.106	SPO2159	0.56	0.025	SPO2160	1.32	0.274	SPO2162	1.05	0.851	SPO2157	0.65	0.029	SPO2155	0.78	0.492	SPO2155	0.53	0.809	SPO2153	1.04	0.671
SPO2162	0.73	0.142	SPO2160	0.55	0.027	SPO2161	1.01	0.883	SPO2163	1.09	0.568	SPO2158	0.98	0.021	SPO2156	0.66	0.765	SPO2156	0.92	0.902	SPO2154	1.82	0.266
SPO2163	0.76	0.35	SPO2161	0.83	0.279	SPO2162	1.11	0.686	SPO2164	1.05	0.387	SPO2159	2.26	0.051	SPO2157	0.43	0.039	SPO2157	0.96	0.966	SPO2155	1.03	0.867
SPO2164	1.17	0.338	SPO2162	0.81	0.088	SPO2163	1.02	0.993	SPO2165	1.04	0.143	SPO2160	2.71	0.046	SPO2158	0.49	0.028	SPO2158	1.00	0.956	SPO2156	0.95	0.965
SPO2165	1.22	0.474	SPO2163	0.99	0.776	SPO2164	1.32	0.595	SPO2166	1.29	0.163	SPO2161	1.84	0.032	SPO2159	2.92	0.025	SPO2159	1.92	0.088	SPO2157	0.98	0.82
SPO2166	1.53	0.024	SPO2164	1.25	0.822	SPO2165	1.03	0.357	SPO2167	1.11	0.142	SPO2162	0.68	0.026	SPO2160	2.88	0.048	SPO2160	1.50	0.221	SPO2158	0.94	0.698
SPO2167	0.92	0.575	SPO2165	1.18	0.432	SPO2166	1.08	0.334	SPO2168	1.05	0.643	SPO2163	0.62	0.103	SPO2161	1.94	0.016	SPO2161	0.86	0.540	SPO2159	1.87	0.041
SPO2168	1.72	0.077	SPO2166	1.39	0.034	SPO2167	1.09	0.193	SPO2169	1.08	0.032	SPO2164	0.97	0.676	SPO2162	0.65	0.021	SPO2162	0.83	0.437	SPO2160	1.46	0.405
SPO2169	0.62	0.992	SPO2167	0.89	0.292	SPO2168	1.18	0.897	SPO2170	1.03	0.236	SPO2165	0.78	0.384	SPO2163	0.62	0.071	SPO2163	0.62	0.144	SPO2161	0.93	0.713
SPO2170	0.38	0.17	SPO2168	1.17	0.396	SPO2169	1.22	0.119	SPO2171	1.19	0.612	SPO2166	0.83	0.004	SPO2164	1.16	0.607	SPO2164	1.05	0.977	SPO2162	0.76	0.198
SPO2171	0.85	0.699	SPO2169	1.51	0.012	SPO2170	1.07	0.588	SPO2173	1.04	0.973	SPO2167	1.56	0.005	SPO2165	0.65	0.037	SPO2165	0.97	0.897	SPO2163	0.61	0.108
SPO2172	1.02	0.422	SPO2170	0.51	0.261	SPO2171	1.47	0.771	SPO2174	1.03	0.814	SPO2168	1.47	0.118	SPO2166	0.64	0.039	SPO2166	0.97	0.772	SPO2164	1.01	0.932
SPO2173	1.08	0.264	SPO2171	0.81	0.327	SPO2173	1.06	0.799	SPO2176	1.03	0.643	SPO2169	1.03	0.581	SPO2167	1.63	0.012	SPO2167	1.01	0.794	SPO2165	0.93	0.287
SPO2174	0.96	0.956	SPO2173	0.93	0.826	SPO2174	1	0.641	SPO2177	1.12	0.976	SPO2170	2.04	0.142	SPO2168	1.39	0.107	SPO2168	1.19	0.671	SPO2166	0.84	0.185
SPO2175	1.15	0.92	SPO2174	1.09	0.135	SPO2176	1.24	0.787	SPO2178	1.08	0.991	SPO2171	1.88	0.075	SPO2169	1.07	0.138	SPO2169	1.19	0.491	SPO2167	1.04	0.326
SPO2176	1.15	0.622	SPO2175	0.88	0.254	SPO2177	1.1	0.967	SPO2179	1.08	0.137	SPO2173	0.83	0.471	SPO2170	1.82	0.250	SPO2170	1.23	0.360	SPO2168	1.19	0.410
SPO2177	0.73	0.35	SPO2176	1.06	0.702	SPO2177	1.09	0.167	SPO2180	1.07	0.829	SPO2174	0.65	0.021	SPO2171	1.21	0.709	SPO2171	1.29	0.921	SPO2169	1.16	0.548
SPO2178	0.75	1.35	SPO2177	1.08	0.71	SPO2179	1.07	0.162	SPO2181	1.27	0.164	SPO2176	0.82	0.208	SPO2173	0.91	0.402	SPO2173	1.05	0.550	SPO2170	1.13	0.038
SPO2179	1.18	0.087	SPO2178	1.1	0.770	SPO2180	1.07	0.66	SPO2182	1.05	0.544	SPO2177	0.91	0.970	SPO2174	1.26	0.289	SPO2174	1.08	0.871	SPO2171	1.12	0.317
SPO2180	1.03	0.589	SPO2180	0.73	0.098	SPO2181	0.99	0.861	SPO2183	1.16	0.84	SPO2178	0.94	0.863	SPO2176	0.97	0.778	SPO2176	1.02	0.782	SPO2173	1.01	0.941
SPO2181	1.04	0.924	SPO2181	1.07	0.268	SPO2182	0.99	0.301	SPO2184	1.34	0.004	SPO2179	0.63	0.089	SPO2177	0.88	0.964	SPO2177	0.92	0.959	SPO2174	1.03	0.547
SPO2182	0.71	0.154	SPO2182	1.05	0.603	SPO2183	1.25	0.889	SPO2185	0.94	0.757	SPO2180	0.72	0.263	SPO2178	0.96	0.821	SPO2178	0.95	0.829	SPO2176	1.05	0.554
SPO2183	0.82	0.167	SPO2183	0.98	0.068	SPO2184	1.03	0.505	SPO2186	1.33	0.649	SPO2181	0.81	0.277	SPO2179	0.58	0.077	SPO2179	0.95	0.892	SPO2177	0.93	0.962
SPO2184	0.79	0.303	SPO2184	0.85	0.065	SPO2185	1.1	0.876	SPO2187	1.26	0.033	SPO2182	0.82	0.309	SPO2180	0.73	0.339	SPO2180	1.57	0.091	SPO2178	0.93	0.851
SPO2185	1.29	0.601	SPO2185	0.82	0.106	SPO2186	1.27	0.825	SPO2188	1.19	0.891	SPO2183	0.78	0.534	SPO2181	0.85	0.584	SPO2181	0.92	0.571	SPO2180	0.93	0.713
SPO2186	1.28	0.601	SPO2186	0.73	0.252	SPO2187	1.04	0.133	SPO2189	1.08	0.137	SPO2184	1.70	0.010	SPO2182	0.79	0.301	SPO2182	1.00	0.888	SPO2180	1.54	0.079
SPO2187	1.27	0.006	SPO2187	0.71	0.015	SPO2188	1.19	0.979	SPO2190	1.03	0.902	SPO2185	1.74	0.036	SPO2183	0.80	0.799	SPO2183	0.84	0.813	SPO2181	0.99	0.948
SPO2188	0.91	0.643	SPO2188	1.25	0.603	SPO2189	1.03	0.393	SPO2191	1.06	0.842	SPO2186	1.87	0.017	SPO2184	2.01	0.001	SPO2184	1.51	0.054	SPO2182	1.01	0.990
SPO2189	0.88	0.892	SPO2189	1.29	0.043	SPO2190	1.11	0.957	SPO2192	1.18	0.861	SPO2187	1.13	0.063	SPO2185	1.85	0.014	SPO2185	1.12	0.586	SPO2183	0.83	0.338
SPO2190	0.82	0.792	SPO2190	1.04	0.646	SPO2191	1.17	0.824	SPO2193	1.11	0.913	SPO2188	1.17	0.759	SPO2186	1.98	0.002	SPO2186	0.97	0.995	SPO2184	1.45	0.028
SPO2191	0.87	0.377	SPO2191	0.93	0.984	SPO2192	1.03	0.826	SPO2194	1.05	0.378	SPO2189	1.12	0.340	SPO2187	1.18	0.005	SPO2187	1.07	1.181	SPO2185	1.10	0.671
SPO2192	1.07	0.636	SPO2192	0.85	0.71	SPO2193	1.08	0.998	SPO2195	1.28	0.481	SPO2190	1.07	0.344	SPO2188	1.14	0.800	SPO2188	1.10	0.904	SPO2186	1.07	0.579
SPO2193	0.91	0.80	SPO2193	0.81	0.219																		

SPO2284	1.37	0.061	SPO2282	1.32	0.078	SPO2283	1.01	0.219	SPO2285	1.23	0.044	SPO2280	0.81	0.335	SPO2278	1.31	0.245	SPO2276	1.31	0.281	SPO2277	1.20	0.033
SPO2285	0.81	0.034	SPO2283	1.95	0.102	SPO2284	1.18	0.476	SPO2287	1.15	0.732	SPO2281	1.69	0.006	SPO2279	1.69	0.051	SPO2278	1.14	0.422	SPO2277	1.10	0.564
SPO2286	0.79	0.716	SPO2284	1.26	0.033	SPO2285	1.11	0.063	SPO2282	1.11	0.602	SPO2286	1.98	0.002	SPO2280	0.76	0.361	SPO2280	0.85	0.290	SPO2278	1.30	0.250
SPO2287	0.50	0.269	SPO2285	0.93	0.093	SPO2286	1.16	0.701	SPO2288	1.16	0.140	SPO2283	0.81	0.151	SPO2282	1.51	0.002	SPO2281	1.04	0.430	SPO2281	1.04	0.039
SPO2288	0.31	0.063	SPO2286	0.73	0.772	SPO2287	1.28	0.689	SPO2289	1.22	0.791	SPO2284	1.35	0.133	SPO2282	1.60	0.019	SPO2280	1.07	0.679	SPO2280	0.83	0.327
SPO2289	0.31	0.168	SPO2287	0.74	0.222	SPO2288	1.01	0.869	SPO2290	0.99	0.167	SPO2285	0.52	0.010	SPO2283	0.70	0.589	SPO2283	1.01	0.883	SPO2281	1.12	0.237
SPO2290	0.58	0.03	SPO2288	1.91	0.066	SPO2289	1.08	0.676	SPO2292	1.19	0.472	SPO2286	0.75	0.764	SPO2284	1.37	0.032	SPO2284	0.85	0.460	SPO2282	1.07	0.536
SPO2292	0.96	0.841	SPO2289	0.38	0.249	SPO2290	1.11	0.193	SPO2293	1.04	0.887	SPO2287	0.40	0.012	SPO2285	0.51	0.001	SPO2285	0.94	0.715	SPO2283	0.84	0.743
SPO2293	0.91	0.426	SPO2290	0.79	0.56	SPO2292	1.05	0.324	SPO2294	1.29	0.806	SPO2288	0.88	0.957	SPO2286	0.65	0.585	SPO2286	0.93	0.952	SPO2284	0.83	0.421
SPO2294	0.75	0.029	SPO2292	0.94	0.71	SPO2293	1.11	0.861	SPO2295	1.08	0.245	SPO2289	4.11	0.085	SPO2287	0.35	0.029	SPO2287	0.98	0.408	SPO2285	0.93	0.330
SPO2295	1.66	0.252	SPO2293	0.98	0.903	SPO2294	1.01	0.811	SPO2296	1.05	0.008	SPO2290	0.75	0.038	SPO2288	0.85	0.896	SPO2288	1.00	0.904	SPO2286	1.00	0.975
SPO2296	0.51	0.269	SPO2294	0.93	0.093	SPO2295	1.05	0.523	SPO2297	1.06	0.443	SPO2291	1.37	0.066	SPO2289	0.89	0.127	SPO2289	1.39	0.697	SPO2287	1.00	0.675
SPO2297	0.81	0.289	SPO2295	1.46	0.216	SPO2296	1.17	0.124	SPO2298	1.11	0.114	SPO2293	0.01	0.854	SPO2289	0.80	0.138	SPO2290	1.06	0.882	SPO2288	0.90	0.684
SPO2298	1.04	0.894	SPO2296	0.54	0.062	SPO2297	1.19	0.24	SPO2298	1.14	0.571	SPO2294	0.54	0.006	SPO2292	1.91	0.022	SPO2292	0.90	0.273	SPO2289	1.48	0.535
SPO2299	0.63	0.474	SPO2297	1.04	0.655	SPO2298	0.98	0.218	SPO2300	1.01	0.922	SPO2295	0.40	0.048	SPO2293	0.97	0.955	SPO2293	1.05	0.846	SPO2290	1.22	0.161
SPO2300	0.89	0.907	SPO2298	0.88	0.638	SPO2299	1.43	0.768	SPO301	1.13	0.813	SPO2296	1.32	0.126	SPO2294	0.51	0.003	SPO2294	1.03	0.155	SPO2292	1.04	0.722
SPO2301	0.67	0.055	SPO2299	0.72	0.136	SPO2300	1.08	0.956	SPO2302	1.29	0.485	SPO2297	0.61	0.030	SPO2295	0.50	0.017	SPO2295	1.04	0.876	SPO2293	1.01	0.913
SPO2302	0.88	0.499	SPO2300	0.97	0.905	SPO2301	1.12	0.822	SPO2303	1.17	0.82	SPO2298	1.56	0.125	SPO2296	1.34	0.121	SPO2296	1.04	0.798	SPO2294	1.07	0.327
SPO2303	1.07	0.577	SPO2301	0.81	0.111	SPO2302	1.09	0.265	SPO2304	1.02	0.331	SPO2299	0.77	0.241	SPO2297	0.56	0.046	SPO2297	0.78	0.071	SPO2295	0.98	1.000
SPO2304	1.17	0.141	SPO2302	0.85	0.298	SPO2303	1.24	0.877	SPO2305	1.16	0.604	SPO2300	0.61	0.162	SPO2298	1.93	0.030	SPO2298	1.02	0.868	SPO2296	1.09	0.611
SPO2305	0.73	0.14	SPO2304	1.05	0.163	SPO2305	1.18	0.371	SPO2307	1.17	0.667	SPO2302	0.93	0.294	SPO2300	0.58	0.024	SPO2300	0.96	0.333	SPO2298	1.03	0.757
SPO2307	1.01	0.636	SPO2305	1.23	0.111	SPO2306	1.22	0.285	SPO2308	1.23	0.217	SPO2303	1.24	0.015	SPO2301	0.40	0.032	SPO2301	1.04	0.850	SPO2299	1.05	0.921
SPO2308	1.1	0.691	SPO2306	0.86	0.414	SPO2307	1.22	0.79	SPO2309	1.11	0.876	SPO2304	1.05	0.643	SPO2302	0.98	0.070	SPO2302	1.11	0.470	SPO2301	1.11	0.585
SPO2309	1.26	0.524	SPO2307	1.1	0.597	SPO2308	1.17	0.154	SPO2310	1.47	0.339	SPO2305	1.24	0.099	SPO2303	1.43	0.097	SPO2303	1.09	0.320	SPO2301	1.02	0.813
SPO2310	1.26	0.290	SPO2308	1.1	0.451	SPO2309	1.02	0.651	SPO2311	1.41	0.697	SPO2306	0.59	0.115	SPO2304	1.04	0.452	SPO2304	0.89	0.633	SPO2302	1.12	0.032
SPO2311	1.07	0.22	SPO2309	1.28	0.789	SPO2310	1.14	0.377	SPO2312	1.11	0.128	SPO2307	0.76	0.020	SPO2305	1.28	0.063	SPO2305	1.16	0.134	SPO2303	1.03	0.873
SPO2312	1.49	0.046	SPO2310	1.24	0.019	SPO2311	1.03	0.331	SPO2313	1.13	0.461	SPO2308	0.74	0.141	SPO2306	0.61	0.144	SPO2306	0.75	0.126	SPO2304	0.93	0.811
SPO2313	1.22	0.137	SPO2311	1.06	0.201	SPO2312	1.15	0.939	SPO2314	1.18	0.922	SPO2311	0.92	0.18	SPO2307	0.75	0.068	SPO2307	1.01	0.149	SPO2305	1.16	0.224
SPO2314	1.31	0.414	SPO2312	1.44	0.089	SPO2313	1.14	0.416	SPO2315	1.17	0.953	SPO2310	0.74	0.081	SPO2308	0.93	0.085	SPO2308	1.07	0.830	SPO2306	0.77	0.137
SPO2315	1.52	0.071	SPO2313	1.33	0.218	SPO2314	1.15	0.813	SPO2316	1.35	0.862	SPO2311	0.57	0.157	SPO2309	0.79	0.755	SPO2309	0.88	0.364	SPO2307	0.86	0.054
SPO2316	1.19	0.781	SPO2314	1.26	0.373	SPO2315	1.12	0.547	SPO2317	1.16	0.52	SPO2312	0.74	0.263	SPO2310	0.74	0.009	SPO2310	0.83	0.194	SPO2308	1.16	0.586
SPO2317	1.38	0.389	SPO2315	1.38	0.057	SPO2316	1.07	0.94	SPO2318	1.22	0.943	SPO2313	0.59	0.022	SPO2311	0.61	0.017	SPO2311	1.24	0.361	SPO2309	0.90	0.864
SPO2318	1.43	0.142	SPO2316	1.11	0.876	SPO2317	1.14	0.707	SPO2319	1.38	0.739	SPO2314	1.01	0.625	SPO2312	0.75	0.501	SPO2312	1.13	0.450	SPO2310	0.81	0.281
SPO2319	1.31	0.57	SPO2317	1.28	0.274	SPO2318	1.11	0.889	SPO2320	1.49	0.544	SPO2315	0.93	0.881	SPO2313	0.95	0.226	SPO2313	0.95	0.738	SPO2311	1.30	0.293
SPO2320	1.87	0.052	SPO2318	1.37	0.163	SPO2319	1.22	0.809	SPO2321	1.07	0.568	SPO2316	1.02	0.925	SPO2314	1.09	0.570	SPO2314	1.09	0.749	SPO2312	1.03	0.743
SPO2321	1.07	0.137	SPO2319	1.06	0.175	SPO2320	1.11	0.375	SPO2322	1.27	0.272	SPO2317	0.92	0.27	SPO2312	0.92	0.18	SPO2312	0.91	0.711	SPO2311	0.83	0.522
SPO2322	0.89	1.146	SPO2320	1.06	0.074	SPO2321	1.11	0.891	SPO2323	1.11	0.883	SPO2318	1.04	0.908	SPO2316	1.00	0.940	SPO2316	0.96	0.948	SPO2314	1.06	0.879
SPO2323	0.68	0.618	SPO2321	1.29	0.038	SPO2322	1.11	0.16	SPO2324	1.21	0.365	SPO2319	0.76	0.739	SPO2317	0.69	0.256	SPO2317	0.79	0.259	SPO2315	1.07	0.344
SPO2324	0.91	0.721	SPO2322	0.96	0.689	SPO2323	1.22	0.898	SPO2325	1.16	0.514	SPO2320	0.66	0.057	SPO2318	0.69	0.668	SPO2325	1.11	0.848	SPO2316	0.98	0.988
SPO2325	1.1	0.995	SPO2323	0.79	0.73	SPO2324	1.17	0.103	SPO2326	1.03	0.248	SPO2321	1.52	0.008	SPO2319	0.69	0.445	SPO2319	0.88	0.814	SPO2317	0.84	0.383
SPO2326	0.66	0.063	SPO2324	1.06	0.742	SPO2325	1.13	0.449	SPO2327	1.01	0.033	SPO2322	1.25	0.004	SPO2320	0.71	0.217	SPO2320	0.96	0.907	SPO2318	1.05	0.908
SPO2327	0.95	0.652	SPO2325	0.91	0.816	SPO2326	1.19	0.234	SPO2328	1.09	0.882	SPO2323	0.89	0.905	SPO2321	1.52	0.003	SPO2321	1.04	0.623	SPO2319	0.98	0.987
SPO2328	0.99	0.935	SPO2326	0.07	0.096	SPO2327	1.39	0.018	SPO2329	1.01	0.414	SPO2324	1.05	0.042	SPO2322	1.19	0.005	SPO2322	0.94	0.887	SPO2320	0.95	0.909
SPO2329	1.49	0.138	SPO2327	0.86	0.857	SPO2328	1.21	0.892	SPO2330	1.25	0.916	SPO2324	1.09	0.501	SPO2323	0.93	0.857	SPO2323	0.93	0.848	SPO2321	0.98	0.942
SPO2330	1.28	0.402	SPO2328	0.94	0.833	SPO2329	1.09	0.42	SPO2331	1.11	0.016	SPO2328	1.22	0.120	SPO2324	0.30	0.032	SPO2324	0.91	0.423	SPO2322	0.99	0.960
SPO2331	1.11	0.027	SPO2329	1.37	0.213	SPO2330	1.17	0.755	SPO2332	1.36	0.04	SPO2327	1.05	0.027	SPO2325	1.05	0.592	SPO2325	0.93	0.863	SPO2323	0.81	0.744
SPO2332	1.52	0.043	SPO2330	1.29	0.447	SPO2331	1.07	0.008	SPO2333	1.34	0.373	SPO2328	1.47	0.024	SPO2326	1.31	0.074	SPO2326	1.34	0.079	SPO2324	0.81	0.487
SPO2333	1.38	0.179	SPO2331	2.06	0.007	SPO2332	1.08	0.008	SPO2334	1.04	0.947	SPO2329	1.70	0.276	SPO2327	0.46	0.028	SPO2327	1.01	0.836	SPO2325	0.97	0.966
SPO2334	1.11	0.909	SPO2332	1.7	0.064	SPO2333	1.23	0.193	SPO2335	1.07	0.644	SPO2330	0.92	0.929	SPO2328	1.42	0.004	SPO2328	1.18	0.117	SPO2326	1.26	0.208
SPO2335	1.42	0.04	SPO2333	1.42	0.063	SPO2334	1.03	0.95	SPO2336	1.06	0.734	SPO2331	0.37	0.009	SPO2329	0.70	0.375	SPO2329	1.10	0.582	SPO2327	0.97	0.957
SPO2336	0.96	0.971	SPO2334	1.04	0.957	SPO2335	1.04	0.467	SPO2337	1.11	0.957	SPO2332	0.51	0.041	SPO2330	0.99	0.016	SPO2330	1.02	0.910	SPO2328	1.27	0.062
SPO2337	1.1	0.06	SPO2335	1.44	0.288	SPO2336	1.11	0.632	SPO2338	1.11	0.764	SPO2334	1.09	0.860	SPO2331	0.99	0.075	SPO2331	0.92	0.783	SPO2329	0.99	0.942
SPO2338	1.54	0.243	SPO2336	1.04																			

SPO2435	0.85	0.701	SPO2433	0.85	0.58	SPO2434	1.14	0.015	SPO2437	1.2	0.915	SPO2429	1.01	0.602	SPO2429	0.97	0.474	SPO2430	1.11	0.809	SPO2426	0.95	0.615
SPO2436	1.2	0.707	SPO2434	0.69	0.041	SPO2435	1.04	0.243	SPO2438	1.06	0.24	SPO2430	1.00	0.573	SPO2430	1.24	0.565	SPO2431	1.00	0.959	SPO2427	0.96	0.789
SPO2437	0.96	0.963	SPO2435	0.93	0.061	SPO2436	1.02	0.891	SPO2439	1.12	0.713	SPO2431	0.83	0.264	SPO2431	0.72	0.065	SPO2432	0.97	0.760	SPO2428	0.99	0.961
SPO2438	1.28	0.993	SPO2444	1.08	0.15	SPO2437	1.15	0.975	SPO2438	1.14	0.649	SPO2432	1.25	0.228	SPO2432	1.32	0.228	SPO2433	1.09	0.934	SPO2430	0.75	0.932
SPO2439	0.89	0.297	SPO2437	1.1	0.876	SPO2439	1.03	0.151	SPO2441	1.32	0.688	SPO2433	1.1	0.98	SPO2433	1.39	0.284	SPO2434	1.01	0.934	SPO2430	1.08	0.832
SPO2440	0.86	0.7	SPO2438	0.72	0.405	SPO2439	1.09	0.779	SPO2442	1.1	0.765	SPO2434	1.75	0.027	SPO2434	1.71	0.018	SPO2435	0.96	0.766	SPO2431	0.98	0.813
SPO2441	0.88	0.319	SPO2439	0.89	0.66	SPO2440	1.07	0.941	SPO2443	1.03	0.293	SPO2435	0.94	0.340	SPO2435	0.97	0.379	SPO2436	0.95	0.849	SPO2432	0.97	0.829
SPO2442	0.88	0.907	SPO2440	0.86	0.198	SPO2441	1.09	0.419	SPO2444	1.34	0.545	SPO2436	0.90	0.932	SPO2436	1.06	0.989	SPO2437	1.05	0.980	SPO2433	1.08	0.789
SPO2443	0.85	0.759	SPO2441	1.02	0.383	SPO2442	1.02	0.858	SPO2445	1.06	0.837	SPO2437	1.50	0.306	SPO2437	1.75	0.515	SPO2438	1.14	0.783	SPO2434	1.11	0.383
SPO2444	1.32	0.039	SPO2442	1.01	0.645	SPO2443	1.15	0.197	SPO2446	1.05	0.349	SPO2438	1.69	0.068	SPO2438	1.57	0.133	SPO2439	1.13	0.585	SPO2435	0.97	0.946
SPO2445	1.23	0.254	SPO2443	0.78	0.305	SPO2444	1.07	0.644	SPO2447	1.54	0.887	SPO2439	1.56	0.204	SPO2439	1.28	0.187	SPO2440	1.02	0.991	SPO2436	0.93	0.904
SPO2446	1.28	0.993	SPO2444	1.1	0.823	SPO2445	1.11	0.71	SPO2448	1.06	0.841	SPO2440	1.24	0.398	SPO2440	1.19	0.38	SPO2441	0.88	0.767	SPO2437	1.07	0.770
SPO2447	0.95	0.789	SPO2445	0.92	0.883	SPO2446	1.06	0.247	SPO2449	1.02	0.819	SPO2441	1.53	0.043	SPO2441	1.41	0.005	SPO2442	0.86	0.770	SPO2438	1.17	0.719
SPO2448	1.25	0.736	SPO2446	1.36	0.028	SPO2447	1.1	0.878	SPO2450	1.08	0.058	SPO2442	0.96	0.952	SPO2442	0.72	0.156	SPO2443	1.14	0.303	SPO2430	1.08	0.566
SPO2449	1.09	0.423	SPO2447	1.22	0.46	SPO2448	1.12	0.956	SPO2451	1.48	0.84	SPO2443	2.56	0.048	SPO2443	2.31	0.014	SPO2444	1.07	0.550	SPO2440	1.02	0.922
SPO2450	0.96	0.996	SPO2448	1.24	0.819	SPO2449	1.18	0.109	SPO2452	1.1	0.842	SPO2444	0.73	0.163	SPO2444	0.70	0.214	SPO2445	0.97	0.888	SPO2441	0.93	0.796
SPO2451	1.03	0.97	SPO2449	1.06	0.678	SPO2450	1.18	0.287	SPO2453	1.09	0.181	SPO2445	0.93	0.735	SPO2445	0.85	0.458	SPO2446	1.19	0.055	SPO2442	0.96	0.460
SPO2452	1.38	0.467	SPO2450	0.7	0.423	SPO2451	1.15	0.96	SPO2454	1.07	0.183	SPO2446	1.40	0.088	SPO2446	1.47	0.007	SPO2447	0.93	0.705	SPO2443	1.01	0.932
SPO2453	0.93	0.426	SPO2451	0.97	0.316	SPO2452	1.27	0.994	SPO2455	1.21	0.828	SPO2447	1.20	0.482	SPO2447	1.18	0.539	SPO2448	0.90	0.930	SPO2444	1.01	0.844
SPO2454	1.33	0.398	SPO2452	1.26	0.649	SPO2453	1.11	0.35	SPO2456	1.16	0.131	SPO2448	1.10	0.759	SPO2448	1.07	0.866	SPO2449	1.05	0.693	SPO2445	1.00	0.984
SPO2455	0.79	0.336	SPO2453	0.93	0.543	SPO2454	1.08	0.205	SPO2457	1.15	0.48	SPO2449	1.08	0.022	SPO2449	0.57	0.021	SPO2450	1.05	0.817	SPO2446	1.09	0.414
SPO2456	1.15	0.223	SPO2454	1.3	0.09	SPO2455	1.03	0.61	SPO2458	1.06	0.982	SPO2450	2.58	0.095	SPO2450	4.36	0.010	SPO2451	1.15	0.894	SPO2447	1.08	0.830
SPO2457	1.1	0.326	SPO2455	0.83	0.484	SPO2456	1.08	0.168	SPO2459	1.09	0.027	SPO2451	0.78	0.924	SPO2451	0.63	0.421	SPO2452	0.98	0.988	SPO2448	0.97	0.911
SPO2458	1.37	0.656	SPO2456	1.15	0.293	SPO2457	1.07	0.467	SPO2458	0.88	0.953	SPO2452	0.76	0.820	SPO2452	0.76	0.820	SPO2453	0.99	0.863	SPO2449	1.07	0.561
SPO2459	0.67	0.009	SPO2457	1.1	0.228	SPO2458	1.1	0.976	SPO2461	1.1	0.907	SPO2453	1.47	0.009	SPO2453	1.45	0.004	SPO2454	1.07	0.511	SPO2450	1.18	0.349
SPO2460	2.07	0.009	SPO2458	1.26	0.783	SPO2459	1.14	0.601	SPO2462	1.01	0.792	SPO2454	0.92	0.937	SPO2454	0.91	0.841	SPO2455	1.00	0.915	SPO2451	1.05	0.896
SPO2461	1.64	0.009	SPO2459	0.71	0.016	SPO2460	1.01	0.815	SPO2463	1.09	0.626	SPO2455	1.00	0.657	SPO2455	1.02	0.487	SPO2456	0.85	0.479	SPO2452	0.91	0.876
SPO2462	1.03	0.652	SPO2460	1.77	0.001	SPO2461	1.17	0.995	SPO2464	1.17	0.699	SPO2456	0.70	0.249	SPO2456	0.65	0.125	SPO2457	0.93	0.723	SPO2453	1.00	0.451
SPO2463	0.82	0.389	SPO2461	1.01	0.667	SPO2462	1.05	0.667	SPO2465	1.1	0.726	SPO2457	0.75	0.987	SPO2457	0.80	0.927	SPO2458	1.09	0.085	SPO2470	1.08	0.851
SPO2464	1.08	0.668	SPO2462	0.95	0.957	SPO2463	1.12	0.752	SPO2466	1.08	0.245	SPO2458	0.76	0.830	SPO2458	0.74	0.808	SPO2459	1.00	0.819	SPO2455	0.99	0.935
SPO2465	1.38	0.118	SPO2463	1.21	0.587	SPO2464	1.11	0.843	SPO2467	1.12	0.928	SPO2459	2.56	0.015	SPO2459	2.76	0.003	SPO2460	1.32	0.243	SPO2456	0.78	0.050
SPO2466	0.59	0.125	SPO2464	1.01	0.808	SPO2465	1.23	0.443	SPO2468	1.05	0.541	SPO2460	0.99	0.924	SPO2460	0.99	0.790	SPO2461	1.32	0.098	SPO2457	0.96	0.883
SPO2467	0.87	0.794	SPO2465	1.16	0.7	SPO2466	1.21	0.176	SPO2469	1.13	0.433	SPO2461	1.21	0.132	SPO2461	1.23	0.153	SPO2462	0.86	0.451	SPO2458	0.94	0.947
SPO2468	0.73	0.022	SPO2466	0.63	0.029	SPO2467	1.29	0.763	SPO2470	1.1	0.589	SPO2462	0.71	0.215	SPO2462	0.69	0.206	SPO2463	1.01	0.931	SPO2459	1.15	0.661
SPO2469	0.97	0.899	SPO2467	1.02	0.899	SPO2468	1.72	0.685	SPO2471	1.16	0.353	SPO2463	1.23	0.291	SPO2463	1.37	0.492	SPO2464	0.96	0.860	SPO2460	1.10	0.226
SPO2470	0.78	0.396	SPO2468	0.82	0.173	SPO2469	1.42	0.666	SPO2472	1.22	0.195	SPO2464	0.97	0.867	SPO2464	1.04	0.713	SPO2465	1.02	0.998	SPO2461	1.19	0.053
SPO2471	1.01	0.791	SPO2469	1.13	0.476	SPO2470	1.44	0.41	SPO2473	1.19	0.553	SPO2472	0.75	0.987	SPO2472	0.80	0.927	SPO2473	1.09	0.085	SPO2470	1.08	0.851
SPO2472	1.15	0.37	SPO2470	0.83	0.654	SPO2471	1.46	0.007	SPO2474	1.13	0.122	SPO2466	0.61	0.017	SPO2466	0.66	0.022	SPO2467	0.83	0.710	SPO2463	1.10	0.839
SPO2473	1.97	0.005	SPO2471	0.84	0.419	SPO2472	1.25	0.719	SPO2475	1.06	0.203	SPO2467	1.01	0.842	SPO2467	1.06	0.777	SPO2468	0.93	0.734	SPO2464	0.98	0.966
SPO2474	1.87	0.016	SPO2472	0.98	0.709	SPO2473	1.11	0.843	SPO2476	1.12	0.019	SPO2468	1.12	0.019	SPO2468	1.19	0.087	SPO2469	0.98	0.705	SPO2465	0.95	0.884
SPO2475	1.3	0.019	SPO2473	1.62	0.008	SPO2474	1.01	0.289	SPO2477	1.2	0.01	SPO2469	0.70	0.011	SPO2469	0.72	0.009	SPO2470	1.03	0.916	SPO2466	1.16	0.331
SPO2476	0.77	0.167	SPO2474	1.66	0.006	SPO2475	1.16	0.396	SPO2479	1.07	0.611	SPO2470	0.99	0.743	SPO2470	0.93	0.939	SPO2471	1.15	0.563	SPO2467	0.85	0.761
SPO2477	1.12	0.412	SPO2475	1.29	0.081	SPO2476	1.2	0.092	SPO2480	1.19	0.413	SPO2471	1.07	0.456	SPO2471	1.10	0.281	SPO2472	1.31	0.450	SPO2468	0.99	0.880
SPO2478	1.29	0.474	SPO2476	0.79	0.327	SPO2477	1.09	0.021	SPO2481	1.08	0.998	SPO2472	1.32	0.628	SPO2472	1.42	0.097	SPO2473	1.07	0.174	SPO2469	0.98	0.910
SPO2479	0.82	0.938	SPO2477	1.11	0.702	SPO2478	1.15	0.862	SPO2482	1.18	0.053	SPO2473	0.75	0.987	SPO2473	0.80	0.927	SPO2474	1.09	0.085	SPO2470	1.08	0.851
SPO2480	1.02	0.927	SPO2479	1.18	0.783	SPO2480	1.28	0.489	SPO2483	1.1	0.914	SPO2474	0.61	0.043	SPO2474	0.57	0.007	SPO2475	1.38	0.143	SPO2471	1.10	0.718
SPO2481	1.02	0.927	SPO2480	0.82	0.22	SPO2481	1.15	0.981	SPO2484	1.06	0.809	SPO2475	0.60	0.009	SPO2475	0.62	0.005	SPO2476	0.91	0.230	SPO2472	1.18	0.592
SPO2482	1.17	0.344	SPO2481	0.88	0.95	SPO2482	1.22	0.255	SPO2485	1.05	0.614	SPO2476	1.15	0.297	SPO2476	1.19	0.160	SPO2477	1.03	0.711	SPO2473	1.04	0.722
SPO2483	1.19	0.57	SPO2482	0.98	0.198	SPO2483	1.06	0.887	SPO2486	1.09	0.734	SPO2477	0.95	0.694	SPO2477	0.94	0.466	SPO2479	1.40	0.350	SPO2474	1.04	0.486
SPO2484	0.88	0.75	SPO2483	1.1	0.355	SPO2484	1.19	0.602	SPO2487	1.13	0.633	SPO2479	0.71	0.133	SPO2479	0.77	0.519	SPO2480	1.12	0.125	SPO2475	1.34	0.099
SPO2485	1.22	0.507	SPO2484	1.16	0.593	SPO2485	1.16	0.273	SPO2488	1.03	0.537	SPO2480	1.12	0.169	SPO2480	1.19	0.350	SPO2481	0.79	0.549	SPO2476	0.94	0.728
SPO2486	1.53	0.317	SPO2485	0.86	0.474	SPO2486	1.32	0.392	SPO2489	1.15	0.544	SPO2481	0.92	0.948	SPO2481	0.82	0.870	SPO2482	0.97	0.915	SPO2477	1.06	0.045
SPO2487	1.01	0.791	SPO2486	1.13	0.875	SPO2487																	

SPO2578	1.11	0.557	SPO2577	0.46	0.064	SPO2578	1.28	0.054	SPO2581	1.14	0.816	SPO2573	1.38	0.002	SPO2573	1.02	0.268	SPO2573	1.53	0.069	SPO2569	1.06	0.842
SPO2579	1.74	0.367	SPO2578	1.02	0.752	SPO2579	1.42	0.222	SPO2582	1.38	0.292	SPO2574	1.49	0.100	SPO2574	1.44	0.055	SPO2574	1.09	0.601	SPO2570	1.06	0.394
SPO2580	1.51	0.093	SPO2579	1.43	0.129	SPO2580	1.03	0.15	SPO2583	1.24	0.267	SPO2575	0.88	0.936	SPO2575	1.26	0.741	SPO2575	1.17	0.872	SPO2571	1.02	0.702
SPO2581	1.07	0.353	SPO2580	1.01	0.333	SPO2581	1.01	0.14	SPO2584	1.08	0.988	SPO2576	1.78	0.036	SPO2576	1.66	0.031	SPO2576	1.86	0.036	SPO2572	1.28	0.626
SPO2582	1.11	1.507	SPO2581	1.08	0.344	SPO2582	1.07	0.448	SPO2585	1.28	0.871	SPO2577	1.59	0.018	SPO2577	1.54	0.059	SPO2577	1.54	0.059	SPO2573	1.55	0.010
SPO2583	0.92	0.389	SPO2582	1.04	0.353	SPO2583	1.04	0.393	SPO2586	1.03	0.667	SPO2578	1.12	0.286	SPO2578	1.13	0.174	SPO2578	1.01	0.866	SPO2574	1.10	0.616
SPO2584	1.08	0.838	SPO2583	0.91	0.26	SPO2584	1.01	0.641	SPO2587	1.22	0.339	SPO2579	0.83	0.432	SPO2579	0.87	0.447	SPO2579	1.03	0.546	SPO2575	1.14	0.883
SPO2585	1.42	0.169	SPO2584	0.99	0.93	SPO2585	1.02	0.656	SPO2590	1.21	0.871	SPO2580	0.26	0.004	SPO2580	0.24	0.003	SPO2580	0.72	0.444	SPO2576	1.91	0.082
SPO2586	1.45	0.11	SPO2585	1.39	0.122	SPO2586	1.17	0.197	SPO2589	1.12	0.768	SPO2581	1.49	0.087	SPO2581	1.50	0.167	SPO2581	0.82	0.613	SPO2577	2.38	0.005
SPO2587	1.58	0.028	SPO2586	1.34	0.101	SPO2587	1.07	0.376	SPO2590	1.21	0.648	SPO2582	0.76	0.130	SPO2582	0.74	0.206	SPO2582	0.92	0.572	SPO2578	1.10	0.918
SPO2588	1.22	0.237	SPO2587	1.41	0.053	SPO2588	1.06	0.721	SPO2591	1.02	0.328	SPO2583	0.83	0.366	SPO2583	0.75	0.242	SPO2583	1.08	0.574	SPO2579	0.90	0.346
SPO2589	1.07	0.35	SPO2588	1.07	0.293	SPO2589	1.09	0.184	SPO2590	1.09	0.14	SPO2584	0.85	0.730	SPO2584	0.85	0.631	SPO2584	0.85	0.748	SPO2583	0.90	0.052
SPO2590	0.68	0.014	SPO2589	1.17	0.338	SPO2590	1.17	0.395	SPO2593	1.09	0.704	SPO2585	1.07	0.205	SPO2585	1.11	0.016	SPO2585	0.83	0.625	SPO2581	0.81	0.504
SPO2591	0.85	0.008	SPO2590	0.78	0.331	SPO2591	1.42	0.102	SPO2594	1.11	0.578	SPO2586	1.14	0.096	SPO2586	1.23	0.018	SPO2586	0.93	0.683	SPO2582	0.90	0.550
SPO2592	1.43	0.518	SPO2591	0.88	0.732	SPO2592	1.17	0.904	SPO2595	1.05	0.8	SPO2587	0.72	0.296	SPO2587	0.68	0.250	SPO2587	0.98	0.627	SPO2583	1.00	0.951
SPO2593	1.04	0.742	SPO2592	1.33	0.584	SPO2593	1.38	0.549	SPO2596	1.1	0.1	SPO2588	1.12	0.202	SPO2588	1.19	0.284	SPO2588	1.05	0.789	SPO2584	0.89	0.842
SPO2594	1.34	0.113	SPO2593	0.99	0.774	SPO2594	1.03	0.262	SPO2597	1.03	0.049	SPO2589	1.21	0.137	SPO2589	1.26	0.419	SPO2589	1.06	0.782	SPO2585	0.98	0.951
SPO2595	1.39	0.759	SPO2594	1.3	0.041	SPO2595	1.11	0.928	SPO2598	1.19	0.958	SPO2590	1.16	0.035	SPO2590	0.97	0.532	SPO2590	0.96	0.933	SPO2586	0.92	0.515
SPO2596	1.5	0.043	SPO2595	1.96	0.471	SPO2596	1.1	0.726	SPO2601	1.05	0.73	SPO2591	0.88	0.962	SPO2591	0.77	0.434	SPO2591	1.00	0.943	SPO2587	0.93	0.711
SPO2597	1.29	0.916	SPO2596	1.41	0.018	SPO2597	1.14	0.304	SPO2602	1.46	0.353	SPO2592	0.88	0.781	SPO2592	0.96	0.321	SPO2592	0.96	0.320	SPO2588	0.98	0.949
SPO2598	1.29	0.196	SPO2597	0.96	0.693	SPO2598	1.06	0.862	SPO2603	1.07	0.512	SPO2593	0.98	0.051	SPO2593	0.72	0.484	SPO2593	1.49	0.518	SPO2589	1.05	0.919
SPO2601	0.91	0.894	SPO2598	1.26	0.347	SPO2601	1.14	0.988	SPO2604	1.96	0.571	SPO2594	0.85	0.028	SPO2594	0.68	0.024	SPO2594	0.80	0.172	SPO2590	1.10	0.722
SPO2602	1.12	0.59	SPO2601	0.96	0.897	SPO2602	1.02	0.639	SPO2605	1.16	0.886	SPO2595	0.41	0.299	SPO2595	0.48	0.452	SPO2595	1.96	0.672	SPO2591	1.02	0.783
SPO2603	0.9	0.948	SPO2602	1.1	0.327	SPO2603	1.18	0.898	SPO2606	1.01	0.017	SPO2596	0.61	0.012	SPO2596	0.59	0.023	SPO2596	1.04	0.535	SPO2600	1.00	0.989
SPO2604	0.93	0.868	SPO2603	1.09	0.216	SPO2604	1.23	0.12	SPO2607	1.03	0.143	SPO2597	0.84	0.211	SPO2597	0.86	0.576	SPO2597	0.94	0.734	SPO2593	1.47	0.426
SPO2605	0.76	0.490	SPO2604	1.1	0.756	SPO2605	1.06	0.656	SPO2608	1.11	0.025	SPO2598	1.11	0.429	SPO2598	1.14	0.540	SPO2598	1.07	0.387	SPO2594	0.92	0.521
SPO2606	0.69	0.189	SPO2605	0.8	0.601	SPO2606	1.08	0.019	SPO2609	1.26	0.691	SPO2601	1.29	0.100	SPO2601	1.39	0.134	SPO2601	0.96	0.800	SPO2595	1.21	0.949
SPO2607	0.62	0.006	SPO2606	0.65	0.054	SPO2607	1.12	0.272	SPO2610	1.38	0.163	SPO2602	1.09	0.859	SPO2602	1.32	0.123	SPO2602	1.09	0.858	SPO2596	0.99	0.929
SPO2608	1.22	0.393	SPO2607	0.66	0.045	SPO2608	1.16	0.948	SPO2611	1.06	0.111	SPO2603	1.18	0.262	SPO2603	1.52	0.036	SPO2603	1.23	0.672	SPO2616	1.06	0.780
SPO2609	0.69	0.086	SPO2608	0.71	0.047	SPO2609	1.04	0.517	SPO2613	1.08	0.704	SPO2604	1.31	0.227	SPO2604	1.07	0.770	SPO2604	1.05	0.855	SPO2598	1.05	0.846
SPO2610	0.68	0.025	SPO2609	0.77	0.319	SPO2610	1.02	0.127	SPO2614	1.27	0.222	SPO2605	1.32	0.383	SPO2605	1.26	0.485	SPO2605	1.06	0.848	SPO2601	1.07	0.398
SPO2612	0.69	0.022	SPO2610	0.77	0.168	SPO2612	1.03	0.868	SPO2615	1.21	0.6	SPO2606	2.25	0.004	SPO2606	2.65	0.000	SPO2606	1.18	0.149	SPO2602	1.07	0.565
SPO2613	1.13	0.465	SPO2612	0.75	0.021	SPO2613	1.04	0.857	SPO2616	1.31	0.222	SPO2607	1.45	0.106	SPO2607	1.49	0.081	SPO2607	1.06	0.323	SPO2603	0.95	0.888
SPO2614	1.1	0.061	SPO2613	1.13	0.631	SPO2614	1.22	0.905	SPO2617	1.29	0.249	SPO2608	1.39	0.146	SPO2608	1.21	0.065	SPO2608	1.08	0.770	SPO2604	0.99	0.749
SPO2615	1.18	0.523	SPO2614	1.11	0.34	SPO2615	1.17	0.359	SPO2618	1.42	0.033	SPO2609	0.88	0.799	SPO2609	0.88	0.799	SPO2609	0.93	0.785	SPO2605	0.99	0.954
SPO2616	0.81	0.019	SPO2615	1.12	0.452	SPO2616	1.22	0.223	SPO2619	1.14	0.938	SPO2610	1.87	0.003	SPO2610	1.96	0.002	SPO2610	1.02	0.376	SPO2606	1.21	0.028
SPO2618	0.79	0.418	SPO2617	0.86	0.232	SPO2618	1.15	0.219	SPO2621	1.03	0.829	SPO2612	1.06	0.029	SPO2612	0.68	0.043	SPO2612	0.93	0.623	SPO2608	1.18	0.209
SPO2619	1.15	0.663	SPO2618	0.92	0.874	SPO2619	1.03	0.672	SPO2622	1.04	0.151	SPO2614	1.08	0.001	SPO2614	1.08	0.001	SPO2614	1.28	0.003	SPO2609	0.95	0.747
SPO2620	0.81	0.46	SPO2619	1.27	0.135	SPO2620	1.2	0.863	SPO2623	1.09	0.788	SPO2615	0.98	0.002	SPO2615	0.95	0.003	SPO2615	1.35	0.444	SPO2610	1.05	0.132
SPO2621	1.5	0.523	SPO2620	0.85	0.098	SPO2621	1.01	0.879	SPO2624	1.22	0.643	SPO2616	0.84	0.052	SPO2616	0.98	0.517	SPO2616	1.18	0.326	SPO2612	0.94	0.668
SPO2622	0.93	0.883	SPO2621	1.27	0.536	SPO2622	1.21	0.48	SPO2625	1.04	0.671	SPO2617	0.42	0.059	SPO2617	0.38	0.040	SPO2617	1.28	0.511	SPO2613	1.00	0.952
SPO2623	0.85	0.875	SPO2622	0.88	0.701	SPO2623	1.07	0.752	SPO2626	1.13	0.022	SPO2618	0.90	0.007	SPO2618	0.45	0.012	SPO2618	1.36	0.167	SPO2614	1.42	0.106
SPO2624	1.28	0.203	SPO2623	0.72	0.481	SPO2624	1.11	0.629	SPO2627	1.21	0.894	SPO2619	1.26	0.017	SPO2619	1.015	0.015	SPO2619	1.29	0.587	SPO2606	1.36	0.282
SPO2625	1.16	0.32	SPO2624	1.26	0.323	SPO2625	1.1	0.725	SPO2628	1.18	0.262	SPO2620	1.52	0.179	SPO2620	0.63	0.008	SPO2620	1.12	0.724	SPO2616	1.06	0.780
SPO2626	1.07	0.53	SPO2625	1.14	0.888	SPO2626	1.16	0.013	SPO2629	1.42	0.198	SPO2621	0.89	0.584	SPO2621	0.56	0.513	SPO2621	0.56	0.979	SPO2617	1.43	0.261
SPO2627	1.3	0.002	SPO2626	1.1	0.086	SPO2627	1.13	0.196	SPO2630	1.24	0.408	SPO2622	1.69	0.073	SPO2622	1.51	0.020	SPO2622	1.11	0.706	SPO2618	1.47	0.034
SPO2628	1.3	0.001	SPO2627	0.53	0.056	SPO2628	1.05	0.002	SPO2631	1.35	0.295	SPO2623	1.03	0.972	SPO2623	0.90	0.612	SPO2623	0.74	0.432	SPO2619	1.32	0.144
SPO2629	1.79	0.91	SPO2628	0.36	0.001	SPO2629	1.11	0.263	SPO2632	1.13	0.102	SPO2624	1.01	0.988	SPO2624	1.02	0.989	SPO2624	0.96	0.649	SPO2620	1.13	0.037
SPO2630	1.81	0.083	SPO2629	1.65	0.02	SPO2630	1.08	0.301	SPO2633	1.1	0.335	SPO2625	0.81	0.871	SPO2625	0.85	0.879	SPO2625	0.96	0.960	SPO2621	0.96	0.939
SPO2631	1.59	0.095	SPO2630	1.63	0.165	SPO2631	1.03	0.18	SPO2634	1.11	0.377	SPO2626	1.51	0.003	SPO2626	1.56	0.006	SPO2626	0.80	1.140	SPO2622	1.17	0.468
SPO2632	1.93	0.004	SPO2631	1.55	0.037	SPO2632	1.24	0.111	SPO2635	1.11	0.106	SPO2627	3.09	0.001	SPO2627	2.88	0.004	SPO2627	0.90	0.735	SPO2623	0.77	0.651
SPO2633	1.68	0.026	SPO2632	1.82	0.055	SPO2633	1.15	0.363	SPO2636	1.11	0.913	SPO2628	0.77	0.000	SPO2628	0.000	0.000	SPO2628	1.24	0.278	SPO2624	0.88	0.875
SPO2634	1.23	0.011	SPO2633	1.67	0.027																		

SPO2720	0.74	0.766	SPO2719	0.98	0.668	SPO2720	1.17	0.857	SPO2723	0.99	0.622	SPO2715	1.14	0.650	SPO2715	1.05	0.840	SPO2715	0.91	0.850	SPO2711	0.88	0.746
SPO2721	0.76	0.254	SPO2720	0.73	0.746	SPO2721	1.09	0.039	SPO2724	1	0.498	SPO2716	0.85	0.431	SPO2716	0.89	0.536	SPO2716	0.89	0.511	SPO2712	1.00	0.992
SPO2722	0.98	0.954	SPO2721	0.88	0.614	SPO2722	1.23	0.022	SPO2725	1.11	0.278	SPO2717	1.37	0.551	SPO2717	1.32	0.585	SPO2717	1.10	0.874	SPO2713	1.01	0.972
SPO2723	0.94	0.850	SPO2722	0.24	0.823	SPO2723	1.21	0.445	SPO2726	1.08	0.907	SPO2718	1.05	0.925	SPO2718	0.98	0.907	SPO2718	1.04	0.874	SPO2714	0.81	0.824
SPO2724	0.74	1.118	SPO2723	0.67	1.223	SPO2724	1.3	0.724	SPO2728	1.05	0.965	SPO2719	1.07	0.680	SPO2719	1.10	0.035	SPO2719	0.88	0.025	SPO2715	0.85	0.739
SPO2725	1.05	0.634	SPO2724	0.79	0.283	SPO2725	1.77	0.545	SPO2730	1.38	0.862	SPO2720	1.07	0.069	SPO2720	0.99	0.912	SPO2720	1.03	0.999	SPO2716	0.88	0.389
SPO2726	0.71	0.52	SPO2725	1.17	0.433	SPO2726	1.15	0.898	SPO2731	1.11	0.01	SPO2721	0.44	0.043	SPO2721	0.38	0.011	SPO2721	0.88	0.672	SPO2717	1.06	0.923
SPO2727	0.79	0.761	SPO2726	0.98	0.947	SPO2729	0.99	0.983	SPO2733	1.01	0.757	SPO2722	0.59	0.090	SPO2722	0.53	0.113	SPO2722	0.85	0.671	SPO2718	0.86	0.804
SPO2730	0.91	0.7	SPO2729	0.8	0.913	SPO2730	1.15	0.874	SPO2734	1.07	0.836	SPO2723	1.11	0.492	SPO2723	1.08	0.495	SPO2723	0.91	0.771	SPO2719	0.85	0.804
SPO2731	1.17	0.424	SPO2730	0.93	0.991	SPO2731	1.01	0.039	SPO2735	1.2	0.902	SPO2724	1.41	0.035	SPO2724	1.35	0.122	SPO2724	0.91	0.571	SPO2720	1.06	0.974
SPO2733	1.22	0.111	SPO2731	1.4	0.017	SPO2733	0.99	0.939	SPO2736	1.04	0.791	SPO2725	0.84	0.087	SPO2725	0.52	0.046	SPO2725	0.83	0.578	SPO2721	0.90	0.261
SPO2734	1.04	0.859	SPO2732	1.04	0.823	SPO2734	1.03	0.444	SPO2738	1.17	0.981	SPO2726	1.21	0.356	SPO2726	0.99	0.709	SPO2726	0.76	0.371	SPO2722	0.86	0.591
SPO2735	1.06	0.637	SPO2733	1.04	0.686	SPO2735	1.11	0.542	SPO2739	1.02	0.641	SPO2729	1.28	0.882	SPO2729	1.19	0.925	SPO2729	1.03	0.986	SPO2723	0.92	0.839
SPO2736	1.67	0.016	SPO2735	1.03	0.649	SPO2736	1.29	0.466	SPO2740	1.11	0.564	SPO2730	0.96	0.519	SPO2730	0.92	0.138	SPO2730	0.85	0.483	SPO2724	0.98	0.914
SPO2738	0.69	0.012	SPO2736	1.44	0.018	SPO2738	1.26	0.015	SPO2741	1.06	0.711	SPO2731	0.52	0.112	SPO2731	0.38	0.004	SPO2731	0.69	0.290	SPO2725	0.72	0.112
SPO2739	1.08	0.399	SPO2738	0.73	0.038	SPO2739	1.2	0.7	SPO2742	1.23	0.96	SPO2733	0.95	0.912	SPO2733	0.93	0.965	SPO2733	1.02	0.836	SPO2726	0.87	0.900
SPO2740	1.11	0.11	SPO2739	1.07	0.027	SPO2740	1.07	0.345	SPO2743	1.17	0.365	SPO2734	1.07	0.519	SPO2734	1.10	0.454	SPO2734	1.06	0.909	SPO2729	0.92	0.958
SPO2741	0.84	0.634	SPO2740	1.04	0.93	SPO2741	1.02	0.769	SPO2744	1.18	0.702	SPO2735	1.07	0.463	SPO2735	1.10	0.359	SPO2735	0.92	0.422	SPO2730	0.83	0.447
SPO2742	1.13	0.629	SPO2741	0.95	0.661	SPO2742	1.01	0.848	SPO2745	1.14	0.933	SPO2736	1.34	0.062	SPO2736	1.39	0.116	SPO2736	1.21	0.450	SPO2731	0.66	0.009
SPO2743	1.39	1.109	SPO2742	1.26	0.31	SPO2743	1.03	0.21	SPO2746	1.11	0.166	SPO2738	1.43	0.030	SPO2738	1.35	0.018	SPO2738	1.00	0.622	SPO2733	1.03	0.699
SPO2744	1.34	0.028	SPO2743	1.31	0.211	SPO2744	1.15	0.908	SPO2747	1.1	0.992	SPO2739	0.86	0.579	SPO2739	0.76	0.505	SPO2739	0.83	0.253	SPO2734	1.01	0.957
SPO2745	1.28	0.83	SPO2744	1.3	0.033	SPO2745	0.99	0.958	SPO2748	1.04	0.889	SPO2740	0.89	0.861	SPO2740	0.92	0.396	SPO2740	0.98	0.926	SPO2735	1.00	0.960
SPO2746	0.66	0.005	SPO2745	1.31	0.726	SPO2746	1.01	0.211	SPO2749	1.22	0.558	SPO2741	1.86	0.232	SPO2741	1.67	0.282	SPO2741	1.08	0.790	SPO2736	1.21	1.110
SPO2747	0.84	0.473	SPO2746	0.7	0.475	SPO2747	1.25	0.117	SPO2750	1.03	0.275	SPO2742	0.93	0.907	SPO2742	0.91	0.890	SPO2742	0.96	0.972	SPO2738	1.06	0.595
SPO2748	1.17	0.506	SPO2747	0.86	0.723	SPO2748	1.17	0.618	SPO2751	0.99	0.957	SPO2743	1.46	0.153	SPO2743	1.33	0.235	SPO2743	1.16	0.625	SPO2739	0.82	0.221
SPO2749	0.88	0.68	SPO2748	1.17	0.488	SPO2749	1.11	0.877	SPO2752	1.16	0.971	SPO2744	1.45	0.021	SPO2744	1.43	0.008	SPO2744	0.99	0.810	SPO2740	0.95	0.693
SPO2750	0.66	0.176	SPO2749	0.96	0.995	SPO2750	1.13	0.526	SPO2753	1.18	0.713	SPO2745	0.76	0.649	SPO2745	0.68	0.578	SPO2745	1.08	0.952	SPO2741	1.12	0.774
SPO2751	1.13	0.849	SPO2750	0.66	0.071	SPO2751	1.13	0.996	SPO2754	1.14	0.743	SPO2746	0.85	0.929	SPO2746	0.88	0.278	SPO2746	1.23	0.074	SPO2742	0.96	0.956
SPO2752	1.08	0.49	SPO2751	1.1	0.275	SPO2752	1.13	0.604	SPO2757	1.15	0.478	SPO2747	0.84	0.384	SPO2747	0.87	0.151	SPO2747	0.97	0.914	SPO2733	1.15	0.891
SPO2753	1.24	0.296	SPO2752	1.15	0.235	SPO2753	1.07	0.561	SPO2756	1.16	0.952	SPO2748	0.93	0.108	SPO2748	0.51	0.086	SPO2748	1.04	0.893	SPO2744	0.97	0.701
SPO2754	1.25	0.432	SPO2753	1.11	0.27	SPO2754	1.05	0.737	SPO2757	1.09	0.014	SPO2749	1.10	0.272	SPO2749	1.16	0.069	SPO2749	0.89	0.113	SPO2745	0.99	0.989
SPO2755	0.79	0.68	SPO2754	1.25	0.386	SPO2755	1.01	0.705	SPO2758	1.26	1.1	SPO2750	0.56	0.057	SPO2750	0.60	0.071	SPO2750	0.81	0.191	SPO2746	1.22	0.070
SPO2756	0.99	0.39	SPO2755	0.73	0.548	SPO2756	1.16	0.913	SPO2759	1.29	0.368	SPO2751	0.85	0.954	SPO2751	0.80	0.917	SPO2751	0.95	0.975	SPO2747	0.97	0.906
SPO2757	0.52	0.021	SPO2756	1.08	0.779	SPO2757	1.2	0.002	SPO2760	1.21	0.744	SPO2752	1.36	0.102	SPO2752	1.49	0.003	SPO2752	1.05	0.756	SPO2748	1.00	0.994
SPO2758	1.07	0.736	SPO2757	0.71	0.437	SPO2758	1.18	0.927	SPO2761	1.94	0.237	SPO2763	0.94	0.007	SPO2763	0.98	0.007	SPO2763	0.84	0.207	SPO2753	0.92	0.880
SPO2759	1.28	1.136	SPO2758	1.08	0.308	SPO2759	1.01	0.512	SPO2762	1.23	0.762	SPO2754	0.78	0.363	SPO2754	0.78	0.345	SPO2754	0.94	0.728	SPO2750	0.87	0.124
SPO2760	1.03	0.663	SPO2759	1.13	0.448	SPO2760	1.34	0.237	SPO2763	1.34	0.075	SPO2765	1.03	0.019	SPO2765	1.01	0.028	SPO2765	1.01	0.821	SPO2759	0.97	0.857
SPO2761	1.03	0.863	SPO2760	1.13	0.148	SPO2761	1.18	0.166	SPO2764	1.18	0.162	SPO2756	1.19	0.814	SPO2756	1.19	0.808	SPO2756	1.00	0.969	SPO2752	1.12	0.052
SPO2762	1.12	0.741	SPO2761	1.01	0.756	SPO2762	1.18	0.808	SPO2765	1	0.21	SPO2757	1.63	0.073	SPO2757	2.08	0.056	SPO2757	1.34	0.004	SPO2753	0.85	0.650
SPO2763	1.27	0.103	SPO2762	1.09	0.7	SPO2763	1.18	0.024	SPO2766	1.1	0.965	SPO2758	0.81	0.745	SPO2758	0.81	0.623	SPO2758	1.21	0.573	SPO2754	0.94	0.870
SPO2764	1.3	0.147	SPO2763	1.08	0.213	SPO2764	1.11	0.754	SPO2767	1.04	0.649	SPO2759	0.76	0.284	SPO2759	0.86	0.544	SPO2759	1.07	0.534	SPO2755	1.12	0.600
SPO2765	1.17	0.043	SPO2764	1.34	0.018	SPO2765	1.02	0.531	SPO2768	1.16	0.299	SPO2760	1.70	0.015	SPO2760	1.61	0.034	SPO2760	0.95	0.641	SPO2756	1.08	0.912
SPO2766	1.14	0.776	SPO2765	1.17	0.069	SPO2766	1.24	0.945	SPO2769	1.26	0.004	SPO2761	1.90	0.046	SPO2761	1.99	0.036	SPO2761	1.16	0.307	SPO2757	1.58	0.003
SPO2767	1.13	0.114	SPO2766	1.17	0.568	SPO2767	1.02	0.015	SPO2770	1.32	0.036	SPO2762	2.08	0.087	SPO2762	2.08	0.128	SPO2762	1.05	0.876	SPO2758	1.16	0.808
SPO2768	1.08	0.96	SPO2767	1.17	0.231	SPO2768	1.87	0.084	SPO2771	1.02	0.591	SPO2763	1.31	0.056	SPO2763	1.39	0.022	SPO2763	1.18	0.041	SPO2759	0.97	0.857
SPO2769	1.06	0.46	SPO2768	1.14	0.196	SPO2769	1.02	0.129	SPO2772	1.04	0.412	SPO2764	1.16	0.060	SPO2764	1.10	0.116	SPO2764	1.02	0.627	SPO2760	0.94	0.809
SPO2770	0.94	0.469	SPO2769	1.12	0.127	SPO2770	1.12	0.127	SPO2773	1.03	0.827	SPO2765	1.67	0.004	SPO2765	1.52	0.006	SPO2765	1.02	0.178	SPO2761	1.12	0.425
SPO2771	1.07	0.414	SPO2770	1.09	0.023	SPO2771	1.14	0.088	SPO2774	1.14	0.014	SPO2766	1.42	0.302	SPO2766	1.34	0.363	SPO2766	0.88	0.887	SPO2762	1.11	0.778
SPO2772	1.2	0.637	SPO2771	1.16	0.322	SPO2772	1.06	0.336	SPO2775	1.17	0.264	SPO2767	1.29	0.074	SPO2767	1.28	0.019	SPO2767	0.86	0.468	SPO2763	1.16	1.090
SPO2773	0.94	0.937	SPO2772	1.18	0.182	SPO2773	1.33	0.9	SPO2776	1.07	0.264	SPO2768	1.36	0.015	SPO2768	1.50	0.025	SPO2768	0.90	0.564	SPO2764	1.03	0.707
SPO2774	0.98	0.793	SPO2773	0.85	0.879	SPO2774	1.01	0.08	SPO2777	1.09	0.506	SPO2769	1.40	0.031	SPO2769	1.38	0.008	SPO2769	1.01	0.898	SPO2765	1.00	0.727
SPO2775	1.24	0.059	SPO2774	0.88	0.547	SPO2775	0.99	0.2	SPO2778	1.08	0.447	SPO2770	1.73	0.015	SPO2770	1.71	0.006	SPO2770	0.95	0.926	SPO2770	0.88	0.957
SPO2776	1.22	0.112	SPO2775	1.14	0.147	SPO2776																	

SPO2863	1.23	0.537	SPO2862	1.06	0.691	SPO2863	1.04	0.729	SPO2866	1.07	0.06	SPO2858	0.86	0.643	SPO2858	0.88	0.896	SPO2858	1.02	0.838	SPO2854	1.19	0.500
SPO2864	0.75	0.261	SPO2863	1.19	0.339	SPO2864	1.01	0.085	SPO2867	1.21	0.477	SPO2869	1.42	0.139	SPO2869	1.51	0.086	SPO2869	0.92	SPO2865	0.98	0.977	
SPO2865	0.85	0.061	SPO2864	0.92	0.125	SPO2865	1.26	0.077	SPO2868	1.04	0.605	SPO2860	1.06	0.932	SPO2860	1.11	0.903	SPO2860	0.86	0.862	SPO2866	1.01	0.570
SPO2866	1.23	0.63	SPO2865	0.86	0.293	SPO2866	1.19	0.383	SPO2869	1.23	0.974	SPO2861	2.95	0.003	SPO2861	0.89	0.003	SPO2861	1.12	0.239	SPO2867	0.94	0.623
SPO2867	0.81	0.6	SPO2866	0.55	0.786	SPO2867	1.08	0.383	SPO2870	1.04	0.354	SPO2862	2.95	0.023	SPO2862	2.95	0.005	SPO2862	1.38	0.079	SPO2868	0.93	0.841
SPO2868	1.81	0.851	SPO2867	0.85	0.834	SPO2868	1.02	0.57	SPO2871	1.14	0.097	SPO2863	1.25	0.548	SPO2863	1.15	0.574	SPO2863	0.93	0.862	SPO2869	1.00	0.968
SPO2869	1.24	0.531	SPO2868	1.18	0.08	SPO2869	1.11	0.922	SPO2872	1.26	0.044	SPO2864	3.25	0.010	SPO2864	2.95	0.003	SPO2864	1.25	0.055	SPO2860	0.86	0.880
SPO2870	1.03	0.70	SPO2869	1.12	0.751	SPO2870	1.03	0.227	SPO2873	1.35	0.669	SPO2865	1.98	0.083	SPO2865	1.82	0.102	SPO2865	1.15	0.474	SPO2861	1.27	0.029
SPO2871	1.01	0.841	SPO2870	1.06	0.636	SPO2871	1.2	0.098	SPO2874	1.07	0.053	SPO2866	2.34	0.007	SPO2866	2.95	0.032	SPO2866	1.30	0.235	SPO2862	1.38	0.012
SPO2872	1.16	0.562	SPO2871	1.04	0.561	SPO2872	1.1	0.122	SPO2875	1.03	0.111	SPO2867	6.39	0.094	SPO2867	5.98	0.106	SPO2867	1.11	0.812	SPO2863	0.95	0.930
SPO2873	1.03	0.84	SPO2872	1.11	0.454	SPO2873	1.09	0.651	SPO2876	1.06	0.393	SPO2868	1.29	0.096	SPO2868	1.33	0.032	SPO2868	1.30	0.081	SPO2864	1.36	0.108
SPO2874	1.11	0.453	SPO2873	0.86	0.749	SPO2874	1.04	0.393	SPO2877	1.12	0.974	SPO2869	1.02	0.856	SPO2869	0.99	0.832	SPO2869	0.86	0.855	SPO2865	1.23	0.076
SPO2875	0.59	0.057	SPO2874	1.06	0.133	SPO2875	1.09	0.324	SPO2878	1.04	0.188	SPO2870	1.29	0.004	SPO2870	1.33	0.021	SPO2870	1.22	0.302	SPO2866	1.28	0.499
SPO2876	0.66	0.125	SPO2875	0.6	0.006	SPO2876	1.02	0.958	SPO2879	1.01	0.205	SPO2871	3.25	0.011	SPO2871	3.00	0.011	SPO2871	1.51	0.130	SPO2867	1.10	0.845
SPO2877	1.12	0.205	SPO2876	0.75	0.361	SPO2877	1.18	0.075	SPO2880	1.07	0.875	SPO2872	3.24	0.038	SPO2872	3.12	0.007	SPO2872	1.21	0.741	SPO2868	1.26	0.112
SPO2878	1.6	0.006	SPO2877	1.07	0.475	SPO2878	1.01	0.806	SPO2881	1.14	0.808	SPO2873	1.51	0.514	SPO2873	1.19	0.623	SPO2873	1.08	0.816	SPO2869	0.98	0.999
SPO2879	1.18	0.313	SPO2878	1.5	0.019	SPO2879	1.05	0.571	SPO2882	1.02	0.338	SPO2874	2.95	0.012	SPO2874	2.67	0.011	SPO2874	1.27	0.100	SPO2870	1.22	0.417
SPO2880	1.06	0.878	SPO2879	1.19	0.152	SPO2880	1.02	0.851	SPO2883	1.17	0.843	SPO2875	2.06	0.003	SPO2875	2.95	0.001	SPO2875	1.13	0.179	SPO2871	1.31	0.218
SPO2881	0.78	0.441	SPO2880	0.93	0.993	SPO2881	1.1	0.798	SPO2884	1.1	0.528	SPO2876	4.56	0.010	SPO2876	3.98	0.016	SPO2876	1.40	0.127	SPO2872	1.27	0.219
SPO2882	0.78	0.819	SPO2881	0.83	0.54	SPO2882	1.04	0.876	SPO2885	1.12	0.895	SPO2877	1.98	0.185	SPO2877	1.82	0.163	SPO2877	1.10	0.193	SPO2873	1.06	0.693
SPO2883	1.01	0.896	SPO2882	0.76	0.801	SPO2883	1.03	0.618	SPO2886	1.2	0.680	SPO2878	0.75	0.058	SPO2878	0.73	0.059	SPO2878	1.16	0.157	SPO2874	1.32	0.028
SPO2884	0.34	0.199	SPO2883	0.93	0.61	SPO2884	1.02	0.559	SPO2887	1.01	0.052	SPO2879	0.99	0.892	SPO2879	0.91	0.736	SPO2879	0.96	0.819	SPO2875	1.09	0.239
SPO2885	0.82	0.256	SPO2884	0.53	0.148	SPO2885	1.26	0.89	SPO2888	1.13	0.208	SPO2880	0.81	0.789	SPO2880	0.89	0.870	SPO2880	0.90	0.867	SPO2876	1.39	0.075
SPO2886	0.91	0.51	SPO2885	0.8	0.041	SPO2886	1.18	0.856	SPO2889	1.02	0.051	SPO2881	0.99	0.689	SPO2881	1.03	0.425	SPO2881	0.78	0.957	SPO2877	1.05	0.871
SPO2887	0.88	0.006	SPO2886	0.97	0.98	SPO2887	1.12	0.021	SPO2890	1.15	0.272	SPO2882	0.93	0.899	SPO2882	0.85	0.790	SPO2882	0.92	0.832	SPO2878	1.08	0.356
SPO2888	1.5	0.098	SPO2887	1.01	0.54	SPO2888	1.06	0.221	SPO2891	1.22	0.881	SPO2883	0.61	0.044	SPO2883	0.67	0.016	SPO2883	0.98	0.842	SPO2879	1.02	0.879
SPO2889	1.03	0.914	SPO2888	1.38	0.039	SPO2889	1.1	0.296	SPO2892	1.18	0.785	SPO2884	0.97	0.929	SPO2884	0.98	0.934	SPO2884	1.03	0.985	SPO2880	1.01	0.994
SPO2890	0.74	0.207	SPO2889	1.06	0.238	SPO2890	1.27	0.574	SPO2893	1.21	0.411	SPO2885	0.61	0.049	SPO2885	0.67	0.013	SPO2885	0.98	0.784	SPO2881	1.03	0.990
SPO2891	0.89	0.931	SPO2890	1.36	0.081	SPO2891	1.08	0.849	SPO2894	1.04	0.849	SPO2886	0.54	0.23	SPO2886	0.68	0.339	SPO2886	0.86	0.339	SPO2882	1.02	0.874
SPO2892	1.14	0.207	SPO2891	0.98	0.996	SPO2892	1.14	0.792	SPO2895	1.19	0.546	SPO2887	1.60	0.002	SPO2887	1.53	0.005	SPO2887	1.07	0.432	SPO2883	0.97	0.874
SPO2893	0.89	0.314	SPO2892	1.07	0.827	SPO2893	1.12	0.969	SPO2896	1.03	0.651	SPO2888	1.65	0.021	SPO2888	1.60	0.035	SPO2888	0.98	0.999	SPO2884	1.08	0.865
SPO2894	1.43	0.181	SPO2893	0.92	0.492	SPO2894	1.04	0.308	SPO2897	1.01	0.286	SPO2889	2.45	0.043	SPO2889	2.50	0.005	SPO2889	1.12	0.837	SPO2885	1.05	0.705
SPO2895	0.96	0.885	SPO2894	1.25	0.216	SPO2895	1.15	0.964	SPO2898	1.1	0.267	SPO2890	1.35	0.457	SPO2890	1.24	0.077	SPO2890	0.74	0.349	SPO2886	0.91	0.440
SPO2896	0.96	0.839	SPO2895	1.01	0.853	SPO2896	1.14	0.989	SPO2899	1.03	0.594	SPO2891	1.57	0.728	SPO2891	1.61	0.727	SPO2891	0.77	0.854	SPO2887	0.95	0.743
SPO2897	0.72	0.29	SPO2896	0.92	0.61	SPO2897	1.01	0.304	SPO2900	1.18	0.569	SPO2892	0.62	0.285	SPO2892	0.61	0.391	SPO2892	0.87	0.621	SPO2888	0.97	0.953
SPO2898	0.52	0.315	SPO2897	0.75	0.002	SPO2898	1.12	0.198	SPO2901	1.01	0.414	SPO2893	0.91	0.819	SPO2893	0.93	0.628	SPO2893	0.94	0.784	SPO2889	1.14	0.248
SPO2899	1.38	0.81	SPO2898	1.25	0.366	SPO2900	1.05	0.511	SPO2903	1.31	0.906	SPO2894	0.92	0.929	SPO2894	0.94	0.929	SPO2894	0.84	0.839	SPO2890	0.84	0.947
SPO2900	1.38	0.81	SPO2899	1.25	0.366	SPO2900	1.05	0.511	SPO2903	1.31	0.906	SPO2895	1.09	0.314	SPO2895	1.03	0.479	SPO2895	1.01	0.831	SPO2891	0.87	0.937
SPO2901	0.89	0.795	SPO2900	1.34	0.085	SPO2901	1.05	0.474	SPO2904	1.13	0.387	SPO2896	0.89	0.949	SPO2896	0.99	0.427	SPO2896	0.99	0.338	SPO2892	0.92	0.862
SPO2902	0.63	0.203	SPO2901	0.87	0.532	SPO2902	1.1	0.559	SPO2905	1.05	0.902	SPO2897	0.90	0.994	SPO2897	0.90	0.863	SPO2897	0.93	0.681	SPO2883	0.96	0.804
SPO2903	1.34	0.709	SPO2902	0.71	0.074	SPO2903	1.08	0.888	SPO2906	1.04	0.524	SPO2898	1.26	0.052	SPO2898	1.30	0.042	SPO2898	0.96	0.888	SPO2884	1.00	0.966
SPO2904	0.88	0.325	SPO2903	1.22	0.776	SPO2904	1.03	0.215	SPO2907	1.18	0.146	SPO2899	0.78	0.411	SPO2899	0.83	0.573	SPO2899	0.98	0.938	SPO2895	0.99	0.949
SPO2905	1.12	0.433	SPO2904	0.84	0.207	SPO2905	1.11	0.882	SPO2908	1.29	0.967	SPO2900	1.30	0.119	SPO2900	1.39	0.044	SPO2900	1.16	0.222	SPO2896	1.02	0.786
SPO2906	1.32	0.029	SPO2905	1.06	0.164	SPO2906	1.08	0.554	SPO2909	1.07	0.823	SPO2901	0.88	0.894	SPO2901	0.95	0.536	SPO2901	1.06	0.392	SPO2897	0.99	0.941
SPO2907	1.15	0.443	SPO2906	1.11	0.443	SPO2907	1.11	0.443	SPO2910	1.04	0.664	SPO2902	0.93	0.256	SPO2902	0.98	0.270	SPO2902	1.11	0.375	SPO2898	1.04	0.637
SPO2908	1.4	0.577	SPO2907	1.26	0.146	SPO2908	1.02	0.936	SPO2911	1.15	0.908	SPO2903	0.87	0.624	SPO2903	0.70	0.716	SPO2903	1.34	0.826	SPO2899	0.93	0.843
SPO2909	1.73	0.358	SPO2908	1.47	0.61	SPO2909	1.09	0.901	SPO2912	1.04	0.584	SPO2904	0.98	0.251	SPO2904	1.02	0.295	SPO2904	0.90	0.388	SPO2900	1.17	0.237
SPO2910	0.88	0.264	SPO2909	1.57	0.361	SPO2910	1.06	0.071	SPO2913	1.07	0.825	SPO2905	1.02	0.634	SPO2905	0.98	0.770	SPO2905	1.00	0.900	SPO2901	1.03	0.795
SPO2911	1.03	0.749	SPO2910	0.93	0.693	SPO2911	1.03	0.718	SPO2914	1.1	0.97	SPO2906	1.23	0.120	SPO2906	1.20	0.089	SPO2906	1.01	0.855	SPO2902	1.17	0.271
SPO2912	0.79	0.015	SPO2911	1.05	0.496	SPO2912	1.33	0.428	SPO2915	1.31	0.32	SPO2907	1.21	0.297	SPO2907	1.30	0.033	SPO2907	1.17	0.395	SPO2903	1.08	0.959
SPO2913	1.06	0.915	SPO2912	0.79	0.007	SPO2913	1.32	0.689	SPO2916	1.02	0.288	SPO2908	0.81	0.898	SPO2908	0.85	0.891	SPO2908	0.96	0.977	SPO2904	0.90	0.548
SPO2914	0.68	0.536	SPO2913	0.97	0.961	SPO2914	1.06	0.815	SPO2917	1.06	0.324	SPO2909	0.70	0.437	SPO2909	0.78	0.617	SPO2909	1.01	1.000	SPO2905	1.02	0.567
SPO2915	0.68	0.119	SPO2914	0.88	0.408	SPO2915																	

SPO3005	1.12	0.889	SPO3004	0.52	1.01	SPO3005	1.06	0.815	SPO3010	1.13	0.896	SPO3000	0.66	0.294	SPO3000	0.56	0.063	SPO3000	0.86	0.412	SPO2996	0.86	0.686
SPO3008	0.82	0.333	SPO3005	1.1	0.89	SPO3008	1.14	0.846	SPO3011	1.04	0.512	SPO3001	0.62	0.599	SPO3001	0.63	0.697	SPO3001	1.04	0.939	SPO2997	0.93	0.754
SPO3009	0.95	0.97	SPO3008	0.76	0.213	SPO3009	1.03	0.85	SPO3012	1.02	0.342	SPO3002	1.38	0.445	SPO3002	1.46	0.061	SPO3002	1.05	0.801	SPO2998	0.93	0.887
SPO3010	1.49	0.59	SPO3010	1.32	0.189	SPO3010	1.07	0.853	SPO3013	1.05	0.941	SPO3003	1.61	0.352	SPO3003	1.64	0.332	SPO3003	0.93	0.968	SPO2999	0.93	0.303
SPO3011	0.97	0.927	SPO3010	0.94	0.953	SPO3011	1.24	0.738	SPO3014	1.1	0.01	SPO3004	2.6	0.071	SPO3004	2.6	0.049	SPO3004	0.96	0.973	SPO3000	0.87	0.512
SPO3012	1.62	0.075	SPO3011	0.94	0.889	SPO3012	1.02	0.551	SPO3015	1.32	0.245	SPO3005	0.65	0.808	SPO3005	0.71	0.896	SPO3005	0.90	0.938	SPO3001	1.04	0.955
SPO3013	0.71	0.402	SPO3012	1.5	0.091	SPO3013	1.12	0.796	SPO3016	1.08	0.568	SPO3008	0.53	0.079	SPO3008	0.51	0.038	SPO3008	0.95	0.712	SPO3002	1.03	0.706
SPO3014	1.74	0.018	SPO3013	0.66	0.372	SPO3014	1.07	0.003	SPO3017	1.12	0.054	SPO3009	2.15	0.027	SPO3009	1.97	0.038	SPO3009	1.24	0.320	SPO3003	0.96	0.966
SPO3015	1.19	0.243	SPO3014	1.38	0.003	SPO3015	1.19	0.329	SPO3018	1.53	0.627	SPO3010	1.12	0.835	SPO3010	1.21	0.057	SPO3010	0.95	0.820	SPO3004	0.97	0.990
SPO3016	0.52	0.027	SPO3015	1.02	0.495	SPO3016	1.02	0.304	SPO3019	1.08	0.479	SPO3011	0.65	0.176	SPO3011	0.65	0.053	SPO3011	0.94	0.602	SPO3005	0.85	0.891
SPO3017	0.77	0.045	SPO3016	1.04	0.004	SPO3017	0.99	0.209	SPO3020	1.1	0.0	SPO3012	0.66	0.266	SPO3012	0.60	0.083	SPO3012	1.62	0.194	SPO3008	0.94	0.783
SPO3018	0.93	0.591	SPO3017	1.36	0.004	SPO3018	1.17	0.875	SPO3021	1.1	0.41	SPO3013	0.77	0.352	SPO3013	0.79	0.332	SPO3013	1.01	0.974	SPO3003	1.21	0.479
SPO3019	1.02	0.75	SPO3018	0.89	0.463	SPO3019	1.06	0.777	SPO3022	1.19	0.882	SPO3014	1.06	0.001	SPO3014	1.06	0.003	SPO3014	1.62	0.038	SPO3010	0.94	0.778
SPO3020	0.85	0.67	SPO3019	0.97	0.962	SPO3020	1.13	0.902	SPO3023	1.07	0.943	SPO3015	1.25	0.249	SPO3015	1.48	0.012	SPO3015	1.38	0.139	SPO3011	0.93	0.697
SPO3021	1.05	0.75	SPO3020	1.05	0.83	SPO3021	1.11	0.965	SPO3024	1.1	0.875	SPO3016	1.97	0.004	SPO3016	1.99	0.001	SPO3016	1.28	0.504	SPO3012	1.26	0.500
SPO3022	1.36	0.388	SPO3022	1.27	0.154	SPO3022	1.07	0.726	SPO3025	1.16	0.376	SPO3017	3.85	0.003	SPO3017	3.76	0.006	SPO3017	1.58	0.019	SPO3013	1.01	0.951
SPO3023	0.94	0.858	SPO3023	1.03	0.586	SPO3023	1.07	0.824	SPO3026	1.02	0.93	SPO3018	0.69	0.105	SPO3018	0.71	0.006	SPO3018	0.95	0.668	SPO3014	2.11	0.024
SPO3024	0.68	0.388	SPO3024	0.81	0.307	SPO3024	0.99	0.655	SPO3027	1.11	0.004	SPO3019	0.60	0.019	SPO3019	0.60	0.004	SPO3019	0.88	0.145	SPO3015	1.32	0.184
SPO3025	0.85	0.123	SPO3025	0.94	0.955	SPO3025	1.41	0.51	SPO3028	1.12	0.743	SPO3020	0.96	0.835	SPO3020	0.94	0.172	SPO3020	0.82	0.457	SPO3016	1.07	0.110
SPO3026	0.83	0.81	SPO3026	0.95	0.897	SPO3026	1.14	0.549	SPO3029	0.99	0.871	SPO3021	1.41	0.392	SPO3021	1.21	0.875	SPO3021	1.07	0.948	SPO3017	1.44	0.079
SPO3027	0.81	0.394	SPO3027	0.75	0.355	SPO3027	1.08	0.027	SPO3030	1.07	0.875	SPO3022	0.65	0.075	SPO3022	0.67	0.077	SPO3022	0.93	0.799	SPO3018	0.94	0.514
SPO3028	1.69	0.019	SPO3028	1.64	0.145	SPO3028	1.15	0.947	SPO3031	1.07	0.976	SPO3023	0.94	0.357	SPO3023	0.96	0.970	SPO3023	1.18	0.103	SPO3019	0.85	0.801
SPO3029	0.93	0.209	SPO3029	0.92	0.346	SPO3029	1.02	0.828	SPO3032	1.22	0.809	SPO3024	1.11	0.925	SPO3024	1.38	0.078	SPO3024	1.42	0.381	SPO3020	0.64	0.151
SPO3030	1.1	0.428	SPO3030	1.2	0.6	SPO3030	1.1	0.5	SPO3033	1.1	0.696	SPO3025	0.63	0.094	SPO3025	0.58	0.033	SPO3025	0.75	0.048	SPO3021	1.02	1.000
SPO3031	2.24	0.36	SPO3031	2.08	0.64	SPO3031	1.08	0.993	SPO3034	1.02	0.557	SPO3026	1.03	0.371	SPO3026	1.10	0.290	SPO3026	1.06	0.522	SPO3022	1.02	0.871
SPO3032	1.74	0.019	SPO3032	1.87	0.163	SPO3032	1.04	0.873	SPO3035	0.99	0.398	SPO3027	0.78	0.006	SPO3027	0.78	0.000	SPO3027	0.822	0.003	SPO3023	1.14	0.425
SPO3033	2.28	0.094	SPO3033	2.28	0.244	SPO3033	1.06	0.796	SPO3036	1.13	0.063	SPO3028	0.72	0.300	SPO3028	0.76	0.463	SPO3028	1.11	0.730	SPO3024	1.14	0.484
SPO3034	1.65	0.029	SPO3034	1.18	0.252	SPO3034	1.25	0.313	SPO3037	1.04	0.448	SPO3029	0.57	0.089	SPO3029	0.56	0.046	SPO3029	0.89	0.596	SPO3025	0.71	0.230
SPO3035	1.31	0.445	SPO3035	1.45	0.065	SPO3035	1.04	0.298	SPO3038	1.14	0.257	SPO3030	0.81	0.321	SPO3030	0.91	0.405	SPO3030	1.13	0.034	SPO3026	1.09	0.604
SPO3036	0.92	0.658	SPO3036	0.9	0.187	SPO3036	1.12	0.245	SPO3039	1.03	0.935	SPO3031	0.93	0.510	SPO3031	0.93	0.488	SPO3031	0.94	0.980	SPO3027	0.99	0.846
SPO3037	0.82	0.188	SPO3037	0.87	0.489	SPO3037	1.06	0.79	SPO3040	1.09	0.991	SPO3032	0.25	0.034	SPO3032	0.25	0.057	SPO3032	0.95	0.762	SPO3028	0.95	0.903
SPO3038	0.93	0.981	SPO3038	1	0.873	SPO3038	1.03	0.542	SPO3041	1.16	0.862	SPO3033	0.25	0.025	SPO3033	0.28	0.073	SPO3033	1.21	0.422	SPO3029	0.91	0.637
SPO3039	0.79	0.591	SPO3039	0.81	0.664	SPO3039	1.08	0.659	SPO3042	1.06	0.432	SPO3034	0.55	0.009	SPO3034	0.60	0.169	SPO3034	0.97	0.818	SPO3030	0.89	0.703
SPO3040	0.91	0.95	SPO3040	0.94	0.984	SPO3040	1.05	0.908	SPO3043	1.25	0.221	SPO3035	0.90	0.912	SPO3035	0.95	0.658	SPO3035	0.97	0.899	SPO3031	0.96	0.987
SPO3041	0.91	0.95	SPO3041	0.77	0.686	SPO3041	1.61	0.549	SPO3044	1.01	0.812	SPO3036	0.74	0.103	SPO3036	0.74	0.382	SPO3036	0.97	0.944	SPO3032	0.99	0.969
SPO3042	0.92	0.922	SPO3042	1.05	0.403	SPO3042	1.05	0.888	SPO3045	1.34	0.257	SPO3037	1.44	0.137	SPO3037	1.38	0.050	SPO3037	1.03	0.789	SPO3033	1.20	0.610
SPO3043	1.41	0.445	SPO3043	1.45	0.065	SPO3043	1.04	0.591	SPO3046	1.14	0.134	SPO3038	0.81	0.321	SPO3039	0.91	0.405	SPO3039	0.84	0.851	SPO3034	1.09	0.620
SPO3044	1.11	0.726	SPO3044	1.12	0.665	SPO3044	1.03	0.816	SPO3047	1.07	0.182	SPO3039	0.92	0.819	SPO3039	1.00	0.951	SPO3039	0.94	0.851	SPO3035	0.96	0.857
SPO3045	0.72	0.5	SPO3045	0.78	0.593	SPO3045	1.03	0.461	SPO3048	1.15	0.706	SPO3040	1.21	0.769	SPO3040	1.05	0.905	SPO3040	1.04	0.988	SPO3036	0.92	0.538
SPO3046	0.86	0.388	SPO3046	0.83	0.093	SPO3046	0.99	0.645	SPO3049	1.08	0.55	SPO3041	0.78	0.377	SPO3041	0.82	0.792	SPO3041	0.82	0.340	SPO3037	1.04	0.762
SPO3047	1.14	0.554	SPO3047	1.13	0.452	SPO3047	1	0.351	SPO3050	1.11	0.197	SPO3042	0.76	0.345	SPO3042	0.74	0.062	SPO3042	0.80	0.143	SPO3038	0.94	0.885
SPO3048	1.22	0.824	SPO3048	1.25	0.805	SPO3048	1.2	0.477	SPO3051	1.1	0.092	SPO3043	1.51	0.277	SPO3043	1.34	0.716	SPO3043	1.05	0.938	SPO3039	0.96	0.881
SPO3049	0.97	0.836	SPO3049	0.9	0.871	SPO3049	1.07	0.66	SPO3052	1.08	0.066	SPO3044	1.05	0.977	SPO3044	0.85	0.677	SPO3044	0.91	0.807	SPO3040	1.00	0.948
SPO3050	1.43	0.1	SPO3050	1.45	0.085	SPO3050	1.41	0.198	SPO3053	1.04	0.822	SPO3045	1.46	0.387	SPO3045	1.49	0.301	SPO3045	1.24	0.605	SPO3041	0.92	0.705
SPO3051	1.21	0.445	SPO3051	1.45	0.065	SPO3051	1.32	0.289	SPO3054	1.28	0.978	SPO3046	1.37	0.112	SPO3046	1.41	0.308	SPO3046	0.96	0.624	SPO3042	0.88	0.461
SPO3052	0.89	0.068	SPO3052	0.95	0.388	SPO3052	1.02	0.069	SPO3055	1.02	0.541	SPO3047	0.83	0.445	SPO3047	0.81	0.197	SPO3047	0.86	0.530	SPO3043	1.17	0.646
SPO3053	1.26	0.41	SPO3053	1.19	0.705	SPO3053	1.04	0.84	SPO3056	1.1	0.376	SPO3048	0.86	0.848	SPO3048	0.77	0.743	SPO3048	0.81	0.833	SPO3044	0.87	0.706
SPO3054	1.11	0.119	SPO3054	1.09	0.303	SPO3054	1.12	0.389	SPO3057	1.05	0.615	SPO3049	1.38	0.395	SPO3049	1.45	0.394	SPO3049	1.44	0.334	SPO3045	1.25	0.549
SPO3055	1.91	0.02	SPO3055	1.7	0.048	SPO3055	1.14	0.052	SPO3058	1.03	0.878	SPO3050	0.68	0.184	SPO3050	0.65	0.103	SPO3050	0.93	0.378	SPO3046	0.96	0.611
SPO3056	0.76	0.178	SPO3056	0.79	0.23	SPO3056	1.35	0.439	SPO3059	1	0.835	SPO3051	0.65	0.057	SPO3051	0.65	0.012	SPO3051	1.01	0.854	SPO3047	0.88	0.479
SPO3057	1.18	0.162	SPO3057	1.02	0.45	SPO3057	1.03	0.594	SPO3060	1.03	0.395	SPO3052	0.74	0.095	SPO3052	0.77	0.214	SPO3052	0.95	0.373	SPO3048	0.81	0.814
SPO3058	1.42	0.472	SPO3058	1.41	0.425	SPO3058	1.04	0.833	SPO3062	1.11	0.124	SPO3053	0.45	0.076	SPO3053	0.42	0.093	SPO3053	0.99	0.963	SPO3049	1.39	0.500
SPO3059	0.91	0.397	SPO3059	0.86	0.419	SPO3059	1.25	0.8															

SPO3149	0.69	0.026	SPO3149	0.65	0.519	SPO3149	1.03	0.611	SPO3152	1.13	0.5	SPO3144	0.62	0.008	SPO3144	0.70	0.304	SPO3144	0.87	0.253	SPO3140	1.07	0.806
SPO3150	1.14	0.899	SPO3150	1.19	0.9	SPO3150	1.04	0.326	SPO3153	0.98	0.693	SPO3145	1.30	0.122	SPO3145	1.26	0.103	SPO3145	1.04	0.924	SPO3141	1.01	0.780
SPO3151	0.87	0.21	SPO3151	0.96	0.957	SPO3151	1.24	0.195	SPO3154	0.99	0.891	SPO3146	1.63	0.064	SPO3146	1.72	0.005	SPO3146	1.20	0.166	SPO3142	0.97	0.848
SPO3152	1.32	0.195	SPO3152	0.82	0.195	SPO3152	1.02	0.195	SPO3157	1.02	0.195	SPO3147	0.47	0.85	SPO3147	1.15	0.354	SPO3147	1.15	0.354	SPO3143	1.21	0.610
SPO3153	0.81	0.807	SPO3153	0.85	0.867	SPO3153	0.99	0.867	SPO3156	1.14	0.336	SPO3148	0.96	0.554	SPO3148	0.99	0.554	SPO3148	0.99	0.554	SPO3144	0.88	0.132
SPO3154	1.29	0.368	SPO3154	1.3	0.187	SPO3154	1.91	0.907	SPO3157	1.06	0.451	SPO3149	0.97	0.906	SPO3149	1.03	0.961	SPO3149	1.06	0.933	SPO3145	1.04	0.700
SPO3155	0.95	0.823	SPO3155	0.95	0.962	SPO3155	1.08	0.268	SPO3158	1.1	0.913	SPO3150	0.76	0.882	SPO3150	0.76	0.882	SPO3150	0.92	0.946	SPO3146	1.09	0.692
SPO3156	1.42	0.063	SPO3156	1.38	0.941	SPO3156	0.99	0.941	SPO3159	1.05	0.513	SPO3151	1.34	0.015	SPO3151	1.30	0.007	SPO3151	1.13	0.226	SPO3147	1.10	0.580
SPO3157	0.9	0.554	SPO3157	1.02	0.633	SPO3157	1.08	0.91	SPO3160	1.72	0.228	SPO3152	1.47	0.084	SPO3152	1.39	0.191	SPO3152	0.90	0.753	SPO3148	0.90	0.373
SPO3158	0.85	0.37	SPO3158	0.87	0.677	SPO3158	1.07	0.953	SPO3161	1.39	0.035	SPO3153	0.93	0.675	SPO3153	0.63	0.437	SPO3153	0.79	0.755	SPO3149	1.08	0.890
SPO3159	1.34	0.299	SPO3159	1.28	0.491	SPO3159	1.01	0.519	SPO3162	1.2	0.727	SPO3154	1.16	0.300	SPO3154	1.13	0.108	SPO3154	1.17	0.168	SPO3150	0.90	0.943
SPO3160	1.49	0.19	SPO3160	1.28	0.008	SPO3160	1.15	0.067	SPO3163	1.14	0.808	SPO3155	1.40	0.096	SPO3155	1.48	0.074	SPO3155	1.03	0.654	SPO3151	1.17	0.953
SPO3161	1.49	0.299	SPO3161	1.28	0.008	SPO3161	1.15	0.067	SPO3164	1.07	0.838	SPO3156	0.81	0.009	SPO3156	0.82	0.078	SPO3156	0.97	0.101	SPO3152	1.00	0.963
SPO3162	1.22	0.161	SPO3162	1.12	0.195	SPO3162	1.18	0.808	SPO3165	1.08	0.544	SPO3157	0.89	0.878	SPO3157	0.81	0.206	SPO3157	0.93	0.679	SPO3153	0.93	0.896
SPO3163	1.07	0.703	SPO3163	1.08	0.71	SPO3163	1.15	0.619	SPO3166	1.07	0.514	SPO3158	0.88	0.267	SPO3158	0.68	0.447	SPO3158	0.92	0.840	SPO3154	1.08	0.628
SPO3164	1.13	0.188	SPO3164	1.01	0.971	SPO3164	1.27	0.138	SPO3167	1.01	0.802	SPO3159	1.17	0.547	SPO3159	1.10	0.695	SPO3159	1.09	0.747	SPO3155	1.05	0.691
SPO3165	0.86	0.080	SPO3165	0.92	0.529	SPO3165	1.15	0.015	SPO3168	1.22	0.404	SPO3160	1.06	0.473	SPO3160	1.03	0.490	SPO3160	0.92	0.778	SPO3156	0.91	0.233
SPO3166	0.61	0.054	SPO3166	0.71	0.101	SPO3166	1.11	0.162	SPO3169	1.06	0.084	SPO3161	0.74	0.210	SPO3161	0.77	0.309	SPO3161	1.24	0.148	SPO3157	0.88	0.504
SPO3167	1.01	0.266	SPO3167	1.17	0.304	SPO3167	1.11	0.089	SPO3170	1.05	0.061	SPO3162	1.03	0.190	SPO3162	1.03	0.190	SPO3162	1.02	0.552	SPO3158	0.92	0.835
SPO3168	0.67	0.097	SPO3168	0.74	0.514	SPO3168	1.05	0.571	SPO3171	1.09	0.312	SPO3163	1.45	0.119	SPO3163	1.33	0.141	SPO3163	1.09	0.558	SPO3159	1.05	0.827
SPO3169	0.99	0.62	SPO3169	0.91	0.553	SPO3169	1.04	0.444	SPO3172	0.97	0.256	SPO3164	1.30	0.008	SPO3164	1.30	0.002	SPO3164	1.08	0.227	SPO3160	1.01	0.951
SPO3170	1.28	0.078	SPO3170	1.26	0.237	SPO3170	1.45	0.084	SPO3173	1.08	0.957	SPO3165	1.98	0.007	SPO3165	1.77	0.008	SPO3165	1.27	0.254	SPO3161	1.04	0.601
SPO3171	1.15	0.401	SPO3171	1.03	0.701	SPO3171	1.04	0.074	SPO3174	1.18	0.895	SPO3166	0.80	0.614	SPO3166	0.79	0.805	SPO3166	0.78	0.229	SPO3162	1.06	0.628
SPO3172	1.62	0.17	SPO3172	1.4	0.059	SPO3172	1.13	0.346	SPO3175	1.09	0.895	SPO3167	0.77	0.426	SPO3167	0.78	0.064	SPO3167	1.01	0.999	SPO3163	1.13	0.411
SPO3173	1.42	0.051	SPO3173	1.23	0.873	SPO3173	1.21	0.441	SPO3176	1.02	0.015	SPO3168	0.79	0.074	SPO3168	0.85	0.013	SPO3168	0.89	0.118	SPO3164	1.15	0.050
SPO3174	0.81	0.075	SPO3174	0.87	0.768	SPO3174	0.99	0.541	SPO3177	1.31	0.819	SPO3169	0.40	0.048	SPO3169	0.45	0.003	SPO3169	1.03	0.623	SPO3165	1.36	0.214
SPO3175	0.97	0.09	SPO3175	0.96	0.956	SPO3175	1.16	0.536	SPO3178	1.13	0.772	SPO3170	0.82	0.217	SPO3170	0.86	0.181	SPO3170	1.00	0.941	SPO3166	0.85	0.342
SPO3176	0.95	0.634	SPO3176	1.01	0.327	SPO3176	1.3	0.009	SPO3179	1.09	0.883	SPO3171	0.57	0.066	SPO3171	0.60	0.155	SPO3171	0.82	0.517	SPO3167	1.06	0.719
SPO3177	1.22	0.503	SPO3177	1.28	0.441	SPO3177	1.34	0.017	SPO3180	1.15	0.918	SPO3172	0.83	0.207	SPO3172	0.85	0.074	SPO3172	1.02	0.854	SPO3168	0.88	0.494
SPO3178	0.53	0.424	SPO3178	0.9	0.936	SPO3178	1.23	0.611	SPO3181	1.07	0.267	SPO3173	0.83	0.096	SPO3173	0.75	0.819	SPO3173	1.02	0.986	SPO3169	1.07	0.194
SPO3179	0.93	0.825	SPO3179	1.13	0.107	SPO3179	0.99	0.462	SPO3182	1.15	0.055	SPO3174	0.52	0.275	SPO3174	0.55	0.423	SPO3174	0.77	0.445	SPO3170	0.88	0.300
SPO3180	1.18	0.221	SPO3180	1.3	0.031	SPO3180	1.3	0.602	SPO3183	1.09	0.472	SPO3175	1.09	0.418	SPO3175	1.00	0.782	SPO3175	0.99	0.987	SPO3171	0.82	0.356
SPO3181	1.66	0.094	SPO3181	1.71	0.063	SPO3181	1.05	0.448	SPO3184	1.09	0.997	SPO3176	1.60	0.026	SPO3176	1.64	0.039	SPO3176	1.35	0.009	SPO3172	0.88	0.383
SPO3182	1.5	0.028	SPO3182	1.34	0.049	SPO3182	1.01	0.098	SPO3185	1.13	0.544	SPO3177	0.98	0.830	SPO3177	0.93	0.901	SPO3177	0.99	0.990	SPO3173	0.96	0.956
SPO3183	1.01	0.807	SPO3183	1.05	0.584	SPO3183	1.32	0.501	SPO3186	1.24	0.467	SPO3178	0.79	0.537	SPO3178	0.74	0.604	SPO3178	0.80	0.610	SPO3174	0.85	0.442
SPO3184	0.92	SPO3184	1.05	0.828	SPO3184	1.32	0.991	SPO3187	1.33	0.989	SPO3179	1.01	0.938	SPO3179	0.99	0.654	SPO3179	1.00	0.923	SPO3175	1.03	0.783	
SPO3185	0.83	0.39	SPO3185	0.95	0.208	SPO3185	1.02	0.847	SPO3190	1.24	0.216	SPO3180	1.42	0.07	SPO3180	1.42	0.07	SPO3180	1.02	0.914	SPO3164	1.07	0.374
SPO3186	1.01	0.891	SPO3186	0.91	0.738	SPO3186	1.28	0.219	SPO3189	1.11	0.958	SPO3181	0.60	0.118	SPO3181	0.50	0.061	SPO3181	0.95	0.922	SPO3177	1.01	0.934
SPO3187	0.88	0.847	SPO3187	0.88	0.801	SPO3187	1.02	0.952	SPO3190	1.23	0.272	SPO3182	1.22	0.032	SPO3182	1.19	0.060	SPO3182	0.92	0.571	SPO3178	1.00	0.965
SPO3188	0.79	0.831	SPO3188	0.92	0.963	SPO3188	1.14	0.78	SPO3191	1.05	0.552	SPO3183	0.80	0.171	SPO3183	0.85	0.292	SPO3183	0.85	0.329	SPO3179	1.02	0.947
SPO3189	0.92	0.948	SPO3189	1.01	0.917	SPO3189	1.25	0.793	SPO3192	1.19	0.664	SPO3184	1.04	0.994	SPO3184	1.02	0.936	SPO3184	1.16	0.759	SPO3180	1.02	0.818
SPO3190	0.61	0.14	SPO3190	0.72	0.131	SPO3190	1.02	0.503	SPO3193	1.45	0.011	SPO3185	1.14	0.301	SPO3185	1.01	0.391	SPO3185	0.89	0.661	SPO3181	0.89	0.634
SPO3191	0.6	0.21	SPO3191	0.68	0.236	SPO3191	1.29	0.369	SPO3194	0.99	0.661	SPO3186	0.93	0.920	SPO3186	0.89	0.773	SPO3186	0.79	0.172	SPO3182	0.96	0.914
SPO3192	1.34	0.007	SPO3192	1.12	0.198	SPO3192	1.16	0.446	SPO3195	1.27	0.709	SPO3187	1.25	0.571	SPO3187	1.43	0.252	SPO3187	1.06	0.981	SPO3183	0.86	0.658
SPO3193	1.12	0.06	SPO3193	1.05	0.208	SPO3193	1.02	0.017	SPO3198	1.24	0.24	SPO3188	1.68	0.588	SPO3188	1.63	0.632	SPO3188	0.88	0.914	SPO3164	1.07	0.374
SPO3194	1.21	1.689	SPO3194	1.01	0.905	SPO3194	1.19	0.641	SPO3197	1.14	0.599	SPO3189	1.10	0.884	SPO3189	1.04	0.995	SPO3189	0.85	0.768	SPO3185	0.93	0.714
SPO3195	0.89	0.756	SPO3195	0.85	0.681	SPO3195	1.08	0.723	SPO3198	1.42	0.226	SPO3190	1.48	0.091	SPO3190	1.60	0.028	SPO3190	0.99	0.864	SPO3186	0.78	0.907
SPO3196	0.78	0.584	SPO3196	0.96	0.949	SPO3196	1.07	0.437	SPO3199	0.98	0.298	SPO3191	1.36	0.243	SPO3191	1.89	0.388	SPO3191	0.93	0.745	SPO3187	1.09	0.884
SPO3197	1.64	0.124	SPO3197	1.29	0.504	SPO3197	0.99	0.74	SPO3200	1.35	0.146	SPO3192	1.17	0.655	SPO3192	1.17	0.617	SPO3192	1.11	0.545	SPO3188	0.91	0.935
SPO3198	1.91	0.018	SPO3198	1.7	0.027	SPO3198	1.01	0.87	SPO3201	1.39	0.262	SPO3193	0.72	0.070	SPO3193	0.71	0.040	SPO3193	0.83	0.231	SPO3189	0.92	0.868
SPO3199	1.18	0.32	SPO3199	1.22	0.027	SPO3199	1.13	0.573	SPO3202	1.01	0.306	SPO3194	0.88	0.931	SPO3194	0.94	0.903	SPO3194	1.07	0.837	SPO3190	1.00	0.915
SPO3200	0.87	0.098	SPO3200	0.92	0.236	SPO3200	1.12	0.441	SPO3203	1.22	0.367	SPO3195	0.62	0.370	SPO3195	0.61	0.339	SPO3195	0.88	0.717	SPO3181	1.01	0.988
SPO3201	0.93	0.59	SPO3201	0.98	0.201	SPO3201																	

SPO3295	1.18	0.341	SPO3295	1.2	0.196	SPO3295	1.07	0.265	SPO3298	1.24	0.249	SPO3290	1.36	0.182	SPO3290	1.29	0.208	SPO3290	0.81	0.478	SPO3286	0.97	0.937
SPO3296	1.15	0.827	SPO3296	1.12	0.872	SPO3296	1.09	0.921	SPO3299	1.0	0.52	SPO3291	1.92	0.108	SPO3291	1.85	0.101	SPO3291	1.06	0.474	SPO3287	0.51	0.014
SPO3297	1.1	0.927	SPO3297	0.97	0.827	SPO3297	1.1	0.704	SPO3300	1.05	0.978	SPO3292	0.97	0.957	SPO3292	1.04	0.908	SPO3292	1.00	0.982	SPO3288	1.14	0.454
SPO3298	0.83	0.289	SPO3298	0.96	0.927	SPO3298	1.11	0.74	SPO3301	1.12	0.229	SPO3293	1.53	0.267	SPO3293	1.58	0.263	SPO3293	0.83	0.723	SPO3289	1.10	0.653
SPO3299	1.28	0.107	SPO3299	1.33	0.089	SPO3299	1.03	0.446	SPO3302	1.14	0.524	SPO3294	1.50	0.196	SPO3294	1.63	0.270	SPO3294	1.00	0.532	SPO3290	0.84	0.403
SPO3300	0.97	0.986	SPO3300	0.96	0.934	SPO3300	1.08	0.996	SPO3303	1.33	0.726	SPO3295	1.56	0.005	SPO3295	1.61	0.024	SPO3295	1.00	0.336	SPO3291	1.04	0.532
SPO3301	1.36	0.087	SPO3301	1.32	0.329	SPO3301	1.13	0.205	SPO3304	1.1	0.862	SPO3296	1.38	0.773	SPO3296	1.37	0.795	SPO3296	0.95	0.950	SPO3292	1.05	0.945
SPO3302	0.57	0.047	SPO3302	0.68	0.113	SPO3302	1.07	0.555	SPO3305	1.15	0.895	SPO3297	1.45	0.337	SPO3297	1.24	0.183	SPO3297	1.23	0.790	SPO3293	0.90	0.581
SPO3303	0.88	0.585	SPO3303	0.85	0.296	SPO3303	1.18	0.519	SPO3306	1.08	0.224	SPO3298	1.42	0.016	SPO3298	1.34	0.102	SPO3298	1.09	0.328	SPO3294	1.07	0.882
SPO3304	1.18	0.078	SPO3304	1.13	0.114	SPO3304	1.28	0.698	SPO3307	1.11	0.292	SPO3299	1.21	0.498	SPO3299	1.62	0.210	SPO3299	1.02	0.938	SPO3295	1.08	0.756
SPO3305	1.24	0.441	SPO3305	1.34	0.416	SPO3305	1.13	0.892	SPO3308	1.1	0.999	SPO3300	1.21	0.640	SPO3300	1.12	0.127	SPO3300	1.02	0.964	SPO3296	0.95	0.947
SPO3306	0.78	0.289	SPO3306	0.96	0.927	SPO3306	1.03	0.6	SPO3309	1.02	0.353	SPO3301	0.95	0.27	SPO3301	0.91	0.065	SPO3301	1.08	0.718	SPO3297	1.10	0.398
SPO3307	0.93	0.201	SPO3307	0.88	0.448	SPO3307	1.2	0.356	SPO3302	1.2	0.356	SPO3302	0.73	0.210	SPO3302	0.70	0.123	SPO3302	1.06	0.816	SPO3298	1.01	0.998
SPO3308	0.98	0.985	SPO3308	0.92	0.692	SPO3308	1.05	0.461	SPO3311	0.98	0.6	SPO3303	1.11	0.400	SPO3303	1.20	0.052	SPO3303	0.99	0.964	SPO3299	1.12	0.671
SPO3309	0.81	0.34	SPO3309	0.87	0.403	SPO3309	1.07	0.138	SPO3312	1.4	0.214	SPO3304	0.88	0.856	SPO3304	0.93	0.822	SPO3304	0.91	0.463	SPO3300	1.03	0.861
SPO3310	0.78	0.417	SPO3310	0.76	0.003	SPO3310	1.13	0.297	SPO3313	1.1	0.504	SPO3305	1.02	0.798	SPO3305	0.96	0.909	SPO3305	1.00	0.799	SPO3301	1.16	0.652
SPO3311	0.53	0.1	SPO3311	0.6	0.06	SPO3311	1.03	0.023	SPO3314	1.19	0.764	SPO3306	1.14	0.047	SPO3306	1.07	0.117	SPO3306	1.07	0.178	SPO3302	1.09	0.626
SPO3312	0.72	0.154	SPO3312	0.77	0.048	SPO3312	1.04	0.177	SPO3315	1.04	0.87	SPO3307	1.02	0.516	SPO3307	0.95	0.880	SPO3307	0.96	0.857	SPO3303	1.02	0.387
SPO3313	0.78	0.365	SPO3313	0.68	0.683	SPO3313	1.13	0.178	SPO3316	1.1	0.888	SPO3308	1.05	0.881	SPO3308	0.98	0.199	SPO3308	0.95	0.819	SPO3304	0.88	0.483
SPO3314	1.51	0.369	SPO3314	1.38	0.381	SPO3314	1.04	0.76	SPO3317	1.03	0.163	SPO3309	1.25	0.179	SPO3317	1.24	0.054	SPO3309	1.09	0.449	SPO3305	1.05	0.828
SPO3315	1.11	0.507	SPO3315	0.98	0.961	SPO3315	1.09	0.617	SPO3318	1.08	0.706	SPO3310	1.24	0.149	SPO3310	1.24	0.022	SPO3310	1.24	0.462	SPO3306	1.10	0.290
SPO3316	1.47	0.377	SPO3316	1.37	0.077	SPO3316	1.91	0.679	SPO3319	1.1	0.68	SPO3311	1.81	0.011	SPO3311	1.90	0.019	SPO3311	1.14	0.139	SPO3307	1.00	0.853
SPO3317	1.17	0.427	SPO3317	1.24	0.012	SPO3317	2.11	0.131	SPO3320	1.06	0.057	SPO3312	1.18	0.024	SPO3312	1.37	0.050	SPO3312	1.14	0.600	SPO3308	1.01	0.869
SPO3318	0.8	0.466	SPO3318	0.81	0.104	SPO3318	1.17	0.317	SPO3321	1.04	0.192	SPO3313	0.67	0.160	SPO3313	0.44	0.097	SPO3313	0.72	0.322	SPO3309	1.18	0.272
SPO3319	0.91	0.867	SPO3319	0.92	0.932	SPO3319	1.32	0.737	SPO3322	1.11	0.454	SPO3314	0.36	0.031	SPO3314	0.37	0.078	SPO3314	1.24	0.772	SPO3310	1.36	0.268
SPO3320	1.29	0.077	SPO3320	1.13	0.134	SPO3320	1.02	0.104	SPO3323	1.22	0.821	SPO3315	0.78	0.428	SPO3315	0.81	0.654	SPO3315	0.83	0.283	SPO3311	1.24	1.147
SPO3321	0.67	0.011	SPO3321	0.65	0.106	SPO3321	2.3	0.407	SPO3324	1.03	0.611	SPO3316	0.66	0.460	SPO3316	0.58	0.324	SPO3316	0.76	0.567	SPO3312	1.16	0.549
SPO3322	0.98	0.033	SPO3322	0.94	0.763	SPO3322	2.0	0.226	SPO3325	1.17	0.333	SPO3317	1.09	0.588	SPO3317	1.03	0.897	SPO3317	0.83	0.733	SPO3313	0.81	0.518
SPO3323	0.86	0.246	SPO3323	0.81	0.404	SPO3323	1.46	0.464	SPO3326	1.08	0.464	SPO3318	1.25	0.034	SPO3318	1.27	0.108	SPO3318	1.06	0.589	SPO3314	1.23	0.752
SPO3324	1.06	0.559	SPO3324	0.93	0.693	SPO3324	1.77	0.981	SPO3327	1.09	0.814	SPO3319	2.15	0.338	SPO3319	2.1	0.341	SPO3319	0.96	0.971	SPO3315	0.81	0.407
SPO3325	0.84	0.226	SPO3325	0.87	0.212	SPO3325	1.08	0.152	SPO3328	1.19	0.894	SPO3320	0.68	0.103	SPO3320	0.68	0.069	SPO3320	0.93	0.360	SPO3329	0.97	0.527
SPO3326	1.05	0.757	SPO3326	1.11	0.548	SPO3326	1.07	0.157	SPO3329	1.08	0.088	SPO3321	1.11	0.295	SPO3321	1.03	0.423	SPO3321	1.12	0.253	SPO3317	0.95	0.510
SPO3327	1.23	0.605	SPO3327	1.18	0.846	SPO3327	1.1	0.783	SPO3330	1.21	0.237	SPO3322	0.88	0.667	SPO3322	1.00	0.365	SPO3322	1.04	0.584	SPO3318	1.02	0.735
SPO3328	1.04	0.766	SPO3328	0.86	0.452	SPO3328	1.26	0.631	SPO3331	1.05	0.995	SPO3323	0.82	0.714	SPO3323	0.83	0.683	SPO3323	1.01	0.942	SPO3319	0.98	0.996
SPO3329	1.3	0.307	SPO3329	1.56	0.033	SPO3329	1.12	0.521	SPO3332	1.03	0.058	SPO3324	0.98	0.575	SPO3324	1.06	0.173	SPO3324	1.17	0.059	SPO3320	0.93	0.719
SPO3330	1.18	0.212	SPO3330	1.11	0.371	SPO3330	1.25	0.107	SPO3333	1.23	0.273	SPO3325	0.69	0.095	SPO3325	0.67	0.001	SPO3325	0.93	0.097	SPO3321	1.14	0.260
SPO3331	1.11	0.943	SPO3331	0.943	0.939	SPO3331	1.17	0.1	SPO3334	1.05	0.323	SPO3326	0.93	0.031	SPO3326	0.78	0.031	SPO3326	0.83	0.887	SPO3323	0.98	0.965
SPO3332	1.74	0.017	SPO3332	1.52	0.044	SPO3332	1.1	0.109	SPO3335	1.1	0.182	SPO3327	0.85	0.788	SPO3327	0.80	0.781	SPO3327	0.85	0.645	SPO3327	1.09	0.598
SPO3333	0.76	0.631	SPO3333	0.81	0.576	SPO3333	1.15	0.41	SPO3336	1.27	0.574	SPO3328	0.62	0.188	SPO3328	0.61	0.096	SPO3328	1.03	0.746	SPO3324	1.25	1.28
SPO3334	0.76	0.15	SPO3334	0.79	0.96	SPO3334	1.14	0.157	SPO3337	0.99	0.186	SPO3329	0.25	0.003	SPO3329	0.31	0.001	SPO3329	1.13	0.550	SPO3325	1.03	0.620
SPO3335	1.90	0.031	SPO3335	1.93	0.029	SPO3335	1.1	0.223	SPO3338	1.65	0.915	SPO3330	1.37	0.165	SPO3330	1.41	0.184	SPO3330	1.01	0.966	SPO3326	0.86	0.605
SPO3336	1.5	0.28	SPO3336	1.44	0.506	SPO3336	1.09	0.529	SPO3339	2.27	0.63	SPO3331	0.62	0.820	SPO3331	0.63	0.827	SPO3331	0.88	0.941	SPO3327	0.83	0.675
SPO3337	1.5	0.069	SPO3337	1.44	0.016	SPO3337	1.04	0.394	SPO3340	1.15	0.721	SPO3332	0.63	0.158	SPO3332	0.68	0.041	SPO3332	1.01	0.935	SPO3328	1.03	0.721
SPO3338	1.15	0.77	SPO3338	1.18	0.635	SPO3338	1.07	0.963	SPO3341	1.33	0.92	SPO3333	3.16	0.004	SPO3333	2.97	0.037	SPO3333	0.97	0.972	SPO3329	1.08	0.646
SPO3339	1.11	0.24	SPO3339	0.98	0.451	SPO3339	1.17	0.383	SPO3342	1.05	0.32	SPO3334	0.98	0.015	SPO3334	0.91	0.012	SPO3334	0.95	0.887	SPO3330	0.98	0.650
SPO3340	1.6	0.016	SPO3340	1.46	0.044	SPO3340	1.13	0.014	SPO3343	2.4	0.943	SPO3335	0.84	0.237	SPO3335	0.93	0.413	SPO3335	0.89	0.436	SPO3331	0.87	0.938
SPO3341	1.1	0.596	SPO3341	0.97	0.943	SPO3341	1.05	0.588	SPO3344	2.35	0.400	SPO3336	3.18	0.206	SPO3336	3.08	0.400	SPO3336	0.66	0.736	SPO3332	0.94	0.453
SPO3342	1.37	0.155	SPO3342	1.27	0.13	SPO3342	1.1	0.787	SPO3345	1.42	0.547	SPO3337	0.58	0.043	SPO3337	0.63	0.098	SPO3337	0.86	0.106	SPO3333	0.99	0.882
SPO3343	0.67	0.46	SPO3343	0.69	0.548	SPO3343	1.08	0.905	SPO3346	1.82	0.389	SPO3338	0.71	0.699	SPO3338	0.71	0.666	SPO3338	0.99	0.981	SPO3334	0.94	0.828
SPO3344	1.24	0.327	SPO3344	1.14	0.261	SPO3344	1.07	0.658	SPO3347	1.13	0.918	SPO3339	0.81	0.315	SPO3339	0.79	0.495	SPO3339	1.03	0.929	SPO3335	0.79	0.223
SPO3345	1.38	0.111	SPO3345	1.17	0.122	SPO3345	1.6	0.373	SPO3348	1.1	0.517	SPO3340	0.96	0.832	SPO3340	0.98	0.705	SPO3340	1.07	0.626	SPO3336	0.71	0.658
SPO3346	1.19	0.222	SPO3346	1.2	0.1	SPO3346	1.53	0.522	SPO3349	1.09	0.251	SPO3341	0.76	0.177	SPO3341	0.78	0.104	SPO3341	0.93	0.853	SPO3337	0.91	0.627
SPO3347	1.58	0.55	SPO3347	1.37	0.616	SPO3347	1.12	0.															

SPO3434	1.11	0.575	SPO3434	1.13	0.551	SPO3434	1.07	0.513	SPO3437	1.1	0.875	SPO3429	0.64	0.445	SPO3429	0.60	0.448	SPO3429	0.85	0.650	SPO3425	1.04	0.733
SPO3435	0.94	0.843	SPO3435	0.83	0.537	SPO3435	1.04	0.621	SPO3438	1.15	0.904	SPO3430	0.93	0.529	SPO3430	0.70	0.795	SPO3430	1.08	0.581	SPO3426	1.08	0.191
SPO3436	1.61	1.06	SPO3436	1.36	1.154	SPO3436	1.11	0.629	SPO3439	0.99	0.795	SPO3431	0.90	0.771	SPO3431	0.91	0.706	SPO3435	0.92	0.577	SPO3428	0.95	0.988
SPO3437	1.33	0.928	SPO3437	1.25	0.395	SPO3437	1.31	0.651	SPO3440	1.18	0.788	SPO3432	1.09	0.712	SPO3432	1.09	0.692	SPO3432	1.14	0.582	SPO3428	1.15	0.739
SPO3438	0.83	0.904	SPO3438	0.97	0.993	SPO3438	1.07	0.976	SPO3441	1.09	0.263	SPO3433	0.98	0.923	SPO3433	0.91	0.572	SPO3433	0.91	0.887	SPO3429	0.85	0.452
SPO3439	1.48	0.234	SPO3439	1.15	0.019	SPO3439	1.06	0.501	SPO3442	1.05	0.857	SPO3434	1.08	0.677	SPO3434	1.05	0.741	SPO3434	0.91	0.739	SPO3430	0.76	0.454
SPO3440	1.09	0.246	SPO3440	1.04	0.448	SPO3440	1.1	0.095	SPO3443	1.05	0.91	SPO3435	0.46	0.078	SPO3435	0.46	0.064	SPO3435	0.96	0.958	SPO3431	0.93	0.736
SPO3441	0.68	1.02	SPO3441	0.75	0.821	SPO3441	1.27	0.492	SPO3444	1.04	0.668	SPO3436	1.05	0.571	SPO3436	1.14	0.279	SPO3436	0.93	0.249	SPO3432	1.13	0.518
SPO3442	1.39	0.41	SPO3442	1.21	0.536	SPO3442	1.24	0.773	SPO3445	1.08	0.116	SPO3437	1.45	0.179	SPO3437	1.45	0.342	SPO3437	1.14	0.302	SPO3433	0.91	0.872
SPO3443	1.12	0.745	SPO3443	1.14	0.76	SPO3443	1.49	0.977	SPO3446	1.03	0.05	SPO3438	0.86	0.929	SPO3438	0.74	0.815	SPO3438	0.85	0.899	SPO3434	0.89	0.622
SPO3444	1.13	0.756	SPO3444	1.13	0.441	SPO3444	1.11	0.761	SPO3447	1.08	0.188	SPO3439	1.51	0.046	SPO3439	1.52	0.071	SPO3439	1.22	0.162	SPO3435	0.95	0.900
SPO3445	0.75	0.028	SPO3445	1.25	0.395	SPO3445	1.05	0.01	SPO3448	1.03	0.788	SPO3440	1.33	0.213	SPO3440	1.37	0.052	SPO3440	1.13	0.173	SPO3436	1.04	0.651
SPO3446	1.34	0.004	SPO3446	1.41	0.024	SPO3446	1.04	0.044	SPO3449	1.01	0.863	SPO3441	1.09	0.288	SPO3441	0.88	0.154	SPO3441	1.25	0.006	SPO3437	1.04	0.810
SPO3447	0.52	0.196	SPO3447	0.62	0.011	SPO3447	1.15	0.021	SPO3450	1.01	0.139	SPO3442	0.79	0.634	SPO3442	0.90	0.758	SPO3442	1.02	0.867	SPO3438	0.91	0.931
SPO3448	0.81	0.296	SPO3448	0.89	0.502	SPO3448	1.06	0.93	SPO3451	1.04	0.376	SPO3443	0.96	0.975	SPO3443	0.93	0.979	SPO3443	0.99	0.988	SPO3439	1.19	0.164
SPO3449	0.71	0.682	SPO3449	0.88	0.718	SPO3449	1.45	0.913	SPO3452	1.11	0.075	SPO3444	1.02	0.861	SPO3444	0.95	0.841	SPO3444	0.97	0.953	SPO3440	1.10	0.216
SPO3450	1.27	0.078	SPO3450	1.23	0.023	SPO3450	2.04	0.366	SPO3453	1.24	0.719	SPO3445	7.72	0.020	SPO3445	7.42	0.004	SPO3445	0.83	0.463	SPO3441	1.32	0.139
SPO3451	0.78	0.223	SPO3451	0.8	0.189	SPO3451	1.69	0.393	SPO3454	1.08	0.152	SPO3446	0.57	0.003	SPO3446	0.53	0.008	SPO3446	0.96	0.946	SPO3442	0.99	0.958
SPO3452	0.74	0.154	SPO3452	0.85	0.389	SPO3452	1.4	0.423	SPO3455	1.26	0.876	SPO3447	1.16	0.151	SPO3447	1.27	0.040	SPO3447	1.08	0.666	SPO3443	0.97	0.599
SPO3453	0.88	0.119	SPO3453	0.88	0.569	SPO3453	1.16	0.574	SPO3456	1.22	0.855	SPO3448	1.26	0.242	SPO3448	1.27	0.175	SPO3448	1.10	0.551	SPO3444	0.95	0.845
SPO3454	1.12	0.031	SPO3454	1.16	0.014	SPO3454	1.21	0.333	SPO3457	1.3	0.51	SPO3449	1.07	0.746	SPO3449	1.02	0.799	SPO3449	1.01	0.947	SPO3445	0.93	0.885
SPO3455	0.95	0.90	SPO3455	0.94	0.845	SPO3455	1.05	0.844	SPO3458	1.54	0.562	SPO3450	0.70	0.096	SPO3450	0.70	0.096	SPO3450	1.17	0.257	SPO3446	0.94	0.689
SPO3456	1.17	0.717	SPO3456	1.34	0.747	SPO3456	1.4	0.855	SPO3459	1.16	0.834	SPO3451	1.97	0.033	SPO3451	1.82	0.062	SPO3451	1.11	0.557	SPO3447	1.04	0.748
SPO3457	1.09	0.359	SPO3457	1.02	0.78	SPO3457	1.29	0.944	SPO3460	1.1	0.042	SPO3452	1.82	0.033	SPO3452	1.94	0.016	SPO3452	1.26	0.299	SPO3448	1.12	0.597
SPO3458	1.04	0.326	SPO3458	1.19	0.19	SPO3458	1.17	0.709	SPO3461	1.06	0.859	SPO3453	0.81	0.226	SPO3453	0.81	0.226	SPO3453	0.92	0.767	SPO3449	1.03	0.923
SPO3459	1.57	0.077	SPO3459	1.34	0.017	SPO3459	1.05	0.069	SPO3462	1.44	0.12	SPO3454	0.92	0.185	SPO3454	0.92	0.185	SPO3454	0.92	0.500	SPO3450	1.09	0.417
SPO3460	0.78	0.232	SPO3460	0.79	0.154	SPO3460	1	0.265	SPO3463	1.81	0.979	SPO3455	0.37	0.199	SPO3455	0.36	0.204	SPO3455	1.00	0.918	SPO3451	1.07	0.572
SPO3461	0.74	0.636	SPO3461	0.81	0.72	SPO3461	1.17	0.789	SPO3464	1.17	0.865	SPO3456	0.97	0.189	SPO3456	0.95	0.409	SPO3456	0.93	0.871	SPO3452	1.16	0.171
SPO3462	0.78	0.632	SPO3462	0.83	0.632	SPO3462	1.01	0.81	SPO3467	1.16	0.334	SPO3457	1.19	0.12	SPO3457	1.19	0.12	SPO3457	0.96	0.893	SPO3453	0.81	0.653
SPO3463	1.04	0.849	SPO3463	0.95	0.792	SPO3463	1	0.602	SPO3466	1.14	0.783	SPO3458	0.73	0.011	SPO3458	0.99	0.020	SPO3458	0.94	0.809	SPO3454	0.95	0.804
SPO3464	0.92	0.738	SPO3464	0.99	0.843	SPO3464	1.44	0.873	SPO3467	1.14	0.93	SPO3459	0.19	0.003	SPO3459	0.21	0.005	SPO3459	1.13	0.461	SPO3455	1.00	0.952
SPO3465	1.15	0.18	SPO3465	1.02	0.509	SPO3465	1.02	0.861	SPO3468	1.47	0.847	SPO3460	0.25	0.02	SPO3460	0.26	0.000	SPO3460	1.05	0.912	SPO3456	1.00	0.882
SPO3466	1.22	0.717	SPO3466	1.11	0.828	SPO3466	1.15	0.617	SPO3469	1.41	0.483	SPO3461	0.20	0.028	SPO3461	0.24	0.016	SPO3461	0.98	0.901	SPO3457	0.95	0.858
SPO3467	0.76	0.012	SPO3467	0.82	0.21	SPO3467	1.14	0.617	SPO3470	1.11	0.507	SPO3462	0.75	0.107	SPO3462	0.75	0.107	SPO3462	1.01	0.967	SPO3458	1.04	0.945
SPO3468	0.69	0.506	SPO3468	0.7	0.148	SPO3468	1	0.938	SPO3471	1.05	0.746	SPO3463	0.56	0.08	SPO3463	0.54	0.116	SPO3463	0.95	0.896	SPO3459	1.11	0.724
SPO3469	0.56	0.039	SPO3469	0.59	0.082	SPO3469	1.03	0.515	SPO3472	1.06	0.517	SPO3464	1.37	0.114	SPO3464	1.44	0.057	SPO3464	1.11	0.748	SPO3460	1.13	0.489
SPO3470	1.15	0.65	SPO3470	1.16	0.34	SPO3470	1.13	0.314	SPO3473	1.17	0.11	SPO3465	0.29	0.01	SPO3465	0.29	0.01	SPO3465	1.12	0.22	SPO3461	0.81	0.623
SPO3471	0.81	0.64	SPO3471	0.88	0.765	SPO3471	1.03	0.814	SPO3474	1.11	0.833	SPO3466	0.99	0.892	SPO3466	0.97	0.905	SPO3466	0.84	0.849	SPO3462	0.96	0.711
SPO3472	0.61	0.034	SPO3472	0.7	0.031	SPO3472	1.12	0.706	SPO3475	1.04	0.486	SPO3467	1.44	0.005	SPO3467	1.37	0.014	SPO3467	1.00	0.847	SPO3463	0.93	0.831
SPO3473	0.83	0.391	SPO3473	0.83	0.643	SPO3473	1.16	0.922	SPO3476	1.41	0.54	SPO3468	1.53	0.071	SPO3468	1.65	0.042	SPO3468	0.95	0.899	SPO3464	1.05	0.874
SPO3474	0.83	0.36	SPO3474	0.88	0.216	SPO3474	1.03	0.385	SPO3477	1.18	0.802	SPO3469	1.58	0.073	SPO3469	1.50	0.079	SPO3469	1.03	0.827	SPO3465	0.99	0.926
SPO3475	0.95	0.25	SPO3475	0.9	0.439	SPO3475	1.06	0.274	SPO3478	1.02	0.892	SPO3470	0.76	0.325	SPO3470	0.79	0.383	SPO3470	0.92	0.795	SPO3466	0.88	0.817
SPO3476	0.89	0.896	SPO3476	0.88	0.548	SPO3476	1.02	0.681	SPO3479	1.16	0.54	SPO3471	0.86	0.870	SPO3471	0.81	0.743	SPO3471	1.02	0.954	SPO3467	0.99	0.997
SPO3477	1.04	0.646	SPO3477	1.04	0.473	SPO3477	1.11	0.598	SPO3480	1.04	0.585	SPO3472	0.99	0.370	SPO3472	0.89	0.369	SPO3472	0.96	0.967	SPO3468	0.98	0.966
SPO3478	1.15	0.65	SPO3478	1.05	0.891	SPO3478	1.13	0.942	SPO3481	1.17	0.11	SPO3473	0.89	0.01	SPO3473	0.89	0.01	SPO3473	1.16	0.138	SPO3469	1.02	0.733
SPO3479	1.18	0.264	SPO3479	1.17	0.176	SPO3479	1.04	0.447	SPO3482	1.13	0.504	SPO3474	0.93	0.741	SPO3474	0.85	0.673	SPO3474	0.90	0.895	SPO3470	0.99	0.983
SPO3480	1.24	0.143	SPO3480	1.27	0.071	SPO3480	1.03	0.381	SPO3483	1.1	0.153	SPO3475	0.81	0.589	SPO3475	0.85	0.700	SPO3475	0.78	0.066	SPO3471	1.01	0.950
SPO3481	1.24	0.378	SPO3481	1.17	0.052	SPO3481	1.03	0.116	SPO3484	1	0.664	SPO3476	0.62	0.040	SPO3476	0.63	0.024	SPO3476	0.99	0.891	SPO3472	1.00	0.860
SPO3482	1.33	0.084	SPO3482	1.36	0.204	SPO3482	1.08	0.04	SPO3485	1.25	0.219	SPO3477	0.84	0.299	SPO3477	0.82	0.191	SPO3477	1.05	0.705	SPO3473	1.16	0.429
SPO3483	1.37	0.043	SPO3483	1.26	0.091	SPO3483	1.12	0.012	SPO3486	1.03	0.073	SPO3478	0.82	0.757	SPO3478	0.77	0.699	SPO3478	0.85	0.802	SPO3474	0.90	0.673
SPO3484	1.29	0.675	SPO3484	1.09	0.86	SPO3484	1.08	0.893	SPO3479	1.08	0.893	SPO3479	0.75	0.159	SPO3479	0.78	0.296	SPO3479	0.73	0.269	SPO3475	0.83	0.161
SPO3485	1.2	0.228	SPO3485	1.08	0.37	SPO3485	1.02	0.418	SPO3488	1.15	0.907	SPO3480	0.71	0.025	SPO3480	0.74	0.211	SPO3480	0.64	0.109	SPO3476	0.99	0.897
SPO3486	0.96	0.867	SPO3486	1.02	0.601	SPO3486	1	0.861															

SPO3575	1.21	0.554	SPO3575	1.13	0.728	SPO3575	1.22	0.855	SPO3578	1.11	0.741	SPO3570	1.86	0.047	SPO3570	1.97	0.005	SPO3570	1.12	0.575	SPO3566	0.97	0.967
SPO3576	0.86	0.424	SPO3576	0.99	0.955	SPO3576	1.24	0.725	SPO3580	1.13	0.953	SPO3571	1.23	0.247	SPO3571	1.43	0.049	SPO3571	1.29	0.417	SPO3567	1.00	0.961
SPO3577	0.97	0.901	SPO3577	0.95	0.945	SPO3577	1.13	0.321	SPO3580	1.22	0.033	SPO3572	0.85	0.781	SPO3572	0.78	0.510	SPO3572	0.93	0.819	SPO3568	1.05	0.702
SPO3578	0.91	0.216	SPO3578	1.11	0.255	SPO3578	1.11	0.255	SPO3581	1.37	0.272	SPO3573	1.37	0.110	SPO3573	1.13	0.326	SPO3573	1.15	0.332	SPO3569	0.86	0.915
SPO3579	0.94	0.944	SPO3579	1.03	0.674	SPO3579	1.11	0.617	SPO3582	1.14	0.447	SPO3574	1.55	0.005	SPO3574	1.70	0.020	SPO3574	1.15	0.754	SPO3570	1.12	0.195
SPO3580	1.05	0.023	SPO3580	0.81	0.081	SPO3580	1.27	0.555	SPO3583	1.12	0.319	SPO3575	0.91	0.879	SPO3575	0.83	0.720	SPO3575	0.76	0.900	SPO3571	1.20	0.457
SPO3581	1.08	0.944	SPO3581	1.04	0.827	SPO3581	1.12	0.76	SPO3584	1.04	0.557	SPO3576	1.38	0.097	SPO3576	1.31	0.079	SPO3576	1.15	0.438	SPO3572	0.95	0.808
SPO3582	1.30	0.030	SPO3582	1.37	0.031	SPO3582	1.15	0.937	SPO3585	1.36	0.805	SPO3577	1.00	0.938	SPO3577	0.99	0.725	SPO3577	0.99	0.865	SPO3573	1.20	1.008
SPO3583	1.02	0.692	SPO3583	1.08	0.269	SPO3583	1.13	0.2	SPO3586	1.47	0.361	SPO3578	0.68	0.041	SPO3578	0.68	0.014	SPO3578	0.89	0.334	SPO3574	0.97	0.916
SPO3584	1.45	0.063	SPO3584	1.44	0.087	SPO3584	1.12	0.364	SPO3587	1.56	0.036	SPO3579	1.47	0.115	SPO3579	1.38	0.072	SPO3579	1.04	0.868	SPO3575	0.80	0.155
SPO3585	0.97	0.936	SPO3585	0.98	0.934	SPO3585	1.02	0.78	SPO3588	1.19	0.591	SPO3580	1.13	0.611	SPO3580	1.99	0.025	SPO3580	1.14	0.539	SPO3576	1.09	0.424
SPO3586	0.75	0.216	SPO3586	0.97	0.897	SPO3586	1.18	0.253	SPO3589	1.26	0.478	SPO3581	1.43	0.336	SPO3581	1.24	0.176	SPO3581	1.12	0.765	SPO3577	1.03	0.989
SPO3587	0.89	0.223	SPO3587	0.86	0.284	SPO3587	1.02	0.245	SPO3590	1.14	0.417	SPO3582	1.00	0.369	SPO3582	0.96	0.449	SPO3582	1.00	0.971	SPO3578	0.90	0.786
SPO3588	1.12	0.525	SPO3588	0.83	0.664	SPO3588	1.31	0.477	SPO3591	1.12	0.114	SPO3583	0.96	0.873	SPO3583	1.13	0.293	SPO3583	1.00	0.930	SPO3579	1.00	0.790
SPO3589	1.1	0.697	SPO3589	1.19	0.093	SPO3589	1.13	0.787	SPO3592	1.12	0.118	SPO3584	0.88	0.580	SPO3584	1.00	0.563	SPO3584	1.00	0.563	SPO3580	1.26	0.277
SPO3590	0.58	0.019	SPO3590	0.67	0.016	SPO3590	1.04	0.103	SPO3593	1.37	0.591	SPO3585	1.07	0.552	SPO3585	1.02	0.564	SPO3585	0.91	0.719	SPO3581	1.07	0.430
SPO3591	1.36	0.006	SPO3591	1.17	0.038	SPO3591	1.15	0.155	SPO3594	1.14	0.842	SPO3586	1.03	0.707	SPO3586	1.06	0.811	SPO3586	1.00	0.939	SPO3582	1.08	0.634
SPO3592	0.88	0.252	SPO3592	0.93	0.662	SPO3592	0.98	0.138	SPO3595	1.17	0.179	SPO3587	1.07	0.030	SPO3587	1.13	0.023	SPO3587	1.16	0.113	SPO3583	1.05	0.796
SPO3593	0.69	0.474	SPO3593	0.75	0.133	SPO3593	1.07	0.885	SPO3596	1.15	0.059	SPO3588	0.83	0.408	SPO3588	0.95	0.516	SPO3588	0.92	0.642	SPO3584	1.02	0.990
SPO3594	1.46	0.022	SPO3594	1.38	0.422	SPO3594	1.19	0.953	SPO3597	1.12	0.551	SPO3589	0.57	0.071	SPO3589	0.71	0.038	SPO3589	0.53	0.091	SPO3585	0.85	0.955
SPO3595	1.04	0.432	SPO3595	1.11	0.385	SPO3595	1.12	0.087	SPO3598	1.12	0.551	SPO3590	0.76	0.185	SPO3590	0.68	0.030	SPO3590	1.06	0.596	SPO3586	1.04	0.749
SPO3596	0.71	0.492	SPO3596	0.76	0.033	SPO3596	1.57	0.03	SPO3599	0.99	0.081	SPO3591	0.58	0.001	SPO3591	0.58	0.001	SPO3591	0.53	0.488	SPO3587	1.20	0.018
SPO3597	1.36	0.379	SPO3597	1.18	0.427	SPO3597	1.06	0.053	SPO3600	1.21	0.041	SPO3592	0.95	0.568	SPO3592	1.00	0.279	SPO3592	1.17	0.560	SPO3588	1.09	0.878
SPO3598	1.25	0.358	SPO3598	1.38	0.003	SPO3598	1.17	0.123	SPO3601	1.09	0.906	SPO3593	0.83	0.467	SPO3593	0.90	0.324	SPO3593	0.90	0.490	SPO3589	0.63	0.400
SPO3599	0.99	0.930	SPO3599	1.28	0.238	SPO3599	1.12	0.601	SPO3602	1.13	0.432	SPO3594	0.92	0.976	SPO3594	0.92	0.958	SPO3594	0.88	0.987	SPO3590	1.08	0.605
SPO3600	0.01	0.033	SPO3600	0.27	0.048	SPO3600	1.11	0.133	SPO3603	1.11	0.94	SPO3595	0.97	0.763	SPO3595	1.03	0.828	SPO3595	0.98	0.287	SPO3591	0.97	0.835
SPO3601	1.01	0.927	SPO3601	1.03	0.655	SPO3601	1.26	0.653	SPO3604	1.06	0.328	SPO3596	0.62	0.551	SPO3596	0.61	0.495	SPO3596	0.86	0.822	SPO3592	1.19	0.348
SPO3602	0.79	0.288	SPO3602	0.85	0.501	SPO3602	1.02	0.683	SPO3605	1.08	0.111	SPO3597	0.56	0.188	SPO3597	0.60	0.066	SPO3597	0.93	0.581	SPO3593	0.92	0.216
SPO3603	0.89	0.799	SPO3603	0.98	0.988	SPO3603	1.63	0.591	SPO3606	1.08	0.849	SPO3598	0.98	0.028	SPO3598	0.98	0.559	SPO3598	0.87	0.355	SPO3594	1.02	0.892
SPO3604	1.29	0.141	SPO3604	1.11	0.358	SPO3604	1.13	0.711	SPO3607	1.14	0.837	SPO3599	1.02	0.180	SPO3599	0.82	0.967	SPO3599	0.88	0.408	SPO3595	1.01	0.922
SPO3605	1.01	0.58	SPO3605	1.05	0.165	SPO3605	1.03	0.183	SPO3608	1.02	0.357	SPO3600	0.26	0.034	SPO3600	0.25	0.027	SPO3600	1.42	0.069	SPO3596	0.87	0.729
SPO3606	1.22	0.129	SPO3606	1.21	0.438	SPO3606	1.05	0.683	SPO3609	1.14	0.867	SPO3601	1.25	0.376	SPO3601	1.12	0.442	SPO3601	0.98	0.909	SPO3597	0.88	0.488
SPO3607	0.56	0.642	SPO3607	0.68	0.789	SPO3607	1.24	0.874	SPO3610	1.54	0.948	SPO3602	1.63	0.028	SPO3602	1.52	0.010	SPO3602	1.02	0.861	SPO3598	0.86	0.350
SPO3608	0.88	0.541	SPO3608	0.85	0.283	SPO3608	1.19	0.263	SPO3611	1.05	0.229	SPO3603	0.90	0.913	SPO3603	0.85	0.982	SPO3603	0.99	0.989	SPO3599	0.95	0.884
SPO3609	1.78	0.025	SPO3609	1.4	0.043	SPO3609	1	0.656	SPO3612	1.11	0.394	SPO3604	0.29	0.014	SPO3604	0.31	0.014	SPO3604	1.15	0.205	SPO3600	1.47	0.138
SPO3610	1.26	0.859	SPO3610	1.16	0.907	SPO3610	1.06	0.95	SPO3613	1.11	0.959	SPO3605	0.46	0.036	SPO3605	0.36	0.010	SPO3605	1.25	0.187	SPO3601	0.90	0.483
SPO3611	0.71	0.071	SPO3611	0.81	0.101	SPO3611	1.01	0.821	SPO3614	1.19	0.206	SPO3606	0.19	0.036	SPO3606	0.23	0.039	SPO3606	1.01	0.943	SPO3610	1.02	0.943
SPO3612	1.36	0.216	SPO3612	1.33	0.051	SPO3612	1.06	0.195	SPO3615	1.25	0.404	SPO3607	0.47	0.523	SPO3607	0.45	0.097	SPO3607	1.75	0.658	SPO3603	1.06	0.894
SPO3613	1.19	0.44	SPO3613	0.99	0.433	SPO3613	1.21	0.768	SPO3616	1	0.514	SPO3608	2.06	0.032	SPO3608	2.05	0.013	SPO3608	1.06	0.495	SPO3604	1.12	0.318
SPO3614	1.02	0.597	SPO3614	1.02	0.425	SPO3614	1	0.288	SPO3617	1.02	0.227	SPO3609	1.67	0.059	SPO3609	1.69	0.008	SPO3609	1.25	1.065	SPO3605	1.25	0.110
SPO3615	0.87	0.591	SPO3615	0.89	0.765	SPO3615	1.02	0.62	SPO3618	1.72	0.996	SPO3610	0.61	0.742	SPO3610	0.67	0.811	SPO3610	0.95	0.971	SPO3606	0.99	0.974
SPO3616	1.62	0.021	SPO3616	1.52	0.028	SPO3616	1	0.468	SPO3619	1.35	0.991	SPO3611	1.46	0.296	SPO3611	1.47	0.042	SPO3611	1.01	0.955	SPO3607	1.65	0.664
SPO3617	1.11	0.174	SPO3617	1.04	0.318	SPO3617	1.2	0.406	SPO3620	1.07	0.659	SPO3612	2.00	0.048	SPO3612	2.00	0.048	SPO3612	0.82	0.301	SPO3608	1.10	0.485
SPO3618	1.41	0.25	SPO3618	1.2	0.611	SPO3618	1.12	0.74	SPO3621	1.18	0.445	SPO3613	0.98	0.006	SPO3613	0.98	0.004	SPO3613	1.05	0.974	SPO3609	1.20	0.312
SPO3619	1.23	0.947	SPO3619	1.12	0.132	SPO3619	1.34	0.753	SPO3622	1.08	0.192	SPO3614	1.14	0.07	SPO3614	1.14	0.07	SPO3614	1.01	0.940	SPO3610	0.88	0.932
SPO3620	0.90	0.963	SPO3620	0.98	0.846	SPO3620	1.17	0.525	SPO3623	1.02	0.32	SPO3615	0.93	0.879	SPO3615	0.90	0.759	SPO3615	1.01	0.978	SPO3611	0.92	0.805
SPO3621	0.8	0.015	SPO3621	0.94	0.428	SPO3621	1.1	0.528	SPO3625	1.07	0.053	SPO3616	0.69	0.031	SPO3616	0.69	0.031	SPO3616	1.04	0.629	SPO3612	0.85	0.276
SPO3622	1.34	0.019	SPO3622	1.25	0.044	SPO3622	1.01	0.065	SPO3626	1.01	0.913	SPO3617	2.12	0.003	SPO3617	2.22	0.000	SPO3617	0.93	0.470	SPO3613	0.98	0.676
SPO3623	1.7	0.033	SPO3623	1.64	0.08	SPO3623	1.12	0.859	SPO3627	1.26	0.914	SPO3618	1.35	0.369	SPO3618	1.45	0.332	SPO3618	1.04	0.876	SPO3614	1.03	0.986
SPO3625	1.12	0.083	SPO3625	0.98	0.916	SPO3625	1.14	0.017	SPO3628	1.03	0.891	SPO3619	1.07	0.154	SPO3619	1.00	0.171	SPO3619	1.00	0.774	SPO3615	0.92	0.609
SPO3626	1.12	0.748	SPO3626	0.98	0.997	SPO3626	1.19	0.827	SPO3629	1.15	0.599	SPO3620	0.97	0.544	SPO3620	0.97	0.427	SPO3620	0.97	0.427	SPO3616	0.99	0.847
SPO3627	1.23	0.597	SPO3627	1.29	0.815	SPO3627	1.03	0.926	SPO3630	1.19	0.477	SPO3621	1.48	0.040	SPO3621	1.51	0.005	SPO3621	1.02	0.852	SPO3617	0.87	0.094
SPO3628	1.32	0.947	SPO3628	1.25	0.132																		

SPO3718	1.18	0.29	SPO3718	1.19	0.057	SPO3718	1.1	0.249	SPO3721	1.34	0.202	SPO3713	1.58	0.005	SPO3713	1.57	0.005	SPO3713	1.06	0.127	SPO3709	0.88	0.934
SPO3719	0.91	0.70	SPO3719	0.99	0.42	SPO3719	1.16	0.148	SPO3722	1.12	0.16	SPO3714	0.60	0.007	SPO3714	0.59	0.007	SPO3714	1.46	0.044	SPO3710	1.00	0.952
SPO3720	1.38	0.05	SPO3720	1.48	0.015	SPO3720	1.09	0.173	SPO3723	0.99	0.416	SPO3715	0.88	0.988	SPO3715	0.83	0.883	SPO3715	1.08	0.737	SPO3711	0.96	0.771
SPO3721	1.43	0.70	SPO3721	1.43	0.147	SPO3721	1.09	0.683	SPO3724	1.04	0.581	SPO3716	1.09	0.366	SPO3716	1.08	0.261	SPO3716	1.23	0.238	SPO3712	1.01	0.783
SPO3722	0.85	0.52	SPO3722	0.9	0.681	SPO3722	1.1	0.769	SPO3725	1.1	0.769	SPO3717	0.89	0.586	SPO3717	0.87	0.599	SPO3717	0.57	0.846	SPO3713	1.08	0.421
SPO3723	1.06	0.38	SPO3723	0.9	0.686	SPO3723	1.1	0.342	SPO3726	1.11	0.997	SPO3718	0.57	0.087	SPO3718	0.53	0.004	SPO3718	0.74	0.015	SPO3714	1.46	0.071
SPO3724	0.94	0.84	SPO3724	1.06	0.552	SPO3724	1.22	0.751	SPO3727	1.32	0.064	SPO3719	0.96	0.517	SPO3719	0.94	0.264	SPO3719	1.00	0.747	SPO3715	1.07	0.737
SPO3725	0.98	0.96	SPO3725	0.98	0.952	SPO3725	0.99	0.732	SPO3728	1.19	0.685	SPO3720	0.58	0.018	SPO3720	0.54	0.009	SPO3720	1.00	0.733	SPO3716	1.07	0.799
SPO3726	1.07	0.714	SPO3726	1.09	0.71	SPO3726	1.05	0.783	SPO3729	1.08	0.041	SPO3721	0.15	0.002	SPO3721	0.14	0.001	SPO3721	0.93	0.679	SPO3717	1.04	0.817
SPO3727	0.86	0.333	SPO3727	0.94	0.813	SPO3727	1.06	0.364	SPO3730	1.06	0.061	SPO3722	0.19	0.001	SPO3722	0.19	0.007	SPO3722	0.99	0.850	SPO3718	0.74	0.113
SPO3728	0.99	0.951	SPO3728	0.97	0.838	SPO3728	1.25	0.811	SPO3731	1.17	0.728	SPO3723	0.44	0.026	SPO3723	0.43	0.021	SPO3723	0.97	0.680	SPO3719	1.04	0.790
SPO3729	1.05	0.701	SPO3729	1.05	0.673	SPO3729	1.05	0.253	SPO3732	1.12	0.357	SPO3724	1.12	0.357	SPO3724	1.12	0.357	SPO3724	1.08	0.361	SPO3724	1.08	0.361
SPO3730	1.61	0.102	SPO3730	1.5	0.075	SPO3730	1.5	0.481	SPO3733	1.01	0.4	SPO3725	1.04	0.566	SPO3725	1.07	0.460	SPO3725	0.88	0.583	SPO3721	1.03	0.937
SPO3731	1.02	0.601	SPO3731	1.05	0.279	SPO3731	1.39	0.278	SPO3734	1.24	0.019	SPO3726	0.94	0.694	SPO3726	0.95	0.480	SPO3726	1.06	0.734	SPO3722	0.96	0.972
SPO3732	1.02	0.651	SPO3732	1.04	0.226	SPO3732	1.14	0.334	SPO3736	1.06	0.911	SPO3727	1.65	0.060	SPO3727	1.55	0.013	SPO3727	1.05	0.600	SPO3723	1.02	0.994
SPO3733	1.1	0.309	SPO3733	1.09	0.221	SPO3733	1.14	0.038	SPO3737	1.05	0.546	SPO3728	1.39	0.020	SPO3728	1.44	0.011	SPO3728	0.88	0.237	SPO3724	1.15	0.734
SPO3734	0.99	0.92	SPO3734	1.06	0.316	SPO3734	1.18	0.432	SPO3738	1.06	0.203	SPO3729	1.43	0.046	SPO3729	1.53	0.022	SPO3729	1.00	0.882	SPO3725	0.91	0.707
SPO3735	1.16	0.399	SPO3735	0.99	0.7	SPO3735	1.02	0.958	SPO3739	1.22	0.888	SPO3730	0.54	0.037	SPO3730	0.61	0.375	SPO3730	1.16	0.119	SPO3726	1.09	0.626
SPO3736	0.99	0.03	SPO3736	1.05	0.665	SPO3736	1.22	0.966	SPO3740	1.05	0.28	SPO3731	2.06	0.046	SPO3731	1.95	0.012	SPO3731	0.85	0.160	SPO3727	1.16	0.063
SPO3737	1.26	0.224	SPO3737	1.25	0.309	SPO3737	1.34	0.309	SPO3741	1.33	0.235	SPO3732	1.05	0.326	SPO3732	1.04	0.349	SPO3732	0.99	0.902	SPO3728	0.92	0.260
SPO3738	1.32	0.068	SPO3738	1.35	0.011	SPO3738	1.31	0.514	SPO3742	1.39	0.71	SPO3733	0.73	0.070	SPO3733	0.73	0.166	SPO3733	1.15	0.157	SPO3729	1.04	0.527
SPO3739	0.79	0.263	SPO3739	0.85	0.835	SPO3739	1.15	0.663	SPO3743	1.23	0.47	SPO3734	1.11	0.718	SPO3734	1.08	0.654	SPO3734	0.96	0.912	SPO3730	1.09	0.249
SPO3740	0.79	0.127	SPO3740	0.75	0.134	SPO3740	1.13	0.307	SPO3744	1.13	0.81	SPO3735	0.88	0.036	SPO3735	0.73	0.086	SPO3735	1.20	0.483	SPO3731	0.98	0.932
SPO3741	0.59	0.029	SPO3741	0.6	0.033	SPO3741	1.42	0.282	SPO3745	1.05	0.379	SPO3736	0.76	0.397	SPO3736	0.74	0.227	SPO3736	1.02	0.868	SPO3732	1.07	0.463
SPO3742	0.74	0.119	SPO3742	0.81	0.274	SPO3742	1.31	0.914	SPO3746	1.13	0.121	SPO3737	0.85	0.437	SPO3737	0.88	0.577	SPO3737	1.08	0.709	SPO3733	1.11	0.434
SPO3743	1.21	0.219	SPO3743	1.18	0.119	SPO3743	1.27	0.578	SPO3747	1.37	0.692	SPO3738	1.46	0.128	SPO3738	1.71	0.001	SPO3738	1.11	0.662	SPO3734	0.94	0.670
SPO3744	0.94	0.853	SPO3744	0.96	0.95	SPO3744	1.23	0.721	SPO3748	1.34	0.791	SPO3739	0.72	0.395	SPO3739	0.66	0.499	SPO3739	0.97	0.952	SPO3735	0.85	0.843
SPO3745	0.97	0.724	SPO3745	1.01	0.723	SPO3745	1.15	0.121	SPO3749	1.22	0.786	SPO3740	0.68	0.095	SPO3740	0.68	0.095	SPO3740	0.97	0.984	SPO3736	1.02	0.816
SPO3746	1.13	0.063	SPO3746	1.13	0.068	SPO3746	1.13	0.068	SPO3750	1.02	0.367	SPO3741	0.41	0.132	SPO3741	0.41	0.132	SPO3741	0.98	0.982	SPO3737	1.05	0.917
SPO3747	0.9	0.194	SPO3747	0.85	0.139	SPO3747	1.04	0.103	SPO3751	1.12	0.238	SPO3742	0.71	0.110	SPO3742	0.76	0.025	SPO3742	0.91	0.397	SPO3738	1.15	0.023
SPO3748	0.75	0.082	SPO3748	0.75	0.029	SPO3748	1.06	0.64	SPO3752	1.18	0.554	SPO3743	0.89	0.706	SPO3743	0.88	0.548	SPO3743	1.05	0.401	SPO3739	0.97	0.943
SPO3749	0.75	0.428	SPO3749	0.68	0.641	SPO3749	1.09	0.671	SPO3753	1.33	0.358	SPO3744	0.77	0.845	SPO3744	0.82	0.998	SPO3744	0.86	0.829	SPO3740	1.03	0.138
SPO3750	0.56	0.083	SPO3750	0.68	0.149	SPO3750	1.05	0.568	SPO3754	1.22	0.301	SPO3745	2.07	0.003	SPO3745	1.73	0.020	SPO3745	1.09	0.453	SPO3741	1.06	0.796
SPO3751	1.5	0.007	SPO3751	1.53	0.025	SPO3751	1.07	0.558	SPO3755	1.03	0.179	SPO3746	1.93	0.015	SPO3746	1.80	0.023	SPO3746	1.00	0.872	SPO3742	0.87	1.171
SPO3752	1.46	0.27	SPO3752	1.53	0.06	SPO3752	1.28	0.574	SPO3756	1.2	0.29	SPO3747	0.88	0.380	SPO3747	0.96	0.506	SPO3747	0.96	0.273	SPO3743	1.01	0.856
SPO3753	1.74	0.138	SPO3753	1.71	0.044	SPO3753	1.11	0.583	SPO3757	1.04	0.822	SPO3748	0.80	0.74	SPO3748	0.75	0.631	SPO3748	0.74	0.504	SPO3744	0.96	0.991
SPO3754	0.71	0.05	SPO3754	0.69	0.05	SPO3754	1.12	0.037	SPO3759	1.11	0.37	SPO3749	1.11	0.37	SPO3749	0.98	0.37	SPO3749	0.98	0.646	SPO3753	0.95	0.917
SPO3755	0.86	0.165	SPO3755	0.91	0.044	SPO3755	1.03	0.05	SPO3759	1.05	0.885	SPO3750	1.43	0.162	SPO3750	1.44	0.088	SPO3750	1.20	0.398	SPO3746	1.02	0.716
SPO3756	1.4	0.383	SPO3756	1.32	0.256	SPO3756	1.12	0.398	SPO3760	1.11	0.357	SPO3751	0.59	0.017	SPO3751	0.60	0.106	SPO3751	1.08	0.825	SPO3747	0.99	0.826
SPO3757	0.9	0.253	SPO3757	0.89	0.444	SPO3757	16.3	0.639	SPO3761	1.1	0.934	SPO3752	0.66	0.027	SPO3752	0.75	0.112	SPO3752	1.06	0.233	SPO3748	0.78	0.202
SPO3758	0.8	0.141	SPO3758	0.85	0.375	SPO3758	7.12	0.229	SPO3762	1.12	0.619	SPO3753	0.55	0.086	SPO3753	0.55	0.017	SPO3753	1.14	0.546	SPO3749	1.00	0.992
SPO3759	1.61	0.128	SPO3759	1.55	0.028	SPO3759	20.8	0.221	SPO3763	1.25	0.968	SPO3754	0.90	0.366	SPO3754	1.00	0.867	SPO3754	1.09	0.313	SPO3750	1.24	0.244
SPO3760	0.97	0.98	SPO3760	1	0.794	SPO3760	9.92	0.308	SPO3764	1.1	0.807	SPO3755	1.29	0.121	SPO3755	1.28	0.172	SPO3755	1.08	0.653	SPO3751	1.21	0.559
SPO3761	1.14	0.335	SPO3761	1.08	0.374	SPO3761	1.33	0.872	SPO3765	1.13	0.566	SPO3756	1.05	0.701	SPO3756	1.08	0.038	SPO3756	1.07	0.556	SPO3752	1.06	0.811
SPO3762	1.61	0.09	SPO3762	1.58	0.09	SPO3762	1.34	0.708	SPO3769	1.07	0.625	SPO3757	0.91	0.763	SPO3757	0.93	0.67	SPO3757	0.91	0.646	SPO3753	1.07	0.670
SPO3763	1.51	0.031	SPO3763	1.56	0.033	SPO3763	1.02	0.904	SPO3767	1.18	0.247	SPO3758	1.29	0.074	SPO3758	1.22	0.027	SPO3758	0.95	0.963	SPO3754	1.04	0.556
SPO3764	1.25	0.135	SPO3764	1.16	0.083	SPO3764	1.01	0.541	SPO3768	1.17	0.021	SPO3759	1.00	0.549	SPO3759	0.98	0.484	SPO3759	1.11	0.318	SPO3755	1.07	0.533
SPO3765	0.75	0.167	SPO3765	0.75	0.311	SPO3765	1.03	0.811	SPO3769	6.08	0.733	SPO3760	1.48	0.322	SPO3760	1.42	0.302	SPO3760	1.18	0.543	SPO3756	1.07	0.336
SPO3766	1.21	0.52	SPO3766	1.21	0.058	SPO3766	1.28	0.614	SPO3770	16.4	0.514	SPO3761	1.16	0.064	SPO3761	1.23	0.014	SPO3761	1.05	0.498	SPO3757	0.91	0.351
SPO3767	0.65	0.012	SPO3767	0.65	0.017	SPO3767	1.17	0.01	SPO3771	7.7	0.865	SPO3762	2.73	0.016	SPO3762	2.88	0.024	SPO3762	1.27	0.160	SPO3758	0.99	0.863
SPO3768	2.2	0.009	SPO3768	1.97	0.002	SPO3768	1.21	0.019	SPO3772	1.25	0.252	SPO3763	1.27	0.047	SPO3763	1.32	0.106	SPO3763	0.96	0.804	SPO3759	1.07	0.566
SPO3769	1.27	0.615	SPO3769	1.28	0.694	SPO3769	1.1	0.685	SPO3774	1.34	0.393	SPO3764	1.04	0.351	SPO3764	1.10	0.226	SPO3764	0.93	0.709	SPO3760	1.20	0.519
SPO3770	0.89	0.779	SPO3770	1.11	0.869	SPO3770	1.07	0.95															

SPO3865	0.88	0.071	SPO3865	0.93	0.087	SPO3864	1.12	0.001	SPO3869	1.01	0.903	SPO3859	1.53	0.086	SPO3859	1.36	0.071	SPO3860	0.89	0.688	SPO3855	0.88	0.375
SPO3866	1.2	0.12	SPO3866	1.08	0.416	SPO3865	1.04	0.135	SPO3870	1.03	0.856	SPO3860	0.79	0.483	SPO3860	0.75	0.058	SPO3861	0.93	0.867	SPO3856	0.85	0.528
SPO3867	1.07	0.72	SPO3867	1.11	0.047	SPO3866	1.08	0.39	SPO3871	1.38	0.945	SPO3861	0.72	0.395	SPO3861	0.68	0.330	SPO3862	0.79	0.878	SPO3853	0.90	0.676
SPO3868	0.91	0.828	SPO3868	0.98	0.374	SPO3867	1.47	0.21	SPO3872	1.43	0.837	SPO3862	0.74	0.33	SPO3862	0.85	0.385	SPO3863	1.03	0.475	SPO3858	0.83	0.107
SPO3869	0.83	0.446	SPO3869	0.86	0.174	SPO3868	1.01	0.292	SPO3873	1.15	0.682	SPO3863	0.90	0.749	SPO3863	0.96	0.976	SPO3864	0.91	0.977	SPO3859	0.74	0.286
SPO3870	1.24	0.107	SPO3870	1.14	0.213	SPO3869	1.16	0.965	SPO3874	1.14	0.893	SPO3864	0.92	0.939	SPO3864	0.91	0.986	SPO3865	1.01	0.972	SPO3860	0.93	0.589
SPO3871	1.02	0.801	SPO3871	1.11	0.59	SPO3870	1.08	0.569	SPO3875	1.26	0.037	SPO3865	0.98	0.223	SPO3865	1.04	0.467	SPO3866	1.07	0.705	SPO3861	0.93	0.874
SPO3872	1.02	0.92	SPO3872	1.02	0.44	SPO3871	1.26	0.474	SPO3876	1.2	0.127	SPO3866	0.79	0.403	SPO3866	0.86	0.454	SPO3867	1.02	0.917	SPO3862	0.85	0.896
SPO3873	0.79	0.052	SPO3873	0.94	0.939	SPO3872	1.06	0.515	SPO3877	1.7	0.912	SPO3867	0.79	0.432	SPO3867	0.85	0.130	SPO3868	0.87	0.278	SPO3863	0.97	0.971
SPO3874	1.62	0.027	SPO3874	1.37	0.147	SPO3873	1.12	0.789	SPO3878	1.3	0.073	SPO3868	0.33	0.034	SPO3868	0.33	0.034	SPO3869	0.98	0.982	SPO3864	0.93	0.364
SPO3875	1.02	0.574	SPO3875	1.03	0.219	SPO3874	1.13	0.607	SPO3879	1.29	0.529	SPO3869	1.09	0.582	SPO3869	1.14	0.219	SPO3870	1.20	0.071	SPO3865	1.01	0.341
SPO3876	0.91	0.828	SPO3876	0.98	0.374	SPO3875	1.35	0.053	SPO3881	1.09	0.54	SPO3870	0.33	0.385	SPO3870	0.89	0.376	SPO3871	1.16	0.445	SPO3866	1.11	0.534
SPO3877	1.02	0.28	SPO3877	1.04	0.362	SPO3876	1.14	0.038	SPO3881	1.09	0.839	SPO3871	1.16	0.291	SPO3871	1.23	0.287	SPO3872	0.93	0.771	SPO3867	0.93	0.453
SPO3878	1.41	0.037	SPO3878	1.16	0.387	SPO3877	1.1	0.975	SPO3882	1.02	0.008	SPO3872	1.18	0.109	SPO3872	1.22	0.066	SPO3873	0.93	0.31	SPO3868	0.88	0.506
SPO3879	0.79	0.868	SPO3879	0.93	0.486	SPO3878	1.42	0.193	SPO3883	1.13	0.319	SPO3873	0.99	0.929	SPO3873	0.88	0.570	SPO3874	0.85	0.290	SPO3869	1.02	0.900
SPO3880	1.36	0.493	SPO3880	1.34	0.348	SPO3879	1.22	0.594	SPO3884	1.44	0.394	SPO3874	1.45	0.013	SPO3874	0.48	0.067	SPO3875	0.91	0.290	SPO3870	1.11	0.441
SPO3881	0.92	0.762	SPO3881	0.87	0.573	SPO3880	1.24	0.532	SPO3885	1.09	0.975	SPO3875	1.03	0.571	SPO3875	1.16	0.096	SPO3876	0.95	0.413	SPO3871	1.07	0.922
SPO3882	0.78	0.013	SPO3882	0.87	0.173	SPO3881	1.05	0.358	SPO3886	1.08	0.076	SPO3876	1.20	0.370	SPO3876	1.22	0.293	SPO3877	1.13	0.526	SPO3872	0.88	0.263
SPO3883	1.65	0.21	SPO3883	1.68	0.177	SPO3882	1.16	0.004	SPO3887	1.1	0.012	SPO3877	1.39	0.314	SPO3877	1.16	0.089	SPO3878	1.00	0.938	SPO3873	0.97	0.754
SPO3884	1.31	0.106	SPO3884	1.27	0.155	SPO3883	1.21	0.494	SPO3888	1.27	0.124	SPO3878	1.14	0.431	SPO3878	1.14	0.549	SPO3879	0.78	0.135	SPO3874	0.74	0.327
SPO3885	1.29	0.559	SPO3885	1.15	0.514	SPO3884	1.22	0.335	SPO3889	1.07	0.34	SPO3879	0.57	0.003	SPO3879	0.60	0.198	SPO3880	1.10	0.713	SPO3875	0.92	0.065
SPO3886	1.13	0.724	SPO3886	1.15	0.568	SPO3885	1.29	0.933	SPO3890	1.15	0.978	SPO3880	0.86	0.350	SPO3880	0.90	0.518	SPO3881	0.99	0.520	SPO3876	0.97	0.726
SPO3887	1.29	0.029	SPO3887	1.11	0.084	SPO3886	1.09	0.437	SPO3891	1.01	0.564	SPO3881	0.64	0.121	SPO3881	0.73	0.042	SPO3882	0.76	0.039	SPO3877	1.15	0.163
SPO3888	0.71	0.006	SPO3888	0.88	0.113	SPO3887	1.12	0.011	SPO3892	1.47	0.159	SPO3882	0.45	0.004	SPO3882	0.35	0.001	SPO3883	1.11	0.514	SPO3878	1.03	0.969
SPO3889	1.14	0.446	SPO3889	1.15	0.429	SPO3888	1.08	0.293	SPO3893	1.13	0.082	SPO3883	0.73	0.373	SPO3883	0.69	0.239	SPO3884	1.11	0.893	SPO3879	0.85	0.688
SPO3890	1.07	0.668	SPO3890	1.07	0.077	SPO3889	1.03	0.444	SPO3894	1.06	0.272	SPO3884	0.87	0.514	SPO3884	0.88	0.624	SPO3885	1.03	0.936	SPO3880	1.05	0.859
SPO3891	1.37	0.137	SPO3891	1.2	0.237	SPO3890	1.01	0.552	SPO3895	1.35	0.793	SPO3885	1.26	0.589	SPO3885	1.45	0.530	SPO3886	1.02	0.940	SPO3881	0.99	0.725
SPO3892	1.17	0.184	SPO3892	1.23	0.042	SPO3891	1.38	0.594	SPO3896	1.1	0.536	SPO3886	0.67	0.451	SPO3886	0.63	0.044	SPO3887	1.01	0.837	SPO3882	0.88	0.208
SPO3893	0.99	0.737	SPO3893	0.73	0.263	SPO3892	1.16	0.011	SPO3897	1.22	0.183	SPO3887	0.98	0.48	SPO3887	0.98	0.48	SPO3888	1.00	0.121	SPO3889	1.06	0.219
SPO3894	1.44	0.042	SPO3894	1.29	0.084	SPO3893	1.05	0.206	SPO3898	1.01	0.167	SPO3888	1.05	0.011	SPO3888	1.03	0.005	SPO3889	0.99	0.814	SPO3884	1.08	0.298
SPO3895	1.27	0.158	SPO3895	1.28	0.132	SPO3894	1.03	0.415	SPO3899	1.14	0.419	SPO3889	0.79	0.081	SPO3889	0.74	0.087	SPO3890	1.07	0.821	SPO3885	1.04	0.914
SPO3896	0.92	0.55	SPO3896	0.88	0.513	SPO3895	1.04	0.908	SPO3900	1.22	0.27	SPO3890	1.27	0.176	SPO3890	1.36	0.102	SPO3891	1.16	0.198	SPO3886	1.00	0.827
SPO3897	0.76	0.475	SPO3897	0.78	0.54	SPO3896	1.03	0.79	SPO3901	1.22	0.869	SPO3891	0.74	0.034	SPO3891	0.71	0.077	SPO3892	0.84	0.346	SPO3887	1.03	0.220
SPO3898	0.9	0.896	SPO3898	1.08	0.324	SPO3897	1	0.559	SPO3902	1.33	0.224	SPO3892	0.79	0.290	SPO3892	0.76	0.294	SPO3893	1.03	0.929	SPO3888	1.01	0.205
SPO3899	0.68	0.28	SPO3899	0.83	0.75	SPO3898	1.3	0.062	SPO3903	1.12	0.676	SPO3893	1.36	0.311	SPO3893	1.42	0.024	SPO3894	0.86	0.260	SPO3889	0.87	0.433
SPO3900	0.98	0.684	SPO3900	0.93	0.915	SPO3899	1.11	0.257	SPO4001	1.12	0.459	SPO3894	1.87	0.077	SPO3894	1.80	0.003	SPO3895	0.92	0.702	SPO3890	1.06	0.819
SPO3901	0.98	0.007	SPO3901	0.93	0.183	SPO3900	1.07	0.17	SPO3902	1.12	0.19	SPO3895	0.52	0.043	SPO3895	0.58	0.029	SPO3900	0.92	0.673	SPO3889	1.06	0.270
SPO3902	0.69	0.007	SPO3902	0.78	0.139	SPO3901	1.16	0.94	SPO4003	1.12	0.212	SPO3896	1.06	0.200	SPO3896	1.11	0.349	SPO3897	1.21	0.356	SPO3892	0.88	0.461
SPO3903	1.79	0.003	SPO3903	1.67	0.011	SPO3902	1.25	0.242	SPO4004	1.08	0.034	SPO3897	1.74	0.196	SPO3897	1.71	0.167	SPO3898	1.15	0.584	SPO3893	1.01	0.689
SPO4001	0.94	0.934	SPO4001	0.95	0.984	SPO3903	1.03	0.047	SPO3906	1.06	0.015	SPO3898	0.92	0.516	SPO3898	1.00	0.970	SPO3899	1.09	0.625	SPO3894	0.86	0.088
SPO4002	1.42	0.147	SPO4002	1.3	0.067	SPO4001	1.25	0.555	SPO4006	1.16	0.065	SPO3899	1.96	0.013	SPO3899	2.05	0.027	SPO3900	1.04	0.720	SPO3895	0.96	0.842
SPO4003	0.81	0.43	SPO4003	0.77	0.097	SPO4002	3.98	0.165	SPO4007	1.16	0.107	SPO3900	1.03	0.784	SPO3900	1.17	0.346	SPO3901	0.97	0.988	SPO3896	0.97	0.927
SPO4004	0.98	0.84	SPO4004	1.03	0.486	SPO4003	2.95	0.341	SPO4008	1.09	0.795	SPO3901	0.66	0.842	SPO3901	0.46	0.623	SPO3902	0.94	0.773	SPO3897	1.28	0.574
SPO4005	1.11	0.662	SPO4005	1.14	0.042	SPO4004	1.24	0.017	SPO4009	1.22	0.219	SPO3902	1.09	0.083	SPO3902	1.02	0.378	SPO3903	1.10	0.703	SPO3898	1.06	0.797
SPO4006	0.98	0.97	SPO4006	0.94	0.869	SPO4005	1.16	0.011	SPO4010	1.15	0.039	SPO3903	0.92	0.15	SPO3903	0.92	0.15	SPO4001	0.92	0.679	SPO4001	1.06	0.710
SPO4007	1.51	0.016	SPO4007	1.47	0.003	SPO4006	1.18	0.162	SPO4011	1.16	0.018	SPO4001	0.90	0.752	SPO4001	0.92	0.417	SPO4002	1.10	0.579	SPO3900	1.14	0.917
SPO4008	0.72	0.281	SPO4008	0.78	0.322	SPO4007	1.11	0.099	SPO4012	1.25	0.102	SPO4002	0.69	0.219	SPO4002	0.75	0.042	SPO4003	1.03	0.907	SPO3901	0.99	0.937
SPO4009	1.18	0.014	SPO4009	1.2	0.018	SPO4008	1.22	0.847	SPO4013	1.17	0.609	SPO4003	0.53	0.070	SPO4003	0.53	0.002	SPO4004	0.92	0.674	SPO3902	0.93	0.239
SPO4010	1.17	0.37	SPO4010	1.11	0.109	SPO4009	1.25	0.162	SPO4014	1.05	0.128	SPO4004	0.37	0.009	SPO4004	0.37	0.002	SPO4005	1.21	0.674	SPO3903	1.09	0.771
SPO4011	1.13	0.046	SPO4011	1.21	0.046	SPO4010	1.14	0.158	SPO4015	1.2	0.843	SPO4005	0.38	0.002	SPO4005	0.38	0.001	SPO4006	1.04	0.723	SPO4001	0.91	0.327
SPO4012	1.29	0.086	SPO4012	1.27	0.183	SPO4011	1.46	0.032	SPO4017	3.97	0.966	SPO4006	0.65	0.125	SPO4006	0.64	0.142	SPO4007	0.93	0.503	SPO4002	0.95	0.749
SPO4013	0.81	0.29	SPO4013	0.83	0.079	SPO4012	2.95	0.369	SPO4018	2.95	0.447	SPO4007	0.80	0.171	SPO4007	0.75	0.080	SPO4008	0.98	0.948	SPO4003	0.97	0.813
SPO4014	1.09	0.749	SPO4014	0.88	0.524	SPO4013																	

SPOA0105	0.88	0.496	SPOA0106	0.83	0.887	SPOA0104	1.31	0.448	SPOA0109	1.14	0.157	SPOA0099	0.84	0.583	SPOA0099	0.74	0.257	SPOA0100	0.88	0.398	SPOA0095	1.09	0.901
SPOA0106	0.92	0.96	SPOA0107	1.05	0.872	SPOA0105	1.04	0.567	SPOA0110	0.98	0.967	SPOA0100	0.88	0.421	SPOA0100	0.74	0.050	SPOA0101	0.81	0.479	SPOA0096	0.91	0.640
SPOA0107	1.05	0.874	SPOA0108	1.09	0.864	SPOA0106	1.21	0.862	SPOA0111	1.01	0.968	SPOA0101	0.99	0.825	SPOA0101	1.02	0.790	SPOA0102	0.86	0.369	SPOA0097	0.88	0.927
SPOA0108	1.07	0.968	SPOA0109	1.07	0.872	SPOA0107	1.07	0.872	SPOA0112	1.01	0.968	SPOA0102	0.81	0.863	SPOA0103	0.81	0.863	SPOA0104	1.13	0.863	SPOA0105	0.81	0.694
SPOA0109	0.6	0.039	SPOA0110	0.67	0.922	SPOA0108	1.43	0.897	SPOA0113	1.1	0.983	SPOA0103	1.67	0.159	SPOA0103	1.63	0.195	SPOA0104	0.81	0.552	SPOA0099	0.84	0.413
SPOA0110	0.93	0.982	SPOA0111	0.93	0.922	SPOA0109	1.01	0.366	SPOA0114	1.03	0.321	SPOA0104	0.54	0.509	SPOA0104	0.96	0.324	SPOA0105	0.93	0.778	SPOA0106	0.76	0.454
SPOA0111	0.75	0.125	SPOA0112	0.81	0.781	SPOA0110	1.17	0.799	SPOA0115	1.06	0.506	SPOA0105	1.33	0.046	SPOA0105	1.07	0.598	SPOA0106	0.88	0.846	SPOA0101	0.90	0.235
SPOA0112	0.82	0.811	SPOA0113	0.81	0.801	SPOA0111	1.07	0.811	SPOA0116	1.11	0.287	SPOA0106	0.97	0.987	SPOA0106	1.33	0.751	SPOA0107	1.01	0.866	SPOA0102	0.85	0.419
SPOA0113	0.84	0.896	SPOA0114	0.76	0.212	SPOA0112	1.18	0.811	SPOA0117	1.18	0.524	SPOA0107	1.80	0.426	SPOA0107	1.68	0.427	SPOA0108	0.79	0.765	SPOA0103	1.30	0.479
SPOA0114	0.71	0.111	SPOA0115	0.8	0.172	SPOA0113	1.18	0.983	SPOA0118	1.06	0.947	SPOA0108	0.81	0.751	SPOA0108	0.85	0.786	SPOA0109	1.12	0.628	SPOA0104	0.61	0.525
SPOA0115	0.69	0.322	SPOA0116	0.76	0.037	SPOA0114	1.14	0.966	SPOA0119	1.19	0.985	SPOA0109	2.99	0.051	SPOA0109	2.97	0.044	SPOA0110	0.81	0.744	SPOA0105	0.93	0.771
SPOA0116	0.67	0.198	SPOA0117	0.67	0.198	SPOA0115	1.03	0.311	SPOA0120	1.12	0.366	SPOA0116	0.99	0.375	SPOA0116	0.99	0.375	SPOA0117	0.99	0.375	SPOA0111	0.99	0.375
SPOA0117	0.93	0.912	SPOA0118	0.83	0.901	SPOA0116	1.18	0.435	SPOA0121	1.28	0.879	SPOA0111	0.90	0.411	SPOA0111	0.88	0.422	SPOA0112	0.83	0.805	SPOA0107	0.94	0.922
SPOA0118	0.9	0.949	SPOA0119	0.86	0.694	SPOA0117	1.16	0.295	SPOA0122	1.37	0.532	SPOA0112	1.24	0.544	SPOA0112	0.96	0.709	SPOA0113	0.97	0.851	SPOA0108	0.84	0.833
SPOA0119	0.95	0.996	SPOA0120	0.76	0.026	SPOA0118	1.36	0.986	SPOA0123	1.24	0.954	SPOA0113	1.28	0.599	SPOA0113	1.05	0.932	SPOA0114	1.13	0.525	SPOA0109	1.21	0.272
SPOA0120	0.72	0.316	SPOA0121	0.98	0.783	SPOA0119	1.1	0.691	SPOA0124	1.28	0.868	SPOA0114	1.58	0.141	SPOA0114	1.25	0.204	SPOA0115	0.88	0.645	SPOA0110	0.78	0.688
SPOA0121	0.96	0.926	SPOA0122	0.88	0.368	SPOA0120	1.23	0.433	SPOA0125	1.11	0.788	SPOA0115	0.93	0.436	SPOA0115	0.85	0.543	SPOA0116	0.96	0.635	SPOA0111	0.76	0.343
SPOA0122	0.71	0.464	SPOA0123	0.88	0.883	SPOA0121	1.22	0.761	SPOA0126	1.44	0.99	SPOA0116	1.45	0.029	SPOA0116	1.60	0.032	SPOA0117	0.96	0.753	SPOA0112	0.96	0.874
SPOA0123	0.9	0.927	SPOA0124	0.81	0.643	SPOA0122	1.18	0.339	SPOA0127	1.04	0.867	SPOA0117	0.88	0.533	SPOA0117	0.86	0.669	SPOA0118	0.97	0.960	SPOA0113	0.95	0.861
SPOA0124	0.74	0.291	SPOA0125	0.88	0.315	SPOA0123	1.13	0.988	SPOA0128	1.11	0.489	SPOA0118	0.99	0.392	SPOA0118	1.01	1.000	SPOA0119	1.04	0.943	SPOA0114	1.14	0.437
SPOA0125	0.64	0.451	SPOA0126	0.93	0.989	SPOA0124	1.16	0.746	SPOA0129	1.03	0.679	SPOA0119	1.30	0.349	SPOA0119	1.36	0.381	SPOA0120	1.04	0.601	SPOA0115	1.01	0.992
SPOA0126	0.82	0.913	SPOA0127	1.02	0.837	SPOA0125	1.21	0.942	SPOA0130	1.15	0.964	SPOA0120	2.10	0.047	SPOA0120	2.08	0.017	SPOA0121	0.96	0.866	SPOA0116	1.06	0.384
SPOA0127	1.01	0.863	SPOA0128	0.48	0.581	SPOA0126	1.1	0.992	SPOA0131	1.31	0.395	SPOA0121	1.37	0.436	SPOA0121	1.31	0.231	SPOA0122	0.85	0.657	SPOA0117	0.88	0.163
SPOA0128	0.58	0.677	SPOA0129	0.84	0.478	SPOA0127	1.24	0.723	SPOA0132	1.09	0.721	SPOA0122	1.01	0.391	SPOA0122	1.01	0.954	SPOA0123	1.01	0.954	SPOA0118	0.96	0.960
SPOA0129	0.74	0.442	SPOA0130	0.94	0.977	SPOA0128	1.13	0.713	SPOA0133	1.13	0.631	SPOA0123	1.05	0.798	SPOA0123	1.08	0.759	SPOA0124	0.91	0.728	SPOA0119	0.98	0.780
SPOA0130	0.87	0.86	SPOA0131	0.88	0.846	SPOA0129	1.01	0.449	SPOA0134	1.27	0.022	SPOA0124	1.15	0.366	SPOA0124	1.06	0.434	SPOA0125	0.94	0.904	SPOA0120	1.04	0.487
SPOA0131	0.96	0.943	SPOA0132	0.81	0.271	SPOA0130	1.11	0.772	SPOA0135	1.1	0.889	SPOA0125	1.27	0.457	SPOA0125	1.26	0.316	SPOA0126	0.84	0.917	SPOA0121	1.03	0.942
SPOA0132	0.76	0.065	SPOA0133	0.81	0.316	SPOA0131	1.07	0.967	SPOA0136	1.13	0.957	SPOA0126	0.75	0.893	SPOA0126	0.69	0.870	SPOA0127	1.00	0.947	SPOA0122	0.85	1.182
SPOA0133	1.23	0.331	SPOA0134	0.93	0.435	SPOA0132	1.27	0.608	SPOA0137	1.07	0.715	SPOA0127	0.98	0.916	SPOA0127	1.01	0.596	SPOA0128	1.09	0.982	SPOA0123	1.09	0.895
SPOA0134	1.43	0.025	SPOA0135	0.93	0.693	SPOA0133	1.1	0.498	SPOA0138	1.22	0.942	SPOA0128	1.26	0.853	SPOA0128	1.42	0.737	SPOA0129	1.04	0.955	SPOA0124	0.93	0.724
SPOA0135	0.81	0.026	SPOA0136	1.02	0.676	SPOA0134	1.02	0.038	SPOA0140	1.11	0.585	SPOA0129	1.12	0.954	SPOA0129	1.04	0.876	SPOA0130	1.15	0.605	SPOA0125	0.97	0.960
SPOA0137	1.01	0.696	SPOA0138	1.35	0.124	SPOA0136	0.98	0.732	SPOA0141	1.1	0.017	SPOA0130	1.61	0.134	SPOA0130	1.46	0.210	SPOA0131	1.06	0.989	SPOA0126	0.93	0.964
SPOA0138	1.62	0.093	SPOA0139	1.3	0.779	SPOA0137	1.14	0.891	SPOA0142	1.21	0.671	SPOA0131	1.33	0.492	SPOA0131	1.52	0.257	SPOA0132	0.78	0.487	SPOA0127	0.93	0.781
SPOA0139	1.35	0.716	SPOA0140	1.36	0.134	SPOA0138	1.01	0.693	SPOA0143	1.19	0.356	SPOA0132	1.11	0.567	SPOA0132	1.12	0.452	SPOA0133	0.90	0.555	SPOA0128	1.17	0.898
SPOA0140	1.29	0.392	SPOA0141	1.32	0.034	SPOA0139	1.02	0.991	SPOA0144	0.96	0.134	SPOA0133	1.45	0.004	SPOA0133	1.42	0.004	SPOA0134	0.68	0.105	SPOA0129	0.91	0.799
SPOA0141	1.57	0.016	SPOA0142	1.18	0.23	SPOA0140	1.1	0.907	SPOA0145	1.06	0.179	SPOA0134	0.53	0.029	SPOA0134	0.45	0.003	SPOA0135	0.80	0.224	SPOA0130	0.97	0.687
SPOA0142	1.33	0.352	SPOA0143	0.95	0.902	SPOA0142	1.11	0.102	SPOA0147	0.99	0.967	SPOA0135	1.11	0.251	SPOA0137	0.83	0.875	SPOA0138	0.97	0.925	SPOA0132	0.85	0.527
SPOA0143	0.88	0.705	SPOA0144	0.71	0.108	SPOA0143	1.15	0.597	SPOA0148	1.12	0.972	SPOA0138	0.93	0.883	SPOA0138	0.98	0.466	SPOA0139	0.93	0.947	SPOA0133	0.99	0.827
SPOA0145	0.77	0.047	SPOA0146	0.93	0.976	SPOA0144	1.13	0.312	SPOA0149	1.03	0.293	SPOA0139	1.06	0.913	SPOA0139	1.06	0.903	SPOA0140	0.87	0.615	SPOA0134	0.64	0.026
SPOA0146	0.87	0.838	SPOA0147	0.97	0.905	SPOA0145	1.03	0.604	SPOA0150	0.98	0.142	SPOA0140	0.85	0.732	SPOA0140	0.78	0.375	SPOA0141	0.88	0.398	SPOA0136	0.85	0.701
SPOA0147	1.04	0.382	SPOA0148	0.89	0.840	SPOA0146	1.56	0.976	SPOA0151	1.24	0.176	SPOA0141	0.57	0.036	SPOA0141	0.54	0.015	SPOA0142	0.91	0.551	SPOA0137	0.89	0.573
SPOA0148	1.13	0.253	SPOA0149	1.34	0.137	SPOA0147	1.12	0.651	SPOA0152	1.0	0.056	SPOA0142	1.26	0.241	SPOA0142	1.21	0.156	SPOA0143	1.07	0.831	SPOA0138	1.02	0.728
SPOA0149	1.29	0.124	SPOA0150	1.21	0.11	SPOA0148	1.22	0.351	SPOA0154	0.98	0.878	SPOA0143	1.07	0.846	SPOA0143	1.14	0.614	SPOA0144	0.81	0.474	SPOA0139	0.91	0.928
SPOA0150	1.23	0.331	SPOA0151	1.19	0.165	SPOA0149	1.14	0.986	SPOA0155	1.05	0.106	SPOA0144	0.56	0.050	SPOA0144	0.53	0.016	SPOA0145	0.93	0.688	SPOA0140	0.84	0.522
SPOA0151	1.23	0.06	SPOA0152	0.97	0.037	SPOA0150	1.1	0.869	SPOA0156	1.13	0.949	SPOA0145	1.00	0.912	SPOA0145	0.92	0.239	SPOA0146	1.01	0.987	SPOA0141	0.85	1.149
SPOA0153	0.83	0.045	SPOA0155	1.87	0.042	SPOA0151	1.38	0.289	SPOA0157	1.07	0.952	SPOA0146	0.68	0.406	SPOA0146	0.70	0.394	SPOA0147	0.88	0.540	SPOA0142	0.83	0.352
SPOA0154	0.91	0.949	SPOA0156	0.85	0.705	SPOA0152	1.25	0.1	SPOA0158	1.18	0.942	SPOA0147	0.73	0.177	SPOA0147	0.76	0.050	SPOA0148	0.80	0.367	SPOA0143	1.00	0.961
SPOA0155	2.04	0.022	SPOA0157	0.99	0.979	SPOA0154	1.01	0.935	SPOA0159	1.11	0.895	SPOA0148	0.59	0.130	SPOA0148	0.55	0.094	SPOA0149	0.90	0.428	SPOA0144	0.77	0.189
SPOA0156	0.85	0.857	SPOA0158	0.77	0.183	SPOA0155	1.14	0.254	SPOA0160	1.68	0.319	SPOA0149	0.89	0.676	SPOA0149	0.92	0.348	SPOA0150	0.97	0.733	SPOA0145	1.02	0.931
SPOA0157	0.91	0.965	SPOA0159	1.12	0.715	SPOA0156	1.16	0.911	SPOA0161	1.1	0.909	SPOA0150	0.99	0.859	SPOA0150	0.94	0.219	SPOA0151	0.95	0.283	SPOA0146	0.96	0.930
SPOA0158	0.79	0.285	SPOA0160	1.21	0.393	SPOA0157	1.05	0.977	SPOA0162	1.32	0.892												

SPOA248	0.77	0.50	SPOA250	0.57	0.286	SPOA247	1.31	0.629	SPOA252	1.47	0.189	SPOA242	1.32	0.585	SPOA241	1.45	0.176	SPOA243	1.09	0.083	SPOA237	1.07	0.918
SPOA249	0.84	0.464	SPOA251	0.89	0.83	SPOA248	1.03	0.342	SPOA253	1.06	0.926	SPOA243	1.07	0.709	SPOA242	1.34	0.436	SPOA244	1.05	0.898	SPOA238	0.82	0.272
SPOA250	0.58	0.346	SPOA252	0.75	0.65	SPOA249	1.08	0.596	SPOA254	1.06	0.995	SPOA244	1.13	0.538	SPOA243	1.07	0.446	SPOA245	0.60	0.499	SPOA239	0.89	0.662
SPOA251	0.71	0.559	SPOA253	1.07	0.83	SPOA250	1.06	0.925	SPOA255	1.06	0.925	SPOA245	1.06	0.925	SPOA244	1.16	0.464	SPOA246	1.21	0.24	SPOA240	1.11	0.703
SPOA252	0.7	0.007	SPOA254	1.07	0.864	SPOA251	1.23	0.841	SPOA256	1.15	0.985	SPOA246	1.91	0.079	SPOA245	0.55	0.637	SPOA247	1.19	0.706	SPOA241	1.11	0.467
SPOA253	0.97	0.959	SPOA255	1.2	0.57	SPOA252	1.09	0.537	SPOA257	1.09	0.825	SPOA247	1.62	0.127	SPOA248	1.72	0.108	SPOA248	1.12	0.919	SPOA242	0.95	0.868
SPOA254	1.36	0.576	SPOA256	1.1	0.78	SPOA253	1.13	0.949	SPOA258	1.09	0.635	SPOA248	1.57	0.414	SPOA247	1.28	0.458	SPOA249	1.05	0.891	SPOA243	1.02	0.876
SPOA255	0.98	0.799	SPOA257	0.93	0.97	SPOA254	1.17	0.99	SPOA259	1.41	0.996	SPOA249	1.95	0.357	SPOA248	1.36	0.504	SPOA250	1.07	0.922	SPOA244	1.11	0.390
SPOA256	1.2	0.656	SPOA258	0.82	0.73	SPOA255	1.12	0.622	SPOA260	1.12	0.827	SPOA250	1.56	0.593	SPOA249	1.87	0.023	SPOA251	1.06	0.749	SPOA245	0.83	0.693
SPOA257	0.84	0.817	SPOA259	0.87	0.508	SPOA256	1.71	0.837	SPOA261	1.32	0.42	SPOA251	1.56	0.510	SPOA250	1.49	0.440	SPOA252	1.17	0.301	SPOA246	1.13	0.785
SPOA258	0.79	0.776	SPOA260	1.04	0.448	SPOA257	1.05	0.999	SPOA262	1.09	0.533	SPOA252	1.37	0.166	SPOA251	0.92	0.644	SPOA253	0.93	0.863	SPOA247	1.17	0.460
SPOA259	0.79	0.871	SPOA261	1.06	0.91	SPOA258	1.16	0.803	SPOA263	1.07	0.363	SPOA253	1.16	0.842	SPOA254	1.15	0.981	SPOA254	1.11	0.989	SPOA248	1.11	0.703
SPOA260	0.92	0.829	SPOA262	1.06	1.17	SPOA259	1.01	0.649	SPOA264	1.19	0.716	SPOA255	1.02	0.951	SPOA253	1.15	0.659	SPOA255	1.11	0.686	SPOA249	1.02	0.844
SPOA261	1.34	0.8	SPOA263	0.76	0.154	SPOA260	1.09	0.887	SPOA265	1.09	0.582	SPOA256	2.12	0.239	SPOA254	0.92	0.746	SPOA256	1.05	0.947	SPOA250	1.16	0.625
SPOA262	1.15	0.079	SPOA264	0.63	0.75	SPOA261	1.15	0.408	SPOA266	1.09	0.585	SPOA256	1.53	0.355	SPOA255	1.87	0.113	SPOA257	0.87	0.658	SPOA251	0.99	0.790
SPOA263	0.85	0.263	SPOA265	0.56	0.514	SPOA262	1.05	0.664	SPOA267	1.06	0.247	SPOA257	1.34	0.737	SPOA256	1.64	0.380	SPOA258	0.93	0.910	SPOA252	1.12	0.959
SPOA264	0.64	0.695	SPOA266	0.55	0.52	SPOA263	1.07	0.022	SPOA268	1.02	0.827	SPOA258	1.17	0.686	SPOA257	1.25	0.772	SPOA259	0.96	0.857	SPOA253	1.06	0.991
SPOA265	0.61	0.53	SPOA267	0.74	0.454	SPOA264	1.07	0.865	SPOA269	1.15	0.985	SPOA259	1.39	0.190	SPOA258	1.07	0.950	SPOA260	1.07	0.906	SPOA254	0.94	0.916
SPOA266	0.7	0.032	SPOA268	0.65	0.971	SPOA265	1.15	0.653	SPOA270	1.96	0.771	SPOA260	1.62	0.029	SPOA259	1.29	0.209	SPOA261	0.87	0.808	SPOA255	1.07	0.809
SPOA267	0.59	0.184	SPOA269	0.8	0.859	SPOA266	1.12	0.222	SPOA271	1.04	0.952	SPOA261	0.70	0.578	SPOA260	1.62	0.099	SPOA262	0.72	0.457	SPOA256	0.98	0.944
SPOA268	0.74	0.531	SPOA270	1.01	0.957	SPOA267	1.12	0.293	SPOA272	1.08	0.974	SPOA262	0.85	0.292	SPOA263	0.65	0.525	SPOA263	1.14	0.149	SPOA257	0.93	0.886
SPOA269	0.85	0.77	SPOA271	0.98	0.869	SPOA268	1.14	0.93	SPOA273	1.09	0.006	SPOA263	1.64	0.148	SPOA262	1.02	0.325	SPOA264	0.95	0.957	SPOA258	1.05	0.97
SPOA270	0.87	0.836	SPOA272	0.5	0.875	SPOA269	1.75	0.967	SPOA274	1.56	0.864	SPOA264	2.35	0.352	SPOA263	1.24	0.035	SPOA265	1.00	0.995	SPOA259	0.94	0.747
SPOA271	0.85	0.795	SPOA273	0.84	0.028	SPOA270	1	0.92	SPOA275	1.26	0.856	SPOA265	1.67	0.409	SPOA264	1.75	0.529	SPOA266	1.05	0.951	SPOA260	0.96	0.834
SPOA272	0.93	0.865	SPOA274	1.02	0.817	SPOA271	1.06	0.564	SPOA276	1.19	0.405	SPOA266	2.25	0.191	SPOA265	1.70	0.422	SPOA267	1.39	0.243	SPOA261	0.85	0.803
SPOA273	0.66	0.009	SPOA275	0.88	0.822	SPOA272	1.01	0.916	SPOA277	1.14	0.856	SPOA267	2.28	0.078	SPOA266	1.51	0.104	SPOA268	0.85	0.667	SPOA262	0.97	0.771
SPOA274	0.86	0.887	SPOA276	1.02	0.763	SPOA273	1.45	0.008	SPOA278	1.02	0.814	SPOA268	0.78	0.442	SPOA267	1.99	0.146	SPOA269	0.98	0.959	SPOA263	1.05	0.637
SPOA275	0.96	0.466	SPOA277	1.07	0.841	SPOA274	1.29	0.957	SPOA279	1.01	0.077	SPOA269	0.96	0.478	SPOA268	0.74	0.460	SPOA270	0.89	0.795	SPOA264	1.04	0.982
SPOA276	1.1	0.728	SPOA278	1.12	0.623	SPOA275	1.07	0.733	SPOA280	1.13	0.744	SPOA270	0.78	0.663	SPOA271	0.99	0.813	SPOA272	0.99	0.814	SPOA265	1.02	0.976
SPOA277	1.01	0.811	SPOA279	0.54	0.053	SPOA276	1.38	0.322	SPOA281	1.14	0.199	SPOA271	1.13	0.892	SPOA270	0.63	0.397	SPOA273	0.99	0.984	SPOA266	1.27	0.213
SPOA278	1.13	0.78	SPOA280	0.66	0.192	SPOA277	1.08	0.849	SPOA282	1.19	0.309	SPOA272	0.70	0.645	SPOA271	0.96	0.205	SPOA274	0.75	0.038	SPOA267	1.21	0.570
SPOA279	0.61	0.192	SPOA281	1.38	0.082	SPOA278	1.37	0.233	SPOA283	1.72	0.118	SPOA273	3.15	0.000	SPOA272	0.68	0.629	SPOA274	1.01	0.985	SPOA268	0.93	0.744
SPOA280	0.65	0.225	SPOA282	1.23	0.203	SPOA279	1.05	0.01	SPOA284	1.09	0.613	SPOA274	1.11	0.866	SPOA273	3.00	0.000	SPOA275	1.02	0.950	SPOA269	0.93	0.868
SPOA281	1.48	0.047	SPOA283	1.14	0.307	SPOA280	1.13	0.68	SPOA285	1.28	0.382	SPOA275	1.11	0.831	SPOA274	0.93	0.610	SPOA276	0.77	0.123	SPOA270	0.91	0.209
SPOA282	1.41	0.188	SPOA284	1.27	0.578	SPOA281	0.99	0.232	SPOA286	0.99	0.379	SPOA276	1.78	0.554	SPOA275	1.14	0.765	SPOA277	0.99	0.874	SPOA271	0.95	0.767
SPOA283	0.95	0.028	SPOA285	0.92	0.44	SPOA282	1.03	0.247	SPOA288	1.16	0.96	SPOA277	1.13	0.354	SPOA276	0.75	0.457	SPOA278	0.97	0.916	SPOA272	0.91	0.891
SPOA284	1.39	0.338	SPOA286	0.87	0.807	SPOA283	1.20	0.772	SPOA289	1.14	0.867	SPOA278	1.41	0.281	SPOA277	1.01	0.377	SPOA279	1.09	0.929	SPOA273	1.09	0.325
SPOA285	0.89	0.646	SPOA288	0.5	0.98	SPOA284	1.02	0.774	SPOA290	1.13	0.92	SPOA279	1.48	0.099	SPOA278	1.04	0.937	SPOA280	1.05	0.903	SPOA274	0.96	0.890
SPOA286	0.52	0.012	SPOA289	0.74	0.405	SPOA285	1.07	0.297	SPOA291	1.06	0.364	SPOA280	1.41	0.187	SPOA279	1.41	0.157	SPOA281	0.93	0.433	SPOA275	1.10	0.658
SPOA287	1.03	0.686	SPOA290	1.01	0.981	SPOA286	1.17	0.141	SPOA292	1.02	0.159	SPOA281	0.85	0.318	SPOA280	1.40	0.125	SPOA282	0.68	0.498	SPOA276	0.77	0.183
SPOA288	0.86	0.934	SPOA291	0.91	0.503	SPOA287	1.09	0	SPOA293	1.12	0.168	SPOA282	0.60	0.127	SPOA281	0.90	0.259	SPOA283	0.65	0.049	SPOA277	0.91	0.778
SPOA289	0.77	0.49	SPOA292	1.3	0.001	SPOA288	1.03	0.926	SPOA294	1.03	0.826	SPOA283	0.73	0.017	SPOA282	0.68	0.017	SPOA284	0.90	0.749	SPOA278	0.94	0.894
SPOA290	1.15	0.856	SPOA293	1.2	0.216	SPOA289	1.17	0.222	SPOA295	1.25	0.86	SPOA284	0.76	0.557	SPOA283	0.72	0.041	SPOA285	0.88	0.394	SPOA279	0.92	0.550
SPOA291	0.82	0.562	SPOA294	1.02	0.518	SPOA290	1.15	0.889	SPOA296	1.39	0.705	SPOA285	0.81	0.129	SPOA284	0.74	0.506	SPOA286	1.09	0.316	SPOA280	1.02	0.949
SPOA292	1.29	0.338	SPOA295	0.98	0.965	SPOA291	1.02	0.698	SPOA297	1.01	0.111	SPOA286	0.95	0.364	SPOA285	0.93	0.016	SPOA287	0.83	0.532	SPOA281	0.92	0.938
SPOA293	1.16	0.055	SPOA296	0.68	0.643	SPOA292	1.29	0.184	SPOA298	1.08	0.242	SPOA287	0.78	0.835	SPOA286	1.00	0.503	SPOA288	0.85	0.864	SPOA282	0.78	0.019
SPOA294	0.99	0.933	SPOA297	0.71	0.102	SPOA293	1.39	0.378	SPOA299	1.18	0.088	SPOA288	3.00	0.176	SPOA287	0.79	0.148	SPOA289	1.04	0.979	SPOA283	0.77	0.033
SPOA295	0.88	0.931	SPOA298	0.66	0.453	SPOA294	1	0.482	SPOA300	1.04	0.814	SPOA289	0.67	0.832	SPOA288	0.60	0.763	SPOA290	0.95	0.979	SPOA284	0.83	0.640
SPOA296	0.72	0.457	SPOA299	0.67	0.508	SPOA295	1.24	0.787	SPOA301	1.16	0.043	SPOA290	0.77	0.078	SPOA289	4.58	0.258	SPOA291	0.86	0.151	SPOA285	0.92	1.033
SPOA297	0.61	0.268	SPOA300	0.57	0.251	SPOA296	1.16	0.538	SPOA302	1.05	0.069	SPOA292	1.12	0.090	SPOA290	0.63	0.808	SPOA292	1.06	0.314	SPOA286	1.04	0.333
SPOA298	0.59	0.254	SPOA301	1.08	0.626	SPOA297	1.06	0.076	SPOA303	1.24	0.189	SPOA293	1.40	0.009	SPOA291	0.74	0.067	SPOA293	1.01	0.887	SPOA287	0.73	0.126
SPOA299	0.6	0.061	SPOA302	0.91	0.732	SPOA298	1.12	0.615	SPOA304	1.08	0.317	SPOA294	1.33	0.054	SPOA292	1.11	0.007	SPOA294	1.05	0.540	SPOA288	0.83	0.862
SPOA300	0.59	0.256	SPOA303	1.3	0.294	SPOA299	1.06																

SPOA0389	1.15	0.396	SPOA0393	4.83	0.011	SPOA0388	1.13	0.52	SPOA0395	1.52	0.006	SPOA0384	0.80	0.683	SPOA0382	0.76	0.675	SPOA0385	0.87	0.899	SPOA0379	0.87	0.488
SPOA0390	0.85	0.224	SPOA0394	2.32	0.026	SPOA0389	1.21	0.122	SPOA0396	1.2	0.004	SPOA0385	1.10	0.952	SPOA0383	0.98	0.968	SPOA0386	0.91	0.847	SPOA0380	0.98	0.949
SPOA0391	0.95	0.932	SPOA0395	3.5	0.036	SPOA0390	1.02	0.961	SPOA0397	1.25	0.08	SPOA0386	0.93	0.841	SPOA0384	0.76	0.718	SPOA0387	0.98	0.935	SPOA0381	1.05	0.731
SPOA0392	7.48	0.001	SPOA0396	5.76	0.008	SPOA0391	1.11	0.789	SPOA0398	1.26	0.003	SPOA0387	1.59	0.379	SPOA0385	1.09	0.965	SPOA0388	0.54	0.165	SPOA0382	0.88	0.822
SPOA0393	4	0.026	SPOA0397	4.06	0.041	SPOA0392	1.42	0.002	SPOA0399	1.19	0	SPOA0388	0.62	0.489	SPOA0386	0.87	0.705	SPOA0389	0.99	0.948	SPOA0383	0.98	0.951
SPOA0394	1.87	0.041	SPOA0398	5.03	0.003	SPOA0393	1.07	0.042	SPOA0400	1.11	0.264	SPOA0389	0.58	0.016	SPOA0387	1.49	0.367	SPOA0390	0.92	0.745	SPOA0384	0.90	0.853
SPOA0395	2.53	0.077	SPOA0399	8.53	0.001	SPOA0394	1.28	0.089	SPOA0401	1.41	0.955	SPOA0390	1.05	0.626	SPOA0388	0.49	0.534	SPOA0391	0.78	0.718	SPOA0385	1.04	0.978
SPOA0396	5.69	0.007	SPOA0400	0.99	0.712	SPOA0395	1.02	0.06	SPOA0402	1.13	0.793	SPOA0391	0.66	0.498	SPOA0389	0.64	0.005	SPOA0392	0.10	0.007	SPOA0386	0.92	0.877
SPOA0397	5.21	0.049	SPOA0401	0.85	0.776	SPOA0396	1.25	0.004	SPOA0403	1.21	0.954	SPOA0392	0.56	0.012	SPOA0390	0.99	0.886	SPOA0393	0.11	0.023	SPOA0387	1.03	0.968
SPOA0398	6.09	0.007	SPOA0402	0.85	0.717	SPOA0397	1.08	0.062	SPOA0404	1.15	0.53	SPOA0393	0.48	0.172	SPOA0391	0.81	0.69	SPOA0394	0.81	0.286	SPOA0388	0.62	0.471
SPOA0399	0.006	SPOA0403	0.99	0.911	SPOA0398	1.07	0	SPOA0405	1.25	0.992	SPOA0394	0.85	0.547	SPOA0392	0.63	0.012	SPOA0395	0.12	0.031	SPOA0389	0.99	0.950	
SPOA0400	1.05	0.291	SPOA0404	8.5	0.023	SPOA0399	1.28	0.002	SPOA0406	1.04	0.863	SPOA0395	0.89	0.292	SPOA0393	0.54	0.110	SPOA0396	0.10	0.008	SPOA0398	0.99	0.983
SPOA0401	0.79	0.066	SPOA0405	0.95	0.989	SPOA0400	1.21	0.47	SPOA0407	1.1	0.861	SPOA0396	0.63	0.221	SPOA0394	0.71	0.122	SPOA0397	0.14	0.057	SPOA0391	0.79	0.736
SPOA0402	0.83	0.661	SPOA0406	0.82	0.076	SPOA0401	1.13	0.921	SPOA0408	1.08	0.876	SPOA0397	0.83	0.236	SPOA0395	0.65	0.377	SPOA0398	0.06	0.001	SPOA0392	0.13	0.005
SPOA0403	0.88	0.926	SPOA0407	0.97	0.943	SPOA0402	1.2	0.773	SPOA0409	1.18	0.712	SPOA0398	0.38	0.032	SPOA0396	0.78	0.072	SPOA0399	0.06	0.002	SPOA0389	0.15	0.007
SPOA0404	0.73	0.02	SPOA0408	1	0.319	SPOA0403	1.12	0.906	SPOA0410	1.07	0.033	SPOA0399	0.37	0.007	SPOA0397	1.51	0.648	SPOA0400	0.84	0.195	SPOA0394	0.85	0.262
SPOA0405	1.01	0.979	SPOA0409	1.02	0.838	SPOA0404	1.01	0.96	SPOA0411	1.05	0.058	SPOA0400	0.97	0.982	SPOA0398	0.42	0.026	SPOA0401	1.00	0.970	SPOA0395	0.12	0.014
SPOA0406	0.88	0.597	SPOA0410	0.46	0.023	SPOA0405	1.05	0.982	SPOA0412	1.19	0.808	SPOA0401	1.17	0.343	SPOA0399	0.33	0.000	SPOA0402	0.90	0.680	SPOA0396	0.09	0.003
SPOA0407	0.93	0.089	SPOA0411	0.68	0.019	SPOA0406	1.15	0.6	SPOA0413	1.41	0.876	SPOA0402	1.35	0.488	SPOA0409	1.07	0.506	SPOA0409	0.83	0.797	SPOA0397	0.22	0.055
SPOA0408	1.02	0.597	SPOA0412	0.71	0.261	SPOA0407	1.04	0.7	SPOA0414	1.15	0.464	SPOA0403	1.02	0.362	SPOA0401	1.22	0.583	SPOA0404	0.85	0.140	SPOA0398	0.09	0.001
SPOA0409	1.01	0.816	SPOA0413	0.67	0.389	SPOA0408	1.09	0.994	SPOA0415	1.08	0.987	SPOA0404	1.30	0.098	SPOA0402	1.18	0.502	SPOA0405	0.85	0.905	SPOA0399	0.06	0.000
SPOA0410	0.38	0.003	SPOA0414	1.08	0.697	SPOA0409	1.21	0.692	SPOA0416	7.11	0.199	SPOA0405	0.69	0.840	SPOA0403	0.96	0.915	SPOA0406	0.93	0.756	SPOA0400	0.87	0.242
SPOA0411	0.41	0.046	SPOA0415	1.08	0.854	SPOA0410	1.23	0.008	SPOA0417	5.97	0.269	SPOA0406	1.30	0.502	SPOA0404	1.11	0.252	SPOA0407	0.81	0.546	SPOA0401	0.99	0.717
SPOA0412	0.77	0.151	SPOA0416	1.09	0.188	SPOA0411	1.13	0.024	SPOA0418	2.34	0.325	SPOA0407	0.88	0.479	SPOA0405	0.75	0.881	SPOA0408	0.80	0.680	SPOA0402	0.91	0.768
SPOA0413	0.74	0.341	SPOA0417	1.2	0.376	SPOA0412	1	0.537	SPOA0419	5.79	0.506	SPOA0408	1.04	0.967	SPOA0406	1.31	0.010	SPOA0409	0.87	0.461	SPOA0403	0.92	0.942
SPOA0414	1.12	0.58	SPOA0418	1.05	0.648	SPOA0413	1.09	0.958	SPOA0420	10.2	0.346	SPOA0409	0.90	0.764	SPOA0407	0.85	0.625	SPOA0410	0.99	0.624	SPOA0404	0.94	0.335
SPOA0415	1.27	0.374	SPOA0419	0.78	0.092	SPOA0414	8	0.55	SPOA0421	4.08	0.871	SPOA0410	2.79	0.009	SPOA0408	1.20	0.490	SPOA0411	3.99	0.044	SPOA0405	0.84	0.862
SPOA0416	0.97	0.843	SPOA0420	0.85	0.36	SPOA0415	8.04	0.94	SPOA0422	11.3	0.245	SPOA0411	1.51	0.076	SPOA0409	0.83	0.522	SPOA0412	0.98	0.911	SPOA0406	0.93	0.796
SPOA0417	1.3	0.222	SPOA0421	0.74	0.389	SPOA0416	1.84	0.407	SPOA0423	16.8	0.401	SPOA0412	2.06	0.039	SPOA0410	1.49	0.305	SPOA0413	0.83	0.488	SPOA0407	0.91	0.703
SPOA0418	1.07	0.643	SPOA0422	0.69	0.116	SPOA0417	1.43	0.095	SPOA0424	1.13	0.818	SPOA0413	1.45	0.414	SPOA0411	1.32	0.026	SPOA0414	0.88	0.703	SPOA0408	1.06	0.922
SPOA0419	0.68	0.107	SPOA0423	0.88	0.049	SPOA0418	7.13	0.252	SPOA0425	1.03	0.676	SPOA0414	1.26	0.255	SPOA0412	2.09	0.003	SPOA0415	1.12	0.729	SPOA0409	0.94	0.703
SPOA0420	0.81	0.163	SPOA0424	0.78	0.282	SPOA0419	5.39	0.035	SPOA0426	1.11	0.715	SPOA0415	1.39	0.366	SPOA0413	1.49	0.428	SPOA0416	0.91	0.285	SPOA0410	1.10	0.143
SPOA0421	0.65	0.372	SPOA0425	0.85	0.793	SPOA0420	1.15	0.23	SPOA0427	1.25	0.219	SPOA0416	1.27	0.087	SPOA0414	1.17	0.423	SPOA0417	0.90	0.400	SPOA0411	3.12	0.051
SPOA0422	0.64	0.009	SPOA0426	1.37	0.011	SPOA0421	16.5	0.407	SPOA0428	1.02	0.95	SPOA0417	0.90	0.482	SPOA0415	1.56	0.333	SPOA0418	1.09	0.723	SPOA0412	1.08	0.643
SPOA0423	0.83	0.129	SPOA0427	1.08	0.37	SPOA0422	1.06	0.413	SPOA0429	1.08	0.407	SPOA0418	1.45	0.220	SPOA0416	1.23	0.142	SPOA0419	1.14	0.285	SPOA0413	0.85	0.653
SPOA0424	0.74	0.347	SPOA0428	0.68	0.306	SPOA0423	1.01	0.158	SPOA0430	1.2	0.076	SPOA0419	1.02	0.979	SPOA0417	0.94	0.591	SPOA0420	0.85	0.068	SPOA0414	0.84	0.443
SPOA0425	0.96	0.907	SPOA0429	1.17	0.292	SPOA0424	1.02	0.683	SPOA0431	1.12	0.005	SPOA0420	0.64	0.039	SPOA0419	1.49	0.217	SPOA0421	0.81	0.422	SPOA0415	0.97	0.983
SPOA0426	1.32	0.085	SPOA0430	0.76	0.024	SPOA0425	1.04	0.78	SPOA0432	1.18	0.253	SPOA0421	1.20	0.606	SPOA0419	1.08	0.686	SPOA0422	0.86	0.343	SPOA0416	0.96	0.564
SPOA0427	1.13	0.695	SPOA0431	1.94	0.003	SPOA0426	1.07	0.091	SPOA0433	1.07	0.657	SPOA0422	1.30	0.482	SPOA0420	0.63	0.020	SPOA0423	0.81	0.124	SPOA0417	0.98	0.874
SPOA0428	0.63	0.999	SPOA0432	1.38	0.21	SPOA0427	1.04	0.699	SPOA0434	1.2	0.587	SPOA0423	0.75	0.065	SPOA0421	1.03	0.887	SPOA0424	1.10	0.830	SPOA0418	1.05	0.855
SPOA0429	1.53	0	SPOA0433	0.78	0.547	SPOA0428	1.21	0.673	SPOA0435	1.02	0.093	SPOA0424	0.93	0.373	SPOA0422	1.45	0.018	SPOA0425	0.70	0.143	SPOA0419	1.04	0.899
SPOA0430	0.71	0.962	SPOA0434	1.09	0.521	SPOA0429	1.1	0	SPOA0436	1.16	0.918	SPOA0425	0.65	0.191	SPOA0423	0.85	0.312	SPOA0426	1.02	0.992	SPOA0420	0.83	0.055
SPOA0431	2.28	0.018	SPOA0435	0.9	0.691	SPOA0430	1.13	0.894	SPOA0437	1.13	0.889	SPOA0426	1.07	0.727	SPOA0424	1.05	0.854	SPOA0427	1.00	0.653	SPOA0421	0.88	0.706
SPOA0432	1.39	0.092	SPOA0436	0.83	0.618	SPOA0431	1.19	0.011	SPOA0438	1.93	0.486	SPOA0427	0.78	0.171	SPOA0425	0.63	0.191	SPOA0428	0.87	0.180	SPOA0422	1.00	0.872
SPOA0433	0.7	0.283	SPOA0437	0.83	0.089	SPOA0432	1.23	0.411	SPOA0439	1.09	0.824	SPOA0428	1.04	0.521	SPOA0426	1.06	0.801	SPOA0430	0.88	0.038	SPOA0423	0.83	0.513
SPOA0434	1.1	0.437	SPOA0438	0.88	0.3	SPOA0433	1.18	0.605	SPOA0440	1.13	0.713	SPOA0429	1.01	0.440	SPOA0427	0.76	0.082	SPOA0431	0.77	0.007	SPOA0424	1.02	0.980
SPOA0435	0.92	0.851	SPOA0439	1.09	0.305	SPOA0434	1.1	0.518	SPOA0441	1.12	0.857	SPOA0430	0.90	0.557	SPOA0428	0.99	0.822	SPOA0432	1.08	0.077	SPOA0425	0.69	0.184
SPOA0436	0.68	0.16	SPOA0440	1.1	0.16	SPOA0435	1.1	0.482	SPOA0442	1.07	0.109	SPOA0431	0.51	0.029	SPOA0429	0.99	0	SPOA0433	1.04	0.785	SPOA0426	1.00	0.965
SPOA0437	0.79	0.136	SPOA0441	0.77	0.904	SPOA0436	1.16	0.919	SPOA0443	0.97	0.902	SPOA0432	0.91	0.902	SPOA0430	0.93	0.700	SPOA0434	1.00	0.709	SPOA0427	0.98	0.983
SPOA0438	1.01	0.853	SPOA0442	0.52	0.035	SPOA0437	1.11	0.881	SPOA0444	1.08	0.495	SPOA0433	0.94	0.783	SPOA0431	0.53	0.001	SPOA0435	1.03	0.919	SPOA0428	0.88	0.474
SPOA0439	1.16	0.139	SPOA0443	0.75	0.049	SPOA0438	2.07	0.267	SPOA0445	1.06	0.011	SPOA0434	0.81	0.063	SPOA0432	0.99	0.57						

Chapter 10 - Bibliography

- Abdul-Tehrani, H., Hudson, A. J., Chang, Y. S., Timms, A. R., Hawkins, C., Williams, J. M., *et al.* (1999). "Ferritin mutants of *Escherichia coli* are iron deficient and growth impaired, and *fur* mutants are iron deficient." *J Bacteriol* **181**: 1415-28.
- Adhikari, P., Berish, S. A., Nowalk, A. J., Veraldi, K. L., Morse, S. A. and Mietzner, T. A. (1996). "The *fbpABC* locus of *Neisseria gonorrhoeae* functions in the periplasm-to-cytosol transport of iron." *J Bacteriol* **178**: 2145-9.
- Agar, J. N., Yuvaniyama, P., Jack, R. F., Cash, V. L., Smith, A. D., Dean, D. R., *et al.* (2000). "Modular organization and identification of a mononuclear iron-binding site within the NifU protein." *J Biol Inorg Chem* **5**: 167-77.
- Ahn, B. E., Cha, J., Lee, E. J., Han, A. R., Thompson, C. J. and Roe, J. H. (2006). "Nur, a nickel-responsive regulator of the *fur* family, regulates superoxide dismutases and nickel transport in *Streptomyces coelicolor*." *Mol Microbiol* **59**: 1848-58.
- Alahari, A., Tripathi, A. K. and Le Rudulier, D. (2006). "Cloning and characterization of a *fur* homologue from *Azospirillum brasilense* sp7." *Curr Microbiol* **52**: 123-7.
- Alavi, M., Miller, T., Erlandson, K., Schneider, R. and Belas, R. (2001). "Bacterial community associated with *Pfiesteria*-like dinoflagellate cultures." *Environ Microbiol* **3**: 380-96.
- Allredge, A. L. and Silver, M. W. (1988). "Characteristics, dynamics and significance of marine snow." *Progress In Oceanography* **20**: 41-82.
- Allredge, A. L., Cole, J. J. and Caron, D. A. (1986). "Production of heterotrophic bacteria inhabiting macroscopic organic aggregates (marine snow) from surface waters." *Limnology and oceanography* **31**: 68-78.
- Altschul, S. F., Madden, T. L., Schaffer, A. A., Zhang, J., Zhang, Z., Miller, W., *et al.* (1997). "Gapped blast and psi-blast: A new generation of protein database search programs." *Nucleic Acids Res* **25**: 3389-402.
- Amin, S. A., D. H. Green, *et al.* (2009). "Photolysis of iron-siderophore chelates promotes bacterial-algal mutualism." *Proc Natl Acad Sci U S A* **106**(40): 17071-17076.
- Anderson, E. S., Paulley, J. T., Martinson, D. A., Gaines, J. M., Steele, K. H. and Roop, R. M., 2nd (2011). "The iron-responsive regulator *irr* is required for wild-type expression of the gene encoding the haem transporter *bhuA* in *Brucella abortus* 2308." *J Bacteriol* **193**: 5359-64.
- Andrews, S. C. (1998). "Iron storage in bacteria." *Adv Microb Physiol* **40**: 281-351.
- Andrews, S. C., Robinson, A. K. and Rodriguez-Quinones, F. (2003). "Bacterial iron homeostasis." *FEMS Microbiol Rev* **27**: 215-37.
- Archer, D. E. and Johnson, K. (2000). "A model of the iron cycle in the ocean." *Global Biogeochem. Cycles* **14**: 269-279.
- Archibald, F. (1983). "*Lactobacillus plantarum*, an organism not requiring iron." *FEMS Microbiol Lett* **19**: 29-32.
- Archibald, F. (1986). "Manganese: Its acquisition by and function in the lactic acid bacteria." *Crit Rev Microbiol* **13**: 63-109.
- Aristegui, Javier, Gasol, Josep, M., Duarte, Carlos, M., *et al.* (2009). "Microbial oceanography of the dark ocean's pelagic realm." Waco, TX, ETATS-UNIS, American Society of Limnology and Oceanography.
- Armstrong, J. E. and Van Baalen, C. (1979). "Iron transport in microalgae: The isolation and biological activity of a hydroxamate siderophore from the blue-green alga *Agmenellum quadruplicatum*." *J Gen Microbiol* **111**: 253-262.
- Arosio, P., Ingrassia, R. and Cavadini, P. (2009). "Ferritins: A family of molecules for iron storage, antioxidation and more." *Biochimica et Biophysica Acta (BBA) - General Subjects* **1790**: 589-599.
- Ayala-Castro, C., Saini, A. and Outten, F. W. (2008). "Fe-S cluster assembly pathways in bacteria." *Microbiol Mol Biol Rev* **72**: 110-25, table of contents.
- Azam, F. and Malfatti, F. (2007). "Microbial structuring of marine ecosystems." *Nat Rev Micro* **5**: 782-791.
- Bagos, P. G., Liakopoulos, T. D., Spyropoulos, I. C. and Hamodrakas, S. J. (2004). "Pred-tmbb: A web server for predicting the topology of beta-barrel outer membrane proteins." *Nucleic Acids Res* **32**: W400-4.
- Bailey, T. L. and Elkan, C. (1994). "Fitting a mixture model by expectation maximization to discover motifs in biopolymers." *Proc Int Conf Intell Syst Mol Biol* **2**: 28-36.

- Bandyopadhyay, S., Chandramouli, K. and Johnson, M. K. (2008). "Iron-sulfur cluster biosynthesis." *Biochem Soc Trans* **36**: 1112-9.
- Baumann, P. and Baumann, L. (1981). The marine gram-negative eubacteria: Genera *Photobacterium*, *Bennekea*, *Alteromonas*, *Pseudomonas*, and *Alcaligenes* in the prokaryotes. H. S. M. P. Starr, H. G. Trüper, A. Balows & H. G. Schlegel., Berlin: Springer-Verlag.: 1302–1331.
- Beier, C. L., Horn, M., Michel, R., Schweikert, M., Gortz, H. D. and Wagner, M. (2002). "The genus *Caedibacter* comprises endosymbionts of *Paramecium* spp. Related to the *Rickettsiales* (alphaproteobacteria) and to *Francisella tularensis* (gamma-proteobacteria)." *Appl Environ Microbiol* **68**: 6043-50.
- Beinert, H. (2000). "Iron-sulfur proteins: Ancient structures, still full of surprises." *J Biol Inorg Chem* **5**: 2-15.
- Beinert, H., Holm, R. H. and Munck, E. (1997). "Iron-sulfur clusters: Nature's modular, multipurpose structures." *Science* **277**: 653-9.
- Bendtsen, J. D., Nielsen, H., Widdick, D., Palmer, T. and Brunak, S. (2005). "Prediction of twin-arginine signal peptides." *BMC Bioinformatics* **6**: 167.
- Beringer, J. E. and Hopwood, D. A. (1976). "Chromosomal recombination and mapping in *Rhizobium leguminosarum*." *Nature* **264**: 291-3.
- Berish, S. A., Mietzner, T. A., Mayer, L. W., Genco, C. A., Holloway, B. P. and Morse, S. A. (1990). "Molecular cloning and characterization of the structural gene for the major iron-regulated protein expressed by *Neisseria gonorrhoeae*." *J Exp Med* **171**: 1535-46.
- Biebl, H., Allgaier, M., Tindall, B. J., Koblizek, M., Lunsdorf, H., Pukall, R., et al. (2005). "*Dinoroseobacter shibae* gen. Nov., sp. Nov., a new aerobic phototrophic bacterium isolated from dinoflagellates." *Int J Syst Evol Microbiol* **55**: 1089-96.
- Biers, E. J., Wang, K., Pennington, C., Belas, R., Chen, F. and Moran, M. A. (2008). "Occurrence and expression of gene transfer agent genes in marine bacterioplankton." *Appl Environ Microbiol* **74**: 2933-9.
- Bijlsma, J. J., Waidner, B., Vliet, A. H., Hughes, N. J., Hag, S., Bereswill, S., et al. (2002). "The *Helicobacter pylori* homologue of the ferric uptake regulator is involved in acid resistance." *Infect Immun* **70**: 606-11.
- Birboim, H. C. and Doly, J. (1979). "A rapid alkaline extraction procedure for screening recombinant plasmid DNA." *Nucleic Acids Res* **7**: 1513-23.
- Blain, S., Queguiner, B., Armand, L., Belviso, S., Bombled, B., Bopp, L., et al. (2007). "Effect of natural iron fertilization on carbon sequestration in the southern ocean." *Nature* **446**: 1070-1074.
- Bollen, A., Lathe, R., Herzog, A., Denicourt, D., Lecocq, J. P., Desmarez, L., et al. (1979). "A conditionally lethal mutation of *Escherichia coli* affecting the gene coding for ribosomal protein s2 (rpsb)." *J Mol Biol* **132**: 219-33.
- Bosello, M., Mielcarek, A., Giessen, T. W. and Marahiel, M. A. (2012). "An enzymatic pathway for the biosynthesis of the formylhydroxyornithine required for rhodochelin iron coordination." *Biochemistry* **51**: 3059-66.
- Bosello, M., Robbel, L., Linne, U., Xie, X. and Marahiel, M. A. (2011). "Biosynthesis of the siderophore rhodochelin requires the coordinated expression of three independent gene clusters in *Rhodococcus jostii* rha1." *J Am Chem Soc* **133**: 4587-95.
- Boyd, P. W., Law, C. S., Wong, C. S., Nojiri, Y., Tsuda, A., Lvasseur, M., et al. (2004). "The decline and fate of an iron-induced subarctic phytoplankton bloom." *Nature* **428**: 549-553.
- Boyd, P. W., Watson, A. J., Law, C. S., Abraham, E. R., Trull, T., Murdoch, R., et al. (2000). "A mesoscale phytoplankton bloom in the polar southern ocean stimulated by iron fertilization." *Nature* **407**: 695-702.
- Boyer, E., Bergevin, I., Malo, D., Gros, P. and Cellier, M. F. (2002). "Acquisition of Mn(II) in addition to Fe(II) is required for full virulence of *Salmonella enterica* serovar Typhimurium." *Infect Immun* **70**: 6032-42.
- Braun, V. and Killmann, H. (1999). "Bacterial solutions to the iron-supply problem." *Trends Biochem Sci* **24**: 104-9.
- Braun, V., Hantke, K. and Koster, W. (1998). "Bacterial iron transport: Mechanisms, genetics, and regulation." *Metal Ions Biol Syst* **35**: 67-145.
- Bruland, K. W., Orians, K. J. and Cowen, J. P. (1994). "Reactive trace metals in the stratified central north pacific." *Geochimica et Cosmochimica Acta* **58**: 3171-3182.
- Brune, I., Werner, H., Huser, A. T., Kalinowski, J., Puhler, A. and Tauch, A. (2006). "The Dtxr protein acting as dual transcriptional regulator directs a global regulatory network involved in iron metabolism of *Corynebacterium glutamicum*." *BMC Genomics* **7**: 21.

- Buck, K. N. and Bruland, K. W. (2007). "The physicochemical speciation of dissolved iron in the Bering Sea, Alaska." *Limnology and Oceanography* **52**: 1800-1808.
- Buesseler, K. O. and Boyd, P. W. (2009). "Shedding light on processes that control particle export and flux attenuation in the twilight zone of the open ocean
- Butler, A. (2005). "Marine siderophores and microbial iron mobilization." *Biometals* **18**: 369-374.
- Butler, A. and Theisen, R. M. (2010). "Iron(III)-siderophore coordination chemistry: Reactivity of marine siderophores." *Coordination Chemistry Reviews* **254**: 288-296.
- Cao, J., Woodhall, M. R., Alvarez, J., Cartron, M. L. and Andrews, S. C. (2007). "Efeub (*ycdnob*) is a tripartite, acid-induced and cpxar-regulated, low-pH Fe^{2+} transporter that is cryptic in *Escherichia coli* K-12 but functional in *E. coli* O157:H7." *Mol Microbiol* **65**: 857-75.
- Carrondo, M. A. (2003). "Ferritins, iron uptake and storage from the bacterioferritin viewpoint." *EMBO J* **22**: 1959-68.
- Cartron, M. L., Maddocks, S., Gillingham, P., Craven, C. J. and Andrews, S. C. (2006). "Feo - transport of ferrous iron into bacteria." *Biometals* **19**: 143-57.
- Cescau, S., Cwerman, H., Letoffe, S., Delepelaire, P., Wandersman, C. and Biville, F. (2007). "Haem acquisition by haemophores." *Biometals* **20**: 603-13.
- Chao, T. C., Becker, A., Buhmester, J., Puhler, A. and Weidner, S. (2004). "The *Sinorhizobium meliloti* fur gene regulates, with dependence on mn(II), transcription of the *sitABCD* operon, encoding a metal-type transporter." *J Bacteriol* **186**: 3609-20.
- Chatfield, C. H., Mulhern, B. J., Burnside, D. M. and Cianciotto, N. P. (2011). "*Legionella pneumophila* lbtu acts as a novel, TonB-independent receptor for the legiobactin siderophore." *J Bacteriol* **193**: 1563-75.
- Cheton, P. L. and Archibald, F. S. (1988). "Manganese complexes and the generation and scavenging of hydroxyl free radicals." *Free Radic Biol Med* **5**: 325-33.
- Chin, N., Frey, J., Chang, C. F. and Chang, Y. F. (1996). "Identification of a locus involved in the utilization of iron by *Actinobacillus pleuropneumoniae*." *FEMS Microbiol Lett* **143**: 1-6.
- Coale, K. H., Fitzwater, S. E., Gordon, R. M., Johnson, K. S. and Barber, R. T. (1996). "Control of community growth and export production by upwelled iron in the equatorial pacific ocean." *Nature* **379**: 621-624.
- Coale, K. H., Johnson, K. S., Chavez, F. P., Buesseler, K. O., Barber, R. T., Brzezinski, M. A., *et al.* (2004). "Southern ocean iron enrichment experiment: Carbon cycling in high- and low-Si waters." *Science* **304**: 408-414.
- Coale, K. H., Johnson, K. S., Fitzwater, S. E., Gordon, R. M., Tanner, S., Chavez, F. P., *et al.* (1996). "A massive phytoplankton bloom induced by an ecosystem-scale iron fertilization experiment in the equatorial pacific ocean." *Nature* **383**: 495-501.
- Cope, L. D., Yogeve, R., Muller-Eberhard, U. and Hansen, E. J. (1995). "A gene cluster involved in the utilization of both free haem and haem:Hemopexin by *Haemophilus influenzae* type b." *J Bacteriol* **177**: 2644-53.
- Cornelis, P. and Andrews, S. C. (2010). Iron uptake and homeostasis in microorganisms. Norfolk, Caister Academic.
- Cornelis, P., Matthijs, S. and Van Oeffelen, L. (2009). "Iron uptake regulation in *Pseudomonas aeruginosa*." *Biometals* **22**: 15-22.
- Cornelissen, C. N. and Sparling, P. F. (1994). "Iron piracy: Acquisition of transferrin-bound iron by bacterial pathogens." *Mol Microbiol* **14**: 843-50.
- Crichton, R. R. and Boelaert, J. R. (2001). "Inorganic biochemistry of iron metabolism : From molecular mechanisms to clinical consequences." Chichester, Wiley.
- Crosa, J. H. and Walsh, C. T. (2002). "Genetics and assembly line enzymology of siderophore biosynthesis in bacteria." *Microbiol Mol Biol Rev* **66**: 223-49.
- Crosa, J. H., Mey, A. R. and Payne, S. M. (2004). "Iron transport in bacteria." Washington, D.C., ASM ; Oxford : John Wiley.
- Cunliffe, M. (2011). "Correlating carbon monoxide oxidation with cox genes in the abundant marine Roseobacter clade." *ISME J* **5**: 685-91.
- da Silva, S. M., Pimentel, C., Valente, F. M., Rodrigues-Pousada, C. and Pereira, I. A. (2011). "Tungsten and molybdenum regulation of formate dehydrogenase expression in *Desulfovibrio vulgaris hildenborough*." *J Bacteriol* **193**: 2909-16.
- Davies, B. W. and Walker, G. C. (2007). "Disruption of *sitA* compromises *Sinorhizobium meliloti* for manganese uptake required for protection against oxidative stress." *J Bacteriol* **189**: 2101-9.

- Delany, I., Spohn, G., Rappuoli, R. and Scarlato, V. (2001). "The fur repressor controls transcription of iron-activated and -repressed genes in *Helicobacter pylori*." *Mol Microbiol* **42**: 1297-309.
- Deneer, H. G., Healey, V. and Boychuk, I. (1995). "Reduction of exogenous ferric iron by a surface-associated ferric reductase of *Listeria* spp." *Microbiology* **141 (Pt 8)**: 1985-92.
- DeRisi, J. L., Iyer, V. R. and Brown, P. O. (1997). "Exploring the metabolic and genetic control of gene expression on a genomic scale." *Science* **278**: 680-6.
- Diaz-Mireles, E., Wexler, M., Sawers, G., Bellini, D., Todd, J. D. and Johnston, A. W. (2004). "The Fur-like protein Mur of *Rhizobium leguminosarum* is a Mn(II)-responsive transcriptional regulator." *Microbiology* **150**: 1447-56.
- Diaz-Mireles, E., Wexler, M., Todd, J. D., Bellini, D., Johnston, A. W. and Sawers, R. G. (2005). "The manganese-responsive repressor Mur of *Rhizobium leguminosarum* is a member of the Fur-superfamily that recognizes an unusual operator sequence." *Microbiology* **151**: 4071-8.
- Doucette, G. J., Erdner, D. L., Peleato, M. L., Hartman, J. J. and Anderson, D. M. (1996). "Quantitative analysis of iron-stress related proteins in *Thalassiosira weissflogii*: Measurement of flavodoxin and ferredoxin using HPLC." *Marine Ecology Progress Series* **130**: 269-276.
- Drechsel, H., Freund, S., Nicholson, G., Haag, H., Jung, O., Zahner, H., et al. (1993). "Purification and chemical characterization of staphyloferrin b, a hydrophilic siderophore from staphylococci." *Biometals* **6**: 185-92.
- Drechsel, H., Tschierske, M., Thielen, A., Jung, G., Zähler, H. and Winkelmann, G. (1995). "The carboxylate type siderophore rhizoferrin and its analogs produced by directed fermentation." *Journal of Industrial Microbiology & Biotechnology* **14**: 105-112.
- Duce, R. A. and Tindale, N. W. (1991). "Atmospheric transport of iron and its deposition in the ocean." *Limnology and oceanography* **36**: 1715-1726.
- Emsley, J. (2001). "Nature's building blocks : An a-z guide to the elements." Oxford, Oxford University Press.
- Entsch, B., Sim, R. G. and Hatcher, B. G. (1983). "Indications from photosynthetic components that iron is a limiting nutrient in primary producers on coral reefs." *Marine Biology* **73**: 17-30.
- Erdner, D. L., Price, N. M., Doucette, G. J., Peleato, M. L. and Anderson, D. M. (1999). "Characterization of ferredoxin and flavodoxin as markers of iron limitation in marine phytoplankton." *Marine Ecology Progress Series* **184**: 43-53.
- Escobar, L., Perez-Martin, J. and de Lorenzo, V. (1999). "Opening the iron box: Transcriptional metalloregulation by the Fur protein." *J Bacteriol* **181**: 6223-9.
- Faraldo-Gomez, J. D. and Sansom, M. S. P. (2003). "Acquisition of siderophores in gram-negative bacteria." *Nat Rev Mol Cell Bio* **4**: 105-116.
- Feely, R. A., Doney, S. C. and Cooley, S. R. (2009). "Ocean acidification : Present conditions and future changes in a high-CO2 world." *Oceanography* **22**: 36-47.
- Felsenstein, J. (1985). "Confidence limits on phylogenies: An approach using the bootstrap." *Evolution* **39**: 783-791.
- Fenton, H. J. H. (1894). "Lxxiii.-oxidation of tartaric acid in presence of iron." *Journal of the Chemical Society, Transactions* **65**: 899-910.
- Fernandes, J. L. (2012). "Iron chelation therapy in the management of transfusion-related cardiac iron overload." [Lid - 10.1111/j.1537-2995.2012.03580.X \[doi\]](https://doi.org/10.1111/j.1537-2995.2012.03580.X).
- Ferreiros, C., Criado, M. T. and Gomez, J. A. (1999). "The *Neisserial* 37 kda ferric binding protein (FbpA)." *Comp Biochem Physiol B Biochem Mol Biol* **123**: 1-7.
- Fontecave, M. and Ollagnier-de-Choudens, S. (2008). "Iron-sulfur cluster biosynthesis in bacteria: Mechanisms of cluster assembly and transfer." *Arch Biochem Biophys* **474**: 226-237.
- Forman, S., Nagiec, M. J., Abney, J., Perry, R. D. and Fetherston, J. D. (2007). "Analysis of the aerobactin and ferric hydroxamate uptake systems of *Yersinia pestis*." *Microbiology* **153**: 2332-41.
- Fricke, B., Parchmann, O., Kruse, K., Rucknagel, P., Schierhorn, A. and Menge, S. (1999). "Characterization and purification of an outer membrane metalloproteinase from *Pseudomonas aeruginosa* with fibrinolytic activity." *Biochim Biophys Acta* **1454**: 236-50.
- Fuangthong, M. and Helmann, J. D. (2003). "Recognition of DNA by three ferric uptake regulator (*fur*) homologs in *Bacillus subtilis*." *J Bacteriol* **185**: 6348-57.
- Gay, P., Le Coq, D., Steinmetz, M., Berkelman, T. and Kado, C. I. (1985). "Positive selection procedure for entrapment of insertion sequence elements in gram-negative bacteria." *J Bacteriol* **164**: 918-21.

- Gledhill, M. and van den Berg, C. M. G. (1994). "Determination of complexation of iron(III) with natural organic complexing ligands in seawater using cathodic stripping voltammetry." *Marine Chemistry* **47**: 41-54.
- Gonzalez, J. M. and Moran, M. A. (1997). "Numerical dominance of a group of marine bacteria in the alpha-subclass of the class proteobacteria in coastal seawater." *Appl Environ Microbiol* **63**: 4237-42.
- Gonzalez, J. M., Kiene, R. P. and Moran, M. A. (1999). "Transformation of sulfur compounds by an abundant lineage of marine bacteria in the alpha-subclass of the class Proteobacteria." *Appl Environ Microbiol* **65**: 3810-9.
- Gonzalez, J. M., Mayer, F., Moran, M. A., Hodson, R. E. and Whitman, W. B. (1997). "*Microbulbifer hydrolyticus* gen. Nov., sp. Nov., and *Marinobacterium georgiense* gen. Nov., sp. Nov., two marine bacteria from a lignin-rich pulp mill waste enrichment community." *Int J Syst Bacteriol* **47**: 369-76.
- Gonzalez, J. M., Simo, R., Massana, R., Covert, J. S., Casamayor, E. O., Pedros-Alio, C., et al. (2000). "Bacterial community structure associated with a dimethylsulfoniopropionate-producing north atlantic algal bloom." *Appl Environ Microbiol* **66**: 4237-46.
- Gordon, R. M., Martin, J. H. and Knauer, G. A. (1982). "Iron in north-east pacific waters." *Nature* **299**: 611-612.
- Granger, J. and Price, N. M. (1999). "The importance of siderophores in iron nutrition of heterotrophic marine bacteria." *Limnology and Oceanography* **44**: 541-555.
- Gresock, M. G., Savenkova, M. I., Larsen, R. A., Ollis, A. A. and Postle, K. (2011). "Death of the TonB shuttle hypothesis." *Front Microbiol* **2**: 206.
- Grifantini, R., Sebastian, S., Frigimelica, E., Draghi, M., Bartolini, E., Muzzi, A., et al. (2003). "Identification of iron-activated and -repressed Fur-dependent genes by transcriptome analysis of *Neisseria meningitidis* group b." *Proc Natl Acad Sci U S A* **100**: 9542-7.
- Güssow, K., Proelss, A., Oeschlies, A., Rehdanz, K. and Rickels, W. (2010). "Ocean iron fertilization: Why further research is needed." *Marine Policy*.
- Haber, F. and Weiss, J. (1932). "Äoerber die katalyse des hydroperoxydes." *Naturwissenschaften* **20**: 948-950.
- Hamza, I., Chauhan, S., Hassett, R. and O'Brian, M. R. (1998). "The bacterial Irr protein is required for coordination of haem biosynthesis with iron availability." *J Biol Chem* **273**: 21669-74.
- Hansel, C. M. and Francis, C. A. (2006). "Coupled photochemical and enzymatic Mn(II) oxidation pathways of a planktonic roseobacter-like bacterium." *Appl Environ Microbiol* **72**: 3543-9.
- Hantke, K. (1981). "Regulation of ferric iron transport in *Escherichia coli* K12: Isolation of a constitutive mutant." *Mol Gen Genet* **182**: 288-92.
- Hantke, K. (2001). "Iron and metal regulation in bacteria." *Curr Opin Microbiol* **4**: 172-7.
- Harle, C., Kim, I., Angerer, A. and Braun, V. (1995). "Signal transfer through three compartments: Transcription initiation of the *Escherichia coli* ferric citrate transport system from the cell surface." *EMBO J.* **14**: 1430-8.
- Hassett, D. J., Sokol, P. A., Howell, M. L., Ma, J. F., Schweizer, H. T., Ochsner, U., et al. (1996). "Ferric uptake regulator (fur) mutants of *Pseudomonas aeruginosa* demonstrate defective siderophore-mediated iron uptake, altered aerobic growth, and decreased superoxide dismutase and catalase activities." *J Bacteriol* **178**: 3996-4003.
- Haygood, M. G., Holt, P. D. and Butler, A. (1993). "Aerobactin production by a planktonic marine *Vibrio* sp." *Limnology and oceanography* **38**: 1091-1097.
- Heemstra, J. R., Jr., Walsh, C. T. and Sattely, E. S. (2009). "Enzymatic tailoring of ornithine in the biosynthesis of the Rhizobium cyclic trihydroxamate siderophore vicibactin." *J Am Chem Soc* **131**: 15317-29.
- Hernandez, J. A., Peleato, M. L., Fillat, M. F. and Bes, M. T. (2004). "Haem binds to and inhibits the DNA-binding activity of the global regulator FurA from *Anabaena* sp. Pcc 7120." *FEBS Lett* **577**: 35-41.
- Hibbing, M. E. and Fuqua, C. (2011). "Antiparallel and interlinked control of cellular iron levels by the Irr and RirA regulators of *Agrobacterium tumefaciens*." *J Bacteriol* **193**: 3461-72.
- Hideki, F., Rumi, S., Toshi, N. and Isao, K. (2007). "Size distribution and biomass of nanoflagellates in meso- and bathypelagic layers of the subarctic pacific." *Aquatic Microbial Ecology* **46**: 203-207.
- Higgs, P. I., Larsen, R. A. and Postle, K. (2002). "Quantification of known components of the *Escherichia coli* TonB energy transduction system: TonB, ExbB, ExbD and FepA." *Mol Microbiol* **44**: 271-81.
- Hoang, T. T., Karkhoff-Schweizer, R. R., Kutchna, A. J. and Schweizer, H. P. (1998). "A broad-host-range FLP-FRT recombination system for site-specific excision of chromosomally-located DNA sequences: Application for isolation of unmarked *Pseudomonas aeruginosa* mutants." *Gene* **212**: 77-86.
- Hobbie, J. E., Daley, R. J. and Jasper, S. (1977). "Use of nucleopore filters for counting bacteria by fluorescence microscopy." *Appl. Environ. Microbiol.* **33**: 1225-1228.

- Hohle, T. H. and O'Brian, M. R. (2009). "The *mntH* gene encodes the major Mn(II) transporter in *Bradyrhizobium japonicum* and is regulated by manganese via the Fur protein." *Mol Microbiol* **72**: 399-409.
- Hohle, T. H., Franck, W. L., Stacey, G. and O'Brian, M. R. (2011). "Bacterial outer membrane channel for divalent metal ion acquisition." *Proc Natl Acad Sci U S A* **108**: 15390-5.
- Holmes, K., Mulholland, F., Pearson, B. M., Pin, C., McNicholl-Kennedy, J., Ketley, J. M., *et al.* (2005). "*Campylobacter jejuni* gene expression in response to iron limitation and the role of Fur." *Microbiology* **151**: 243-257.
- Homann, V. V., Sandy, M., Tincu, J. A., Templeton, A. S., Tebo, B. M. and Butler, A. (2009). "Loihichelins a-f, a suite of amphiphilic siderophores produced by the marine bacterium *Halomonas lob-5*." *Journal of Natural Products* **72**: 884-888.
- Homuth, M., Valentin-Weigand, P., Rohde, M. and Gerlach, G. F. (1998). "Identification and characterization of a novel extracellular ferric reductase from *Mycobacterium paratuberculosis*." *Infect Immun* **66**: 710-6.
- Hopkinson, B. and Morel, F. (2009). "The role of siderophores in iron acquisition by photosynthetic marine microorganisms." *Biometals* **22**: 659-669.
- Hopkinson, B. M. and Barbeau, K. A. (2012). "Iron transporters in marine prokaryotic genomes and metagenomes." *Environ Microbiol* **14**: 114-28.
- Hutchins, D. A., Rueter, J. G. and Fish, W. (1991). "Siderophore production and nitrogen fixation are mutually exclusive strategies in anabaena 7120." *Limnology and oceanography* **36**: 1-12.
- Hutchins, D. A., Witter, A. E., Butler, A. and Luther, G. W. (1999). "Competition among marine phytoplankton for different chelated iron species." *Nature* **400**: 858-861.
- Ito, Y. and Butler, A. (2005). "Structure of synechobactins, new siderophores of the marine cyanobacterium *Synechococcus* sp. Pcc 7002." *Limnology and oceanography* **50**: 1918-1923.
- Jakubovics, N. S. and Jenkinson, H. F. (2001). "Out of the iron age: New insights into the critical role of manganese homeostasis in bacteria." *Microbiology* **147**: 1709-18.
- Jeblick, J. and Kusch, J. (2005). "Sequence, transcription activity, and evolutionary origin of the R-body coding plasmid pKAP298 from the intracellular parasitic bacterium *Caedibacter taeniospiralis*." *J Mol Evol* **60**: 164-73.
- Jickells, T. D., An, Z. S., Andersen, K. K., Baker, A. R., Bergametti, G., Brooks, N., *et al.* (2005). "Global iron connections between desert dust, ocean biogeochemistry, and climate." *Science* **308**: 67-71.
- Johnson, H. A. and Tebo, B. M. (2008). "In vitro studies indicate a quinone is involved in bacterial Mn(II) oxidation." *Arch Microbiol* **189**: 59-69.
- Johnson, K. S., Gordon, R. M., Coale and K, H. (1997). "What controls dissolved iron concentrations in the world ocean?" Amsterdam, PAYS-BAS, Elsevier.
- Johnston, A. W. B., Setchell, S. M. and Beringer, J. E. (1978). "Interspecific crosses between *Rhizobium leguminosarum* and *R. Meliloti*: Formation of haploid recombinants and of R-primes." *J Gen Microbiol* **104**: 209-218.
- Johnston, A. W., Todd, J. D., Curson, A. R., Lei, S., Nikolaidou-Katsaridou, N., Gelfand, M. S., *et al.* (2007). "Living without Fur: The subtlety and complexity of iron-responsive gene regulation in the symbiotic bacterium *Rhizobium* and other alpha-proteobacteria." *Biometals* **20**: 501-11.
- Jones, D. T., Taylor, W. R. and Thornton, J. M. (1992). "The rapid generation of mutation data matrices from protein sequences." *Comput Appl Biosci* **8**: 275-82.
- Juretic, D., Zoranic, L. and Zucic, D. (2002). "Basic charge clusters and predictions of membrane protein topology." *J Chem Inf Comput Sci* **42**: 620-32.
- Kammler, M., C. Schon, *et al.* (1993). "Characterization of the ferrous iron uptake system of *Escherichia coli*." *J Bacteriol* **175**(19): 6212-6219.
- Karner, M. B., DeLong, E. F. and Karl, D. M. (2001). "Archaeal dominance in the mesopelagic zone of the Pacific ocean." *Nature* **409**: 507-510.
- Keele, B. B., Jr., McCord, J. M. and Fridovich, I. (1970). "Superoxide dismutase from *Escherichia coli* B. A new manganese-containing enzyme." *J Biol Chem* **245**: 6176-81.
- Keen, N. T., Tamaki, S., Kobayashi, D. and Trollinger, D. (1988). "Improved broad-host-range plasmids for DNA cloning in gram-negative bacteria." *Gene* **70**: 191-7.
- Kehres, D. G., Janakiraman, A., Slauch, J. M. and Maguire, M. E. (2002a). "Regulation of *Salmonella enterica* serovar Typhimurium MntH transcription by H₂O₂, Fe(2+), and Mn(2+)." *J Bacteriol* **184**: 3151-8.

- Kehres, D. G., Janakiraman, A., Slauch, J. M. and Maguire, M. E. (2002b). "SitABCD is the alkaline Mn²⁺ transporter of *Salmonella enterica* serovar Typhimurium." *J. Bacteriol.* **184**: 3159-3166.
- Kehres, D. G., Zaharik, M. L., Finlay, B. B. and Maguire, M. E. (2000). "The NRAMP proteins of *Salmonella typhimurium* and *Escherichia coli* are selective manganese transporters involved in the response to reactive oxygen." *Mol Microbiol* **36**: 1085-100.
- Kelm, S., Shi, J. and Deane, C. M. (2009). "Membrane: Homology-based membrane-insertion of proteins." *Bioinformatics* **25**: 1086-8.
- Kim, H., Lee, H. and Shin, D. (2012). "The FeoA protein is necessary for the FeoB transporter to import ferrous iron." *Biochemical and Biophysical Research Communications* **423**: 733-738.
- Kioerboe, T. and Jackson, G. A. (2001). "Marine snow, organic solute plumes, and optimal chemosensory behavior of bacteria." *Limnology and Oceanography* **46**: 1309-1318.
- Kirchman, David, L., Elifantz, Hila, Dittel, Ana, I., et al. (2007). "Standing stocks and activity of archaea and bacteria in the western arctic ocean." Waco, TX, ETATS-UNIS, *American Society of Limnology and Oceanography*.
- Kranzler, C., Lis, H., Shaked, Y. and Keren, N. (2011). "The role of reduction in iron uptake processes in a unicellular, planktonic cyanobacterium." *Environ Microbiol* **13**: 2990-9.
- Köster, W. (2001). "ABC transporter-mediated uptake of iron, siderophores, haem and vitamin B₁₂." *Research in Microbiology* **152**: 291-301.
- Landing, W. M. and Bruland, K. W. (1987). "The contrasting biogeochemistry of iron and manganese in the pacific ocean." *Geochimica et Cosmochimica Acta* **51**: 29-43.
- Law, N. A., Caudle, M. T., Pecoraro, V. L. and Sykes, A. G. (1998). "Manganese redox enzymes and model systems: Properties, structures, and reactivity." *Advances in inorganic chemistry*, Academic Press. **Volume 46**: 305-440.
- Legrain, M. I., Mazarin, V. r., Irwin, S. W., Bouchon, B., Quentin-Millet, M.-J., Jacobs, E., et al. (1993). "Cloning and characterization of *Neisseria meningitidis* genes encoding the transferrin-binding proteins Tbp1 and Tbp2." *Gene* **130**: 73-80.
- Letoffe, S., Ghigo, J. M. and Wandersman, C. (1994). "Iron acquisition from haem and hemoglobin by a *Serratia marcescens* extracellular protein." *Proc Natl Acad Sci U S A* **91**: 9876-80.
- Li, L., Chen, O. S., McVey Ward, D. and Kaplan, J. (2001). "Ccc1 is a transporter that mediates vacuolar iron storage in yeast." *J Biol Chem* **276**: 29515-9.
- Lin, S., Sandh, G., Zhang, H., Cheng, J., Perkins, K., Carpenter, E. J., et al. (2009). "Two flavodoxin genes in *Trichodesmium* (oscillatoriales, cyanophyceae): Remarkable sequence divergence and possible functional diversification." *Journal of Experimental Marine Biology and Ecology* **371**: 93-101.
- Locher, K. P., Rees, B., Koebnik, R., Mitschler, A., Moulinier, L., Rosenbusch, J. P., et al. (1998). "Transmembrane signaling across the ligand-gated FhuA receptor: Crystal structures of free and ferrichrome-bound states reveal allosteric changes." *Cell* **95**: 771-8.
- Lorain, S., Lecluse, Y., Scamps, C., Mattei, M. G. and Lipinski, M. (2001). "Identification of human and mouse hira-interacting protein-5 (hirip5), two mammalian representatives in a family of phylogenetically conserved proteins with a role in the biogenesis of Fe-S proteins." *Biochim Biophys Acta* **1517**: 376-83.
- Maddocks, S. E. and Oyston, P. C. (2008). "Structure and function of the lysr-type transcriptional regulator (LtrR) family proteins." *Microbiology* **154**: 3609-23.
- Mahowald, N., Kohfeld, K., Hansson, M., Balkanski, Y., Harrison, S. P., Prentice, I. C., et al. (1999). "Dust sources and deposition during the last glacial maximum and current climate: A comparison of model results with paleodata from ice cores and marine sediments." *J. Geophys. Res.* **104**: 15895-15916.
- Makui, H., Roig, E., Cole, S. T., Helmann, J. D., Gros, P. and Cellier, M. F. (2000). "Identification of the *Escherichia coli* K-12 NRAMP orthologue (MntH) as a selective divalent metal ion transporter." *Mol Microbiol* **35**: 1065-78.
- Maniatis, T., Fritsch, E. F. and Sambrook, J. (1982). "Molecular cloning : A laboratory manual." Cold Spring Harbor, N.Y., Cold Spring Harbor Laboratory.
- Maranger, R., Bird, D. F. and Price, N. M. (1998). "Iron acquisition by photosynthetic marine phytoplankton from ingested bacteria." *Nature* **396**: 248-251.
- Marrs, B. (1974). "Genetic recombination in *Rhodospseudomonas capsulata*." *Proc Natl Acad Sci U S A* **71**: 971-3.
- Martin, J. H., Coale, K. H., Johnson, K. S., Fitzwater, S. E., Gordon, R. M., Tanner, S. J., et al. (1994). "Testing the iron hypothesis in ecosystems of the equatorial pacific ocean." *Nature* **371**: 123-129.

- Martin, J. H., Gordon, R. M. and Fitzwater, S. E. (1990). "Iron in antarctic waters." *Nature* **345**: 156-158.
- Martin, J. H., Gordon, R. M. and Fitzwater, S. E. (1991). "The case for iron." *Limnology and oceanography* **36**: 1793-1802.
- Martin, J., Ito, Y., Homann, V., Haygood, M. and Butler, A. (2006). "Structure and membrane affinity of new amphiphilic siderophores produced by *Ochrobactrum* sp. Sp18." *Journal of Biological Inorganic Chemistry* **11**: 633-641.
- Martinez, J. S., Zhang, G. P., Holt, P. D., Jung, H. T., Carrano, C. J., Haygood, M. G., et al. (2000). "Self-assembling amphiphilic siderophores from marine bacteria." *Science* **287**: 1245-1247.
- Martinez, M., R. A. Ugalde, et al. (2005). "Dimeric *Brucella abortus* Irr protein controls its own expression and binds haem." *Microbiology* **151**(Pt 10): 3427-3433.
- Masse, E. and Gottesman, S. (2002). "A small RNA regulates the expression of genes involved in iron metabolism in *Escherichia coli*." *Proc Natl Acad Sci U S A* **99**: 4620-5.
- Massé, E., Salvail, H., Desnoyers, G. and Arguin, M. (2007). "Small RNAs controlling iron metabolism." *Curr Opin Microbiol* **10**: 140-5.
- Massé, E., Vanderpool, C. K. and Gottesman, S. (2005). "Effect of RyhB small RNA on global iron use in *Escherichia coli*." *J Bacteriol* **187**: 6962-71.
- Mawji, E., Gledhill, M., Milton, J. A., Tarran, G. A., Ussher, S., Thompson, A. (2008). "Hydroxamate siderophores: Occurrence and importance in the Atlantic Ocean." *Environ Sci Technol* **42**: 8675-8680.
- Measures, C. I., Landing, W. M., Brown, M. T. and Buck, C. S. (2008). "High-resolution Al and Fe data from the Atlantic Ocean Clivar-CO₂ repeat hydrography a16n transect: Extensive linkages between atmospheric dust and upper ocean geochemistry." *Global Biogeochem. Cycles* **22**: GB1005.
- Mendez, J., Guieu, C. and Adkins, J. (2010). "Atmospheric input of manganese and iron to the ocean: Seawater dissolution experiments with Saharan and North American dusts." *Marine Chemistry* **120**: 34-43.
- Merlin, C., McAteer, S. and Masters, M. (2002). "Tools for characterization of *Escherichia coli* genes of unknown function." *J Bacteriol* **184**: 4573-81.
- Mey, A. R., E. E. Wyckoff, et al. (2005). "Iron and *fur* regulation in *Vibrio cholerae* and the role of Fur in virulence." *Infect Immun* **73**(12): 8167-8178.
- Middag, R., de Baar, H. J. W., Laan, P., Cai, P. H. and van Ooijen, J. C. (2011). "Dissolved manganese in the Atlantic sector of the Southern Ocean." *Deep Sea Research Part II: Topical Studies in Oceanography* **58**: 2661-2677.
- Miethke, M., Hou, J. and Marahiel, M. A. (2011). "The siderophore-interacting protein YqjH acts as a ferric reductase in different iron assimilation pathways of *Escherichia coli*." *Biochemistry* **50**: 10951-64.
- Miller, T. R. and Belas, R. (2004). "Dimethylsulfoniopropionate metabolism by *Pfiesteria*-associated *Roseobacter* spp." *Appl Environ Microbiol* **70**: 3383-91.
- Millero, F. J. (2006). "Chemical oceanography." Boca Raton ; London, Taylor Francis.
- Millero, F. J., Woosley, R., DiTrolio, B. and Waters, J. (2009). "Effect of ocean acidification on the speciation of metals in seawater." *Oceanography* **22**.
- Mitsui, A. and Arnon, D. I. (1971). "Crystalline ferredoxin from a blue-green alga, *Nostoc* sp." *Physiologia Plantarum* **25**: 135-140.
- Moore, J. K., Doney, S. C., Glover, D. M. and Fung, I. Y. (2001). "Iron cycling and nutrient-limitation patterns in surface waters of the world ocean." *Deep Sea Research Part II: Topical Studies in Oceanography* **49**: 463-507.
- Moran, M. A., Belas, R., Schell, M. A., Gonzalez, J. M., Sun, F., Sun, S., et al. (2007). "Ecological genomics of marine *Roseobacter* spp." *Appl Environ Microbiol* **73**: 4559-69.
- Moran, M. A., Buchan, A., Gonzalez, J. M., Heidelberg, J. F., Whitman, W. B., Kiene, R. P., et al. (2004). "Genome sequence of *Silicibacter pomeroyi* reveals adaptations to the marine environment." *Nature* **432**: 910-3.
- Morel, F. M. M. and Price, N. M. (2003). "The biogeochemical cycles of trace metals in the oceans." *Science* **300**: 944-947.
- Morris, R. M., Frazar, C. D. and Carlson, C. A. (2012). "Basin-scale patterns in the abundance of SAR11 subclades, marine actinobacteria (om1), members of the *Roseobacter* clade and SAR116 in the South Atlantic." *Environ Microbiol* **14**: 1133-44.
- Morris, R. M., Rappe, M. S., Connon, S. A., Vergin, K. L., Siebold, W. A., Carlson, C. A., et al. (2002). "SAR11 clade dominates ocean surface bacterioplankton communities." *Nature* **420**: 806-10.

- Nakagawa, T., Nakamura, S., Tanaka, K., Kawamukai, M., Suzuki, T., Nakamura, K., *et al.* (2008). "Development of r4 gateway binary vectors (r4pgwb) enabling high-throughput promoter swapping for plant research." *Biosci Biotechnol Biochem* **72**: 624-9.
- Neilands, J. B. (1952). "A crystalline organo-iron pigment from a rust fungus (*Ustilago sphaerogena*)." *Journal of the American Chemical Society* **74**: 4846-4847.
- Nienaber, A., Hennecke, H. and Fischer, H. M. (2001). "Discovery of a haem uptake system in the soil bacterium *Bradyrhizobium japonicum*." *Mol Microbiol* **41**: 787-800.
- Niven, D. F., Ekins, A. and al-Samaurai, A. A. (1999). "Effects of iron and manganese availability on growth and production of superoxide dismutase by *Streptococcus suis*." *Can J Microbiol* **45**: 1027-32.
- Noinaj, N., Guillier, M., Barnard, Travis J. and Buchanan, S. K. (2010). "TonB-dependent transporters: Regulation, structure, and function." *Annual Review of Microbiology* **64**: 43-60.
- Noya, F., Arias, A. and Fabiano, E. (1997). "Haem compounds as iron sources for nonpathogenic *Rhizobium* bacteria." *J Bacteriol* **179**: 3076-8.
- O'Brien, I. G. and Gibson, F. (1970). "The structure of enterochelin and related 2,3-dihydroxy-n-benzoylserine conjugates from *Escherichia coli*." *Biochim Biophys Acta* **215**: 393-402.
- Ochsner, U. A. and Vasil, M. L. (1996). "Gene repression by the ferric uptake regulator in *Pseudomonas aeruginosa*: Cycle selection of iron-regulated genes." *Proc Natl Acad Sci U S A* **93**: 4409-14.
- Oeffelen, L., Cornelis, P., Delm, W., Ridder, F., Moor, B. and Moreau, Y. (2008). "Detecting *cis*-regulatory binding sites for cooperatively binding proteins." *Nucl. Acids Res.* **36**: 46.
- Oh, H. M., Kang, I., Lee, K., Jang, Y., Lim, S. I. and Cho, J. C. (2011). "Complete genome sequence of strain IMCC9063, belonging to SAR11 subgroup 3, isolated from the Arctic Ocean." *J Bacteriol* **193**: 3379-80.
- Oh, H. M., Kwon, K. K., Kang, I., Kang, S. G., Lee, J. H., Kim, S. J., *et al.* (2010). "Complete genome sequence of *Candidatus puniceispirillum marinum* IMCC1322, a representative of the SAR116 clade in the alphaproteobacteria." *J Bacteriol* **192**: 3240-1.
- Oliveros, J. (2007). "Venny. An interactive tool for comparing lists with venn diagrams." from citeulike-article-id:6994833.
- Palenik, B., Brahamsha, B., Larimer, F. W., Land, M., Hauser, L., Chain, P., *et al.* (2003). "The genome of a motile marine *Synechococcus*." *Nature* **424**: 1037-1042.
- Palenik, B., Ren, Q., Dupont, C. L., Myers, G. S., Heidelberg, J. F., Badger, J. H., *et al.* (2006). "Genome sequence of *Synechococcus* 9311: Insights into adaptation to a coastal environment." *Proceedings of the National Academy of Sciences* **103**: 13555-13559.
- Palmer, T. and Berks, B. C. (2012). "The twin-arginine translocation (TAT) protein export pathway." *Nat Rev Microbiol* **10**: 483-96.
- Pandey, A., Bringel, F. and Meyer, J.-M. (1994). "Iron requirement and search for siderophores in lactic acid bacteria." *Applied Microbiology and Biotechnology* **40**: 735-739.
- Pankowski, A. and McMinn, A. (2009). "Iron availability regulates growth, photosynthesis, and production of ferredoxin and flavodoxin in antarctic sea ice diatoms." *Aquatic Biology* **4**: 273-288.
- Parker, D., Kennan, R. M., Myers, G. S., Paulsen, I. T. and Rood, J. I. (2005). "Identification of a *Dichelobacter nodosus* ferric uptake regulator and determination of its regulatory targets." *J Bacteriol* **187**: 366-75.
- Patzer, S. I. and Hantke, K. (1998). "The ZnuABC high-affinity zinc uptake system and its regulator Zur in *Escherichia coli*." *Mol Microbiol* **28**: 1199-210.
- Patzer, S. I. and Hantke, K. (2001). "Dual repression by Fe(2+)-Fur and Mn(2+)-MntR of the MntH gene, encoding an NRAMP-like Mn(2+) transporter in *Escherichia coli*." *J Bacteriol* **183**: 4806-13.
- Peter, D. C., Rebecca, J. G., Mark, R. D., Pratik, S., Julie, M. R. and David, A. C. (2007). "Distinct protistan assemblages characterize the euphotic zone and deep sea (2500 m) of the western North Atlantic (Sargasso Sea and gulf stream)." *Environmental Microbiology* **9**: 1219-1232.
- Peters, J. W. and Broderick, J. B. (2012). "Emerging paradigms for complex iron-sulfur cofactor assembly and insertion." *Annu Rev Biochem* **81**: 429-50.
- Petersen, T. N., Brunak, S., von Heijne, G. and Nielsen, H. (2011). "Signalp 4.0: Discriminating signal peptides from transmembrane regions." *Nat Methods* **8**: 785-6.
- Petursdottir, S. K. and Kristjansson, J. K. (1997). "*Silicibacter lacuscaerulensis* gen. Nov., a mesophilic moderately halophilic bacterium characteristic of the blue lagoon geothermal lake in Iceland." *Extremophiles* **1**: 94-9.
- Peuser, V., B. Remes, *et al.* (2012). "Role of the Irr Protein in the Regulation of Iron Metabolism in *Rhodobacter sphaeroides*." *PLoS One* **7**(8): e42231.

- Peuser, V., Metz, S. and Klug, G. (2011). "Response of the photosynthetic bacterium *Rhodobacter sphaeroides* to iron limitation and the role of a Fur orthologue in this response." *Environmental Microbiology Reports* **3**: 397–404.
- Peuser, V., Remes, B. and Klug, G. (2012). "Role of the Irr protein in the regulation of iron metabolism in *Rhodobacter sphaeroides*." *PLoS One* **7**: e42231.
- Platero, R., de Lorenzo, V., Garat, B. and Fabiano, E. (2007). "*Sinorhizobium meliloti* Fur-like (Mur) protein binds a Fur box-like sequence present in the MntA promoter in a manganese-responsive manner." *Appl Environ Microbiol* **73**: 4832-8.
- Platero, R., Peixoto, L., O'Brian, M. R. and Fabiano, E. (2004). "Fur is involved in manganese-dependent regulation of *mntA* (*sitA*) expression in *Sinorhizobium meliloti*." *Appl Environ Microbiol* **70**: 4349-55.
- Pohl, E., Haller, J. C., Mijovilovich, A., Meyer-Klaucke, W., Garman, E. and Vasil, M. L. (2003). "Architecture of a protein central to iron homeostasis: Crystal structure and spectroscopic analysis of the ferric uptake regulator." *Molecular Microbiology* **47**: 903-915.
- Pollack, J. R. and Neilands, J. B. (1970). "Enterobactin, an iron transport compound from *Salmonella Typhimurium*." *Biochem Biophys Res Commun* **38**: 989-92.
- Pollard, R. T., Salter, I., Sanders, R. J., Lucas, M. I., Moore, C. M., Mills, R. A., *et al.* (2009). "Southern Ocean deep-water carbon export enhanced by natural iron fertilization." *Nature* **457**: 577-580.
- Pond, F. R., Gibson, I., Lalucat, J. and Quackenbush, R. L. (1989). "R-body-producing bacteria." *Microbiol Rev* **53**: 25-67.
- Posey, J. E. and Gherardini, F. C. (2000). "Lack of a role for iron in the Lyme disease pathogen." *Science* **288**: 1651-1653.
- Puehringer, S., Metlitzky, M. and Schwarzenbacher, R. (2008). "The pyrroloquinoline quinone biosynthesis pathway revisited: A structural approach." *BMC Biochem* **9**: 8.
- Puigbo, P., Guzman, E., Romeu, A. and Garcia-Vallve, S. (2007). "Optimizer: A web server for optimizing the codon usage of DNA sequences." *Nucleic Acids Res* **35**: W126-31.
- Puri, S., Hohle, T. H. and O'Brian, M. R. (2010). "Control of bacterial iron homeostasis by manganese." *Proc Natl Acad Sci U S A* **107**: 10691-5.
- Qi, Z. and O'Brian, M. R. (2002). "Interaction between the bacterial iron response regulator and ferrochelatase mediates genetic control of haem biosynthesis." *Mol Cell* **9**: 155-62.
- Qi, Z., Hamza, I. and O'Brian, M. R. (1999). "Haem is an effector molecule for iron-dependent degradation of the bacterial iron response regulator (Irr) protein." *Proc Natl Acad Sci U S A* **96**: 13056-61.
- Quatrini, R., Lefimil, C., Holmes, D. S. and Jedlicki, E. (2005). "The ferric iron uptake regulator (Fur) from the extreme acidophile *Acidithiobacillus ferrooxidans*." *Microbiology* **151**: 2005-15.
- Que, Q. and Helmann, J. D. (2000). "Manganese homeostasis in *Bacillus subtilis* is regulated by MntR, a bifunctional regulator related to the diphtheria toxin repressor family of proteins." *Mol Microbiol* **35**: 1454-68.
- Rajasekaran, M. B., Nilapwar, S., Andrews, S. C. and Watson, K. A. (2009). "EfeO-cupredoxins: Major new members of the cupredoxin superfamily with roles in bacterial iron transport." *Biometals* **23**: 1-17.
- Rakin, A. and Heesemann, J. (1995). "Yersiniabactin/pesticin receptor: A component of an iron uptake system of highly pathogenic *Yersinia*." *Contrib Microbiol Immunol* **13**: 244-7.
- Ramakrishnan, G., Meeker, A. and Dragulev, B. (2008). "FslE is necessary for siderophore-mediated iron acquisition in *Francisella tularensis* schu s4." *J Bacteriol* **190**: 5353-61.
- Ramakrishnan, G., Sen, B. and Johnson, R. (2012). "Paralogous outer membrane proteins mediate uptake of different forms of iron and synergistically govern virulence in *Francisella tularensis*." *J Biol Chem* **287**: 25191-202.
- Rappe, M. S., Connon, S. A., Vergin, K. L. and Giovannoni, S. J. (2002). "Cultivation of the ubiquitous SAR11 marine bacterioplankton clade." *Nature* **418**: 630-3.
- Raymond, K. N., Dertz, E. A. and Kim, S. S. (2003). "Enterobactin: An archetype for microbial iron transport." *Proc Natl Acad Sci U S A* **100**: 3584-8.
- Reddy, K. J., Bullerjahn, G. S., Sherman, D. M. and Sherman, L. A. (1988). "Cloning, nucleotide sequence, and mutagenesis of a gene (*irpA*) involved in iron-deficient growth of the cyanobacterium *Synechococcus* sp. Strain pcc7942." *J Bacteriol* **170**: 4466-76.
- Reid, R. T., H., L. D., Faulkner, J. and Butler, A. (1993). "A siderophore from a marine bacterium with an exceptional ferric ion affinity constant." *Nature* **366**: 455-458.

- Resch, M., Dobbek, H. and Meyer, O. (2005). "Structural and functional reconstruction *in situ* of the active site of carbon monoxide dehydrogenase from the carbon monoxide oxidizing eubacterium *Oligotropha carboxidovorans*." *J Biol Inorg Chem* **10**: 518-28.
- Roche, J. L., Murray, H., Orellana, M. and Newton, J. (1995). "Flavodoxin expression as an indicator of iron limitation in marine diatoms." *Journal of Phycology* **31**: 520-530.
- Rodionov, D. A., Gelfand, M. S., Todd, J. D., Curson, A. R. and Johnston, A. W. (2006). "Computational reconstruction of iron- and manganese-responsive transcriptional networks in alpha-proteobacteria." *PLoS Comput Biol* **2**: e163.
- Rodriguez, G. M., Voskuil, M. I., Gold, B., Schoolnik, G. K. and Smith, I. (2002). "*ideR*, an essential gene in *Mycobacterium tuberculosis*: Role of *ideR* in iron-dependent gene expression, iron metabolism, and oxidative stress response." *Infect Immun* **70**: 3371-81.
- Ruangkiattikul, N., S. Bhubhanil, et al. (2012). "*Agrobacterium tumefaciens* membrane-bound ferritin plays a role in protection against hydrogen peroxide toxicity and is negatively regulated by the iron response regulator." *FEMS Microbiol Lett* **329**(1): 87-92.
- Rudolph, G., Semini, G., Hauser, F., Lindemann, A., Friberg, M., Hennecke, H., et al. (2006). "The iron control element, acting in positive and negative control of iron-regulated *Bradyrhizobium japonicum* genes, is a target for the Irr protein." *J Bacteriol* **188**: 733-44.
- Rue, E. L. and Bruland, K. W. (1995). "Complexation of iron(III) by natural organic ligands in the central North Pacific as determined by a new competitive ligand equilibration/adsorptive cathodic stripping voltammetric method." Amsterdam, PAYS-BAS, Elsevier.
- Rue, E. L. and Bruland, K. W. (1997). "The role of organic complexation on ambient iron chemistry in the equatorial pacific ocean and the response of a mesoscale iron addition experiment." Waco, TX, ETATS-UNIS, American Society of Limnology and Oceanography.
- Rueter, J. G. and Unsworth, N. L. (1991). "Response of marine *Synechococcus* (cyanophyceae) cultures to iron nutrition." *Journal of Phycology* **27**: 173-178.
- Runyen-Janecky, L., Dzenski, E., Hawkins, S. and Warner, L. (2006). "Role and regulation of the *Shigella flexneri* Sit and MntH systems." *Infect Immun* **74**: 4666-72.
- Rusch, D. B., Halpern, A. L., Sutton, G., Heidelberg, K. B., Williamson, S., Yooseph, S., et al. (2007). "The sorcerer II global ocean sampling expedition: Northwest atlantic through eastern tropical pacific." *PLoS Biol* **5**: e77.
- Rutherford, K., Parkhill, J., Crook, J., Horsnell, T., Rice, P., Rajandream, M. A., et al. (2000). "Artemis: Sequence visualization and annotation." *Bioinformatics* **16**: 944-5.
- Sabri, M., Leveille, S. and Dozois, C. M. (2006). "A SitABCD homologue from an avian pathogenic *Escherichia coli* strain mediates transport of iron and manganese and resistance to hydrogen peroxide." *Microbiology* **152**: 745-58.
- Saitou, N. and Nei, M. (1987). "The neighbor-joining method: A new method for reconstructing phylogenetic trees." *Mol Biol Evol* **4**: 406-25.
- Sambrook, J., Fritsch, E. F. and Maniatis, T. (1989). Molecular cloning. Cold Spring Harbor, N.Y., Cold Spring Harbor Laboratory Press.
- Sandmann, G., Peleato, M. L., Fillat, M. F., Lázaro, M. C. and Gómez-Moreno, C. (1990). "Consequences of the iron-dependent formation of ferredoxin and flavodoxin on photosynthesis and nitrogen fixation on *Anabaena* strains." *Photosynthesis Research* **26**: 119-125.
- Schafer, A., Tauch, A., Jager, W., Kalinowski, J., Thierbach, G. and Puhler, A. (1994). "Small mobilizable multi-purpose cloning vectors derived from the *Escherichia coli* plasmids pk18 and pk19: Selection of defined deletions in the chromosome of *Corynebacterium glutamicum*." *Gene* **145**: 69-73.
- Schauer, K., Rodionov, D. A. and de Reuse, H. (2008). "New substrates for TonB-dependent transport: Do we only see the tip of the iceberg?" *Trends in Biochemical Sciences* **33**: 330-338.
- Schroder, I., Johnson, E. and de Vries, S. (2003). "Microbial ferric iron reductases." *FEMS Microbiol Rev* **27**: 427-47.
- Schryvers, A. B. and Morris, L. J. (1988). "Identification and characterization of the transferrin receptor from *Neisseria meningitidis*." *Mol Microbiol* **2**: 281-8.
- Schwartz, C. J., Giel, J. L., Patschkowski, T., Luther, C., Ruzicka, F. J., Beinert, H., et al. (2001). "IscR, an Fe-S cluster-containing transcription factor, represses expression of *Escherichia coli* genes encoding Fe-S cluster assembly proteins." *Proc Natl Acad Sci U S A* **98**: 14895-900.

- Schwyn, B. and Neilands, J. B. (1987). "Universal chemical assay for the detection and determination of siderophores." *Anal Biochem* **160**: 47-56.
- Shaw, A. K., Halpern, A. L., Beeson, K., Tran, B., Venter, J. C. and Martiny, J. B. (2008). "It's all relative: Ranking the diversity of aquatic bacterial communities." *Environ Microbiol* **10**: 2200-10.
- Shi, D., Xu, Y., Hopkinson, B. M. and Morel, F. M. M. (2010). "Effect of ocean acidification on iron availability to marine phytoplankton." *Science* **327**: 676-679.
- Sies, H. (1993). "Strategies of antioxidant defense." *Eur J Biochem* **215**: 213-9.
- Singleton, C., White, G. F., Todd, J. D., Marritt, S. J., Cheesman, M. R., Johnston, A. W., *et al.* (2010). "Haem-responsive DNA binding by the global iron regulator Irr from *Rhizobium leguminosarum*." *J Biol Chem* **285**: 16023-31.
- Small, S. K., Puri, S., Sangwan, I. and O'Brian, M. R. (2009). "Positive control of ferric siderophore receptor gene expression by the Irr protein in *Bradyrhizobium japonicum*." *J Bacteriol* **191**: 1361-8.
- Smillie, R. M. (1965). "Isolation of phytoflavin, a flavoprotein with chloroplast ferredoxin activity." *Plant Physiology* **40**: 1124-1128.
- Smith, D. P., Kitner, J. B., Norbeck, A. D., Clauss, T. R., Lipton, M. S., Schwalbach, M. S., *et al.* (2010). "Transcriptional and translational regulatory responses to iron limitation in the globally distributed marine bacterium *Pelagibacter ubique*." *PLoS One* **5**: e10487.
- Smith, M. J., Shoolery, J. N., Schwyn, B., Holden, I. and Neilands, J. B. (1985). "Rhizobactin, a structurally novel siderophore from *Rhizobium meliloti*." *Journal of the American Chemical Society* **107**: 1739-1743.
- Sogin, M. L., Morrison, H. G., Huber, J. A., Mark Welch, D., Huse, S. M., Neal, P. R., *et al.* (2006). "Microbial diversity in the deep sea and the underexplored "Rare biosphere". " *Proc Natl Acad Sci U S A* **103**: 12115-20.
- Spaink, H. P., Okker, R.J.H., Wijffelman, C.A., Pees E., and Lugtenberg B.J.J. (1987). "Promoters in the nodulation region of the *Rhizobium leguminosarum sym* plasmid pRL11." *Plant Mol Biol* **9**: 27-39.
- Spatafora, G. A. and Moore, M. W. (1998). "Growth of *Streptococcus mutans* in an iron-limiting medium." *Methods in Cell Science* **20**: 217-221.
- Stadtman, E. R., Berlett, B. S. and Chock, P. B. (1990). "Manganese-dependent disproportionation of hydrogen peroxide in bicarbonate buffer." *Proc Natl Acad Sci U S A* **87**: 384-8.
- Stingl, U., Tripp, H. J. and Giovannoni, S. J. (2007). "Improvements of high-throughput culturing yielded novel SAR11 strains and other abundant marine bacteria from the oregon coast and the Bermuda Atlantic time series study site." *ISME J* **1**: 361-71.
- Stojiljkovic, I. and Hantke, K. (1992). "Haemin uptake system of *Yersinia enterocolitica*: Similarities with other tonB-dependent systems in gram-negative bacteria." *EMBO J* **11**: 4359-67.
- Stojiljkovic, I., Baumber, A. J. and Hantke, K. (1994). "Fur regulon in gram-negative bacteria. Identification and characterization of new iron-regulated *Escherichia coli* genes by a fur titration assay." *J Mol Biol* **236**: 531-45.
- Stojiljkovic, I., Cobeljic, M. and Hantke, K. (1993). "*Escherichia coli* K-12 ferrous iron uptake mutants are impaired in their ability to colonize the mouse intestine." *FEMS Microbiol Lett* **108**: 111-5.
- Stojiljkovic, I., Larson, J., Hwa, V., Anic, S. and So, M. (1996). "HmbR outer membrane receptors of pathogenic *Neisseria* spp.: Iron-regulated, hemoglobin-binding proteins with a high level of primary structure conservation." *J Bacteriol* **178**: 4670-8.
- Stumm, W. and Morgan, J. J. (1981). "Aquatic chemistry : An introduction emphasizing chemical equilibria in natural waters." New York ; Chichester, Wiley.
- Sun, S., Chen, J., Li, W., Altintas, I., Lin, A., Peltier, S., *et al.* (2010). "Community cyberinfrastructure for advanced microbial ecology research and analysis: The CAMERA resource." *Nucleic Acids Res* **39**: D546-51.
- Sunda, W. G., Huntsman and S. A. (1998). "Interactive effects of external manganese, the toxic metals copper and zinc, and light in controlling cellular manganese and growth in a coastal diatom." Waco, TX, ETATS-UNIS, American Society of Limnology and Oceanography.
- Sunda, W. G. (2010). "Iron and the carbon pump." *Science* **327**: 654-655.
- Sunda, W. G. and Huntsman, S. A. (1994). "Photoreduction of manganese oxides in seawater." *Marine Chemistry* **46**: 133-152.
- Sunda, W. G. and Huntsman, S. A. (1995). "Iron uptake and growth limitation in oceanic and coastal phytoplankton." *Marine Chemistry* **50**: 189-206.

- Szklarczyk, D., Franceschini, A., Kuhn, M., Simonovic, M., Roth, A., Minguéz, P., *et al.* (2011). "The string database in 2011: Functional interaction networks of proteins, globally integrated and scored." *Nucleic Acids Res* **39**: D561-8.
- Tagliabue, A., Bopp, L., Aumont, O. and Arrigo, K. R. (2009). "Influence of light and temperature on the marine iron cycle: From theoretical to global modeling." *Global Biogeochem. Cycles* **23**: GB2017.
- Tai, S. S., Yu, C. and Lee, J. K. (2003). "A solute binding protein of *Streptococcus pneumoniae* iron transport." *FEMS Microbiol Lett* **220**: 303-8.
- Tamura, K., Peterson, D., Peterson, N., Stecher, G., Nei, M. and Kumar, S. (2011). "MEGA5: Molecular evolutionary genetics analysis using maximum likelihood, evolutionary distance, and maximum parsimony methods." *Mol Biol Evol* **28**: 2731-9.
- Tegen, I. and Fung, I. (1995). "Contribution to the atmospheric mineral aerosol load from land surface modification." *J. Geophys. Res.* **100**: 18707-18726.
- Todd, J. D., G. Sawers, *et al.* (2006). "The *Rhizobium leguminosarum* regulator IrrA affects the transcription of a wide range of genes in response to Fe availability." *Mol Genet Genomics* **275**(6): 564-577.
- Todd, J. D., Kirkwood, M., Newton-Payne, S. and Johnston, A. W. (2011). "DddW, a third DMSP lyase in a model Roseobacter marine bacterium, *Ruegeria pomeroyi* DSS-3." *ISME J* **6**: 223-6.
- Todd, J. D., M. Wexler, *et al.* (2002). "RirA, an iron-responsive regulator in the symbiotic bacterium *Rhizobium leguminosarum*." *Microbiology* **148**(Pt 12): 4059-4071.
- Todd, J. D., Sawers, G. and Johnston, A. W. (2005). "Proteomic analysis reveals the wide-ranging effects of the novel, iron-responsive regulator RirA in *Rhizobium leguminosarum* bv. *viciae*." *Mol Genet Genomics* **273**: 197-206.
- Todd, J. D., Sawers, G., Rodionov, D. A. and Johnston, A. W. (2006). "The *Rhizobium leguminosarum* regulator IrrA affects the transcription of a wide range of genes in response to Fe availability." *Mol Genet Genomics* **275**: 564-77.
- Todd, J. D., Wexler, M., Sawers, G., Yeoman, K. H., Poole, P. S. and Johnston, A. W. (2002). "RirA, an iron-responsive regulator in the symbiotic bacterium *Rhizobium leguminosarum*." *Microbiology* **148**: 4059-71.
- Tong, Y. and Guo, M. (2009). "Bacterial haem-transport proteins and their haem-coordination modes." *Arch Biochem Biophys* **481**: 1-15.
- Torres, E. and Ayala, M. (2010). "Biocatalysis based on haem peroxidases: Peroxidases as potential industrial biocatalysts." Heidelberg, Springer.
- Tortell, P. D., Maldonado, M. T., Granger, J. and Price, N. M. (1999). "Marine bacteria and biogeochemical cycling of iron in the oceans." *FEMS Microbiology Ecology* **29**: 1-11.
- Traxler, M. F., M. R. Seyedsayamdost, *et al.* (2012). "Interspecies modulation of bacterial development through iron competition and siderophore piracy." *Mol Microbiol*.
- Trick, C. G. (1989). "Hydroxamate-siderophore production and utilization by marine eubacteria." *Current Microbiology* **18**: 375-378.
- Tsolis, R. M., Baumler, A. J., Heffron, F. and Stojiljkovic, I. (1996). "Contribution of TonB- and Feo-mediated iron uptake to growth of *Salmonella* Typhimurium in the mouse." *Infect Immun* **64**: 4549-56.
- Tsuda, A., Takeda, S., Saito, H., Nishioka, J., Nojiri, Y., Kudo, I., *et al.* (2003). "A mesoscale iron enrichment in the western subarctic pacific induces a large centric diatom bloom." *Science* **300**: 958-961.
- Uchino, Y., Hirata, A., Yokota, A. and Sugiyama, J. (1998). "Reclassification of marine *Agrobacterium* species: Proposals of *Stappia stellulata* gen. Nov., comb. Nov., *Stappia aggregata* sp. Nov., nom. Rev., *Ruegeria atlantica* gen. Nov., comb. Nov., *Ruegeria gelatinovora* comb. Nov., *Ruegeria algicola* comb. Nov., and *Ahrensia kieliense* gen. Nov., sp. Nov., nom. Rev." *J Gen Appl Microbiol* **44**: 201-210.
- Untergasser, A., Nijveen, H., Rao, X., Bisseling, T., Geurts, R. and Leunissen, J. A. (2007). "Primer3plus, an enhanced web interface to primer3." *Nucleic Acids Res* **35**: W71-4.
- van den Berg, C. M. G. (1995). "Evidence for organic complexation of iron in seawater." *Marine Chemistry* **50**: 139-157.
- Van Trappen, S., Mergaert, J. and Swings, J. (2004). "*Loktanella salsilacus* gen. Nov., sp. Nov., *Loktanella fryxellensis* sp. Nov. And *Loktanella vestfoldensis* sp. Nov., new members of the Rhodobacter group, isolated from microbial mats in antarctic lakes." *Int J Syst Evol Microbiol* **54**: 1263-9.
- Vartivarian, S. E. and Cowart, R. E. (1999). "Extracellular iron reductases: Identification of a new class of enzymes by siderophore-producing microorganisms." *Arch Biochem Biophys* **364**: 75-82.

- Vassinova, N. and Kozyrev, D. (2000). "A method for direct cloning of Fur-regulated genes: Identification of seven new fur-regulated loci in *Escherichia coli*." *Microbiology* **146 Pt 12**: 3171-82.
- Venter, J. C., Remington, K., Heidelberg, J. F., Halpern, A. L., Rusch, D., Eisen, J. A., *et al.* (2004). "Environmental genome shotgun sequencing of the sargasso sea." *Science* **304**: 66-74.
- Veyrier, F. J., Boneca, I. G., Cellier, M. F. and Taha, M. K. (2011). "A novel metal transporter mediating manganese export (MntX) regulates the Mn to Fe intracellular ratio and *Neisseria meningitidis* virulence." *PLoS Pathog* **7**: e1002261.
- Vollack, K. U., Hartig, E., Korner, H. and Zumft, W. G. (1999). "Multiple transcription factors of the FNR family in denitrifying *Pseudomonas stutzeri*: Characterization of four FNR-like genes, regulatory responses and cognate metabolic processes." *Mol Microbiol* **31**: 1681-94.
- Wachtershauser, G. (2000). "Origin of life. Life as we don't know it." *Science* **289**: 1307-8.
- Wan, X. F., Verberkmoes, N. C., McCue, L. A., Stanek, D., Connelly, H., Hauser, L. J., *et al.* (2004). "Transcriptomic and proteomic characterization of the Fur modulon in the metal-reducing bacterium *Shewanella oneidensis*." *J Bacteriol* **186**: 8385-400.
- Wandersman, C. and Delepelaire, P. (2004). "Bacterial iron sources: From siderophores to hemophores." *Annu Rev Microbiol* **58**: 611-647.
- Wang, Z., Kadouri, D. E. and Wu, M. (2011). "Genomic insights into an obligate epibiotic bacterial predator: *Micavibrio aeruginosavorus* ARL-13." *BMC Genomics* **12**: 453.
- Webb, E. A., Moffett, J. W. and Waterbury, J. B. (2001). "Iron stress in open-ocean cyanobacteria (*Synechococcus*, *Trichodesmium*, and *Crocospaera* spp.): Identification of the IdiA protein." *Appl. Environ. Microbiol.* **67**: 5444-5452.
- Wells, M. L., Price, N. M., Bruland and K. W. (1995). "Iron chemistry in seawater and its relationship to phytoplankton: A workshop report." Amsterdam, PAYS-BAS, Elsevier.
- Wexler, M., Todd, J. D., Kolade, O., Bellini, D., Hemmings, A. M., Sawers, G., *et al.* (2003). "Fur is not the global regulator of iron uptake genes in *Rhizobium leguminosarum*." *Microbiology* **149**: 1357-65.
- White, G. F., Singleton, C., Todd, J. D., Cheesman, M. R., Johnston, A. W. and Le Brun, N. E. (2011). "Haem binding to the second, lower-affinity site of the global iron regulator Irr from *Rhizobium leguminosarum* promotes oligomerization." *FEBS J* **278**: 2011-21.
- Whitman, W. B., Coleman, D. C. and Wiebe, W. J. (1998). "Prokaryotes: The unseen majority." *Proc Natl Acad Sci U S A* **95**: 6578-83.
- Wilhelm, S. W., Macauley, K, Trick and C, G. (1998). "Evidence for the importance of catechol-type siderophores in the iron-limited growth of a cyanobacterium." Waco, TX, ETATS-UNIS, American Society of Limnology and Oceanography.
- Williams, K. P., Sobral, B. W. and Dickerman, A. W. (2007). "A robust species tree for the alphaproteobacteria." *J Bacteriol* **189**: 4578-86.
- Wood, P. M. (1978). "Interchangeable copper and iron proteins in algal photosynthesis." *European Journal of Biochemistry* **87**: 9-19.
- Wu, J. and Luther, G. W. (1995). "Complexation of Fe(III) by natural organic ligands in the northwest Atlantic Ocean by a competitive ligand equilibration method and a kinetic approach." *Marine Chemistry* **50**: 159-177.
- Wyckoff, E. E., Mey, A. R., Leimbach, A., Fisher, C. F. and Payne, S. M. (2006). "Characterization of ferric and ferrous iron transport systems in *Vibrio cholerae*." *J. Bacteriol.* **188**: 6515-6523.
- Wyckoff, E. E., Stoebner, J. A., Reed, K. E. and Payne, S. M. (1997). "Cloning of a *Vibrio cholerae* vibriobactin gene cluster: Identification of genes required for early steps in siderophore biosynthesis." *J Bacteriol* **179**: 7055-62.
- Xu, Q., Rawlings, N. D., Farr, C. L., Chiu, H. J., Grant, J. C., Jaroszewski, L., *et al.* (2011). "Structural and sequence analysis of imelysin-like proteins implicated in bacterial iron uptake." *PLoS One* **6**: e21875.
- Yang, J., Ishimori, K. and O'Brian, M. R. (2005). "Two haem binding sites are involved in the regulated degradation of the bacterial iron response regulator (Irr) protein." *J Biol Chem* **280**: 7671-6.
- Yasmin, S., Andrews, S. C., Moore, G. R. and Le Brun, N. E. (2011). "A new role for haem, facilitating release of iron from the bacterioferritin iron biomineral." *J Biol Chem* **286**: 3473-83.
- Yeoman, K. H., Curson, A. R., Todd, J. D., Sawers, G. and Johnston, A. W. (2004). "Evidence that the rhizobium regulatory protein RirA binds to *cis*-acting iron-responsive operators (IROs) at promoters of some Fe-regulated genes." *Microbiology* **150**: 4065-74.

- Yeoman, K. H., M. J. Delgado, et al. (1997). "High affinity iron acquisition in *Rhizobium leguminosarum* requires the *cycHJKL* operon and the *feuPQ* gene products, which belong to the family of two-component transcriptional regulators." *Microbiology* **143** (Pt 1): 127-134.
- Yooseph, S., Sutton, G., Rusch, D. B., Halpern, A. L., Williamson, S. J., Remington, K., et al. (2007). "The *Sorcerer II* global ocean sampling expedition: Expanding the universe of protein families." *PLoS Biol* **5**: e16.
- Yu, N. Y., Wagner, J. R., Laird, M. R., Melli, G., Rey, S., Lo, R., et al. (2010). "PsortB 3.0: Improved protein subcellular localization prediction with refined localization subcategories and predictive capabilities for all prokaryotes." *Bioinformatics* **26**: 1608-15.
- Zhang, L., McSpadden, B., Pakrasi, H. B. and Whitmarsh, J. (1992). "Copper-mediated regulation of cytochrome *c553* and plastocyanin in the cyanobacterium *Synechocystis* 6803." *Journal of Biological Chemistry* **267**: 19054-19059.
- Zhou, D., Hardt, W. D. and Galan, J. E. (1999). "*Salmonella* Typhimurium encodes a putative iron transport system within the centisome 63 pathogenicity island." *Infect Immun* **67**: 1974-81.
- Zhou, D., Qin, L., Han, Y., Qiu, J., Chen, Z., Li, B., et al. (2006). "Global analysis of iron assimilation and Fur regulation in *Yersinia pestis*." *FEMS Microbiol Lett* **258**: 9-17.
- Zhu, H., Alexeev, D., Hunter, D. J., Campopiano, D. J. and Sadler, P. J. (2003). "Oxo-iron clusters in a bacterial iron-trafficking protein: New roles for a conserved motif." *Biochem J* **376**: 35-41.
- Zhuang, G., Duce, R. A. and Kester, D. R. (1990). "The dissolution of atmospheric iron in surface seawater of the open ocean." *J. Geophys. Res.* **95**: 16207-16216.
- Wexler, M., K. H. Yeoman, et al. (2001). "The *Rhizobium leguminosarum* TonB gene is required for the uptake of siderophore and haem as sources of iron." *Mol Microbiol* **41**(4): 801-816.
- Wyckoff, E. E., A. R. Mey, et al. (2006). "Characterization of Ferric and Ferrous Iron Transport Systems in *Vibrio cholerae*." *J. Bacteriol.* **188**(18): 6515-6523.